STATE OF NEVADA

AGENCY FOR NUCLEAR PROJECTS/ NUCLEAR WASTE PROJECT OFFICE

BOB MILLER
Governor

ROBERT R. LOUX
Executive Director

STATE OF NEVADA
AGENCY FOR NUCLEAR PROJECTS
NUCLEAR WASTE PROJECT

NWPO-TR-015-90

QUATERNARY GEOLOGY AND NEOTECTONIC ACTIVITY ALONG THE FISH LAKE VALLEY FAULT ZONE, NEVADA AND CALIFORNIA

BY

THOMAS LEN SAWYER
UNIVERSITY OF NEVADA, RENO

AUGUST, 1990

THE NEVADA AGENCY FOR NUCLEAR PROJECTS/NUCLEAR WASTE PROJECT OFFICE (NWPO) WAS CREATED BY THE NEVADA LEGISLATURE TO OVERSEE FEDERAL HIGH-LEVEL NUCLEAR WASTE ACTIVITIES IN THE STATE. SINCE 1985, IT HAS DEALT LARGELY WITH THE U.S. DEPARTMENT OF ENERGY'S SITING OF A HIGH-LEVEL NUCLEAR WASTE REPOSITORY AT YUCCA MOUNTAIN IN SOUTHERN NEVADA. AS PART OF ITS OVERSIGHT ROLE, NWPO HAS CONTRACTED FOR STUDIES OF VARIOUS TECHNICAL QUESTIONS AT YUCCA MOUNTAIN.

THIS STUDY WAS FUNDED BY DOE GRANT NUMBER DE-FG08-85-NV10461.

UNIVERSITY OF NEVADA
RENO

QUATERNARY GEOLOGY AND NEOTECTONIC ACTIVITY ALONG THE FISH LAKE VALLEY FAULT ZONE, NEVADA AND CALIFORNIA

A thesis submitted in partial fulfillment of the
requirements for the degree of Master of Science in Geology.

by

Thomas Len Sawyer

August, 1990

UNIVERSITY OF NEVADA
RENO

Center for Neotectonic Studies
Mail Stop 168
Mackay School of Mines
Reno, Nevada 89557-[illegible]
Phone (702) 784-[illegible]
Phone (702) 784-[illegible]
FAX (702) 784-[illegible]

July 16, 1991

Carl Johnson
Administrator of Technical Programs
State of Nevada
Nuclear Waste Projects Office

Dear Carl:

Enclosed is a copy of Tom Sawyer's newly completed Master of Science thesis, entitled, "Quaternary geology and neotectonic activity along the Fish Lake Valley fault zone, Nevada and California," which was supported by Task 5 and the General Task of the Yucca Mountain Project of the Center for Neotectonic Studies, UNR, with funds provided by your office.

Tom's thesis is the first detailed study of the structure, neotectonic setting, and paleoseismicity of the Fish Lake Valley fault zone, which is the accessible northern continuation of the Furnace Creek fault zone in Death Valley. The latter fault is acknowledged to be the most significant active right-lateral fault in the western Great Basin. This study suggests that, near its northern termination, the zone has a minimum slip rate of 0.7-0.8 mm/yr. Evidence is presented for three discrete slip events in the last 4000 to 2000 years, with the youngest large event about 1000 years ago. If the characteristic earthquake scenario applies, magnitudes of 7.1 $\pm$ 0.3 are suggested. Tom's work underscores the importance of careful studies of paleoseismicity and structure along Quaternary faults in the southwestern Great Basin, in regions near Yucca Mountain.

This is the second of three recently completed theses on neotectonics and active faulting supported by Task 5 that I will be sending you. These studies provide an important body of new information about the neotectonic framework of the Yucca Mountain region. We are grateful for the support provided by your office that made these studies possible.

With best regards,

Rich Schweickert

Richard A. Schweickert
Professor of Geology

ACKNOWLEDGEMENTS

This study has profoundly benefitted from the participation of several individuals. Doug Rennie, who joked that he spent more time in the field on this thesis project than his own, freely shared with me his Quaternary geologic knowledge and personal philosophy. Doug, its too late to thank you now and again, I and many others miss you greatly. I especially thank Marith Reheis for assisting me in a variety of tasks in the field and for lending professional advice on many occasions. I very much appreciate the competent field assistance of Scott Lewis, Steve Nitchman, Pat Goldstrand and Janet Slate. Special thanks to Alan Ramelli, Marith Reheis, Doug Rennie, John Caskey and Nick Varnum for participating with logging trenches under adverse conditions.

This document has been improved as a result of careful editorial consideration by Rich Schweickert, Burt Slemmons, and Fred Peterson, the thesis committee. Sections of this document have been critically edited by Greg Vick and Joanne Hoffard.

This study was funded in part through the Center for Neotectonic Studies, UNR, by a grant from the Nuclear Waste Project Office, Carson City, Nevada. The Nevada Bureau of Mines and Geology and Woodward-Clyde Consultants made computer equipment available to me for the production of this document.

My understanding of several of the aspects of this study has been greatly improved via lengthy conversations with Alan Gillespie, Jennifer Harden, Chester Beaty, and Craig dePolo, in addition to several of the people listed above.

Janet Sawyer has assisted me in virtually every aspect of this study and has somehow managed to endure it.

Finally, I am grateful to Paul Pace for helpful instruction on the use of surveying equipment and for assistance with organizing survey projects.

ABSTRACT

The right-divergent Fish Lake Valley fault zone (FLVFZ), a 80 KM-long component of the northern Death Valley fault system, comprises contemporaneous NW-striking dextral faults, N-striking normal faults, NE-striking left(?)-divergent faults, and locally WNW-striking contractional faults. The fault zone terminates in a horsetail splay where the minimum right-slip rate is 0.7-0.8 mm/yr.

The styles and rates of faulting are based on a sequence of morphostratigraphic units disrupted by the FLVFZ. Geomorphic surface correlations, radiocarbon analyses, tephrochronology, and soil development studies were used to estimate unit ages.

Paleoseismicity studies have identified three discrete slip events in the last 4 to 2 ka on the northern FLVFZ. The last two significant events were similar, suggesting a characteristic earthquake behavior and magnitudes of 7.1 ± 0.3. The last large event occurred 1 ka (±0.6, -0.5) and comparable events have repeated every 1.1 Ka (+2.3, -0.5). Source structure characteristics suggest a MCE of M 7.3 ± 0.4.

TABLE OF CONTENTS

LIST OF TABLES

LIST OF FIGURES

CHAPTER I
INTRODUCTION AND METHOD OF STUDY

STATEMENT OF PROBLEM

Yucca Mountain, Nevada is currently the only site under consideration as the first high-level nuclear waste repository in the United States for storage of commercially spent fuel. Since the waste will remain hazardous for most or all of a 10,000 year isolation period, protracted environmental stability of the site is crucial. Therefore, it is imperative to assess all aspects of the Yucca Mountain region for possible adverse effects on the site proper. Particularly important is the seismic potential of regional and local seismic-source structures.

The longest seismic-source structure in the Yucca Mountain region and within the southern Basin and Range Province, is the Death Valley-Furnace Creek fault zone, herein termed the "Death Valley fault system" (DVFS). The dextral DVFS is an intercontinental transform fault (using Sylvester's [1988, p. 1668] classification) that separates regional domains of conspicuously contrasting tectonic styles and rates in the southwestern province. The nearly 350 km long late Quaternary fault system (comparable in length to the Wasatch fault zone in Utah) lies less than 50 km from the proposed repository at Yucca Mountain, Nevada (Fig. 1).

Although the DVFS was recognized as a Quaternary structure of regional significance near the turn of the century (e.g., Ball, 1907), the neotectonic development and seismic potential of this fundamental crustal structure are poorly understood. This is especially true of the northernmost component of the fault system, the Fish Lake Valley fault zone (FLVFZ) in Fish Lake Valley, Nevada and California (Fig. 1).

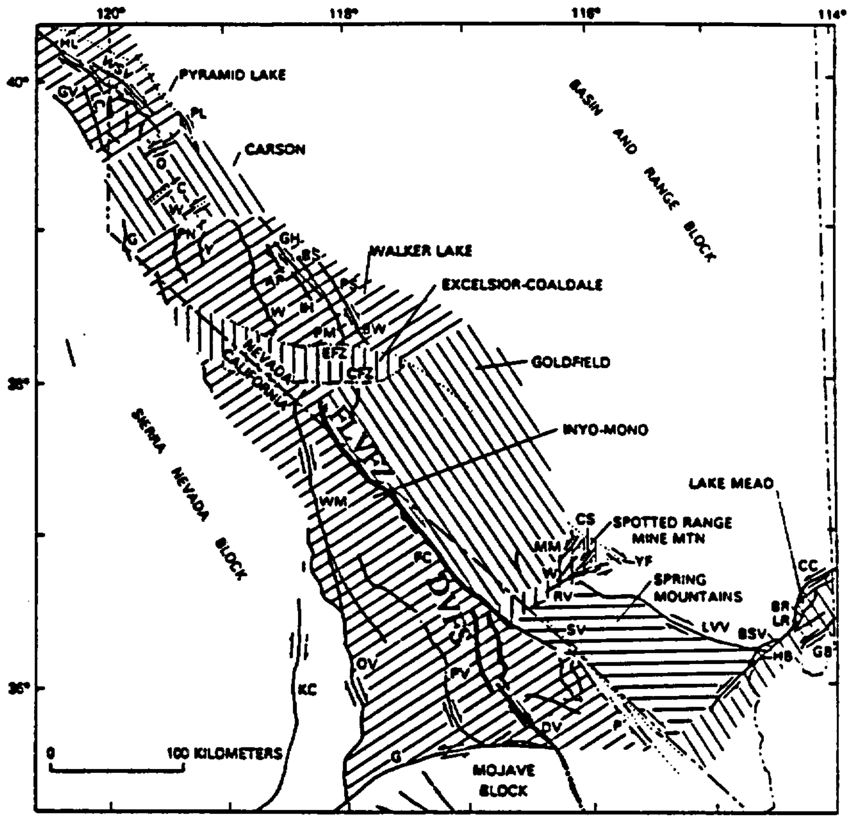

FIG. 25-3. Regional structural blocks and major faults in Walker Lane belt. Arrows indicate relative movement on strike-slip faults. Major faults or fault zone listed by structural blocks: PYRAMID LAKE BLOCK: HL, Honey Lake; GV, Grizzly Valley; LC, Last Chance; WSV, Warm Springs Valley; PL, Pyramid Lake. CARSON BLOCK: O, Olinghouse; C, Carson; W. Wabuska. WALKER LAKE BLOCK: G, Genoa; PN, Pine Nut; Y, Yerington; W, Wassuk; AP, Agai Pah Hills; GH, Gumdrop Hills; IH, Indian Head; BS, Benton Spring; PS, Petrified Springs; PM, Pilot Mountains; BW, Bettles Well. EXCELSIOR-COALDALE BLOCK: EFZ, Excelsior; CFZ, Coaldale. INYO-MONO BLOCK: KC, Kern Canyon; I, Independence; WM, White Mountain; OV, Owens Valley; FC, Furnace Creek; PV, Panamint Valley; DV, Death Valley; G, Garlock; SV, Stewart Valley; P, Pahrump. SPOTTED RANGE-MINE MOUNTAIN BLOCK: MM, Mine Mountain; W, Wahmonie; RV, Rock Valley; CS, Cane Spring; YF, Yucca-Frenchman. SPRING MOUNTAINS BLOCK: LVV, Las Vegas Valley. LAKE MEAD BLOCK: BSV, Bitter Spring Valley; HB, Hamblin Bay; CC, Cabin Canyon; BR, Bitter Ridge; LR, Lime Ridge; GB, Gold Butte.

Figure 1. Stewart's (1988) subdivision of the Walker Lane belt (i.e. WLSZ). The Death Valley fault system (DVFS), including the Fish Lake Valley fault zone (FLVFZ) are shown modified in heavy lines.

The length, geomorphic character, late Quaternary activity, neotectonic influence, and proximity of the DVFS to the Yucca Mountain site mandate a thorough assessment of its seismic potential. This thesis examines the Quaternary tectonics and stratigraphy along the northern DVFS as a basis for characterizing the seismic potential of the FLVFZ.

OBJECTIVES

Assessing the seismic potential of the FLVFZ is the principal objective of this thesis (as stated above). The assessment is largely an attempt to identify the expectable size and frequency of significant earthquakes along the FLVFZ. Understanding rates, styles of faulting, and the Holocene paleoseismic behavior of the fault zone are aspects essential to the assessment of seismic potential.

Several other objectives are fundamental to this study. These objectives include various aspects of Quaternary geology, and provide the basis for assessing the tectonic history, Holocene paleoseismic behavior and seismic potential of the FLVFZ. The most noteworthy of these objectives is establishing a soil-stratigraphic framework that can be extrapolated throughout the region.

The various objectives summarized below are discussed further in the appropriate chapter(s) that follow.

GENERAL STATEMENTS

LOCATION OF STUDY AREA

Fish Lake Valley is near the western margin of the Basin and Range Province, situated between the lofty White Mountains on the west and the Silver Peak range on the east. The study area extends the full length of western Fish Lake Valley and is bounded on the west by the White Mountains and northernmost Inyo Mountains, on the north by the Volcanic Hills and by the Sylvania Mountains and Last Chance Range on the south (Fig. 2). The study area comprises the extensive piedmont slope flanking the eastern White Mountains and a large playa/alluvial flat in the southern part of the valley. Both the FLVFZ and the border between east-central California and southwestern Nevada are straddled by the study area (Fig. 2).

PHYSIOGRAPHY AND DRAINAGE

The majestic White Mountains, the highest of all ranges in the Basin and Range Province, rise in excess of 2700 m (9000 ft) above the floor of Fish Lake Valley. The range culminates in White Mountain Peak at 4341 m (14,242 ft) and forms the highest point in Nevada, Boundary Peak, at 4006 m (13,143 ft). Pellisier Flats forms the broad flattish crest of the range between the two elevated peaks. The eastern margin of the crest is scalloped by deep head cirques of major perennial drainages, glaciated during the Quaternary. Reentrants in the mountain front are common where these streams débouch onto the extensive piedmont slope flanking the eastern White Mountains. Nearly all perennial streams have been artificially diverted for agricultural purposes, but most would otherwise flow across the piedmont slope to the valley floor.

Fish Lake Valley is an alluviated structural basin of largely internal drainage. The valley is apparently named for a small lake fed by springs and surrounded by marshy lowlands in the east-central part of the valley. Both the western and eastern margins of the valley are flanked by extensive piedmont slopes, in particular that along the northwestern margin. Playas and alluvial flats occur in the northeastern and southern parts of this boot-shaped valley. There are two points, one at each end of the valley, through which external drainage occurs. The Gap forms the northern "spill-point" that served as a conduit for external drainage northward into Columbus Salt Marsh, Nevada during July, 1967 (Nurmi, J., 1967, personal commun., in Beaty, 1968). Horse Thief Canyon drains a relatively small area in southernmost Fish Lake Valley, southeastward into Eureka Valley, California (Fig. 2). Although Fish Lake Valley is in part externally drained, the physiographic character of the basin is that of a bolson (i.e., "an internally drained intermontane basin" as defined by Peterson, 1981).

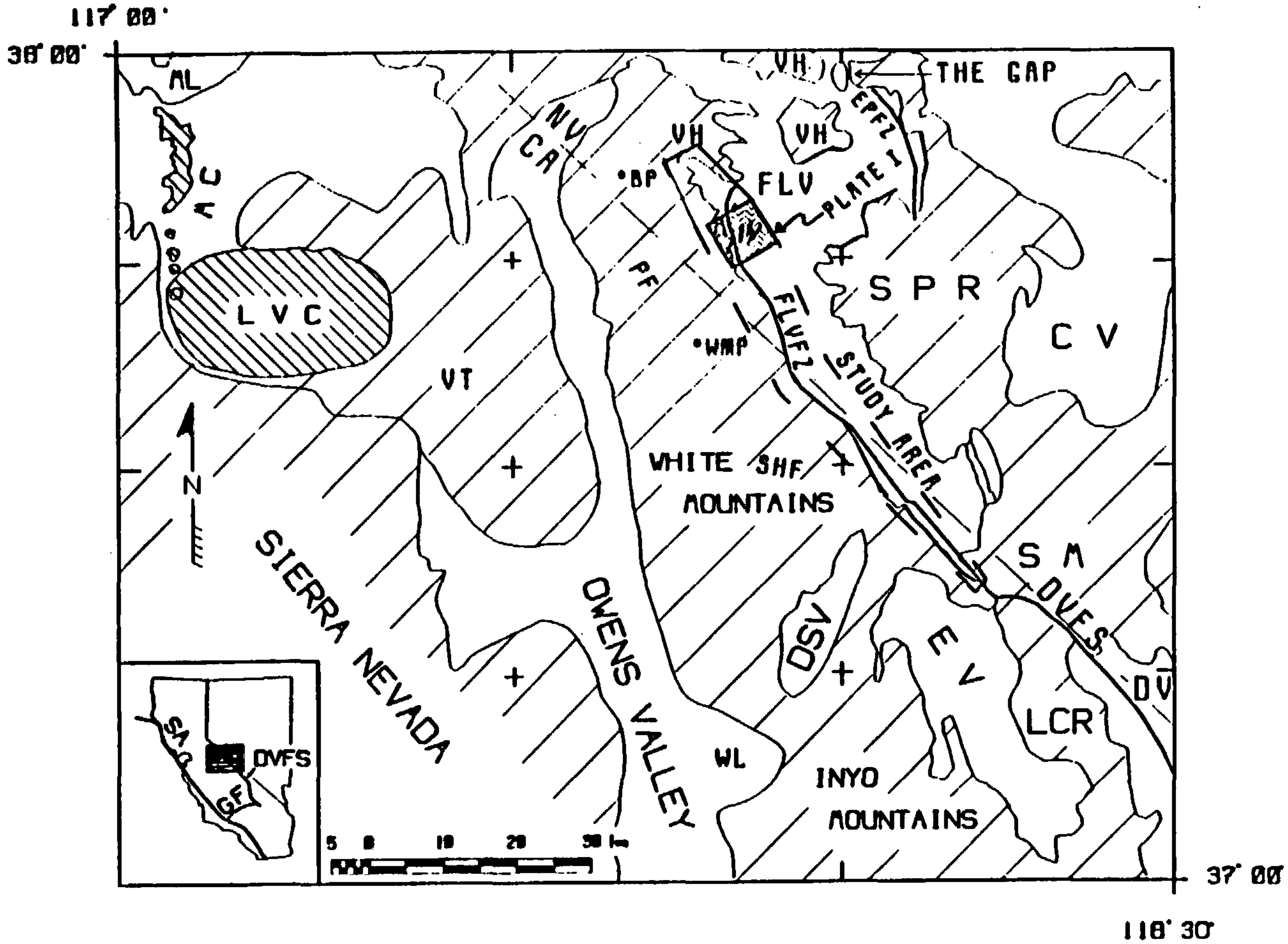

Figure 2. Regional map showing the study and detailed map areas, and selected features: CV, Clayton Valley; DSV, Deep Springs Valley; DV, Death Valley; DVFS, Death Valley fault system; EPFZ, Emigrant Peak fault zone; EV, Eureka Valley; FLV, Fish Lake Valley; FLVFZ, Fish Lake Valley fault zone; GF, Garlock fault; LCR, Last Chance Range; LVC, Long Valley Caldera; MC, Mono Craters; ML, Mono Lake; SA, San Andreas fault; SM, Sylvania Mountains; SPR, Silver Peak Range; VH, Volcanic Hills,; VT, Volcanic Tablelands; WL, Waucoba Lakebeds.

CLIMATE

In this thesis, as in virtually all studies of Quaternary soil-stratigraphy, it is necessary to assess the impact of present and paleoclimatic conditions on soils of the study area.

PRESENT CLIMATE

Fish Lake Valley is in the northern Sonoran Desert and within the precipitation shadow of the Sierra Nevada and the White Mountains. The climate of the region is arid, characterized by hot dry summers and mild winters. Average annual precipitation is about 10 cm (U.S. Weather Bureau, 1948 to 1964) to nearly 13 cm (1903 to 1919, Eakin and Mason, 1950) on the floor of central and southern Fish Lake Valley. Along the semiarid crest of the White Mountains, average precipitation is approximately 40 cm per year (U.S. Weather Bureau, 1951 to 1957). Precipitation is commonly associated with cyclonic to monsoonal storms during winter and early spring, with isolated summer thunderstorms, which have resulted in intense local downpours. Temperatures occasionally exceed 56 C (100° F) in summertime and are infrequently below -18 C (0° F) during wintertime. The mean annual temperature in the valley is about 28 C (50°F)(U.S. Weather Bureau). The arid climate of the Fish Lake Valley region favors preservation of geomorphic features, hence is ideally suited for morphologic studies.

PALEOCLIMATE

The White Mountains experienced several major glaciations during the Pleistocene. Elliott-Fisk (1987) proposed that glacial erratics occur on the flattish crest of the White Mountains. Blackwelder (1934, p. 220) suggested that glaciers formed during the Sherwin glaciation (roughly 1 Ma) extended beyond the front of the east-central White Mountains, based on the distribution of till (?) and gross canyon morphology. Similar conclusions were reached by LaMarche (1965), Elliott-Fisk (1987), and Swanson and others (1988), but questioned by Beaty (1960). The last major glaciation in the White mountains occurred before 18,500 yrB.P., with the innermost moraine constructed before 12,700, based on ^{14}C analysis of organic matter in varnish (Elliott-Fisk and Dorn, 1987). On the floors of the highest cirque in the northern part of the range, "extremely fresh" appearing moraines suggest a relatively minor, early Holocene glaciation (Elliott-Fisk, 1987).

LaMarche (1973) inferred Holocene climatic fluctuations from the position of the upper treeline of Bristlecone pines (Pinus longaeva Bailey) in the White Mountains, a feature that is closely related to warm-season temperatures. LaMarche indicated that from about 4000 to 900 yrB.P. the regional climate was drier and cooler than that during the preceding several thousand years. After 900 yrB.P. and until recently, summers have been cooler and annual conditions drier than previously (LaMarche, 1973).

VEGETATION

The type and distribution of vegetation in the Fish Lake Valley region is largely governed by climatic gradients associated with orographic influences, and the availability of water. Riparian vegetation, including willows, birches and cottonwoods grow along perennial streams and serve as an example of the latter.

A variety of desert shrubs sparsely (20 to 40%) cover the extensive eastern piedmont slope of the White Mountains. The Great Basin sagebrush (Artemisia tridentata) is the predominant plant species. Relatively minor occurrences of bitterbrush (Purshia tridentata), a variety of buckwheats (Eriogonum sp.) and cholla cactus are also present. Near the front of the range desert shrubs are intermixed with Pinyon pine (Pinus monophylla) and at higher elevations within many of the mountain canyons, they are intermixed with juniper (Juniperus californica).

In southern Fish Lake Valley, sagebrush is scarce, whereas rabbit brush (Chrysothamnus sp.), salt brush (Atriplex sp.), greasewood (Sarcobatus vermiculatus), spiny hop sage (Grayia spinosa), and other lowland plants are common. These plant species occur with Joshua trees and abundant cholla cactus in the southernmost part of the valley.

METHODS OF STUDY

More than 100 days of field investigations were conducted from the winter of 1986 through the summer of 1989 as part of this research project. Field work involved geomorphic and stratigraphic analyses of Quaternary alluvial fans, structural analysis of the FLVFZ, surveying offset surficial features, mapping geomorphic surfaces, describing pedogenic soils, and general reconnaissance of the region. Examination of large scale (1:12,000), low sun-angle, aerial photography (Univ. of Nevada, Reno) supplemented nearly all phases of this project. The various methods used are summarized below and described further in the appropriate chapter(s) that follow.

MAPPING

Near the northwestern termination of the DVFS in northwest Fish Lake Valley, an area of about 100 km was mapped at 1:12,000 scale (Fig. 3; Plate I). Approximately 80 percent of this area was mapped from field investigations, using 1:12,000 air-photos as a compilation base. Mapping involved physically tracing fault scarps and contacts between soil-stratigraphic units, and examining, describing and/or measuring associated surface and soil characteristics. The photo-map data was transferred to a topographic base using a Bausch & Lomb zoom transfer scope.

In addition, the full extent of the FLVFZ was mapped from low sun-angle, large-scale (1:12,000) and small scale (1:48,000 to 1:60,000; Plates IIB, C, D, and E) conventional aerial photography, coupled with extensive field verification.

DESCRIPTION OF SOILS

Soil profiles were described to an average depth of 170 cm in hand-dug soil-pits according to standard methods and nomenclature of the Soil Conservation Service (Soil Survey Staff, 1951 and 1981)(Appendix II). The assignment of morphological stages of pedogenic carbonate follows the classification scheme of Gile and others (1965 and 1966), and that for secondary silica follows Taylor's

(1986) scheme. Two informal postscripts for master horizon notation, "j" and "v", identify horizons with sparse, or juvenile accumulations of carbonate or silica, and A horizons with coarsely-vesicular pores.

Pedon description sites are on geomorphically stable, flattish summits of remnantal landforms having gentle easterly slopes, that occur at 1600 to 1900 m elevation. Parent materials are well-drained, gravelly to very gravelly sandy loam, and calcareous throughout. These materials consist primarily of granitic alluvium with varying amounts of metasedimentary, limestone and volcanic rocks, and minor fine-grained eolian sediment.

INDEX OF SOIL DEVELOPMENT

Soil field properties (Appendix II) are quantitatively indexed utilizing the soil development index of Harden (1982) and Harden and Taylor (1983). The various soil development indices were calculated by interactive operation of a computer-template developed by Taylor (1988) and executed with LOTUS 123™ (Appendix III).

COLLECTION OF SAMPLES FOR RADIOCARBON ANALYSES

More than thirty wood and charcoal samples have been collected by the author, with the intent of submitting the organic materials to commercial laboratories for ^{14}C analysis. To date several radiocarbon dates are available (Appendix IV). The method of sampling generally followed the guidelines proposed by Curtis (1981).

SURVEYING

The amount and style of displacement along the FLVFZ has been evaluated from three separate surveying projects of offset geomorphic features (Appendix V). A Topcon electronic distance meter (EDM) coupled with a Wild theodolite were operated following technical procedures conveyed to the author on three separate occasions by P.S. Pace (1987 and 1988, personal commun., Registered Land Surveyor, State of Nevada).

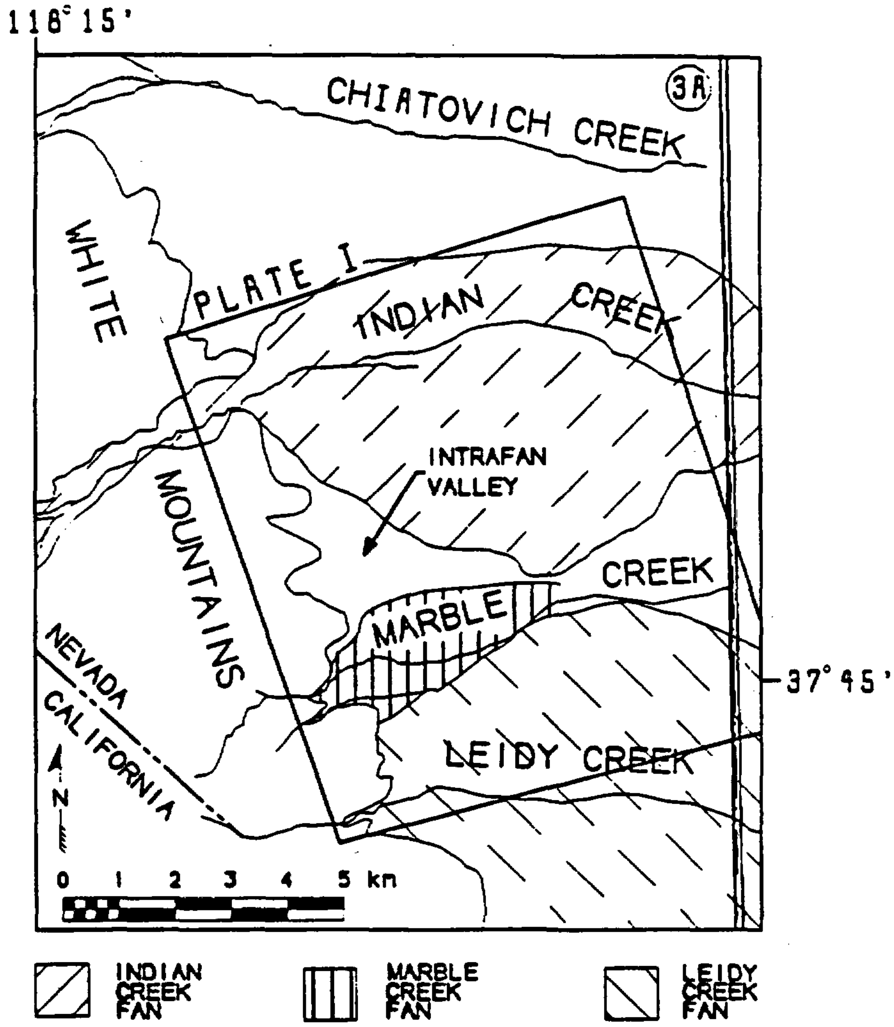

Figure 3. Map showing the area mapped in detail (i.e., Plate I) in northwestern Fish Lake Valley, Nevada. Indian Creek and Leidy Creek are perennial streams that have formed large alluvial fans, whereas Marble Creek is an ephemeral stream that has formed a relatively small fan.

Several topographic profiles (Appendix VI), primarily of fault scarps, were constructed following the Brunton and slope-stick method of Buckman and Anderson (1979).

PREVIOUS STUDIES

Several previous studies have examined the FLVFZ, or portions thereof, and the surficial geologic relations along the fault zone. Anderson (1933) was the first to map traces of the northern FLVFZ. Blackwelder (1934) recognized prominent faulting along the central FLVFZ. Bryson (1937) locally mapped traces of the fault zone and the surficial geology at Perry Aiken Creek. Portions of the fault zone were mapped, from north to south, by Albers and Stewart (1965 and 1972), Robinson and Crowder (1973), Krauskopf (1971 and 1974), Stewart and others (1974), Strand (1967), Ross (1967), and McKee and Nelson (1967). Most recently, Bryant (1988) and Reheis (in press) have evaluated and mapped the southern FLVFZ. Brogan's (1979) mapping of the FLVFZ is the most comprehensive and is being revised by Brogan and others (in press).

The seismic potential of the FLVFZ was postulated by Ryall (1973), Ryall and Ryall (1983), and Wentworth (1982). Vetter (1984) conducted a preliminary examination of seismicity associated with the fault zone.

Various aspects of this thesis project have been reported in Sawyer and Reheis (1987), Sawyer (1988a, 1988b, and 1988c), Sawyer and Slemmons (1988), and Nitchman and others (1990).

CHAPTER II
GENERAL GEOLOGY

PRE-TERTIARY ROCKS

PREBATHOLITHIC ROCKS

Prebatholithic sedimentary and metamorphic rocks constitute much of the bedrock of the White Mountains (Fig. 4). These rocks are part of the Cordilleran miogeocline, a thick sedimentary sequence deposited along the passive western margin of North America. The deposits accumulated from Precambrian to the Devonian in a westward thickening wedge of shallow-water terrigenous detrital and carbonate strata on the east and, farther west, deep-water facies (Stewart, 1978).

The core of the central and southern White Mountains comprise strongly deformed sedimentary strata having a thickness of more than 3 km (Bateman and others, 1965). The prebatholithic sedimentary rocks of this region have been studied in considerable detail (Fiedler (1937), Krauskopf (1971), Crowder and others (1972), Robinson and Crowder (1973), and Hanson and others (1987)). The sedimentary sequence includes the Precambrian Wyman, the lower Cambrian Reed, Deep Spring and Campito Formations, the Cambrian Poleta Formation, and a complex of Triassic (possibly Permian?) and Jurassic metasedimentary and metavolcanic rocks.

The Wyman Formation comprises primarily thin-bedded siltstone, claystone, and limestone with minor amounts of dolomite and sandstone metamorphosed to phyllite and marble. The Wyman Formation crops out along the south fork of Indian Creek and along the upper reaches of Marble Creek. The Reed Dolomite overlies the Wyman and has been metamorphosed to fine-grained white marble. The Deep Spring Formation comprises interbedded quartzite, shale, limestone and dolomite. The Campito Formation, composed of well-stratified shale, siltstone and sandstone, is overlain by the Poleta Formation. The Poleta consists of thin-bedded limestone with minor interbedded phyllite. A complex of slightly

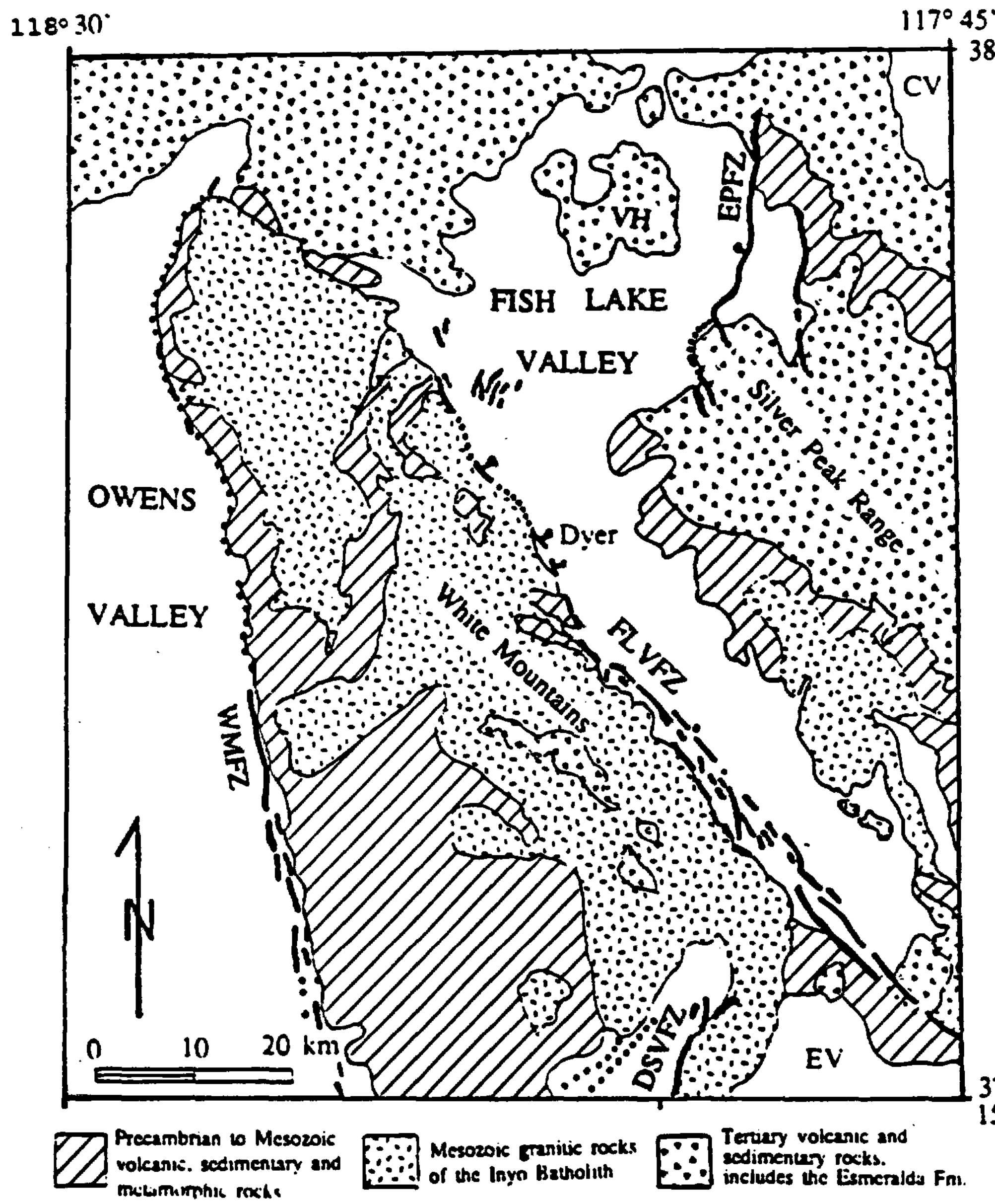

Figure 4. Generalized map showing the bedrock setting of the Fish Lake Valley, Nevada and California, region (modified from Stewart and Carlson, 1978).

metamorphosed sedimentary and volcanic rocks, which form a "horseshoe-shaped" pendant across the northern White Mountains (Hanson and others, 1987), crops out immediately downstream from the head cirque of Indian Creek (Krauskopf, 1971). The metavolcanic rocks are correlated with lithologically similar rocks in the Sierra Nevada batholith to the west, that are in part Early Jurassic, and with volcanic rocks to the northeast in Mineral County, Nevada that are Permian (?) in age (Crowder and others, 1972).

BATHOLITHIC ROCKS

The northern third and much of the eastern White Mountains are underlain by late Mesozoic intrusive igneous rocks of the multipluton Inyo Batholith, a satellite of the Sierra Nevada batholith (McKee, 1982). These rocks were studied in detail by Emerson (1966), Emerson and others, (1987), McKee (1982), McKee and Nash (1967), Albers and Stewart (1972), Anderson (1933, 1937), Crowder and others (1972), and Krauskopf (1971). The Jurassic to Cretaceous plutonic rocks intruded sedimentary and volcanic rocks, resulting in small-scale folding, local shearing and contact metamorphism. The intrusive rocks range in composition from diorite to granite, with granodiorite and adamellite occurring most abundantly. Aplitic and mafic dikes occur in all pluton rocks.

The batholithic rocks include the Jurassic granodiorite of Cabin Creek, the Cretaceous quartz monzonite of both Leidy Creek and Marble Creek, and the Adamellite of Boundary Peak (Fig. 4). The granodiorite of Cabin Creek (Cabin granodiorite of Emerson, 1966) is a medium-grained biotite-hornblende granodiorite, locally porphyritic and foliated. The quartz monzonite of Leidy Creek (same as Leidy adamellite of Emerson, 1966) is a fine- to medium-grained, highly felsic biotite quartz monzonite. The quartz monzonite of Marble Creek is a medium-grained, biotite-hornblende quartz monzonite, highly variable in texture and composition. The adamellite of Boundary Peak is a medium-grained biotite adamellite, named for characteristic outcrops on Boundary Peak. Southeast of Boundary Peak the adamellite is correlative with plutonic rocks of the Mount Barcroft quadrangle, which yield K-Ar dates on biotite of Cretaceous (80-90 m.y.)

age (Krauskopf, 1971).

TERTIARY ROCKS

Rocks of Tertiary age are extensive along the eastern flank of the White Mountains, in the Volcanic Hills in northern Fish Lake Valley, and in the central Silver Peak Range, bordering the valley on the east (Fig. 4). The Tertiary rocks consist of sedimentary, volcanic, and volcaniclastic rocks. The principal volcanic rock units were described by Albers and Stewart (1972) and Robinson and Crowder (1973). Detailed descriptions of the sedimentary units were given by Suthard (1966) and Robinson and others (1968).

Andesite, basalt, and minor amounts of rhyolite are extensive along the northeastern flank of the White Mountains. The greatest thickness of volcanic rocks here is probably the andesite of Davis Mountain, which may be as much as 250 m thick (Robinson and Crowder, 1973). The andesite is probably very late Pliocene or possibly Pleistocene in age (Albers and Stewart, 1972). M.C. Reheis (1989, personal commun.) obtained K-Ar dates of 3.0 to 3.9 ± 0.1 m.y. where these rocks crop out near Indian Creek. This unit forms a "bench" (the "lower east slope" surface of DePolo, 1989) between Indian Creek on the south and Middle Creek on the north. The andesite of Davis Mountain overlies the andesite of Trail Canyon, which includes andesite flows, breccia, and tuffaceous sediment.

The sequence of Tertiary rocks in the Volcanic Hills comprises welded and nonwelded ash flows, andesite and andesitic breccia, tuffaceous sedimentary rocks, and rhyolite and latite flows and tuffs. Basalt flows, possibly correlative with the andesite of Davis Mountain, cap extensive areas of the Volcanic Hills (Albers and Stewart, 1972). Tilted basaltic flows and at least one remnant of a cinder cone occurs northwest of the junction of Highways 3A and 6, in northernmost Fish Lake Valley.

Volcanic rocks of the Silver Peak Range are predominantly rhyolite and trachyandesite flows and tuffs, with lesser exposures of basalt and andesite flows and breccias. The oldest of these rocks consist of welded and nonwelded ash flow tuffs, exposed in the northern Silver Peak Range. The tuffs, which lie unconformably on pre-Tertiary rocks, have a K-Ar date of 21.5 m.y. (Robinson and others, 1968, Table 1). The volcanic rocks associated with a caldera-like structure in the central Silver Peak Range (Albers and Stewart, 1972) are middle to late Pliocene (4.8 to 6.1 m.y.) in age and interfinger with the upper part of the Esmeralda Formation (Robinson and others, 1968).

The Esmeralda crops out in northeastern and in extreme southern Fish Lake Valley where it comprises predominantly fine-grained, well-sorted tuffaceous sandstone interbedded with ash flow and water-laid tuffs of rhyolitic composition. The thick sedimentary sequence was deposited under fluctuating fluciatile and lacustrine conditions. The oldest dated rocks in the Esmeralda Formation are in southernmost Fish Lake Valley, and have a K-Ar date of 13.1 m.y. (Robinson and others, 1968). Volcanic ash in the middle part of this thick (over 800 m) sedimentary sequence is Pliocene to early Quaternary in age (Reheis, 1990a) . In the northern part of the valley the youngest date (4.3 m.y., K-Ar) is from a tuff that is overlain by more than 400 m of the Esmeralda Formation (Robinson and others, 1968).

QUATERNARY STRATIGRAPHY

Deposits of Quaternary age in the Fish Lake Valley region include till, glacial outwash(?), alluvium, colluvium, and fluvial, playa and eolian sediment. Till occurs at higher elevations along all major east-flowing drainages of the White Mountains. Fish Lake Valley is separated from adjacent highlands by extensive, dominantly alluvial deposits that interfinger with subordinate fluvial deposits. The older alluvial deposits are typically mantled with a thin layer of silt and fine sand of probable eolian origin (discussed below; Appendix I). Some fluvial and minor colluvial deposits occur in all mountain canyons. Playa and shallow lacustrine (?) sediments are widespread in the northern and southern parts of the valley.

ALLUVIAL AND FLUVIAL DEPOSITS

Alluvial fan deposits represent a significant portion of the Quaternary stratigraphic record in Fish Lake Valley, as in the Basin and Range Province as a whole. Two ages of Quaternary fan deposits have been mapped along the eastern flank of the White Mountains (Krauskopf, 1971; Robinson and Crowder, 1973; Stewart and others, 1974; Stewart, 1975). The older alluvial unit is generally preserved as uplifted remnants adjacent to the range front and the younger unit occurs valleyward, where it overlaps the older. The principal exception to this pattern of distribution occurs in the northwestern part of the valley, where the older unit of alluvial fans of Indian Creek and Chiatovich Creek extends as much as 10 km beyond the range front. Alluvial fan deposits are presently aggrading in the mid and lower fan positions and generally degrading in the upper fan position. This pattern of erosion and deposition suggests that the loci of deposition has migrated downfan through time (discussed in the Chapter IV).

The regional significance of two general ages of alluvial fan deposits suggests either that the interim was a period of nondeposition, or that the loci of deposition for both intermediate and younger age deposits coincided remarkably. The latter case is preferred based on an on-going study by J.W. Harden (U.S. Geological Survey, Menlo Park), A.R. Gillespie (Univ. of Washington), and J. Slate (Univ. of Colorado), which is discussed below.

The ancestral drainage of Trail Canyon was diverted southeastward by the Tertiary rocks of the Volcanic Hills. Eventually the Trail Canyon fanhead aggraded to the level of the volcanic rocks, at which point the Trail Canyon drainage flowed across the Volcanic Hills and captured a minor drainage (A.R. Gillespie, 1989, personal comm.). Significant incision of the Trail Canyon fanhead followed. This "inverted" stream capture resulted in the preservation of alluvial fan surfaces of intermediate age (J.W. Harden and J. Slate, 1989, personal comm.), which are not recognized elsewhere along the eastern front of the White Mountains. This suggests deposition occurred during the interim between the older and younger alluvial units, and that the younger unit generally buries that of intermediate age.

Within the area mapped in detail (Figs. 2 and 3; Plate I), the upper 20 to

60 m of the alluvial deposits are exposed along the fanhead trenches of Marble Creek and Indian Creek. Here, individual deposits can be observed to extend laterally for several decimeters. The exposed deposits are crudely stratified and poorly sorted, with sedimentary structures such as large-scale scour-and-fill channels and infrequent small scale cross-bedding of fine-grained sand lenses. The deposits comprise materials of diverse composition, reflecting the lithologic inhomogeneity of their province, and range broadly in size from silt and clay to boulders; one boulder on the Marble Creek fanhead is about 8 m in diameter. The angular to subangular coarse lithic fragments are embedded in, and generally supported by, sandy materials. Small lenses of finely-laminated sand occur infrequently.

The fan deposits consist of interbedded debris flows and subordinate water-laid deposits. The identification of individual debris flow lobes and levees both in the field and on low-altitude aerial photographs supports this interpretation. Kesseli and Beaty (1959, p. 75) and Beaty (1960, 1963, 1968 and 1970) concluded, from extensive field studies in the White Mountains region, that alluvial fans form primarily by debris flow deposition. Numerous stratigraphic and geomorphic observations made in the present study (e.g. described above) support this conclusion.

Thus, fan deposits of all ages are similar in regard to sorting, sedimentary structure, texture, and within an individual fan, lithology. Therefore, there is no practical way to recognize and correlate deposits in the field by their composition, and no attempt was made to do so. For this reason, geomorphic surfaces and associated soil characteristics of alluvial fans were mapped rather than "surficial deposits" (Plate I). The genetic relationship between surfaces and soils and their associated deposits is difficult to assess - exceedingly so for erosional surfaces. Such relations are assessed in the present study only where stratigraphic or geomorphic evidence or both permits. Map units are defined and described in detail in Chapters IV and V.

OTHER QUATERNARY DEPOSITS

GLACIAL DEPOSITS

The White Mountains were repeatedly and perhaps extensively glaciated during the Pleistocene. Glacial deposits have been described in many of the canyons draining the eastern slopes of the range (Anderson, 1933, 1937; Blackwelder, 1931, 1934; Fiedler, 1937; LaMarche, 1965; Elliott-Fisk, 1987; Elliott-Fisk and Dorn, 1987a, 1987b; Swanson and others, 1988). These deposits are shown on surficial geologic maps of Krauskopf (1971), Crowder and others (1972), Crowder and Sheridan (1972), Robinson and Crowder (1973), and Albers and Stewart (1972). The lowest elevation of glacial till in canyons of the White Mountains increases slightly from north to south. Glacial deposits, still retaining much of their depositional morphology in the northern part of the range, occur as low as 2550 m (e.g., along Middle Creek), whereas in the southern part of the range such deposits apparently do not occur below about 3100 m (e.g., along the South Fork of Cottonwood Creek).

Glacial deposits in the White Mountains form lateral, medial and terminal moraines, outwash terraces and broad hummocky ground moraines. Well-preserved lateral moraines occur along Davis Creek to about 4 km from the range front. Broad, hummocky ground moraines occur in the higher elevations of many east-sloping canyons, including that of Indian Creek. Repeated Pleistocene glaciations produced broad, U-shaped canyons with lower gradients than adjacent, non-glaciated canyons. This is evident by a comparison of the cross profiles of the glaciated Indian Creek canyon and the nonglaciated Marble Creek canyon (Fig. 5). The broad, U-shaped cross profiles of Middle Creek, Chiatovich Creek, and Indian Creek extend to the eastern front of the range. This led Blackwelder (1934), LaMarche (1965), and Elliott-Fisk (1987) to postulate an extensive Pleistocene glacial event.

Elliott-Fisk (1987) and Swanson and others (1988) believed that this glaciation, which they termed the Dyer Glaciation, is equivalent to the Sherwin Glaciation of the Sierra Nevada to the west, that occurred roughly 1.0 m.y. ago. Blackwelder (1934) also proposed this correlation.

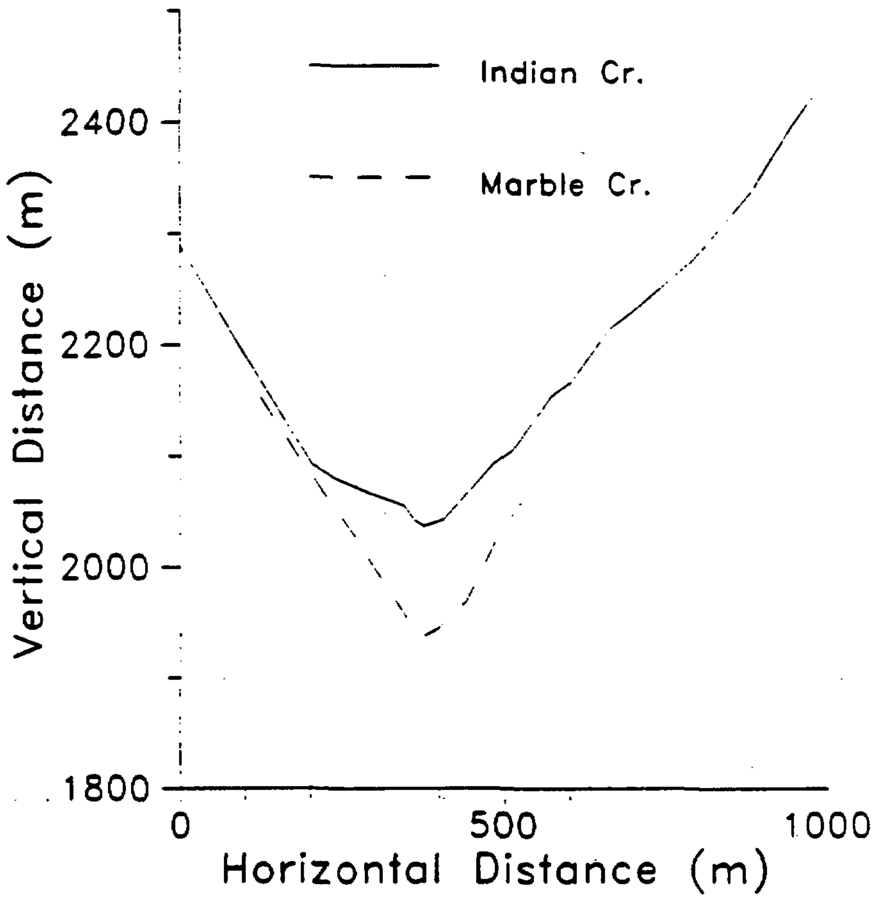

Figure 5. Topographic profiles across the mountain canyons of Indian Creek and Marble Creek (about 1 km from the range front). The broad floor morphology of the Indian Creek canyon is similar to other glaciated canyons in the White Mountain, whereas the "V" shaped morphology of the Marble Creek canyon is similar to other nonglaciated canyons of the region.

The latest Pleistocene Middle Creek Glaciation, reached maximum extent before 18,500 yr B.P. with the innermost moraine developed before 12,700 yr B.P., based on radiocarbon analysis of organic materials in varnish coatings on surficial till boulders (Elliott-Fisk and Dorn, 1987). On the floors of the highest cirques, such as those of the North and South Forks of Chiatovich Creek and Davis Creek, there are very small and "extremely fresh" appearing moraines that may be early Holocene in age (Elliott-Fisk, 1987).

The Pleistocene alluvial fans flanking the eastern White Mountains are comprised primarily of glacial outwash deposits, as proposed by Blackwelder (1934), Albers and Stewart (1972) and recently by Elliott-Fisk (1987). The degree to which glacial scouring has modified major canyons of the range, seemingly necessitates that such deposits are incorporated into the fans. Broad, deep (some nearly 1000 m) head-cirques and U-shaped canyons testify to the erosive strength of Pleistocene glaciers. Undoubtedly, materials removed during formation of the glacial canyons must underlie the flanking Pleistocene piedmont slope and the bolson of Fish Lake Valley to the east. The extent of glacial deposits under the piedmont slope is uncertain, but Pleistocene alluvial fans are most extensive downstream from glaciated mountain canyons. This suggests glacial outwash may be extensive in these alluvial fans.

EOLIAN DEPOSITS

Fine-grained, well-sorted sediment, composed primarily of very fine sand and silt, occur as thin caps or mantles on many piedmont slopes and lava flows in arid regions of the Great Basin, including Fish Lake Valley. The thickness of these deposits often increases downwind from interpluvial playas, suggesting that most of the fine-grained materials in these deposits are eolian in origin. Eolian deposits of Holocene age were recognized by Chadwick and Davis (1988) in the pluvial Lake Lahontan basin, of the northwestern Great Basin. In the southern Great Basin, Davis and Chadwick (1988) concluded that deposits of similar texture, sorting, and age in Las Vegas Valley are of eolian origin. Taylor (1980) and Peterson (1988) suggested that eolian sediment has infiltrated soils on alluvial fans in the Nevada

Test Site region. In the Cima volcanic field of southeastern California, deposits ascribed to an eolian origin form thin mantles over lava flows (McFadden and others, 1986; McFadden and others, 1987). In the Silver Lake region of the eastern Mojave Desert, southeastern California, Wells and others (1987) have concluded that eolian deposits cover large areas of the landscape.

The older alluvial units in northwestern Fish Lake Valley are capped by thin, extensive veneers of similar fine-grained deposits. Laboratory particle size analysis (written comm., M.C. Reheis, 1987) and field textures of the deposits indicate they are primarily composed of silt, very fine and fine sands. The bulk of these deposits is attributed to an eolian origin (Appendix I). Such deposits are referred to herein as "desert loess". Often old fan surfaces mantled with relatively thick desert loess deposits are broken by fairly uniformly spaced steps, oriented roughly parallel to contours, which show a progressive increase in height and decrease in length with increasing surface slopes.

These micro-relief steps were first noted in Fish Lake Valley by Anderson (1933) and first described in some detail by Beaty (1969). Similar features have been identified in the Amargosa Valley region by Denny (1965, 1967), in Death Valley by Hunt and Washburn (1960), and Hunt and Mabey (1964), in Crater Flat, southern Nevada by Peterson (1988) and throughout much of the western Great Basin by Sawyer (1988a; see Fig. 1A, Appendix I). The patterned ground features are the result of downslope movements of desert loess by a unique process of solifluction first described by Sawyer (1988) and discussed extensively in Appendix I.

Eolian deposits also form sand dunes marginal to playas and extensive, typically vegetated sand-sheets elsewhere on the bolson floor of Fish Lake Valley.

CHAPTER III
TECTONIC SETTING AND STRUCTURE

REGIONAL TECTONIC SETTING

WESTERN GREAT BASIN

Fish Lake Valley is one of several tectonically depressed block-faulted basins that lie along or near the margin of the western Great Basin. Contemporaneous strike-slip and normal faults are prominent elements of the tectonic framework within this marginal region. To the west of the Great Basin along the transform boundary of western North America, the San Andreas fault system is the prominent tectonic element. There, dextral strike-slip and contractional faulting are the dominant styles of deformation. The region between the San Andreas and the Colorado Plateau has been interpreted as a broad, "soft" boundary, characterized by distributed dextral movement related to shear stress generated by the relative Pacific-North America plate motions (Atwater, 1970; Atwater and Molnar, 1973). Scholz and others (1971) proposed that along the western margin of the Great Basin, shear stress is superimposed on east-west extension, which is related to crustal spreading in the Basin and Range Province.

Zoback and others (1987) concluded from borehole elongations, earthquake focal mechanisms, and *in situ* stress measurements that the direction of maximum horizontal compressive stress along the San Andreas fault, in central California, is northeast. Similar techniques combined with trends of young (<2 m.y.) volcanic alignments indicate that the direction of maximum horizontal compression in the Basin and Range Province is about N20°E (Zoback and Zoback, 1980). The present extension direction throughout most of the Basin and Range Province is about N65°W (Zoback and Thompson, 1978). Carr (1974) determined from trends of Quaternary faulting and *in situ* stress and strain measurements that the extension direction of the Nevada Test Site region in the south-central Great Basin is approximately N50°W. In Dixie Valley, Nevada, Thompson and Burke (1973) have shown by the attitude of large slickenside grooves on fault planes that the extension direction is approximately N55°W.

Wright (1976) and Zoback and Zoback (1980) suggested that contemporaneous strike-slip and normal faults in the western Great Basin indicate that the relative magnitudes of the vertical and greatest horizontal stresses are nearly equal and that they are interchangeable. Zoback and Beanland (1986) proposed that the exchange of the stresses occurs because of large temporal fluctuations in the relative magnitude of the maximum horizontal stress.

FISH LAKE VALLEY TECTONIC SETTING

The right-lateral strike-slip Death Valley-Furnace Creek fault zone, termed the Death Valley fault system (DVFS), dominates the tectonic setting of the Fish Lake Valley region. The nearly 350 km long DVFS (Fig. 1), comparable in length to the Wasatch fault in Utah, is the longest strike-slip fault in the Basin and Range Province. Large magnitude right-slip (60 to as much as 100 km) characterizes the protracted history of the DVFS. Carr (1984) suggested that the DVFS functions to relieve shear stress related to the transform plate boundary of western North America and further appears to suppress strain accumulation in regions to the east and northeast. At the northern termination of the DVFS, in northwestern Fish Lake Valley, right slip on northwest-striking faults transfers to normal slip on north to north-northeast-striking faults, and possibly left-divergent slip (?) on northeasterly-striking faults. Localized extension appears to be related to strike-slip faulting. Structural and geomorphic evidence supporting this hypothesis are presented in Chapter VI. This region may also transfer movement to areas north and east of the valley.

Although the modern extension direction is consistently northwest-southeast in much of the Great Basin, along its western margin extension is nearly east-west. P- and T-axes of earthquake focal mechanisms in the northern Silver Peak Range, immediately east of northern Fish Lake Valley, suggest EW extension (Smith and Lindh, 1978). From these data Zoback and Zoback (1980) inferred that the maximum horizontal stress in the region is nearly north-south. Speed and Cogbill (1979) determined N82°W extension, based on fault-plane striae in the Candelaria Hills, about 30 km north of the valley. The east-west extension of these regions is in accord with the N80°W extension direction inferred from focal mechanisms and fault-slip analysis to the west in Owens Valley, California (Zoback and Beanland. 1986 and 1988). Focal mechanisms in northwestern and east-central Fish Lake Valley, however, suggest about N60°W extension (Vetter, 1984, Table 2).

STRUCTURE OF THE FISH LAKE VALLEY REGION

This structurally-complex region has experienced late Paleozoic to Mesozoic compressional orogenies, late Mesozoic plutonism, widespread Cenozoic volcanism, and large magnitude late Cenozoic to Recent translational and extensional deformation (Stewart, 1978; 1980). The latest deformational episode is still in progress as suggested by recent earthquake and volcanic activity in this region.

PRE-LATE CENOZOIC STRUCTURE

The structural evolution of the region involved several contractional events including the Paleozoic Antler orogeny, the late(?) Paleozoic and early Mesozoic Sonoma orogeny, the Mesozoic Sevier orogeny, and the Late Cretaceous and early Cenozoic Laramide orogeny. The Late Devonian to Early Mississippian Antler orogeny resulted in emplacement of deep-water strata of the Roberts Mountains allochthon eastward over coeval shelf rocks. The Sonoma orogeny, in Late Permian and Early Triassic time, also resulted in the eastward emplacement of deep-water facies, such as those of the Golconda allochthon, over shallow-water facies (Stewart, 1980). The latest Jurassic to latest Cretaceous Sevier orogeny and the latest Cretaceous to middle or late Eocene Laramide orogeny affected a region in southeastern Nevada (Stewart, 1978).

During the Mesozoic era, an Andean-type subduction zone existed along the west coast of western North America (Burchfiel and Davis, 1975). In the Jurassic and Cretaceous, western Nevada and eastern California were extensively intruded by granitic rocks (McKee and Nash, 1967; Stewart, 1978). The plutonic rocks, which include the Sierra Nevada and Inyo batholiths, were intensely eroded during an interval that extended well into the Tertiary (Albers and Stewart, 1972). This period of erosion, together with limited variability in the thickness of extensive mid-Tertiary ash-flow tuffs in the western Great Basin, indicates a period with little tectonic activity (Stewart, 1980).

Mesozoic structures within the White Mountains include a west vergent thrust fault that emplaces the Barcroft Granodiorite (160-165 Ma) over Mesozoic metasedimentary and volcanic rocks. The McAfee Creek Granite (100 $\pm$ 1 Ma, U/Pb zircon age) postdates this thrust faulting episode (Hanson and others, 1987). Cretaceous thrusting along the White Mountain shear zone, a zone of strongly foliated rocks along the northwest edge of the range, places Paleozoic strata over metavolcanic rocks (Hanson, 1986; reported in Hanson and others, 1987). The footwall of the Last Chance thrust, the highest of several pre-Jurassic thrusts in the region, extends beneath the White-Inyo Mountains (Schweickert and others, 1988).

LATE CENOZOIC STRUCTURE

About 10 Ma the onset of extensional (Scholz and others, 1971) and strike-slip faulting (McKee, 1968), and a change from calc-alkaline to basaltic volcanism significantly influenced the tectonic development of the Basin and Range Province (Christiansen and Lipman, 1971).

About 4 Ma, the tectonic regime of North America changed, as a result of an approximately 20° clockwise rotation (i.e., from N56°W to N35°W) in the relative motions of the Pacific and North American plates (Harbert and Cox, 1989). A cross-over from a regime of extension to one of contraction occurred at that time within the coast ranges of California. The change in plate motions at 4 Ma appears to be closely coincident with the onset of regional uplift and associated block-faulting in the western Great Basin (Nitchman and others, 1990; Caskey, 1990). This latest deformational episode developed the present topography of the western Great Basin (Noble, 1972; Robinson and others, 1968; Gilbert and others, 1968;

Bateman, 1965; and Bachman, 1978). The historical earthquake activity in the region indicates it is still active.

BASIN AND RANGE FAULTING

The significance of crustal spreading and related Basin and Range extensional faulting has been a subject of interest for more than a century, yet considerable debate and controversy still exist. Several models for the structural development of Basin and Range Province have been proposed by Stewart (1978 and 1980b), Scholz and others (1971), Wright (1976), Wernicke (1981 and 1984), Hill (1982), and Wernicke and others (1988).

High-angle, north- to northeast-striking normal faults and associated major fault-block ranges characterize Basin and Range faulting. Furthermore, tilting of fault blocks is a characteristic structure of the province (Stewart, 1980b). Two distinct episodes of late Cenozoic normal faulting occurred in the western part of the Basin and Range Province (Stewart, 1978; Robinson and others, 1968). Normal faulting in much of the Great Basin commenced in the mid Miocene, about 17 m.y. ago (Stewart, 1980; Noble, 1972), and was accompanied by a transition from subduction zone related calc-alkalic volcanism to basaltic volcanism, related to extensional tectonics (Stewart, 1978). An interval of tectonic stability prevailed in the late Miocene and early Pliocene (Robinson and others, 1968), and was accompanied by extensive erosion and planation of the western Great Basin (Albers and Stewart, 1972).

A second episode of block faulting probably began in the late Pliocene and early Pleistocene in the westernmost Great Basin and Sierra Nevada (Noble, 1972). This latest episode resulted in the formation of many of the present basins and ranges in the region, including Fish Lake Valley and valleys to the east and northeast (Robinson and others, 1968), Mono Lake basin to the northwest (Gilbert and others, 1968), and the Sierra Nevada, White-Inyo Mountains, and Owens Valley to the west (Axelrod, 1957; Bateman, 1965; and Bachman, 1978).

By late Tertiary time an extensive erosion surface of low relief had developed in the western Great Basin (Robinson and others, 1968) and extended into the Sierra Nevada (Gilbert and others, 1968). At that time, drainage was probably to the west across the present site of the Sierra Nevada (Axelrod, 1950, p. 226). Basin and Range deformation disrupted the external drainage and produced many well-defined sedimentary basins by about 11 to 13 Ma (Axelrod, 1957; Gilbert and Reynolds, 1973). In the present Fish Lake Valley region, two northwest-trending basins apparently developed, and within them the middle Miocene to early Pleistocene, Esmeralda Formation was deposited (Moiola, 1969; Robinson, 1964; Reheis, 1990c). Subsequent disruption of the northern Esmeralda basins in late-middle or early-late Pliocene time (Moiola, 1969) and the southern basin in the mid Quaternary (Reheis, 1990c), is associated with the latest and ongoing deformational episode.

This latest deformational episode produced widespread uplift, regional arching, and extensive high-angle normal faulting of the Sierra Nevada, White Mountains and adjacent parts of Nevada. The present relief of this region is largely a product of this deformational episode (Axelrod, 1957; Knopf, 1918; Bateman, 1965).

Fish Lake Valley is largely a post-Miocene structural depression formed in part by normal faulting which is still in progress (Reheis, 1988; see Chapters VI and VII). Development of the valley was accompanied by eastward tilt of the bounding blocks and probably the Fish Lake Valley structural block itself. Late Cenozoic uplift and eastward tilt of the White Mountains horst block is evident from the asymmetric east-west physiography of the range (Knopf, 1918; Anderson, 1933; Fiedler, 1937, p. 13, 36; Bryson, 1937), the gentle tilt of basaltic lava flows (Bryson, 1937; Albers and Stewart, 1972), the eastward slopes of erosional surfaces within the range (Marchand, 1974), rates of displacement of range bounding faults (discussed below), and by geophysical studies (Pakiser and Kane, 1964, p. 54-55). These data suggest that uplift was greater along the west margin of the range.

Pakiser and Kane (1965) inferred from gravity studies that the total vertical displacement along faults bounding the west side (i.e., the White Mountains fault zone) of the White Mountains is as much as 4000 m. Bachman (1978) used Hay's (1966, p.20) K-Ar date from the upper part of the Waucobi Lake beds and gravity data from Pakiser and others (1964) to postulate as much as 2300 m of vertical displacement during the last 2.3 Ma along White Mountain fault zone (Fig. 1). These data suggest an average Quaternary uplift rate of 1 mm/yr along the western margin of the range. Wallace (1984) suggested the uplift rate of the northwestern White Mountains is about 0.8 mm/yr. Detailed study of the White Mountains fault zone by DePolo (1989) suggests that the average Quaternary uplift rate is as high as about 0.7 mm/yr.

In contrast to the western margin of the range, uplift along the eastern margin was less significant. Between Trail Canyon and Davis Canyon the andesite of Davis Mountain caps alluvial gravels. These gravels are from 100 to nearly 300 m above the present fans, probably as a result of uplift by faulting (Anderson, 1933, p.62, 162). K-Ar dates of 3.0 to 3.9 ±0.1 Ma (M.C. Reheis, 1988, personal commun.) from the andesite of Davis Mountain suggest relatively low, long-term uplift rates (about 0.03 to 0.09 mm/yr minimum). As discussed in Chapter VI, the late Pleistocene uplift rate along the master fault of the northern FLVFZ is about 0.2 mm/yr (preferred estimate).

A prominent topographic escarpment along the northeastern front of the range suggests that an earlier period of faulting extended farther northwestward than at present. The linear north-northwest-trending rangefront north of Chiatovich Creek is fault controlled (Anderson, 1933). Detailed field studies by Anderson (1933) showed that faulting occurred prior to, or accompanied, extrusion of basaltic flows, but ceased before the cessation of the volcanic episode.

Pellisier, Chiatovich, and Sage Hen Flats, which lie along the crest of the range (Fig. 2), are erosional surfaces of low to gently rolling relief (Marchand, 1974; Anderson, 1933; Fiedler, 1937, Beaty, 1960). These surfaces presumably formed as part of an extensive erosion surface that developed across the westernmost Great Basin and extended into the Sierra Nevada during the Miocene (Bateman and others, 1965). Sage Hen Flat is partially covered by basaltic flows, with K-Ar ages of 10.8 Ma (Dalrymple, 1963). Fiedler (1937) postulated that the erosional surfaces may have formed level with adjacent blocks that now form Fish Lake Valley and Owens Valley. If correct, these data suggest 2900 m of uplift within the last 10.8 m.y. yielding an uplift rate of about 0.3 mm/yr. However, Bachman (1978) indicated that most of this uplift occurred within the last 2.3 m.y. The erosional surface and overlying basalts have been tilted eastward and offset vertically nearly 1500 m by faulting along the south end of the range (Marchand, 1974).

In late-early to middle Pliocene time, fine-grained sediment was deposited at the present site of the central Silver Peak Range, suggesting that a connection existed between Fish Lake Valley and Clayton Valley to the east at that time. The sediment has been uplifted at least 900 m since extrusion of trachyandesite flows K-Ar dated at 5.9 m.y. Uplift may be related to volcanic activity of the Silver Peak volcanic center (Robinson and others, 1968) a caldera-like structure (Albers and Stewart, 1972). Eastward tilt during early to mid Pliocene time (Albers and Stewart, 1972) apparently accompanied uplift of the range. The present topography of the Silver Peak range was established by the late Pliocene (Robinson and others, 1968).

The upper Tertiary Esmeralda Formation in northeastern Fish Lake Valley is generally tilted from 15° to 30° eastward (Robinson and others, 1968). The upper Tertiary volcanic rocks in the northwestern part of the valley have similar eastward tilts (Crowder and others, 1972; Robinson and Crowder, 1973). Collectively, these data suggest that at least northern Fish Lake Valley has functioned structurally as a quasi-rigid block that was tilted eastward as a result of block faulting. This interpretation is in accord with Stewart's (1980b) interpretation that northern Fish Lake Valley is an east tilted fault block.

<u>Walker Lane shear zone</u>

The Walker Lane was originally defined by Locke and others (1940) as a linear belt of low topography separating north-northeast trends of the Basin and Range Province from northwest trends of the Sierra Nevada. The belt includes a region of predominantly northwest-striking dextral faults. Stewart (1988) depicted the Walker Lane shear zone (WLSZ) as a northwest-striking belt of strike-slip faulting that is approximately 700 km long and 100 to 300 km wide (Fig. 1). Rather than consisting of a single thoroughgoing strike-slip fault, the WLSZ comprises several regional blocks that either contain or are bounded by major strike-slip faults (Stewart, 1988).

Displacement along the WLSZ may have began as early as Late Triassic or Jurassic, possibly in response to oblique subduction along the western margin of North America (Stewart, 1988) - i.e., a trench-linked strike-slip fault using Sylvester's (1988) classification. Late Cenozoic lateral displacement within the WLSZ may be associated with the development of the San Andreas transform system (Zoback and others, 1981).

Atwater (1970) and Atwater and Molnar (1973) suggested that a significant portion of the transform motion between the Pacific and North American plates is not accounted for by displacement along the San Andreas fault alone. They proposed that a portion of the relative plate motion is absorbed within the Basin and Range Province. Albers (1967) indicated that the total right-lateral displacement within the western Great Basin (i.e., the WLSZ) may be as large as 130 to 200 km, occurring as both slip along faults and related crustal folding or oroflexural bending (Albers, 1967; Stewart and Poole, 1974). Recent palinspastic reconstruction of Mesozoic thrust faults by Wernicke and others (1988) suggests that when resolved parallel to the San Andreas, 214 $\pm$ 48 km of northwest translation has occurred between the Sierra Nevada Province and the Colorado Plateau. Argus and Gordon (1989) determined from Very Long Baseline Interferometry data collected over a four year period that extension within the Basin and Range Province is characterized by N45°W displacement at a rate of ~10 mm/yr. Hence, transform deformation associated with the western margin of North America is apparently superimposed on the western part of the Basin and Range Province.

The WLSZ contains several subparallel northwest to north-northwest-striking and a few east-west-striking strike-slip faults of regional significance. The largest of these is the Death Valley fault system (Figs. 1 and 6; discussed in the next section), along which right-lateral displacement may be as much as 100 km (Poole and others, 1967). Another fault of regional consequence is the right-lateral Las

Vegas shear zone (Fig. 6). Forty to 65 km of displacement on the shear zone has been suggested from studies of isopachs and facies trends of Precambrian and Paleozoic strata (Stewart, 1967; Ross and Longwell, 1964) and by offset Mesozoic thrust faults (Longwell, 1960; Burchfiel, 1965; Wernicke and others, 1988). This deformation probably occurred between 15 and 11 Ma (Fleck, 1970; Longwell, 1974). Sixteen to 19 km of right-lateral offset has been suggested on the Pahrump fault zone, another northwest-striking fault within the southern WLSZ, from studies of Precambrian and Paleozoic rocks (R.L. Christiansen, in Stewart and others, 1968).

The north-striking Owens Valley-White Mountain fault system is the second longest fault system in the WLSZ, at about 300 km in length (Fig. 6). Moore and Hopson (1961) suggested that the Independence dike swarm crosses the Owens Valley fault zone with no obvious displacement. However, Schweickert (1981) suggested that about 19 km of left-lateral offset of the dike swarm is possible across Owens Valley. Martel (1984) interpreted the Quaternary structure of the Owens Valley fault zone to indicate right-lateral strike-slip movement. Bonilla (1968) and Beanland and Clark (1987) noted right-lateral displacement along the Owens Valley fault zone, associated with the 1872 Owens Valley earthquake. DePolo and Ramelli (1987) determined from the geometry and character of ground fractures along the White Mountain fault zone related to the 1986 Chalfant Valley earthquake sequence, that right-lateral displacement was predominant.

An earlier history of left-lateral offset of the late Jurassic Independence dike swarm along the Owens Valley fault zone may be consistent with Stewart's (1985) postulated late Mesozoic stress regime. This regime accounts for an earlier period of right-lateral movement along the easterly-striking Coaldale and Excelsior fault zones during the late Mesozoic, and in this regime north-striking faults should experience displacement. If this hypothesis is correct, then the formerly left-lateral Owens Valley-White Mountain fault system would have been reactivated as a predominantly right-lateral strike-slip fault system during the latest Cenozoic.

The northwest-striking Hunter Mountain fault zone (Fig. 6) between Saline and Panamint Valleys has experienced from 8-10 km of right-slip during the last 3.0 m.y., with no evidence of pre-late Cenozoic displacement (Burchfiel and others,

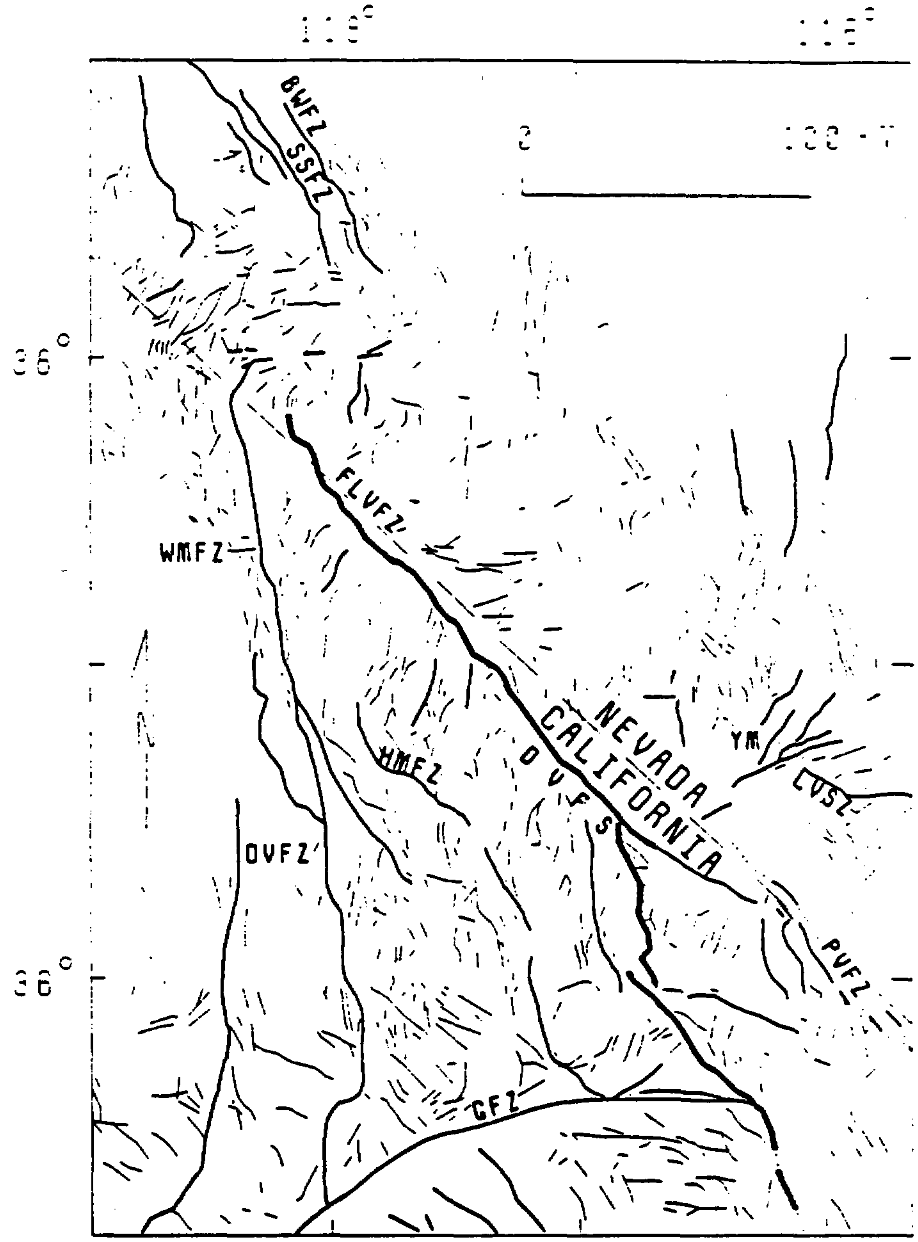

Figure 6. Map showing major late Cenozoic faults in the western Great Basin. The heaviest lines are faults of the Death Valley fault system; intermediate lines are other major faults, dotted where inferred; and fine lines are minor faults (modified from Stewart, 1988, Fig. 25-2). BWFZ, Beatties Wells fault zone; DVFS, Death Valley fault system; FLVFZ, Fish Lake Valley fault zone; GFZ, Garlock fault zone; HMFZ, Hunter Mountain fault zone; LVSZ, Las Vegas Valley shear zone; OVFZ, Owens Valley fault zone; PVFZ, Pahrump Valley fault zone; SSFZ, Soda Springs fault zone.

1987). Saline Valley and northern Panamint Valley are pull-apart basins that developed at either end of the Hunter Mountain fault zone as a result of lateral movement along the structure (Burchfiel and others, 1987; Zellmer, 1983).

Two of the more significant strike-slip faults of the central WLSZ are the Soda Springs and Bettles Well faults (Fig. 6). The northwest-striking Soda Spring Valley fault has from a few kilometers (Speed and Cogbill, 1979) to as much as 16 km (Nielsen, 1965) of right-lateral displacement, which began late in the Miocene and continued to the Recent (Nielsen, 1965). The Bettles Well fault is subparallel to the Soda Spring Valley fault and may have had initial movement during the Mesozoic (Albers, 1967). However, most of the lateral movement occurred in late Cenozoic time (Stewart, 1985). Hardyman and others (1975) indicated 32 km of late Cenozoic right-lateral displacement has occurred along the Bettles Well fault. Both the Soda Spring Valley and the Bettles Well faults terminate to the south at the east-west-striking Excelsior fault zone (Stewart, 1985).

In the region between the Soda Spring Valley fault and northern Fish Lake Valley is a zone about 25 km wide that contains several east-west to east-northeast-trending strike-slip faults (Fig. 6). The most prominent structures in this region include the Excelsior, Coaldale, and Candelaria fault zones. The main movement along the Coaldale and Excelsior faults occurred prior to late Oligocene time. The distribution of pre-Cenozoic rocks suggests 60 to 80 km of right-lateral offset along the Coaldale fault and 45 to 55 km along the Excelsior fault (Stewart, 1985). The Coaldale and Excelsior faults were reactivated in many places, possibly by left slip during the late Tertiary and Quaternary (Stewart, 1985). Left slip initiated along the Candelaria fault zone in Oligocene time, possibly before 24 m.y. B.P. (Speed and Cogbill, 1979). Speed and Cogbill (1979) postulated about 900 m of left-lateral displacement along the Candelaria fault zone in the last 2.8 m.y. Left-lateral displacement associated with the 1934 Excelsior Mountain earthquake (Callaghan and Gianella, 1934) indicates that the regional system of east-west-striking left-lateral faults is still active.

As both the Death Valley and the Owens Valley-White Mountain fault systems approach the Coaldale fault zone from the south they curve eastward and terminate against it (Stewart, 1985, p. 547, and 1988). The Emigrant Peak fault zone in northeastern Fish Lake Valley also terminates at this structure (Fig. 6). Stewart (1985) suggested that the eastward curve in the fault patterns may be related to drag folding along the Coaldale fault zone. Stewart (1970 and 1985) suggested that the northern Death Valley fault system may once have been connected with the Bettles Well fault, but that 30 to 40 km of right-lateral movement along the Coaldale fault zone may have resulted in their separation.

Death Valley Fault System: The longest fault within the WLSZ is the nearly 350 km-long DVFS (Figs. 6 and 7). The fault system is the longest strike-slip fault in the Basin and Range Province, extending from south of the Garlock fault (Brady and Troxel, 1981; Brady and Verosub, 1984) in southeastern California, through Death Valley and Fish Lake Valley, and perhaps to the Coaldale fault zone (Stewart, 1985, p. 547) in west-central Nevada (Fig. 6). The DVFS has a protracted history of large magnitude right slip, which possibly was initiated as early as the Middle Jurassic (McKee, 1968).

The DVFS is an intracontinental transform fault (following Sylvester's, 1988 classification of strike-slip faults) and is similar in many respects to the Garlock fault. The fault system fundamentally separates regional domains of contrasting tectonic styles. Areas west of the DVFS have high-strain rates (Dohrenwend, 1987), abundant evidence of Quaternary and some historic right-lateral faulting on northwest-striking faults (Smith, 1979; Bonilla, 1968; Slemmons and others, 1968; DePolo and Ramelli, 1987; Beanland and Clark, 1987; Zellmer, 1983; Burchfiel and others, 1987; Chapter VI), and west-northwestward extension (Wright, 1976; Zoback and Beanland, 1986; Zoback and Zoback, 1980; Chapter VI). In contrast, areas to the east of the DVFS have predominantly low strain rates (Dohrenwend, 1987), a near absence of northwest-striking Quaternary structures (Carr, 1974, p.29), and a more northerly orientation of extension (Zoback and Zoback, 1980; Zoback and Thompson, 1978; Carr, 1974).

The DVFS as defined here is essentially the same as the Death Valley and Furnace Creek fault zones of Noble and Wright (1954). The fault system consists of five interconnected fault zones in kinematic correspondence. From south to north

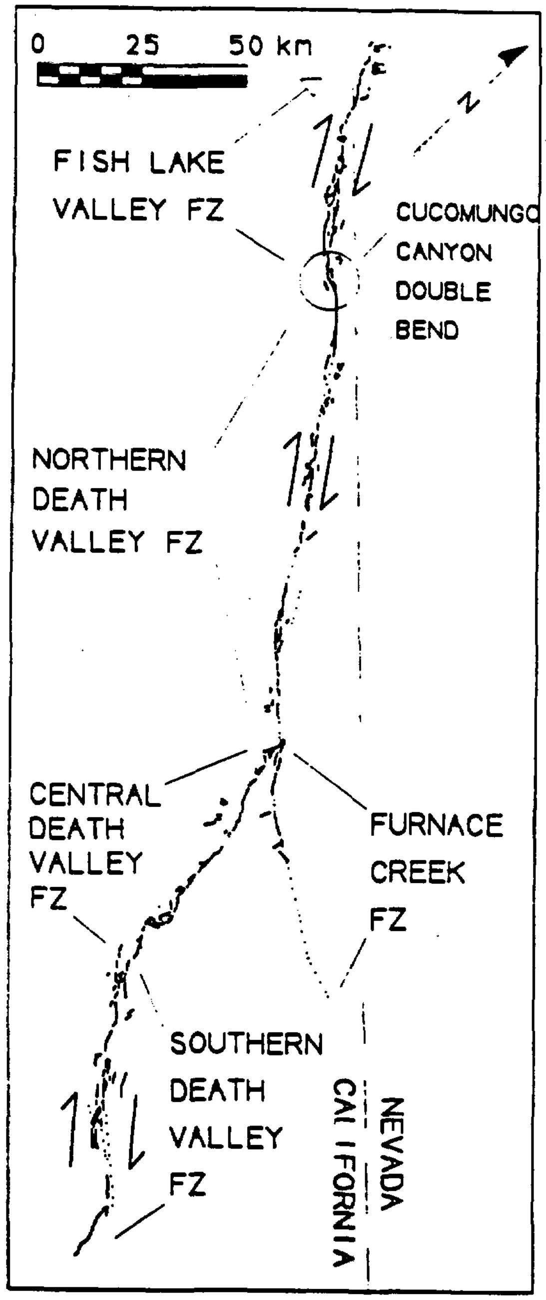

Figure 7. Map showing the major fault zones of the dextral Death Valley fault system. Jennings and others (1975) and Stewart and Carlson (1978) were used as sources for the map.

they are the northwest-striking Southern Death Valley fault zone, the northerly-striking Central Death Valley fault zone, and the northwest-striking Northern Death Valley and Fish Lake Valley fault zones (Fig. 7). This subdivision of the DVFS accords with suggestions made to the author by L. Wright (1987, personal commun.). Right-lateral strike-slip faulting predominates along the DVFS (Curry, 1938a; Noble and Wright, 1954; Hill and Troxel, 1966; Albers, 1967; Stewart, 1967, 1983; McKee, 1968; Stewart and others, 1968, 1970; Brogan and Slemmons, 1970; Buckley, 1974; Reynolds, 1976; Brogan, 1979; Oakes, 1987; Butler and others, 1988; Chapter VI). Right-divergent slip occurs along the northerly-striking Central Death Valley fault zone (Burchfiel and Stewart, 1966; Wright and others, 1974; Wright and Troxel, 1967; Stewart, 1983; Noble and Wright, 1954) and along faults of similar orientation in west-central and northwestern Fish Lake Valley (Chapter VI).

The considerable variance of estimated magnitudes of right-lateral offset of upper Precambrian and Paleozoic rocks across the DVFS presents an enigma. There are two general ranges in estimates of the magnitude of displacement. The larger estimates range from 40 to as much as 100 km (Stewart, 1967; Poole and others 1967, 1977, Stewart and others, 1968; McKee, 1968; Oakes, 1977), whereas the lower estimates are 11 km or less (Wright and Troxel, 1967, 1970; Davis, 1977).

Stewart (1967) indicated that the apparent offset in isopach trends of Stirling Quartzite, Wood Canyon Formation, and Zabriskie Quartzite suggests 80 km of right-lateral offset on the DVFS. Poole and others (1967), based on similar stratigraphic trends of Precambrian, Cambrian, and Devonian rocks, suggested as much as 100 km of right-lateral displacement is possible on the DVFS. Along the northern part of the DVFS, McKee (1968) correlated two parts of a Middle Jurassic pluton across the fault system, based on similar lithology and K-Ar ages. McKee suggested that the distribution of the granitic bodies indicates 48 km of right-lateral displacement on the northern DVFS. This estimate of displacement generally agrees with that suggested by Saleeby and others (1985), based on about 40 km of right lateral offset of the Sr_i 0.706 line across the northern DVFS in Fish Lake Valley. Snow and Wernicke (1988) correlated three Mesozoic thrust faults across the DVFS in northern Death Valley, indicating 68 ± 4 km of right-lateral offset. Oakes (1987) suggested that a 7.3 to 7.9 Ma (McKee, 1985) granitic pluton in the northern Last Chance Range is offset 32 km along the northern part of the DVFS from "identical-appearing" granitic rocks in the northern Grapevine Mountains in northern Death Valley.

In contrast, significantly less displacement has apparently occurred along the DVFS in central Death Valley. Wright and Troxel (1967) described several linear features, such as the intersection between two regional unconformities, margins of sedimentary wedges, and facies changes in late Precambrian and Cambrian sedimentary units. These throughgoing linear features place a limit of 11 km of right-lateral displacement on the central part of the DVFS (Wright and Troxel, 1967; 1970). Davis (1977) suggested that Precambrian stratigraphic trends across the central Death Valley area indicate about 8 km of displacement.

Burchfiel and Stewart (1966) interpreted central Death Valley as a pull-apart basin lying obliquely between the ends of two én echélon strike-slip faults (i.e., Northern and Southern Death Valley fault zones). They inferred that the cumulative right-lateral offset on the Southern Death Valley fault zone is of comparable magnitude to that on the northern part of the DVFS.

Butler and others (1988) have subsequently shown that 35 ± 5 km of right-lateral offset occurred on the Southern Death Valley fault zone between the mid-Miocene and about 1 Ma based on matching ancient fan gravels with their source area. They indicated that this displacement is consistent with the geometry of Burchfiel and Stewart's (1966) pull-apart basin in central Death Valley.

There are several hypotheses that attempt to reconcile the differences in estimates of the magnitude of right-lateral offset on the DVFS. Wright and Troxel (1970) suggested that greater extension on the southwest side of the DVFS in northern Death Valley would result in progressively greater displacements to the northwest, allowing for significantly less offset in the central Death Valley area. Stewart (1967, Fig. 6) indicated however, that displacement increases toward the southeast. Stewart and others (1970) suggested that oroflexural bending, mostly in the Black Mountains, may have absorbed some of the right-lateral displacement that is apparent in northern Death Valley. Wright and Troxel (1970) argued however, that the proposed oroclinal flexure is not supported by structural data, because several northwest-trending linear features pass through the proposed flexure without bending. Further, neither hypothesis considers large lateral displacements along the southern Death Valley fault zone (Wright and Troxel, 1967).

Stewart (1983) proposed that if displacement was synchronous on the left-lateral Garlock fault and the right-lateral northern DVFS, then the triangular-shaped wedge between these faults would be translated roughly N55°W. In effect this wedge extended and tracked the northwestward migration of the Sierra Nevada Province (Wright, 1976; Albers, 1967, p.147). Therefore, northwestward translation of the Panamint Range from the Black Mountains would not result in significant right-lateral offset of the northwest-trending features in central Death Valley identified by Wright and Troxel (1967) and by Davis (1977). Thus, this model accounts for larger displacement along the northern DVFS and smaller displacement along the central DVFS. However, the model requires little if any right-lateral offset on the southern Death Valley fault zone (Stewart, 1983), but apparently does not preclude the possibility of such displacement.

Albers (1967, p. 151) discussed another enigma with regard to displacements on the DVFS that is not satisfactorily resolved. The question is how does a fault having a ratio of lateral displacement to fault length as large as 1:3 terminate in a short distance? Stewart (1967) proposed that both the DVFS and the Las Vegas shear zone die out to the northwest into large oroflexural folds. Albers (1967, p. 151 and Fig. 4) indicated that this hypothesis is in good agreement with observed facts. Albers argued that the Silver Peak-Palmetto-Montezuma oroflex is a gigantic dextral drag fold related to the northern DVFS, and which developed along an arcuate contractional fault (Albers, 1967, Fig. 3). Therefore, according to Albers right-lateral strike-slip displacement was "absorbed" by folding and thrust faulting. However, Stewart's and Albers' hypotheses do not account for the termination of the DVFS during latest Cenozoic time, since from late Tertiary to Recent the Fish Lake Valley region was dominated by master normal faults (Albers and Stewart, 1972).

The northwestern termination of the Quaternary DVFS (i.e., FLVFZ) may differ greatly from Stewart's (1967) model of oroflexural folding. Fish Lake Valley offers a unique opportunity to study the termination of a major strike-slip fault. As discussed in Chapter VI, the Fish Lake Valley fault zone (FLVFZ) terminates in the northwestern part of the valley by splaying, bending, and transferring right-slip on north-northwest-striking faults to normal-slip on north- to northeast-striking faults. Apparently transform faulting is taken-up or consumed by localized crustal extension. This interpretation of the northwestern termination of the FLVFZ is supported by geomorphic and structural evidence presented in Chapter VI.

The FLVFZ is described in detail in Chapters VI, VII, and VIII.

CHAPTER IV
QUATERNARY GEOLOGY OF FISH LAKE VALLEY

INTRODUCTION

Assessing the Quaternary geologic setting is germane to virtually all detailed studies in neotectonics, particularly those involving investigations of paleoseismicity. The identification and interpretation of sequences of geomorphic surfaces and their genetically related soils are necessary to provide a stratigraphic framework with chronologic controls. The movement histories of faults displacing these surfaces and the Quaternary stratigraphic history of a region can then be deciphered.

In this chapter, six distinct and regionally extensive geomorphic surfaces with characteristic soils are identified and described. The individual units, termed morphostratigraphic units (defined in a following section), are from youngest to oldest, the "late", "middle", and "early Marble", "Leidy", "Indian", and "McAfee Creek" units. The numerical ages assigned to the various units are based on radiocarbon-dated organic carbon (detrital wood) and tentative correlations of volcanic ash layers in alluvial fan deposits with established tephrochronologies.

The stratigraphic framework (established in this chapter) is evaluated in light of previous climatic studies of the region to provide a perspective on possible influences of Holocene climatic fluctuations on the stratigraphic record of the area.

GEOMORPHIC SETTING OF THE STUDY AREA

The White Mountains, immediately west of Fish Lake Valley, are the highest range in the Basin and Range Province. The western and eastern flanks of the range are bordered by extensive Quaternary piedmont slopes. These piedmont slopes were studied by Kesseli and Beaty (1959), Beaty (1960, 1963, 1968a, 1968b, 1970), Filipov (1986), and DePolo (1989).

The northwestern slope of the White Mountains forms an abrupt and impressively steep escarpment, with relief of 1800 to 3000 m in a horizontal distance of 6 to 10 km. In contrast, the eastern slope is gradual and has similar relief over a distance of 15 to more than 20 km. Reentrants in the mountain front (piedmont embayments) are common along the scalloped northeastern margin of the range, but are nearly absent along the linear western margin.

The gross morphology of the western and eastern piedmont slopes differs in a manner analogous to the slopes of the range. Alluvial fans bordering the range on the west are generally younger, smaller, and steeper than those on the east as, for example, in northwestern Fish Lake Valley.

The topographic asymmetry of the White Mountains and the gross morphological differences of the marginal piedmont slopes are attributed to differential vertical tectonism along range-bounding faults. Specifically, higher rates and magnitudes of uplift along the western margin (i.e., the White Mountains fault zone), and associated eastward tilt of the White Mountains fault block during the Pliocene and Quaternary (discussed in a following section) have prominently influenced the morphology of both the range and the piedmont slopes.

Virtually all alluvial fans of the White Mountains, including those along the southern margin of the range in Deep Spring Valley (Lustig, 1965), are undergoing fanhead dissection while their lower parts are actively enlarging. This is true for nearly all fans of the Fish Lake Valley and Death Valley region (Beaty, 1961; Hunt and Mabey, 1966; and Denny, 1967) and throughout the Basin and Range Province (Peterson, 1981; Christenson and Purcell, 1975). The pattern and possible significance of erosion and sedimentation on alluvial fans of the study area are discussed in following sections of this chapter.

GEOMORPHIC SETTING OF THE DETAILED MAP AREA

Nowhere are the marginal piedmont slopes of the White Mountains more extensive than in northwestern Fish Lake Valley. Sediment is supplied to the piedmont slope by drainages that head along the 3800 m to 4300 m range crest. The broad piedmont slope extends as far as 13 km from the eastern front of the range to the valley floor below, dropping from 400 to 800 m along slopes of 2.5° to 4.5°.

The area mapped in detailed in northwestern Fish Lake Valley spans more than 85 km² and includes, from north to south, alluvial fans of Indian Creek, Marble Creek, and part of the fan of Leidy Creek (Fig. 3; Plate I). The Indian Creek and Leidy Creek fans are among the largest components of the White Mountains eastern piedmont slope. These two large fans converge downslope and partially enclose a triangular-shaped interfan valley (Hawley, 1980). The Marble Creek fan is considerably smaller in size and lies along the northern margin of the Leidy Creek fan within the interfan valley. North of the Marble Creek fan, the interfan valley comprises several even smaller alluvial fans, or fanlettes, that issue from minor ephemeral drainages that head along (or near) the eastern front of the range. These drainages coalesce downslope and exit the interfan valley through a rather narrow restriction, formed by the southern margin of the Indian Creek fan and the northern margin of Leidy Creek fan.

The Indian Creek, Marble Creek, and Leidy Creek alluvial fans have several common characteristics. Their active channel crosses the apex and upper one-third to one-half of these fans as a narrow, deeply-incised channel, i.e., a fanhead trench (Eckis, 1928). Commonly, suites of terraces occur within and along the fanhead trenches of major Pleistocene fans. Actually, these topographically arranged geomorphic surfaces are inset alluvial fans, as evident by their convex lateral profiles, longitudinal profiles that grade to well-defined fan surfaces, and by observed stratigraphic relations (e.g., buttress unconformity). Furthermore, the mid and lower parts of the major fans are actively aggrading and their fantoes are prograding. Nearly all of the alluvial fans in the study area exhibit a similar morphology.

The depth of incision across the upper portions of the fans decreases downfan to a point where the active drainage emerges from the fanhead trench and flows on the mid- to lower-fan surface. The transition from channelized to non- (or shallowly-) channelized flow occurs at the intersection point (e.g., Hooke, 1967; Wasson 1974, 1975). Above the intersection point, fan surfaces are largely relict i.e., remnants of former fan surfaces because they are incised and thus bypassed by the active drainages. This relict portion of the fan is dissected by numerous, subparallel onfan drainages that separate broad, flattish interfluves, and broad, well-rounded ridgeline remnants or ballenas (terminology of Peterson, 1981). Such morphological features indicate this portion of the fan is undergoing destruction. The intersection point is approximately at the apex of the actively forming part of the fan. Downstream from this point is the locus of current deposition. This aggrading portion of the fan has a distributary, braided system of shallowly incised drainages. The micro-topography of the active, or recently active, fan surfaces is characterized by discontinuous swales separated by debris flow levees and lobes.

An additional aspect shared by the Indian Creek, Marble Creek, Leidy Creek fans and several other fans in the study area is that their morphology is clearly and markedly influenced by deformation along and adjacent to the Fish Lake Valley fault zone (FLVFZ). The influence of the Quaternary FLVFZ on stratigraphic and morphologic aspects of alluvial fans is discussed at length in a following section, "Distribution of Units Mapped", and in Chapter VI.

INDIAN CREEK ALLUVIAL FAN

The Indian Creek fan is the largest single alluvial fan of the White Mountains. The fan is approximately 12 km long, 5 km wide, and from apex to toe, 460 m high. The Indian Creek fanhead trench provides the best example of stepped fan surfaces within the detailed map area (Fig. 8). Sixfold stepped fan surfaces occur upstream from where the master fault of the northern FLVFZ traverses Indian Creek. This suggests that vertical movements on the fault have influenced the locus and rate of channel incision along this reach of Indian Creek.

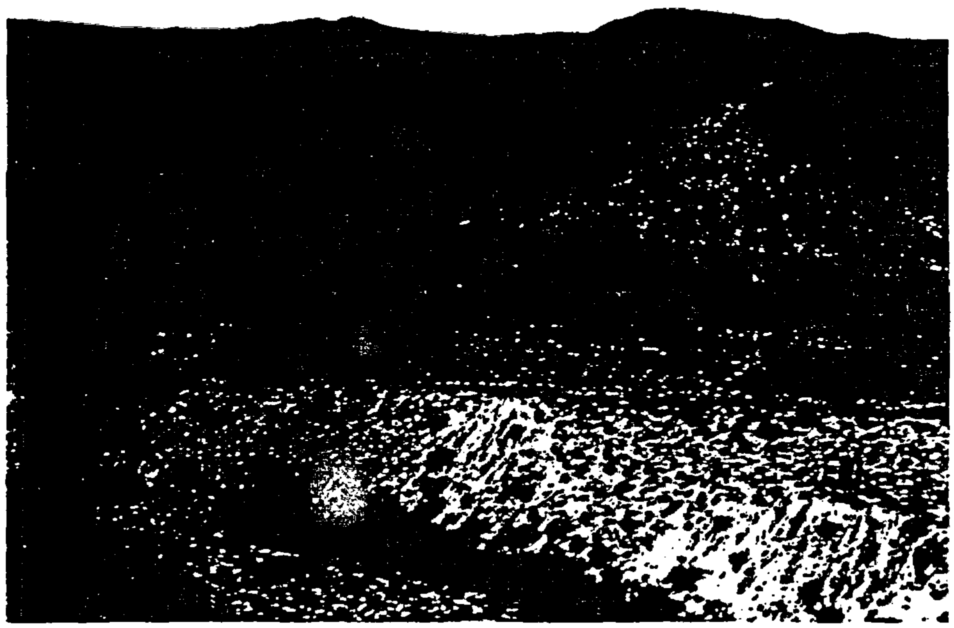

Figure 8. Photograph taken to the west-northwest of morphostratigraphic units in stepped sequence within the Indian Creek fanhead trench, courtesy of Steven P. Nitchman. MM, middle Marble; EM, early Marble; L, Leidy; I, Indian; MC, McAfee Creek (lowest\youngest to highest\oldest).

The Indian Creek stepped sequence consists of geomorphic surfaces at several different levels and therefore ages. That is, the lowest surface is the youngest, higher surfaces are progressively older, and the highest and generally farthest from the active channel is the oldest. The surface remnants are generally paired across Indian Creek and have transversely convex profiles. This suggests the surfaces are coeval remnants of once more extensive fans. Several of these fan remnants can be traced continuously (or nearly so) from within the Indian Creek fanhead trench across the master fault and subsidiary faults of the northern FLVFZ, to where they grade into fan surfaces of equivalent age (Plate I). The southern half of the Indian Creek fan comprises a relatively large, erosional fan remnant with flattish, topographically concordant, relict summits separated by incised onfan drainages. The northern half of the Indian Creek fan, in contrast, comprises active and recently active fan surfaces. This currently aggrading area on the Indian Creek fan exhibits a shallowly incised, braided drainage system, and swale and levee interfluve microtopography characteristic of Holocene fan surfaces of the study area.

MARBLE CREEK ALLUVIAL FAN

The Marble Creek fan is considerably smaller than the Indian Creek and Leidy Creek fans (Fig. 3), which corresponds to its small drainage-basin. The Marble Creek fan is about 4 km long, less than 2 km wide and is approximately 270 m high. An uplifted, erosional fan remnant forms the upper third of the Marble Creek fan. This portion of the fan surface has been stripped off to a large extent by erosion, and is partially buried by younger alluvium. Drainage dissection and associated surface truncation have been accelerated by uplift of the fan remnant along the southeastern continuation of the master fault.

Marble Creek is an ephemeral stream that crosses the uplifted Marble Creek fan remnant in a deeply incised channel. This fanhead trench is incised to a depth of 8 to 40 m, and provides illuminating exposures of the fan stratigraphy (discussed in a following section). The Marble Creek fanhead trench terminates downfan at the master fault of the northern FLVFZ. This suggests fanhead entrenchment has been influenced by vertical displacement on the master fault, as was proposed for the Indian Creek fanhead trench (previous section).

An unnamed minor drainage crosses the Marble Creek fanhead in a shallowly incised and terraced channel about a half kilometer south of Marble Creek. The character of this drainage also changes from channelized to non-channelized where it crosses the master fault. The drainage forms an alluvial fanlette that is actively aggrading by a distributed system of drainages below the fault (i.e., intersection point). Young debris-flow lobes and levees characterize the surface of this fanlette and the lower Marble Creek fan.

LEIDY CREEK ALLUVIAL FAN

The detailed map area includes a portion of the northern Leidy Creek fan (Fig. 3; Plate I). However the entire fan was carefully examined by field reconnaissance and air-photo analysis. Leidy Creek is a perennial stream that débouches from the White Mountains into a large piedmont embayment and forms the extensive Leidy Creek fan. The apex of this fan is about 350 m above the floor of Fish Lake Valley. The fan is about 10 km long, 5 km wide, and exhibits a prominent sequence of stepped fan surfaces within the fanhead trench.

Most of the Leidy Creek fanhead, south of Leidy Creek, is an uplifted erosional fan remnant. In contrast, north of Leidy Creek, most of the fan surface has recently aggraded; the Indian Creek fan exhibits a similar relationship (discussed in a previous section). A pair of broadly rounded ballenas are prominent on the northern Leidy Creek fanhead. Ballenas represent the final morphological stage in the erosional destruction of a once continuous alluvial fan surface (Peterson, 1981). Most of the mid and lower parts of the Leidy Creek fan are accessible to deposition, and hence these are in a constructional phase.

DESCRIPTION OF MORPHOSTRATIGRAPHIC UNITS

OPERATIONAL DEFINITION AND USAGE

Frye and Willman (1960, p. 7) first proposed the informal term, morphostratigraphic unit, to "a body of rock that is identified primarily from the surface form it displays". Frye and Willman (1962, p. 113) indicated that the morphostratigraphic unit may be applied to the classification of alluvial fans of the Basin and Range Province, as Gile and others (1981, p. 24) and Ruhe (1974, p.487) have done.

Peterson (1981, p.1) suggested that "landform recognition merges with the concept of the geomorphic surface that is so valuable for mapping soils". Hence, it is necessary to define a stratigraphic unit that combines the form of a body of sediment with surface and soil characteristics. This section attempts to define such a stratigraphic unit by building on Frye and Willman's (1960, 1962) definition of a morphostratigraphic unit.

The "morphostratigraphic" units, as defined here, has three-dimensional form and may, or may not, comprise a relict geomorphic surface and a pedogenic soil. These units have regional stratigraphic significance and are considered to be of fundamental importance to Quaternary geologic studies in the Basin and Range Province. Some of the criteria used in the definition of morphostratigraphic units in this section are from Frye and Willman (1960, 1962), from Peterson's (1981, p. 42-43) definition of a geomorphic surface, and from definitions of various formal stratigraphic units (none of which are widely applicable to the present study) outlined by the North American Stratigraphic Code (1983).

Morphostratigraphic units are mappable, stratified bodies of sediment that are primarily identified by their three-dimensional form, but can also be identified by distinguishing characteristics of geomorphic surfaces and (or) pedogenic soils that the units may comprise. The primary deposit(s) can be of diverse composition and age, but must be of a thickness that will accommodate the development of a pedogenic soil, i.e., about 50 cm (Peterson, 1981, p. 43).

Each morphostratigraphic unit may have an unique assemblage of surface and soil characteristics that are primarily the products of weathering. These characteristics, which may vary systematically with the duration of exposure to the weathering environment, are observed or measured in the field. Soils genetically related to morphostratigraphic units may be members of regionally extensive chronosequences (i.e., a sequence of soils such that one soil differs from another primarily as a result of soil age, Jenning, 1941).

The units provide a means of recognizing and isolating weathering phenomena based on relative age relations. Ideally, the criteria used to define a unit should be clearly documented where the relative age of that unit is known from geomorphic evidence (e.g., stepped sequence). The units should be chosen to represent different intervals of regional landscape stability and soil formation.

Correlation of morphostratigraphic units may be accomplished by tracing unit boundaries from within stepped sequences (i.e., where their relative age is known), or by comparative analysis of diagnostic weathering characteristics with those exhibited within stepped sequences. Infrequently, correlation is established by stratigraphic relations and radiocarbon dates, or by tephrochronologic correlations.

Morphostratigraphic units are not recognized on the basis of primary properties of the stratiform body (e.g., initial composition, texture, color, and sedimentary structure and fabric of the deposit). Therefore, morphostratigraphic units do not uniquely define lithic units (i.e., "surficial deposits"). However, if the fan surface is unmodified or only slightly modified (i.e., is a relict surface), then the unit may delineates a surficial deposit.

DIAGNOSTIC CRITERIA FOR RECOGNITION AND CORRELATION

The diagnostic criteria used for recognition and correlation of morphostratigraphic units (Table 1) show systematic changes with increasing unit age. These changes are used to infer relative age relations. The various relative-age criteria begin to develop at the time of stabilization of the land surface, and not necessarily at the time of deposition of the surficial deposit.

Depth of Incision

Detailed mapping indicates that the relative depth of incision is a useful relative age indicator within the stepped sequences of fanhead trenches. This criterion provides a means of recognizing and correlating morphostratigraphic units with a high degree of confidence in the fanhead area.

However, downfan from the intersection point, the relative depth of incision may provide ambiguous or erroneous results. Older units are typically overlapped by younger units in this portion of the fan, and thus topographic separation of units is minor. In different tectonic settings, the depth of incision may produce erroneous results, since tectonic influences may vary rapidly along fault strike. Furthermore, since the depth of incision depends on the competency of a drainage to down-cut, drainages with large catchment areas tend to be incised to a depth greater than drainages with small catchment areas. For this reason, Indian Creek is incised somewhat more deeply than Marble Creek.

Drainage Pattern

The pattern of drainageways is easily assessed from air photos and is a useful indicator of relative age throughout the alluvial fan environment. In general, the number of drainages is inversely proportional to the age of the unit, and the magnitude of incision is directly proportional to age (above). Shallowly incised, distributed and braided drainage systems characterize young, aggrading alluvial fan surfaces. Older units (Pleistocene fan surfaces) are deeply dissected by a few onfan drainages which are arranged in parallel to dendritic patterns.

Surface Topography

Through time the constructional morphology of an alluvial fan surface is progressively modified by weathering processes. The microtopography becomes smoother on successively older fan surfaces, as is evident from air-photo analysis and field reconnaissance. Rough, angular bar-and-swale microtopography is characteristic of young surfaces. Such features are commonly absent or subdued on late Pleistocene surfaces of the study area. Hence, the degree of preservation of primary depositional features, such as bar-and-swale microtopography and debris-flow levees and lobes, provides an indication of relative age.

The modification of alluvial fan surfaces is in part due to burial by eolian sediment, and to saturated flow or solifluction within these desert loess mantles (Sawyer, 1988). Denny (1965; 1967) and Denny and Drewes (1965) referred to this process as creep-smoothing, although the process of creep is probably minor relative

TABLE 1: DIAGNOSTIC SURFICIAL CRITERIA FOR RECOGNITION AND CORRELATION OF MORPHOSTRATIGRAPHIC UNITS

Stratigraphic units: Unit Name	Approximate Age[1] (ka or epoch)	Surficial Criteria for Recognition and Correlation
late Marble	0.1	Shallowly (< 2m) incised; distributary drainage pattern with numerous channels; preserved debris flow lobes & levees, and bar & swale microtopography; pavement and varnish are absent; frequently forms low flood plains along modern channels and fan aprons & skirts in lower fan positions, with limited occurrence within fanhead trenches; geomorphic evidence of faulting is absent; consists of essentially raw alluvium.
middle Marble	1.0	Moderately incised (2 to 6 m), distributary drainage pattern; slightly subdued debris flow lobes & levees, and bar & swale microtopography; pavement and varnish are absent; forms the first prominent, commonly paired, terrace (or inset fan) in stepped sequences and frequently forms fanlettes at the base of large fault scarps; forms the youngest, clearly faulted surface (scarp height ≤ 1 m); only incipient accumulations of eolian? silts and fine sands.
early Marble	1.8	Moderately incised (4 to 12 m),distributary drainage pattern; subdue bar and swale topography, commonly dissected (or buried) near modern drainages; has incipient pavettes with first occurrence of varnish within "pits" in lithic fragments; forms prominent, paired, inset fan remnants in stepped sequences; scarp height ≤ 2 m; generally ≤ 5 cm thick fine-grained eolian? caps.

TABLE 1: Continued.

Stratigraphic units Unit Name	 Approximate Age[1] (ka or epoch)	Surficial Criteria for Recognition and Correlation
Leidy	mid-Holocene to latest Pleistocene	Moderately (3 to 6 m) incised by parallel onfan, and deeply (<15 m) by trunk, drainages; bar & swale topography is latest absent; pavettes beginning to interlock, but not sorted, with clastsembedded in prominent accumulations of eolian? sediment (about 5 cm thick); varnish forms weak discontinuous coatings - shiny in pits; typically forms uplifted, broad flattish, erosional fan remnants; fault scarps 2 to 4 m in height; some gruss derived from granitic boulders and limestone fragments are slightly etched.
Indian	late Pleistocene	Deeply dissected (10 to 40 m) by trunk streams and moderately dissected ($\leq$10 m) by well-established, parallel onfan drainageways; prominent solifluction steps with well sorted, interlocked pavettes on treads; varnish coatings may be moderate to thick, continuous, and shiny; forms extensive erosional fan remnants and infrequent ballenas; prominently (in places pervasively) faulted with scarps $\leq$ 40 m high, and offset about 120 m in a right lateral sense on Indian Creek fan; some granitic, volcanic, and most limestone boulders are deeply etched; thick (15-30 cm), fine-grained eolian? caps are common.
McAfee Creek	late-middle Pleistocene	Very deeply dissected ($\leq$80 m); relict surface is commonly stripped; erosional surfaces may have pavements that contain abundant carbonate rubble, are moderately to well packed and sorted, with varnish coatings on pavement chips that are moderate to thick and shiny; forms the highest fan remnants with some gross morphology preserved; extensively faulted.

[1] See text for discussion of approximate ages of morphostratigraphic units and Tables 2 and 3.

to solifluction (Appendix I). The solifluction process is unique because it depends on time, pedogenic processes, eolian sediment influx, and does not require frigid climatic conditions. Solifluction within desert loess mantles on Pleistocene fan remnants results in the formation of micro-relief steps. The solifluction steps produce a distinctive pattern of tonal bands that can be typically recognized on air photos of 1:24,000 and larger scales. The pattern consists of alternating light and dark stripes which impart a "wrinkled" or "shingled" appearance to the fan remnants (Appendix I, Figs. A2 and A3).

The patterns of solifluction steps allow reliable recognition and correlation of the late Pleistocene Indian morphostratigraphic units throughout northwestern Fish Lake Valley.

Desert Pavement

Stone pavements are surface concentrations of lithic fragments arranged in a layer one or two clasts thick. In arid regions, pavements (or desert pavements) form on flattish, geomorphically-stable alluvial fan surfaces. Typically, fine-grained, gravel-free Av horizons (in probably desert loess) occur beneath such pavements.

With time, desert pavements become prominent, well-sorted and tightly-packed. Pavement is absent or incipient on the surfaces of late Holocene units, but is prominent on Pleistocene surfaces in the study area. Commonly, the lithic fragments of prominent pavements are shallowly embedded within a thin, slightly harder, surficial layer or crust, comprised of fine-grained vesicular materials. Clasts of incipient pavements, in contrast, rest on coarse alluvial materials.

Field studies indicate that the degree of pavement development is useful for recognition and correlation of intermediate and older morphostratigraphic units in the study area, provided that weathering-resistant pavement fragments occur in sufficient quantities.

Desert Varnish

Desert varnish comprises manganese, iron oxides, clay, trace minerals, and sparse organic matter (Dorn and DeNiro, 1985). Coatings of varnish form on pavement clasts and surficial boulders. Initially, the coatings are thin and discontinuous, but with time, they become thick, black and continuous.

On the surfaces of Holocene units, varnish coatings are absent or discontinuous, and occur only within small recessed areas ("pits") in rock fragments. Intermediate-age units (latest Pleistocene to Holocene) have thin, discontinuous coatings on most exposed areas of lithic fragments and relatively thick varnish coatings within some pits. Thick, nearly continuous, "greasy"-feeling, shiny-appearing, purplish-black, varnish coats the pavement of older units of the study area.

Hence, the prominence of desert varnish is a useful indicator of relative age for all morphostratigraphic units in the study area. The prominence of desert varnish can be assessed from air photos as tonal differences between surfaces of contrasting age. However, mafic or other dark colored lithic fragments may influence tonal contrasts. Desert varnish development, like pavement development, depends on an abundance of lithic clasts that are resistant to weathering.

Landform Pattern

The relationships between landforms frequently can be used to infer relative age. Peterson (1981) indicated that recognition of the types of remnant landforms, which are extensive in the upper piedmont slope of the study area, is a fundamental tool in establishing the relative age of geomorphic surfaces. For example, inset or stepped relations between geomorphic surfaces clearly demonstrate relative age. Ruhe (1967) showed that an inset fan is younger than the relict fan surface in which it is emplaced. The elevation of a morphostratigraphic unit within a stepped sequence is the operational definition of relative age. Hence, the higher the unit within the sequence, the greater is its age.

The morphology of landforms also suggests age relations. The constructional form of young landforms is well preserved. Remnants of young and intermediate age tend to have angular shoulders. In contrast remnants of older landforms have well-rounded shoulders.

Morphostratigraphic units of the study area commonly occupy specific positions in the local landscape. Holocene units occur most extensively within the interfan valley, along modern and active channels, and in mid to lower positions of Pleistocene fans (Plate I). The Holocene units also occur as inset fans within fanhead trenches. The older units are extensive along and near the eastern front of the White Mountains and occur less commonly in the mid and lower piedmont position.

Other Criteria

A number of other criteria also provide information about relative age. Among these are boulder weathering, stratigraphic relations, and accumulations of fine-grained (eolian?) materials on fan surfaces. Soil development is another important indicator of relative age and is discussed in considerable detail in Chapter V.

Weathering of surficial boulders depends in part upon time and lithology. Given sufficient time and exposure to weathering processes, the relative resistance to weathering of a mafic dike in granite, or a clastic-rich interbed in a carbonate rock, is revealed by a difference in surface relief. Boulders on the younger units have no appreciable relief between such features. In contrast, on older units, boulders may have marked surface relief (5-10 cm) between such features. Older units generally lack surficial boulders, suggesting that they have been buried or have disintegrated.

Traditional stratigraphic relations such as superposition and cross-cutting relations provide conclusive evidence of relative age. However, such relations are rarely observed on the piedmont slope beyond the fanhead trenches and thus have limited application to correlation and discrimination of units in the study area.

Accumulations of well sorted, virtually gravel-free, fine-grained materials occur on the older units, generally beneath tightly-packed stone pavements. This material, probably eolian in origin, only occurs where pavements have developed, and therefore are absent on the younger units. These fine-grained materials are generally thickest on the older units. Hunt and Mabey (1966, p. A67 and A68) suggested that thicknesses of silt layers on "old" surfaces in Death Valley are greater than on younger surfaces. However, Peterson (1988) cautioned against indiscriminant use of the thickness of such capping deposits as an indicator of relative age, since infiltration of eolian material into the soil occurs naturally and therefore it is not simple to establish the base of the eolian layer, or the volume of eolian material that has been infiltrated.

AGES OF MORPHOSTRATIGRAPHIC UNITS

Numerical age ranges have been assigned to the Holocene morphostratigraphic units of the map area, based primarily on radiocarbon dating of detrital wood incorporated in alluvial fan deposits. Additionally, age assignments for Holocene and Pleistocene units have been based on tentative correlations of volcanic ash layers intercalated in fan alluvium to established tephrochronologic units. An additional age dating technique, dendrochronology (i.e., tree-ring analysis), was employed to date a buried Bristlecone pine (Pinus longaeva Bailey) log. The results however, proved to be inconclusive (Harlin, T., 1988, written commun., Laboratory of Tree-Ring Research, University of Arizona).

Factors that complicate the assignment of ages to morphostratigraphic units include the limited number of radiocarbon dates, and the lack of convincing correlations to established time scales (e.g., tephrochronologic units and dated soil sequences). Age assignments are further complicated by uncertainty about relationships between dated features, their host deposits, and the respective morphostratigraphic units.

Radiocarbon Age Determination

The radiocarbon dating method is based on the fact that carbon dioxide in the atmosphere contains stable ^{12}C and ^{13}C and minor amounts of radioactive ^{14}C. The various isotopes of carbon are incorporated in organism in their atmospheric ratios. Upon death of the organism, the radioactive decay of ^{14}C begins to reduce the ratio of ^{14}C to ^{12}C. The ^{14}C isotope decays at a known and constant rate. Therefore, by measuring the current ratio of ^{14}C to ^{12}C in a sample of organic material, the age of that sample can be determined (Bradley, 1985).

As a result of fluctuations in atmospheric ^{14}C during the past, radiocarbon ages are only approximations of the historical age reported in calendar years (Stuiver, 1982). Several schemes have been developed to calibrate radiocarbon ages through dendrochronology, based in part on Bristlecone pines in the White Mountains (e.g., LaMarche, 1973; Stuiver, 1982; Stuiver and Pearson, 1986). The calibrated ^{14}C age is a close approximation of the historical age, but is expressed in dendroyears rather than calendar years, because of possible errors in tree-ring counting "probably no more than a couple years" (Stuiver, 1982).

The convention in reporting radiocarbon ages, adopted herein, is to convert ^{14}C ages to calibrated dendroyear ages using the current high-precision calibration schemes of Stuiver and Pearson (1986, their Figs. 1 & 2).

More than thirty samples of detrital wood and charcoal were collected by the author during field investigations in the study area. To date, radiocarbon analyses are available for eight detrital wood samples (Appendix II; see Plate I, and Table 2). The conventional radiocarbon ages and their calibrated mean ages, denoted herein as calB.P. (calibrated years B.P.), are shown in Table 2.

Commonly, the relative ages of morphostratigraphic units are known unequivocally from morphostratigraphic relations. All radiocarbon ages must be shown to be internally consistent and consistent with relative age relations if they are to be considered plausible. The radiocarbon ages reported in Table 2 are both internally consistent, and consistent with known relative ages of the various morphostratigraphic units (Fig. 9).

Table 3 and Figure 9 depict the stratigraphic relations of radiocarbon-dated samples to their host deposits and to individual morphostratigraphic units. It is here assumed that the elapsed time between death of the tree and its incorporation in the alluvial fan gravels is negligible. It is recognized that a radiocarbon-dated sample of detrital wood (taken at face value) can be as old as or older than its host deposit.

A radiocarbon-dated sample that occurs stratigraphically above a morphostratigraphic unit provides the minimum possible chronologic age for that unit ("limiting minimum" age). A radiocarbon-dated sample that occurs stratigraphically within the deposit that forms the relict surface of a particular morphostratigraphic unit provides a date that is the "most probable" age for that unit. For example, the limiting minimum age for the middle Marble unit is 680 calB.P., since the host deposit is stratigraphically above the middle Marble unit (Fig. 9). The most probable age for the middle Marble unit is 1065 calB.P., since the date is from the deposit that forms the relict surface of this unit. It is less straightforward to determine the "limiting maximum" age of a unit.

Stratigraphic relations shown in Figure 9 illustrate that morphostratigraphic units are genetically associated with cut-fill episodes on the piedmont slope (discussed in detail in a following section). Downfan from the fanhead trench, the units may only be associated with depositional periods, because erosion in these areas is generally negligible. Each period of deposition or fill episode is associated with several individual deposits (Fig. 9). Since it is unlikely that any particular deposit (e.g., debris flow) would occupy all areas accessible to deposition, a single phase of deposition may result in the formation of several geomorphic surfaces, all closely spaced in age. Therefore, a radiocarbon date from the basal deposit of a fill assemblage is taken to represent the limiting maximum age for the morphostratigraphic unit formed within that assemblage. Hence, the limiting maximum age for the late Marble unit is about 680 calB.P. (see Fig. 9).

Radiocarbon Site 1: Radiocarbon Site 1 is along Marble Creek, about where the northwestward projection of the master fault of FLVFZ would intersect Marble Creek (Plates I and IIB; 37°45'02" N. Lat., 118°09'35" Long.). At this site, Marble Creek is incised about 2 m into the late Marble surface (Fig. 10). The surface was formed upon a young, clearly traceable debris flow deposit. This deposit spread laterally upon issuing from the fanhead trench and can be traced at least 3 km downfan.

Morphostratigraphic relations in the immediate area of Radiocarbon Site 1 provide unequivocal evidence of the relative age of the late Marble unit. This unit can be traced physically from where it occurs below the middle Marble unit within the fanhead trench, to where it overlies the middle Marble and Leidy units beyond the fanhead trench.

TABLE 2: RADIOCARBON AND CALIBRATED AGES

[n.a., not available; yr B.P., years before AD 1950; cal B.P., calibrated years before AD 1950]

Sample Number	Sample Site[1]	Laboratory Number[2]	^{14}C Age (yrB.P.)[3]	DEL ^{14}C (‰)	Calibrated Age (calB.P.)[4]
5-TS-1-51MC-I	RC-1	Beta-26169	140 ± 40	n.a.	120 ± 45
5-TS-1-7MC	RC-1	A-4765	660 ± 40	-23.6	660 ± 50
5-TS-1-49-B	RC-1	A-5068	755 ± 60	-22.6	680 ± 65
5-TS-1-52	RC-4	Beta-26170	1160 ± 50	n.a.	1065 ± 55
5-TS-1-28FC	RC-3	A-4768	1670 ± 40	-23.5	1555 ± 45
5-TS-1-22A	RC-2	A-4767	2170 ± 45	-22.0	2155 ± 50
5-TS-1-10MC	RC-2	A-4766	2290 ± 50	-20.5	2340 ± 55

[1] Sample sites are plotted on Plate 1.

[2] A-# - University of Arizona, Laboratory of Isotope Geochemistry-Environmental Isotope Research; Beta-# - Beta Analytic Inc., Coral Gables, Florida.

[3] Based on the "Libby" half-life (5568 yr) of the radioactive disintegration process, and normalized to Del. ^{14}C = -25 per mil.

[4] The conversion of radiocarbon ages to calibrated ages is based on the current calibration schemes of Stuiver and Pearson (1986). If the calibrated age, as determined from their Figure 1, is not unique, then the calibrated age is determined from their Figure 2; if still not unique the calibrated age that most closely matches the radiocarbon age is reported.

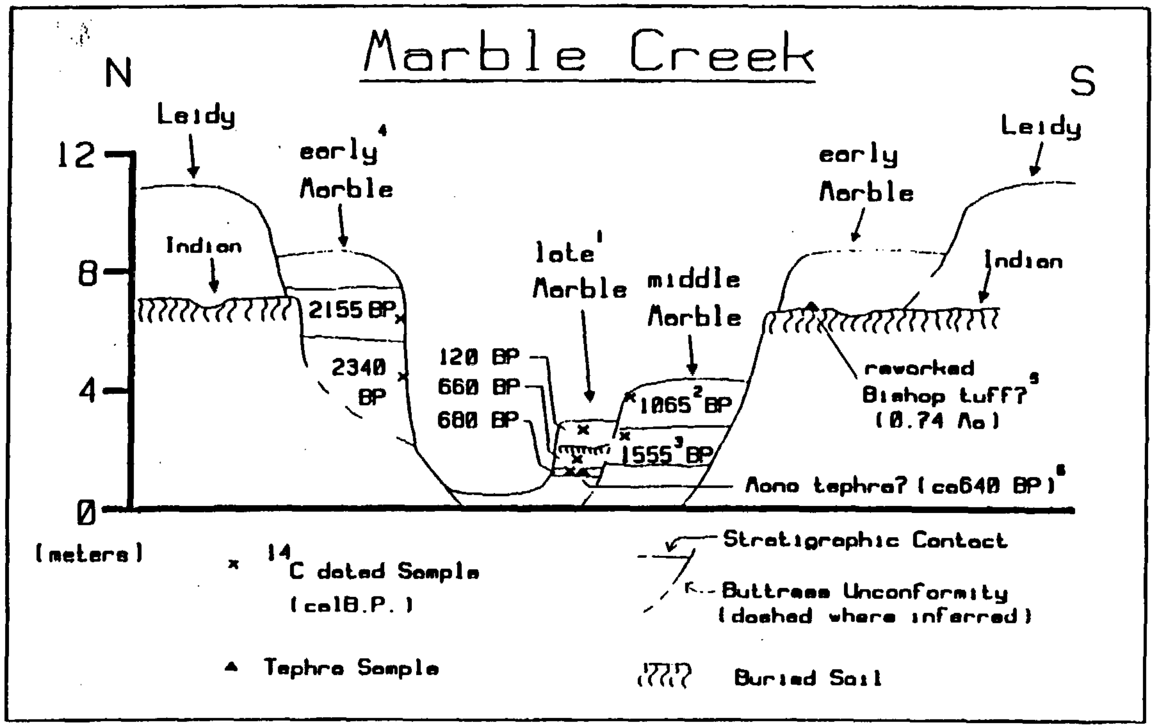

Figure 9. Composite and schematic cross section of morphostratigraphic units at Marble Creek in the vicinity of Radiocarbon Site 2, showing the stratigraphic positions of radiocarbon dates and tephra layers. The deposits stratigraphically above a buttress unconformity form the fill assemblage related to the overlying morphostratigraphic unit. [1]Dates from Radiocarbon Site 1 and Tephra Site 1; [2]Date from Radiocarbon Site 4; [3]Date from Radiocarbon Site 3; [4]Dates from Radiocarbon Site 2, which is the approximate location of the section; [5]Date from Tephra Site 3.

TABLE 3: AGE CONTROLS FOR MORPHOSTRATIGRAPHIC UNITS IN NORTHWESTERN FISH LAKE VALLEY

[n.a., not available; a.d., available, but not dated]

Morpho-Strat. units	Calibrated mean Radiocarbon ages (calB.P.)[1]			Inferred age of tephra layers, stratigraphically below unit[2] (ka)	Approx. age of Morpho-strat. units (ka)	Inferred age uncertainty of age est. (ka or epoch)
	Stratigraphically above unit (limiting minimum)	Within unit ("most probable")	Stratigraphically below unit (limiting maximum)			
late Marble	Historic?	120 (Beta-26169)	660 (A-4765)	0.64 (5-TS-1-7MC-C)	0.1	0 to <0.7
middle Marble	680 (A-5068)	1065 (Beta-26170)	1555 (A-4768)	3.4-4.1 (5-TS-1-28FC-B)	1.0	0.6 to 1.6
early Marble	1555 (A-4768)	a.d.	2155 (A-4767)	n.a.	1.8	1.5 to 2.3
Leidy	2340 (A-4766)	n.a.	n.a.	n.a.	13[3]	>2.2 to latest Pleistocene
Indian	n.a.	n.a.	n.a.	740-1,000 (5-TS-1-17MC)	230	late to late middle Pleistocene
McAfee Creek	n.a.	n.a.	n.a.	740-1,000	500 (M.C. Reheis, person. comm.)	late middle Pleistocene

[1] Calibrated ages from Table 2; Numbers in parentheses refer to laboratory and sample for radiocarbon ages reported in Table 2 and Appendix IV. See Text for explanation of "most probable" age.

[2] "Best" correlation of tephra layers based on chemistry as proposed by Andrei Sarna-Wojcicki (1987, 1989, USGS, written commun.) based on scanning electron microscope electron probe analyses performed by Charlie Mayer (1987, USGS, in Sarna-Wojcicki, 1987, USGS, written commun.) on volcanic-glass separated from tephra samples; all tephra samples were collected from positions stratigraphically below the morphostratigraphic unit (i.e., surface deposit); ages reported in yr B.P., unless specified otherwise.

[3] See text for approximate age of Unit 5.

The fan gravels within which the late Marble unit is developed at Radiocarbon Site 1 contain abundant detrital wood fragments, including a log more than 2 m long (Fig. 10). Radiocarbon dates are available for three separate detrital wood samples. The relation of the dated samples to morphostratigraphic units of the Marble Creek fan is as follows:

The uppermost of three dated samples (Fig. 10, "A") at Radiocarbon Site 1 comprises several small fragments of wood that were collected 5 to 26 cm below the relict surface of the late Marble unit in a soil pit 6 m south of Marble Creek (Pedon Site 4). The host deposit of the dated sample is the debris flow upon which the late Marble surface formed. Therefore, the stratigraphic position of the upper most sample should provide a date that is the "most probable" age of the late Marble unit. The age of the uppermost sample, hence the most probable age estimate for the late Marble unit, is 120 calB.P. (Beta-26169).

From a subjacent deposit, at a depth of about 80 cm, the intermediate radiocarbon dated sample was collected from a 2.3 m long detrital log. A date of 660 calB.P. (A-4765) has been obtained from this sample. The lowermost date of 680 calB.P. (A-5068) is from a wood fragment collected from a Mono(?) tephra layer (discussed in "Tephra Site 1"), at a depth of about 2 m. The stratigraphic position of the lowermost dated sample is probably near the base of the late Marble "fill-assemblage," but definitive relations are concealed. The limiting maximum age of the late Marble is estimated from the lowermost date of 680 calB.P. (A-5068).

All three radiocarbon dates at this site are internally consistent with their relative stratigraphic positions (Fig. 9). This suggests that radiocarbon dates provide reasonable chronologic constraints for the various morphostratigraphic units.

Immediately upstream from Radiocarbon Site 1, the late Marble unit is inset into the middle Marble unit. Therefore, the lowermost dated sample at Radiocarbon Site 1 should be younger than the middle Marble unit. This date, 680 calB.P. (A-5068), is considered to represent the limiting minimum age for the middle Marble unit.

<u>Radiocarbon Site 2</u>: Radiocarbon Site 2 is approximately 1 km upstream from

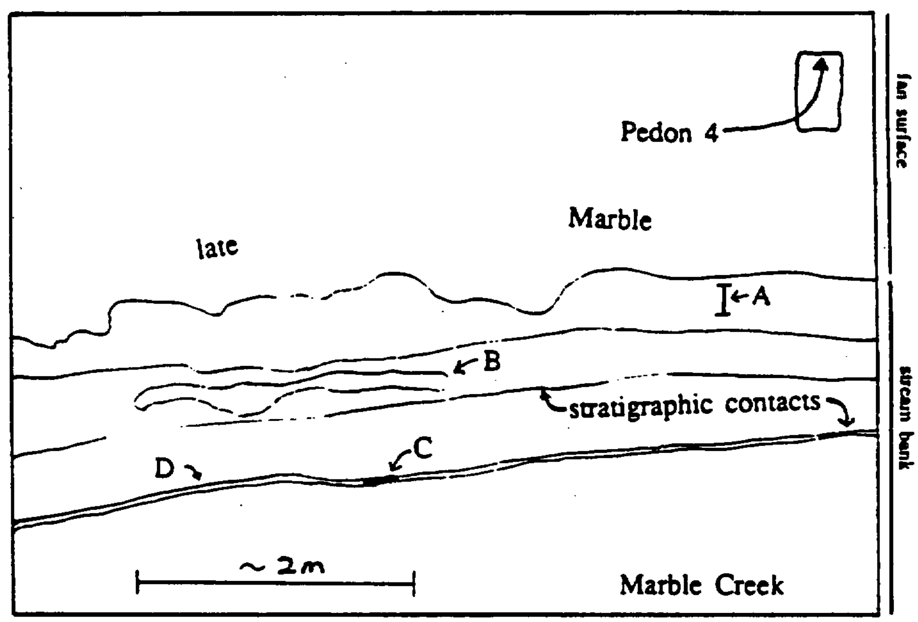

Figure 10. Sketch of Radiocarbon Site 1/Tephra Site 1 showing the stratigraphic relations of radiocarbon dated samples ("A", relative position of 5-TS-1-51MC-I; "B", 5-TS-1-7MC; "C", 5-TS-1-49-B) and a probable Mono tephra layer ("D", 5-TS-1-7MC-C) to the late Marble morphostratigraphic unit, which forms the surface. The sketch is of a hand held photograph of a stream cut along Marble Creek that was taken to the south (see Plate I for location).

Radiocarbon Site 1, within the Marble Creek fanhead trench (Fig. 11; Plates I and IIB; 37°45'02" N. Lat., 118°09'46" Long.). Imbricate cut-and-fill alluvial assemblages observed in exposures in the walls of the fanhead trench clearly illustrate age relations of various morphostratigraphic units (Figs. 9 and 11).

At Radiocarbon Site 2, the early Marble fill-assemblage is inset into the Indian unit (observed) and the Leidy unit (inferred from morphological relations). Locally, the fill assemblage can be observed 8 m above the active channel of Marble Creek, forming a 2 to 3 m thick cap overlying the paleosol of the Indian unit (Fig. 11). A gnarled Bristlecone pine (Pinus longaeva Bailey) log, more than 3 m long and 40 cm in diameter, is exposed in the north wall of the Marble Creek fanhead trench at this site (Fig. 11, "C"). The log is 2.2 m below the early Marble relict surface and is incorporated in the associated fill assemblage. A sample of wood, collected from the outermost part of the log near preserved bark, has a radiocarbon date of 2155 calB.P. (A-4767). Until an overlying sample (discussed below) is dated, the age of this log (2155 calB.P.) is taken to be greater than, or equal to, the most probable age of the early Marble unit (Table 3). Tom Harlin (Univ. of Arizona, 1988, written commun.) attempted to date this detrital log by dendrochronologic techniques. Harlin identified 211 tree rings in a slab cut from this remarkably well-preserved log. More than 100 of the tree rings appear suitable for correlation to the established Bristlecone pine (Pinus longaeva) tree-ring chronology in the White Mountains. However, Harlin was unable to make a convincing correlation.

A small detrital wood fragment (Fig. 11, "D") was collected at a depth of 1 m below the early Marble surface and 1.2 m above the Bristlecone pine log. If dated, this sample would provide a better estimate of the most probable age for the early Marble unit.

Approximately 20 m downstream from the Bristlecone pine log, a second detrital log is exposed about 5 m below the relict surface of the early Marble unit. This log is enclosed within, and apparently lies near the base of, the early Marble fill assemblage (Fig. 11, "E"). Although the stratigraphic relations are partially obscured by colluvial debris, a radiocarbon date of 2340 calB.P. (A-4766) from this

(b)

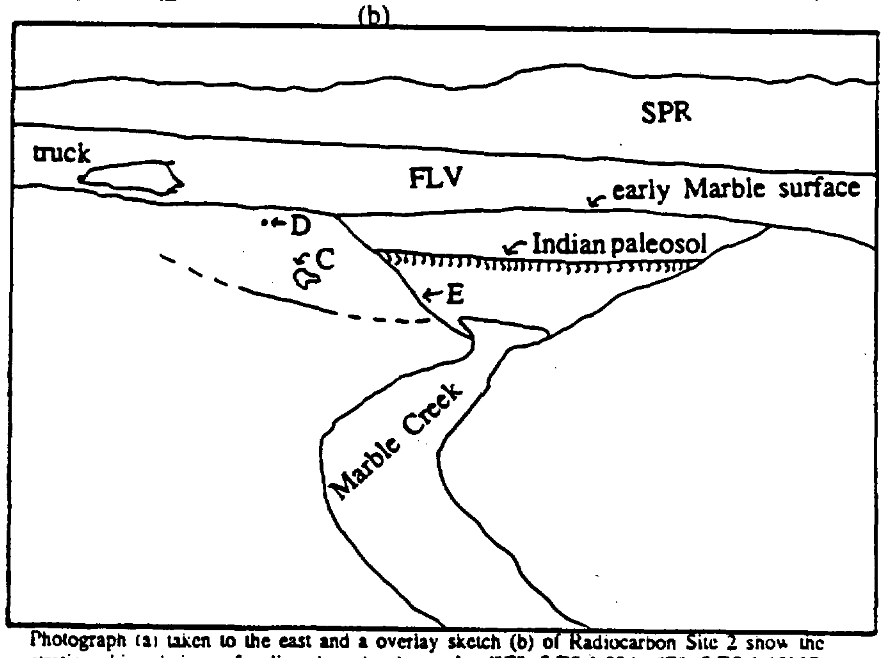

Figure 11. Photograph (a) taken to the east and a overlay sketch (b) of Radiocarbon Site 2 show the stratigraphic relations of radiocarbon dated samples ("C", 5-TS-1-22A; "E", 5-TS-1-10MC) to the early Marble (EM) morphostratigraphic unit, which forms the surface. A third sample ("D", 5-TS-1-10A-C), if radiocarbon dated, should provide the most probable age of the early Marble unit. Note that the early Marble fill assemblage buries the paleosol of the Indian unit (I). The truck provides a scale for the middle ground. FLV, Fish Lake Valley; SPR, Silver Peak Range.

log most likely provides the limiting maximum age for the early Marble unit. Further, the age of the log is equal to, or less than the limiting minimum age of the Leidy unit (Table 3) since, the deposit containing the dated log is interpreted to be inset into the Leidy unit (Fig. 11).

Radiocarbon Site 3: Approximately 0.5 km south of Radiocarbon Site 1, a small, unnamed drainage crosses the master fault of the northern FLVFZ. The drainageway emerges from the channel and forms an alluvial fanlette, on the downthrown side of the fault. Radiocarbon Site 3 is located at the apex of the fanlette, about 20 m upstream from the fault (Plates I and IIC; 37°44'48" N. Lat. 118°09'28" Long.).

At Radiocarbon Site 3, the middle Marble unit is inset into the Leidy unit. Upstream, the late Marble through Leidy units occur in stepped sequence. These morphostratigraphic relations establish the relative ages of the various units.

A detrital log, exposed approximately 50 cm below the relict middle Marble surface, has a radiocarbon date of 1555 calB.P. (see Plate III). Stratigraphically, the log is incorporated within the middle Marble fill assemblage, perhaps near its base. The age of the log (1555 calB.P.) provides an estimate of the limiting maximum age of the middle Marble unit. In addition, the date also provides the limiting minimum age for the early Marble unit, since the dated sample is in a deposit younger than this unit.

Radiocarbon Site 4: Radiocarbon Site 4 is about 2.5 km north of Marble Creek, along an unnamed drainage that heads near knob 7917 on the Davis Mtn., NV-CA, 15' Quadrangle (Plates I and IIB; 37°46'18" N. Lat. 118°10'25" Long.). Here, the middle Marble unit lies 2 to 3 m above the active wash. Immediately downstream the late Marble unit partially buries the middle Marble unit.

A detrital log, exposed 40 to 50 cm below the relict surface of the middle Marble unit, has a date of 1065 calB.P. (Fig. 12, "C"). The middle Marble surface is developed upon the host deposit of the log. Therefore, the age of the log (1065 calB.P.) provides the most probable age estimate for the middle Marble unit.

(a)

(b)

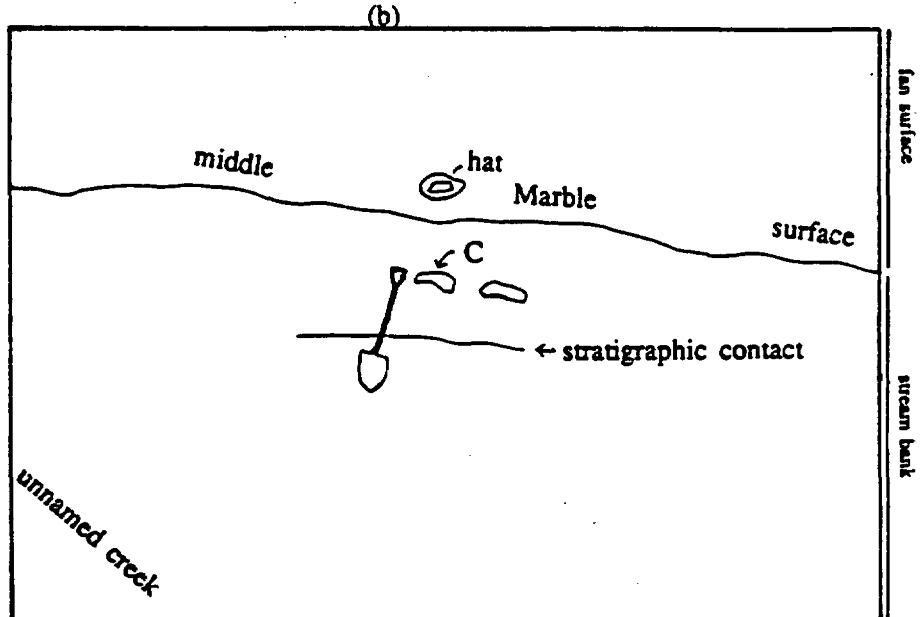

Figure 12. Photograph (a) taken to the southeast and a sketch (b) of Radiocarbon Site 4 show the stratigraphic relations of a radiocarbon dated sample ("C", 5-TS-1-52) to the middle Marble morphostratigraphic unit, which forms the surface (see Plate I for location). Short handle shovel (1 m long) provides a scale.

Tephrochronologic Age Determinations

Volcanic ash layers are key stratigraphic markers because they form geologically instantaneous deposits that are generally widespread. Correlation of ashes based on chemical "fingerprints" can extend age constraints from an area where dates exist to other areas where dates might not otherwise be available.

One of the most volcanically active regions in the Basin and Range Province during the Quaternary lies between the White Mountains and the Sierra Nevada. The region comprises the Long Valley-Mono Craters-Glass Mountain volcanic complex (Fig. 2). Fish Lake Valley is 80 km east, or leeward, of the volcanic complex and is known from the present study to contain ashes erupted from these volcanic centers.

All volcanic ash correlations discussed here have been provided by A. Sarna-Wojcicki (1987, 1989; written commun.; USGS, Menlo Park; Appendix II), and are provisional in nature. Therefore, the ages of the volcanic ashes listed in Table 3 and Appendix IV are only "tentative guides" to the age of a particular ash. Electron microprobe analyses of volcanic glass separated from the various ashes, performed by C. Meyer (USGS, Menlo Park), provide the basis for correlation. The correlations represent the "best" matches to ashes that are of similar composition.

Late Holocene volcanic ashes of Mono Craters, two of which are reported below, are very similar in composition, and therefore are difficult to identify and correlate (Sarna-Wojcicki, 1989, written commun.). The result is a decreased probability of a unique correlation and increased uncertainty in the age of the ash.

All volcanic ash or tephra layers sampled in the study area have been reworked. The reworked layers are therefore younger than the deposits from which they were derived. Thus, volcanic ash ages listed in Table 3 probably represent maximum ages for the reworked tephra.

Tephra Site 1: Tephra Site 1 is at the same location as Radiocarbon Site 1, on the Marble Creek fan (Plates I and IIB; 37°45'02" N. Lat. 118°09'35" Long.). A tephra layer, composed of pods or lenses of volcanic ash, is exposed about 2 m below the late Marble surface. As discussed earlier, the stratigraphically lowest radiocarbon date of 680 calB.P. (A-5068) is from this tephra layer. A radiocarbon date of 660 calB.P. is from a detrital wood fragment in the deposit that overlies the tephra layer. Hence, redeposition of the tephra probably occurred near or sometime after 660-680 calB.P.

The tephra is similar in composition to volcanic ashes erupted from the Mono Craters (Sarna-Wojcicki, 1987; written commun.)(Fig. 2). The best correlation, in view of the radiocarbon ages, is with an ash erupted from Panum Crater in the Mono Crater Chain erupted ca 640 ^{14}C yr B.P. (Wood and Brooks, 1979). This date supports the limiting maximum age for the late Marble unit of about 660 yr (Table 3).

Tephra Site 2: Tephra Site 2 is about 0.5 km south of Marble Creek, and coincides with Radiocarbon Site 3 (Plates I and IIC; 37°44'48" N. Lat. 118°09'28" Long.). An exploratory trench was excavated across the master fault of the FLVFZ at this site. A layer of reworked tephra occurs 1.8 m below the relict middle Marble surface, shown as stratigraphic unit 2 in Plate 3. As discussed earlier, a detrital log that has a radiocarbon date of 1555 calB.P. (A-4768) occurs above the tephra layer. Hence, the tephra was redeposited prior to 1555 calB.P.

The composition of the tephra layer (sample 5-TS-1-28FC-B) compares most closely with several volcanic ashes erupted from the Mono Craters Chain between 3400 to 4100 yr B.P. Apparently less significant comparisons have been made with ashes as old as 8000 yr B.P. (Appendix II).

The age range for the tephra, 3400-4100 to 8000 yr B.P., may be too old for its stratigraphic position, because the layer probably occurs within the early Marble fill assemblage (Plate 3), which has dates of 2340 calB.P. and younger at Radiocarbon Site 2.

Tephra Site 3: Tephra Site 3 is in the south wall of the Marble Creek fanhead trench, near the mouth of the canyon (Plates I and IIC; 37°44'40" N. Lat. 118°14'07" Long.). Here, as elsewhere on the Marble Creek fanhead, the relict surface of the Indian unit is truncated. The truncated Indian surface (and soil) is partially buried by Leidy and younger alluvium (Fig. 9).

A layer of reworked tephra (5-TS-1-17MC), 4 to 15 cm thick, rests unconformably on a formerly exhumed Bk horizon of the Indian paleosol (Fig. 9).

The tephra is correlative with the Bishop tuff or with several other ashes erupted from the Long Valley-Mono-Glass Mountain complex that range in age from about 0.74 to 1.0 Ma. The apparently equivalent tephra occurs at the mouth of McAfee Creek, 5.6 km to the south, and is reworked there as well (M.C. Reheis and J. Slate, 1989, personal commun.). The McAfee Creek unit, which is older than the Indian unit, overlies the tephra. These relations suggest that both the McAfee Creek and Indian units are younger than about 0.74 to 1.0 Ma.

AGES ASSIGNED TO MORPHOSTRATIGRAPHIC UNITS

The radiocarbon and tephrochronologic age data (discussed above), and their relations to morphostratigraphic units are shown in Table 3. These age data provide the primary basis for assigning (estimating) numerical ages and associated uncertainties to the various morphostratigraphic units.

Late Marble Unit: The approximate age of the late Marble unit, about 0.1 ka, is based on age data from Radiocarbon Site 1 (Table 3). The date of 120 calB.P. (Beta-26169) on wood fragments at this site provides the most probable age for the late Marble unit. The stratigraphically lower wood fragment with a date of 660 calB.P. (A-4765) provides the limiting maximum age for the unit. The limiting maximum age is also supported by an estimated age of 640 ^{14}C yr B.P. for a volcanic ash layer at this site. The limiting minimum age may be within Historic time. Therefore, the late Marble unit is assigned an age of 0.1 ka, but may be as old as 0.7 ka.

Middle Marble Unit: The oldest date of 680 calB.P. (A-5068) from Radiocarbon Site 1 is inferred to represent the limiting minimum age for the middle Marble unit. At Radiocarbon Site 3, a date of 1555 calB.P. (A-4768) provides the limiting maximum age for this unit. The most probable age for the middle Marble unit is provided by a date of 1065 calB.P. (Beta-26170) from Radiocarbon Site 4. The middle Marble unit is therefore assigned an age of 1.0 ka and a range of uncertainty from 0.6 to 1.6 ka.

Early Marble Unit: The limiting minimum age of the early Marble unit is inferred from a date of 1555 calB.P. (A-4768) from Radiocarbon Site 3. A limiting maximum age of 2155 calB.P. (A-4767) is provided by a date at Radiocarbon Site 2. The most probable age of the unit is undetermined, but suitable materials that could provide this age have been collected. The early Marble unit therefore has a range of uncertainty of 1.6 to 2.2 ka, with 1.8 ka assumed to be an approximate age (Table 3).

Leidy Unit: The Leidy unit is older than the date of 2340 calB.P. (A-4766) from the basal fill associated with the early Marble unit at Radiocarbon Site 2. Unfortunately, this is the only age data pertinent to this unit. Morphostratigraphic relations suggest that the Leidy unit is not substantially older than the early Marble unit. The Leidy soil, discussed in Chapter V, has limited accumulations of pedogenic clay that are apparently similar to desert soils of the southwestern United States that formed during the last 12,000 years (e.g., Gile, 1975; Nettleton and others, 1975). The Leidy unit is assigned a limiting minimum age of 2.3 ka and an inferred limiting maximum age of latest Pleistocene (18 ka). The approximate age of the Leidy unit is assumed to be 13 ka (Table 3).

Indian and McAffee Creek Units: The various criteria used for recognition and correlation of morphostratigraphic units (Table 1) strongly support an age assignment for the Indian unit that is significantly older than the Leidy unit. Soil properties (Appendix II) known from the present study to be an important indicator of relative age (Chapter V) also suggest a considerably older age for the Indian unit. The Indian unit is probably substantially younger than the McAfee Creek unit, as suggested by many of the above criteria, including relative depths of incision. Thus, the Indian unit is intermediate in age between the Leidy and McAfee Creek units. Before discussing the age of the Indian unit further, it is necessary first to discuss the age of the McAfee Creek unit.

In Plate I the McAfee Creek unit occurs only on an erosional remnant, perched high above Indian Creek at the mouth of the canyon. The relict surface of this remnant landform is truncated, as is suggested by a merger of its shoulder slope components (criterion suggested by Peterson, 1981). Therefore, relative dating criteria such as surface weathering characteristics and soil development are of limited usefulness since their "clocks" have essentially been reset. These indicators of relative age are not associated with stabilization and inception of the McAfee Creek surface, but with the subsequent erosional surface. However, even though these indicators are probably less well developed than those associated with the relict McAfee Creek surface, they clearly are more prominent than those associated with the relict Indian surface. This supports that the McAfee Creek unit is significantly older than the Indian unit.

The McAfee Creek unit at the mouth of McAfee Creek (Plate IIC) overlies a thick reworked section of the Bishop (?) tuff (740 ka)(M.C. Reheis and J. Slate, 1989, personal commun.; collaborative endeavors between Reheis, Slate and the author, 1989). Fill alluvium overlying the tuff and underlying the McAfee Creek unit is 50 m or more thick. These stratigraphic relations indicate the McAfee Creek unit is younger than the redeposited Bishop (?) tuff upon which it rests. The thick sequence of fill alluvium separating the McAfee Creek surface from the underlying tuff suggests that the McAfee Creek unit could be significantly younger than the tuff. The age of the Bishop tuff, 740 ka, is therefore considered to be greater than the limiting maximum age of the McAfee Creek unit.

Morphostratigraphic relations along the east flank of the White Mountains (described above) indicate that the Indian unit is significantly older than the mid-Holocene to latest Pleistocene Leidy unit, but substantially younger than the McAfee Creek unit. The Indian unit shares surface and soil characteristics with the Yucca and the early Black Cone geomorphic surfaces in Crater Flat, southern Nevada (e.g., Peterson, 1988)(discussed in Appendix VII, "Case Study 1"). The Yucca surface has cation-ratio dates of 360 to 380 ka and the early Black Cone surface has dates of 128 to 137 ka, from desert varnish collected from surficial lithic fragments (Dorn, 1987). Based on available data, the Indian unit is inferred to be late (possibly late middle?) Pleistocene in age (100 to 360 ka) and the McAfee Creek unit is inferred to be late middle (?) Pleistocene (less than 740 to 1000 ka).

POSSIBLE INFLUENCE OF CLIMATE ON HOLOCENE ALLUVIATION AT MARBLE CREEK

The well dated series of late Holocene morphostratigraphic units and associated deposits of the Marble Creek fan contribute a perspective on the dynamics of sedimentation and erosion in the alluvial fan environment, that for the arid Basin and Range Province is in rare chronologic detail. The following is a comparison of the timing of depositional episodes on the Marble Creek fan with that of Holocene climatic fluctuations and widespread episodes of Holocene alluviation in the southwestern United States. Based on this comparison, fan-building episodes on the Marble Creek fan appear to coincident with Holocene climatic fluctuations. This suggests that Holocene climatic fluctuations have influenced alluviation in the study area and further implies similar, but more significant influences were associated with the dramatic fluctuations in Pleistocene climates.

The morphostratigraphic relations of Holocene units along Marble Creek are shown schematically in Figure 9. These relations provide a chronology of cut-fill episodes along the Marble Creek. This alluviation history is compared to the occurrence of Holocene climatic variations in the White Mountains (LaMarche, 1973), to severe droughts of the western United States (Antevs, 1955), and to glacial advances of the region (Elliott-Fisk, 1987; and Curry, 1969, 1971). A further comparison is made with stratigraphic sequences in the southwestern United States inferred to have climatic significance (Gile, 1975; Haynes, 1965).

This comparison shows general to close temporal agreement between the occurrence of cut-fill episodes at Marble Creek, regional Holocene climatic fluctuations, and severe droughts and climatically influenced Holocene depositional events of the western United States. Alluviation on the Marble Creek fan is apparently initiated by changes to more arid and/or warmer climatic conditions (discussed in a following section).

DESCRIPTION OF CUT-FILL EPISODES

Three late Holocene cut-fill episodes and one mid-Holocene to latest-Pleistocene episode are suggested from stratigraphic relations along the Marble Creek fanhead trench (Fig. 9). Two cut-fill episodes are indicated at Radiocarbon Site 2 and a third at Radiocarbon Site 1. Collectively, the relations suggest a minimum of six debris flows along Marble Creek fan in 2300 years, or an average of at least one every 380 years. This rate is consistent with a 300 year recurrence of debris flows estimated by Beaty (1960) for White Mountain canyons, in general, and with the 300 year repeat time determined by Filipov (1986) for drainages on the west side of the range.

Figure 9 shows schematically the composite morphostratigraphic relations of cut-fill alluvial assemblages along the Marble Creek fanhead trench in the general vicinity of Radiocarbon Site 2. Incision associated with the first cut-fill episode initiated after surfaces of Leidy age began to form geomorphically stable sites, or sometime before about 2400 yr B.P. The early Marble fill-assemblage was deposited after about 2300 yr B.P., and before about 1600 yr B.P. The second cut-fill episode was associated with construction and isolation (incision) of middle Marble surfaces and ceased about 1000 yr B.P. A hiatus in deposition (i.e., a period of incision) occurred between construction of middle Marble surfaces and initiation of the latest cut-fill episode that began before about 700 yr B.P. This latest episode was interrupted by a depositional hiatus and associated incipient soil development (buried soil below late Marble surface, Fig. 9; Appendix II, Pedon 4), between about 600 and 150 years ago. The latest phase of the third depositional episode resulted in construction of late Marble surfaces and probably is ongoing.

POSSIBLE CLIMATIC INFLUENCES ON ALLUVIATION

Holocene climate variations may have significantly and repeatedly influenced the processes of erosion and deposition within the Marble Creek drainage-fan system. The influence of climate on sedimentation and erosion was postulated, near the turn of this century, by Huntington (1907, p. 358 & 359) who stated:

> "In arid regions during a moist epoch... the processes of weathering are more active...than in a dry epoch. Moreover, the moisture causes vegetation to flourish to a degree impossible under drier conditions. The vegetation holds the new-formed soil in place... If the moist epoch last long, the mountains...become well shrouded with rock waste. On the advent of a dry epoch... part of the vegetation disappears; and the contrast between dry seasons and wet seasons is more marked than formerly...The soil on the mountains is no longer protected by roots and leaves, and is exposed at intervals to violent erosion, because rain runs off quickly, now that the protecting cover of plants is removed. The rock waste mantling the slopes is washed down into the valleys, and accumulates there because the heavily loaded stream can not carry it all away. In the course of time the slopes are stripped of loose material, or else the climate again becomes moist and vegetation becomes abundant. In either case the load of the stream is less heavy than formerly, and rivers begin to dissect the deposits on top of which they have hitherto been flowing. Thus, apparently a ['fill'] terrace is formed; and a repetition of the process gives rise to a series..."

Similar models of climatic influences on alluviation in the southwestern United States have been proposed by several subsequent investigators (e.g., Metcalf, 1967 and 1969; Hooke, 1972, p.2094; Bull, 1979; Bull and Schick, 1979; Gile, 1975, p. 544; Gile and others, 1981; Taylor, 1986; Wells and McFadden, 1987; this chapter).

Huntington (1907) proposed that mountain streams respond to the onset of drier climatic conditions by eroding and eventually stripping rock waste from adjacent slopes. The result is that the stream channel first aggrades with the increased supply of colluvial materials, but as rock waste mantling slopes diminishes so does the supply. The stream then responds by dissecting the valley fill deposits on which it flows.

Bull and Schick (1979) suggested that a change from a semiarid to a drier and/or warmer early Holocene climate resulted in stripping of late Pleistocene colluvium from valley slopes. Valley alluviation occurred until the slopes were completely stripped and sediment yields declined, causing entrenchment of the valley fill.

Bull and Knuepfer (1987) suggested that with the onset of aridity, sediment yield from hillsides increases and the piedmont reach of drainages aggrades. With the return of moister conditions sediment decreases and entrenchment of piedmont reaches results.

In drainage-fan systems, like that of Marble Creek, periods of valley fill incision correspond to episodes of fan building. It is likely that periods of fan building lag somewhat behind the actual change to drier conditions however. Incision of the fan occurs when vegetation again stabilizes the mountain slopes, or when both the slopes and the valley are striped of colluvium. This cycle of deposition and incision in response to climatic changes results in the formation of sequences of inset fans. If correct, and inset fan formed in this manner is genetically related to a change to greater aridity. This hypothesis is evaluated by comparing the occurrence of cut-fill episodes on the Marble Creek fan with the timing of local and regional climatic variations in the following section.

HOLOCENE CLIMATIC VARIATIONS

Local Climatic Variations

LaMarche (1973) inferred variations in Holocene climate from fluctuations in the position of the upper treeline of Bristlecone pines (Pinus longaeva Bailey) at high elevations in the White Mountains; located about 25 km south of the Plate I area. The elevation of the upper treeline has been shown by experimental and empirical evidence to be closely related to warm-season temperatures, but its response probably lags behind the climatic fluctuation (LaMarche, 1973). LaMarche dated treeline fluctuations by tree-ring and radiocarbon analyses of standing snags and fallen logs above the present position of the upper treeline. LaMarche's inferred climatic variations are shown in a graphical comparison with Marble Creek depositional episodes in Figure 13.

LaMarche (1973) indicated that at least until about 4000 yr B.P. the regional climate was characterized by "unusual summer warmth." During the period from 4000 to about 900 yr B.P. climatic conditions were drier and cooler than during the preceding several thousand years. A lowering of the tree-line position after about 2500 yr B.P. may have been a response to drier and cooler conditions. An abrupt drop in treeline position after 900 yr B.P. suggests a response to either much colder summers, or to fairly cold summers and generally drier annual conditions. Similar conditions have prevailed until recently (LaMarche, 1973).

There appears to be a close temporal correlation between the cut-fill episodes at Marble Creek and LaMarche's climatic variations (Fig. 13). The first of the three late Holocene cut-fill episodes (early Marble) along Marble Creek began before about 2400 yr B.P., and may have coincided with LaMarche's transition from

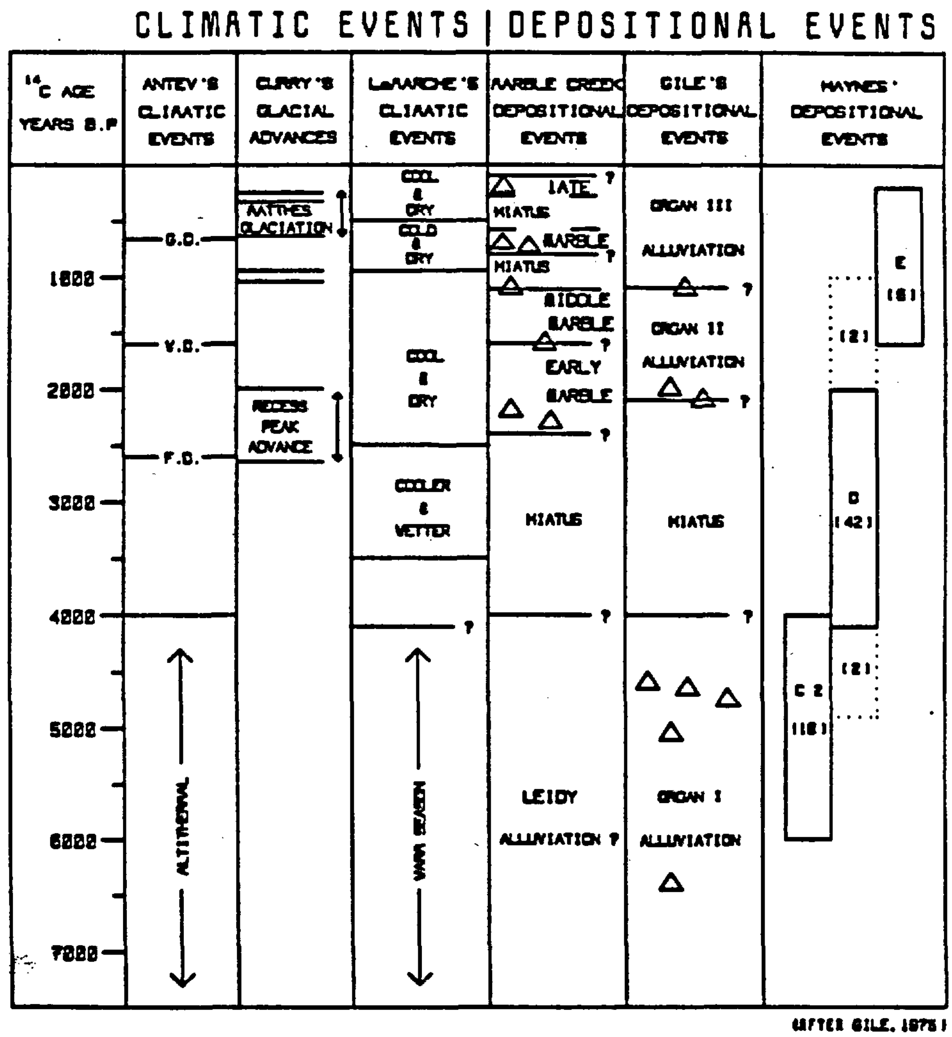

Figure 13. A comparison of depositional episodes at Marble Creek with climatic events and periods of alluviation in the southwestern United States, which have occurred during the Holocene.

a period of "cooler and wetter" to a period of "cool and dry" conditions, at about 2500 years ago. The second cut-fill episode (middle Marble), that began about 1600 yr B.P. and ceased about 1000 yr B.P., is coincident with the later part of LaMarche's "cool and dry" period that ended about 1000 yr B.P. The third cut-fill episode (late Marble) began before or at about 700 yr B.P. and thus closely follows LaMarche's transition to a period of "cold and dry" conditions at about 900 yr B.P. (Fig. 8).

Severe Droughts

Episodes of Holocene alluviation on the Marble Creek fan also appear to correlate closely with the onset of Antevs' (1955) severe droughts in the western United States (Fig. 13). The onset of the early Marble depositional episode (before or at about 2400 yr B.P.) closely followed Antevs' "Fairbank Drought," at about 2600 yr B.P. Furthermore, the onset of the middle Marble depositional episode (about 1600 yr B.P.) essentially matches that of the "Whitewater Drought," at about 1600 yr B.P. Remarkably, another drought from 675 to 650 yr B.P. appears to coincide with the onset of the late Marble depositional event (around 700 yr B.P.). The close temporal-occurrence of severe droughts in the southwestern United States and depositional episodes on the Marble Creek fan suggest a climatic influence on alluviation.

Gile (1975) also proposed that radiocarbon dated depositional episodes, in southern New Mexico, were influenced by Antevs' (1955) Holocene droughts. However, the relationship between depositional episodes and severe droughts of Antevs' is even more convincing in the present study than that of Gile (cf., Fig. 13).

Glacial Advances

Glacial advances during the Holocene also appear to have influenced alluviation on the Marble Creek fan. Bryan and Ray (1940) argued that mountain streams are heavily loaded during glacial advances and therefore aggrade their channels. Bryan and Ray further suggested that during deglaciation streams dissect their alluviated channels, due to a larger volume of water and decreased sediment load. This invites the speculation that the Indian and McAfee Creek units, which occur most extensively at the mouths of formally glaciated canyons, are genetically associated with waning middle and late Pleistocene glacial periods. Such speculation however is only supported by circumstantial evidence.

It follows that glacial periods correspond to intervals of little or no fan deposition, hence to intervals of landscape stability. Furthermore, waning of glacial periods corresponds to episodes of fan building. The above effects probably influence nonglaciated drainages of the region, but to a lesser degree. The Leidy depositional episode along Marble Creek therefore, may correspond to waning of the latest Pleistocene glaciation in the region, between about 18 and 12.5 ka (Elliott-Fisk, 1987).

Curry (1969) studied Holocene glacial deposits in the central Sierra Nevada, California, and approximately dated the deposits by several techniques including radiocarbon, lichenometry, palynology, variation in tree rings, and timberline position. Curry concluded that at least four periods of multiple glacial advances have occurred in the Sierra Nevada during the last 10,000 years.

Three of Curry's (1969) glacial advances appear to coincide temporally to periods of nondeposition on the Marble Creek fan (Fig. 13). The Recess Peak Advance, that tentatively occurred between about 2000 and 2600 years ago, possibly coincided with the depositional hiatus between the early Marble and Leidy depositional episodes (from 2300 to 4000? yr B.P.). Another multiple advance around a 1000 years ago appears to have coincided with the hiatus separating the middle Marble episode (from about 1600 to 1000 yr B.P.) from the late Marble episode (after 700 yr B.P.). A third advance, the Matthes glaciation (Birman, 1964), occurred between 650 and 300 years ago (Curry, 1969), and closely coincides with the depositional hiatus that occurred during the late Marble episode, between about 600 and 150 yr B.P.

The close agreement between the timing of glacial advances in the Sierra Nevada and depositional hiatuses on the Marble Creek fan suggest that the former influences the latter (i.e., a genetic relationship).

COMPARISON WITH OTHER DEPOSITIONAL SEQUENCES

The chronology of depositional events at Marble Creek, based primarily on radiocarbon dated deposits, agrees closely with that demonstrated for radiocarbon dated depositional events in the southwestern United States that Gile (1975) and Haynes (1965) postulate were climatically influenced (Fig. 13).

The Leidy depositional episode is inferred to have coincided with the Organ I depositional event of Gile (1975) and the "C2" event of Haynes (1965)(Fig. 13). The early and middle Marble depositional episodes appear to coincide with the Organ II event of Gile (1975). The late Marble depositional episode corresponds closely with Gile's Organ III event, and generally with the "E" event of Haynes (1965). However, there is no equivalent to Haynes' "D" unit in the present study, nor that of Giles.

The coincidence between depositional events at Marble Creek and those of Gile (1975) and Haynes (1965) further support a climatic influence on alluviation at Marble Creek.

DISCUSSION OF CLIMATIC INFLUENCES

The rather remarkable coincidence between the onset of depositional episodes on the Marble Creek fan and those elsewhere in the southwestern United States (Gile, 1975; Haynes, 1965), and with the occurrence of climatic fluctuations (LaMarche, 1973) and severe droughts (Anteves, 1955), strongly supports Holocene alluviation during periods of drier climatic conditions. Further supporting evidence, and equally remarkable, is the coincidence between periods of fan stability and glacial advances (Curry 1969, 1971). These similarities suggest that Holocene climatic fluctuations have significantly influenced alluviation in the Fish Lake Valley region.

The Marble Creek drainage system is apparently sensitive to climatic influences on alluviation and erosion, owing largely to the nonglacial physiography of its mountain canyon. There are few sites on the steep walls of the V-shaped Marble Creek canyon for residence of colluvial materials (Fig. 5). During intervals of greater slope instability (i.e., greater aridity) colluvium accumulates on the bedrock-floored channel. Subsequent dissection of the canyon fill, perhaps associated with stripping of rock waste from adjacent slopes or with waning glacial periods, results in depositional episodes on the Marble Creek fan. Dissection of the fan deposits is related to isolation and stabilization of geomorphic surfaces, from which morphostratigraphic units form.

If the depositional episodes at Marble Creek are genetically associated with Holocene climate changes - as suggested in the present study - then it is possible that the Leidy depositional event was also influenced by a climatic change. In which case the Altithermal period (4000 to 7500 yr B.P.) of Antevs (1955), that apparently corresponds to LaMarche's (1973) "warm season" (between about 4000 and 8300 yr B.P.), is a candidate. However, it is possible that the Leidy depositional event coincided with waning of the latest Pleistocene glaciation, by about 12,500 yr B.P. (Elliott-Fisk, 1987).

The Leidy depositional event appears to be coincident with either the Altithermal period (4000 to 7,500 yr B.P.) or the transition from full-glacial to inter-glacial at the Pleistocene/Holocene boundary (12,500 to 18,000 yr B.P.). Of these two scenarios the latter is currently preferred. The preference is based on comparing soil properties (Appendix II) and general morphostratigraphic characteristics of the Leidy unit with those of the early Marble unit (Table 1).

The relatively minor Holocene climatic changes of the region have apparently resulted in complex and multiple interactions between erosion and sedimentation throughout an entire drainage-fan system. Hence, much greater effects may be expected from the marked climatic changes of the Pleistocene.

It is therefore tempting to speculate (as was done in the previous section) that the Indian and McAfee Creek depositional episodes - which are apparently regionally correlative (based on collaborative studies between M.C. Reheis and J. Slate and the author) and occur most extensively in drainage-fan systems that experienced Pleistocene glaciations - were influenced by climatic change, perhaps characterized by a change from glacial to interglacial in a manner similar to that described by Bryan and Ray (1940).

DISTRIBUTION OF MORPHOSTRATIGRAPHIC UNITS

Morphostratigraphic units of all ages occupy specific positions in the regional landscape of the study area. The oldest units, which retain little, if any, of their relict surface morphology, are extensive along the eastern front of the White Mountains. These Pleistocene units are commonly entrenched by drainageways, thus providing channelized reaches across the upper-fan through which debris is transported to the mid- and lower-fan. The alluvial debris, including that reworked from older units, forms a mosaic of equitant Holocene deposits, valleyward of the Pleistocene units.

A series of Holocene units, characterized by well-preserved depositional morphology (e.g., levees and swale microtopography), have formed within the mid- to lower-fan sedimentary mosaics. The Holocene units also form on inset fan remnants within many fanhead trenches and below high standing Pleistocene interfluves. Within the interfan valley, north of the Marble Creek fan, Holocene units (Leidy and younger) are extensive, whereas Pleistocene units are absent (Plate I).

The most notable departure from the above described distribution pattern of morphostratigraphic units - i.e., where older units fringe the range front and younger units form valleyward - is shown by the late Pleistocene Indian unit, on the southern Indian Creek fan (Plate I). The Indian unit occupies an alluvial fan remnant that extends from the fanhead to nearly the valley floor. This fan remnant is displaced in a right-divergent style along the master fault of the FLVFZ, as suggested by an offset drainage channel (discussed in Chapter VI). Hence, the rather unusual position of the Indian unit probably result from lateral translation and therefore removal from an otherwise inevitable fate of burial by Holocene sediment.

Morphostratigraphic relations observed in the field show that older units have steeper longitudinal gradients than younger units, and form the highest remnants within fanhead trenches. Units of all ages converge downfan and coalesce where older units are buried by younger units. These observations indicate that the loci of deposition has varied both temporally and spatially. That is, with time, depositional loci have migrated downfan. Furthermore, the stepped sequences within the fanhead trenches suggest episodic, rather than gradual, shifts in depositional loci; since stepped sequences reflect several intervals of regional instability with subsequent periods of aggradation (Gile and others, 1981; Lustig, 1965; previous section).

POSSIBLE INFLUENCES ON THE DISTRIBUTION OF MORPHOSTRATIGRAPHIC UNITS

Determining the causative factor(s) for the distribution and downstream convergence of morphostratigraphic units in the study area is largely problematic. Most likely, there are several independent factors. The influence of each is superposed and is reflected in the distribution of the units. The three causative factors deemed most significant, are discussed below.

Commonly cited factors affecting erosion and sedimentation on alluvial fans in the southwestern United States include climatic fluctuations (e.g., Eckis, 1928, p. 237; Davis, 1938, p. 1349; Blissenbach, 1954; Lustig, 1965; Bull, 1961, 1964; Cooke and Warren, 1973; Wasson, 1977; Bull and Schick, 1979; Christenson and Purcell, 1985; Gile and others, 1981; Hawley, 1980; and Harden and others, 1985), tectonic perturbations (Beaty, 1961; Denny, 1965, 1967; Hooke, 1967, 1972; Bull, 1961, 1964, 1977; and Christenson and Purcell, 1985), and baselevel changes (Eckis, 1928; Ruhe, 1964; Bull, 1964; and Harden and others, 1985). The following subsections comprise an introductory discussion of each of the three factors.

Virtually all alluvial fans in Fish Lake Valley have fanheads that are older and dissected to a greater degree than lower fan positions. This pattern occurs in the Death Valley region (Beaty, 1961; Denny, 1965, 1967; Hunt and Mabey, 1966; Hooke,1967; Lustig, 1965; personal observation) and throughout the Basin and Range Province (Peterson, 1981; Christenson and Purcell, 1985). As pointed out by Lustig (1965) the widespread occurrence of fans having similar characteristics requires a regional explanation. This has lead some investigators (e.g., Royse and Barsch, 1971) to discount the influence of tectonic perturbations and to advocate that of climatic fluctuations (e.g., Hawley, 1980).

Influence of Climate Fluctuations

The possible influence of climate change on erosion and sedimentation of alluvial fans is summarized here. As previously discussed, a change to greater aridity results in a decrease in production of vegetation. This has the effect of increasing runoff and rates of erosion on formally vegetation-stabilized slopes of the catchment area. Colluvial materials derived from the destabilized slopes accumulates on the canyon floor, where this material is transported to the fan primarily by debris flows. Thus, in this manner a change to aridity corresponds to an episode of fan-building (alluviation).

A subsequent climate change to moister conditions would increase production of vegetation, thereby decreasing erosion rates and sediment supply to the fans. With greater moisture and less stream load entrenchment of the alluvial fans results. Hence, declines in sediment yield to the fan coincide with the onset of moister conditions. Such a change could therefore influence dissection of alluvial fan and the downfan migration of the loci of deposition.

Lustig (1965) studied the alluvial fans of Deep Springs Valley and several fans in the surrounding valleys, including those in Fish Lake Valley. Lustig noted several features that are characteristic of fans in this region. Such as prominent fanhead trenches, downfan shifts in the loci of deposition to midfan positions, and terraces that are continuous with downstream fan surfaces. Lustig suggested that these similarities result from climatic change.

Influence of Tectonic Perturbations

A tectonic explanation for the widespread similarities among alluvial fans in the Fish Lake Valley and Death Valley region has been discounted by Lustig (1965) as it requires nearly simultaneous tectonic uplift of the region. However, the major structural blocks of this region experienced latest Cenozoic (last 3 to 4 Ma) uplift and tilt (Knopf, 1918; Axelrod, 1950, 1957; Bateman and others, 1965; Gilbert and others, 1968; Robinson and others, 1968; Moiola, 1969; Noble, 1972; Bachman, 1978; Stewart, 1980) that continued into the Holocene (Hunt and Mabey, 1966; Hooke, 1972; dePolo, 1989; Chapter VI) and can be anticipated in the future

(Chapters VIII and IX). Hence, tectonic perturbations may account for the widespread occurrence of similar alluvial fans in the region.

The influence of tectonic perturbations on dissection and deposition of alluvial fans generally stem from differential vertical displacement, tectonic tilting, or both. These tectonic perturbations and their associated influences are summarized in the following sub-sections.

Differential Vertical Movements: Uplift of a catchment area relative to an alluvial fan, along a range-bounding fault, results in nongraded drainage-fan systems. Within catchment areas stream gradients and flow velocities increase as a result of uplift. This accelerates erosion and entrenchment of the mountain canyon. On the downdropped alluvial fan the stream responds by aggrading. Simultaneous erosion of the catchment area and deposition on the fan will, in time, reestablish a graded profile.

There are many examples in the study area of intermittent vertical displacements on intra-piedmont faults (i.e., non-range bounding faults). Drainages traversed by these faults respond to the vertical component of displacement by dissection of the footwall and, concurrently, deposition on the hangingwall. Thus, reestablishing a graded profile, and in the process forming paired-fan remnants and alinements of alluvial fanlette apices.

Blackwelder (1934) reached the inescapable conclusion (author's opinion) that vertical displacement on the FLVFZ (i.e., the Dyer sub-zone) has resulted in prominent entrenchment of the Perry Aiken Creek fan. A conclusion also reached by Bryson (1937).

Tectonic Tilting: Tectonic tilting can produce or enhance many features that are characteristic of the alluvial fans in the study area. Hunt and Mabey (1966), Hooke (1972) and Denny (1965) described fans flanking the Panamint Range with similar characteristics. They suggested the character of these fans were strongly influenced by eastward tilt of the Panamint structural block.

Hunt and Mabey (1966, p.A100, A105 & A106) suggested the eastern shoreline of a Recent lake in Death Valley, dated by archaeological means at about 2000 yr B.P. (p. A79), is 20 ft (6 m) lower than the correlative shoreline on the west side; with about half of the differential displacement occurring along a scarp at the foot of the Black Mountains. Hunt and Mabey (p. A105) also suggested that a Lake Manly - upper Pleistocene pluvial lake - shoreline is tilted 200 ft (60 m) down to the east and 300 ft (90 m) to the north, however correlation of the shoreline is uncertain.

Hunt and Mabey (1966, p. A87, A106) compared the morphology of alluvial fans on the west side of Death Valley at the foot of the Black Mountains, with those on the east side at the foot of the Panamint Range. They observed that east side fans are small relative to west side fans that are longer and higher. Hunt and Mabey suggested that these differences result from eastward tilting of the valley during Pleistocene to Recent time.

Hooke (1972) noted that the youngest fan gravels were near the fanhead on the east side of Death Valley, but always near the fantoe on the west side. This pattern of erosion and deposition results from eastward tilt of the Death Valley-Panamint Range structural block (Hooke, 1972).

Denny (1965) suggested that fans on the east side of Death Valley are small relative to their source area. This relationship results from eastward tilt of the valley floor, associated with vertical displacement on the central Death Valley fault zone (Denny, 1965).

The pattern of fanhead entrenchment, downfan convergence of fan surfaces and advancement of fantoes along the east side of the White Mountains are similar to fans influenced by tectonic tilting on the west side of Death Valley (c.f. Denny, 1965; Hunt and Mabey, 1966; Hooke, 1972). It is probable that eastward tilt of the White Mountains and Fish Lake Valley structural blocks produced or enhanced the morphology of fans along the eastern flank of the range.

Several characteristics of alluvial fans along the western side of the White Mountains (c.f. Beaty, 1960, 1968) in Owens Valley are similar to those along the west side of the Black Mountains in Death Valley (c.f. Hunt and Mabey, 1966; Hooke, 1972). A similar comparison can be made between alluvial fans along the east side of the White Mountains (this study) and those along the east side of the Panamint Range (c.f. Denny, 1965; Hunt and Mabey, 1966; Hooke, 1972). The similarities between fans flanking the White Mountains and those in Death Valley, and the differences between the fans on either side of the range, suggest that eastward tilt of the White Mountains structural block (discussed in Chapter III) has influenced alluvial fans of the study area.

Influence of non-tectonic Base Level Changes

Both regional and local (non-tectonic) baselevel changes may affect erosion and sedimentation of alluvial fans (Bull, 1964, p. 99). Ruhe (1964, p. 157) suggested that differences in the gradients of fan surfaces near Las Cruces, New Mexico, indicate the baselevel to which these surfaces were graded varied in elevation. Harden and others (1985) suggested that downstream convergence of terrace gradients on alluvial fans in southeastern Utah could result from valley subsidence.

Fish Lake Valley is essentially a closed basin or bolson that has very nearly reached its "spill-point". Actually, at either end of the valley external drainage does occurs, but has not significantly impacted the physiography of the basin. Hence, base level changes for drainages in the study area are probably negligible.

The late Pleistocene to latest-Holocene fan surfaces, in northwestern Fish Lake Valley, graded to similar baselevels (i.e., roughly that of the present bolson floor). This suggests little or no baselevel change is required.

Significance of Possible Influences

The above relations suggest that baselevel changes during the late Quaternary did not significantly influence alluvial fans in the study area. Hence, such changes apparently do not account for the characteristic morphology of alluvial fans flanking the eastern White Mountains.

Undoubtedly, both tectonic perturbations and climate changes have influenced the alluvial fans of the study area. Ascertaining their relative significance however, is somewhat more difficult. The difficulty stems from recognizing and isolating the prospective influences of these two factors.

The influence of tectonic activity on alluvial fans of the area of study is clearly shown by prominent fault scarps and uplifted and tilted, small-scale fault blocks. The proximity of morphostratigraphic unit boundaries, mouths of onfan drainageways, and alinement of fanlette apices along known faults (Plate I) also suggest a tectonic influence. The upstream proximity of both prominently displayed stepped sequences and fanhead trenches to the FLVFZ further suggests influence by vertical tectonism.

Recurrent vertical displacement on the FLVFZ has resulted in relative uplift and dissection of the older units fringing the eastern front of the White Mountains. The tectonic activity also enhances the preservation of these older map units (e.g., Indian and McAfee Creek units) by isolating them from active drainages. As a consequence of uplift, depositional loci have shifted downfan, hence, restricting younger units to lower fan positions.

Bull (1964a and 1968) suggested that thick (greater than 100 m) alluvial fans, such as the Indian Creek and Leidy Creek fans, represent orogenic deposits, not climatically related deposits (Bull and McFadden, 1973; Bull, 1977). This also suggests a tectonic influence on the fans of the study area.

Lateral displacement on the right-divergent FLVFZ has also influenced fans traversed by the fault. For example, the Indian unit of the southern Indian Creek fan has been translated southeastward along the master fault of the FLVFZ (Chapter VI). Lateral translation of the Indian unit is also shown on the northern Leidy Creek fan (Chapter VI).

Eastward tilting of the White Mountains and Fish Lake valley structural blocks could result in fanhead dissection, downfan migration of depositional loci, and downstream convergence of fan surfaces bordering the valley on the west. Alluvial fans bordering Death Valley on the west exhibit similar features and are tilted (Denny, 1965; Hunt and Mabey, 1966; Hooke, 1972). The differences between fans on either side on the White Mountains (discussed previously) can also be accounted for by tectonic tilting. The White Mountains and apparently Fish Lake Valley structural blocks were tilted eastward, thus influencing alluvial fan of the study area.

Locally, the influence of tilting is shown by the patten of erosion and sedimentation on the lower Indian Creek fan. One, or more, small-scale fault blocks have apparently been tilted eastward, resulting in dissection and deposition on the up-tilted and down-tilted ends of the block, respectively. Hence, providing a small-scale example of the types of influences that probably have occurred regionally.

The influence of Holocene climate change on alluvial fans of the study area is apparently significant (discussed in previous sections). It is therefore likely that marked changes in Pleistocene climatic conditions prominently influenced construction and dissection of these fans as well. The pervasive tectonic overprint on the morphology of the fans, however, makes assessing the influence of climate change more difficult.

In an effort to isolate possible climatic influences from tectonic influences, the Marble Creek drainage-fan system is compared to that of Indian Creek, as follows. The influence of tectonic perturbations is roughly similar for both drainage-fan systems, but climatic influence differs importantly. The Marble Creek drainage was not glaciated during the Pleistocene, as is evident from the narrow, V-shaped morphology (Fig. 5) of its bedrock floored canyon. Indian Creek, in stark contrast, was repeatedly glaciated during the Pleistocene (e.g., LaMarche, 1965; Elliott-Fisk, 1987). The Indian Creek canyon is several times larger than that of Marble Creek, and is broad, stepped, and deeply alluviated. Indian Creek and apparently Marble Creek have incised their prospective mountain canyons since the basalts of Davis Mountain were extruded (about 3.0 to 3.9 ± 0.1 Ma, M.C. Reheis, USGS, personal commun., 1989). Incision of the canyons is due, in part, to longterm uplift and eastward tilt of the White Mountains. The Marble Creek canyon is floored by bedrock, whereas the Indian Creek canyon is deeply alluviated. Hence, Marble Creek continues to downcut while Indian Creek flows on valley-fill debris. This difference suggests the influence of climate is greater on the Indian Creek drainage-fan system than on that of Marble Creek. Further, that erosion associated with glacial periods exceeds that in response to uplift.

This conclusion is supported by features of the Chiatovich Creek and Middle Creek alluvial fans, northwest of the area of study. Entrenchment of the upper reaches of these fans occurred largely independent of faulting. Both of their drainages were glaciated during Pleistocene time (LaMarche, 1965; Elliott-Fisk, 1987). This suggests that climatic changes significantly influenced the morphology of these alluvial fans.

In summary, the widespread occurrence of alluvial fans having similar morphological features is attributed to tectonic perturbation (i.e., both uplift and tilt - in order of probable importance) and to Quaternary climatic changes. The relative importance of these two influences is uncertain. Finally, late Pleistocene baselevel changes are likely to have been minor and probably had little or no influence.

CHAPTER V
EVALUATION OF SOIL DEVELOPMENT

INTRODUCTION

Pedogenic soils were described to an average depth of 170 cm in hand-dug soil pits at the various numerical age control sites (described in Chapter IV) and elsewhere in the Plate I area. The soils were described according to methods and nomenclature of the Soil Survey Staff (USDA, 1951), that were subsequently partially revised (USDA, 1981, p. 39-49 & 105-107). The morphology of pedogenic carbonate was described following the classification scheme of Gile and others (1965, 1966), and Taylor's (1986) scheme was used for that of pedogenic silica. Soil field descriptions (Appendix II) are evaluated using soil development indices developed by Harden (1982) and Harden and Taylor (1983). Taylor's (1988) computer template, executed by LOTUS 123™, was used for compilation of soil indices (Appendix III).

Radiocarbon and preliminary tephrochronologic ages are used to date soils at the various numerical age determination sites. The dated soils, which are members of the regional chronosequence (described in next section), provide a means of chronologically calibrating the various soil development indices. The soil indices in turn provide a means of extrapolating age data. That is, a soil (and many of its properties) described where numerical age control is lacking can be compared by soil indices to dated soils (i.e., those described at numerical age control sites). Thereby, estimating a rough numerical age for the soil (morphostratigraphic unit).

Each morphostratigraphic unit has only one soil component, with an allowable degree of variation (described in Chapter IV). Therefore, morphostratigraphic relations and surface weathering characteristics serve not only as the basic tool for predicting the distribution of the units, but also their associated soils. Since, soil patterns commonly coincide with landform patterns (Peterson, 1981, p. 1; Ruhe, 1974) this application of morphostratigraphic units is feasible, further its practical.

DESCRIPTION OF CHRONOSEQUENCE

DEFINITION OF CHRONOSEQUENCE

The sequence of soils associated with morphostratigraphic units constitute a chronosequence. Jenny (1941, 1946, 1961) defined a chronosequence as a series of related soils in an arrangement, such that one differs from another primarily as a result of the soil-forming factor, time. For clarity and convenience, Jenny (1941, 1946) expressed the soil state as a mathematical relationship, involving at least five soil-forming factors. Jenny's equation is expressed as follows:

$$S = f(cl, o, r, p, t, \ldots)$$

Jenny (1946) expressed individual soil properties (s) as a function of the genetic soil forming factors, where:

$$s = f(cl, o, r, p, t, \ldots)$$

The soil (S), or soil property (s), is the dependent variable, and soil forming factors (cl, o, r, p, t,...) are independent variables. The two most important aspects of the environmental climate (cl) are temperature and annual precipitation (Birkeland, 1984, p. 275). The soil-forming factor, organism (o), refers to the kinds and frequency of species of vegetation and animals (Jenny, 1946, p. 375) in the surrounding region. Relief (r) is the topography, morphology, and hydrologic character of the area (Jenny, 1946, p. 375). The parent material (p) is the state of the soil at its inception (Jenny, 1946). Time (t), as a soil-forming factor, is the interval during which the parent material has been, or was, exposed at the surface (Birkeland, 1984, p. 164), and thereby subjected to pedogenic processes. Genetic soil-forming factors of the soil description sites are shown in Table 4.

Soils are directly related to time, under the condition that all other factors (cl, o, r, p, ...) are constant (Jenny, 1941). Jenny expressed such conditions mathematically as a chronofunction, where:

$$S = f(t)\ cl, o, r, p, \ldots$$

Jenny (1946) pointed out that under field conditions it is extremely difficult to satisfy the requirement of constancy. However, within a given area, for single-factor functions such as chronofunctions, this requirement may be relaxed (Jenny, 1946, p. 376) provided one of the following two conditions is satisfied. Either the variance of one factor (e.g., time) greatly exceeded the variance of the other factors; or (2) one or more factors varied considerably, but only one (e.g., time) is important in determining differences in soil properties. Jenny (1946) suggested that these circumstances are frequently obtained in under field conditions.

It is perhaps fortuitous in chronosequence analyses that the variance of time is always unidirectional and constant. The same cannot be said of any other genetic factors. Hence, soil properties related to time should ideally be enhanced, and thus dominate those properties that are related to randomly varying factors.

This argument can be likened to a photograph of Grand Central Station, in New York City. The exposure time for the photograph was several hours. During that time thousands of people passed in front of the cameras lens. Since their positions were random in space and time, their images were not recorded. The interior structure of the building was recorded however, because its position remained constant.

Time-dependent soil properties are enhanced in an analogous manner to the buildings interior structure. Whereas properties related to randomly varying factors are not enhanced (at least not to the same degree), similar to the images of the passers-by.

REQUISITES OF PEDON DESCRIPTION SITES

Soil-forming factors make up a complex multi-component system that is amenable to chronofunction analyses only when pedon (i.e., a body of soil that includes representative variations, USDA, 1975, p. 5) description sites are selected with considerable care. In this study, each pedon description site conforms to a

TABLE 4: CRITERIA FOR GENETIC SOIL-FORMING FACTORS AT PEDON DESCRIPTION SITES

Soil-forming factors	Description of Pedon Site Requirements
Climate	Warm-mesic temperature regime[1] (mean annual temperature[2], 28 C); semi-arid moisture regime (mean annual precipitation[2] 8.2 cm [1948-57], 12.5 cm [1954-64]).
Organism	Sparse vegetation in Sagebrush Steppe (Sagebrush [Artemisia tridentata], Rabbit Brush, Grease Wood, Shadscale [Artiplex confertifolia], Spinney Hop sage), with rare juniper (Juniper utahensis) above about 1800 m.
Relief	Topographic highs; transversely level; 0-6 percent longitudinal slopes; easterly aspects; well-drained[3]; vertical range 1590-1915 m; geomorphically sle sites generally lacking evidence of erosion[4].
Parent Material	Gravelly to very gravelly sandy-loamy, poorly sorted and stratified, alluvium of primarily quartz monzonitic composition with subordinate limestone, and metasedimentry and/or volcanic fragments and fined-grained eolian? sediment; fine earth is strongly calcareous throughout.
Time (ka, epoch)	0.1 to late middle Pleistocene

[1] Schmidlin and others (1983, Fig. 2).
[2] U.S. Weather Bureau (Nevada), Annual Summary (1948-57), data from Dyer, Nevada (elevation 1520 m).
[3] The Indian and McAfee Creek soils at present are somewhat poorly drained, resulting form prominent argillic and indurated Bk and K horizons.
[4] The present McAfee Creek surface clearly exhibits evidence of soil truncation, and therefore is an exception to the requirement of geomorphic stability.

host of requirements that attempt to insure consistency among all soil-forming factors, except time. These requirements are listed in Table 4. Pedon description sites are located on geomorphically-stable, flattish remnantal landforms having gentle easterly slopes, occurring within a limited range of elevation and comprising well drained parent material.

The parent material is typically gravelly to very gravelly sandy loam in texture, calcareous throughout, and composed primarily of granitic alluvium with varying amounts of metasedimentary, limestone, and volcanic lithic fragments. Eolian sediments probably occur in all soils to some degree and are thought to be an important source of silts, very fine sand, clay, carbonate, and salts. The high carbonate content and coarse texture of the parent materials allows maximum translocation of pedogenic carbonate, as determined for example by Gile and others (1966) and Gile (1975). Hence, carbonate morphology provides relatively high temporal-resolution among the soils, thus is well suited for chronofunction analysis.

REPRESENTATIVE SOIL PROFILE CHARACTERISTICS

Soils representative of the various morphostratigraphic units were described to an average depth of 170 cm in hand-dug soil-pits and trenches. Detailed descriptions of the various pedons are shown in Appendix II and are highlighted below.

Parent materials relatively unaltered by pedogenic processes were rarely observed, owing to the rate and depth of carbonate accumulation. Thus, the total thickness of the soil profiles is only infrequently known with certainty.

LATE MARBLE SOILS

Pedon 4 and Pedon 13 illustrate soil features representative of the late Marble morphostratigraphic unit (Appendix II). The late Marble soils lack vesicular surficial horizons (Av horizons) and have only very minimal evidence of pedogenesis. The most prominent evidence of pedogenesis is an "early-Stage I" (denoted I-) horizon of very modest carbonate accumulation (Bkj). The underside of pebbles in this horizon may have "powdery", thin, discontinuous filaments of pedogenic carbonate in dendritic arrangements - as if formed along fine roots. Pedon 4 was described at Radiocarbon Site 1. The AB horizon contained several wood fragments that were collected and dated as a bulk sample at 120 cal B.P. (Beta-26169). This horizon has unusually distinct angular and subangular blocky structure, perhaps related not to pedogenesis, but to dissection of the fine-grained parent materials. These materials overly a buried soil, as suggested by organic materials apparently in growth position along the contact and by radiocarbon dates at this site.

The upper most horizon (2Bkqb horizon) of the buried soil displays thin, discontinuous carbonate coats and "flakes" of opal on pebble-bottoms. A detrital log from this horizon has a radiocarbon date of 660 cal B.P. (A-5068). Mottles of 10YR hue occur in the 2Bk2 and 2CB horizons of this pedon (Pedon 4), probably related to a periodic shallow groundwater table, since the soil-pit is close to the active channel of Marble Creek.

MIDDLE MARBLE SOILS

Pedons 1, 2, 8, and 11 illustrate characteristic pedogenic properties of the middle Marble soils (Appendix II). Both pedons 1 and 2 are at Radiocarbon Site 3. At this site a detrital log, about 50 cm below the middle Marble surface, has a radiocarbon date of 1555 cal B.P.(A-4768). Pedon 11 was described at Radiocarbon Site 4. At this site a detrital log, dated at 1065 cal B.P.(Beta-26170), was collected from the Bk2 horizon at a depth of 40-50 cm below the middle Marble surface.

The Av horizon of these pedons is thin (3 to 5 cm thick), light colored (2.5Y6.5 to 8/2, dry), sandy loam to sandy textured, and forms a crust with coarse vesicular pores. The Av horizons are present only between coppice dunes, where an incipient concentration of lithic fragments or proto-pavements occur. The Stage I Bk horizons are prominent and have continuous (or nearly so), thin, powdery carbonate coatings on the underside of pebbles and cobbles. Carbonate is only very rarely observed as nodules within the fine-grained matrix of the parent material of these horizons. Stage I opal accumulations, in the Bkq horizons of Pedons 1, 2, and 8, have discontinuous thin coatings on the underside of pebbles. The middle Marble pedons are strongly calcareous throughout, regardless of the coarse lithic constituents of the parent materials.

EARLY MARBLE SOILS

Soil characteristics of the early Marble soils are shown by Pedons 3 and 9 (Appendix II). These pedons display prominently vesicular Av horizons that have sandy loam textures, and a massive upper sub-horizon and a weakly platy lower sub-horizon. Near the base of the Av horizons, weak Stage I carbonate morphology infrequently occurs between platy peds. The relative abundance of silt and very fine sand, and the slightly sticky wet consistence of these horizons is largely attributed to the accumulation and infiltration of fine-grained eolian sediment.

The Bw horizons of Pedons 3 and 9 have subangular blocky structure and negligible illuvial accumulations of carbonate (Stage I-) and opal (Stage I-). The underlying Bk horizons contain significantly more carbonate and therefore serve as evidence of chemical alteration (i.e., eluviation of carbonate) of the Bw horizons. Thus, the Bw horizon of Pedon 9 is a cambic horizon and that of Pedon 3 a cambic-like horizon; since it does not meet the 25 cm depth requirement for the base of the horizon (USDA, 1975). The upper Bk horizons of early Marble soils have Stage I carbonate and opal accumulations coatings on pebble-bottoms. Prominent "late-Stage I" (I+) to early Stage II (II-) carbonate coats occur as botryoidal to stalactite-like pendants on pebble-bottoms in the Bk1 horizon of Pedon 9. This, suggests that opal (silica) constitutes a significant part of the coatings (Taylor, 1980; M.C. Reheis, 1987, personal commun.), probably Stage II (II-) opal accumulation.

LEIDY SOILS

Pedon 6 and Pedon 10 illustrate Leidy soils, below loosely packed, weakly to moderately sorted, desert pavements (pavettes). The mid-Holocene to latest-Pleistocene Leidy soils are the youngest within the area studied to have clear evidence of silicate clay translocation (e.g., clay films). Both pedons have weak Bt horizons, however probably are not argillic horizons, and have common, thin bridges of pedogenic clay between mineral grains and a few thin films on pores. The Bt horizons have little or no reaction when treated with dilute HCl, suggesting that they are leached of carbonate. Similar accumulations of clay in Leidy soils were observed in several shallow "test-pits." Thus, the presence of a weak Bt horizon is an apparently reliable indicator for distinguishing soils of Leidy age from all those younger.

The most prominent pedogenic features of the Leidy soils is not the Bt horizons however, but the Stage II Bk horizons. Moderately thick, continuous carbonate coats (Stage II) with stalactite-like pendants (i.e., Stage II opal) occur in the upper Bk horizons. Thus, Leidy soils are also the youngest soils to display rather prominent Stage II carbonate morphology. This contributes to the uniqueness of the Leidy soils. Carbonate also forms small, weakly cemented nodules and lenses within the interstitial fine-earth materials in the B horizons of these soils. Carbonate Stage I, Bk horizons were observed at the base of the soil pits (185 and 205 cm for Pedons 6 and 10, respectively).

Leidy soils exhibit moderately thick, very-slightly-sticky Av horizons that form massive, prominent crusts in their upper sub-horizon and medium to coarse, distinctly platy structure in the lower sub-horizon. Av horizons were not observed beneath coppice dunes, perhaps due to their coarser texture. Powdery carbonate forms between some platy peds, particularly near the base of the Av horizons. The bulk of the fine-grained material in the Av and Bt horizons is probably eolian sediment that infiltrated the soil profiles.

INDIAN SOILS

Pedons 5 and 7 illustrate the strongly differentiated horizons of the late Pleistocene Indian soils, below well sorted, moderately to tightly packed desert pavements (Appendix II). Pedon 5 was described below the tread of a prominent solifluction step (Appendix I, Fig. I4). The generally gravel-free Avk horizons of these pedons are coarsely-vesicular and form prominent crusts with very-coarse-columnar and subangular blocky compound structure. Near their base, coarse platy structure is distinctly visible. Carbonate forms between platy peds, and Stage I coats on the underside of pebbles.

Underlying the Avk horizons are BA horizons that have platy structure, vesicular pores and modest carbonate accumulations. The Avk and BA horizons probably have formed within layers of desert loess (Appendix I).

Below the BA horizon of Pedons 5 and 7, formed in the alluvial parent materials, are thick (30 to 40 cm) Bt horizons of prominent silicate clay accumulation and 10YR hue. Stage I opal and Stage I to Stage II carbonate accumulations occur on pebble-bottoms, and Stage I carbonate occurs on ped faces. In the lower part of these argillic horizons, nodules and lenses are cemented by carbonate and opal. Illuvial accumulations of oriented clay form common, thin, bridges between mineral grains, films on pore walls, and a few colloid stains on grains.

Pedons 5 and 7 comprise a partially indurated Bkm horizon. Opal also occurs in these horizons, as is suggested from soaking a sample of the Pedon 5 Bkm horizon in an approximately 1N HCL solution for about 48 hours and observing an insoluble residue; i.e., following procedures outlined by the USDA (1975). Hence, these horizons are probably duripans. The Stage III, Bkm horizons lack a continuous laminar Stage IV carbonate cap. Infiltration rates are probably reduced by these horizons, and thus encouraging solifluction of surficial loess layers (Appendix I). Below the Bkm horizons of these pedons are Stage I+ to Stage II Bk horizons with thick, continuous carbonate coatings and whitened interpebble fine earth. These horizons extend at least to the bottom of the exposures.

Discussion of Indian Soils

The formation of the Avk and BA horizons in Indian soils is largely attributed to accumulation and infiltration of eolian sediment. These vesicular horizons form in desert loess that accumulates in thin caps or veneers on the surface of stable remnantal landforms. The hypothesis that the fine-grained surficial layers is loess is supported by their narrow particle size range and regional continuity on landforms that are otherwise isolated from receiving sediments (Sawyer, 1988;

Appendix I). As pointed out by Peterson (1988), it is generally accepted, among most current workers in soil genesis, that the formation of Av horizons is largely attributed to dust accumulation.

Marchand (1970) demonstrated that soils in a subalpine, semi-arid environment of the White Mountains, about 40 km south of the Plate I area, have as much as 34 % eolian constituents in the total soil material. Chadwick and Davis (1988) and Davis and Chadwick (1988) suggested episodic eolian dustfall events contribute fine particles to soils in the Great Basin and influence local and regional pedogenesis. McFadden and others (1986), Wells and others (1987), McFadden and others (1987), and McFadden and Tinsley (1985) worked in the eastern Mojave Desert of California and reached the similar conclusion that eolian sediment influx markedly influences soil genesis. Gile and others (1966) indicated that the rate of carbonate accumulation, in soils formed from calcareous verses non-calcareous parent materials, is virtually nullified by contributions of carbonate in the from of eolian sediments.

The Av and BA horizons of Indian soils are very dilatent (i.e., the "viscous-liquid like behavior of saturated soil material with high contents of silt and very fine sand" (Peterson, 1988). Dilatent behavior is indicated by viscous flow structures (similar in appearance to wax that has flowed down and solidified on the side of a candle) observed in the Pedon 5 soil pit a few weeks after a thunderstorm. The flow structures issued from below the crusting sub-horizon of the Avk horizon, resulting in lowering or subsidence of the pavement surface by 3 to 4 cm.

The presence of vesicular pores and surficial crusts in the Av horizons provides further evidence of the dilatent behavior of desert loess. Miller (1971) demonstrated that vesicular pores form in fine-grained soils when they are in a semi-fluid state that is "very unstable". Nettleton and Peterson (1983) ascribed the formation of both surficial crusts and vesicular pores to repeated saturation of low-humus, loamy soil material. They indicated that the saturated soil material or "plasma" is mobile and free to move. Peterson (1987, personal commun.) suggested that Av horizons form only when the surficial layer is saturated. Therefore, the presence of vesicular pores, surficial crusts and observed flow structures, suggest that these horizons, which are formed in probable eolian parent material, are very dilatent.

In Appendix I, the dilatent behavior of desert loess in the area of study and elsewhere in the western Great Basin is discussed in considerable detail. It is concluded that relatively thick, desert loess layers on gently sloping Pleistocene landforms are highly susceptible to saturated flow or solifluction (Appendix II). The solifluction processes is encouraged by less-permeable soil horizons (e.g., argillic and K horizons) below desert loess layers (Sawyer, 1988c).

The formation of argillic horizons is encouraged during periods of relatively high precipitation (e.g., pluvial climates), characterized by more effective leaching (Gile and Grossman, 1968). Nettleton and Peterson (1983) suggested that in arid environments clay is deposited at shallower depths than carbonate. Wilding and others (1983) suggested that carbonate, even in modest amounts, inhibits dispersion and eluviation of clay. Therefore, the eluvial portion of the soil-profile must be leached of readily mobile carbonate prior to eluviation of clay. Hence, accumulations of carbonate above a noncalcareous argillic horizon and engulfing its basal part are evidence of polygenesis.

Polygenic soils form under conditions that have changed importantly with time. For example, gross shifts in climate, landscape position, soil truncation and sedimentation result in the formation of polygenetic soils (Gile and others, 1966). Of these possible changes, that in climate is likely responsible for polygenesis of the Indian soil. Locally, soil truncation and sedimentation are also important in the development of polygenetic Indian soils.

The A horizons are too thin and the clay content of the parent material too low to be the source of clay in the thick argillic horizons. Gile and others (1981) found that even in the oldest argillic horizons in southern New Mexico, the primary minerals were only slightly weathered. Apparently *in situ* weathering does not account for the clay content of the argillic horizons. Infiltrated eolian sediments probably represent the significant source of clay in argillic horizons of Indian soils.

McAFEE CREEK SOILS

Pedon 12 illustrates soil properties of the McAfee Creek soil, formed below tightly packed, moderately to well sorted pavement. The McAfee Creek soil formed on the crest of a narrowly-rounded ballena, the highest fan remnant in the Indian Creek stepped sequence (Plate I). Truncation of the remnant is suggested by the ballena morphology.

The McAfee Creek soil has a thick, gravel-free Avk horizon with thin carbonate coats (Stage I) on pebble bottoms and between platy peds (Appendix II). This horizon exhibits distinct, coarse columnar and moderately distinct medium platy compound structure. The subjacent horizon is also nearly gravel-free and exhibits compound structure consisting of moderately distinct very coarse subangular blocky and fine platy structures. Fine vesicular pores occur throughout, as does Stage III carbonate and Stage II opal morphology. The carbonate results in whitening (paling and lightening) of the horizon (Appendix III).

The Km horizon, a probable duripan, of the McAfee Creek soil is 40 cm thick and is strongly cemented. The K horizon is "a soil horizon so strongly carbonate-impregnated that their morphology is determined by the carbonate" (Gile and others, 1965, p. 82). This horizon exhibits a massive, carbonate Stage III "plugged" zone, as suggested by a 2 to 3 cm thick, well indurated, but discontinuous capping sub-horizon of inter-laminar carbonate and opal (Stage IV). Below the Km horizon and extending to a depth of at least 145 cm is a carbonate Stage III, opal Stage II Bk horizon with well-indurated lenses of carbonate.

Discussion of McAfee Creek Soils

Because the McAfee Creek soil is truncated the present soil properties, illustrated by Pedon 12 (Appendix II), are partially and genetically related to the exhumed surface of the post-McAfee Creek erosional landform. Hence, soil properties "date" from or sometime after the McAfee Creek unit was stabilized. Hence, properties of Pedon 12 represent the minimal degree of development for this soil.

The Km horizon of Pedon 12 is considered to be a remnantal horizon that was truncated and subsequently buried by the eolian parent materials. The McAfee Creek soil is polygenetic in nature, as a result of deep dissection and related soil truncation (accelerated by more than 50 to 60 m of uplift; Chapter VI), climate changes, and burial by eolian sediment.

EVALUATION OF SOIL GENESIS WITH TIME

The previously established absolute and relative age control of morphostratigraphic units (Chapter IV) provides chronologic constraints on soil genesis. The radiocarbon dated detrital wood fragments are particularly important, since they lie within or below genetic horizons and therefore allow description of soil genesis in relation to soil age.

Soils of morphostratigraphic units in stepped sequence exhibit more prominent pedogenic features, and more distinct horizonation with progressively higher (i.e., older) positions in stepped sequences. Undoubtedly, soil age (time) is the most significant genetic factor that accounts for the differences in these soils.

The degree of soil development is well related to soil age. Shaw (1928) was one of the first to recognize a systematic increase in the development of soil properties with soil age. Several other investigators, for example Jenny (1941), Harden and Marchand (1977), Gile and others (1966), Burke and Birkland (1978), Ruhe (1983), and Harden (1987) have shown similar relationships between soil genesis and soil age.

Several factors complicate assessing pedogenesis with increasing soil age. These factors include a limited number of absolutely dated soils, soil truncation (and/or burial), additions of fine-grained eolian sediment, and Quaternary climatic change. The influence of solifluction on pedogenesis is uncertain, however it is likely a common process in desert soils in the western Great Basin (Sawyer, 1988; Appendix I). Cumulative soils (i.e., those formed in two or more strata [i.e., parent materials] that may be of significantly different age) present an added complication.

Even with these and other complicating factors (not listed here), the relative degree of soil development is the most useful and reliable indicator of relative age employed in the present study. Various developmental trends in pedogenesis with soil age are evaluated in the following sections.

TRENDS IN SOIL GENESIS WITH TIME

MORPHOLOGY OF PEDOGENIC CARBONATE

Carbonate accumulation is promoted by the well-drained, gravelly to very gravelly parent materials of the study area. In part, because as clast size increases, specific area decreases. Thus, relatively less secondary carbonate is needed to coat larger clasts (Peterson, 1985, personal commun.), hence less time is required. Only soils formed primarily in gravelly to very gravelly sand loams were described (Table 4; Appendix II) in an attempt to minimize the textural influence of parent materials on carbonate morphology.

Carbonate is readily available from the fine-grained fraction of the calcareous to highly calcareous parent materials. This contributes to the rate of carbonate accumulation. The term carbonate, as used here, refers primarily to secondary calcium carbonate ($CaCO_3$), perhaps with minor opal, soluble salts, and gypsum.

In areas where soils receive carbonate in the form of atmospheric dust, carbonate morphology is independent of carbonate content of the parent material (Gile and others 1965; and Gile, 1975). The calcareous nature of the desert loess layers on geomorphic surfaces in the study area suggest that carbonate is a constitute of atmospheric dust. Infiltration of eolian carbonate may "normalize" the minor variance in carbonate content of the parent materials.

Carbonate morphology, in soils of all ages, is the pedogenic feature that best discriminates soils of different age (Table 5). Secondary carbonate accumulates in a step-wise morphological sequence that generally follows Gile and others' (1966) morphogenetic classification of pedogenic carbonate in gravelly soils of the desert southern New Mexico. Soils of the Plate I area exhibit morphological development of authigenic carbonate with soil age (Table 6) that generally accords with that

TABLE 5: ILLUSTRATIVE SOIL PROPERTIES OF MORPHOSTRATIGRAPHIC UNITS

[n.a., not applicable]

Morpho-Strat. Unit	Maximum Stage of Carbonate Accumulation	Maximum Stage of Opal Accumulation	Diagnostic Subsurface Horizons	Vesicular Surface Horizon
late Marble	n.a.	n.a.	n.a.	absent
middle Marble	I[1]	I-	Bk	incipient & thin
early Marble	II-	I	Bw to Cambic[2]	easily observable & thin
Leidy	II	I+ to II-	Bw to Cambic[2]	prominent & dilatent
Indian	III	II to III	Argillic & K horizons	prominent, thick, & very dilatent
McAfee Creek	IV	IV	K horizon	prominent, thick, & very dilatent

[1] *Discontinuous Stage I+ carbonate occurs infrequently.*

[2] Typically, the base of the horizon does not meet the arbitrary 25 cm depth requirement of cambic horizons, in which case the horizon is technically not an cambic horizon.

TABLE 6: COMPARSION OF STAGES OF CARBONATE MORPHOLOGY WITH TIME

Stage of Carbonate Accumulation in Gravelly Soils	Youngest Unit on which Stage of Horizon Occurs and age - ka or epoch: Present Study	Gile and others, 1981[1]
I	middle Marble 0.6 to 1.6	Fillmore 0.1 to 7.0
II	Leidy 4.0? to latest Pleistocene (18?)	Isaack's Ranch 8.0 to 15.0
III	Indian late Pleistocene	Jornada II[2] late Pleistocene
IV	McAfee Creek late middle Pleistocene	Jornada I late middle Pleistocene

[1] From their Table 21, p. 68.

[2] The Jornada II geomorphic surface also exhibits Stage IV.

determined by Gile and others (1981).

Accumulations of secondary carbonate are the most prominent evidence of pedogenesis in the area mapped, due in part to their durability. Gravelly soils of a hundred to several hundred (0.6 to 0.2-0.7 ka) years old have no, or only incipient accumulations of carbonate (e.g., Appendix II, Pedons 4 and 13). In gravelly soils of late Holocene age (0.6 to 2.2 ka) Stage I carbonate accumulations are prominent and common (e.g., Pedons 1-3, 8 and 9). The mid Holocene (4? ka) to latest Pleistocene (18? ka) soils exhibit horizons of Stage II carbonate morphology (Pedons 6 and 10). Late Pleistocene soils display massive Stage III K horizons (Pedons 5 and 7) and late-middle Pleistocene soils have continuous and well indurated Stage IV sub-horizons (e.g., Pedon 12).

Often thin, powdery filaments in dendritic arrangement on pebble bottoms provide the primary evidence of pedogenesis in late Marble soils. At Radiocarbon Site 1/Tephra Site 1 a radiocarbon date of 120 cal B.P. (Beta-26169) was obtained on detrital wood fragments collected from an AB horizon (Appendix II ,Pedon 4). This horizon has only a modest trace of secondary carbonate. Stratigraphically below this date a second radiocarbon date of 660 cal B.P. (A-4765) was obtained on detrital wood from a buried, early Stage I (I-) Bk horizon. At a depth of about 2 m, in parent materials displaying little or no evidence of pedogenesis, another detrital wood fragment provides a date of 680 cal B.P. (A-5068). The late Holocene middle and early Marble soils have Stage I Bk horizons and accumulations of carbonate to considerable depths (commonly 1.5 m, or more). The middle Marble soil at Radiocarbon Site 3 (Appendix II, Pedons 1 & 2) has a Stage I Bk horizon, radiocarbon dated at 1555 cal B.P. (A-4768). The middle Marble soil at Radiocarbon Site 4 (Pedon 11) also has a Stage I Bk horizon, dated at 1065 cal B.P. (Beta-26170). The Bk horizon of the early Marble soil (Pedon 3) at Radiocarbon Site 2 displays prominent Stage I (I+) morphology and overlies a detrital log dated at 2155 cal B.P. (A-4767). The early Marble soil at Pedon 9 also exhibits a Stage I+ (or II-) Bk horizon.

A transition from Stage I to Stage II Bk horizons is shown by early Marble (Table 3, 1.5 to 2.4 ka) soils and Leidy (mid-Holocene to latest-Pleistocene) soils.

This transition provides a useful means of distinguishing soils of Leidy age from those of Marble age (late Holocene). The Leidy soils of Pedons 6 and 10 (Appendix II) display Stage II morphology, whereas the maximum developmental stage exhibited by early Marble (late Holocene) soils is Stage I (I+).

The accumulation of pedogenic carbonate in the late Pleistocene Indian soil form Stage III morphology and have pervasive K fabric. The Indian soils of Pedons 5 and 7 exhibit Stage III K horizons that are weakly to moderately indurated. These horizons lack a laminar cap or subhorizon, suggesting the K horizons are not yet "plugged" (i.e., impermeable).

Within the map area, plugging and associated development of laminar carbonate morphology (Stage IV) occur only in soils associated with the post-Bishop Tuff ($\leq$ 740 ka) age McAfee Creek unit. McAfee Creek soils along the eastern piedmont slope of the White Mountains are generally truncated and probably illustrate only minimal soil development. That is, relative to where these soils occur on relict McAfee Creek surfaces, perhaps on the Trail Canyon fanhead. Nevertheless, the McAfee Creek soil exhibits the most significant accumulations of carbonate in the area of study. The above relations suggest carbonate morphology is useful for recognition and correlation of morphostratigraphic units that range in age several magnitudes (i.e., from latest Holocene to late-middle Pleistocene).

ACCUMULATION OF SECONDARY CLAY

The presence of illuvial, or secondary, silicate clays in argillic horizons provide evidence of geomorphic stability of the soil surface (USDA, 1975, p. 20). Prominent argillic horizons occur in late Pleistocene and older soils of the desert southwestern United States (Peterson 1980) suggesting they formed primarily during the Pleistocene (Gile and Grossman, 1968). However, argillic horizons have formed in soils younger than 12,000 yr old within this region (Nettleton and others, 1975). In southern New Mexico a few argillic horizons formed during the Holocene, but most are older than 7500 yr B.P. (Gile, 1975). Argillic horizons in southeastern California (actually natric horizons -i.e., sodium enriched argillic horizons, USDA, 1975, p. 28) have formed in less than 3,500 years and probably in less than 2,000 years under the influence of significant eolian influx of both sodium and clay (Peterson, 1980).

Soluble salts are only infrequently observed on the eastern piedmont slope of the White Mountains, and therefore do not appear to significantly influence clay accumulation. Eolian additions of clay however, are probably important in argillic horizon development.

Dispersion, eluviation and illuviation of clays, associated with the development of Bt and argillic horizons, is inhibited by carbonate occurring even in modest amounts (Wilding and others, 1983). Hence, readily available carbonate must be leached from the soil profile before translocation of clays. Illuviation of oriented clays is favored during periods of high precipitation (Gile and Grossman, 1968, p. 12), characterized by more effective leaching. Argillic horizons engulfed by carbonate provide evidence of polygenesis, possibly associated with less effected leaching during a subsequent period of relatively low precipitation.

Oriented secondary clays have not formed in Marble soils (late Holocene). This suggests the duration of soil formation (i.e., time since surface stabilization) is insufficient to have effectively leached available carbonate from the calcareous parent materials, and for translocation and illuviation of clays in these late Holocene soils.

The mid Holocene (4 ka?) to latest-Pleistocene Leidy soil is the youngest to exhibit secondary clay accumulations in the map area. This provides another useful criterion for distinguishing the Leidy soil from those younger. The Bt (possibly argillic) horizons of the Leidy soil (e.g., Pedons 6 and 10) have infrequent, thin clay films on pores and skeletal grains. These limited clay accumulations are apparently comparable to those in desert soils of the southwestern United States formed during the Holocene (Gile, 1975; younger than 12,000 yr old, Nettleton and others, 1975). This supports the mid Holocene to latest Pleistocene age assignment for the Leidy morphostratigraphic unit (Table 3).

The late Pleistocene Indian soil exhibits prominent, thick (30-35 cm) argillic horizons. Secondary clays form frequent medium-thick films on pores and bridges between, and colloid stains on mineral grains (Appendix II, Pedons 5 and 7). Carbonate has engulfed and discontinuously cemented the base of these argillic horizons.

The prominent argillic horizons (and K horizons) of the Indian soil probably developed during a period characterized by more effective leaching of carbonate and translocation of clays, associated with K and argillic horizon development. Shallow, presumably Holocene Stage I carbonate has formed above the argillic horizons. The general bimodal distribution of carbonate in the Indian soil profiles suggests leaching is less effective at present, then during argillic and K horizon development. This also suggests the Indian soil is polygenetic in nature.

The post-Bishop tuff (?) McAfee Creek soil lacks an argillic horizon (Pedon 12) where it formed from the highest fan remnant within the Indian Creek piedmont embayment (Plate I). Presumably a prominent argillic horizon was associated with the late-middle Pleistocene McAfee Creek soil, but was truncated when the subjacent K horizon was exhumed.

J.W. Harden (USGS, Menlo Park) and A.R. Gillespie (Univ. of Washington) excavated a probable McAfee Creek relict surface (equivalent) on the abandoned Trail Canyon fanhead. Preliminary examination of these excavations suggests the relict McAfee Creek soils have prominent, thick argillic horizons.

OTHER TRENDS WITH SOIL AGE

Several other trends in soil genesis are apparent. The most noteworthy of these are the formation of diagnostic horizons (i.e., Av, Bw and cambic horizons) and secondary opal (silica) accumulations.

Vesicular A Horizon Formation

Peterson (1988, p. 11) referred to vesicular A horizons (informally denoted Av) as:

> " surface horizons...that crust and crack into coarse 'polygons' (coarse prismatic structure) when dry, that...are either massive or massive in the upper part and platy in the lower part...[that have] coarse vesicular pores in at least the upper part...[and] may occur under pavement, but is less gravelly than the parent material...; is light colored and low in humus...[and] has a high percentage of very fine sand and/or silt that encourages 'dilatancy' [i.e., viscous-liquid like behavior] when saturated."

Av horizons are absent in the late Marble soil (less than 0.6 ka), incipient in middle Marble soil (less than 1.5 ka), and thin (2-4 cm), generally discontinuous in soils of early Marble age (1.5-2.0 ka). The mid Holocene to latest Pleistocene Leidy soil has a prominent, thick (5 cm or more) and weakly dilatant Av horizons (Table 5).

The late Pleistocene Indian soil exhibits thick, nearly gravel-free Av horizons that are strongly dilatant. These horizons commonly underlie an armament of moderately- to tightly-packed, well-sorted pavement on treads of solifluction steps but are generally absent on risers where biocoppices are common. These Av horizons have compound very coarse prismatic and subangular blocky structure in the upper subhorizon and platy structure in the lower subhorizon.

The McAfee Creek soil at Indian Creek has a discontinuous, but thick, Av horizon that is frequently absent (probably stripped). Where Av horizons occur (i.e., between bio-coppices) they display compound structures, similar to those of the Indian soils.

Cambic Horizon Formation

The diagnostic cambic horizon is a subsurface soil horizon that has evidence of alteration, e.g., redistribution of carbonate, structural and/or color development, with negligible illuvial material and a bottom that is 25 cm or more below the surface (USDA, 1975, p. 36). Cambic horizons are Bw horizons that display prominent evidence of pedogenesis.

The late Marble soil lacks a Bw horizon, the middle Marble soil has a Bw horizon (probably not cambic) and the early Marble soil displays a Bw horizon that meets the alteration and structural requisites of cambic horizons, but not the depth requirement (USDA, 1975, p. 36). The Bw horizons of the Leidy soils also fail the arbitrary depth requirement, but otherwise are cambic-like. "Cambic" horizons within the Plate I area have formed in soils as young as early Marble (1.6-2.2 ka) and Leidy (older than about 4 ka) ages. In southern New Mexico cambic horizons formed in 2200 to 4600 years (Nettleton and Peterson, 1983). Thus, the rate of cambic horizon formation in this area (Table 5), like that of carbonate morphology

(Table 6), is apparently similar to desert soils in southern New Mexico.

Secondary Silica Accumulations

Secondary silica, i.e., pedogenic opal, has accumulated in virtually all soils of the study area, except for the late Marble soil. Progressively more distinct accumulations of opal occur in successively older soils, with the most prominent accumulations in the McAfee Creek soil (Table 5). In this section, the morphology of opal accumulations are described following the four-stage morphogenetic classification scheme of Taylor (1986). Table 5 shows the youngest morphostratigraphic unit to exhibit a particular morphological stage.

The buried soil at Radiocarbon Site 1/Tephra Site 1 is the youngest in the Plate I area to have pedogenic opal accumulations (Appendix II) . This soil is dated at about 0.6 to 0.8 ka, and has discontinuous coatings and small flakes of opal (Stage I-) on pebble undersides. The middle Marble soil of Pedons 1, 2 and 8 (Appendix II), also have Stage I- opal morphology.

The early Marble (1.6 to 2.2 ka) soils (Pedons 3 and 9) and Leidy (mid Holocene to latest Pleistocene) soils (Pedons 6 and 10) roughly illustrate the transition from Stage I to Stage II opal morphology (Appendix II; Table 5); similar but perhaps not as reliable as that for carbonate morphology (discussed in a previous section). Stage II opal morphology in Leidy soils is suggested from carbonate-silica pendants on the underside of pebbles. The late Pleistocene Indian soils has Bkm horizons with Stage II to III opal morphology (Pedons 5 and 7). Infrequently, thin (1 mm or less) light pink, opal lamina are interstratified with carbonate lamina in these horizons.

The Kqm horizons of the McAfee Creek soils have prominent accumulations of pedogenic opal. A thick (about 1 to 2 cm), laminar coating of inter-banded carbonate and opal was removed from Pedon 12 (Appendix II) and treated with dilute (about 10%) HCL acid. Several, thin (approximately 1-3 mm) flakes of opal remained insoluble after soaking more than 48 hours in the acidic solution. This suggests that in addition to carbonate, opal is a cementing agent in these possible duripans (i.e., silica cemented subsurface horizons).

In summary, secondary opal is absent in the late Marble soil, forms Stage I- coatings in the middle Marble soil, and Stage I coatings in the early Marble soil. Stage I+ (infrequently II-) accumulations of opal forms in the Leidy soil. Pleistocene soils have Stages II to III (Indian soil) and Stage IV (McAfee Creek soil) opal morphology (Table 5).

Weathering of volcanic ash high in bases can "liberate soluble silicates at a rapid rate" (USDA, 1975, p. 41). Several volcanic ash deposits are known (e.g., from the present study and cooperative studies between the author and M.C. Reheis, J.W. Harden [USGS], A.R. Gillespie [Univ. of Washington], and J., Slate [Univ. of Colorado]) to be intercalated in the alluvial soils of Fish Lake Valley. Marchand (1970) determined that volcanic ash is a significant constituent (30%) of soils in a sub-alpine region of the southern White Mountains, about 40 km south of the Plate I area. King and Elliot-Fisk (1988) found volcanic ash in soils on the crest of the range, about 15 km west of this area.

It, therefore, seems probable that volcanic ash is a significant source of readily soluble silica in soils of the Fish Lake Valley region. The relative rapid development of silica morphology, as compared to that shown by Taylor (1986) for the Nevada Test Site area, southern Nevada, may be attributed to volcanic ash.

INDICES OF SOIL DEVELOPMENT

SOIL DEVELOPMENT INDEX

Soil field properties (Appendix II) were quantitatively indexed using the soil development index (SDI) of Harden (1982) and Harden and Taylor (1983). Soil development indices were calculated by interactive operation of a computer-template developed by Taylor (1988) and executed with LOTUS 123™ (Appendix III).

The SDI permits evaluating the present state of the soil in terms of the degree of pedogenic alteration of the parent material (Harden, 1982). The SDI is used to compare the relative degree of soil development among soils of different ages. Numerical calibration of the SDI is based primarily on radiocarbon dated soils. The calibrated Holocene SDI provides an important means of evaluating pedogenesis with increasing soil age, and is used for general temporal-correlation of soils in the Plate I area. Hence, the SDI can be used for demarcation of soils, based on soil age.

Calculation of the SDI involves first describing the soil profile (pedon) and assessing the parent material(s). Then field properties of each horizon are quantified by assigning values for the amount of change from the parent material to the present soil state. The quantified properties are normalized and summed. This value is divided by the number of properties and multiplied by the thickness of the horizon. The SDI is the sum of the products from each of the horizons within the soil profile (Harden, 1982; Harden and Taylor, 1983).

In addition to calculation of the SDI, Taylor's (1988) template allows the user to select specific soil properties for calculation of the selected property index. The template can also calculate the profile property index, which is an assessment of soil properties on an individual basis.

Since buried soil horizons are not genetically associated with the overlying soil, nor the present geomorphic surface, they are excluded from calculations of soil development indices (Appendix III).

Calculation of the SDI involves assessing the parent material(s) of a particular soil (pedon). Parent materials are assessed to be gravely sandy loam in texture, 2.5Y7/2 to 6/3 (dry) and 2.5Y 5/3 to 4/2 (moist) colors, loose to slightly hard dry, loose to very friable moist, and non-sticky and non-plastic when wet. All properties attributed to soil parent materials were observed in the immediate area of the pedon description sites and elsewhere in the Plate I area.

Values of Soil Development Indices

Values of six (of ten possible) profile property indices are shown in Table 7. These indices are paling, lightening, structure, dry consistence, carbonate, and clay films. The value of each is systematically greater in progressively older soils, hence the various indices can be used to identify soils of different age.

In Figure 14, all but one of the six profile property indices are regressed on the approximate age of Holocene soils (Table 3). Holocene soils were chosen as

TABLE 7: SOIL DEVELOPMENT INDEX VALUES[1]

Morpho-strat. Unit	Pedon Number	Profile Property Index Values						Selected Property Index[2]
		Paling	Light	Struct.	Dry Consist.	Clay Films	Carb	
late Marble	4	0.00	0.00	16.83	2.70	0.00	0.00	0.90
	13	0.00	0.00	10.50	2.30	0.00	0.50	0.77
middle Marble	1	7.00	5.75	47.83	16.40	0.00	2.63	4.65
	2	3.50	8.50	59.42	15.80	0.00	2.83	3.13
	8	2.50	6.25	40.83	19.75	0.00	2.08	7.28
	11	3.83	9.63	48.75	15.70	0.00	3.21	6.30
early Marble	3	9.67	12.25	54.33	22.00	0.00	6.42	8.94
	9	6.33	13.75	55.42	26.70	0.00	4.46	9.55
Leidy	6	8.67	8.50	64.58	34.40	5.77	6.08	15.42
	10	5.50	13.63	68.08	31.75	3.46	9.01	12.22
Indian	5	24.50	21.13	64.17	35.10	14.54	30.58	26.74
	7	17.67	18.50	53.42	32.15	16.31	24.46	24.31
McAfee Creek	12	19.33	37.75	75.54	43.70	13.77	60.83	39.43

[1] Soil development index values were calculated in Appendix III from soil field descriptions in Appendix II.

[2] Selected properties are dry consistency, carbonate morphology, and clay films.

their ages are best constrained, and because they are of greatest interest to the assessment of Holocene paleoseismicity of the FLVFZ (Chapter VII). The profile clay film index was not regressed with soil age, as only one Holocene (?) soil (that of Leidy age) displays clay films. The three properties that are best related to soil age (i.e., have the largest determination coefficient, R^2 value; R^2 value of 1 indicates a perfect relationship between the independent variable, age and the dependent variable, the SDI), are carbonate and clay morphologies and dry consistency.

These three properties are used in calculation of the selected property index (Table 7). Two properties, dry consistence and carbonate, have the most significant relations to age (i.e, greatest R^2 value). The third, clay films, warrants inclusion in calculation of the selected property index, because it distinguishes the Leidy soil from all those younger, and it also allows for better characterization of Indian soil (Fig. 15). The relationship of the selected property index to Holocene soil age is statistically significant (as indicated by an R^2 value of 0.74; Fig. 16). That is, this index is related to soil age.

In Figure 15, the average value of the selected property index for all morphostratigraphic unit is regressed separately for Holocene and Pleistocene soils. The "Holocene-regression line" is clearly steeper than the "Pleistocene-regression line," indicating the rate of Holocene soil development is significantly greater than of Pleistocene soils.

Factors such as soil truncation and the polygenetic nature of Pleistocene soils may account for some, perhaps only a minor amount, of the discrepancy in the relative rates of soil formation. Harden (1982) and Harden and Taylor (1983) have shown a similar difference in the relative rates of Holocene and Pleistocene soil genesis.

<u>Estimated Ages of Holocene Soils based on Selected Property Index</u>

Soil development indices suggest a clear relationship between soil age and the degree of soil development (e.g., Figs. 14, 15, and 16). Thus, supporting the previous claim that the sequence of soils constitutes a chronofunction. Hence time, is the single most important genetic factor influencing soils of the Plate I area.

(a)

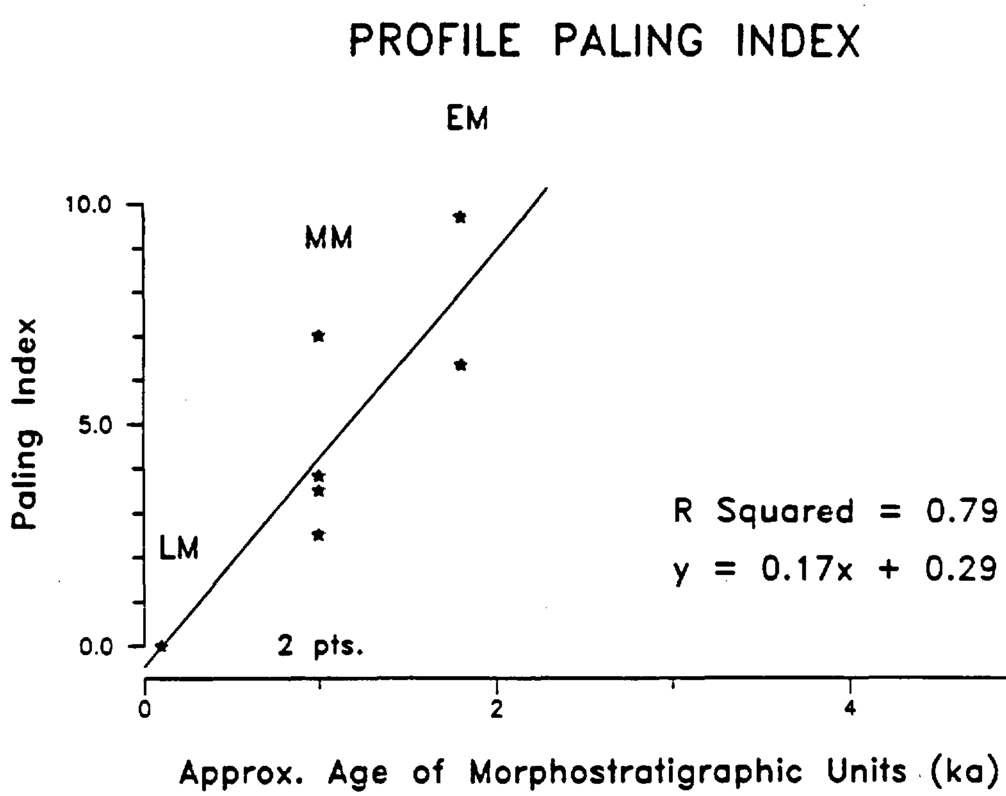

Figure 14. Regression analyses of various profile property indices and approximate ages of the late, middle, and early Marble morphostratigraphic units. (a) Profile paling index; (b) Profile lightening index; (c) Profile dry consistence index; (d) Profile structure index; (e) Profile carbonate index.

(b)

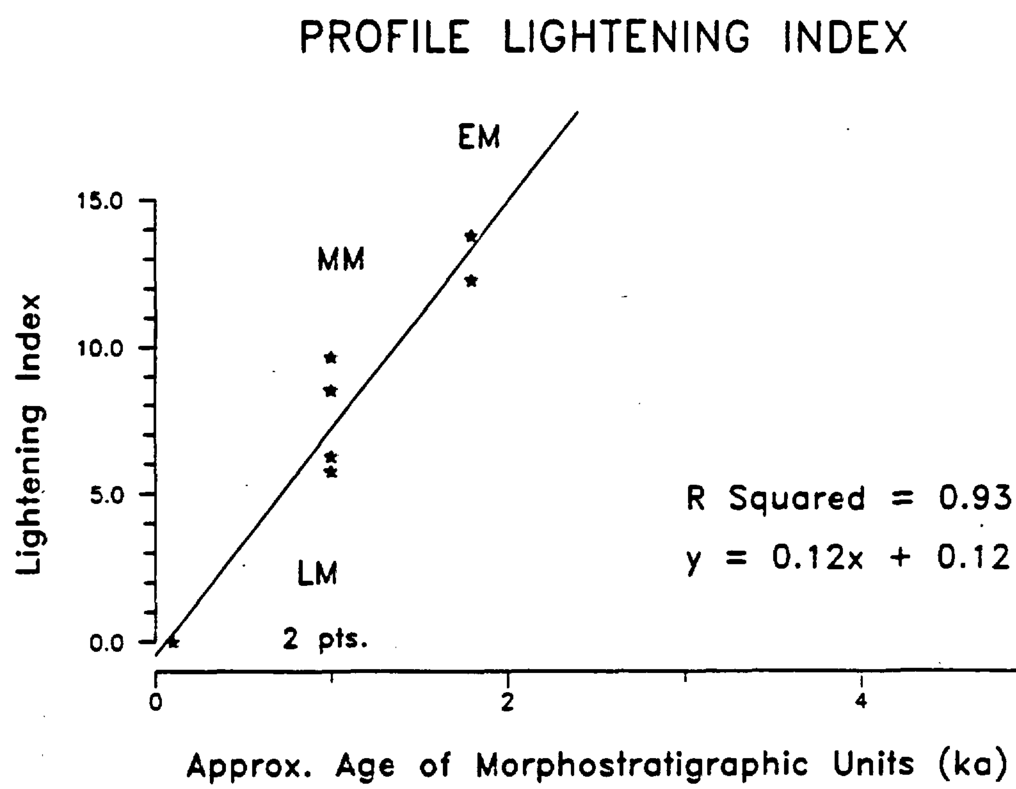

Figure 14. Continued

(c)

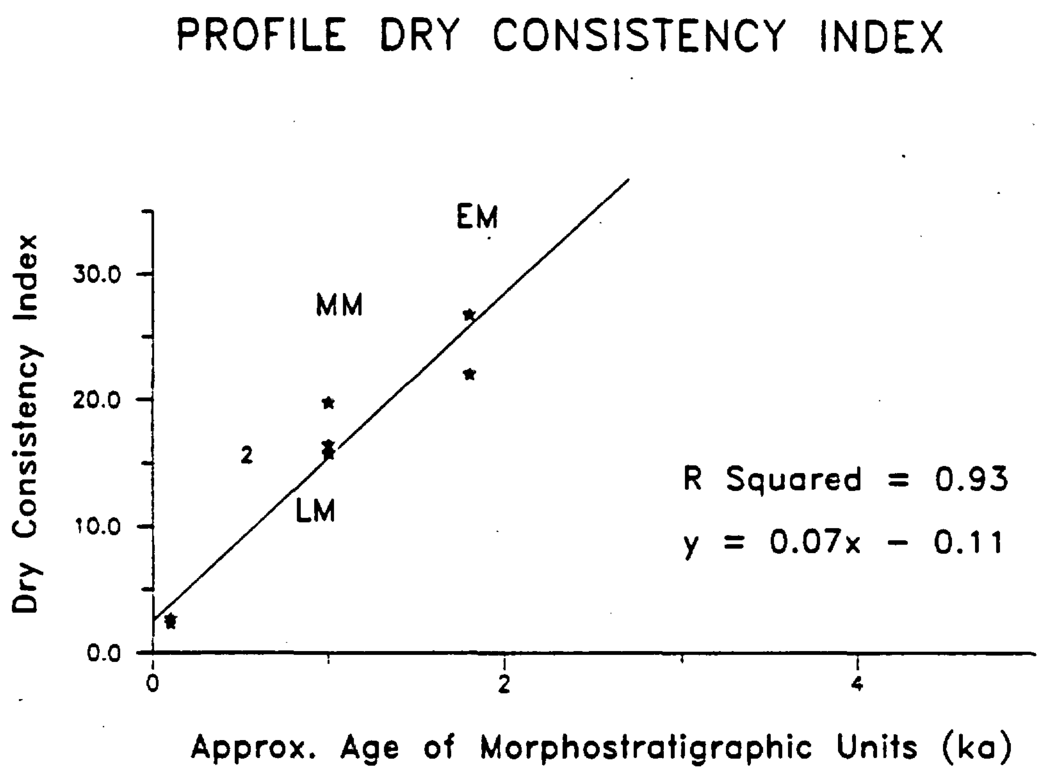

Figure 14. **Continued**

(d)

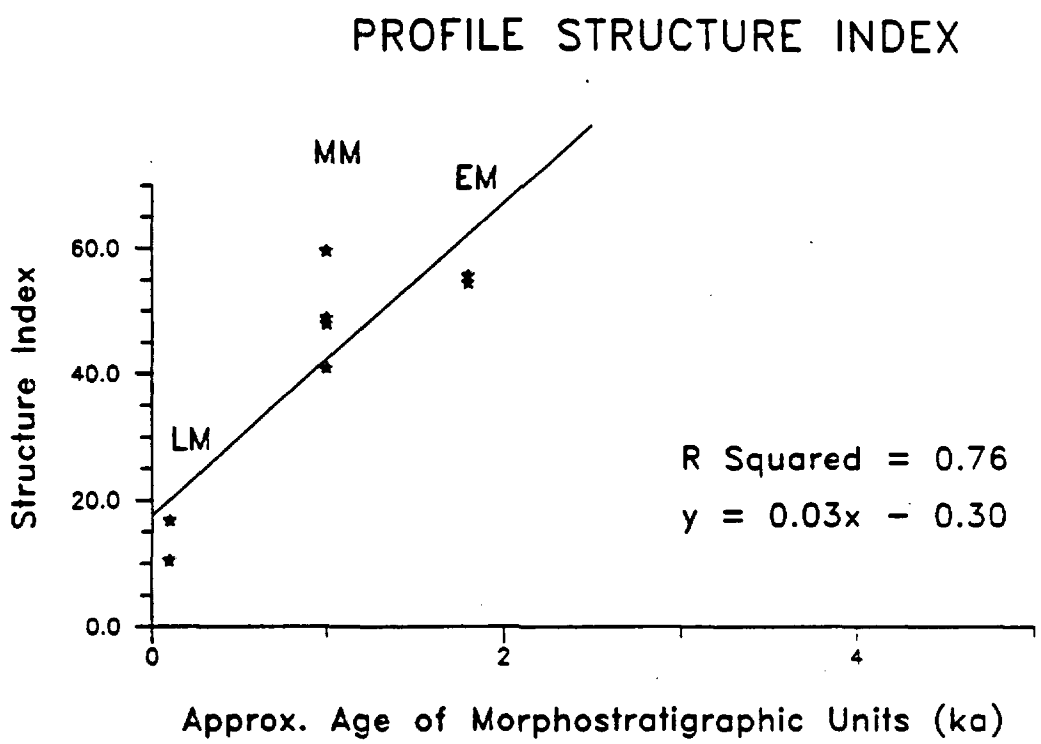

Figure 14. Continued

(e)

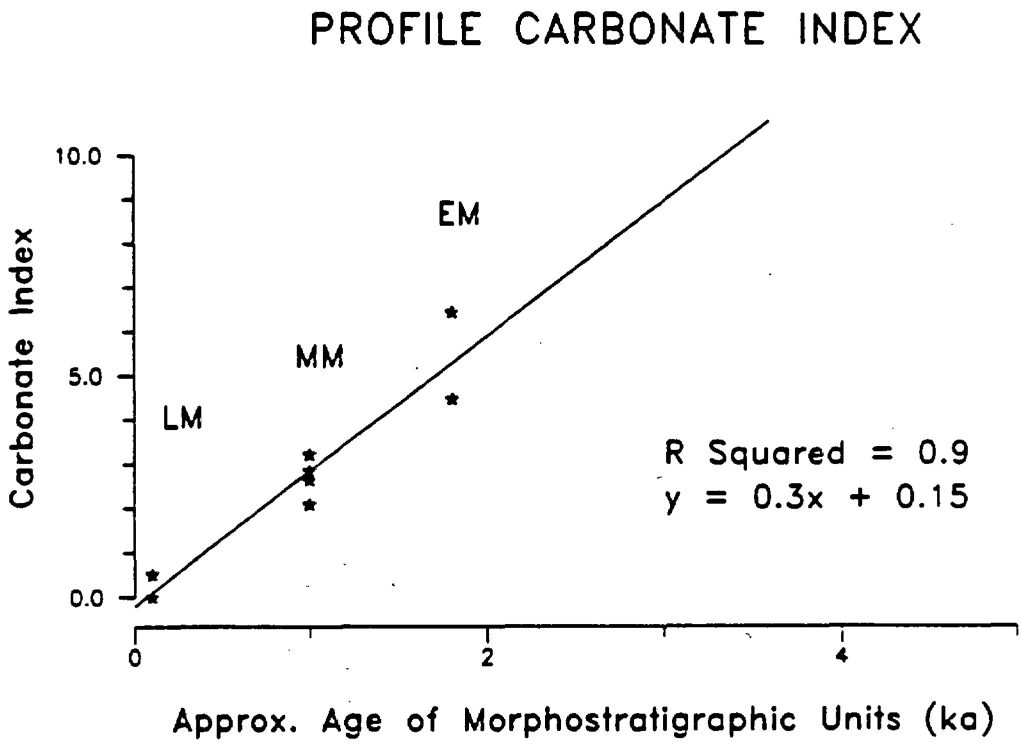

Figure 14. Continued

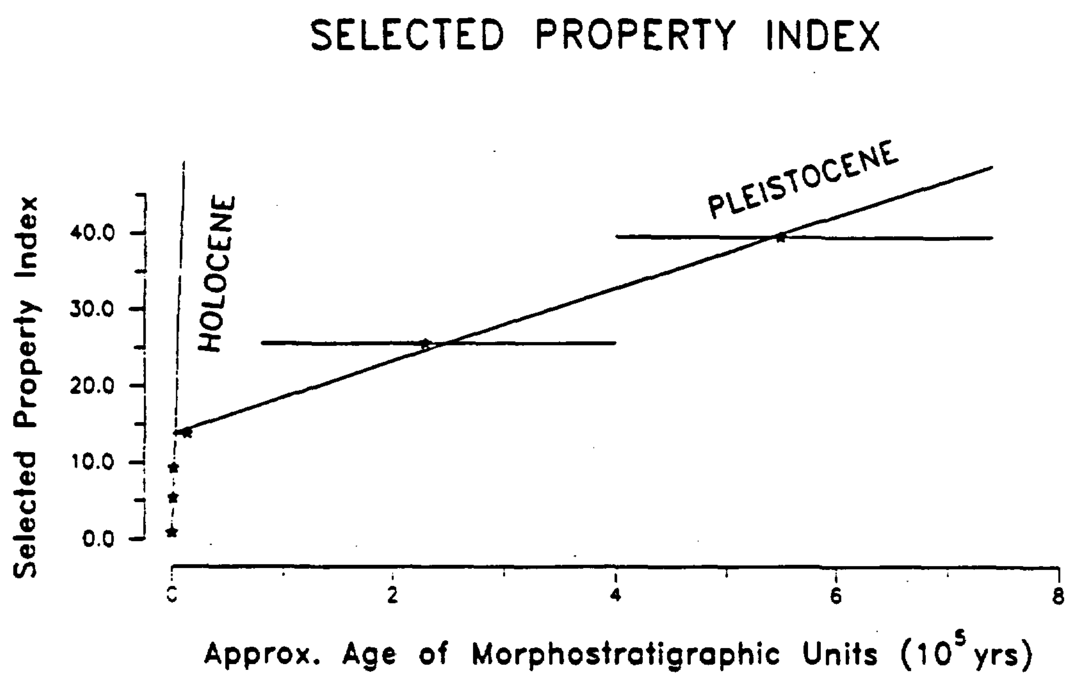

Figure 15. Regression analyses of the selected property index and approximate ages of Holocene and Pleistocene morphostratigraphic units.

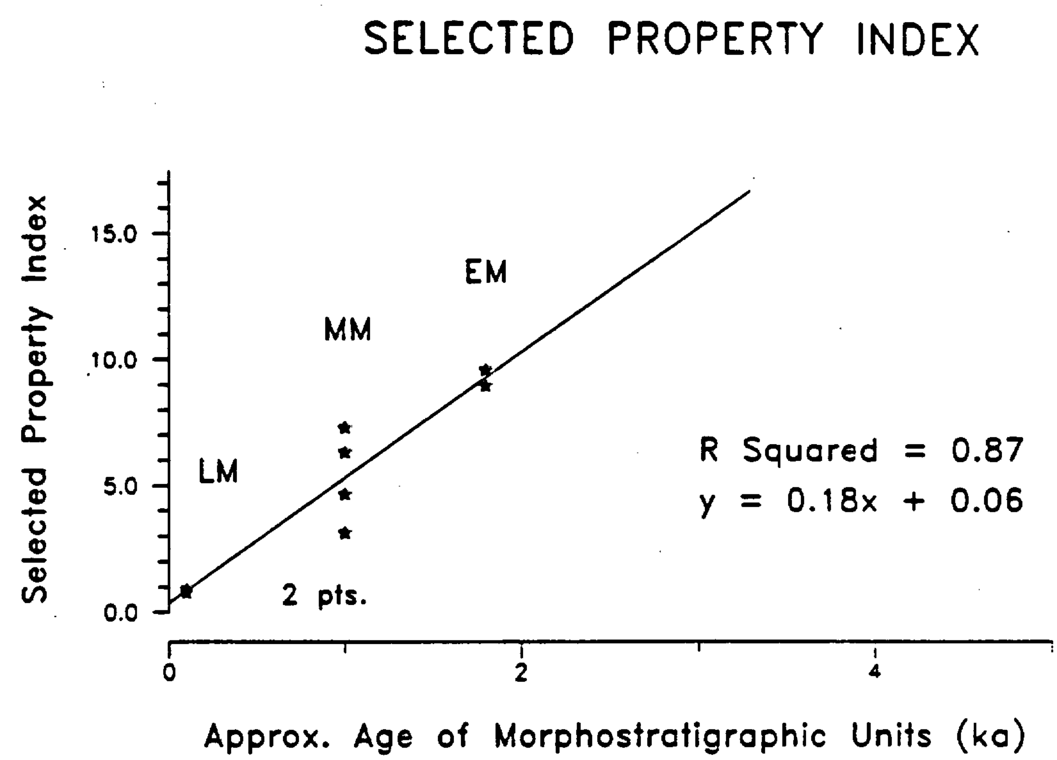

Figure 16. Regression analyses of the selected property index and approximate ages of the late, middle, and early Marble morphostratigraphic units.

It is therefore possible to estimate soil ages based on soil development indices. When time is evaluated as the dependent variable, the indices provide a means of estimating soil age (i.e., independent variable). Thus, soil development indicies for radiocarbon dated soils can be compared to undated soils, thereby extending (locally) general numerical age constraints to soils where none existed before.

In Figure 17, the selected Property index is shown as the independent variable from which soil ages are estimated as dependent variables. The selected property index was used to estimate soil ages, because it incorporates the properties that are most clearly related to the soil-forming factor, time (i.e., carbonate morphology, dry consistence and accumulations of clay). Soil ages estimated by the calibrated selected property index are listed in Table 8. Minimum and maximum ages represent the standard deviation of the predicted age value about the regression line. Ages are reported in soil development index years before present (sdiB.P.) to reflect the uncertainty in the estimated values. Uncertainties in soil ages may be significant (80%, Harden, 1989), and stem from soil variability, a limited number of detailed pedon descriptions, and uncertainties in age estimates of "dated" soils. Therefore, the estimated soil ages serve as general numerical "guides" to what the ages of the soils may actually be. They are not absolute ages, nor can they treated as such.

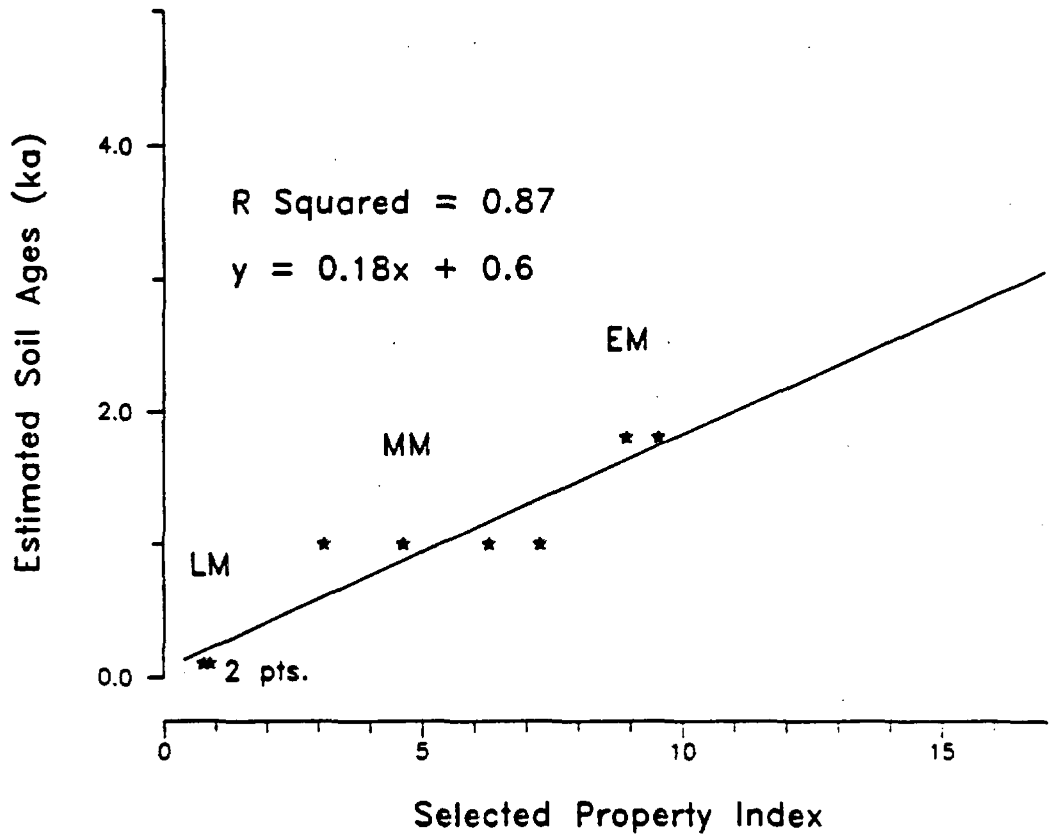

Figure 17. Regression analyses of approximate ages and the selected property index of the late, middle, and early Marble morphostratigraphic units. This calibrated selected property index is used to estimate soil ages.

TABLE 8: ESTIMATED HOLOCENE SOIL AGES BASED ON SELECTED PROPERTY INDEX[1]

[n/a, not available, since negative soil ages are unreasonable]

Morphostrat. Unit	Pedon Number	Estimated Soil Ages			Estimated Mean Soil Ages		
		Soil Age	Max. Age	Min. Age	Soil Age	Max. Age	Min. Age
late Marble	13	0.1	0.5	n/a	0.1	0.5	n/a
	4	n/a	0.5	n/a			
middle Marble	11	1.2	1.5	0.9	0.9	1.3	0.7
	1	0.9	1.2	0.6			
	2	0.6	0.9	0.4			
	8	1.4	1.6	1.1			
early Marble	3	1.7	1.9	1.4	1.6	2.0	1.4
	9	1.8	2.0	1.5			

[1] All estimates of soil ages are expressed in 10^3 soil development index years before present (sdi B.P.), and were determined in Appendix III.

CHAPTER VI
SURFACE FAULTING ALONG THE FISH LAKE VALLEY FAULT ZONE

INTRODUCTION

One of the longest interconnected fault systems within the Basin and Range Province is the right-lateral Death Valley fault system (DVFS; Figs. 6 and 7). The DVFS, equal in length to the Wasatch fault zone in Utah, is the longest strike-slip fault in the province. The fault system was one of the first in the western United States recognized as exhibiting Pleistocene activity (e.g., Ball, 1907; Anderson, 1933). Yet, little is known about the Quaternary tectonic history and seismic potential of this regionally extensive Quaternary fault system, which passes less than 50 km from the proposed high-level nuclear waste repository site at Yucca Mountain, Nevada.

The FLVFZ is a significant structural component of the DVFS, and extends the entire length of western Fish Lake Valley, Nevada and California, a distance of about 80 km. The fault zone separates the White Mountains on the west from the valley on the east (Fig. 18). The FLVFZ is predominantly a right-lateral strike-slip fault, having a variable but pervasive component of down to the east vertical displacement. Hence, right-divergent-slip (valley side relatively downdropped) characterizes the style of faulting along the fault zone. The fault zone comprises contemporaneous northwest- to north-northwest-striking right-slip to right-divergent-slip faults, and north-striking prominent normal faults. The kinematic style of the FLVFZ therefore is similar to the DVFS as a whole (cf., Burchfiel and Stewart, 1966; Wright and Troxel, 1967; Brogan, 1979), and is generally consistent with the east-west (Smith & Lindh, 1978) to N80°W (Zoback and Zoback, 1980; Zoback and Beanland, 1986) extension direction of the region.

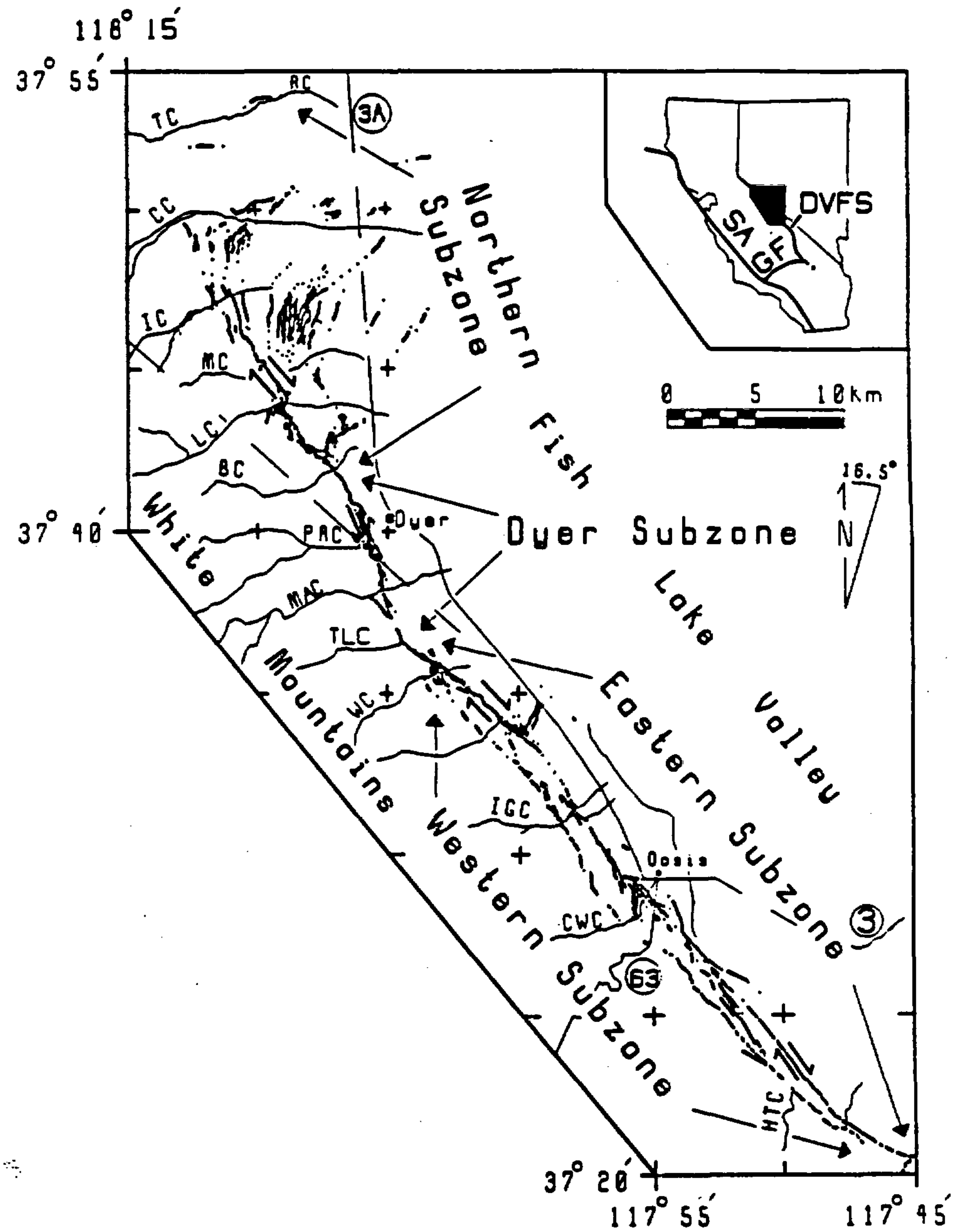

Figure 18. Map of the Fish Lake Valley fault zone showing the various subzone that it comprises. BC, Busher Creek; CC Chiatovich Creek; CWC, Cottonwood Creek; DVFS, Death Valley fault system; GF, Garlock fault; HTC, Horse Thief Canyon; IC, Indian Creek; IGC, Indian Garden Creek; LC, Leidy Creek; MAC, McAfee Creek; MC, Marble Creek; PAC, Perry Aiken Creek; RC, Rock Creek; SA, San Andreas fault system; TC, Trail Canyon; TLC, Toler Creek; WC, Wildhorse Creek.

In the present chapter, structural analysis of Quaternary fault patterns and geomorphological evaluation of displaced surficial features, are the basis for inferring the style(s) of faulting at selected sites along the FLVFZ. Regional seismicity and geophysical studies also aid in such evaluations. Near the northwestern terminus of the fault zone, styles of faulting are determined in part from three EDM/theodolite surveys of offset geomorphic features (Appendix V). The fault pattern is assessed with reference to the Quaternary morphostratigraphic framework (Chapters III and IV), thus providing a partial tectonic history of the fault zone. The tectonic history coupled with the survey data, form a means of estimating average late Quaternary slip-rates along the northern FLVFZ (Appendix VII).

A regional synthesis, or kinematic model, is developed based on styles, patterns and rates of faulting measured, estimated, or inferred from informative sections of the FLVFZ. The models suggest that the style of faulting along the fault zone is influenced by the relative motion of the White Mountains and Fish Lake Valley structural blocks and the geometry of their mutual boundary - i.e., the strike of the FLVFZ. This model is consistent with late Cenozoic movements along the DVFS (e.g., Burchfiel and Stewart, 1966; Wright and Troxel, 1967; Stewart, 1983; and discussed in Chapter III). Further, the model suggests that the White Mountains structural block is tracking the northwest translation of the Sierra Nevada Province (Wright, 1976).

PATTERNS AND STYLES OF SURFACE FAULTING

Along its approximately 80 km extent, the FLVFZ separates the White Mountains, northern Inyo Mountains and the northern Last Chance Range from Fish Lake Valley and the Sylvania Mountains on the east (Fig. 2). The fault zone, along virtually its entire extent, has abundant and prominent geomorphic and structural evidence of late Pleistocene to Holocene (even late Holocene in places; Chapter VII) surface faulting. Evidence of surface faulting includes: fault scarps, some of which display opposing vertical displacements along strike; small-scale, occasionally tilted or (and) rhombohedral-shaped fault blocks in distributed, én echélon or anastomosing arrangements; shutter and pressure (?) ridges; side-hill benches and ridge-crest saddles; vegetation lineaments delineating faults in playa sediments; and deflected, offset, beheaded, and related abandonment and/or catchment of drainages. Several of these geomorphic features decidedly indicate a component of strike-slip displacement along the FLVFZ during the Quaternary.

The FLVFZ connects with the Northern Death Valley fault zone, through a large-scale, left-step (a probable restraining-bend) of about 5 to 6 km (Fig. 7). This step, or bend, is referred to as the "Cucomungo Canyon double restraining bend." Within the bend faults locally strike N80°W, but resume northwestward (N35° to 40°W, average) strikes, where they extend into southern most Fish Lake Valley. The fault zone continues northwestward and maintains two distinct splays that join in the west-central part of the valley. The fault zone to the north comprises a principal displacement zone or master fault that strikes approximately N35°W, and bends northward (about N15°W), branches and eventually terminates in northwesternmost Fish Lake Valley.

Tectonic, geomorphic, and structural evidence indicate that Quaternary tectonic activity on the northwest-striking FLVFZ is predominantly right-lateral strike slip (right slip) in style. The evidence suggests that right slip predominates where the fault zone strikes northwest, right-divergent slip (normal component is dominantly down to the east) where the fault strikes north-northwest and normal slip where the fault zone strikes north to apparently northeast. The styles of faulting along the FLVFZ are influenced by the orientation of the fault; similar to the pull-apart argument for central Death Valley (Burchfiel and Stewart, 1966; Wright and Troxel, 1967; Stewart, 1983; discussed in Chapter III).

The fault zone is herein subdivided into the southern FLVFZ, which is comprised of the "Eastern" and "Western" subzones (Fig. 19), and the northern FLVFZ, comprised of the "Southern" and "Northern" subzones (Fig. 20). Although this subdivision is in part for ease of discussion, the subzones have contrasting structural patterns and apparently faulting styles. The subzones are not necessarily

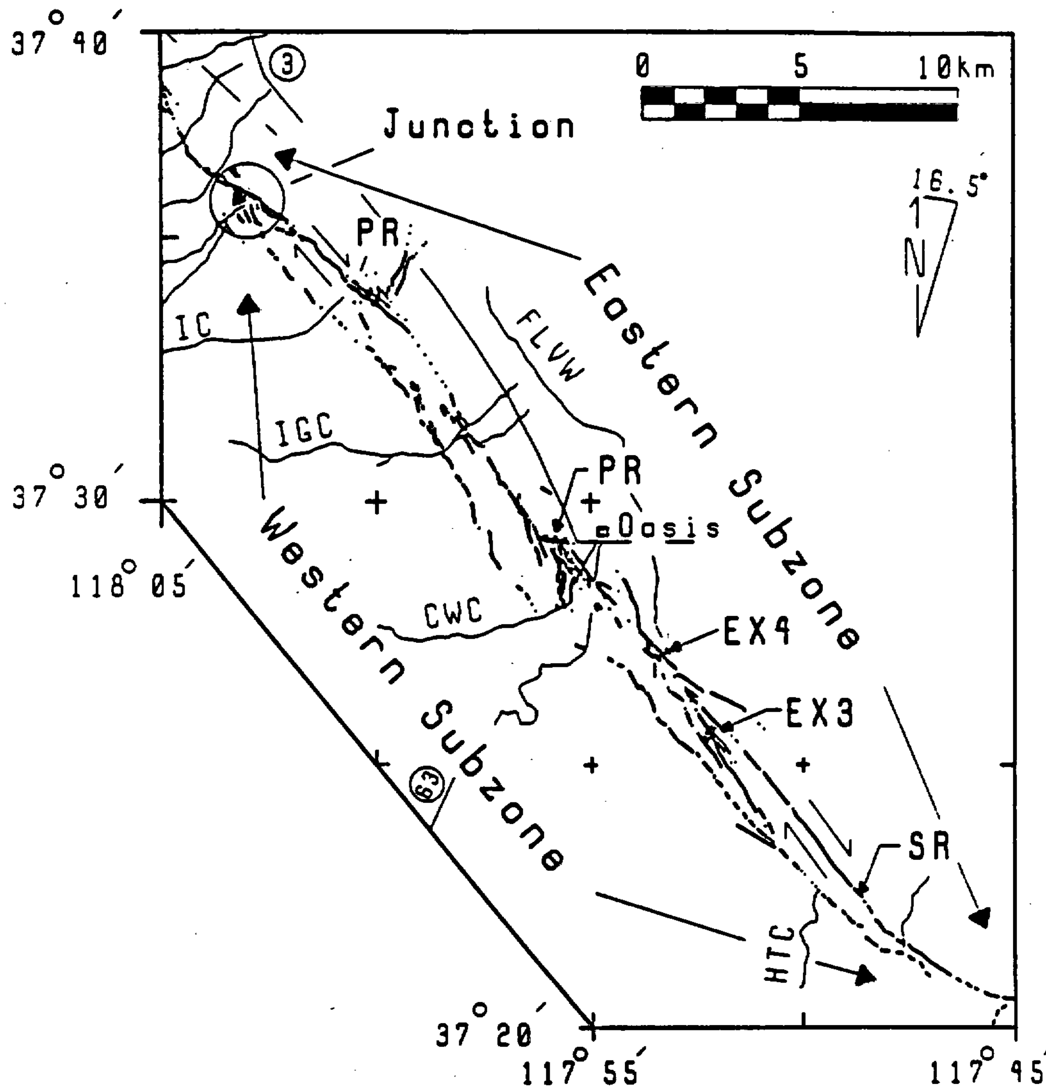

Figure 19. Map of the southern Fish Lake Valley fault zone showing the Western and Eastern subzones and Excavation Sites 3 and 4 (EX3 and 4). Compare with Figure 18 for the location of drainages. PR, pressure ridge; SR, shutter ridge.

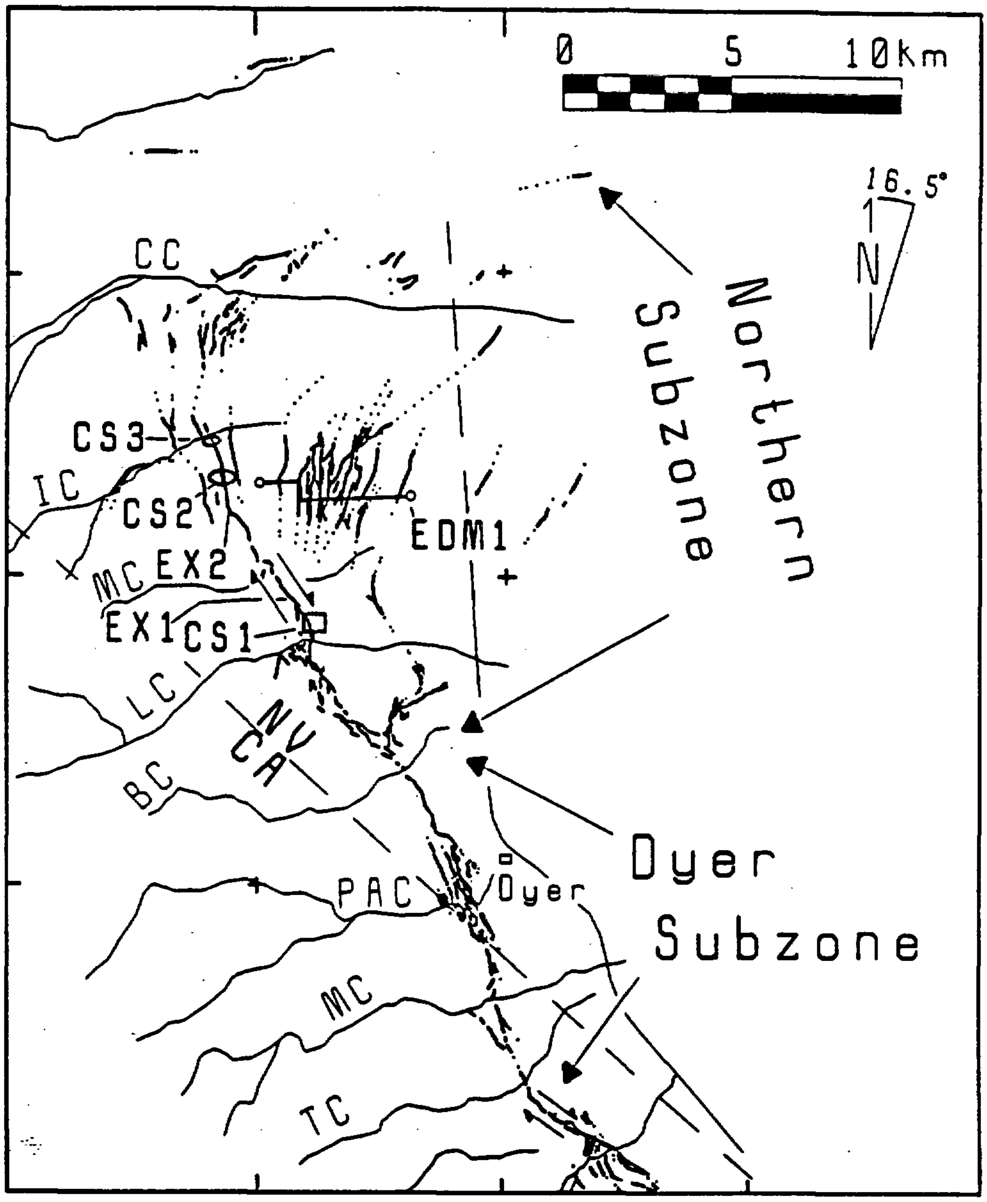

Figure 20. Map of the northern Fish Lake Valley fault zone showing the Dyer and Northern subzones and Excavation Sites 1 and 2 (EX1 and 2). Compare with Figure 18 for the location of drainages. OC, offset channel; SR, shutter ridge.

"earthquake rupture segments" -i.e., that portion of an active fault that has continuity, character, and orientation suggesting that a segment will rupture as a unit (Slemmons, 1982), which will be assessed in Chapter VIII.

SOUTHERN FISH LAKE VALLEY FAULT ZONE

The Cucomungo Canyon double restraining bend separates the southern FLVFZ from the Northern Death Valley fault zone (Fig. 7). The bend is defined by a continuous zone of sub-parallel faults, characterized by right slip, apparently coupled with a reverse component (Reheis, 1990a & b). The fault zone locally trends N80°W and separates highly deformed Mesozoic granitic rocks to the east from similarly deformed Paleozoic rocks to the west (McKee and Nelson, 1967). The profound structural complexity of the bend, which McKee (1968) refers to as a "crushed" zone, is testament of a protracted geometry of the fault zone between these valleys.

North of the restraining bend, the southern FLVFZ forms a narrow (about 1 km wide), fault-trough (Fig. 19) between the northern Inyo Mountains and the Sylvania Mountains. The east bounding fault extends northward and forms a down to the west scarp in probable Holocene alluvium. The fault extends into the valley fill where it forms numerous vegetation lineaments in én echélon arrangement. Still further northwestward, the fault zone traverses several White Mountains alluvial fans and forms a braided and anastomosing pattern of individual fault traces that define small-scale fault blocks; herein referred to as the Eastern subzone of the southern FLVFZ (Fig. 19).

The Western subzone comprises the west bounding fault of the structural trough, which forms the eastern front of the northern Inyo Mountains. Northward the subzone forms the irregular western margin of the valley and eventually joins the Eastern subzone, in a complex pattern of surface faulting (Fig. 19). The two subzones are characterized by contrasting fault patterns and apparently styles of faulting (discussed herein).

<u>EASTERN SUBZONE</u>

The northwest-striking Eastern subzone forms a prominent, down to the west fault scarp, that separates uplifted and deeply dissected fan gravels from the fault trough of southernmost Fish Lake Valley. Here a minor drainage (unnamed) of the Sylvania Mountains has recently breached a ridge that had previously diverted it northward, thereby shortening and steeping its reach to the fault-trough (Plate IIE); where it is actively forming an alluvial fanlette. The recent stream adjustment provides a well-exposed cross section through the ridge. The ridge is within the Eastern subzone and lies between two major faults with opposing components of vertical displacement. The drainage exposure indicates that the ridge is internally deformed by pervasive, near vertical and relatively low-angle (as low as about 45°) faults.

Stratigraphic relations observed in the recently formed exposure, also indicate that light-colored alluvial sediment composed primarily of granitic alluvium is in fault contact along a steeply east dipping (80° to 70°E) fault, with darker-colored alluvium containing basalt and some metasedimentary clasts, on the west. The sediment on the east is overlapped by similar light-colored alluvium, but of probable Holocene age, that appear to be dammed against the east-flanking scarp in a buttress unconformable relationship. However, closer examination may reveal that a fault forms this contact. The light-colored alluvium was apparently deposited by the drainage prior to its recent adjustment. The ridge comprises materials from the surrounding and deeply dissected older alluvium (Tl, as mapped by Reheis, 1990b). These relations suggest that the drainage was diverted by a shutter ridge, and therefore that strike-slip faulting has occurred along the southern part of the Eastern subzone, probably during the Holocene.

To the north, the Eastern subzone displaces probable Holocene alluvial fan surfaces and extends into and across the bolson floor. A series of vegetation lineaments, the larger of which form a left-stepping én echélon pattern, occur on the playa of southern Fish Lake Valley (Fig. 21). The vegetation lineaments are surficial expressions of faults as suggested by their linear form and the fact that some are physically continuous with well-defined fault scarps. Exposures in two

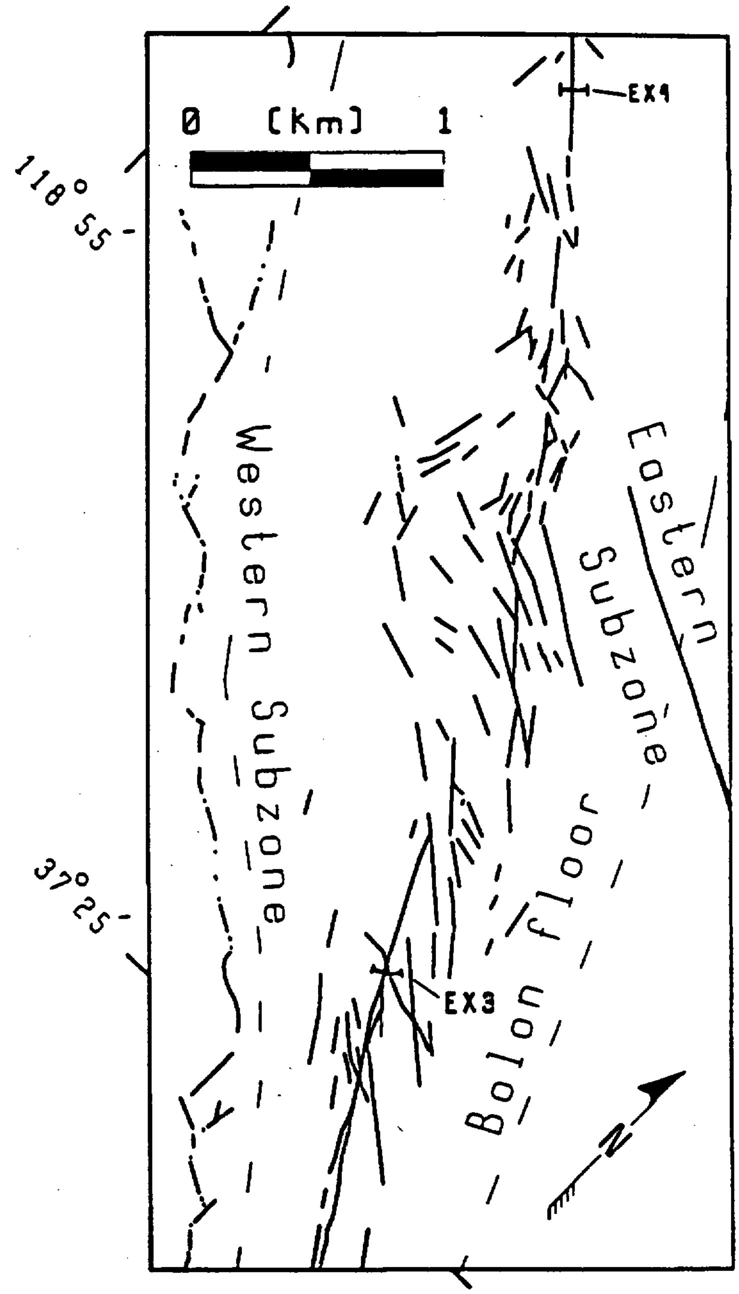

Figure 21. Detailed map of a portion of the southern Fish Lake Valley fault zone showing the pattern of vegetation lineaments on the bolson floor of southern Fish Lake Valley. At Excavation Sites 3 and 4 (EX3 and 4) exploratory trenches were excavated across prominent vegetation lineaments. Large-scale (1:12,000), low-sun-angle aerial photographs were used for a map base.

exploratory trenches excavated across three of these features support a fault related origin. Trench exposures (Plates V and VI) indicate that fracturing and in at least one trench (i.e., at Excavation Site 3) faulting of playa sediments directly below the vegetation lineaments (discussed in Chapter VII).

On the bolson floor of southern Fish Lake Valley a throughgoing fault is absent, and instead several discontinuous northwest- and north-northwest-striking faults form an én echélon arrangement (Fig. 21). The longest faults (up to about 3 km in length) tend to have average strikes of about N40° to 45°W, faults of intermediate length strike about N60°W, and those having the shortest lengths strike about N15° to 30°W. Many of the north-northwest-striking faults are about 30° (or less) east of the northwest-striking faults, suggesting that they are Riedel (R) shears developed within a northwest-striking right-slip fault zone. If this is the case, then northwest-striking faults may be P-shears. Due to their orientation, P-shears theoretically should display a component of convergence. A slight apparent reverse displacement is shown in Plate V where the trench at Excavation Site 3 crosses a vegetation lineament (Fig. 21), supporting the hypothesis that the lineaments delineate shears developed in a right-slip fault zone.

The patterns of the above shears (Fig. 21) are similar to those developed in clay filled shear boxes under initial or early strain states (e.g., Tchalenko, 1970, Fig. 4). Experimentally formed fractures have orientations and respective lengths that are similar to those developed in the valley fill, suggesting that the latter developed within a right-lateral strike-slip fault zone. Furthermore this structural pattern, when evaluated in context of the evolution of a strike-slip fault zone (cf. Harding and Longwell, 1979), appears to resemble that of an incipient or proto strike-slip strike-slip fault. Perhaps the rate of sedimentation in southern Fish Lake Valley is sufficiently high to prevent the southern FLVFZ from being displayed as a more mature fault zone, as it is to the northwest.

The Eastern subzone extends northwestward (N35° to 40 °W) across the piedmont slope flanking the eastern White Mountains, and forms a prominent down to the east, degraded scarp. In contrast to the southern extension of the subzone, the northern extent appears to have been less active during the Holocene, based on geomorphic evidence.

West of Oasis and between the piedmont and valley-floor traces, there is a small-scale (about 3/4 km) left-step in the Eastern subzone. "Cemetery" ridge lies within the step, oriented diagonally between two prominent fault traces (Plate IIE). The west-northwest-striking (about N75°W) ridge is strongly asymmetric in north-south profile, exhibiting steeper slopes along its south side. The prominent fault trace that forms the western leg of the step continues southward past the ridge, and then bends westward, where it apparently joins with the Western subzone near Cottonwood Creek (Fig. 18). A group of more than 5 subparallel fault traces abut the south side of the ridge and are not expressed north of it. The easternmost fault trace continues to the south and forms a scarp in Holocene alluvium that is delineated by springs. Prominent well-defined geomorphic features displayed by this trace indicate that it is the most active of the group. Fault traces become progressively more degraded and apparently less active to the west.

The proximity of the ridge to the step, its orientation and asymmetric profile, and its relationship to the group of subparallel faults (i.e., they are apparently terminated by it), suggest that it is a pressure ridge formed by movement along a south-southwest vergent contractional fault within a restraining step of the Eastern subzone. Further, these relations suggest eastward migration of the active fault trace south of the ridge, and related eastward propagation of the contractional fault along which the pressure ridge developed.

To the north (about 10 km), there is a gradual westward bend of approximately 30° in the Eastern subzone (Fig. 19). The average strike changes from N35°W, where a down to the east normal component of displacement is prominent, to N50°W with less significant vertical displacement, and eventually (between Iron and Wildhorse Creeks, Fig. 18) to about N65°W with variable vertical displacements. The more westerly trending sections of the subzone exhibit braided and anastomosing patterns of individual fault traces.. The larger faults define small-scale fault blocks, generally less than 1 km in length, that are obliquely traversed by relatively minor traces (Fig. 22). Typically, adjacent blocks along strike display opposing vertical displacements, where one block is relatively uplifted and another is

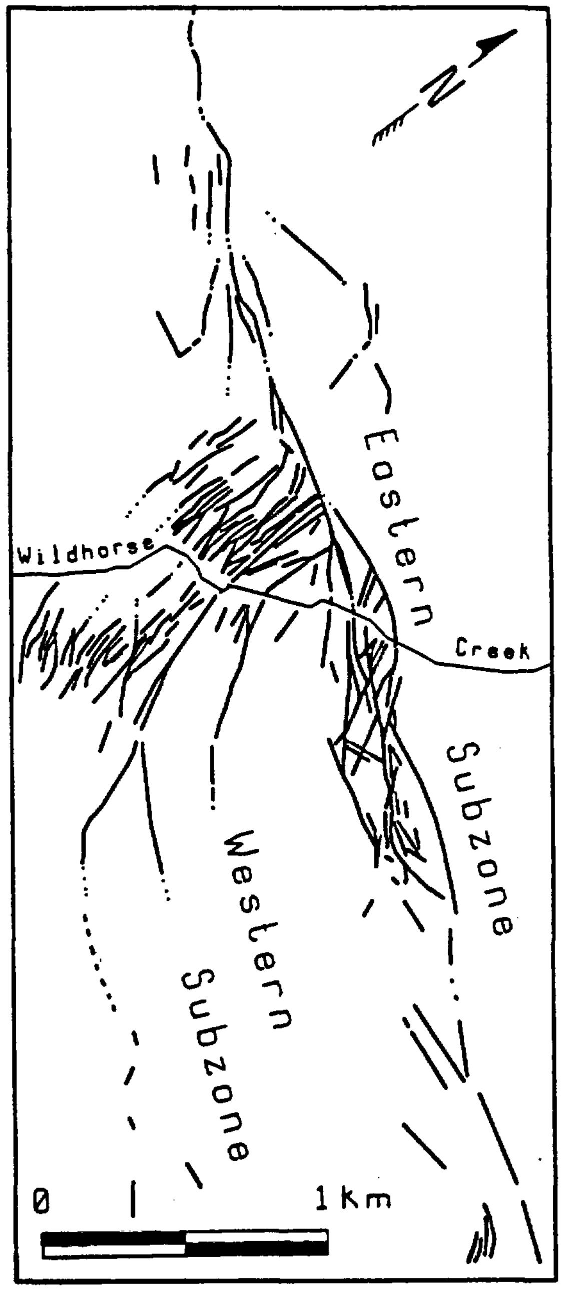

Figure 22. Detailed map of the junction of the Eastern and Western subzones of the southern Fish Lake Valley fault zone on the Wildhorse Creek fan in west-central Fish Lake Valley. Note the braided pattern of the Eastern subzone and the arcuate pattern of the Western subzone as it approaches the former. Large-scale (1:12,000), low-sun-angle aerial photographs were used for a map base.

downdropped and commonly buried by fine-grained ponded sediment. Some of the uplifted blocks (e.g., on the southern Furnace Creek fan) stand as much as 40 m above the surrounding fan surfaces and generally display little evidence of dissection.

Fine-grained ponded sediment has accumulated within a small enclosed basin atop a downdropped fault block on the Furnace Creek fan. M.C. Reheis (1989, personal commun.) augered a hole by hand into the fine-grained sediment. At a depth of about 1.5 m the Mazama ash (ca 6700 ka) was encountered - this is its southernmost known occurrence. At no depth in the approximately 6 m-deep hole were gravel or sand layers encountered, suggesting a considerable thickness of the fine-grained sediment and a comparable amount of relative downdrop of the fault block. If the rate of sedimentation within the enclosed basin was constant, which is not known, then the base of the hole encountered sediments that are roughly 30 to 35 ka old. Since deposition of the ponded sediment, and probably much longer, thefault block remained relatively downdropped, indicating that the braided pattern of faulting has persisted.

Braided structural patterns of the fault zone and variable vertical displacements along short sections of linear faults are a common characteristic of strike-slip faults. Thus the character of the northern section of the Eastern subzone, indicates strike-slip faulting. Further, the character of the fault zone here is similar to that displayed by strike-slip faults of "mature" structural development (cf., Harding and Longwell, 1979). The character of the fault zone therefore indicates that strike-slip movement predominates and has for some time (during at least the late Pleistocene). However, vertical displacements within and across the fault zone suggest the faulting style is right divergent.

The predominantly right slip style of faulting along this section of the FLVFZ is generally consistent with that determined by Brogan (1979). Brogan proposed that three abandoned drainages on the southern Furnace Creek fan exhibit 60 to 120 m of right slip with insignificant vertical slip across two sub-parallel faults (valley side relatively downdropped), thus indicating a predominance of right slip.

Evidence supporting predominantly right slip along the Eastern subzone of the FLVFZ includes: stratigraphic and structural relations exposed along a breached shutter ridge and in two exploratory trenches within the southern part of the subzone; a series of fault traces in playa sediments arranged similar to those developed in shear box experiments and characteristic of proto-strike-slip fault zones; a probable pressure ridge oriented obliquely within an apparent restraining left step; and furthermore a pattern similar to that of a "mature" strike-slip faults displayed by the northern part of the subzone. Additionally, a systematic and rather predictable change in the style of faulting with changes in fault orientation, also infers a strike-slip style.

WESTERN SUBZONE

The western subzone of the southern FLVFZ forms the linear eastern rangefront of the northeasternmost Inyo Mountains (Fig. 2). Here the fault is inferred primarily from the linearity of the rangefront. However, there are few subdued fault scarps in Pleistocene alluvium along this portion of the subzone. Additionally, a few faults branch northward, extend to the valley floor, and apparently join with the Eastern subzone (Fig. 21).

Along the Western subzone to the northwest, where Highway 63 enters Fish Lake Valley from the west, there is a little more than a 0.5 km left step in the front of the range; this is the somewhat arbitrary boundary between the northern Inyo Mountains and southern White Mountains (Plates IIA and IIE). The step coincides closely with the projection (through alluvium) of an unnamed, northeast striking, left-lateral strike-slip fault, as shown by McKee and Nelson (1967). Presumably, they determined the sense of movement from an apparent mismatch (of roughly 1.2 km) of the Cambrian Mule Spring Limestone and rocks of the Saline Valley Formation (which have limited extent in the immediate area) and two Jurassic plutonic bodies across the structure. It is tempting to speculate that the left step in the rangefront is a result of left slip on the northeast-striking fault. However, the movement history of the fault has not been established. Recent mapping by Reheis (1990c) suggests that Cottonwood Creek flowed southeastward across this fault around the time of the Bishop tuff eruption (0.74 Ma). The projection of this former drainage crosses the fault with no apparent deviation, suggesting that significant left slip has not occurred since eruption of the tuff.

Between Highway 63 and Cottonwood Creek (to the north), the Western subzone is poorly expressed, whereas several more northerly-striking branch faults are prominent and join with the Eastern subzone (Figs. 16 and 17). The subzone strikes N35°W (average) from Cottonwood Creek to just south of Furnace Creek and forms small, well-defined, fault scarps where it displaces probably late Holocene fan surfaces (i.e., equivalent to the middle or early Marble surfaces) and oversteepened, larger, somewhat degraded fault scarps in older surfaces. It is the opinion of the author that these "fresh" appearing scarps represent a recent (possibly late Holocene) paleoseismic surface faulting event(s) (described in Chapter VIII).

The Western subzone north of Furnace Creek is poorly expressed by short discontinuous scarps in alluvium and by apparently truncated bedrock salients (i.e., triangular facets) along the front of the range. It is of interest to note that roughly where the Western subzone becomes poorly expressed to the north, the Eastern subzone exhibits "fresh" appearing scarps in most probably Holocene alluvium, whereas the opposite is apparently true as far south as Oasis, California. This suggests that recent activity has stepped back and forth from the Western to the Eastern subzones.

This portion of the Western subzone (i.e., that north of Highway 63) forms the rather sinuous rangefront of the southeastern White Mountains. The sinuous range-bounding pattern, the apparently consistent magnitude of vertical displacement, and the absence of features characteristic of strike-slip faults, suggests that the normal component of displacement is significant (dominant?) along this part of the Western subzone. If the inference is correct, then in addition to activity alternating between the subzones, the Eastern and Western subzones function to partition strain, with right-divergent slip and normal slip concentrated along the subzones (respectively).

JUNCTION OF SUBZONES

The Eastern and Western subzones join in a complex and informative surface faulting pattern, in west-central Fish Lake Valley (Fig. 22). As the Western subzone approaches the junction on the WildHorse Creek fan (Fig. 18), it splays into numerous arcuate traces that bend abruptly north-northeastward as they near the Eastern subzone. Most of the arcuate traces are truncated, but a few bend into near parallelism with the throughgoing Eastern subzone (Fig. 22). The arcuate to Z-shaped traces of the Western subzone appear to have been drag-folded by right slip along the dominant Eastern subzone.

NORTHERN FISH LAKE VALLEY FAULT ZONE

The northern FLVFZ comprises the "Dyer" and "Northern" subzones (Fig. 20). North of the previously described junction, the principal displacement zone bends northward and forms the eastern front of the White Mountains. This northerly striking portion of the fault zone, about 10 km in length, is the Dyer subzone. The Dyer subzone connects the northwest-striking Eastern and Northern subzones in a large-scale, én echélon, right step in the central FLVFZ. The Northern subzone steps out about 1 km from the range front at Leidy Creek, branches north to northeastward, and eventually terminates by bending east-northeastward in northwestern Fish Lake Valley (Fig.18). A few nearly east-west striking, down to the south fault scarps have been identified (in this study) as far north as the upper part of the abandoned Trail Canyon fan and along Rock Creek, where it traverses Wildhorse Flat (about 3 and 5 km north of the prominent surface faulting, Fig.18).

Geomorphic and structural (i.e., patterns of surface faulting) evidence, supplemented by regional seismicity and gravity studies are presented in the following subsections. These data indicate that the style of faulting along the northern FLVFZ varies systematically with changes in strike of the fault zone, similar to the southern fault zone. Specifically, right slip on northwest striking faults, right-divergent slip on north-northwest striking faults, and normal slip (and possibly left-divergent slip?) on north- to northeastward-striking faults. Additionally, faults of all orientations and apparent styles of faulting disrupt the late Pleistocene Indian unit. This suggests contemporaneous activity on faults having several different orientations and styles.

DYER SUBZONE

The Dyer subzone extends from north of the junction between the Eastern and Western subzones in west-central Fish Lake Valley (Fig. 20), to about Busher Creek, northwest of Dyer, Nevada (Figs. 18 and 20). The northerly-striking subzone comprises a single master fault that bends about 35° northward (from N50°W to N15°W), on the Toler Creek fan and forms a linear escarpment along the eastern front of the White Mountains. Compound fault scarps as much as 80 m or more high, on the Perry Aiken Creek and McAfee Creek fans near Dyer, Nevada, are evidence of a substantial component of vertical displacement on the Dyer subzone.

Bryson (1937) studied the faulted fanhead of the Perry Aiken Creek fan, southwest of Dyer. Bryson measured compound scarps 80 m or more high with slope of 30° to 35°, that display little evidence of dissection. The extensively faulted fanhead is probably equivalent in age to the late Pleistocene Indian unit. Bryson also noted that the amount of vertical displacement along the FLVFZ varied systematically, but was most prominent where the fault zone had a northerly strike (N15°W). Bryson considered strike-slip faulting to explain the variation in magnitude of vertical displacement along the FLVFZ, but dismissed it in favor of normal faulting on a moderately dipping (70°E) fault plane.

Bryson (1937) also observed that the bedrock escarpment above the Perry Aiken Creek fan is an exhumed and older fault plane that forms prominent triangular facets. The triangular facets are comprised of quartz monzonite of Marble Creek (Bryson's "Pellisier Granite") and display what appears from a distance to be "pseudo-sedimentary" structures (Emerson, 1966). These subparallel bands were first noted by Anderson (1937) and subsequently were considered examples of granitization (e.g., Longwell and Flint, 1962; as pointed out by Emerson, 1966). Emerson concluded that the bands are iron-stained weathering zones that developed along the contact between bedrock and fan gravels. Further that the bands, which are spaced about 6 m apart, were exposed by intermittent movements along the Dyer subzone. Emerson postulated that the intermittent displacements were comparable in size to the spacing between bands (i.e., dip-slip displacements of about 6 m per event).

The Bishop (?) tuff (0.74 ma) outcrops below the McAfee Creek surface, within the McAfee Creek fanhead trench (M.C. Reheis and J. Slate, 1988, personal commun.). The McAfee Creek surface is uplifted (relatively) about 60 m along the master fault. South of McAfee Creek, the fault displaces the Indian surface about 35 m, valley side down. Prominent fault scarps also occur in younger fan surfaces. Hence, significant vertical displacement characterizes the Dyer subzone, and has since at least the mid Pleistocene.

The relative significance of vertical displacement on the northern FLVFZ, is shown by comparing the area of drainage basins to that of alluvial for some of the larger drainage-fan systems in the study area (below). The basic premise is that intermittent uplifts of the White Mountains structural block along the fault zone result in offset of stream channels, and thus in non-graded drainage-fan systems. These systems responded by incising their uplifted reaches and aggrading their downdropped reach, and with time, reestablishing a graded profile. This results in enlargement of drainage basins and in burial of alluvial fans. Thus, rather than prograding into the valley as fans in the Plate I area have done (e.g., those of Indian Creek and Leidy Creek), the Perry Aiken Creek and McAfee Creek fans aggrade. Thereby increasing the ratio of drainage-basin area to fan area.

Bull (1962 and 1964) showed that the area of an alluvial fan increases at about the same exponential rate as the drainage-basin area increases (i.e., the ratio of areas is commonly about 1:1), even where there are considerable differences in lithology. This is generally the case for the Indian Creek and Leidy Creek fans, which have ratios of drainage-basin area to fan area of 1.4 and 2.1 (respectively). In marked contrast, the Perry Aiken Creek and McAfee Creek drainage-fan systems have ratios of 15.1 and 25.2. Beaty (1960) noted that the latter two systems comprised among the largest drainage basins in the White Mountains, that of Perry Aiken Creek is the largest, but have "ridiculously" small fans. Clearly, as Beaty concluded, recent vertical movements along the Dyer subzone have uplifted the fanheads and downfaulted the mid- and lower-fan position, resulting in burial of the latter. It is evident from these ratios that vertical displacement is much more significant along the Dyer subzone than along the Northern subzone.

It is perhaps coincidental that the highest point along the crest of the White Mountains, White Mountain Peak at 4,342 m (14,246 ft), is along that portion of the FLVFZ (i.e., Dyer subzone) that is characterized by the highest fault scarps anywhere in Fish Lake Valley. If this relationship is not merely coincidental, which is strongly advocated by the author, then it suggests that vertical slip along the Dyer subzone have had long-term significance. It is probable that uplift along this section of the FLVFZ coupled with probably greater uplift along the White Mountain fault zone (at western front of the range) have contributed to the considerable height of the range crest.

Long-term importance of vertical movements along the Dyer subzone is supported by an isostatic residual gravity survey of the region (unpub. data, B. Mcffee, 1987, written commun. to C.M. DePolo). A well-defined gradient in the survey data immediately valleyward of the Dyer subzone indicates a prominent gravity low (about 18 mgal) in this part of the valley. The gravity low suggests the presence of a substantial thickness of low density sediment, probably interfingered fan alluvium and valley fill. The apparent thickness of the sediment suggests the Fish Lake Valley structural block has been downdropped considerably, relative to the White Mountains block along the Dyer subzone. This supports the inferred significance of vertical displacements along the Dyer subzone.

NORTHERN SUBZONE

The Northern subzone extends northwestward from a probable releasing bend, which connects on the south to the northerly striking Dyer subzone (Fig. 20). North of the bend, the subzone comprises a master fault and several subparallel subsidiary faults that form a distributive left-stepping structural pattern. A few faults branch northeastward from just north of the bend, and form a right-stepping én echélon pattern that traverses the lower Leidy Creek fan (Fig. 18). Most of the branch faults extend to the valley floor, where they are apparently buried by valley fill. However, a few faults on the lower Leidy fan splay northwestward from these branch faults, and may connect to a group of northerly striking faults on the lower Indian Creek fan (Fig. 18; discussed below). The left-stepping pattern north of the bend and the right-stepping pattern of branch faults are consistent with right-slip and left-slip on northwest- and northeast-striking (conjugate?) faults, respectively.

Fish Lake Valley broadens markedly along the strike of the northeast-striking branch faults. When projected about 4 km across the valley, the branch faults are approximately on strike with the southern Emigrant Peak fault zone, a prominent, distributive (4 km or more wide), normal fault (Reheis, 1990) that essentially forms the northeastern margin of Fish Lake Valley. It is possible, as discussed below ("Kinematic Model"), that displacement on the FLVFZ may be transferred across northern Fish Lake Valley to the Emigrant Peak fault zone. In that case, the northeast-striking branch faults on the Leidy Creek fan, those on the Indian Creek and Chiatovich Creek fans, and those along the southern boundary of the Volcanic Hills (discussed below), may transfer displacement from one fault zone to another. In this view, northern Fish Lake Valley is a region of extension, associated with strike-slip faulting along the FLVFZ (discussed further in following sections).

The Northern subzone forms a right step, or more correctly a double bend, of about 1 km at Leidy Creek (Fig. 18). Within the double-bend, the master fault strikes northward (N5°E) and is delineated by a continuous, geomorphically "youthful" fault scarps in Leidy to middle Marble fan surfaces. West of the bend, the late Pleistocene Indian unit forms the uplifted Leidy Creek fanhead. This fanhead remnant is disrupted by more than 15 well-defined faults in a distributive zone, more than 1 km wide. North of the bend, the master fault strikes northwest (N35°W) and exhibits clear evidence of right slip (discussed in "Case Study 1").

The double bend is probably divergent in character, resulting from right slip along two én echélon portions of the northwest-striking Northern subzone. This apparent divergent double bend is consistent with, but on a smaller scale than, the divergent character of the Dyer subzone, which obliquely connects the predominantly right slip Eastern and Northern subzones of the central FLVFZ (discussed above).

North of the bend, the master fault of the Northern subzone strikes N35°W (average) and maintains a distance of about 1 km valleyward of the eastern front of the White Mountains. Several northerly striking faults on the mid and lower Indian Creek fan appear to be splays of the master fault on the Marble Creek fan (Figs. 18 and 20), although the structural relations are mostly buried by late Holocene alluvium. North of Marble Creek, the master fault gradually bends northward and strikes about N15°W across the Indian Creek fanhead.

The master fault and branch faults of the Northern subzone have different orientations and apparent styles of faulting. Geomorphological and structural evidence suggests that the Quaternary tectonic activity along this subzone is characterized by right slip on northwest-striking faults, right-divergent slip on north-northwest-striking faults, and normal slip on north-striking faults (discussed below). Left slip may occur on northeastward-striking faults, but supporting evidence is largely circumstantial.

Northwestward-Striking Faults

The principal displacement zone of the Northern subzone comprises a master fault and several subparallel subsidiary faults. This group of northwestward-striking (N35°W) faults cross the Marble Creek fan and bend northward within the interfan valley. The master fault strikes north-northwest (N15°W) across the Indian Creek fanhead (Fig. 18). Where the master fault traverses Marble Creek it apparently branches northward into a group of north- to north-northeast-striking faults on the mid and lower Indian Creek fan (discussed in the next section). Geomorphic evidence from the northern Leidy Creek ("Case Study 1") and southern Indian Creek fans ("Case Study 2") indicate right-slip is the dominant component of displacement on the northwest- to north-northwest-striking master fault of the Northern subzone.

Where the master fault traverses the northern Leidy Creek fan the style of faulting is determined from an EDM/theodolite survey (Appendix V, EDM Project

2; see "Case Study 1") of a pair of offset ballenas; i.e., well-rounded ridgeline remnants of fan alluvium (Peterson, 1981). These fan remnants are offset in a dextral sense along the master fault. The ballena remnants east of the fault form shutter ridges that divert onfan drainages northward along the fault. The characteristic pattern of solifluction steps, supported by a host of other surficial characteristics and morphostratigraphic relationships indicate that the ballenas are remnants of an late Pleistocene Indian fan surface, and therefore the ballenas are post-Indian in age.

Figure 23 is a topographic map based on the survey data that shows probable projections of the ballena crests. The longitudinal profiles of the ballena crests are shown in Figure 24. In the next section (Case Study 1), the survey data is used to suggests that the northern ballena crest is displaced about 90 m (+15/-20 m) by right slip with little (about 5 ± 5m, apparent reverse), if any, vertical slip. The minor vertical displacement that is suggested, is reverse in style, and perhaps is related to the arcuate trace on the master fault (Figs. 20 and 23).

On the Marble Creek fan, unequivocal evidence of strike-slip faulting has not been recognized. However, the fault pattern and at least one geomorphic feature suggest strike-slip displacement. The master fault traverses the Marble Creek fan without deviation in strike (Plate I). This suggests a high-angle fault plane, consistent with strike-slip faulting. The master fault forms an asymmetric fault scarp where it crosses a flattish interfluve on the southern Marble Creek fan. The scarp is prominent on the northern shoulder of the interfluve, but is nearly absent on the southern shoulder. This suggests that the "nose" of the interfluve was displaced right laterally. These relations suggest that right-oblique slip predominates on the northwest-striking master fault where it traverses the Marble Creek fan.

The master fault of the Northern subzone forms a nearly continuous zone of well-defined scarp in Holocene fan surfaces in the interfan valley between the Marble Creek and Indian Creek fans (Plate I). Structural and stratigraphic relations exposed in an exploratory trench at Excavation Site 2 (Fig. 20) suggest recurrent Holocene activity has occurred on the master fault (discussed in Chapter VII).

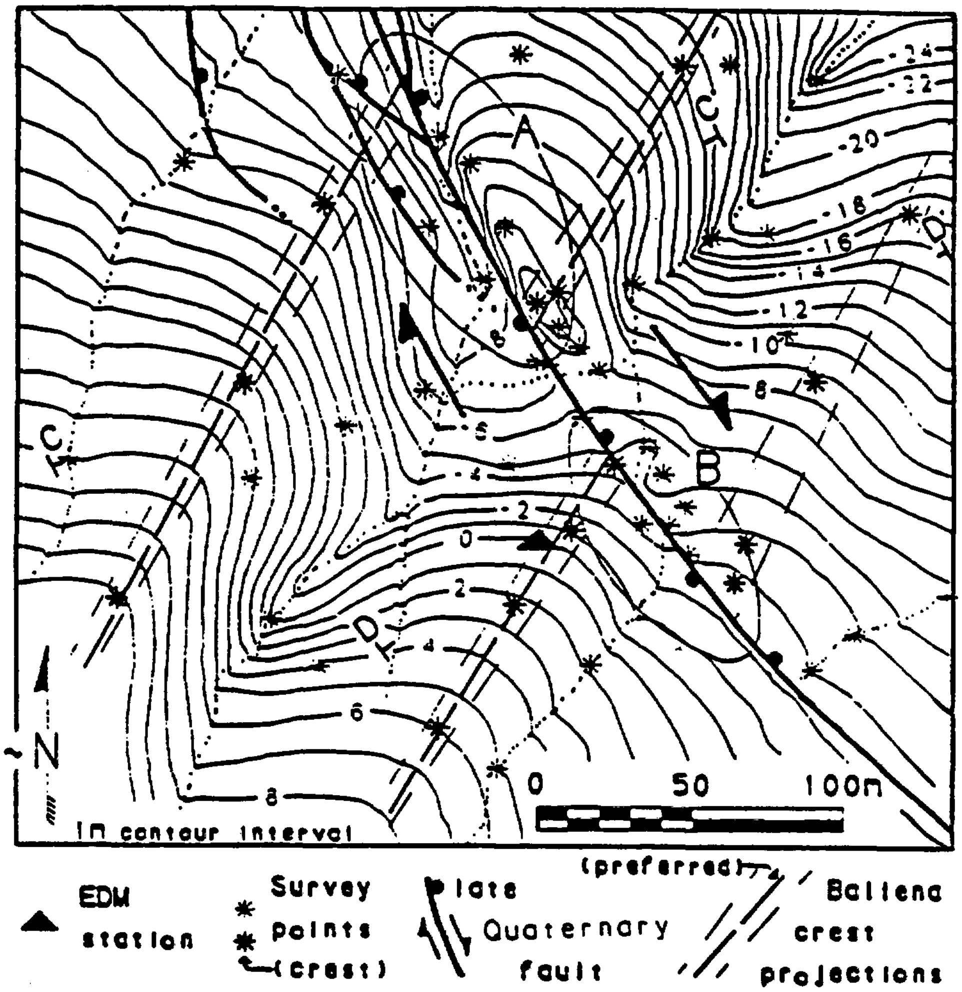

Figure 23a. Large-scale topographic map of a pair of ballenas offset in a right lateral sense across the Northern subzone of the Fish Lake Valley fault zone. See shutter ridge in Figure 20 for location. The map is based on a EDM/theodolite survey (Appendix V, EDM Project #2). Note that there is no preferred projection of the southern ballena remnant east of the fault, because it has been significantly modified by erosion.

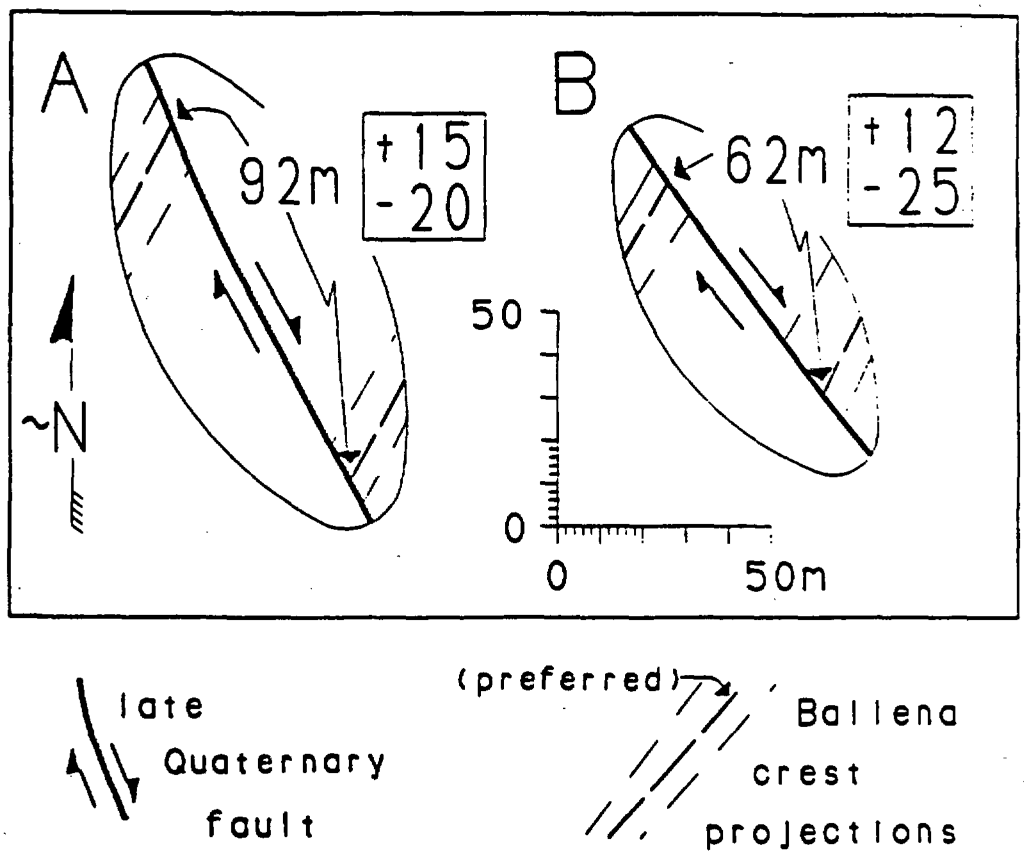

Figure 23b. "A" and "B" are enlargements from Figure 23a showing the amount of right lateral offset of the ballena crests across the Northern subzone.

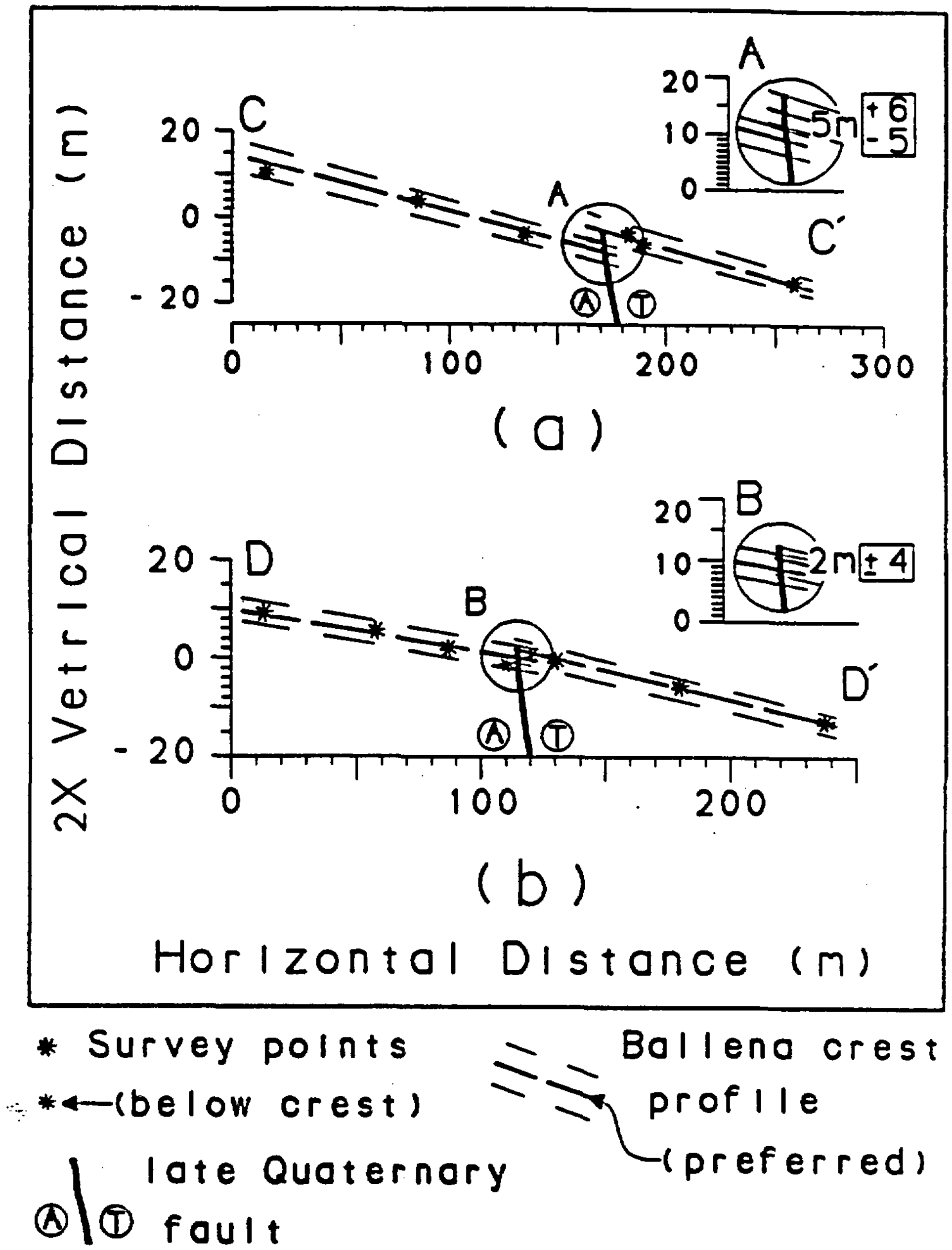

Figure 24. Longitudinal profiles showing the vertical separation of the northern (a) and southern (b) ballenas crests in Figure 23 (C-C' and D-D'). Note that little if any vertical separation is required, however that which is allowed is reverse in nature.

The master fault, where it traverses the southern Indian Creek fan, forms a continuous, large (up to about 50 m high), down-to-the-east scarp, that shows little evidence of dissection. A subsidiary fault strikes subparallel to the master fault and is located about 350 m to the east (Plate I). A branch fault extends northeastward from a 15° to 20° bend in the master fault, near the southern margin of the Indian Creek fan. This down-to-the-south branch fault lies diagonally between and connects the master fault with the subsidiary fault, forming a small-scale, rhombohedral-shaped fault block.

The north-northwest-striking (N20°W) master fault displaces an abandoned drainage channel on the Indian Creek fanhead. The channel can be physically traced from west of the master fault, across it and the subsidiary fault to the east, and about 1 km beyond (Plate I). The channel is only shallowly incised into the Indian surface and is flanked by degraded lateral debris flow levees, that have solifluction steps. These relations suggest that the channel was transporting debris to and across the Indian surface. Therefore, the drainage developed during, or shortly after, the late Pleistocene Indian surface.

An EDM/theodolite survey of the offset channel provides the basis for determining the style of faulting along the N20°W-striking master fault of the Northern subzone (Appendix V, EDM Project 3). Figure 25 shows probable and conservative projections of the displaced channel. In a following section ("Case Study 2"), these projections are used to suggest about 120 m (± 40 m) of right slip along the master fault during the late Pleistocene.

Figure 26 shows longitudinal projections of the channel. The survey data, when erosional modifications are considered, suggests that the present thalweg of the channel is displaced vertically about 40 m (± 13 m) (east side relatively downfaulted) across the master fault. Little (or no?) lateral displacement of the channel is required where it crosses the subsidiary fault to the east (Plate I), but perhaps as much as 15 to 20 m of right slip is possible.

The survey data from the Indian Creek fanhead indicates that right-divergent slip characterizes the N20°W-striking master fault of the Northern subzone. Further, the data suggests lateral to vertical displacement ratios of 2:1 to about 5:1.

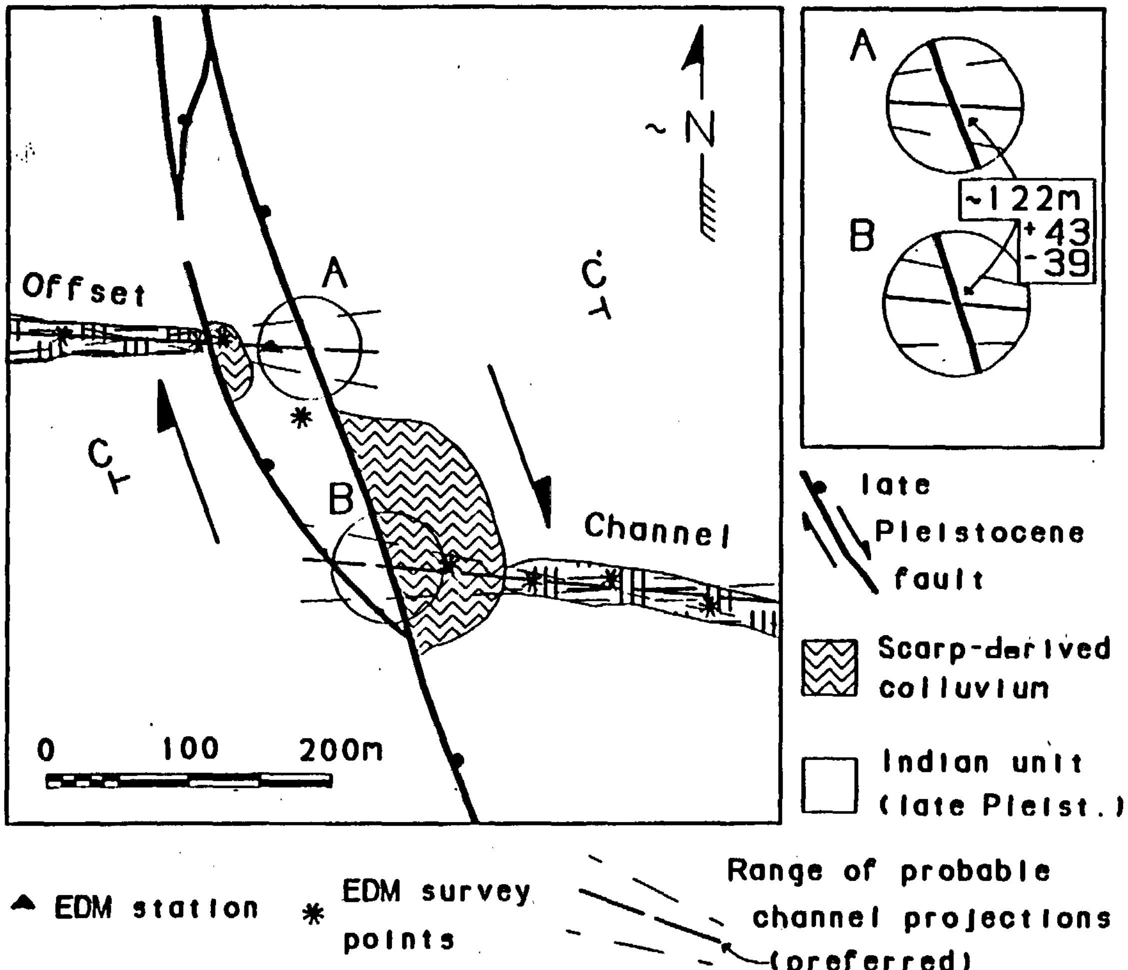

Figure 25. Large-scale map of a drainage channel offset across the Northern subzone of the Fish Lake Valley fault zone on the Indian Creek fanhead, based on a EDM/theodolite survey (Appendix V, EDM Project 3). See offset channel in Figure 20 for location. In the upper right corner of the figure, are enlargements of "A" and "B" showing the amount of right lateral offset.

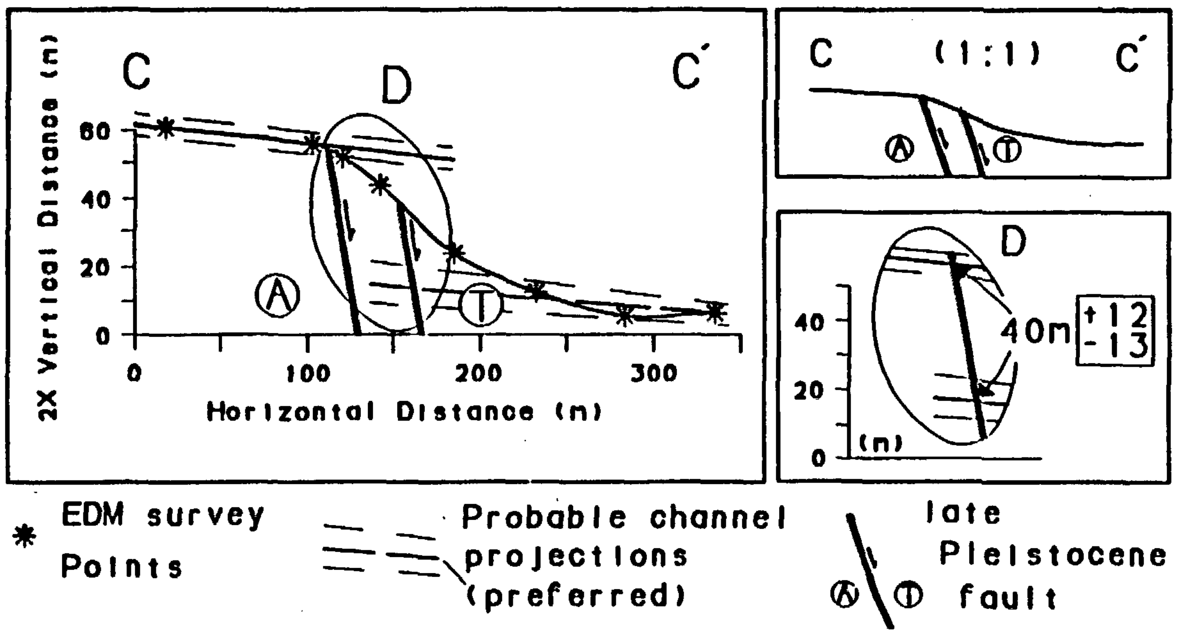

Figure 26. Longitudinal profile of the offset drainage channel in Figure 25 (C-C') across the Northern subzone. The profile in the upper right corner of the figure is shown without vertical exaggeration. In the lower left corner, inset "D" shows the amount of vertical separation of the channel.

The northward extension of the master fault, where it traverses the northern Indian Creek fan, displays a distinct left-stepping pattern, suggestive of right-slip (Figs. 18 and 20). Immediately south of the point where the fault crosses Indian Creek, it forms a well-defined scarp (Appendix VI, Profile P23) in a Leidy age (mid Holocene to latest Pleistocene) inset fan remnant. A small onfan drainage is shallowly incised into the inset fan and appears to be offset right laterally across the fault. The displacement of the channel is evaluated in a the following section ("Case Study 3"). This evaluation suggests that the drainage is displaced less than 15 m and more than about 3 m in a right lateral sense across the master fault. The vertical displacement of the Leidy surface is about 1 ± 0.3 m (Appendix VI, Profile P23). These data support the existence of predominantly right-divergent slip on the north-northwest-striking (N20°W) master fault of the Northern subzone.

To the north on the Chiatovich Creek fan, the master fault and associated north-northwest-striking faults abruptly bend north-northeast to northeastward and a few eventually bend to the east-northeast (Figs. 18 and 20). Some of these faults are delineated by vegetation lineaments on the floor of northwestern Fish Lake Valley. The projection of these faults is essentially on strike with those faults along the southern Volcanic Hills, about 3 or 4 km across the valley. The possible kinematic relationship between these faults is discussed in a following section ("Kinematic Model"). The northernmost geomorphic evidence of Quaternary surface faulting identified in the present study, is provided by two east-west-striking down-to-the-south fault scarps (both a few hundred meters in length) on the upper Trail Creek fan and along Rock Creek where it traverses Wildhorse Flat (Fig. 18).

North- to North-Northeast-Striking Faults

The north- to north-northeastern-striking group of faults prominently deform the late Pleistocene Indian surface on the mid and lower Indian Creek fan (Plate I). There are more than 20 individual, anastomosing and subparallel faults within this group that form a distributed zone, which is at least 4 km wide. The total width of the FLVFZ on the Indian Creek fan is 10 km or more in wide.

The north- to north-northeast-striking closely-spaced group of faults on the Indian Creek fan forms an extensive graben complex. A multitude of small scale fault blocks that average about 300 m in width, but range from nearly 3/4 km to a few tens of meters, occur within this area of rather intense deformation. A few fault blocks east of the central graben, have probably been tilted eastward a few degrees. Differential displacement between adjacent blocks results in numerous beheaded and abandoned channels and in several diverted drainages. Of the abandoned channels that cross the north- to north-northeast-striking faults, none appear to display evidence of lateral displacement, but virtually all display prominent evidence of vertical displacements (Plate I).

The intense faulting of the mid and lower Indian Creek fan is evaluated by analysis of EDM/theodolite survey (EDM Project 1, Appendix V) and by scarp profile data (Appendix VI). Figure 27 shows a topographic profile of the Indian surface across the graben-complex, based on a nearly 3 km long EDM/theodolite survey. Each of the faults traversed by the survey line were profiled in detailed (Appendix VI) by the slope-stick method of Buchman and Anderson (1979).

In Figure 28 EDM Projects 1 and 3 are linked together via a topographic map. This figure documents the deformation of the Indian surface across the most significant faulting along the northern FLVFZ. Prominent, extension accompanied by significant vertical displacement (roughly 150 m), and tilted fault blocks characterize this portion of the FLVFZ.

Near the confluence of the south and north forks of Indian Creek in the Indian Creek canyon, there are two linear well-defined scarps. These northeastward-striking scarps project up the south fork to a fault mapped in the Precambrian Wyman Formation (Krauskopf, 1971). Anderson (1933) was the first to note the scarps and inferred that they were related to faulting. Bryson (1937) rejected this origin and considered them to be fluvial scarps. It is the author's opinion that the scarps are in fact of tectonic origin, and possibly are related to reactivation of an older bedrock fault. The scarps differ from the fluvial scarps of Indian Creek in that they are linear. Although they occur above the lowest obvious fluvial scarp (terrace riser), which is comparable in height and formed in similar materials, they

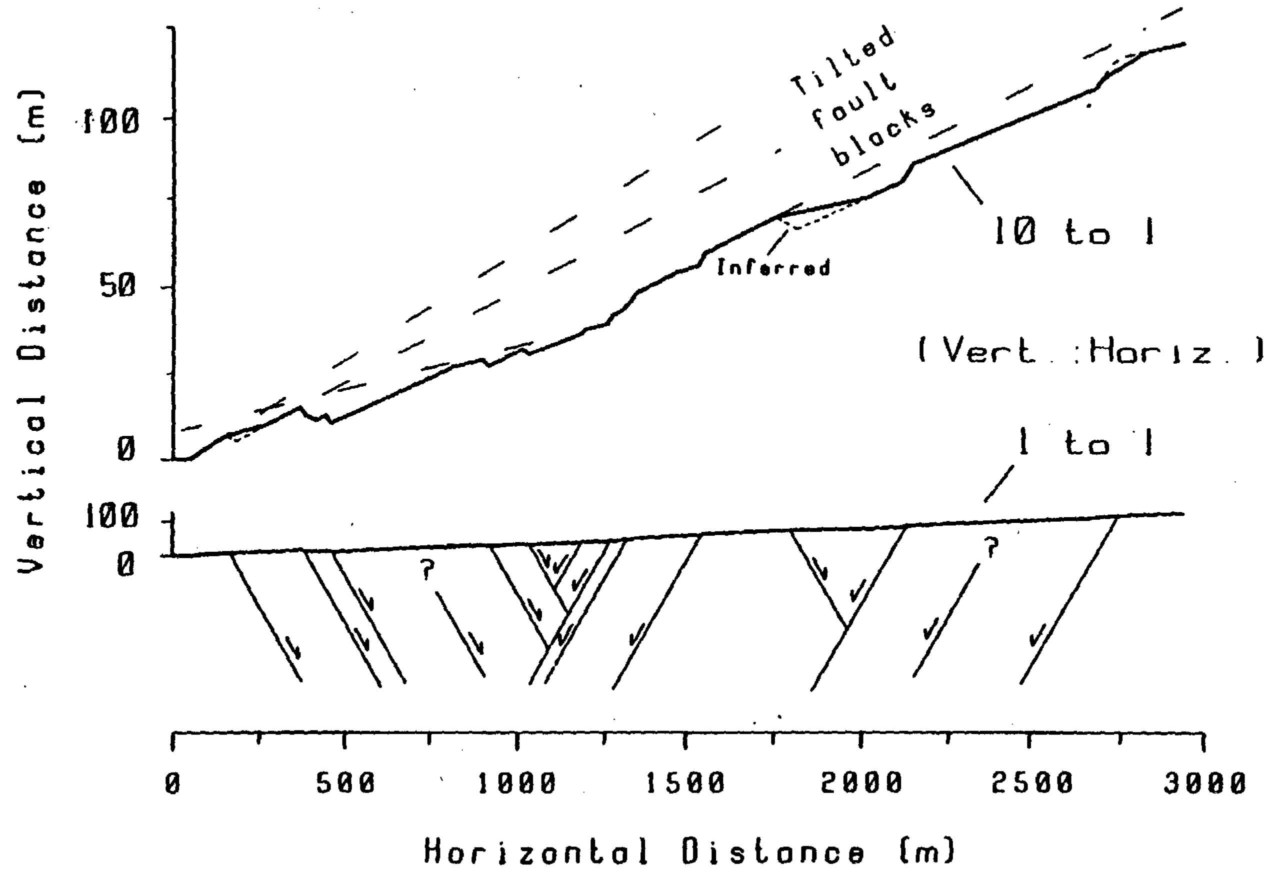

Figure 27. Topographic profile of the late Pleistocene Indian morphostratigraphic unit on a portion of the mid and lower Indian Creek fan based on a EDM/theodolite survey (Appendix V, EDM Project 1). See Plate I and Figure 29 for location of survey. The subsurface structure has been inferred from the style of surface deformation. Note that several small-scale fault blocks have apparently been tilted.

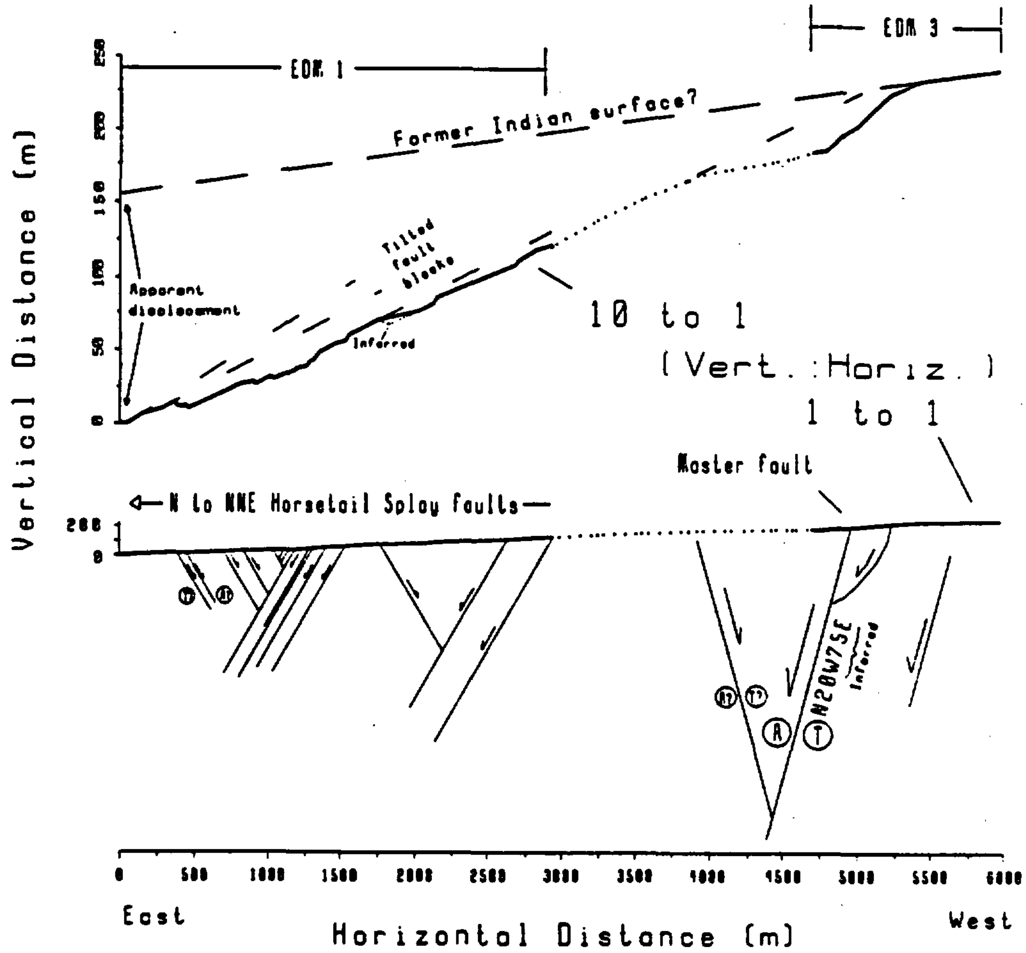

Figure 28. Topographic profile of the Indian morphostratigraphic unit on the Indian Creek fan based on two EDM/theodolite surveys (Appendix V, EDM Projects 1 and 3), which were connected using the Davis Mountain 15' Quadrangle (dotted line). A projection of the former Indian surface suggests that it has been displaced about 160 m vertically. The subsurface structure has been inferred from surface deformation.

have steeper slope angles. If they were fluvial scarps, they would be older than the lower fluvial scarp and therefore should have more gentle slopes. However, their slopes are steeper, supporting a tectonic origin and suggesting rejuvenation by intermittent faulting.

Termination of the Fish Lake Valley Fault Zone

Background Studies: Northwestern Fish Lake Valley provides a unique opportunity to study the termination of a regional scale strike-slip fault. Several studies have addressed the termination of the DVFS, including those by Albers (1967), Stewart (1967, 1970, 1985) and Albers and Stewart (1972). Albers (1967, p. 151 and Fig. 4) and Stewart (1967) proposed that the DVFS dies out to the northwest into large oroflexural folds, or contractional features of regional-scale. Thus, inferring that right slip on the FLVFZ is "absorbed" by folding and thrust faulting.

This model is in direct contradiction with the Quaternary tectonic setting of northern Fish Lake Valley, based on structural and geomorphic evidence presented in this study. The northwestern termination of the Quaternary FLVFZ (i.e., DVFS), probably differs greatly from Alber's (1967) and Stewart's (1967) models of oroflexural folding and contractional faulting. Rather, northern Fish Lake Valley is a region of marked extension and normal faulting associated with right slip on the FLVFZ.

The large-scale normal faults and widespread volcanism in northern Fish Lake Valley support the hypothesis that northern Fish Lake Valley is a region of extension. Carr (1984) indicated that volcanism is concentrated where right-lateral strike-slip faults terminate or connect with northeast striking left-lateral strike-slip faults. Such may be the case in northern Fish Lake Valley.

Northwestern Termination of the FLVFZ: In northwestern Fish Lake Valley the FLVFZ terminates by splaying, gradually bending northward, and eventually abruptly bending northeastward (Figs. 18 and 20). The closely spaced faults that prominently disrupt the middle and lower Indian Creek fan are branch faults splaying north to north-northeastward in a horsetail splay pattern (e.g., Sylvester, 1988, his Fig. 18) from the master fault of the Northern subzone. The intersection between the master fault and the branch faults is apparently buried by latest Holocene (mostly late Marble in age) alluvial deposits of the Marble Creek fan (Plate I).

The master fault and associated north-northwestward-striking faults of the northern FLVFZ make an approximately right-angle bend at Chiatovich Creek (Fig. 18). Between the northern margin of the Indian Creek fan and that of Chiatovich Creek fan, a distance of about 3 km, the north-northwest-striking (N15°W) master fault bends abruptly northeastward (N60°E) and displays a few nearly east-west (N75°E) striking fault scarps south of Wildhorse Flat. East-west-striking scarps have also been identified on the upper part of the abandoned Trail Canyon fan (3 km north), along Rock Creek just south of Pinto Hill (9 km north), and about 2 km up the Indian Creek canyon, near the confluence of the south and north forks of Indian Creek (discussed previously).

Where the FLVFZ terminates in northwestern Fish Lake Valley (Fig. 29), well-defined fault scarps occur from within the White Mountains to just west of Highway 3A (Plate IIB). Vegetation lineaments occur on the bolson floor and extend at least 1 km valleyward of the highway. The vegetation lineaments are similar to those known from exploratory trench studies in southern Fish Lake Valley (e.g., Plate V) to be faults. The distributive pattern of the northernmost FLVFZ is at least 10 km or more wide.

The lineaments and fault scarps on the lower Chiatovich fan, are generally on strike with the fault scarps at the foot of the southern Volcanic Hills. The two sets of faults are separated by 5 km (or less) of probable Holocene valley fill, which may conceal a throughgoing fault zone. In that case, the FLVFZ is joined in the subsurface to the faults at the foot of the southern Volcanic Hills. The northwestern termination would therefore be an intersection between the northwest striking FLVFZ and the northeastward striking faults of the southern Volcanic Hills.

Henceforth, "termination" simply implies the end of prominent surface faulting that characterizes the FLVFZ to the south. It does not preclude the possibility that the FLVFZ terminates at an intersection with northeast-striking (transfer?) faults, or that displacement is transferred to the Emigrant Peak, Coaldale,

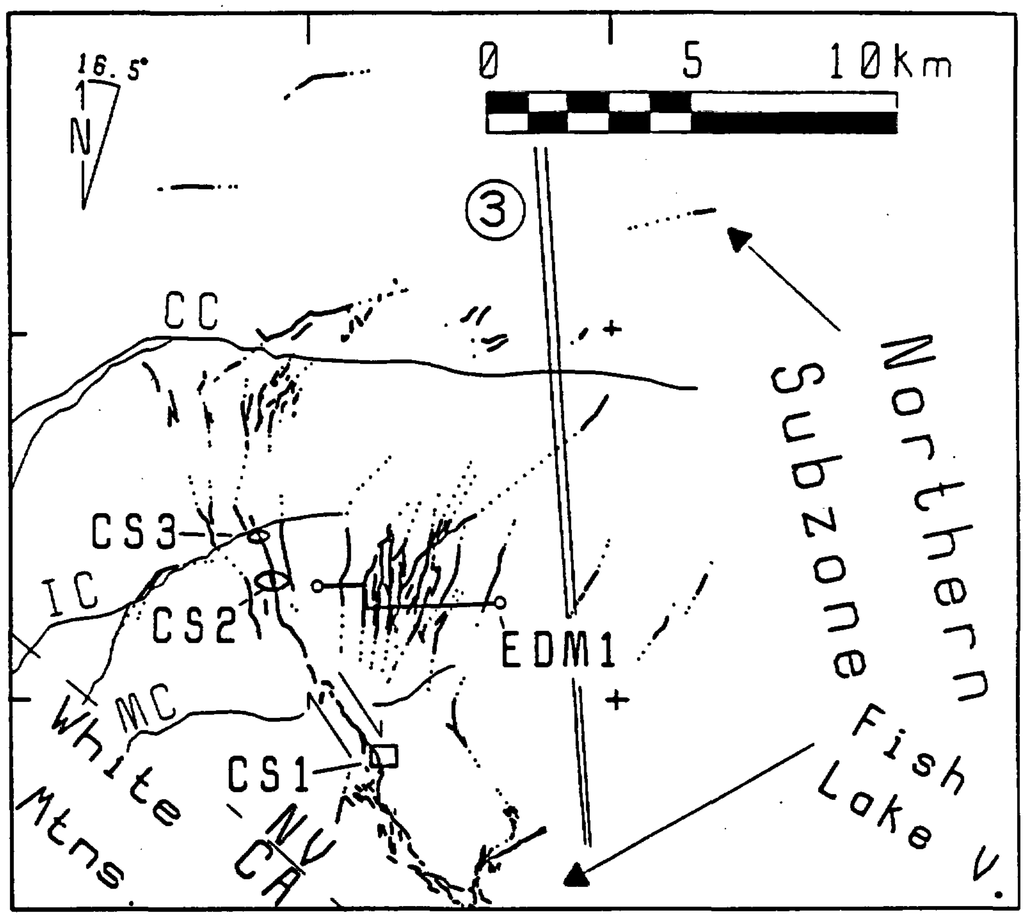

Figure 29. Map of the Northern subzone of the Fish Lake Valley fault zone showing that the fault zone terminates to the north in a horse tail splay pattern. The faults are dotted where inferred. Compare with Figure 18 for location of drainages. CS1, 2, and 3; Case Studies 1, 2, and 3; EDM1; EDM Project 1 (Appendix V); EX1 and 2; Excavation Sites 1 and 2.

and (or) other fault zones to the north and east.

The broad, distributive fault pattern of the northern FLVFZ (e.g., Figs. 18, 20, and 29) and prominent vertical displacements of the Indian morphostratigraphic unit (e.g., Figs. 24, 25 and 26) suggest general east-west (to west-northwest/east-southeast) extension during the late Pleistocene. This inferred extension direction accords well with that determined by Smith and Lindh (1978), Speed and Cogbill (1979), and Zoback and Beanland (1986 and 1988) for the surrounding region. Furthermore, the extension direction is supported by the northerly strikes of faults having a significant or dominant component of vertical displacement within the FLVFZ and the Emigrant Peak fault zone (Reheis, 1990).

Seismicity at the Northwest Termination of the FLVFZ: Earthquake epicenters within the southern Basin and Range Province typically do not show alignments along known surface faults (Ryall, 1973), but do tend to cluster at the ends or intersections of faults (Ryall and Ryall, 1980). The DVFS is no exception to these general observations. There are very few epicenters that can reasonably be shown to lie within the fault system (e.g., Real and others, 1978). A prominent cluster of seismicity, the most prominent anywhere along the nearly 350 km-long DVFS, occurs where the FLVFZ abruptly bends at its northern end (e.g., Fig. 30; Ryall and Ryall, 1983, Fig. 1; Slemmons and others, 1965, Fig. 3). Since 1910 there have been 48 earthquakes on magnitude (M_L) 4.0 or greater within this temporally persistent cluster of seismicity (Fig. 30), the largest of which was a magnitude 5.5. An earthquake of $M_L = 5.3$ occurred during a swarm of earthquakes in 1982 and 1983 (Univ. of Nevada, Reno, seismology laboratory, unpub. data) within this cluster. Only recently (1-14-90) a $M_L = 4.6$, followed by a energetic aftershock sequence lasting a few days, occurred in the northwestern corner of the valley (Univ. of Nevada, Reno, Seismological Laboratory). The inferred significance of clusters of seismicity (above) supports the hypothesis that the FLVFZ terminates, or intersects the northeast striking faults of the southern Volcanic Hills.

Vetter (1984) determined focal mechanisms for several earthquakes within the cluster of seismicity at the northern end of the FLVFZ, the larger of which are shown in Figure 31. Nodal plane solution for the various focal mechanisms indicate

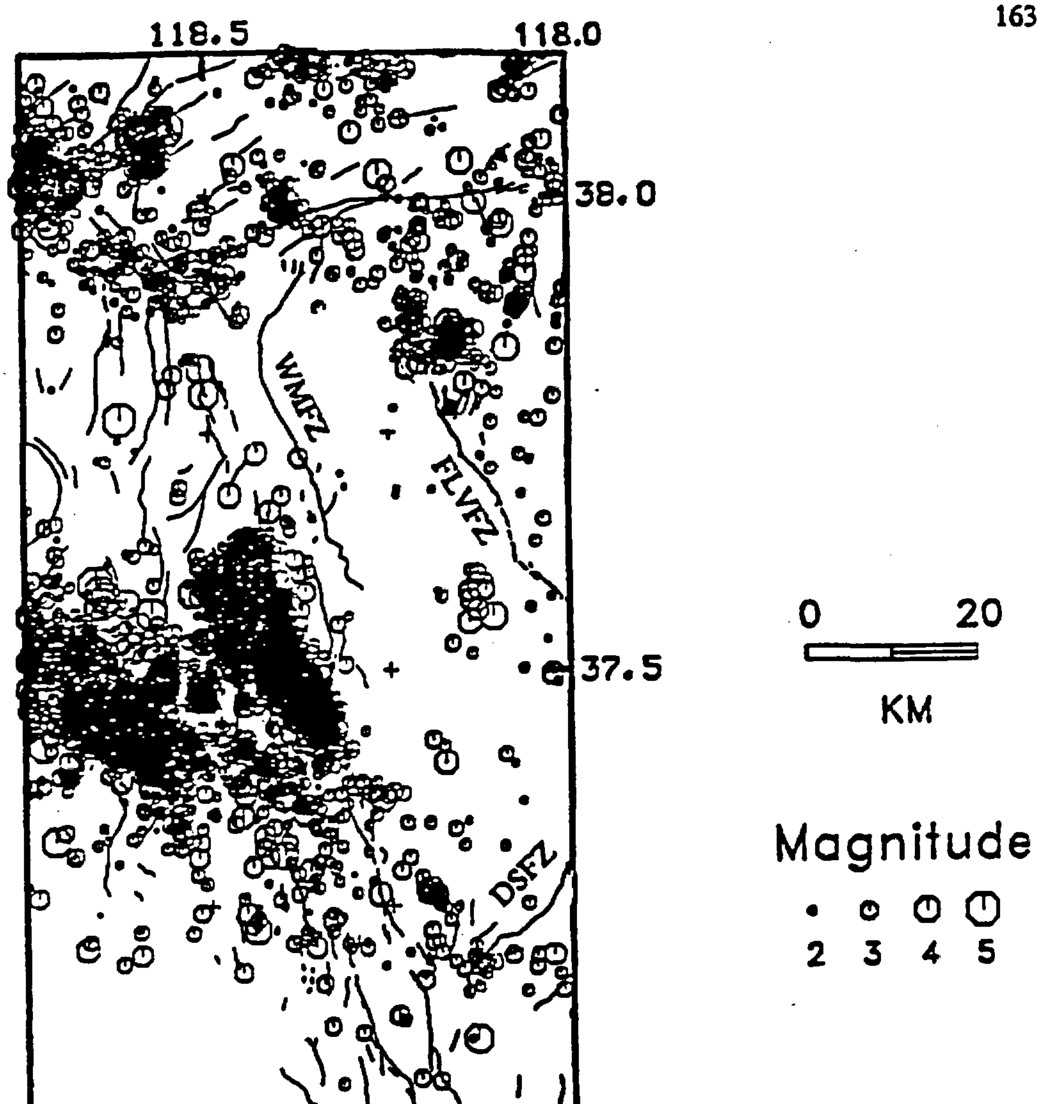

Figure 30. Map showing the distribution of epicenter in the Fish Lake Valley region from 1970 to 1988 (source Univ. of Nevada, Reno, Seismology Laboratory). Note the cluster of seismicity at the northern end of Fish Lake Valley fault zone (FLVFZ). DSFZ, Deep Springs Valley fault zone; WMFZ, White Mountains fault zone.

either right-lateral strike-slip faulting on northwest- to north-northwest-striking faults or left-lateral strike-slip faulting on northeast- to east-northeast-striking faults. The two smallest events however, have normal and reverse components of displacement. Right slip on northwestward-striking faults agrees well with that the structural and geomorphic evidence presented above, and left slip on northeastward-striking faults is at least permissible based on this evidence.

Discussion of Northwest Termination of the FLVFZ: In summary, northern Fish Lake Valley appears to be a region of extension related to right slip on the FLVFZ. Horsetail splaying and bending northeastward characterizes the northwestern termination of the fault zone (Fig. 29). Here, right slip on northwest- to north-northwest-striking faults is converted to normal slip and associated extension on northward-striking normal faults, and possibly left-lateral strike-slip faulting on northeast-striking faults. Hence, northern Fish Lake Valley is a region of extension related to right slip on the northwest-striking FLVFZ.

Qidong and Peizhen (1984) and Ron and Eyal (1985) proposed similar structural patterns and faulting styles at strike-slip fault terminations. Qidong and Peizhen (1984) suggested that strike-slip faults commonly terminate by an abrupt change in strike, where strike slip is converted to dip slip on normal faults. This is exemplified in northern Israel where both the right-lateral Zarit and the left-lateral Pegiin faults terminate by splaying, bending, and transferring lateral slip to normal slip (Ron and Eyal, 1985).

A kinematic transfer from right slip to normal slip at the terminus of a strike-slip fault apparently occurred during the 1979 M_L 6.6 Imperial Valley earthquake. The earthquake ruptured the northwest-striking Imperial fault continuously for about 35 km, before terminating by splaying northward into several faults, with normal displacement (Sibson, 1986).

RATES OF QUATERNARY FAULTING

Several displaced geomorphic features clearly reveal the style of movement along the FLVFZ. EDM/theodolite surveys (Appendix V) and slope-stick profiles

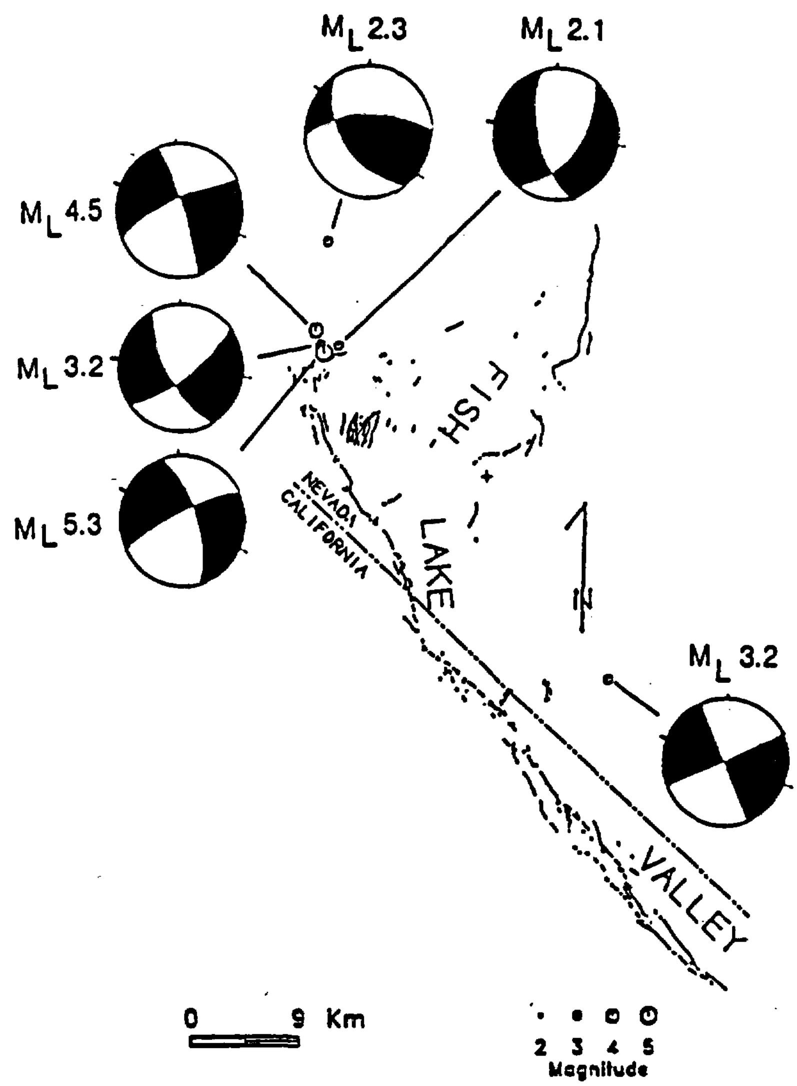

Figure 31. Lower hemisphere fault-plane solutions for selected earthquakes in Fish Lake Valley, which were determined by Vetter (1984). EPFZ, Emigrant Peak fault zone; FLVFZ, Fish Lake Valley fault zone.

(Appendix VI) of such features are used to document the amount and style of displacement along the Northern subzone. The morphostratigraphic framework of the study area (Chapters IV and V) provides general age constraints for offset features, and hence the duration of slip accumulation. The displacement estimates and the inferred slip durations are used to estimate average slip rates on the northern FLVFZ, during specified intervals of the late Quaternary (Appendix VII).

The geometrical and mathematical relations between various components of displacement have been determined by methods of Clark and others (1984), and shown modified in Figure 32. Where T is the amount of total slip, H_t is the amount of horizontal slip, D is the amount of the dip slip component. The dip slip component has both a vertical (V) and a horizontal component (H_d). The angle α is equal to 90° less the dip of the fault. The various components of slip are used in the following evaluations of average slip rates along three sections of the northern FLVFZ.

RATES FROM LEIDY CREEK FAN

CASE STUDY 1

The northwest-striking (N35°W) master fault of the northern FLVFZ (Fig. 18), where it traverses the northern Leidy Creek fan, clearly and unequivocally displaces two alluvial fan remnants (ballenas) in a right-lateral sense (Fig. 23). These remnants are the most convincing indicators of lateral displacement identified in this study anywhere along the nearly 80 km-long FLVFZ. The ballenas are remnants of the Indian unit, and therefore are younger than this late Pleistocene unit by some undetermined amount of time. This contributes to the uncertainty in determining the average slip rate at this site.

Without numerical age constraints, determining the age of the ballenas is problematic. It is possible that the ballenas are significantly younger than the late Pleistocene Indian unit. Peterson (1981) suggested that ballenas essentially represent the final morphological stage in the erosional truncation and destruction of once more extensive alluvial fan surfaces. Therefore, the approximate age of the Indian

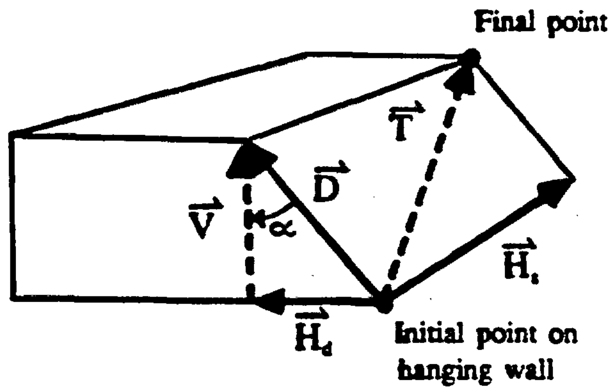

Style Components

$\vec{D}$ = dip slip
$\vec{H}_d$ = horizontal component of dip slip
$\vec{V}$ = horizontal component of dip slip
$\vec{H}_s$ = horizontal slip
$\vec{T}$ = total slip = $\vec{H}_s + \vec{D} = \vec{H}_s + \vec{H}_d + \vec{V}$

Figure 32. Diagram and definitions of displacement components (modified from Clark and others, 1984) used in slip rate calculations (Appendix VII).

unit (Table 3) represents the maximum duration of slip accumulation.

The solifluction steps on the crests and shoulders of the ballenas require that a rather thick layer of desert loess caps these fan remnants, and that their soils have prominent clay and/or carbonate accumulations, which promote solifluction. Such steps are absent on Leidy age and younger fan surfaces in the study area, and probably do not occur on Holocene or latest Pleistocene surfaces of region (discussed in Appendix I). The treads of the steps display well sorted, interlock pavements with dark, continuous varnish coats on lithic fragments, similar to features characteristic of the Indian surface (Table 1). It is herein assumed that the ballenas are roughly half the age of the Indian unit (Table 3), for the purpose of estimating slip rates (Appendix VII).

It is difficult when dealing with displaced erosional landforms to determine the degree of post-offset modification of their morphology. Although the solifluction steps result from downslope movement, their presence suggests that the ballenas have been stable for a considerable period of time. Erosional modifications of the ballenas may have shifted the ballena crests as much as roughly 7 m laterally and perhaps 3 m vertically. These uncertainties are represented by the size of the EDM survey points in Figure 23, from which displacement measurements are made. These uncertainties do not however, account for the relatively significant erosional modification of the southern ballena remnant east of the fault (discussed in Appendix VII).

Figure 23 shows probable projections of the two ballena crests, based on the EDM/theodolite survey (Appendix V, EDM Project 2). The projections suggest that the northern and southern ballena crests are displaced about 92 m (+15/-20 m) and 62 m (+12/-25 m), respectively, in a right-lateral style along the master fault of the northern FLVFZ (Fig. 23). Modification of the southern remnant results in a estimate of displacement.

Figure 24 shows that little vertical displacement (≤5 m +6/-5m), if any, is required to match the longitudinal projections of the Ballena crests across the northwest-striking (N35°W) master fault. The minor vertical displacement suggested shows that the valley side of the fault is upthrown relative to the mountain side.

This suggests a minor reverse component of displacement, perhaps related to the arcuate trace of the master fault (Fig. 23).

In Appendix VII, slip rates are calculated from displacement measurements and inferred age of the ballenas. Table 9 shows estimates of the average slip rates at the Case Study 1 site on the northern Leidy Creek fan. These estimates suggest the preferred total (T) slip rate for the master fault is about 0.8 mm/yr (0.4 to 2.4 mm/yr).

RATES FROM THE INDIAN CREEK FAN

CASE STUDY 2

Right-divergent slip on the north-northwest-striking (N20°W) master fault, where it traverses the southern Indian Creek fan, is evident form an abandoned and offset drainage channel (Plate I). The offset channel can be physically traced eastward from west of the master fault, across it and a subsidiary fault to the east, and about 1 km beyond. The channel is only shallowly incised into the Indian surface of the upper Indian Creek fan, and apparently is graded to this surface in the midfan area. Degraded lateral debris flow levees, mantled with prominent solifluction steps, flank the extent of the channel. These relations suggest the drainage channel transported debris to and across the Indian surface, and therefore developed during, or shortly after, the surface stabilized. The age of the drainage channel is assumed to be the same as the Indian morphostratigraphic unit (Table 3).

The master fault traverses the southern Indian Creek fan and forms a large (roughly 30 m to as much 50 m high), continuous, down-to-the-east scarp exhibiting little evidence of dissection. Where the fault displaces the abandoned channel it consists of two closely-spaced parallel traces, but movement on the western trace is relatively minor. An EDM/theodolite survey (EDM Project 3, Appendix V) of the offset channel, across the N20°W-striking master fault on the southern Indian Creek fan, indicates a predominance of right slip. Figure 25 shows probable and conservative projections of the offset channel, based on survey data and considering erosional modifications (discussed below).

TABLE 9: SLIP RATE ESTIMATES FOR THE NORTHERN FLVFZ[1]

LATE PLEISTOCENE SLIP RATES

CASE STUDY 1:
NORTHERN BALLENA REMNANTS

Style Component	Estimated Slip Rate (mm/yr) Minimum	Maximum	Preferred
H_s - right slip	0.4	2.1	0.8
V - vertical slip (reverse)	0.0	0.2	<0.1
D - dip slip (reverse)	0.0	0.2	<0.1
T - right-oblique slip	0.4	2.4	0.8

SOUTHERN BALLENA REMNANTS

Style Component	Estimated Slip Rate (mm/yr) Minimum	Maximum
H_s - right lateral	≥0.2	≥1.5
V - vertical slip (normal)	≥0.0	≥0.1
V - vertical slip (reverse)	≥0.0	≥0.1
D - dip slip	≥0.0	≥0.1
T - right-oblique slip	≥0.2	≥1.6

CASE STUDY 2:

Style Component	Estimated Slip Rate (mm/yr) Minimum	Maximum	Preferred
H_s - right slip	0.2	1.7	0.5
V - vertical slip (normal)	0.1	0.5	0.2
D - dip slip (normal)	0.1	0.6	0.2
T - right-divergent slip	0.3	2.3	0.7

LATEST PLEISTOCENE TO HOLOCENE SLIP RATES

CASE STUDY 3:

Style Component	Estimated Slip Rate (mm/yr) Minimum	Maximum	Preferred
H_s - right slip	0.2	<2.5	0.4
V - vertical slip (normal)	<0.1	0.3	0.1
D - dip slip (normal)	<0.1	0.4	0.1
T - right-divergent slip	0.2	<2.8	0.5

[1] Slip rates are estimated in Appendix VII.

As in Case Study 1 (above), it is necessary to consider lateral shifts of the displaced geomorphic feature, related to post-offset modifications. This task is simplified by the lateral debris flow levees, that flank the offset channel. The reason is debris levees are depositional features having an initial morphology comparable to those formed by recent debris flows, that issued from other White Mountain canyons (e.g. Kesseli and Beaty, 1959, Figs. 24 and 40; Beaty, 1968, Fig. 18). Hence, by comparing the present degraded morphology of the displaced levees to that of "fresh" debris flow levees in the region, post-offset modifications can be evaluated.

This comparison suggests the levee crests were lowered, rounded, and thus broadened. The prominent solifluction steps on the levees suggest this modification resulted, in part, from "smoothing" effects of solifluction (Appendix I). Based on this comparison, the post-offset modifications may have conservatively shifted the channel laterally by as much as about 7 m. When modifications are considered the survey data suggests the channel is offset about 122 m (+43/-39 m) in a right lateral sense along the master fault (Fig. 25).

Figure 26 shows projections of the longitudinal profile of the offset channel. The vertical displacement of the channel is somewhat more difficult to determine. This determination is complicated by probable post-offset incision (< 3 m) of the channel reach, east of the master fault. The uncertainty in determining the amount of vertical displacement is reflected in the size of the EDM survey points in Figure 26. The survey data suggests the thalweg of the channel is displaced vertically 40 m (+12/-13m, east side relatively downfaulted).

The survey data suggests the channel is displaced about 120 ±40m laterally, and about 42 ± 8 m vertically. Therefore, right-divergent-slip, characterizes by displacement ratios of 2:1 to 5:1 (lateral:vertical), predominates on the N20°W-striking master fault of the northern FLVFZ.

The dip of the fault is uncertain, but the somewhat curvealinear expression of the fault suggests that it dips to the east. Less than 1 km to the west, a parallel secondary fault is exposed in bedrock and dips about 65° to 70°E. The southern extension of the master fault is exposed in an exploratory trench at Excavation Site

2 (Fig. 20), where it is nearly vertical (Plate IV). Hence, in calculating average slip rates (Appendix VII), the fault dip is assumed to range from vertical to 60°E (75°, preferred).

The estimates of the average slip rates at this site are reported in Table 9. The total (T) slip rate on the master fault on the Indian Creek fan is 0.7 mm/yr (0.3 to 2.2 mm/yr) and the dip slip (normal) rate is 0.2 mm/yr (0.1 to 0.5 mm/yr).

CASE STUDY 3

The Case Study 3 site is located about a one kilometer northward of the previous site, along the same master fault of the northern FLVFZ (Fig. 29). Here a small, onfan drainage is shallowly incised into the surface of a Leidy age inset fan remnant. The drainage channel is younger than the Leidy surface into which it is inset. Further, morphostratigraphic relations suggest the channel developed before the early Marble surface, probably about when the Leidy surface stabilized. Thus, the age of the channel is inferred to be the same as for the Liedy unit (Table 3).

This drainage channel is diverted for a short reach southward along the base of a down to the east scarp, formed by the master fault. The channel adjacent to the fault on the downthrown side, is wider then on the upthrown side. This suggests, lateral-erosion of the southern channel margin on the east side of the fault. Therefore, the right-lateral displacement of the channel is in part apparent. However, channel modifications do not account for the mismatch of the northern channel margin across the master fault. The morphology and possible projections of the offset channel were closely evaluated in the field. The field studies suggest the northern margin of the channel is offset as little as about 5 ± 2 m, in a right lateral sense across the master fault. Whereas, the southern channel margin is apparently displaced by as much as about 15 m. The latter displacement estimate is considered to be greater than the "true" lateral displacement (>H_t), due to lateral erosion of the channel reach east of the fault.

The vertical displacement of the Leidy surface across the master fault at this site, was measured from a slope-stick/Brunton profile (Appendix VI, Profile 23). The profile was measured immediately north of the western channel remnant, where the upper and lower relict Leidy surfaces are well preserved, and the scarp clearly defined. The profile data suggests 1 ± 0.3 m of vertical displacement of the Leidy surface across the master fault near Indian Creek.

The displacement data supports right-divergent slip (valley side down) on the N20°W-striking master fault of the northern FLVFZ. The displacement data coupled with an estimate of the duration of slip accumulation (i.e., age of the Leidy unit) provides a preferred total (T) slip rate of 0.8 mm/yr (0.2 to <2.8 mm/yr)(Table 9; Appendix VII). Hence, the latest Pleistocene to Holocene style and rate of faulting is apparently similar to the late Pleistocene style and rate of faulting.

COMPARISON WITH SLIP RATES ALONG THE DVFS

Several geomorphic and structural features along the DVFS indicate a predominance of right-lateral strike-slip displacement during the Quaternary. The amount of slip and the interval during which it accumulated has been determined for a few of these features, thus yielding estimates of average slip rates. The following is a brief summary of long term, lateral slip rates along the DVFS.

Cinder Hill, in southcentral Death Valley, is a basaltic cinder cone that straddles a trace (probably the master trace) of the southern Death Valley fault zone (Troxel and Butler, 1986). The cinder cone, K-Ar dated at about 700 ka by R. L. Drake (in Wright and Troxel, 1984), is offset approximately 200 m in a right lateral sense along the fault trace (Troxel and Butler, 1986). The data suggests a lateral slip rate of about 0.3 mm/yr for this trace of the Southern Death Valley fault zone.

Along the Northern Death Valley fault zone, Oakes (1987) examined an offset pluton, half of which is in the northern Last Change range and the other half in the northern Grapevine Mountains. The pluton is K-Ar dated at 7.3 to 7.9 Ma, and is displaced approximately 32 km. These data yield an estimated slip rate for the Northern Death Valley fault zone of about 4.1 to 4.4 mm/yr.

McKee (1968) proposed as much as about 900 m of right slip along the southern FLVFZ in southernmost Fish Lake Valley, based on a postulated mismatched of sediments from a late Pliocene drainage system. McKee reported a

K-Ar date on biotite of 3.5 ± 0.2 m.y., collected from near the base of the sedimentary sequence. These relations, suggest a rough estimate of about 0.3 mm/yr on the southern FLVFZ, since the late Pliocene. However, recent mapping by Reheis (1990c) suggests that McKee's proposed correlation may be incorrect.

McKee (1968) also proposed that quartz monzonite in the Sylvania Mountains was once continuous with rocks of similar lithology and age (160 Ma) in the southeastern White Mountains, but they have been offset about 50 km in a right lateral sense along the DVFS. These data suggest an average slip rate of about 0.3 mm/yr.

Reheis (1990c) estimates that faulting began on the southernmost FLVFZ between 11.5 and 8.2 Ma. Reheis suggests that if McKee's 50 km of cummulative slip occurred since the onset of faulting (11.5 to 8.2 Ma), then the average slip rate is 4.3 to 6.1 mm/yr. Which, as Reheis noted, agrees well with the average rate (4.1 to 4.4 mm/yr) reported by Oakes (1987) for the Northern Death Valley fault zone.

The average slip rates estimated in this study along the northern FLVFZ (Table 10) generally do not agree with the long-term slip rates summarized above. The slip rates listed in Table 10 were determined for only the master fault near the northwestward termination of FLVFZ. Therefore, it is probable that the late Quaternary slip rate is higher than those listed in Table 10.

KINEMATIC MODEL OF QUATERNARY FAULTING

Geomorphic and structural analyses indicate the northwest-striking FLVFZ is predominantly a zone of right slip. However, a down-to-the-east (i.e., valley side) normal component of displacement is generally evident to prominent, and locally may be significant or even be dominant (e.g., Dyer subzone). The style of faulting along the fault zone is influenced by the strike of individual faults. On a regional scale, the style is governed by the relative motion of the White Mountains and Fish Lake Valley structural blocks, and the geometry of their faulted boundary (i.e., strike of the FLVFZ). These relationships form the bases of the kinematic model proposed in this section.

Styles of faulting along the FLVFZ (discussed in previous sections) are influenced by the orientation of individual faults. Northwest- to north-northwest-striking faults generally display a dominant component of right slip with a variable, but generally minor to insignificant component of vertical slip. North- to north-northeast-striking faults have dominant normal displacement with no (or little ?) lateral displacement. Where the fault zone strikes west-northwest local areas of apparent contraction occur within the fault zone. Hence, the northwest-striking FLVFZ has a predominance of right-divergent slip.

In this section, a kinematic model is developed for the FLVFZ. The model is a regional synthesis that incorporates styles of faulting determined from structural and geomorphic evidence along the fault zone (described in previous sections).

The kinematic model of the FLVFZ is shown in Figure 33. The model is based on northwest (N35°W) translation of the White Mountains structural block relative to the Fish Lake Valley block along the FLVFZ, and on a east-west to west-northwest extension direction.

The translation direction (N35°W) is inferred from a pair of ballenas offset in a right lateral sense along the master fault on the Leidy Creek fan (see Case Study 1). The extension direction is inferred from the orientation of prominent normal faults within the FLVFZ. Hence these strain orientations are inferred from structural and geomorphic analyses of the FLVFZ, and agree closely with the regional tectonic setting (Chapter III). Therefore, the model suggests that the style of faulting along the FLVFZ agrees kinematically with the DVFS to the south.

The northerly-striking (N15°W) Dyer subzone connects the northwest-striking, én echélon Eastern and Northern subzones. Normal displacement is significant (perhaps dominant?) on the Dyer subzone, whereas right slip predominates on the other two subzones. The model suggests that the Dyer subzone functions kinematically as a releasing step, and forms a small-scale pull apart basin along the central FLVFZ. This interpretation is in good agreement with the prominent vertical displacements and apparently deep valley fill along the Dyer subzone. Further, the interpretation is seemingly supported by the gross morphology

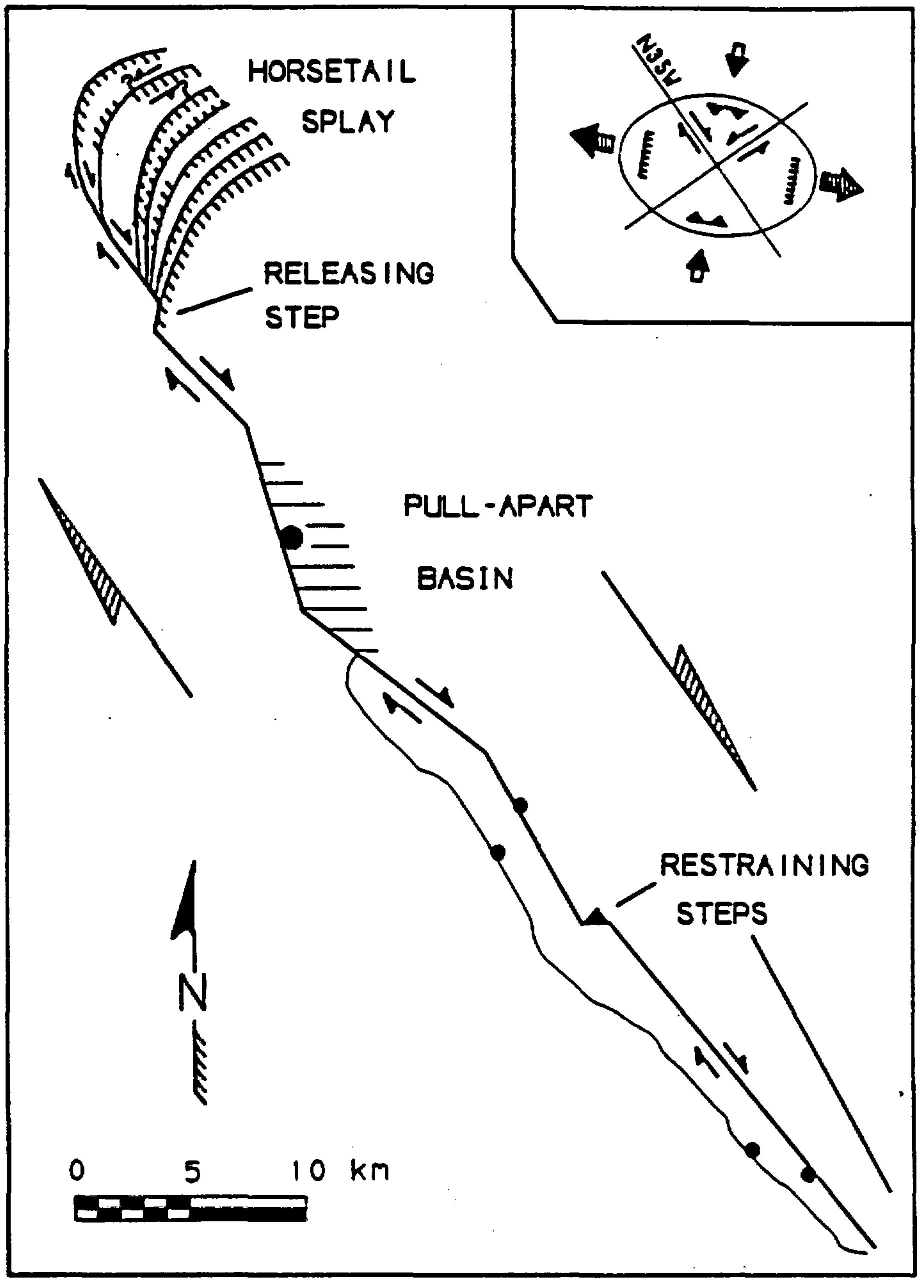

Figure 33. Kinematic model of the Fish Lake Valley fault zone based on this study. The preferred direction for right slip is about N40°W, which is based on analysis of displaced geomorphic features and fault patterns along the fault zone. Note that where the fault zone deviates from a northwest strike a dip slip component is present.

of the range, i.e., the pull apart basin lies opposite the highest point along the crest of the range.
Hence, the Dyer subzone is a mirror analog of the Central Death Valley fault zone, which forms a releasing right step between two right slip fault zones, the Northern and Southern Death Valley fault zones (Burchfiel and Stewart, 1966; Wright and Troxel, 1967; Stewart, 1983; discussed in Chapter III).

The model suggests the FLVFZ terminates in a region where right slip is converted to dip slip and east-west (west-northwest) extension. Thus, the model can account for: 1) right slip predominating on northwestward-striking faults, for example the master fault on the Leidy Creek fan (Fig. 23); 2) right-divergent slip on north-northwest-striking faults, for example the master fault where it traverses the Indian Creek fan (Fig. 25); and 3) the east-west extension of the Indian Creek fan (Figs. 27 and 28). The extension direction (east-west to west-northwest) is similar in orientation to the minimum horizontal stress (σ_3) in the surrounding region (e.g., Smith and Lindh, 1978; Zoback and Zoback, 1980; and Zoback and Beanland, 1986 and 1988). This seemingly supports as "Andersonian" fault mechanism (c.f., Anderson, 1905), i.e., uniform relation between stress and strain.

The left step in the Eastern subzone near Oasis, California (Figs. 18 and 19), according to the model, should function as a restraining step. This is consistent with the pressure ridge interpretation for this feature (discussed in a previous section).

In summary, the kinematic model accounts for variations in faulting styles with changes in the orientation of the FLVFZ, in an analogous manner to the DVFS to the south (c.f. McKee, 1968; Brogan and Slemmons, 1970; Reynolds, 1976; Brogan, 1979; Sawyer, 1988a, b, and c; Reheis, 1990c). This suggests that the FLVFZ is an integral structure of, and kinematically linked to the DVFS.

The translation direction of the White Mountains structural block (N35°W) is similar to that of the Sierra Nevada Province (northwest)(c.f. Wright, 1976; Arugs and Grodon, 1989). This suggests that the White Mountains block is tracking, at a minimum rate of 0.7-0.8 mm/yr but could be in excess of 2.3-2.4 mm/yr, the northwest translation of the Sierra Nevada Province. The only significant aspect of the FLVFZ that the model does not account for, is normal displacements where the fault zone strikes northwest and west-northwest. For example, prominent normal displacement along the northernmost section of the northwest-striking Eastern subzone (Fig. 18), which however may be explained as an edge effect of the Dyer pull apart basin. This deficiency may also stems from modeling the FLVFZ as a pure right-slip fault zone, rather than as a right-divergent slip fault zone.

CHAPTER VII
PALEOSEISMICITY OF THE FISH LAKE VALLEY FAULT ZONE

INTRODUCTION

Establishing the long-term behavior of seismogenic faults is invaluable to assessments of seismic potential and to characterization of earthquake hazards associated with active faults. Detailed studies of paleoseismicity often provide the only means of establishing fault behavior during intervals of geologic time. Examination of the Holocene paleoseismic record, including the most recent surface faulting event, is fundamental because this portion of the paleoseismic record may best represent expectable behavior of the fault. These points are particularly appropriate in regions such as the Basin and Range Province where historical and instrumental records are short compared to recurrence rates of large earthquakes.

An objective of this paleoseismicity study is to establish the most recent history of surface faulting along the FLVFZ. Thus, the youngest morphostratigraphic units disrupted by the fault were closely examined. This examination provides important characteristics of the paleoseismic behavior of the FLVFZ, including the number, relative size, and, in some cases, timing of the most recent paleoseismic surface faulting events. Paleoseismic ruptures along the FLVFZ are identified and described in Chapter VIII.

In this chapter, the Holocene paleoseismic record of the FLVFZ is assessed by examining the relationships between faults and alluvial fan stratigraphy in exploratory trenches. Individual and sequential prehistoric earthquakes are identified, for example, by: (1) faults that displace older fan deposits, but not younger deposits, or (2) displace an older morphostratigraphic unit more than a younger unit; (3) discrete colluvial aprons (wedges) deposited on the downthrown side of the fault;

and (4) distinct crevices within the fault zone, which have been infilled by surficial materials.

Stratigraphic and structural relations exposed in exploratory trenches across the master fault of the northern FLVFZ constrain the relative timing of prehistoric earthquakes. This relative paleoseismic record has been evaluated in the context of the morphostratigraphic framework established in Chapters IV and V. This evaluation provides general timing constraints, where age data is absent or lacking. Materials suitable for numerical age determination (e.g., organic matter or volcanic ash) have been collected from all four exploratory trenches, and presently provide direct timing constraints at one excavation site.

In addition to morphostratigraphy, soil age estimates (Fig. 17 and Table 8), based on a radiocarbon-calibrated selected property index (Chapter V), are used to estimate general timing constraints. Such constraints often provide the most conservative timing estimates.

Historical surface faulting in various places worldwide has occurred mainly during large earthquakes (M_l 5.0 and greater)(Bonilla, 1986). However, a few surface ruptures are associated with smaller earthquakes, and some ruptures have occurred aseismically by fault creep. I assume that large earthquakes on the FLVFZ resulted in surface faulting, whereas moderate-sized earthquakes and creep did not, or at least not to the degree that is recognizable in the paleoseismic record.

The following exploratory trench studies suggest that deformation along the FLVFZ occurs episodically by discrete surface faulting events, which are apparently associated with extensive surface ruptures. This supports the assumption that creep is negligible or absent and that large, rather than moderate, earthquakes are associated with surface faulting. Successive Holocene surface faulting events have ruptured the master fault of the northern FLVFZ in a similar manner, which suggests a characteristic earthquake behavior (described below).

EXPLORATORY TRENCH STUDIES

Detailed examinations of mesoscopic structural and stratigraphic relations exposed in exploratory trenches across the master or suspected faults of the FLVFZ has led to recognition and characterization of paleoseismic events. The detail or resolution of the paleoseismic record depends largely on the continuity of the stratigraphy exposed in the trenches. Hence, the exploratory trench sites were selected in areas that have received frequent and recent deposition, e.g. alluvial fanlette apices and playa/lake plains.

A problem common to exploratory trench studies, including the present study, is that a trench provides only a two-dimensional (vertical) account of three-dimensional deformation associated with earthquakes. This is particularly a problem for evaluating the paleoseismic character of strike-slip faults, as the most significant deformation occurs along the fault strike. However, the right-divergent slip FLVFZ has had a minor to significant component of vertical slip (Chapter VI). Thus, paleoseismic events are represented by vertical offsets of alluvial fan deposits, which were measured directly from trench exposures.

Since right slip has predominated along the FLVFZ, vertical separations give apparent rather than net slip. In addition, variations in thickness and orientation of stratigraphic units juxtaposed along the fault occur as a result of right slip. I assume in this study that the difference between the measured vertical separation and the "actual" vertical slip is negligible.

EXCAVATION SITE 1

The Marble Creek fanhead has been truncated by prominent, down-to-the-east slip on the northwest-striking (N30°W) master fault of the northern FLVFZ. The fact that progressively larger fault scarps occur in successively older morphostratigraphic units suggests that this section of the master fault has had recurrent activity. About a half kilometer south of Marble Creek an unnamed small drainage crosses the master fault. The drainage reach on the upthrown side of the fault is shallowly incised into the Leidy alluvial fan remnant, and has formed paired early and middle Marble inset fan remnants (Plate I). The drainage is actively aggrading on the downdropped side of the fault, forming an alluvial fanlette with middle and late Marble surfaces. Vertical slip on the master fault has controlled the loci of deposition for this relatively minor drainage, and thus has localized the apex of this alluvial fanlette along the master fault.

Excavation Site 1 is on the faulted apex of this inset alluvial fanlette (Plate I). The master fault of the FLVFZ displaces the middle Marble surface about one third of a meter (Profile P20, Appendix VI), near where a hand-dug exploratory trench was excavated across this fault. Radiocarbon Site 3, Tephra Site 2, and Pedons 1 and 2 (Appendix II) are all in the immediate area (Plate I).

Geomorphic features indicating the sense of net slip on the master fault have not been recognized at Excavation Site 1. However, 0.8 km southeastward along the master fault, the sense of slip is shown by an EDM/theodolite survey (Fig. 23) of a pair of offset ballenas (Case Study 1). The survey data suggests that right slip has predominated during the late Pleistocene along the master fault. Displacement ratios of 6:1 (lateral:vertical) to pure strike slip are suggested from this survey. An offset Leidy surface immediately south of the ballenas suggests a similar style of latest Pleistocene to Holocene surface faulting.

The displacement ratio apparently decreases northwestward along the master fault, perhaps due to a slight northward bend of 5° to 10° in fault strike. At Excavation Site 1 the displacement ratio is inferred to be roughly 10:1 to 4:1. This is based on the fact that larger scarps occur at Excavation Site 1 than in the same units adjacent to the ballenas, and on the inference that an increase in vertical slip, related to a more northerly fault strike, is accompanied by a corresponding decrease in lateral slip (i.e., conservation of slip).

A lateral component of displacement is supported by structural and stratigraphic relations observed in the exploratory trench at this site. Structural relations include vertical to near-vertical fault planes arranged in a "flower" structure (Plate III). Stratigraphic evidence of lateral slip includes stratigraphic thickness and/or facies changes and discontinuity of sedimentary structures (e.g., cross bedded sand lenses) across observed faults and fractures.

SUMMARY OF SEPARATION DATA

Vertical separations of stratigraphic units were measured directly from exposures on the north wall of the exploratory trench at Excavation Site 1. Lateral separations are inferred to be roughly 4 to 10 times greater than measured vertical separations (described above).

Plate III is a graphical log of the north wall of the exploratory trench at Excavation Site 1, which is shown in simplified form in Figure 34. Ten stratigraphic units, composed largely of debris flow deposits with subordinate water lain sediment, are designated I through X.

Units I and II, and the lower contact of unit III, have cumulative vertical separations of 33 to 35 cm (± 3 cm), east-side-down (i.e., valley-side-down), across the main fracture (Plate III, near meter 6). Vertical separations were not observed where these stratigraphic units are traversed by other fractures. However, small-scale sedimentary structures are apparently truncated along some of these fractures (e.g., Plate III, Annotations #24 and #25), suggesting lateral slip.

The upper contact of unit III, and the lower contacts of units IV through VI, and IX have cumulative vertical separations of 17 to 21 cm (± 2 cm; valley side down). Units IV, V, and VII through X appear to be cut by a secondary fracture (Plate III, near meter 9) and separated as much as 2? or 3? cm.

PALEOSEISMICITY AT EXCAVATION SITE 1

A paleoseismic record based on the structural and stratigraphic relations described above is developed in this section. The record is shown schematically in Figure 35 as a sequence of successive prehistoric earthquakes. Figure 35a shows units I, II and III in their initial unfaulted state. These units were subsequently displaced about 15 cm vertically during "Event A1" (Fig. 35b), i.e., the first paleoseismic event identified at Excavation Site 1. The upper contact of unit III may have formed the early Marble surface as suggested by what appears to be a buried soil formed in this unit. If correct, Event A1 occurred after the early Marble

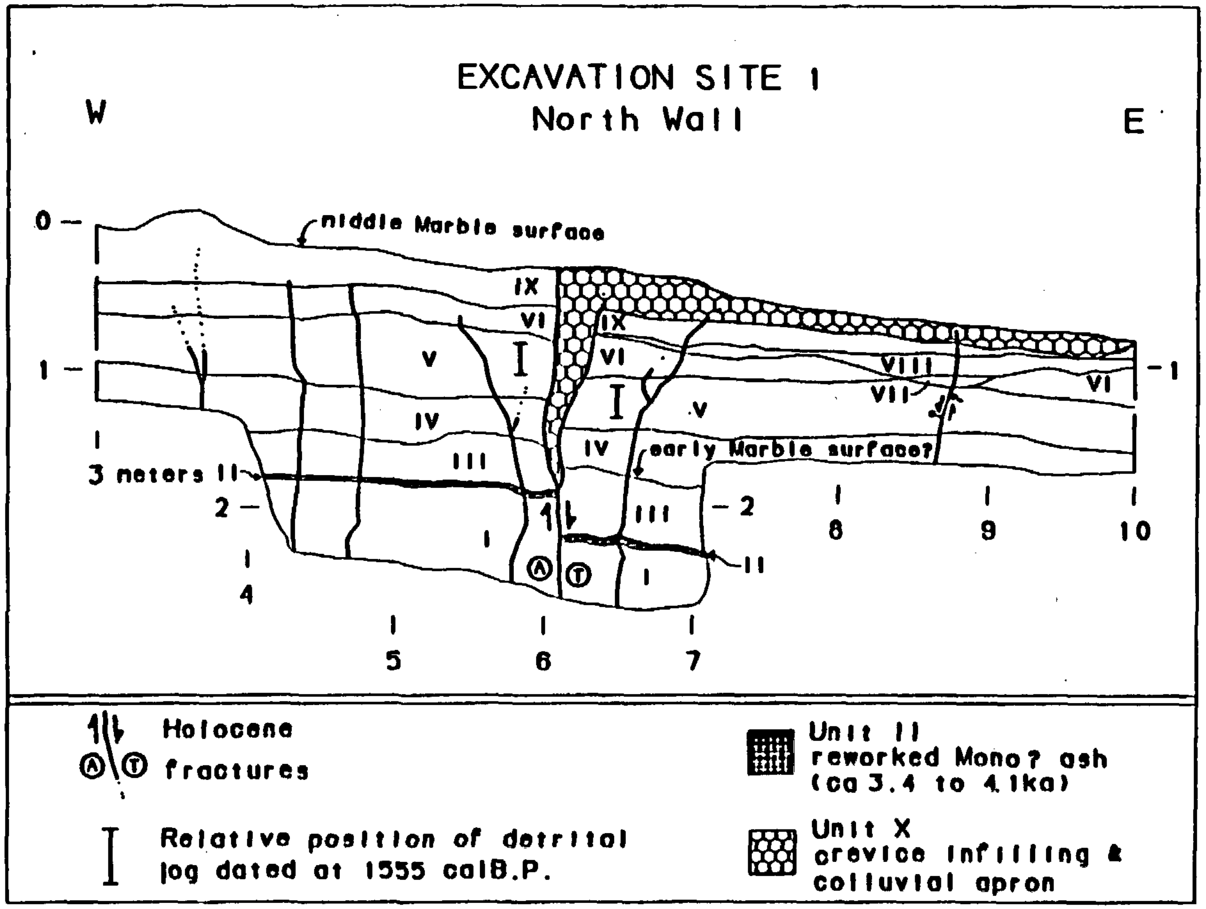

Figure 34. Simplified log of a portion of the exploratory trench at Excavation Site 1. The late Holocene middle Marble unit forms the present land surface and has been faulted. A deposit (Unit V) radiocarbon dated at 1555 calB.P. is offset about half as much as the underlying Mono(?) tephra layer (ca 3400 to 4100 yrB.P.).

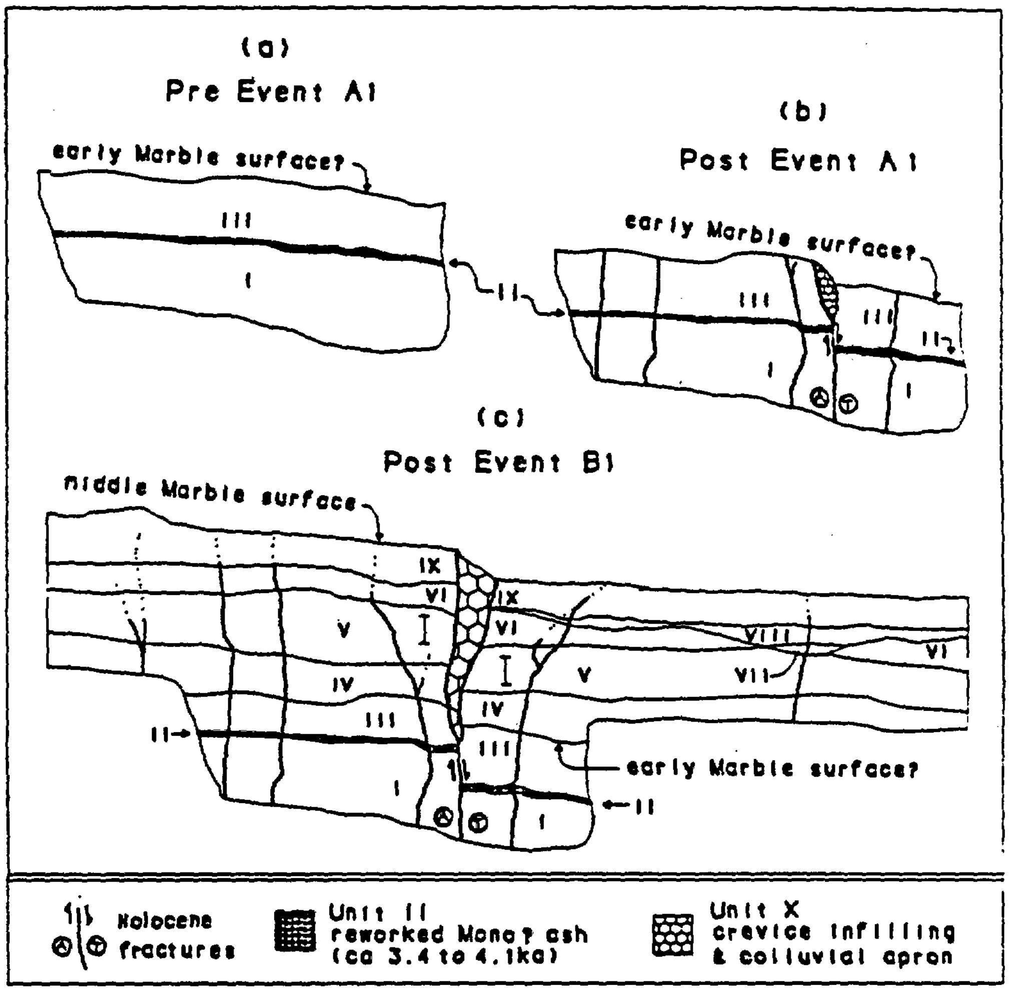

Figure 35. Palinspastic reconstruction of the deposits exposed in the exploratory trench at Excavation Site 1, showing the prefaulting (a), the post Event A1 (b), and the post Event B1 (c) states. See Figure 34 for the post (postulated) Event C1.

surface was stabilized. This event also formed a crevice along the main fault (Fig. 34, near meter 6), that is infilled by unit X. Following Event A1, unit III was truncated on the upthrown side of the fault, resulting in nearly complete removal of the Event A1-scarp. Then unit III was buried by units IV through IX.

The second event at Excavation Site 1, "Event B1," displaced units IV through VI, and IX and the middle Marble surface (Fig. 35c) about 16 to 18 cm (vertically) across the master fault. Unit X comprises colluvial deposits that infilled a crevice and form a colluvial apron derived from the Event B1 scarp.

A suspect third event, "Event C1" is weakly suggested from fractures (Fig. 34 and Plate III) and perhaps 2 to 3 cm of vertical separation of unit X, near meter 9. This event is considered possible, but supporting structural and stratigraphic relations are uncertain. The uncertainty results from the small amount of apparent separation relative to the size of irregularities in the stratigraphic contacts, and from disturbance of the fan surface in the immediate vicinity of the fracture.

<u>Timing of Paleoseismicity</u>

The timing of individual events is based on radiocarbon dates, provisional tephrochronology, and ages of morphostratigraphic units (Table 3) and associated soils (Fig. 17 and Table 8).

Stratigraphic units I, II and III were deposited before Event A1 (Fig 35b). Unit II is a tephra layer that is compositionally most similar to several volcanic ashes erupted from the Mono Crater Chain of east-central California (Fig. 2), that range in age from about 3400 to 4100 yr B.P. (Appendix IV). However, one is as old as 8000 yr B.P. (Sarna-Wojcicki, 1987, written commun.). Therefore, Event A1 occurred after 4100 to 3400 yr B.P., i.e., the "best" estimated age of the tephra.

The "tephra" layer (unit II) consists of weakly laminated ashy sand to sandy ash with minor lenses or pods of nearly sand-free volcanic ash. This suggests the tephra is reworked, and therefore the age of the tephra does not necessarily accord with its stratigraphic context. The age of the tephra layer is considered too old for its stratigraphic position (discussed in "Tephra Site 2"), since it apparently lies in fill alluvium of the early Marble unit (Figs. 34 and 35). The most likely age of the tephra (4100 to 3400 yr B.P.) is taken to represent the maximum timing of Event A1 (Table 10).

Unit V overlies the degraded Event A1-scarp, and was offset about 16 to 18 cm (vertically) during Event B1 (Fig. 35c). Hence, unit V was deposited during the interseismic interval.

The bounding surfaces of unit V were traced physically and continuously for a distance of about 20 m, beyond the west end of Plate III. At which point a 0.5 m long (15 to 30 cm in dia.) log is incorporated into the unit V debris flow deposit ("Radiocarbon Site 3"). The detrital log has a radiocarbon date of 1555 (±45) calB.P. (Appendix IV, A-4768).

This radiocarbon date directly provides the minimum possible timing for Event A1 of about 1.5 ka and the maximum possible timing of Event B1 of about 1.6 ka. The overlap in the timing of these events represents the uncertainty of the radiocarbon date. Event B1 also occurred after stabilization of the middle Marble surface, because this surface was displaced during the event (Figs. 34 and 35c).

The middle Marble surface formed from stratigraphic unit IX, which overlies the radiocarbon-dated unit V. Units VII and VIII rest unconformably on units V and VI (east half of Plate III), suggesting a depositional hiatus. Thus, the middle Marble surface is probably significantly younger than the radiocarbon date of 1555 ± 45 calB.P. The "most probable" age of the middle Marble unit is about 1.0 ka (+0.6/-0.4 ka; Table 3).

Therefore, Event B1 occurred after about 1.6 ka, and probably after 1.0 ka. Event B1 occurred before stabilization of the late Marble morphostratigraphic unit, as there is no evidence that the late Marble surface was faulted. The late Marble unit is younger than about 0.7 ka and probably older than about 0.1 ka (Table 3). Hence, Event B1 occurred before, and suspected Event C1 occurred after, about 0.7 to 0.1 ka.

Since this paleoseismic sequence disrupts late Holocene morphostratigraphic units, the estimated age of associated soils (Fig. 15 and Table 8) can be used to provide general timing constraints. Soil ages are expressed in soil development index years before present (sdiB.P.) to reflect a greater (perhaps considerable)

TABLE 10: ESTIMATED TIMING OF PALEOSEISMIC EVENTS ON THE NORTHERN FISH LAKE VALLEY FAULT ZONE

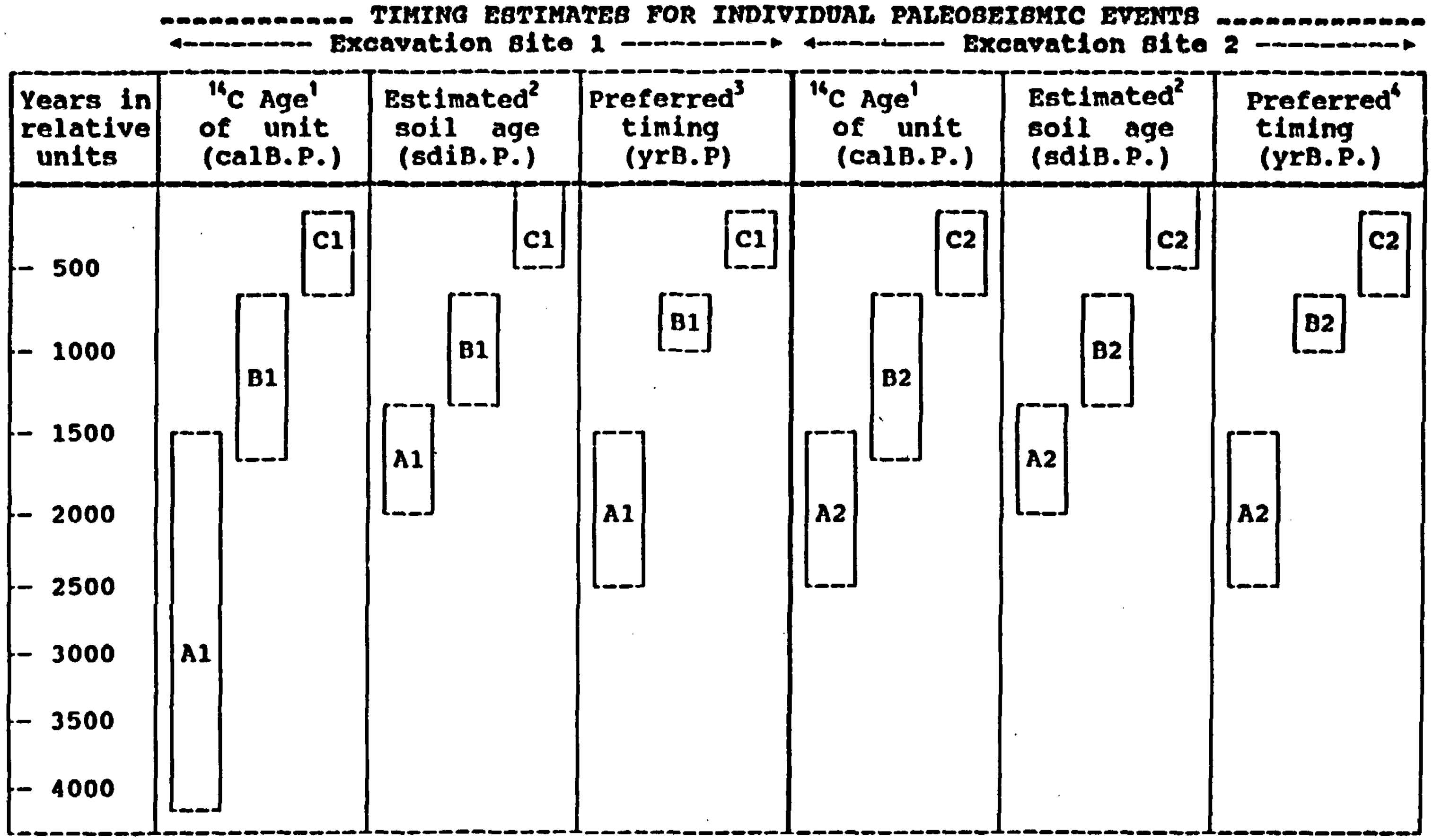

TABLE 10: Continued

Dashed lines indicate that the relationship between the event and the soil is uncertain, or in the case of Event C1, that the event itself is uncertian.

Timing estimates based on: [1] a radiocarbon dated detrial log, preliminary tehrochronology, and assigned age of morphostratigraphic units (Table 3); [2] estimated ages of soils (Table 8); [3] preferred timing discussed in text; and [4] assigned ages of morphostratigraphic units (Table 3).

degree of uncertainty in the reported value. Ages estimated for the early Marble soil range from about 4000 to 2000 sdiB.P., for the middle Marble soil from about 2500 to 500 sdiB.P., and for the late Marble soil from 600 sdiB.P. to the present (Table 8).

Based on estimated soil ages, Event A1 occurred after about 4 to 2 ka but before Event B1, which occurred after 2.5 ka and probably before about 0.5 ka. While this chronology is more conservative (i.e., it has greater uncertainty), it contradicts some observed and inferred timing relations. For example, Event B1 could not have occurred as early as about 2.5 ka, based on an offset radiocarbon-dated deposit (described above). Hence, a few timing constraints based on soil age estimates must be rejected.

The suspected Event C1 apparently fractured, and possibly faulted, a colluvial apron (Fig 35c, unit X), associated with degradation of the Event B1-scarp. If correct, this event occurred sometime after Event B1 and possibly before the late Marble surface stabilized. Thus, this relatively minor event occurred within the last 600 years.

Timing constraints for the paleoseismic history at Excavation Site 1 are shown in Table 10, which includes the preferred or "most probable" history. The preferred history is summarized as follows: Event A1 occurred sometime after 4.1 to 3.4 ka (i.e., "most-likely" age of tephra layer, unit II, Fig. 34) and before about 1.5 ka (^{14}C date from a detrital log contained in unit V). Event B1 probably occurred after 1.0 ka ("most-probable age" of the middle Marble unit, Table 3), but before about 0.6 ka (i.e., minimum estimated age of the middle Marble soil and the approximate limiting maximum age of the late Marble unit). Lastly, the postulated third and most recent event (Event C1) is estimated to have occurred after 0.6 ka and before about 0.1 ka (i.e., the approximate age of the late Marble unit).

EXCAVATION SITE 2

Excavation Site 2 is near the southern margin of the Indian Creek fan, 4.5 km northwest of Excavation Site 1 (Plate I). The master fault of the northern

FLVFZ forms a prominent and continuous down-to-the-east scarp in all but late Marble fan surfaces between the two sites and beyond.

At Excavation Site 2, the north-south-striking (N5°W) master fault forms a 1.3 m (± 0.3 m) high scarp in the middle Marble surface (Appendix VI, Profile 21). At this site, a hand-dug exploratory trench was excavated across the master fault. The south wall of the trench was graphically logged (Plate IV). Pedons 8 and 13 (Appendix II) were also described at this site (Plate I).

To the north the master fault bends westward, to about N20°W, and displaces an abandoned drainage channel associated with the relict Indian surface on the southern Indian Creek fan (Figs. 25 and 26; Plate I). An EDM/theodolite survey of the offset channel (Appendix VII, EDM Project 3) suggests right-divergent slip characterized by displacement ratios of 7:1 to 2:1 (lateral:vertical) on the master fault. Farther north along Indian Creek, the middle Marble surface is displaced about 0.5 m vertically (Appendix VI, Profile 24) and the Leidy surface about 1 m vertically (Profile 23) and perhaps 5 m laterally across the master fault (see Chapter VI, "Case Study 3").

The style of faulting along the FLVFZ is influenced by changes in fault strike (as discussed in Chapter VI), which suggests that vertical displacements are greater on northerly-striking faults (e.g. the master fault at Excavation Site 2) than on northwest-striking faults (e.g., the master fault in "Case Study 1"). The increase in vertical displacement is assumed to be coupled with a decrease in right slip. Therefore, the displacement ratio of the northerly striking master fault at Excavation Site 2 is inferred to be about 3:1 to 1:1 (lateral:vertical), based on a reduction in the 2:1 to 7:1 displacement ratios determined for the same fault about 1 km to the north where it strikes N20°W (see "Case Study 2 and 3"). Hence, vertical separations measured in the exploratory trench are probably comparable to, or roughly one-third of the lateral separations associated with the same event.

Lateral slip along the master fault at Excavation Site 2 is suggested by near vertical fault planes that form a "flower" structure, some of which exhibit apparent reverse separation (Plate IV). Changes in the thickness of stratigraphic units and minor facies changes across faults exposed in the trench also suggest a strike-slip component.

SUMMARY OF SEPARATION DATA

Plate IV is a graphical log of the south wall of the trench at Excavation Site 2, which is shown in simplified form in Figure 36. Ten stratigraphic units, composed primarily of gravelly debris flow and minor colluvial deposits, were identified and designated I to X (Fig. 36).

Stratigraphic unit I and the bottom contact of unit II have cumulative vertical separations of about 60 to 68 cm, valley side down, across the main fault zone in the trench, between meters 1 and 2 (Plate IV). The upper contact of unit II, and units III through V, have cumulative separations from 32 to 36 cm across this fault zone. The bottom of unit V also displays reverse separation east of the main fault. The lower contact of unit VIII is displaced about 6 to 8 cm vertically by the main fault. Unit X forms the late Marble surface and is apparently unfaulted (Fig. 36 and Plate IV).

PALEOSEISMICITY AT EXCAVATION SITE 2

The paleoseismic record, based on stratigraphic, structural, and morphostratigraphic relations at this site, is shown schematically in Figure 37. Stratigraphic units I and II were unfaulted prior to "Event A2" (Fig. 37a), the first event identified at this site, and were displaced about 27 cm (east-side-down) in association with this event (Fig. 37b). Unit VI is associated with Event A2 and consists of colluvial deposits that infilled a crevice. Following Event A2, unit II was truncated on the upthrown side of the fault, and the Event A2-scarp was partially degraded. Then unit II was buried by units III through V.

Units III through V were unfaulted prior to "Event B2" and were separated about 28 cm vertically during this second event (Fig. 37c). The crevice that initially formed during Event A2 (Fig. 37b) subsequently was enlarged during Event B2 (Fig. 37c). Unit VII forms a colluvial apron derived from degradation of the Event B2 fault scarp, thus accounting for the eastward thinning of unit V west of the main fault (Figs. 36 and 37d).

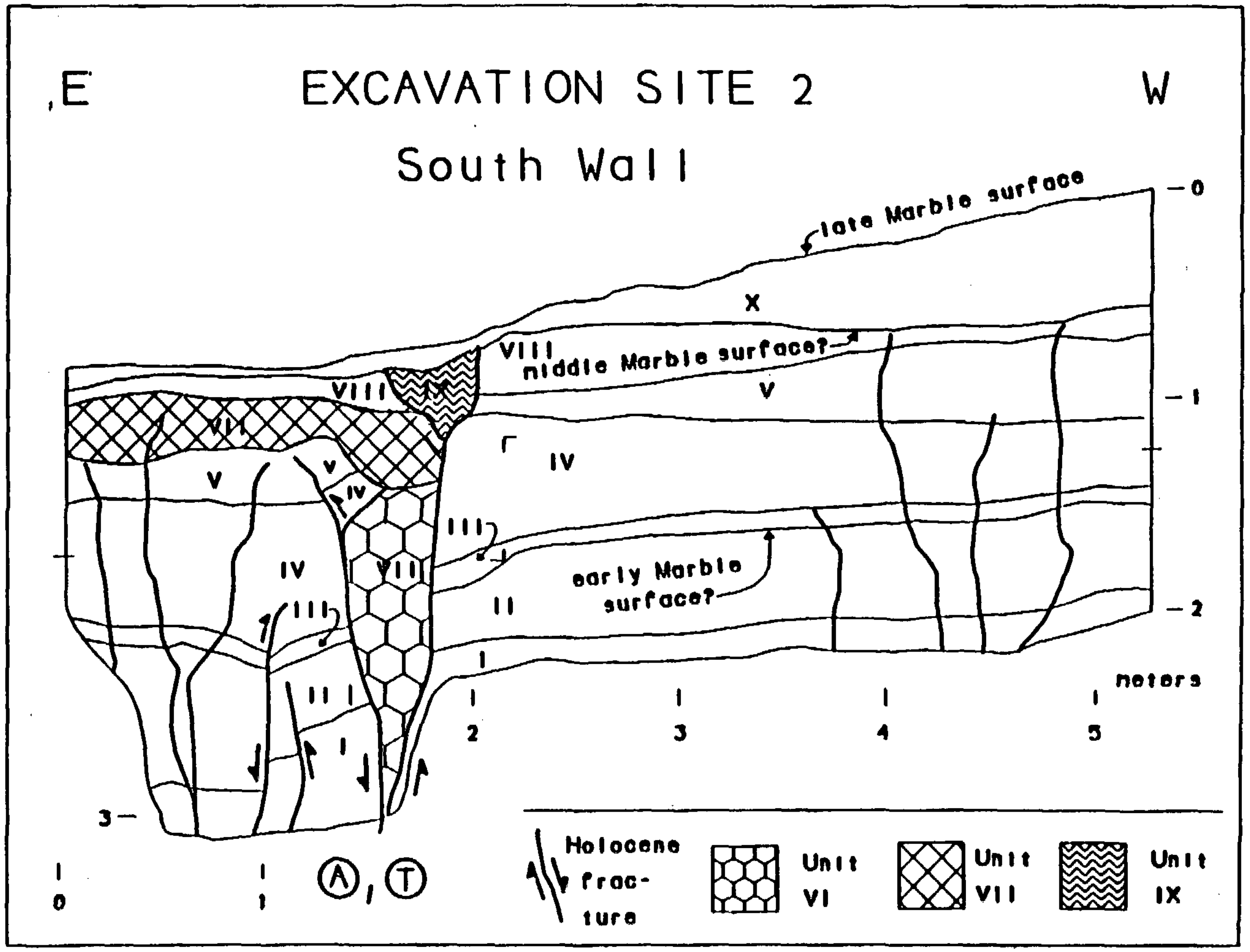

Figure 36. Simplified log of the exploratory trench at Excavation Site 2. The latest Holocene late Marble unit forms the present land surface and is unfaulted, whereas the underlying middle Marble unit has been faulted. The stratigraphic units shown with patterns (Units VI, VII, and IX) are related to successive surface faulting events (Events A2, B2, and C2, respectively).

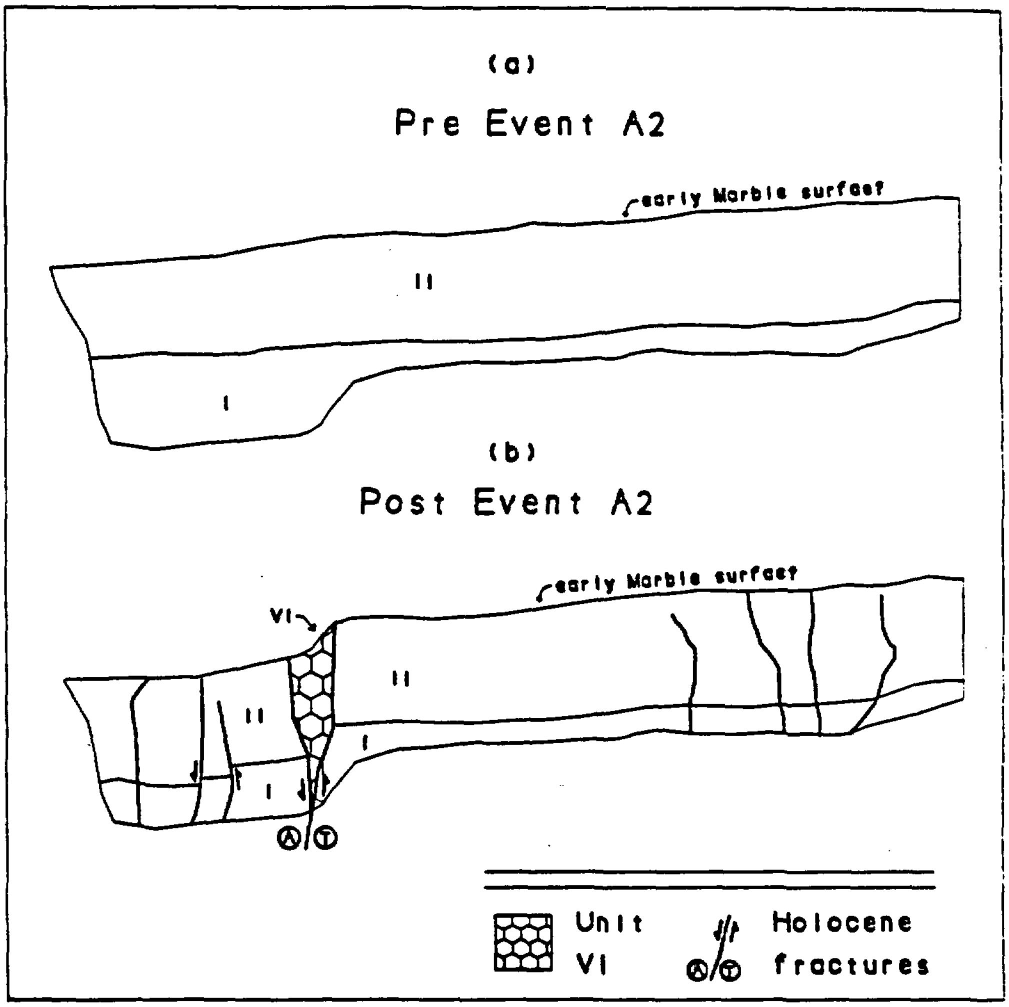

Figure 37. Palinspastic reconstruction of the deposits exposed in the exploratory trench at Excavation Site 2, showing the prefaulting (a) and the post Event A2 (b) states.

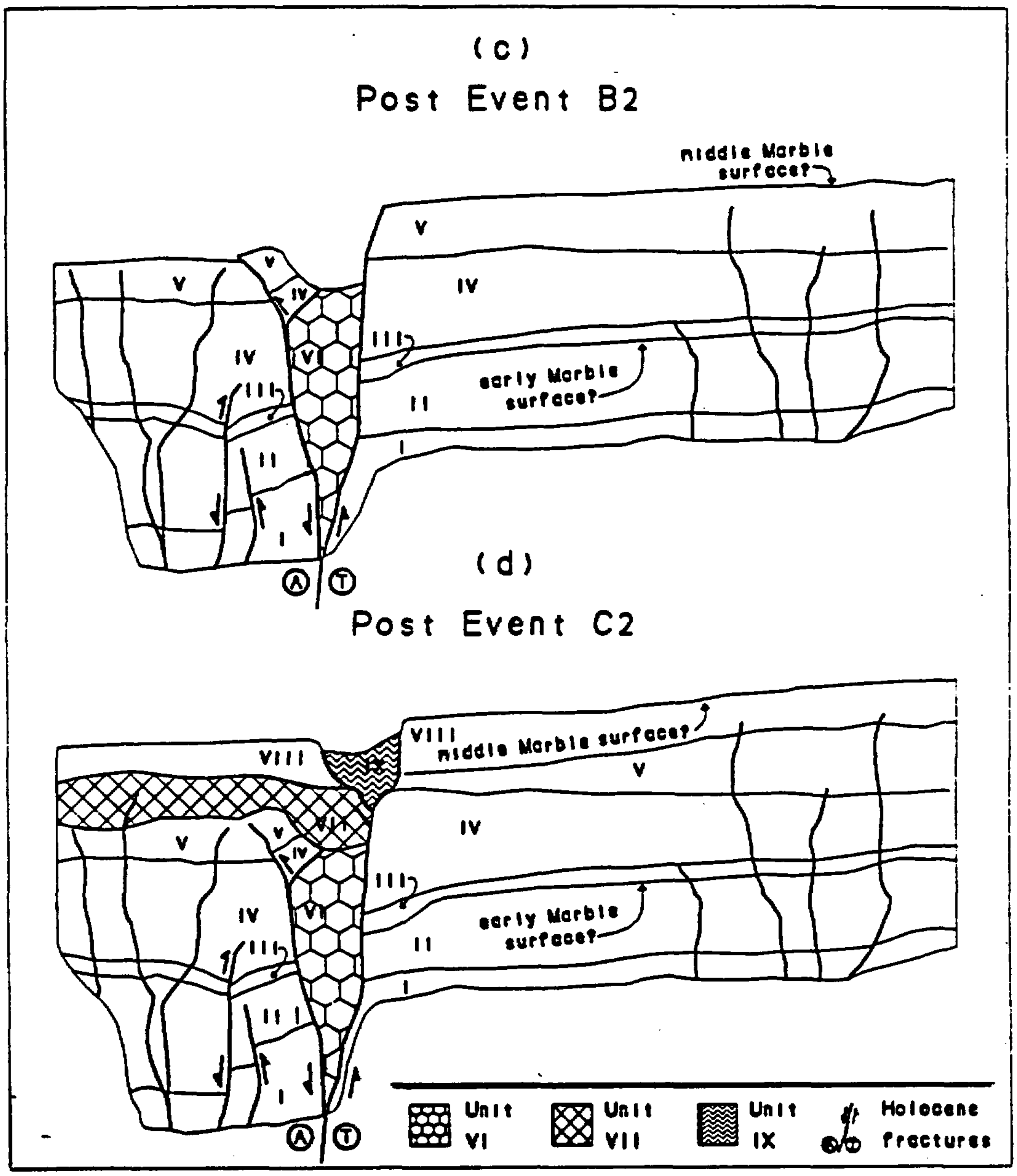

Figure 37. Continued

Unit VIII was deposited on the degraded Event B2-scarp, and subsequently was displaced about 6 to 8 cm during "Event C2" (Fig. 37d), the third and most recent event at this site. Unit IX forms a "keystone" block, which was down-dropped during this latest event. Unit X was deposited after the sequence of three surface-faulting events and is apparently unfaulted (Fig. 37).

Timing of Paleoseismicity

Unfortunately there are no direct age controls to constrain the timing of paleoseismicity at Excavation Site 2. Organic materials (5-TS-2-49B) were collected from unit VIII on the downthrown side of the fault (Plate IV, annotation 9). The sample was submitted for radiocarbon age determination, but not dated, because it was too small for conventional radiocarbon analysis after pretreatment (M. Tumers, 1988, written commun., Beta Analytic Inc., Appendix IV).

General timing constraints for individual events at Excavation Site 2 are based on assigned ages of morphostratigraphic units (Table 3), and estimated soil ages (Table 8).

The following summary of the paleoseismic history at Excavation Site 2 is based on morphostratigraphic relations. Event A2 may have occurred after the early Marble surface stabilized, and before the middle Marble surface formed. This is suggested by a buried early Marble (?) soil disrupted during Event A2 (Fig. 37b). The early Marble unit is assigned a "most probable" age of 1.8 (+0.5/-0.3) ka and the middle Marble unit is assigned an age of 1.0 (+0.6/-0.4) ka (Table 3). This suggests Event A2 occurred after about 2.3 ka, and probably before about 1.5 ka. It is possible however, that this event occurred before the early Marble surface formed, and thus the upper timing limit for the event is uncertain (Table 10).

Surface faulting associated with Event B2 disrupted the middle Marble surface (Fig. 37c). Thus, Event B2 occurred after about 1.6 ka and probably before 0.6 ka (Table 10).

Event C2 occurred after Event B2, since it displaces stratigraphic unit VIII, which buries the degraded Event B2-scarp and associated colluvial apron (Fig. 37d). Event C2 apparently occurred before the late Marble unit was stabilized (0.7 to 0.1

ka), as it does not displace unit X. Therefore, Event C2 is inferred to have occurred after about 0.7 ka and before about 0.1 ka.

Soil ages may also be used to bound the paleoseismic history, since the relative timing of paleoseismic events at Excavation Site 2 with respect to the Marble soils is known. Soil ages were estimated by means of a radiocarbon-calibrated soil development index, established for Holocene soils in Chapter IV (Fig. 17 and Table 8).

The soil ages suggests Event A2 probably occurred before about 2400 to 2000 sdiB.P., but possibly as early as about 4000 sdiB.P. Event B2 occurred between about 2400 to 2000 sdiB.P. and 500 sdiB.P., and Event C2 after about 600 sdiB.P.

The paleoseismic history at Excavation Site 2, based on ages assigned to morphostratigraphic units and estimated soil ages, generally agrees with the paleoseismic record at Excavation Site 1 (Table 10; discussed below).

DISCUSSION OF PALEOSEISMICITY AT EXCAVATION SITES 1 AND 2

The records of paleoseismicity at Excavation Sites 1 and 2 are similar in several regards. Most notably, two relatively large surface faulting events have been identified from stratigraphic and structural relations at these sites. Furthermore, the timing of events, estimated from ages of morphostratigraphic units and associated soils, suggests that the events may have been contemporaneous at the two sites.

I therefore suggest that the same two events are represented at both excavation sites. Since the sites are separated only by 4.5 km along the master fault of the northern FLVFZ (Plate I) and have experienced similar paleoseismic histories, this inference appears to be reasonable. Thus, Events A1 and B1 at Excavation Site 1 are inferred to correlate with Events A2 and B2, respectively, at Excavation Site 2. The suspected Event C1 may correspond to Event C2.

The paleoseismic character of the first two events at Excavation Sites 1 and 2 is rather similar. The first event ("Event A") was associated with about 15 cm (average) of vertical slip at Excavation Site 1, and about 27 cm at Excavation Site 2. Vertical slip associated with "Event B" was about 17 and 28 cm at the respective sites. Furthermore, deformation associated with Event B essentially mimicked that of Event A. That is, the same fault plane ruptured by the first event was reruptured to a comparable degree and in a similar manner by the second event (Figs. 35 and 37). The hypothesis that the same paleoseismic sequence is represented at both excavation site is supported by the estimated timing of the events (Table 10).

Empirical displacement-magnitude relations based on historical surface faulting events (e.g., Slemmons, 1982; Bonilla and others, 1984) suggest that Events A and B may have been associated with rupture lengths of 20 to 50 km or more. Since these rupture lengths are several times longer than the distance between the trenches, Events A and B should be anticipated in the paleoseismic records of the two sites.

A zone of small, well-defined fault scarps and scarplets occur in all but the latest Holocene fan surfaces from Chiatovich Creek southward, through both excavation sites and beyond Busher Creek. This 20 to 25 km (or more?) zone of scarps along the master fault of the northern FLVFZ is associated with Events A and B at Excavation Sites 1 and 2. The scarps delineate a zone of repeated mid to late Holocene surface faulting (discussed in Chapter VIII). The length and continuity of this paleoseismic rupture zone further suggests the same events are represented at both sites.

Similarities between successive prehistorical earthquakes along a fault or fault segment provide the primary means of identifying a "characteristic" earthquake. The paleoseismic character of Events A and B (described above) suggests a characteristic earthquake behavior for at least part of the northern FLVFZ.

However, the character of the most recent surface faulting event, "Event C", differs markedly from that of the first two events. Event C was associated with minor vertical slip at Excavation Site 2 (6 to 8 cm) and fracturing and perhaps relatively minor vertical slip at Excavation Site 1. This suggests that Event C was a relatively minor earthquake, one that is only well-represented at the northern site (Excavation Site 2).

EXCAVATION SITES 3 AND 4

Numerous vegetation lineaments traverse the bolson floor of southernmost Fish Lake Valley (Fig. 21). The larger of which are left stepping and én echélon, similar to Riedel shears formed in a clay-filled shear box under progressive simple shear (cf., Tchalenko, 1970). These vegetation lineaments appear to delineate faults of the southern FLVFZ, which is supported by evidence exposed in exploratory trenches at Excavation Sites 3 and 4.

Excavation Sites 3 and 4 are within the network of lineaments on the bolson floor of southernmost Fish Lake Valley (Fig. 21; Plate IIE). At these sites, exploratory trenches were excavated by a backhoe across three prominent and extensive vegetation lineaments that occur in the fine-grained playa (lake?) sediment.

An objective of these exploratory trenches was to determine if the vegetation lineaments are surficial traces of faults. As with Excavation Sites 1 and 2 (described above), additional objectives were to document the number, relative size and, if possible, timing of surface faulting events.

Structural and stratigraphic relations exposed in trenches at Excavation Sites 3 and 4 indicate that fractures occur in the fine-grained sediment directly beneath the vegetation lineaments (Plates V and VI). Furthermore, apparent reverse stratigraphic offsets were measured at Excavation Site 3 beneath a northwest-striking (N35°W) lineament. I conclude that the lineaments delineate faults and tectonic fractures that were produced in association with right slip on the southern FLVFZ.

Several detrital charcoal samples have been collected at Excavation Sites 3 and 4, but as yet have not been dated. Therefore, direct timing constraints on faulting and fracturing events are currently unavailable. At the excavation sites, the morphostratigraphic characteristics of the bolson floor (playa) differ markedly form those of alluvial fan surfaces (e.g., Table 1). Thus, such characteristics can not be compared with dated fan surfaces as a means of estimating age relations at Excavation Sites 3 and 4.

The uppermost playa sediment is probably mid Holocene, or perhaps late Holocene, in age. This is based on the apparent interfingering relationship between the playa sediment and the marginal alluvial fans, which have morphostratigraphic characteristics equivalent to those of the early and middle Marble units. Reheis (1990b) recently mapped the marginal alluvial fan deposits as mid to late Holocene in age (Qfcl and Qfce).

EXCAVATION SITE 3

At Excavation Site 3, a chevron-shaped trench was excavated across two well-defined vegetation lineaments that intersect in an acute angle (approximately 30°), 20 m north of the exploratory trench. The stratigraphic and structural relations exposed in the north trench wall are shown in Plate V. Several stratigraphic units, composed primarily of silt and very fine to fine sands, were identified and designated A through I. Most (all?) of these units are fractured and in places have been faulted.

Stratigraphic offsets measured in the exploratory trench are summarized as follows. Units E, C, D, and I are offset in an apparent reverse sense across a zone of fractures located between meters 12 and 13 (Plate V). The upper contact of unit E, unit D, and the lower contact of unit C are separated vertically about 10 cm (average). The upper contacts of units C and I display approximately half as much separation (about 5 cm) across the same zone of fractures.

The difference in stratigraphic offsets between units D and I (Plate V) could suggest recurrent movement along the fault zone. However, it is also permissible that stratigraphic separations diminished toward the surface as a result of distributed slip within the broad (approximately 20 cm wide) zone of fractures.

Units G and H and the lower contact of unit E are not obviously displaced across the fracture zone, which seemingly contradicts the stratigraphic offsets of the overlying units. However, the bounding surfaces of these units are irregular (Plate V), and thus the units may have deformed plastically under saturated conditions. Evidence of small-scale plastic deformation was observed along a fracture near meter 7 (Plate V), where unit H was apparently injected about 5 cm along the fracture into the overlying unit (unit G).

Thus, the vegetation lineaments at Excavation Site 3 are associated with fracturing, faulting and perhaps soft sediment deformation. Stratigraphic and structural relations indicate at least one discrete faulting event, which resulted in apparent reverse offsets.

EXCAVATION SITE 4

Excavation Site 4 is on the bolson floor of southernmost Fish Lake Valley, about 3 km northwest of Excavation Site 3 (Fig. 21; Plate IIE). An exploratory trench was emplaced across the most continuous and prominent vegetation lineament in the area. The lineament forms the well-defined eastern margin of a small playa. This suggests that fine-grained sediment has been "ponded" by down-to-the-west vertical displacements across the lineament (probable fault).

Plate VI is a graphical log of the north wall of the exploratory trench at Excavation Site 4. In this trench there was a general lack of visible stratigraphy, which greatly inhibited deciphering the paleoseismic record. However, four poorly defined stratigraphic units were identified and designated A through D. None of these units appears to be offset.

The apparent restriction of unit B to the playa side of the main fracture zone (Plate VI, near meter 12) suggests down-to-the-west displacement. Unit B appears to be dammed against the fracture as a result of similar displacement on the fault. However, unit D occurs primarily to the east of the main zone of fractures, suggesting the opposite sense of vertical slip.

In summary, fractures occur in the fine-grained sediment beneath the lineament at Excavation Site 4, but in contrast to Excavation Site 3, convincing offsets of stratigraphic units were not observed. The lack of observed offsets does not preclude the possibility that the lineament is associated with a fault, which is considered probable.

CHAPTER VIII
SEISMIC POTENTIAL OF THE FISH LAKE VALLEY FAULT ZONE

INTRODUCTION

In this chapter, the FLVFZ is treated as an earthquake source structure that is independent of the DVFS, although scenarios are developed that involve part or all of the DVFS. The assessment of the seismic potential of the FLVFZ involves several strategies that incorporate morphostratigraphic, structural, and paleoseismic data presented in Chapters IV through VII. The various strategies combine the above data with geomorphic observations, regional seismicity and geophysical studies, and the character of historical surface faulting events. Collectively, these data are used to characterize the prospective behavior (i.e., seismic potential) of the FLVFZ.

GENERAL STATEMENT

The seismic potential of the FLVFZ warrants particular concern. The surface ruptures of the 1872 Owens Valley earthquake (M 7.8) and the 1932 Monte Cristo Valley earthquake (M 7.2) form a large-scale, right-stepping, én echélon pattern (Fig. 38). The region between these historical ruptures has been identified by seismicity and geologic data as a seismic gap, termed the "White Mountain" seismic gap, i.e., a region of low seismicity suggested to be the most likely location for the next large earthquake (Bullen and Bolt, 1985). Ryall (1973) suggested Fish Lake Valley is one of several regions in the western Great Basin with a relatively high potential for large earthquakes. Furthermore, the FLVFZ is an important (80 km-long) component of the DVFS, which is a nearly 350 km-long system of

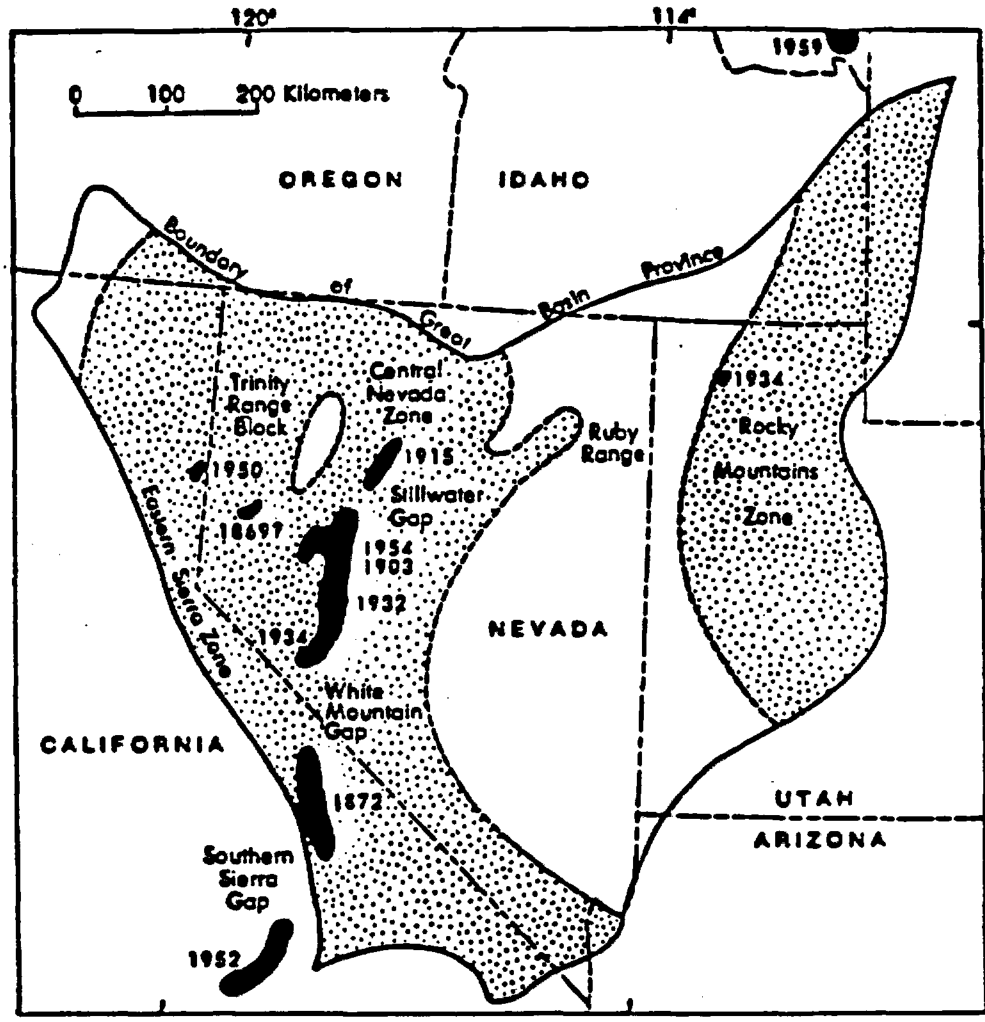

SURFACE FAULTING IN THE GREAT BASIN PROVINCE

1915		
HISTORIC FAULTING $3x10^{-4}$ > event > $1x10^{-4}$ per year per 1000 KM^2	**HOLOCENE FAULTING** (last 12,000 years) $5x10^{-4}$ > event > $5x10^{-5}$ per year per 1000 KM^2	**NO LATE QUATERNARY EVENTS** (last $5x10^4$ years)

NOTE: An event is an occurrence of surface faulting large enough to have produced an earthquake >M7. Earthquakes of 1869, 1903, 1934 and 1950 were <M7. Those of 1872, 1915, 1932, 1952 and 1954 were >M7.

Figure 38. Map showing selected surface faulting events and inferred seismic gaps, including the White Mountain seismic gap, in the Great Basin Province (from Wallace, 1978).

kinematically linked faults (Fig. 7).

Surface ruptures associated with several large historical earthquakes in the western Basin and Range Province have occurred in a region known as the central Nevada-eastern California Seismic Belt (NCSB)(Wallace, 1978). The White Mountain seismic gap is a 130 km segment of the NCSB that has not ruptured in historical time (Fig. 38), except for the 1986 Chalfant Valley earthquake sequence (M 6.2), which resulted in minor ground fracturing along the White Mountain fault zone (DePolo and Ramelli, 1987; Lienkaemper and others, 1987).

Slemmons and others (1959) were the first to note this seismic gap, and it has subsequently been studied by Ryall (1966), Ryall and Ryall (1983), Ryall and VanWormer (1980), VanWormer and Ryall (1980), Wallace (1978 and 1984), and Wallace and others (1983). However, until recently (e.g., Ryall and Ryall, 1983), the FLVFZ had not been identified within the seismic gap, and thus was not considered as a potential source for the next "gap-filling" earthquake.

The location and orientation of the FLVFZ within the White Mountain seismic gap, the Quaternary tectonic activity, paleoseismic behavior, and geomorphic character strongly suggest that this regional source structure poses the greatest seismic potential in the Fish Lake Valley region and perhaps within the White Mountain seismic gap.

SIZE DETERMINATION OF EARTHQUAKES

The size of large historical earthquakes, frequently expressed in surface wave magnitude (M_s), is related to surface rupture parameters that can be measured in the field. Tocher (1958) was the first to estimate the magnitude of an earthquake from empirical relations that utilize fault-rupture lengths and (or) maximum displacements associated with historical events. Bonilla (1967), Brune (1968), Bonilla and Buchan (1970), Slemmons (1977 and 1982), Slemmons and others (1986), Bonilla and others (1984), and Lienkaemper (1984), for example, have subsequently developed empirical relations to estimate earthquake magnitudes from various parameters of historical surface ruptures.

In this section, paleoseismic data, geomorphic analyses, and other aspects are used to estimate rupture parameters, which in turn are used with the empirical relations to estimate the size (i.e., M_s) of the maximum credible and characteristic earthquakes along the FLVFZ.

PALEOSEISMIC APPROACH TO SIZE DETERMINATION

EXPLORATORY TRENCH STUDIES

As determined in Chapter VII, the paleoseismic character of Events A and B may represent a "characteristic" earthquake for the northern FLVFZ. If these events are characteristic, their associated displacements can be used in regression analyses to estimate the magnitude of a "characteristic" earthquake along the northern FLVFZ. The resulting estimates of magnitude are only approximations of the earthquake size owing to several factors, including: 1) the statistical uncertainty of the empirical relations; 2) right slip predominates on this part of the master fault but only vertical displacement data is directly available; and 3) the displacement data does not necessarily represent the maximum possible displacements, since the primary objective of exploratory trench studies was to document a complete paleoseismic record and not necessarily the most dramatic.

The average vertical displacement associated with paleoseismic Events A and B is about 15 and 30 cm (average) at Excavation Sites 1 and 2, respectively. The estimates of lateral displacement conservatively range from as little as a 1/2 meter to as much as 2 m (or more).

Using empirical regressions to estimate the magnitude of a characteristic earthquake for the (northern?) FLVFZ (Appendix VIII), the displacement data yields estimates of magnitudes from 6.6 to 7.1 (M_s), as shown in Table 11. The characteristic earthquake size is discussed further in a following section.

EVALUATION OF PALEOSEISMIC RUPTURE ZONES

Geomorphic analysis of surface ruptures associated with paleoseismic events

TABLE 11: EMPIRICAL RELATIONS OF MAGNITUDE AND DISPLACEMENT[1] DATA

Data collection site/ Regression and data set	Empirical Estimation of Earthquake Magnitude[2]			
	<--- Estimated Magnitudes -->			Uncertainty
	Minimum Magnitude	Maximum Magnitude	Mean Magnitude	of Mag.est. (±1 stn. dev.)
Excavation Site 1				
Slemmons (1982)				
All Events	6.6	7.1	6.9	± 0.331
Strike slip	6.8	7.2	7.1	± 0.323
Bonilla and others (1984)				
All Events	6.8	7.2	7.0	± 0.323
Strike slip	6.8	7.3	7.1	± 0.331
Western N. Am.	6.8	7.2	7.1	± 0.442
Excavation Site 2				
Slemmons (1982)				
All Events	6.3	6.8	6.6	± 0.331
Strike slip	6.5	6.9	6.7	± 0.323
Bonilla and others (1984)				
All Events	6.5	6.9	6.7	± 0.323
Strike slip	6.5	7.0	6.8	± 0.331
Western N. Am.	6.5	6.9	6.7	± 0.442

[1] Lateral displacements inferred from vertical displacement data measured during trench studies, coupled with locally determined displacement ratios (see discussion in text).

[2] Earthquake magnitudes are estimated by emprical relations of magnitude and displacement in Appendix VIII.

on the FLVFZ is used to quantify surface rupture parameters. This data is then compared with empirical relations based on surface rupture lengths and maximum displacements related to large historical earthquakes to estimate earthquake size (Appendix VIII).

Northern Paleoseismic Rupture Zone

The master fault of the northern FLVFZ forms a low, well-defined, and nearly continuous zone of scarps and scarplets in the late Holocene middle Marble surfaces (e.g., Profiles 20, 21, and 24, Appendix VI). The master fault forms progressively higher scarps in successively older surfaces that are generally oversteepened at their bases (e.g., Profile 25). The character of the scarps along this portion of the FLVFZ suggest they represent a continuous zone of paleoseismic surface rupturing. This is supported in part by exploratory trench studies (Chapter VII).

The "fresh" appearance of scarps and scarplets along the probable paleoseismic rupture zone is shown on 1:12,000 low-sun-angle photographs (Univ. of Nevada, collection). The rupture zone was identified from air photo analysis and field examination. The zone (Fig. 38) extends from Chiatovich Creek, essentially the northern end of the FLVFZ, through both excavation sites to about Perry Aiken Creek (Fig. 18), a distance of about 25 km. The southern reach of the rupture zone appears to be superimposed on, and thus is obscured masked by, the large scarps (as much as 80 m high) along the Dyer subzone.

The Dyer subzone exhibits a significant component of vertical displacement, based on the height of fault scarps, which are the highest along the FLVFZ and most, if not all of the DVFS, and by White Mountain drainage-fan systems that are traversed by the subzone. The latter comprise the largest drainage basins in the range (Beaty, 1960), with the greatest relief, but having disproportionately small alluvial fans. The style and apparent rate of slip along the Dyer subzone, together with the large drainage basins, form some of the most dynamic alluvial fans in the Fish Lake Valley-Death Valley region. As a result, evidence of late Holocene surface faulting along the Dyer subzone is largely obscured by recent to historic debris flows, and/or the rupture trace merges indistinguishably with the prominent fault scarps.

The late Holocene rupture zone along the northern FLVFZ probably extends into and possibly through the 10 km length of the Dyer subzone. However, only a few discontinuous scarps have been identified as candidates for delineation of the rupture zone along this section of the central FLVFZ.

The geomorphically youthful appearance of the paleoseismic rupture zone is well defined from the northwestern terminus of the FLVFZ to the north end of the Dyer subzone, a minimum distance of 20 km along strike (Fig. 39). The maximum length of the rupture zone is not known, but could be 30 km or more if the rupture extends through the Dyer subzone.

The length of the northern paleoseismic rupture zone, together with empirical regressions of Bonilla and others (1984) and Slemmons and others (1989) indicate magnitudes of 6.7 to 7.1 (Table 12; Appendix VIII).

The vertical displacement of the middle Marble surface along the paleoseismic rupture zone was measured by Brunton and slope-stick profiles. Profiles 20 and 21 (Appendix VI) were measured at Excavation Sites 1 and 2 (respectively), and Profile 24 near Indian Creek (Plate I). These scarps formed largely during paleoseismic Events A and B, and therefore their height is roughly twice the amount of displacement associated with the individual events.

Profile 20 shows about 30 cm of vertical displacement of the middle Marble surface at Excavation Site 1. Since the scarp formed during two events, each event probably resulted in roughly 15 cm of vertical displacement, which is about the same as that measured in the exploratory trench at this site (Chapter VII). Lateral displacements are inferred to range from about 0.7 m to as much as 1.5 m per event, based on locally determined displacement ratios. The vertical and inferred lateral displacements yield magnitude estimates that range from 6.8 to 7.0 (Table 12; Appendix VIII). In a similar manner, measured and inferred displacement data from Profiles 21 and 24 suggest magnitude estimates of 6.8 to 7.0 (Table 12).

TABLE 12: EMPIRICAL RELATIONS OF MAGNITUDE AND PALEOSEISMIC RUPTURE ZONE PARAMETERS

Rupture zone and length/ Regression and data set	Empirical Estimation of Earthquake Magnitude[1] <--- Estimated Magnitudes ---> Minimum Magnitude	Maximum Magnitude	Mean Magnitude	Uncertainty of Mag. est. (±1 stn. dev.)
Northern Paleoseismic Rupture zone:				
Rupture length: 20 to 30 km				
Slemmons and others (1988)				
All Events	6.7	6.9	6.8	± 0.83
Strike slip	6.7	6.9	6.8	± 0.22
Extensional Events only				
All Events	6.7	6.9	6.8	± 0.22
Strike slip	6.6	6.8	6.7	± 0.25
Bonilla and others (1984)				
All Events	7.0	7.1	7.0	± 0.323
Strike slip	7.0	7.2	7.1	± 0.331
Western N. Am.	6.8	7.0	6.9	± 0.442
Displacement data from fault scarp profile (Appendix VI);				
Slemmons (1982)				
All Events	6.7	7.1	6.8	± 0.331
Strike slip	6.8	7.2	7.0	± 0.323
Bonilla and others (1984)				
All Events	6.8	7.2	7.0	± 0.323
Strike slip	6.8	7.2	7.0	± 0.331
Western N. Am.	6.8	7.2	7.0	± 0.442
Southern Paleoseismic Rupture zone:				
Rupture length: 30 to 40 km				
Slemmons and others (1988)				
All Events	6.9	7.0	7.0	± 0.83
Strike slip	6.9	7.0	7.0	± 0.22
Extensional Events only				
All Events	6.9	7.0	6.9	± 0.22
Strike slip	6.8	7.0	6.9	± 0.25
Bonilla and others (1984)				
All Events	7.1	7.2	7.1	± 0.323
Strike slip	7.2	7.2	7.2	± 0.331
Western N. Am.	7.0	7.2	7.1	± 0.442

[1] Earthquake magnitudes estimated in Appendix VIII.

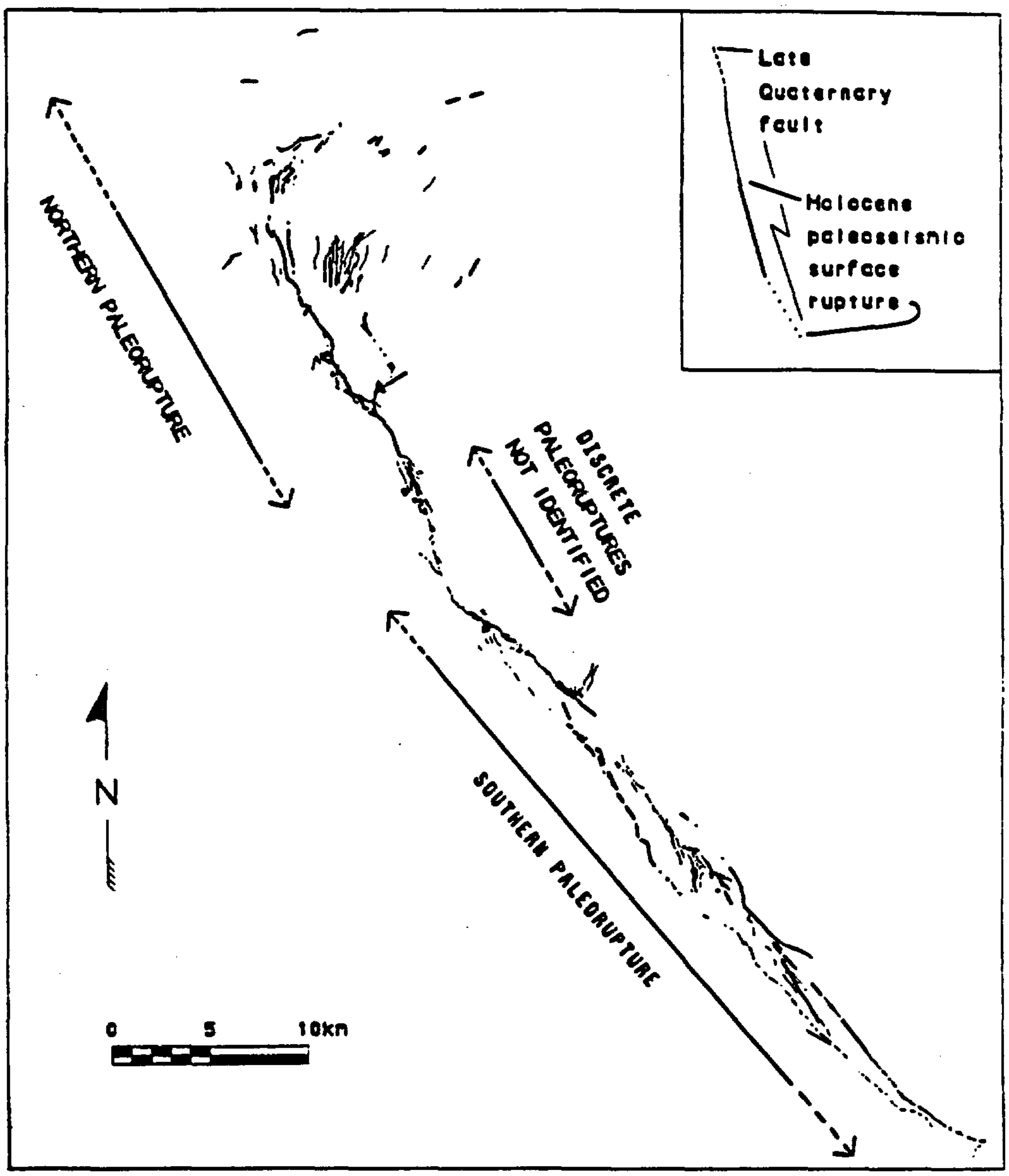

Figure 39. Map showing discrete paleoseismic rupture zones along the Fish Lake Valley fault zone based on the youthful morphology of fault scarps, which have not been identified along the central portion of the fault zone.

<u>Southern Paleoseismic Rupture Zone</u>

The southern part of the FLVFZ forms a second probable mid to late Holocene paleoseismic rupture zone (Fig. 39). The rupture zone is evident from geomorphic and photogrammatic analyses of fault scarps in probable early and middle Marble surface equivalents. The northernmost extent of the rupture zone is poorly delineated by scarplets along the Eastern subzone of the FLVFZ (Fig. 39), about 1 km south of Wildhorse Creek (Fig. 18). The continuity of the zone is apparent at Furnace Creek and southward along the Eastern subzone. A well-defined trace of the rupture zone is shown by abrupt, geomorphically youthful fault scarps about 2 to 3 km north of Indian Garden Creek, formed in Marble surface equivalents along the Western subzone. The rupture trace is prominently and continuously displayed southward along the range front, extending to a point just south of Buck Mine (Plate IIE).

Where the Western subzone displays prominent evidence of recent paleoseismic activity, the subparallel Eastern subzone displays little or no evidence of such activity. For example, the rupture zone is diffuse along the Western subzone south of Buck mine, while in contrast, the Eastern subzone displays geomorphically youthful scarps in probable Marble fan surfaces (or their equivalents), near Oasis, California (Fig. 39). These relations suggest that recent surface faulting events have alternately ruptured both subzones with apparently limited amounts of overlap.

South of Oasis to the point where Highway 63 enters the valley on the west (Fig. 18), the rupture zone is prominently displayed and comprises several scarps with irregular traces that branch from the Eastern subzone (Fig. 39). At least one of these fault scarps continues southward across the bolson floor of southernmost Fish Lake Valley, where its character and orientation change. This prominent vegetation lineament was examined in an exploratory trench at Excavation Site 4 (Plate VI). This feature is probably a fault, but definite offsets were not identified in the trench. Numerous other vegetation lineaments occur across most of the bolson floor to the south (Fig. 21). Stratigraphic and structural relations exposed in a trench at Excavation Site 3 (Plate V) show that one of these lineaments is associated with faults and fractures of tectonic origin.

Across the valley on the opposing lower piedmont slope of the Sylvania Mountains, Reheis (1990c) recently mapped well-defined scarps in Marble age alluvium that show features suggestive of right slip. These scarps probably represent the southern continuation of the paleoseismic rupture zone. The rupture zone may extend southward to the area where Holocene surface faulting was suggested from evidence exposed in a breached shutter ridge along the Eastern subzone (discussed in Chapter VI).

South of this point, the FLVFZ enters the prominent Cucomungo Canyon double restraining bend. The double bend connects the southern FLVFZ with the Northern Death Valley fault zone (Fig. 7). The bend occurs in a region of mountainous bedrock terrain, and thus the fault zone is rarely exposed in alluvium. It is difficult to evaluate the continuity of the paleoseismic rupture zone through the double bend. Mapping by Reheis (1990c) shows no scarps in mid to late Holocene alluvium within the bend. The southern extent of the rupture zone is uncertain, but it probably does not extend much beyond where it enters the double bend (Fig. 39).

In summary, the paleoseismic rupture zone along the southern FLVFZ (Fig. 39) extends southeastward from Furnace Creek to Horse Thief Canyon (Fig. 18), a straight line distance of 30 to 40 km. These rupture lengths, used in regression analyses of Bonilla and others (1984) and Slemmons and others (1989), suggest the southern rupture zone is associated with earthquakes of magnitude 6.9 to 7.2 (Table 12; Appendix VIII).

CHARACTERIZATION OF SOURCE STRUCTURE FOR SIZE DETERMINATION

LENGTH OF RUPTURE

In this section, total and half rupture lengths and lengths of desecrate rupture segments are used to estimate magnitudes of earthquakes on the FLVFZ. Total and half rupture lengths are also considered for the DVFS. Empirical relations between rupture lengths and earthquake magnitudes developed by Bonilla and others (1984) and Slemmons and others (1988) are used in Appendix VIII.

Total Fault Length

Since few historic earthquakes have ruptured the entire length of their source fault zones, regressions based on total fault length generally are considered to yield maximum estimates of magnitude.

Death Valley Fault System: The DVFS extends 320 to 350 km (Fig. 7) from southernmost Death Valley to northernmost Fish Lake Valley. It is unlikely that the total length of the DVFS has ever ruptured during a single event, although a few historic strike-slip earthquakes on the San Andreas fault system have resulted in surface ruptures of that length or longer, e.g. the 1857 and 1906 earthquakes (358 km; Sieh, 1978 and 444 km; Evernden and others, 1981, respectively).

Nevertheless, a scenario involving rupture of the total length of the DVFS is a worthwhile exercise, since the resulting magnitude estimates are considered the maximum that could occur along the fault system. Hence, these estimates represent the maximum or maximum credible earthquake, using terminology of Slemmons (1982), for the DVFS.

This rupture scenario, involving the total length of the DVFS, provides magnitude estimates of 7.8 to 8.3 (Table 13; Appendix VIII).

Fish Lake Valley Fault Zone: The FLVFZ, which is approximately 80 km-long, has prominent and nearly continuous latest Pleistocene and Holocene surface ruptures (Chapters VI and VII; Fig. 39). The entire length of the FLVFZ could have ruptured during a single event, but the most recent rupture events apparently did not (discussed in following section).

Regressions suggest that, if ruptured, the total extent of the FLVFZ would produce earthquakes of magnitudes 7.2 to 7.5 (Table 13).

Half Fault Length

Wentworth and others (1969) first proposed using half the total length of a fault in regression analyses of earthquake magnitude. Freeman and others (1986) argued that regression analyses based on half fault length provide reasonable

TABLE 13: EMPIRICAL RELATIONS OF MAGNITUDE AND LENGTH OF RUPTURE

Length of Rupture/ Regression and data set	Empirical Estimation of Earthquake Magnitude[1] <--- Estimated Magnitudes ---> Minimum Magnitude	Maximum Magnitude	Mean Magnitude	Uncertainty of Mag. est. (±1 stn. dev.)
Total length of the Death Valley fault system; 320 to 350 km				
Slemmons and others (1988)				
All Events	8.0	8.0	8.0	± 0.83
Strike slip	7.9	7.9	7.9	± 0.22
Extensional Events only				
All Events	7.8	7.8	7.8	± 0.22
Strike slip	8.0	8.0	8.0	± 0.25
Bonilla and others (1984)				
All Events	7.8	7.8	7.8	± 0.323
Strike slip	7.8	7.8	7.8	± 0.331
Western N. Am.	8.3	8.3	8.3	± 0.442
Total length of the Fish Lake Valley fault zone; 70 to 80 km				
Slemmons and others (1988)				
All Events	7.3	7.4	7.3	± 0.83
Strike slip	7.3	7.3	7.3	± 0.22
Extensional Events only				
All Events	7.2	7.2	7.2	± 0.22
Strike slip	7.2	7.3	7.3	± 0.25
Bonilla and others (1984)				
All Events	7.3	7.4	7.4	± 0.323
Strike slip	7.4	7.4	7.4	± 0.331
Western N. Am.	7.5	7.5	7.5	± 0.442
Half the length of the Fish Lake Valley fault zone; 35 to 40 km				
Slemmons and others (1988)				
All Events	7.0	7.0	7.0	± 0.83
Strike slip	7.0	7.0	7.0	± 0.22
Extensional Events only				
All Events	6.9	7.0	6.9	± 0.22
Strike slip	6.9	7.0	6.9	± 0.25
Bonilla and others (1984)				
All Events	7.1	7.2	7.2	± 0.323
Strike slip	7.2	7.2	7.2	± 0.331
Western N. Am.	7.1	7.2	7.1	± 0.442

[1] Earthquake magnitudes are estimated by empirical relations of magnitude and rupture length in Appendix VIII.

estimates of the size of events in Basin and Range Province.

Death Valley Fault System: The DVFS is perhaps capable of producing an earthquake associated with rupture of half the length of the fault system (i.e., 160 to 180 km). If so, estimates of magnitude range from 7.6 to 8.0 (Appendix VIII).

Fish Lake Valley Fault Zone: The FLVFZ is probably capable of producing an earthquake that would rupture half of its length. In fact, the southern paleoseismic rupture zone shown in Figure 39 may represent such an event. Regressions based on half the total length of the FLVFZ (35 to 40 km) yield magnitude estimates of 6.9 to 7.2 (Table 13). Hence, magnitude estimates based on half fault lengths are similar to those based on the length of paleoseismic rupture zones along the FLVFZ (cf. Tables 12 and 13).

LENGTH OF RUPTURE SEGMENTS

G.K. Gilbert, more than a century ago, argued for segmentation of seismogenic faults. The 1872 Owens Valley earthquake (M_s 7.8) apparently influenced Gilbert (1884, p.52), who stated:

> "the accumulated earthquake force is for the present spent, and many generations will probably pass before it again manifests itself... The spot which is the focus of an earthquake...is thereby exempt from earthquake for a long time. And conversely, any locality on the fault line...which has been exempt from earthquake for a long time, is by so much nearer to the date of recurrence."

This testament to Gilbert's unusual insight contains the fundamental elements of the concept of earthquake rupture segments and of the "earthquake cycle".

The fault segmentation model was formally developed by Schwartz and Coppersmith (1984). The model has been widely used in assessment of seismic potential in a variety of seismotectonic settings. The basic premise of the segmentation model is that surface rupture occurs repeatedly and rather characteristically along discrete rupture segments of a fault or fault zone. This is consistent with geological and historical observation which indicate that faults (e.g., San Andreas and Wasatch faults) typically do not rupture their total length, but rather some fraction thereof (Knuepfer, 1989).

In this study, smaller segments are considered to rupture more frequently and with smaller magnitude earthquakes than larger segments. The larger segments may in turn represent failure of multiple smaller segments. For example, the Northern and Southern paleoseismic zone of the FLVFZ (Fig. 39) apparently ruptured independently during the mid to late Holocene (discussed in a previous section), but it is also possible that they ruptured (or have ruptured) during the same large earthquake.

In addition, the DVFS probably exhibits segmentation behavior. Such behavior is suggested from paleoseismic rupture zones identified along the FLVFZ (Fig. 39), and along the Central Death Valley fault zone (Wills, 1989). Therefore, the application of the segmentation model to the DVFS and the FLVFZ appears to be warranted.

In this section, lengths of inferred rupture segments are used in regression analyses to estimate earthquake size (Appendix VIII).

<u>Criteria used to Identify Rupture Discontinuities</u>

Historical and geological observations suggest surface ruptures can be inhibited or conserved by structural, geometrical, geological, behavioral, paleoseismic, geomorphological, geophysical and rheological characteristics of the fault zone (Schwartz and Coppersmith, 1984, 1986; Slemmons and DePolo, 1986; Sibson, 1986; Wheeler and Krystinik, 1988; Knuepfer, 1989).

Criteria used by DePolo and others (1990) to evaluate historic rupture characteristics of faults in the Basin and Range Province have generally been followed in this section to identify possible rupture discontinuities along the FLVFZ. In this study, the seismic character of faults is included as a behavioral criterion.

Paleoseismic rupture zones provide direct evidence of past surface rupture events on the FLVFZ, and thus best illustrate expectable rupture behavior. These rupture zones have been used to evaluate the influence of possible rupture discontinuities along the fault zone.

The identification of possible rupture discontinuities along the FLVFZ has been based on morphostratigraphic, structural, paleoseismic, and geomorphological information presented in Chapters IV through VII.

Possible Rupture Discontinuities along the FLVFZ

A total of 13 possible rupture discontinuities have been identified along the FLVFZ (Fig. 40); the possible rupture end-points, are designated from north-to-south, 1 through 13. Each of these discontinuities in the fault zone is described in the following subsections.

Rupture Discontinuity 1: The northwestern terminus of the FLVFZ is a possible rupture discontinuity based on a number of criteria, including branching (i.e., structural criterion), gradual to abrupt bending of the traces (i.e., geometrical), marked widening of the zone (i.e., rheological), clustering of seismicity, variation from right slip to dip slip (i.e., behavioral), and associated local extension (Fig. 40a, #1). Furthermore, the northern end of the northern paleoseismic rupture zone (Fig. 39) apparently coincides with this discontinuity.

Knuepfer (1989) examined characteristics of rupture end points of more than 75 historical surface ruptures worldwide. He suggested that rupture end points occur where there is a change in the primary sense of slip from strike slip to dip slip along a fault. Knuepfer considers such changes as diagnostic of segment boundaries. In which case, Discontinuity #1 represents a rupture end point.

Rupture Discontinuity 2: A divergent double bend in the master fault of the FLVFZ, where it traverses the Leidy Creek fan, is considered a discontinuity on the basis of geometrical, structural, behavioral, and geomorphological evidence (Fig. 40a, #2). The double bend is approximately 0.7 km wide and separates a distributive, range bounding network of faults on the south from the predominantly right slip master fault to the north.

Theoretically, divergent double bends in strike-slip fault zones can arrest rupture propagation (Sibson, 1985). However, historical surface rupture data compiled by Knuepfer (1989) suggests that releasing bends less than 2 km wide were often ruptured through.

Thus, its small size suggests this bend is probably insufficient to serve as a rupture end point. This is supported by fact that the northern paleoseismic rupture zone is well defined through the double bend (cf. Figs. 39 and 40). I infer that this divergent bend has limited influence on propagation of surface ruptures.

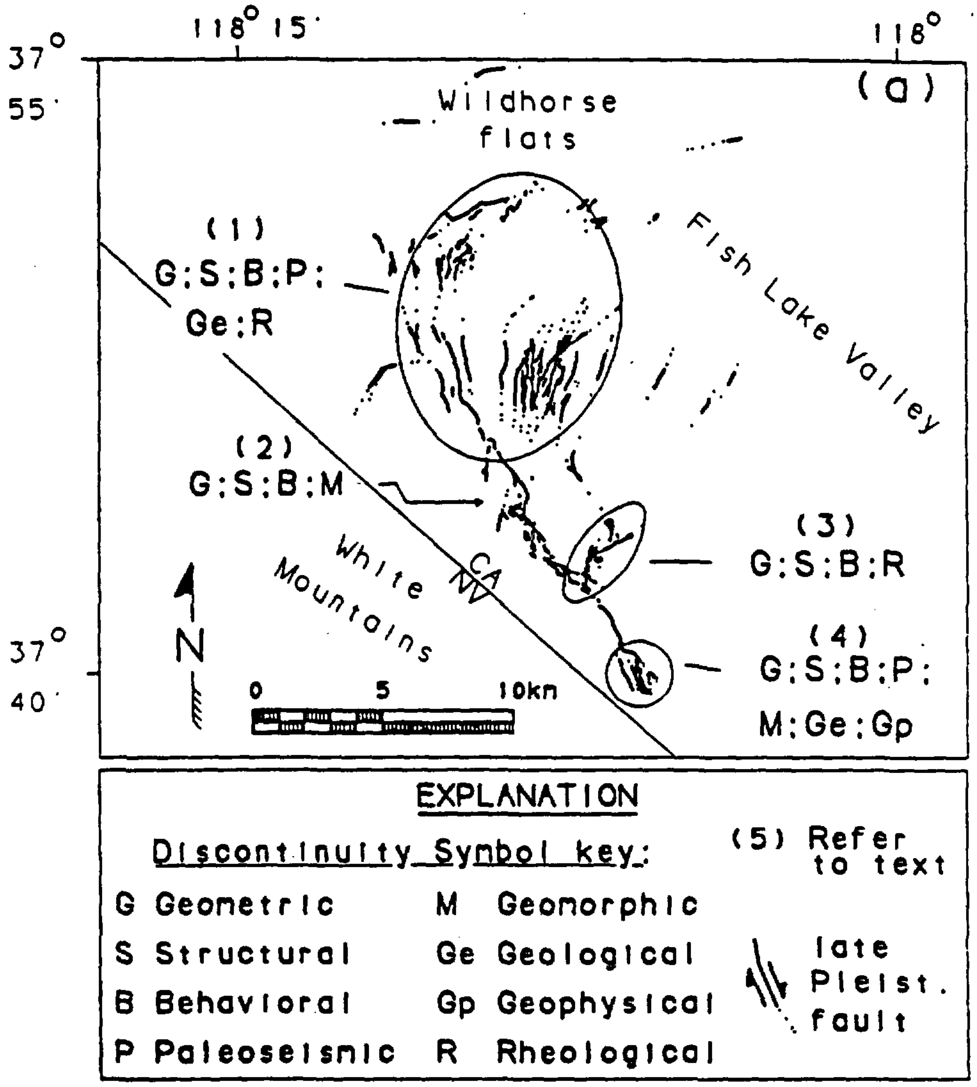

Figure 40. Map showing possible rupture discontinuities along the northern (a), central (b), and southern (c) portions of the Fish Lake Valley fault zone. The various discontinuities were identified based on the criteria listed in the explanation. Compare with Figure 18 for the location of drainages.

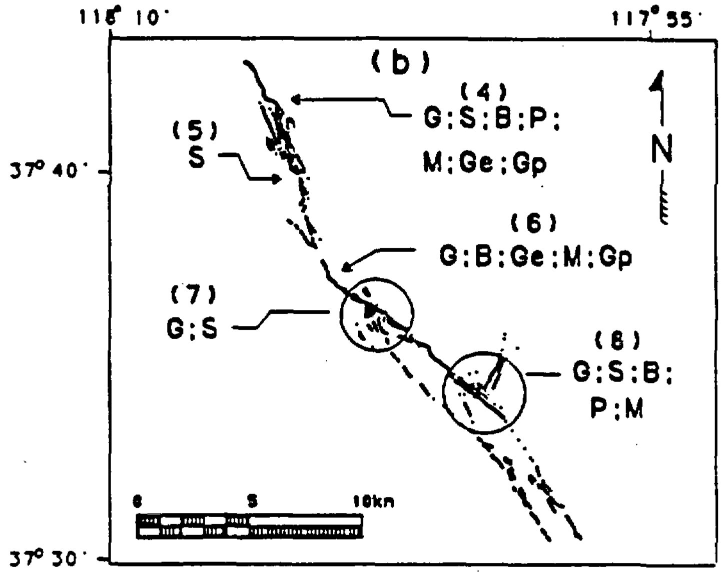

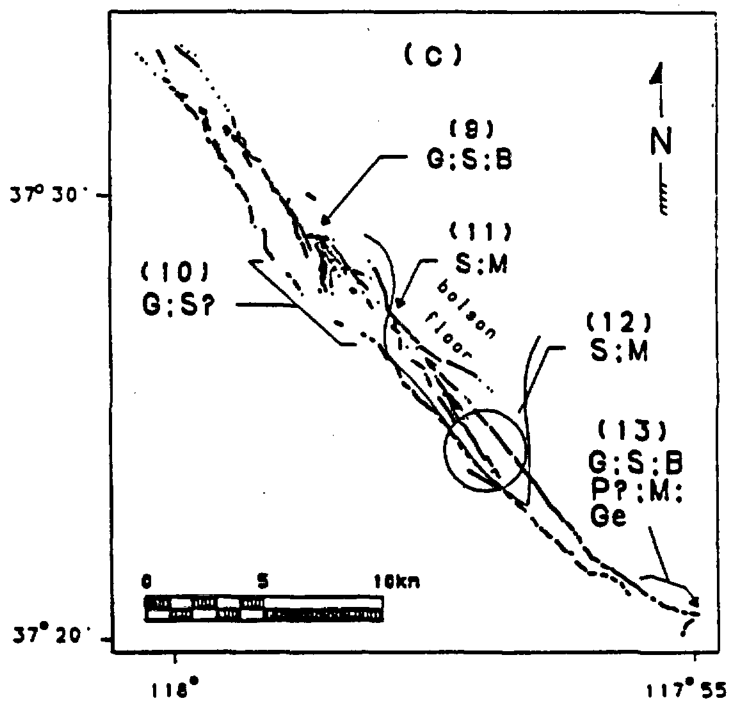

Figure 40. Continued

Rupture Discontinuity 3: Between Leidy Creek and Busher Creek, the FLVFZ bends about 20° westward, and forms a distributive pattern of subparallel faults (Fig. 18). Several right-stepping én echélon branch faults extend northeastward from this apparent releasing bend in the northern FLVFZ. North of this bend, the fault zone is more than 3 km wide, while to the south it is less than 1 km wide. Hence, the bend is identified as a possible rupture discontinuity (Fig. 40a, '3). The northern paleoseismic rupture zone also extends through this bend (Fig. 39), and therefore the discontinuity is not considered to have a large influence on rupture propagation.
Rupture Discontinuity 4: The northern paleoseismic rupture zone (Fig. 39) extends from the northernmost discontinuity (Fig. 40a, '1), through two more discontinuities ('2 and '3), and apparently ends near the fourth discontinuity, which occurs at the northern end of the Dyer subzone (Fig. 40a, '4). This subzone forms a small-scale (about 3 km) pull-apart basin between the én echélon, predominantly right slip Northern and Eastern subzones of the FLVFZ (Chapter VI). As shown in Figure 40a, this discontinuity is defined in part by gravity data that suggests a thick sequence of low density sediment occurs adjacent to the subzone. A change from predominantly right slip to right-divergent slip with a significant dip-slip component characterizes the central FLVFZ along the Dyer subzone.

DePolo and others (1989) examined the relationship between surface rupture propagation and fault zone characteristics for 17 historic surface faulting events in the Basin and Range Province. Several of these surface ruptures had identifiable end points such as extensional basins, cross faults and branch faults. Hence, Discontinuity '4, at the northern end the pull apart basin, is a likely rupture end point.
Rupture Discontinuity 5: The Dyer subzone south of Perry Aiken Creek changes from a widely distributive fault pattern to essentially a single master fault (Fig. 18). The change in the fault pattern is identified as a structural discontinuity that probably has only limited (if any) influence on rupture propagation (Fig. 40b, '5).
Rupture Discontinuity 6: The master fault of the central FLVFZ abruptly bends 35° northwestward where the Dyer subzone is linked to the Eastern subzone (Fig. 18). The range-bounding master fault north of the bend has significant vertical

displacement. In contrast, south of the bend the fault zone is distributed and contains a series of faults on the piedmont slope that have a predominance of right slip (discussed in Chapter VI). Therefore, the bend (Fig. 40b, *6) is a probable rupture end point.

<u>Rupture Discontinuity 7</u>: The junction of the Eastern and Western subzones (Fig. 22) on the Wildhorse Creek fan is identified as a discontinuity from geometric and structural relations (Fig. 40b, *7). However, this structural intersection does not appear to be a discontinuity that would significantly inhibit rupture propagation.

<u>Rupture Discontinuity 8</u>: South of Furnace Creek, the Eastern subzone changes along strike from a braided network of faults with opposing vertical displacements to a single master fault (Figs. 18 and 19) that forms large down-to-the-east scarps. The change in fault pattern is broadly coincident with a gradual 30° bend in the fault zone, and with the branching relationship of several northeast-striking subsidiary faults (Fig. 40b, *8).

Discontinuity *8 approximately coincides with the northernmost scarplets that are clearly associated with the Southern paleoseismic rupture zone (cf. Figs. 39 and 40). However, the rupture zone could have extended into or through the Dyer subzone, as suggested by the oversteepened bases of large fault scarps along this section of the fault zone. The discontinuity may inhibit rupture propagation, but it would be unlikely to serve as a rupture end point. Perhaps this discontinuity together with others to the north (i.e. *6 and *7) would have the cumulative effect of arresting surface ruptures, thus forming a "soft" rupture segment boundary.

<u>Rupture Discontinuity 9</u>: The Eastern subzone of the southern FLVFZ forms a left step of approximately 0.75 km near the town of Oasis (Figs. 18 and 19). A highstanding, asymmetric ridge within this probable restraining step (discussed in Chapter VI) lies obliquely (N70°W) to the northwestward-striking subzone (N35°-30°W).

This step is identified as a discontinuity based on geometrical, structural and behavioral criteria (Fig 40c, *9). The southern paleoseismic rupture zone (Fig. 39) is represented by fault scarplets on either side of the step, but the rupture apparently skirted around the eastern end of the ridge because the most prominent scarplets occur east and north of the step. This discontinuity (Fig 40c, '9) apparently had little influence on the last paleoseismic rupture event, probably due to its small size (cf. Knuepfer, 1989). Hence, Discontinuity '9 is not considered a rupture end point.

Rupture Discontinuity 10: The Western subzone has a general lack of surface expression (a "gap") southwest of Oasis (Fig. 19). The gap approximately marks the intersection of the subzone with a northeastward projection of a left-slip fault in the White Mountains mapped by McKee and Nelson (1967), although the proposed intersection is unexposed at the surface.

This gap is considered to be a discontinuity from geometrical and structural relations (Fig. 40c, '10). The geomorphic expression of the Southern paleoseismic rupture zone diminishes southward along this portion of the Western subzone. In contrast, this paleorupture zone is continuous and well defined along the subparallel Eastern subzone (Fig. 39). Thus, it is possible that Discontinuity '10 inhibits rupture along this portion of the Western subzone.

The gap in the Western subzone is minor relative to the 10 km or more gap in surface ruptures associated with the 1932 Cedar Mountain earthquake (DePolo and others, 1987). Hence, this discontinuity probably exerted little influence on propagation of surface ruptures along the fault zone as a whole.

Rupture Discontinuity 11: The structural and geomorphic character of the Eastern subzone changes where it crosses from piedmont alluvium to fine-grained playa (lake?) sediment of the bolson floor of southern Fish Lake Valley. In alluvium, the northerly-striking master fault (N15°W, average) forms a down-to-the-east scarp delineated by an alinement of springs. Near the boundary of the piedmont slope with the bolson floor the master fault bends 30° westward (to N45°W) and forms a vegetation lineament lacking morphological expression. This is one of several lineaments that form an én echélon pattern on the bolson floor (Fig. 21).

These structural and morphological changes in the Eastern subzone suggest a possible rupture discontinuity (Fig 40c, '11). However, these changes probably reflect different mechanical properties of the geological materials in which the fault is expressed, and hence they should conserve slip. This is supported by the southern paleoseismic rupture zone (Fig. 39) which apparently extends through the

Discontinuity *11.

Rupture Discontinuity 12: Similar structural and morphological changes occur where the Eastern subzone leaves the bolson floor and traverses the piedmont slope on the opposite side of southern Fish Lake Valley (Fig. 40c, *12). These changes are likely to conserve slip, for the same general reasons stated above. The southern paleorupture zone (Fig. 39) also extends through this proposed discontinuity.

Rupture Discontinuity 13: The southern FLVFZ is separated from the Northern Death Valley fault zone by the Cucomungo Canyon double-restraining bend in the DVFS (Fig. 7). This approximately 6 km wide restraining bend forms the southernmost discontinuity to surface ruptures along the FLVFZ (Fig. 40c, *13).

The restraining bend is identified as a discontinuity, based on geometrical, structural, behavioral, and geomorphological criteria. The southern paleoseismic rupture zone apparently ended at the bend (Fig. 39), as suggested by a general lack of Holocene scarps within the bend (Reheis, 1990b). Hence, this discontinuity probably inhibits propagation of surface rupture.

None of the historical surface ruptures studied by Knuepfer (1989) propagated through restraining-double bends wider than about 5 km. Hence, the large-scale Cucomungo Canyon double-restraining bend in the DVFS (Fig. 40c, *13) probably is a rupture end point. However, the possibility that ruptures have propagated through the bend and along some portion of the FLVFZ and (or) the Northern Death Valley fault zone cannot be eliminated. Such a surface rupture event has apparently has not occurred during the middle or late Holocene, based on recent mapping by Reheis (1990b).

Scenarios for Segmentation of Ruptures

In this section, segmentation scenarios are developed for the FLVFZ based on the possible rupture discontinuities identified in the previous section. Rupture segments are considered both to represent independent seismic sources and to operate as coupled-source segments associated with failure of two or more smaller segments. The length of rupture segments is used in regression analyses to characterize earthquakes size (Appendix VIII).

Only two of the 13 discontinuities identified along the FLVFZ would likely terminate propagation of surface ruptures. These discontinuities are defined as rupture segment boundaries, based on several different criteria (discussed above). The criteria include changes in the predominant sense of slip in association with geometric changes in the fault zone. Additionally, the paleoseismic rupture zones along the FLVFZ apparently end at or near these discontinuities.

The inferred segment boundaries (discontinuities) are at either end of the FLVFZ. The northern boundary is formed by the northwestern termination of the fault zone, in an area of extension (Fig. 40a, •1). The southern boundary (Fig. 40c, •13) is formed by the large-scale, restraining, double bend in the DVFS (Fig. 7). If these are the only two segment boundaries (i.e., Fig. 40, •1 and •13), then the FLVFZ would behave as a single rupture segment (Fig. 41). This scenario for the FLVFZ yields magnitude estimates of 7.2 to 7.5 (Table 14). As might be expected, these results are equivalent to those determined from total fault length analysis (Table 13).

The FLVFZ may also comprise multiple rupture segments, as suggested by two apparently unrelated paleoseismic rupture zones (Fig. 39). In this case, the most likely rupture discontinuities would be associated with the pull-apart basin along the central FLVFZ. The 3 km-wide extensional basin was formed by right-divergent slip on the northerly-striking Dyer subzone, and right slip on the northwest-striking, én echélon Northern and Eastern subzones (Fig. 18).

Surface rupturing may be inhibited by two prominent discontinuities in the central FLVFZ at either end of the Dyer subzone (Fig. 40b, •4 and •6). The lack of evidence of late Holocene ruptures between these discontinuities (cf. Figs. 39 and 40) suggests they have functioned as rupture end points.

A 20 to 25 km-long rupture segment (Fig. 41) is suggested to occur between the northwestern termination of the FLVFZ (Fig. 40a, •1) and the northern end of the Dyer subzone (Fig. 40a, •4). Regression analyses of Slemmons and others (1988) and Bonilla and others (1984) provide estimates of magnitude that from 6.7 to 7.1 for this "Northern" rupture segment (Table 14).

The southern end of the Dyer subzone (Fig. 40b, •6) may represent a

TABLE 14: EMPIRICAL RELATIONS OF MAGNITUDE AND RUPTURE-SEGMENT LENGTH

Segment and length/ Regression and data set	Empirical Estimation of Earthquake Magnitude[1] <--- Estimated Magnitudes ---> Minimum Magnitude	Maximum Magnitude	Mean Magnitude	Uncertainty of Mag. est. (±1 stn. dev.)
FLVFZ (coupled-source) Segment; 65 to 75 km				
Slemmons and others (1988)				
All Events	7.3	7.3	7.3	± 0.83
Strike slip	7.3	7.3	7.3	± 0.22
Extensional Events only				
All Events	7.2	7.2	7.2	± 0.22
Strike slip	7.2	7.3	7.2	± 0.25
Bonilla and others (1984)				
All Events	7.3	7.4	7.3	± 0.323
Strike slip	7.4	7.4	7.4	± 0.331
Western N. Am.	7.4	7.5	7.5	± 0.442
Northern Segment; 20 to 25 km				
Slemmons and others (1988)				
All Events	6.7	6.8	6.8	± 0.83
Strike slip	6.7	6.8	6.8	± 0.22
Extensional Events only				
All Events	6.7	6.8	6.7	± 0.22
Strike slip	6.6	6.7	6.7	± 0.25
Bonilla and others (1984)				
All Events	7.0	7.0	7.0	± 0.323
Strike slip	7.0	7.1	7.1	± 0.331
Western N. Am.	6.8	6.9	6.8	± 0.442
Dyer Segment[2]; 10 to 18 km				
Slemmons and others (1988)				
All Events	6.4	6.7	6.6	± 0.83
Dip slip	6.4	6.7	6.5	± 0.34
Extensional Events only				
All Events	6.4	6.6	6.5	± 0.22
Dip slip	6.4	6.7	6.6	± 0.35
Bonilla and others (1984)				
All Events	6.7	6.9	6.8	± 0.323
Western N. Am.	6.4	6.7	6.6	± 0.442

TABLE 14: Continued.

Segment and length/ Regression and data set	Empirical Estimation of Earthquake Magnitude[1] <--- Estimated Magnitudes --> Minimum Magnitude	Maximum Magnitude	Mean Magnitude	Uncertainty of Mag. est. (±1 stn. dev.)
Southern Segment: 22 to 36 km				
Slemmons and others (1988)				
All Events	6.8	7.0	6.9	± 0.83
Strike slip	6.8	7.0	6.9	± 0.22
Extensional Events only				
All Events	6.7	6.9	6.8	± 0.22
Strike slip	6.7	6.9	6.8	± 0.25
Bonilla and others (1984)				
All Events	7.0	7.1	7.1	± 0.323
Strike slip	7.1	7.2	7.1	± 0.331
Western N. Am.	6.8	7.1	7.0	± 0.442

[1] Earthquake magnitudes are estimated by empirical relations of magnitude and length of rupture in Appendix VIII.

[2] Since the Dyer Segment (subzone) has a significant or prehaps dominant dip slip component, regressions based on dip slip data sets are used in addition to other relations in Appendix VIII.

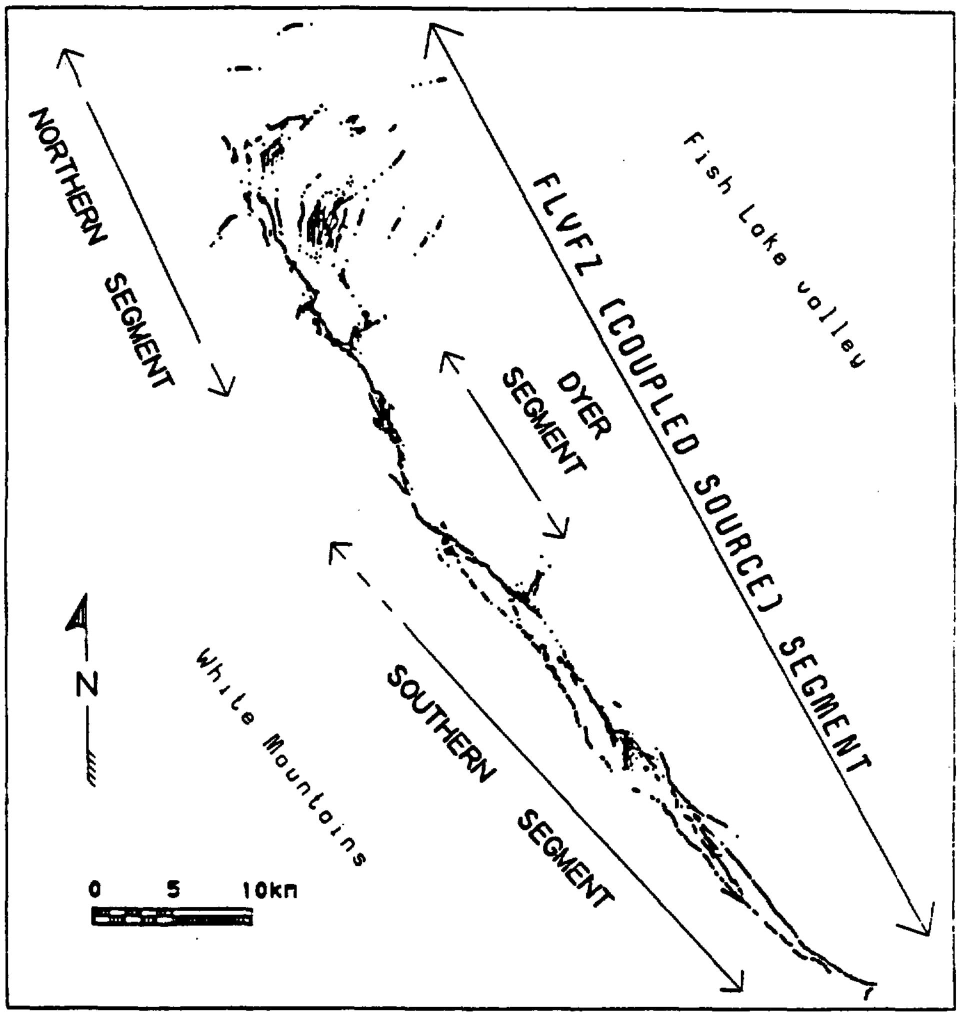

Figure 41. Possible earthquake rupture segments along the Fish Lake Valley fault zone, which are based on the influence that the discontinuities shown in Figure 40 are inferred to have on surface rupture processes.

somewhat diffuse rupture end point, possibly involving other discontinuities to the south (i.e., •7 and •8). Hence, the Dyer subzone may represent a single rupture segment (Fig. 41, "Dyer" segment).

The Dyer segment is from 10 to 18 km in length, depending on the position of its southern end point. Regressions developed by Slemmons and others (1988) for dip-slip faults are used in addition to those developed for other fault types (e.g., Bonilla and others, 1984)(Appendix VIII), because this section of the FLVFZ displays a significant vertical slip component. The resulting estimates of magnitude range from 6.4 to 6.9 (Table 14).

The "Southern" segment of the FLVFZ (Fig. 41) extends southeastward from the Dyer segment (i.e., Fig. 40b, •6 to •8) to the large-scale, restraining double bend (Fig. 40c, •13). This predominantly right slip rupture segment is from 22 to 36 km long. These rupture lengths correspond to magnitudes of 6.7 to 7.1 (Table 14).

DISCUSSION OF EARTHQUAKE SIZE

MAXIMUM CREDIBLE EARTHQUAKE

Slemmons and Chung (1982) defined a maximum credible earthquake (MCE) "as the strongest earthquake that is likely to be generated along an active fault zone." A somewhat more conservative definition of MCE is the largest or maximum earthquake that appears capable along a fault or in an area (California Division of Mines and Geology, 1975). The MCE is generally referred to by news media and layman as "The Big One."

The various approaches used above to estimate the earthquake potential of the FLVFZ are considered in this section in the evaluation of a MCE.

The total fault length and single rupture segment scenarios yield the largest magnitude estimates that can be associated with this fault zone as a seismic source independent of the DVFS to the south. The maximum estimates of magnitude based on these scenarios range from 7.2 to 7.5 M_s (mean magnitudes). When half the total length is used, maximum earthquake magnitudes of 7.0 to 7.2 are estimated

(Table 13). Earthquake magnitudes estimated from the lengths of paleoseismic rupture zones range from 6.8 to 7.2 M_s (Table 12).

When the statistical uncertainty associated with the regression analyses is added to the estimates of maximum magnitude, the resulting range is from magnitude 7 to as high as 8. The mean of these estimates of maximum magnitude is about 7.0, and the mean plus one standard deviation of the regression techinque is about 7.5. The MCE magnitude for the FLVFZ is taken to be 7.3 ± 0.4 (M_s).

The data presented in this thesis does not preclude, but instead suggests, the possibility of multiple rupture segments failing in association with a single large earthquake. In addition, if the FLVFZ is a seismic source that ruptures together with the DVFS, the resulting magnitude estimates could be a full magnitude value higher than the MCE estimated for the FLVFZ alone.

CHARACTERISTIC EARTHQUAKE SCENARIO

The master fault of the northern FLVFZ has ruptured repeatedly and apparently in a similar manner, during the late-middle to late Holocene, as determined from paleoseismicity data (Chapter VI and previous section). Exploratory trench studies and geomorphological analysis of paleo-rupture zones suggest a characteristic behavior for two of the most recent surface faulting events on the northern FLVFZ.

A scenario involving a "characteristic" earthquake on the northern paleo-rupture zone (Fig. 39), is supported by the paleoseismic record at Excavation Sites 1 and 2 (discussed in Chapter VII). The last two significant surface rupturing events on the northern FLVFZ were apparently similar in rupture character. However, a more complete record spanning several rupture events is needed to confirm the characteristic earthquake behavior.

Both single-event displacement data from exploratory trench studies and the length of the northern paleo-rupture zone are used to evaluate a characteristic earthquake. These data suggest magnitudes ranging from 6.7 to 7.2. The mean of these magnitude estimates is 7.1 and the mean plus one standard deviation of the regression techinque is 7.4. The characteristic earthquake on the northern FLVFZ is assigned a magnitude of 7.1 ± 0.3.

Up to this point, the Northern and Southern paleo-rupture zones (Fig. 39) have been considered to be unrelated. However, it is possible that these zones ruptured in association with the same large event (Fig. 41). In this case, the characteristic earthquake magnitude would be equivalent to the MCE magnitude (discussed above).

COMPARISON WITH PREVIOUS SIZE ESTIMATES

Several previous studies have addressed the seismic potential of the White Mountain seismic gap, the DVFS, and the Death Valley region. However, few studies have directly addressed the seismic potential of the FLVFZ. The following is a brief summary of selected assessments of the seismic potential of the DVFS, the White Mountain seismic gap, and the FLVFZ.

Thenhaus and Wentworth (1982) tentatively defined regions (or zones) of the Basin and Range Povince based on different surface faulting characteristics, including repeat times and prehistoric earthquake magnitudes. Thenhaus and Wentworth identified the DVFS as the eastern boundary of a region characterized by recurrent Holocene faulting and earthquake magnitudes as large as 8 (their Zone 3).

Ryall (1973) identified Fish Lake Valley as one of several regions that should be considered as having a relatively high potential for large earthquakes. Ryall and VanWormer (1980) suggested that Fish Lake Valley and Death Valley have the potential for earthquakes of maximum magnitude 8.0 or greater, based on regression analyses of fault lengths.

Wills (1989) examined the Central Death Valley fault zone and determined that the most recent surface faulting event occurred during Holocene time. Wills suggested that the magnitude of the faulting event was 6.5 or larger based on regression analysis using the smallest incremental displacement (i.e., assumed single-event slip).

Wallace (1978) identified three seismic gaps in the western Great Basin, of which the White Mountain seismic gap was suggested to be the most likely candidate for the next magnitude 7 to 8 earthquake (Wallace and others, 1983).

Ryall and Ryall (1983) recognized the potential for faults in the White Mountain seismic gap to produce earthquakes of magnitude 7+. They suggested the possibility of surface rupture along a number of faults, including the northern FLVFZ.

Magnitude estimates from the above studies are generally consistent with the MCE assigned to the FLVFZ in this study. The characteristic earthquake magnitude estimated in this study is slightly greater than the estimated magnitude of the most recent earthquake along the Central Death Valley fault zone (Wills, 1989).

FREQUENCY AND RECENCY OF PALEOSEISMIC ACTIVITY

The recency and frequency of paleoseismic events are essential aspects to all assessments of seismic potential. In this section, the frequency and recency of surface rupturing events along the northern FLVFZ are summarized from exploratory trench studies (Chapter VII). The paleoseismic history of surface faulting events along the northern FLVFZ is shown in Table 10 and summarized below.

The first event occurred after about 4.1 to 3.4 ka and preferably after 2.4 ka, but before about 1.5 ka. The second event was similar in rupture character to the first event and occurred after 1.6 ka and preferably after about 1.0 ka, but before about 0.5 ka. The third event occurred after about 0.7 ka (Table 10). Relative to the first two paleoseismic events along the northern FLVFZ, the most recent event was insignificant. Hence, this minor event is not considered below. The paleoseismic record suggest a recurrence rate for characteristic events of about 1100 ± 600 years (preferred estimate), but could be as long as about 3000 years.

SUMMARY: IMPLICATIONS FOR SEISMIC POTENTIAL

The seismic potential of the FLVFZ has been characterized by estimating the size, frequency and recency of paleoseismic activity along the fault zone during the mid to late Holocene, and by examining source structure characteristics (above). This assessment has important implications for the seismic potential of the FLVFZ.

The FLVFZ is an active fault with a mid to late Holocene paleoseismic behavior characterized by recurrent surface faulting events of magnitude 7 or larger. The last such event on the northern FLVFZ probably occurred after 1600 and before about 500 years ago. The recurrence rate of characteristic earthquakes is about 1100 years on the northern FLVFZ, but may range from 500 to about 3000 years.

Source structure characteristics of the FLVFZ suggest the fault zone is capable of producing a MCE of about M_s 7.3 (±0.4). If the FLVFZ ruptures in association with part or all of the DVFS, magnitudes of 8 or larger are possible (Appendix VIII).

No attempt has been made to forecast the occurrence of the next large earthquake along the FLVFZ. At this point, the database does not support such speculation.

CHAPTER IX
SUMMARY AND CONCLUSIONS

Fish Lake Valley, Nevada and California, contains extensive Quaternary alluvial fan deposits from streams that débouch eastward from major canyons of the majestic White Mountains. Formed in the surficial fan alluvium is a morphostratigraphic sequence composed of six distinct and regionally correlative units. Each member of the sequence is associated with a general period of landscape stability, and thus provides a record during depositional hiatuses. Morphostratigraphic units are defined and distinguished by their form, and generally supported by characteristics of geomorphic surfaces and pedogenic soils. Numerical ages for these units are estimated by radiocarbon dates and by preliminary tephrochronology.

Morphostratigraphic units occupy specific positions in the regional landscape. The mid to late Pleistocene units retain little, if any, of their relict bar-and-swale surface morphology and most are preserved as uplifted fan remnants fringing the eastern front of the White Mountains. The latest Pleistocene to Holocene morphostratigraphic units have relatively unmodified relict surfaces, and are most extensive within the alluvial mosaics that fringe the valleyward margin of the older Pleistocene units. Holocene units also form inset fan remnants within fanhead trenches, and alluvial fanlettes aligned along major faults of the FLVFZ.

A comparison of the timing of multiple Holocene fan-building episodes with local and regional climatic fluctuations supports previous arguments that sedimentation is synchronous with changes to greater aridity (e.g., Huntington, 1907). Furthermore, depositional hiatuses, i.e., periods of fan surface stability, appear to be simultaneous with glacial advances. These relations suggest that the relatively minor climatic fluctuations of the Holocene have controlled the major alluviation events in the region.

The minor Holocene climate changes apparently influenced erosion and sedimentation throughout entire drainage-fan systems of the eastern White Mountains. This implies that the profound climatic changes during the Pleistocene had similar, but significantly greater, influence on these drainage-fan systems. This is indicated by deep head cirques and by the broad U-shaped morphology of canyons at higher elevations of eastern White Mountains, and by the voluminous Pleistocene alluvial fan deposits in western Fish Lake Valley.

The late Pleistocene Indian morphostratigraphic unit is characteristically capped by fine-grained eolian deposits. Formed within these probable desert loess layers are flights of small-scale steps. These micro-relief features are oriented perpendicular to local slope and increase in height and decrease in width with increasing slope. This microtopographic steps results from downslope movements of water-saturated desert loess layers on gently sloping fan surfaces, by solifluction. This process is rather unique, since it depends less on the prevailing climatic conditions than on time, pedogenic processes and eolian sediment influx. Solifluction steps are diagnostic features of many mid to late Pleistocene alluvial fan remnants in the western Great Basin.

The relative degree of soil development is a useful and reliable indicator of relative age of morphostratigraphic units. Soils have more prominent pedogenic features in progressively older units of the series. Undoubtedly, time is the most significant genetic factor accounting for differences in soils. Morphostratigraphic units are therefore members of the regional chronosequence, and thus provide a means of evaluating pedogenesis with increasing soil age.

The morphology of carbonate accumulations in soils is the pedogenic feature that best discriminates morphostratigraphic units. In part, this is due to the durability of secondary carbonate, and the rate at which it accumulates in the gravelly, calcareous parent materials of the Plate I area. Gravelly soils a hundred to several hundred years old have incipient (or no) accumulations of pedogenic carbonate. The late Holocene (3 to 1 ka) soils have prominent Stage I Bk horizons, and the mid Holocene to latest Pleistocene (4?to 18? ka) soils have Bk horizons of Stage II carbonate morphology. The late Pleistocene soils contain massive, Stage III Bk (to K) horizons, and the late-middle Pleistocene (post 740 ka) soils have Stage

IV horizons. Thus, carbonate morphology is useful for recognition and correlation of morphostratigraphic units that range in age from latest Holocene to at least late-middle Pleistocene.

Soil field properties were semi-quantitatively evaluated using the soil development index of Harden (1982) and Harden and Taylor (1983). The relationship between soil ages and the degree of soil development is clearly indicated by soil development indices. The selected property index was chronologically calibrated using radiocarbon-dated soils, and provides an important means of estimating Holocene soil ages where geochronological age control is lacking.

The morphology of alluvial fans in western Fish Lake Valley clearly and dramatically records tectonic activity along the Quaternary FLVFZ. Tectonic perturbations are recorded by fault scarps, small-scale fault blocks, shutter and pressure ridges, side-hill benches and ridge-crest saddles, vegetation lineaments, and drainages that are deflected, offset, abandoned or captured, and beheaded. Furthermore, the upstream proximity of prominent stepped sequences and large fanhead trenches to the FLVFZ result from intermittent vertical displacements. The alluvial fans have also been disrupted by lateral displacements along the FLVFZ, in addition to regional and local tectonic tilting during the Quaternary.

As a direct consequence of tectonic perturbations, alluvial fan remnants along the eastern White Mountains have been uplifted and deeply dissected. This resulted in downfan migration of depositional loci and downstream convergence of alluvial fan surfaces. Thus, alluvial fans of the study area are in part orogenic deposits, characterized by actively aggrading mid and lower fan surfaces and degrading fanheads. Holocene deposition was clearly influenced by vertical movements on the FLVFZ. This is indicated by the alignment of Holocene fan apices along the bases of prominent fault scarps.

The tectonic setting of the western Great Basin is dominated by the major, predominantly right-slip WLSZ. The longest, and perhaps most significant, structural element of the shear zone is the nearly 350 km-long DVFS. This Quaternary fault system separates regional domains of conspicuously contrasting tectonic styles and rates. The orientation, style, and timing of faults, and the translation directions of crustal-scale blocks in the western Great Basin and the Sierra Nevada Province, suggests that strain related to the post-4 Ma North America-Pacific plate boundary has been superimposed on the structural fabric of the region.

The FLVFZ is a regionally significant component of, and is kinematically linked with, the DVFS. This northwest-striking predominantly right-slip fault zone has a variable, but generally minor, vertical-slip component. The FLVFZ comprises contemporaneous west-northwest-striking contractional faults, northwest- to north-northwest-striking right-slip to right-divergent slip faults, north- to north-northeast-striking normal faults, and northeast-striking, possibly left-divergent slip faults.

The FLVFZ terminates in northwestern Fish Lake Valley by branching into numerous faults in a horsetail splay pattern, and abruptly bends to the northeast. At the termination of the fault zone, right slip on the northwest-striking master and subsidiary faults is transferred to normal slip on the north- to northeast-striking branch faults. This conversion of the primary sense of slip results in east-west to west-northwest extension. Thus, northwestern Fish Lake Valley is an extensional basin related to strike-slip faulting along the FLVFZ.

A pull-apart basin, developed within a right step in the central FLVFZ, provides a small-scale analog of the tectonic setting of central Death Valley. This extensional basin was produced by divergent movement on the northerly-striking Dyer subzone, and right slip on the northwest-striking, én echélon Eastern and Northern subzones. This apparently deep sedimentary basin lies opposite White Mountain Peak (14,246 ft), the highest point along the crest of the White Mountains. The relationship between the step in the fault zone, the height of the range, and the apparent depth of the basin argue for significant long-term vertical slip along the Dyer subzone, and a protracted geometry of the central FLVFZ.

The style of faulting along the FLVFZ is dictated by the relative motion of the White Mountains and Fish Lake Valley structural blocks, and the geometry of their faulted boundary (i.e., strike of the FLVFZ). The White Mountains massif apparently tracks the northwest translation of the Sierra Nevada Province at a minimum rate of 0.7 to 0.8 mm/yr, but could exceed 2.3 to 2.4 mm/yr, relative to the Fish Lake Valley block. The style of faulting along the FLVFZ is therefore consistent with late Cenozoic style of the DVFS, and with the generally east-west extension in the western Great Basin.

The paleoseismic behavior of the FLVFZ has been characterized by detailed examination of structural and stratigraphic relations exposed in exploratory trenches, and by geomorphic evaluation of paleorupture zones. The mid to late Holocene paleoseismic behavior is characterized by recurrent large earthquakes associated with prominent surface ruptures along extensive portions the FLVFZ. The character and extent of the last two significant surface rupture events is similar, suggesting a characteristic earthquake behavior for at least the northern FLVFZ.

A variety of approaches involving morphostratigraphic, structural, and paleoseismic data have been used to estimate the size, frequency, and recency of large earthquakes on the FLVFZ. This assessment of seismic potential suggests that the most recent characteristic earthquakes on the northern FLVFZ were 7.1 ± 0.3 M_w. Paleoseismicity studies suggest the last such event occurred after 1.6 ka, probably after 1.0 ka, and before 0.5 ka. These studies further suggest that similar events rupture the northern FLVFZ about once every 1.1 ka, but could occur every 0.5 ka to as much as 3.0 ka.

Segmentation scenarios for the FLVFZ are based on examination of possible rupture discontinuities. Only two of 13 identified discontinuities are likely to function as rupture end points. They are the northwestern termination of the fault zone and the large-scale, restraining double bend at the southern end of the FLVFZ, suggesting the 80 km-long fault zone could rupture as a single segment. However, the pull-apart basin (or some portion thereof) along the central FLVFZ, could function as a diffuse segment boundary, in which case two or possibly three rupture segments may exist.

If the FLVFZ behaves as a single rupture segment, it is capable of producing earthquakes of magnitude 7.4 or greater. Earthquakes of magnitude 7.1 or greater are suggested in the case of multiple rupture segments along the FLVFZ. The latter scenario is supported by two apparently discrete paleoseismic rupture zones identified along the fault zone.

Source structure characteristics of the FLVFZ yield magnitude estimates of 7.2 to 7.5, based on half and total fault lengths.

The assessment of seismic potential of the FLVFZ, based on paleoseismic data, segmentation, and source characteristics, suggests a MCE of 7.3 ± 0.4 M_L. If the FLVFZ ruptures in association with other parts, or all, of the DVFS, earthquakes of magnitude 8 and larger are possible. The data presented in this thesis does not preclude the possibility that a single large earthquake may rupture multiple segments on the FLVFZ and on the DVFS.

In short, the White Mountains massif moves northwestward along the FLVFZ at a minimum rate of 0.7 to 2.4 mm/yr, relative to the Fish Lake Valley structural block. Translation is characterized by right-divergent slip, and results from repeated large magnitude (7+) earthquakes. These events are associated with extensive surface ruptures (from 20 to 40 km in length, but may be 80+ km) and interseismic intervals of 1.1 ka (+2.0/-0.5 ka). The last such event occurred about 1.0 ka (± 0.5 ka).

The FLVFZ is unquestionably capable of producing a large magnitude, damaging earthquake. Future studies of the White Mountain seismic gap need to consider the FLVFZ as a candidate for the next gap-filling event.

REFERENCES

Albers, J. P., and Stewart, J. H., 1965, Preliminary Geologic Map of Esmeralda County, Nevada: U.S. Geological Survey Mineral Inv. Field Studies Map MF-298.

_____1967, Belt of Sigmoidal Bending and Right-Lateral Faulting in the Western Great Basin: Geological Society of America Bulletin v. 78, p. 143-156.

_____and Stewart, J. H., 1972, Geology and Mineral Deposits of Esmeralda county, Nevada: Nevada Bureau of Mines and Geology, Bulletin 78, 80 p.

Anderson, J. G., 1906, Solifluction, a component of subaerial denudation: Jour. Geology. v. 14, p. 91-112.

Anderson, G. H., 1933, Geology of the North Half of the White Mountain Quadrangle, California - Nevada: California Institute of Technology, Ph.D. Dissertation, 237 p., (unpublished).

_____1937, Granitization, Albitization, and Related Phenomena in the Northern Inyo Range of California-Nevada, Geological Society of America, Bulletin, 48, p. 1-74.

Antevs, E., 1955, Geologic-Climatic Dating in the West: American Antiquity, Vol. XX, No. 4, pp. 317-335.

Argus, D. F. and Gordon, R. G., 1989, Comparison of Pacific-North America Motion Averaged Over the Past Few Years to its Motion Averaged Over the Past Few Million Years; Sierra Nevada-North America Motion and Kinematics of the Great Basin and San Andreas Fault: Geological Society of America Abstracts with Program, v. 21.

Atwater, T., 1970, Implications of Plate Tectonics for the Cenozoic Tectonic Evolution of Western North America: Geological Society of America, Bulletin, v. 81, p. 3513-3536.

_____and Molnar, P., 1973, Relative Motion of the Pacific and North American Plates Deduced From Sea-Floor Spreading in the Atlantic, Indian, and South Pacific Oceans.

Axelrod, D. I., 1950c, Evolution of Desert Vegetation in Western North America: Carnegie Inst. Wash. Pub. 590, p. 215-306.

_____1957, Late Tertiary Floras and the Sierra Nevadan Uplift, Geological Society of America, Bulletin, v. 68, p. 19-46.

Bachman, S. B., 1978, Pliocene-Pleistocene Break-up of the Sierra Nevada-White-Inyo Mountains Block and Formation of Owens Valley: Geology, v. 6, P. 461.

Ball, S. H., 1907, Geologic Reconnaissance in Southwestern Nevada and Eastern California: U.S. Geological Survey, Bulletin 308, 218 p.

Bateman, P. C., 1965, Geology and Tungsten Mineralization of the Bishop District, California: U.S. Geological Survey, Professional Paper 470, 208 p.

Beaty, C. B., 1960, Gradational Processes in the White Mountains of California and Nevada: University of California-Berkeley, Ph.D. Dissertation, 260 p. (unpublished).

_____1961, Topographic Effects of Faulting: Death Valley, California, Assoc. of American Geographers Annals, v. 51, no. 2, p. 234-240.

_____1963, Origin of Alluvial Fans, White Mountains, California and Nevada: Assoc. of American Geographers Annals, v. 53, p. 516-535.

_____1968, Sequential Study of Desert Flooding in the White Mountains of California and Nevada: U.S. Army Natick Laboratories, Technical Report 68-31-ES, 96 p.

_____1969, Terraces on an Alluvial Fan, Western Nevada, USA: Communications, VIII Congress, International Union for Quaternary Research, Paris, p. 6.

_____1970, Age and Estimated Rate of Accumulation of an Alluvial Fan, White Mountains, California, USA: American Journal of Science, v. 268, p. 50-77.

Benedict, J. B., 1976, Frost Creep and Gelifluction Features: A Review, Quaternary Research, v. 6, p. 55-76.

Birkeland, P. W., 1984, Soils and Geomorphology: New York, Oxford University Press, 352 p.

Blackwelder, E., 1931, Pleistocene Glaciation in the Sierra Nevada and Basin Ranges: Geological Society of America Bulletin, v. 42, p. 865-922.

_____1934, Supplementary Notes on Pleistocene Glaciation in the Great Basin: Journal of the Washington Academy of Science, v. 24, p. 217-222.

Bonilla, M. G., Mark, R. K. and Lienkaemper, J. J., 1984, Statistical Relations Among Earthquake Magnitude Surface Rupture Length, and Surface Fault Displacement: Bulletin of the Seismological Society of America, v. 74, No. 6, pp. 2379-2411.

Bradley, R. S., 1985, Quaternary Paleoclimatology, Methods of Paleoclimatic Reconstruction: Boston, Allen & Unwin, 231 p.

Brady, R. H. III, and Troxel, B. W., 1981, Eastward Termination of the Garlock Fault in the Avawatz Mountains, San Bernardino County, California: Geological Society of America Abstracts with Programs, v. 13, p. 46.

Brogan, G. E. and Slemmons, D. B., 1970, Late Quaternary Fault Patterns Along the Death Valley - Furnace Creek Fault Zones, Death Valley and Fish Lake Valley, California and Nevada: Geological Society of America Abstracts with Programs, v. 2, no. 2, p. 74.

_____1979, Late Quaternary Faulting along the Northern Death Valley-Furnace Creek Fault System, California and Nevada: University of Nevada, Reno, unpublished Ph.D. thesis, 250 p., 2 appendices, 10 plates, (work in progress).

Brune, J. N., 1968, Seismic Movement, Seismicity and Rate of Slip Along Major Fault Zones: Journal of Geophysical Research, v. 73, p. 777-784.

Bryan, K., 1928, Historic Evidence on Changes in the Channel of Rio Puerco, A Tributary of the Rio Grande in New Mexico: The Journal of Geology, v. XXXVI.

Bryant, W. A., 1988, Northern Death Valley - Furnace Creek Fault Zone Southern Mono and Eastern Inyo Counties, California, California Division of Mines and Geology Fault Evaluation Report FER-193.

Bryson, R. P., 1937, Faulted Fanglomerates at the Mouth of Perry Aiken Creek Northern Inyo Range, California-Nevada, M.S. thesis, California Institute of Technology, 50 p.

Bucknam, R. C. and Anderson, R. E., 1979, Estimation of Fault-Scarp Ages from a Scarp-Height-Slope-Angle Relationship: Geology, v. 7, p. 11-14.

Bull, W. B., 1968, Alluvial Fans: Jornal of Geology 16, 101-6.

_____1977, The Alluvial-Fan Environment, Progress in Physical Geography, v. 1, no. 2, p. 222-270.

Burchfiel, B. C., and Stewart, J. H., 1966, "Pull-Apart" Origin of the Central Segment of Death Valley, California: Geological Society of America, Bulletin, v. 77, p. 439-442.

_____1975, Nature and Controls of Cordilleran Orogenesis, Western United States - Extensions of an Earlier Synthesis: American Journal of Science, v. 275-A, p. 363-396.

_____, Hodges, K. V., and Royden, L. H., 1987, Geology of Panamint Valley - Saline Valley Pull-Apart System, California: Palinspatic Evidence for Low-Angle Geometry of a Neogene Range-Bounding Fault: Journal of Geophysical Research, v. 92, no. B10, p. 10,422-10,426.

Burke, R. M. and Birkeland, P. W., 1978, Reevaluation of Multiparameter Relative Dating Techniques and Their Application to the Glacial Sequence Along the Eastern Escarpment of the Sierra Nevada, California: Quaternary Research 11, p. 21-51.

Butler, P. R., Troxel, B. W., and Verosub, K. L., 1988, Late Cenozoic History and Styles of Deformation along the Southern Death Valley Fault Zone, California: Geological Society of America Bulletin, v. 100, p. 402-410.

California Division of Mines and Geology, 1975, Recommended Guidelines for Determining the Maximum Credible Earthquake and the Maximum Probable Earthquakes: California Division of Mines and Geology, Note 43, 1 p.

Carr, W. J., 1974, Summary of Tectonic and Structural Evidence for Stress Orientation at the Nevada Test Site: U.S. Geological Survey Open File Report 74-176, 53 p.

_____1984, Regional Structural Setting of Yucca Mountain, Southwestern Nevada, and Late Cenozoic Rates of Tectonic Activity in Part of the Southwestern Great Basin, Nevada and California, U.S. Geol. Soc. Am., Open-file Report 84-854, 99 p.

Chadwick, O. A. and Davis, J. O., 1988, Soil-forming Intervals Caused by Eolian Sediment Pulses in the Lahontan Basin, Northwestern Nevada: Geological Society of America, v. 20, no. 7, p. A207.

Christenson, G. E. and Purcell, C., 1985, Correlation and Age of Quaternary Alluvial-fan Sequences, Basin and Range Province, Southwestern United States: in Weide, D. L., ed., Soils and Quaternary Geology of the Southwestern United States, Special Paper 203, p. 115-122.

Clark, M. M., Harms, K. K., Lienkaemper, J. J., Harwood, D. S., Lajoie, K. R., Matti, J. C., Perkins, J. A., Rymer, M. J., Sarna-Wojcicki, A. M., Sharp, R.

V., Sims, J. D., Tinsley, III, J. C. and Ziony, J. I., 1984, Preliminary Slip-Rate Table and Map of Late-Quaternary Faults in California: U.S. Geological Survey, Open-file Report 84-106, 12 p.

Cooke, R. U., 1970, Stone Pavements in Deserts: Annals of the Association of American Geographers, v. 60, no. 3, p. 560-577.

_____ and Warren, A., 1973, Geomorphology in Deserts: University of California Press, Berkeley and Los Angeles, 374 p.

Coppersmith, K. J. and Schwartz, D. P., Introduction to the Special Section on Fault Behavior and the Earthquake Generation Process: Journal of Geophysical Research, v. 89, no. B7, p. 5669-5673.

Corte, A. E., 1963, Particle Sorting by Repeated Freezing and Thawing: Bulletin Periglacial, v. 15, p. 175-240.

Crowder, D. F. and Sheridan, M. F., 1972, Geologic Map of the White Mountain Peak Quadrangle, Mono County, California: U.S. Geological Survey Geol. Quad. Map CQ-1012.

Curry, R. R., 1969, Holocene Climatic and Glacial History of the Central Sierra Nevada, California: Geological Society of America, Special Paper 123.

_____1971, Glacial and Pleistocene History of the Mammoth Lakes Sierra, a Geologic Guidebook: Univ. of Montana Dept. of Geology Publication No. 11, Missoula, Montana, 49 p.

Dalrymple, G. B., 1963, Potassium-argon Dates of Some Cenozoic Volcanic Rocks of the Sierra Nevada, California: Geological Society of America, Bulletin, v. 74, p. 379-390.

Dan, J., Yaalon, D. H., Moshe, R., and Nissum, S., 1982, Evolution of Reg Soils in Southern Israel and Sinai: Geoderma, v. 28, p. 173-202.

Davies, J. L., 1969, Landforms of Cold Climates: Massachusetts Institute of Technology Press, 200 p.

Davis, J. O. and Chadwick, O. A., 1988, Late Quaternary Fine Sediment Flux in the Great Basin: Pedogenic, Climatic, and Stratigraphic Implications: Geological Society of America, v. 20, no. 7, p. A207.

Davison, C., 1889, On the Creeping of the Soil-cap Through the Action of Frost: Geological Magazine, v. 6, p. 255.

Denny, C. S., 1965, Alluvial Fans in the Death Valley Region, California and Nevada: U.S. Geol. Survey Prof. Paper 466, p. 1-19.

_____, 1965, Alluvial Fans in the Death Valley Region, California and Nevada, U. S. Geological Survey Professional Paper 466, p. 1-19.

_____, 1967, Fans and Pediments: American Journal of Science, v. 265, p. 81-105.

_____, and Drewes, H., 1965, Geology of the Ash Meadows Quadrangle, Nevada-California: U.S. Geological Survey Bulletin 1181-L, 56 p.

dePolo, C. M. and Ramelli, A. R. 1987, Preliminary Report on Surface Fractures Along the White Mountains Fault Zone Associated with the July 1986 Chalfant Valley Earthquake Sequence: Bulletin of the Seismological Society of America, Vol. 77, No. 1, pp. 290-296.

_____, Bell, J. W., and Ramelli, A. R., 1987, Geometry of Strike-Slip Faulting Related to the 1932 Cedar Mountain Earthquake, Central Nevada, Geological Society of America, Abstracts with Programs, v. 19, p. 371.

_____, Clark, D. G., Slemmons, D. B. and Aymard, W. A., 1990, Historical Basin and Range Province Surface Faulting and Fault Segmentation, in Workshop on Fault Segmentation and Controls of Rupture Initiation and Termination: U.S. Geological Survey, Open-file Report, 31 p.

Dohrenwend, J. C., 1982, Map Showing Late Cenozoic Faults in the Walker Lane 1° by 2° Quadrangle, Nevada-California: U. S. Geological Survey, Miscellaneous Field Studies Map MF 1382-D, 1:250,000.

_____1987, Morphometric Comparison of Tectonically Defined Areas Within the West-Central Basin and Range, California and Nevada: U. S. Geological Survey, Open-file Report 87-83, 26 p.

Dorn, R. I., 1987, A Critical Evaluation of Cation-Ratio Dating of Rock Varnish and an Evaluation of its Application to the Yucca Mountain Repository by the Department of Energy and its Subcontractors: Nevada Bureau of Mines and Geology (unpubl. report), 59 p.

Eckis, R., 1928, Alluvial Fans of the Cucamonga District, Southern California: The Journal of Geology, v. XXXVI, p. 224-247.

Elliott-Fisk, D. L., 1987, Glacial Geomorphology of the White Mountains, California and Nevada: Establishment of a Glacial Chronology: Physical Geography, v. 8, p. 299-323.

Emerson, D. O., 1966, Granitic Rocks of the Mt. Barcroft Quadrangle, Inyo Batholith, California-Nevada: Geological Society of America Bulletin, v. 77, p. 127-152.

Fielder, W. M. 1937, Structure and Stratigraphy of a Section Across the White Mountains, California: California Institute of Technology, Masters Thesis, 55 p. (unpublished).

Filipov, A. J., 1986, Sedimentology of Debris-Flow Deposits, West Flank of the White Mountains, California: Univ. of Massachusetts, Masters Thesis, 207 p., (unpublished).

Frye, J. C. and Willman, H. B., 1962, Stratigraphic Commission: Bulletin of the American Association of Petroleum Geologists, v. 46, no. 1, p. 112-113.

Gianella, V. P. and Callaghan, E., 1934, The Earthquake of December 20, 1932 at Cedar Mountain, Nevada and its Bearing on the Genesis of the Basin Range Structure: The Journal of Geology, v. XLII, no. 1, 22 p.

Gilbert, C. M. , Christensen, M. N., Al-Rawi, Y. and Lajoie, K. R., 1968, Structural and Volcanic History of Mono Basin, California-Nevada: Geological Society of America Memior 116, p. 275-327.

_____ and Reynolds, M. W., 1973, Character and Chronology of Basin Development, Western Margin of the Basin and Range Province: Geological Society of America, Bulletin, v. 84, p. 2489-2510.

Gilbert, G. K., 1883, A Theory of the Earthquakes of the Great Basin, with a Practical Application: American Journal of Science - Third Series, v. XXVII, no. 157, p. 49-53.

Gile, L. H., Peterson, F. F. and Grossman, R. B., 1965, The K Horizon: A Master Soil Horizon of Carbonate Accumulation: Soil Science, v. 99, no. 2, p. 74-82.

_____ 1974, Holocene Soils and Soil-Geomorphic Relations in an Arid Region of Southern New Mexico: Quaternary Research 5, pp. 321-360.

_____, Peterson, F. F., and Grossman, R. B., 1966, Morphological and Genetic Sequences of Carbonate Accumulation: Soil Science, v. 101, p. 347-360.

_____ and Grossman, R. B., 1967, Morphology of the Argillic Horizon in Desert Soils of Southern New Mexico: Soil Science, v. 106, no. 1, p. 6-15.

_____, Hawley J. W. and Grossman, R. B., 1981, Soils and Geomorphology in the Basin and Range Area of Southern New Mexico-Guidebook to the Desert Project: New Mexico Bureau of Mines & Mineral Resources Memoir 39.

Harden, D. R., Biggar, N. E. and Gillam, M. L., 1985, Quaternary Deposits and Soils in and Around Spanish Valley, Utah: in Weide, D. L., ed., Soils and Quaternary Geology of the Southwestern United States, Special Paper 203, p. 43-64.

Harden, J. W., 1982, A Quantitative Index of Soil Development from Field Descriptions: Examples from a Chronosequence in Central California: Geoderma, 28, p. 1-28.

_____1987, Soils Developed in Granitic Alluvium near Merced, California: U.S. Geological Survey Bulletin 1590-A, 65 p.

_____and Taylor, E. M., 1983, A Quantitative Comparison of Soil Development in Four Climatic Regimes: Quaternary Research 20, p. 342-359.

_____and Matti, J. C., 1989, Holocene and Late Pleistocene Slip Rates on the San Andreas Fault in Yucaipa, California, Using Displaced Alluvial-fan Deposits and Soil Chronology: Geological Society of America Bulletin, v. 101, p. 1107-1117.

Hawley, J. W., 1980, Geology and Geomorphology (Section 2): in Gile, L. H., Hawley, J. W., and Grossman, R. B., Soils and Geomorphology in a Basin and Range Area of Southern New Mexico - Guidebook to the Desert Project, New Mexico Bureau of Mines and Mineral Resources, Memoir 39.

Hay, E. A., 1976, Cenozoic Uplifting of the Sierra Nevada in Isostatic Response to North American and Pacific Plate Interactions: Geology, v. 4, p. 763-766.

Hay, R. L., 1966, Zeolites and Zeolitic Reactions in Sedimentary Rocks: Geological Society of America, Special Paper 85, 130 p.

Haynes, Jr., C. V., 1965, Geochronology of Late-Quaternary Alluvium: in eds. Morrison, R. B. and Wright, Jr., H. E., Means of Correlation of Quaternary Successions, Proceedings VII Congress, International Assoc. for Quaternary Research, v. 8, p. 591-631.

Hill, D. P., 1982, Contemporary Block Tectonics: California and Nevada: Journal of Geophysical Research, v. 87, no. B7, p. 5433-5450.

Hooke, R. L., 1967, Processes on Arid-Region Alluvial Fans: The Journal of Geology, v. 75, p.439-460.

Hunt, C. B., and Washburn, A. L., 1960, Salt Features that Simulate Ground Patterns Formed in Cold Climates: U.S. Geological Survey Professional Paper 400-B, p. B403.

_____, and Washburn, A. L., 1966, Pattern ground, in Hunt, C.B., Robinson, T.W., Bowles, W.A., and Washburn, A.L., Hydrologic basin, Death Valley, California: U.S. Geol. Survey Prof. Paper 494-B, p. B104-B133.

_____, and Mabey, D. R., 1966, Stratigraphy and Structure Death Valley, California: U. S. Geological Survey Professional Paper 494-A, 162 p.

Huntington, E., 1907, Some Characteristics of the Glacial Period in Non-Glaciated Regions: Geological Society of America, Bulletin, v. 18, p. 351-388.

Jennings, C. W. 1975, Fault map of California with Locations of Volcanoes, Thermal Springs and Thermal Wells, California Division of Mines and Geology.

Jenny, H., 1941, Factors of Soil Formation, McGraw-Hill, New York, 281 p.

_____1946, Arrangement of Soil Series and Types According to Functions of Soil-Forming Factors.

_____1961, Derivation of State Factor Equations of Soils and Ecosystems: Soil Sci. Soc. Am. Proc. 25, p. 385-388.

Kesseli, J. E. and Beaty, C. B., 1959, Desert Flood Conditions in the White Mountains of California and Nevada: U.S. Army, Environmental Protection Research Division, Technical Report EP-108, 107 p.

Knopf, A., 1918, A Geologic Reconnaissance of the Inyo Range and the Eastern Slope of the Southern Sierra Nevada, California: U. S. Geological Survey Professional Paper 110, 130 p.

Krauskopf, K. B., 1971, Geologic Map of the Mt. Barcroft Quadrangle, California and Nevada: U. S. Geological Survey, Geologic Quadrangle Maps GQ-960, 1:62,500.

Knuepfer, P. L. K., 1989, Implications of the Characteristics of End-Points of Historical Surface Fault Ruptures for the Nature of Fault Segmentation, U. S. Geological Survey Open File Report, Conference on Fault Segmentation.

LaMarche, V. C., Jr., 1965, Distribution of Pleistocene Glaciers in the White Mountains of California and Nevada: U. S. Geological Survey Professional Paper 525-C, p. C146-C147.

_____1973, Holocene Climatic Variations Inferred from Treeline Fluctuations in the White Mountains, California: Quaternary Research 3, pp. 632-660.

_____ and Harlan, T. P., 1973, Accuracy of Tree Ring Dating of Bristlecone Pine for Calibration of the Radiocarbon Time Scale: Journal of Geophysical Research, v. 78, no. 36, p. 8849-8858.

Lienkamper, J. J., Pezzopane, S. K., Clark M. M. and Rymer, M. J., 1987, Fault Fractures Formed in Association with the 1986 Chalfant Valley, California, Earthquake Sequence: Preliminary Report: Bulletin of the Seismological Society of America, Vol. 77, No. 1, pp. 297-305.

Locke, A., Billingsley P. R. and Mayo, E. B., 1940, Sierra Nevada Tectonic Pattern: Geological Society of America, Bulletin, v. 51, p. 513-540.

Longwell, C. R., 1960, Possible Explanation of Diverse Structural Patterns in Southern Nevada: Am. Jour. Sci., v. 258A, p. 192-203.

_____1974, Measure and Date of Movement on Las Vegas Shear Zone, Clark County Nevada, Geological Society of American Bulletin, v. 85, p. 985-990.

Lustig, L. K., 1965, Clastic Sedimentation in Deep Springs Valley California, U. S. Geological Survey Professional Paper 352-F, 192 p.

Mahacek-King, V. L., Onken, J., Elliott-Fisk D. L. and Bettinger, R. L., 1987, Quaternary Silicic Tephras in the White Mountains, CA-NV, Depositional Environments and Geomorphic History, Geological Society of America, Abstracts with Programs, v. 19, p. 756.

Malde, H. E., 1961, Patterned Ground of Possible Solifluction Origin at Low Altitude in the Western Snake River Plain, Idaho: in Short Papers in the Geologic and Hydrologic Sciences, Articles 1-146, U.S. Geological Survey Professional Paper 424-B, p. B170-B173.

Marchand, D. E., 1970, Soil Contamination in the White Mountains, Eastern California, Geological Society of America Bulletin, v. 81, p. 2497-2506.

_____1974, Chemical Weathering, Soil Development, and Geochemical Fractionation in a Part of the White Mountains, Mono and Inyo Counties, California: U. S. Geological Survey Professional Paper 352-J, 424 p.

McFadden, L. D. and Tinsley, J. C., 1982, Soil Profile Development in Xeric Climates, in Tinsley, J. C., Matti, J. C. and McFadden, L. D., eds., Late Quaternary Pedogenesis and Alluvial Chronologies of the Los Angeles and San Gabriel Mountains Areas, Southern California, and Holocene Faulting and Alluvial Stratigraphy Within the Cucamonga Fault Zone: A Preliminary view: Geological Society of America, Cordilleran Section Field Trip 12, p. 15-20.

_____and Tinsley, J. C., 1985, The Rate and Depth of Accumulation of Pedogenic Carbonate Accumulation in Soils: Formation and Testing of a Compartment Model, in Weide, D. W. ed., Soils and Quaternary Geology of the Southwestern United States, Geological Society of America Special Paper 203, p. 23-42

_____, Wells, S. G. and Dohrenwend, J. C., 1986, Influences of Quaternary Climatic Changes on Processes of Soil Development on Desert Loess Deposits of the Cima Volcanic Field, California: Catena, v. 13, pp. 361-389.

_____, L. D., Wells, S. G. and Jercinovich, M. J., 1987, Influences of Eolian and Pedogenic Processes on the Origin and Evolution of Desert Pavements, Geology, v. 15, pp. 504-508.

McKee, E. H. and Nelson, C. A., 1967, Geologic Map of the Soldier Pass Quadrangle, California and Nevada: Geologic Quadrangle Map, Soldier Pass Quadrangle, California-Nevada, CQ-654, 1:62,500.

_____1968, Age and Rate of Movement of the Northern Part of the Death Valley-Furnace Creek Fault Zone, California, Geol. Soc. of Am., Bull. v. 79, p. 509-512.

_____, Diggles, M. F., Donahoe, J. L. and Elliot, G. S., 1982, Geologic Map of the White Mountain Wilderness and Roadless Areas, California and Nevada: U.S. Geological Survey Miscellaneous Field Studies Map MF-1361-A, scale 1:62,500.

Meremonte, M. E. and Rogers, A. M., 1980, Historical Catalog of Southern Great Basin Earthquakes 1868-1978: U. S. Dept. of Interior, Geological Survey, USGS-OFR-87-80, 29 p.

Miller, D. E., 1971, Formation of Vesicular Structure in Soil: Soil Science Society of America Proceedings, v. 35, pp 635-637.

Miller, W. J., 1928, Geology of Deep Spring Valley, California: The Journal of Geology, v. XXXVI, p. 510-525.

Mooney, H. A., St. Andre, G. and Wright, R. D., 1962, Alpine and Subalpine Vegetation Patterns in the White Mountains of California: The American Midland Naturalist, v. 68, p. 257-273.

Nettleton, W. D. and Peterson, F. F., 1983, Aridisols, in, Wilding, L. P., Smeck, N. E. and Hall, G. F., eds., Pedogenesis and Soil Taxonomy. Vol. II: The Soil Orders. Elsevier, Amsterdam, p. 165-216

Noble, D. C., 1972, Some Observations on the Cenozoic Volcano-Tectonic Evolution of the Great Basin, Western United States: Earth and Planetary Science Letters 17, p. 142-150.

North American Stratigraphic code, 1983, The American Association of Petroleum Geologists Bulletin, v. 67, no. 5., p. 841-875.

Oakes, E. H., 1987, Age and Rates of Displacement Along the Furnace Creek Fault Zone, Northern Death Valley, California: Programs, 83rd Annual Geological Society of America Cordilleran Section Meeting, v. 19, no. 6.

Ollier, C. D., 1966, Desert gilgai: Nature, v. 212, p. 581-583.

Pakisear, L. C., Kane, M. F. and Jackson, W. H., 1964, Structural Geology and Volcanism of Owens Valley Region, California - A Geophysical Study: U. S. Geological Survey, Professional Paper 438, 68 p.

Paterson, T. T., 1940, The Effects of Frost Action and Solifluction Around Baffin Bay and in the Cambridge District: Geol. Soc. London Quart. Jour., v. 96, pp. 99-130.

Peterson, F. F., 1980, Holocene Desert Soil Formation under Sodium Salt Influence in a Playa-Margin Environment: Quaternary Research 13, p. 172-186.

_____1981, Landforms of the Basin and Range Province, Defined for soil survey: University of Nevada Reno, technical Bulletin 28, 52 p.

_____1988, Consultant's Report: Soil-Geomorphology Studies in the Crater Flat, Nevada, Area: for Task 1, Evaluation of the Geologic Relations and Seismotectonic Stability of the Yucca Mtn. Area, Nevada Nuclear Waste Site Investigation (NNWSI), 44 p.

Powell, D. R., 1963, Physical Geography of the White Mountains California-Nevada: University of California-Berkeley, Masters Thesis, 140 p., unpublished.

Price, L. W., 1974, The Developmental Cycle of Solifluction Lobes: Annals of the Association of American Geographers, v. 64, no. 3, pp. 430-438.

Reheis, M.C., 1990a, Preliminary Map of Late Cenozoic Deposits and faults in the Soldier Pass 15' Quadrangle, Esmeralda and Inyo Counties, California and Nevada, U.S. Geological Survey Miscellaneous Field Investigations Map (work in progress).

_____1990b, Preliminary Map of Late Cenozoic Deposits and Faults in the Western Part of the Rhyolite Ridge 15' Quadrangle, Esmeralda County, Nevada, U.S. Geological Survey Miscellaneous Field Investigations Map (work in progress).

_____1990c, Preliminary Observations on Late Cenozoic Motion on the Northern Part of the Furnace Creek Fault Zone, California and Nevada (work in progress).

_____and Noller, J. S., 1989, New Perspectives on Quaternary Faulting in the Southern Walker Lane, Nevada and California, in Ellis, M.A., ed., Late Cenozoic Evolution of the Southern Great Basin--Selected Papers from the Workshop: Nevada Bureau of Mines and Geology Open File 89-1, p. 57-61.

Revel, R. D., 1980, Periglacial Features from Morfee Mountains, North-central British Columbia: Arctic, v. 33, no. 2, p. 349-356.

Reynolds, M. W., 1976, Geology of the Grapevine Mountains, Death Valley, California: A Summary; California Division of Mines and Geology Special Report 106, p. 19-25.

Robinson, P. T., McKee, E. H. and Moiola, R., 1968, Cenozoic Volcanism and Sedimentation, Silver Peak Region, Western Nevada and Adjacent California, in Studies in Volcanology: Geological Society of America, Memoir 116, p. 577-611.

_____and Crowder, D. F., 1973, Geologic Map of the Davis Mountain Quadrangle, Esmeralda and Mineral Counties, Nevada and Mono County, California: U. S. Geological Survey, Geologic Quadrangle Maps, GQ-1078, 1:62,500.

Ron, H. and Eyal, Y., 1985, Intraplate Deformation by Block Rotation and Mesostructures Along the Dead Sea Transform, Northern Israel: Tectonics, v. 4., no. 1, p. 85-105.

Ruhe, R. V., 1956, Geomorphic Surfaces and the Nature of Soils: Soil Science, v. 82, Vol. 6, p. 441-455.

_____1967, Geomorphic Surfaces and Surficial Deposits in Southern New Mexico, New Mexico Bureau of Mines and Mineral Resources Memoir no. 18.

_____1975, Geomorphology, Geomorphic Processes and Surficial Geology: Houghton Mifflin Company, 240 p.

Ryall, A., Slemmons, D. B. and Gedney, L. D., 1966, Seismicity, Tectonism, and Surface Faulting in the Western United States During Historic Time: Seismological Society of America, Bulletin, v. 56, p. 1105-1135.

_____1973, Earthquake Potential in Western Nevada: Presented at an ASCE Seminar on Engineering Problems Associated with Earthquake Hazards in Western Nevada, Carson City, January 29, 1973, 19 p.

_____and VanWormer, J. D., 1980, Estimation of Maximum Magnitude and Recommended Seismic Zone Changes in the Western Great Basin: Bulletin of the Seismological Society of America, v. 70, no. 5, p. 1573-1581.

_____and Ryall, F. D., 1983, Increased Potential for a Major Earthquake in the White Mountains Seismic Gap, California and Nevada: Unpublished Report, Seismological Laboratory University of Nevada, Reno.

Sawyer, T. L., 1988, Terrace-Forms of Possible Solifluction Origin on Piedmont Slopes of the Western Great Basin, Geological Society of America, Abstracts with Programs, v20, no 7, p. A374.

_____1988, Paleoseismicity of the Fish Lake Valley Fault Zone: A Component of the Death Valley Fault System, Fish Lake Valley, Nevada: The South Coast Geological Society Death Valley Guidebook, p. 260-275.

_____1989, Late Holocene Paleoseismicity of the Northern Death Valley Fault System, Fish Lake Valley, Nevada, in Tectonic Evolution of the Southern Great Basin: Nevada Bureau of Mines and Geology, Open-file Report, 16 p.

_____, and Slemmons, D. B., 1988, Chronology of Late Holocene Paleoseismicity of the Northern Death Valley-Furnace Creek Fault Zone, Fish Lake Valley, California-Nevada, Geological Society of America, Abstracts with Programs, v20, no. 3, p. 228.

Schmidlin, T. W., Peterson, F. F. and Gifford, R. O., 1983, Soil Temperature Regimes in Nevada: Soil Science Society of America Journal, v. 47, no. 5, p. 977-982.

Scholz, C. H., Barazangi, M. and Sbar, M. L., 1971, Late Cenozoic Evolution of the Great Basin, Western United States, as an Ensialic Interarc Basin: Geological Society of America Bulletin, v. 82, p. 2979-2990.

Schwartz, D. P. and Coppersmith, K. J., 1984, Fault Behavior and Characteristic Earthquakes: Examples From the Wasatch and San Andreas Fault Zones: Journal of Geophysical Research, v. 89, no. B7, p. 5681-5698.

_____ and Coppersmith, K. J., 1986, Seismic Hazards: New Trends in Analysis using Geologic Data: in Active tectonics, National Academy Press, Washington D.C., p. 215-230.

Schweickert, R. A., 1981, Tectonic Evolution of the Sierra Nevada Range, in Ernst, W. G., ed., The Geotectonic Evolution of California: Ruby Volume I, Prentice-Hall, p. 87-130.

_____, Lahren, M. M. and Caskey, S. J., 1988, Major Triassic Thrust Belt in Eastern Sierra Nevada (ESN) and White-Inyo Mountains (WIM) [abst.]: A New Hypothesis: Geological Society of America, Abstracts with Programs, v. 20, p. A273.

Scuderi, L. A., 1987, Late-Holocene Upper Timberline Variation in the Southern Sierra Nevada: Nature, v. 325, p. 242-244.

Shimazaki, K., and Nakata, T., 1980, Time-predictable Recurrence Model for Large Earthquakes, Geophysical Research Letters, v. 7, p. 279-282.

Sibson, R. H., 1985, Stopping of Earthquake Ruptures at Dilational Fault Jogs, Nature 316, p. 248-251.

_____1986, Rupture Interaction with Fault Jogs: in Das, S., Boatwright, J., Scholz, C. H., eds., Earthquake Source Mechanics, Geophysical Monograph 37, Maurice Ewing Volume 6, p. 157-168.

Sieh, K. E., 1978, Slip Along the San Andreas Fault Associated with the Great 1857 Earthquake, Bulletin of the Seismological Society of Ammerica 68, p. 1421-1448.

Slemmons, D. B., Jones, A. E. and Gimlett, J. I., 1065, Catalog of Nevada Earthquakes, 1852-1960: Bulletin of the Seismological Society of America, v. 55, p. 537-583.

_____1977, Faults and Earthquakes Magnitude: U. S. Army Engineers Waterways Experiment Station, State of the Art for Assessing Earthquake Hazards in the United States, Report 6, Miscellaneous Paper S-73-1, 129 p.

_____1982, Determination of Design Earthquake Magnitudes for Microzonation: Proceedings of the Third International Earthquake Microzonation Conference, Vol. 1, p. 119-130.

_____ and Chung D. H., 1982, Maximum Credible Earthquake Magnitudes for the Calaveras and Hayward Fault Zones, California: California Division of Mines and Geology, Special Paper 62, p. 115-124.

_____and DePolo, C. M, 1986, Evaluation of Active Faulting and Associated Hazards: in Active Tectonics, National Academy Press, p. 45-62.

Smith, R. B. and Lindh, A. G., 1978, Fault-plane Solutions of the Western United States: A Compilation: Geological Society of America, Memoir 152, p. 107-109.

Smith, R. S. U., 1979, Holocene Offset and Seismicity Along the Panamint Valley Fault Zone, Western Basin and Range Province, California: Tectonophysics, 52, p. 411-415.

Smith, T. U., 1949, Physical Effects of Pleistocene Climatic Changes in Nonglaciated Areas: Eolian Phenomena, Frost Action, and Stream Terracing: Geological Society of America, Bulletin, v. 60, p. 1485-1516.

Soil Conservation Service, 1981, Examination and Description of Soils in the Field: in Soil Survey Manual (USDA-SCS), U. S. Government Printing Office Washington, D.C.

Soil Survey Staff, 1975, Soil Taxonomy, U.S. Dept. Agriculture, Agriculture Handbook 436, U. S. Government Printing Office, Washington, D. C., 753 p. Southern Sierra Nevada: Nature Vol. 325, pp. 242-244.

Speed, R. C. and Cogbill, A. H., 1979, Candelaria and Other Left-Oblique Slip Faults of the Candelaria Region, Nevada: Geological Society of America Bulletin, Part I, v. 90, p. 149-163.

Springer, M. E., 1958, Desert Pavement and Vesicular Layer of Some Soils of the Desert of the Lahontan Basin, Nevada: Soil Science Society of America, Proceedings. 22, p. 63-66.

Stewart, J. H., 1966, Correlation of Lower Cambrian and Some Precambrian Strata in the Southern Great Basin, California and Nevada: in Geological Survey Research, U.S. Geol. Survey Professional Paper 550-C, p. C66-C72.

_____1967, Possible Large Right-Lateral Displacement Along Fault and Shear Zones in the Death Valley-Las Vegas Area, California and Nevada, Geol. Soc. of Am., Bull. v. 78, p. 131-142.

_____1978, Basin-Range Structure in Western North America: A Review: Geological Society of America Memoir 152, 31 p.

_____1980, Regional Tilt Patterns of Late Cenozoic Basin-Range Fault Blocks, Western United States: Geological Society of America Bulletin, Part I, v. 91, p. 460-464.

_____1983a, East-Trending Dextral Faults in the Western Great Basin: An Explanation for Anomalous Trends of Precenozoic Strata and Cenozoic Faults: Tectonics, v. 4, no. 6, p. 547-564.

_____1983b, Extensional Tectonics in the Death Valley Area, California: Transport of the Panamint Range Structural Block 80 km Northwestward: Geology, v. 11, p. 153-157.

_____1988, Tectonics of the Walker Lane Belt, Western Great Basin: Mesozoic and Cenozoic Deformation in a Zone of Shear, in Ernst, W. G., ed., Metamorphism and Crustal Evolution of the Western United States: Rubey Volume VII, Prentice-Hall, pub., p. 683-713.

_____,Ross, D. C., Nelson, C. A., and Birchfiel, B. C., 1966, The Last Chance Thrust - A Major Fault in the Eastern Part of Inyo County, California, p. D-23 - D-24 in Geological Survey Research, U.S. Geological Professional Paper 550-D, 267 p.

_____, Albers, J. P., and Poole, F. G., 1968, Summary of Regional Evidence for Right-lateral Displacement in the Western Great Basin: Geological Society of America Bulletin, v. 79, p. 1407-1413.

_____, Albers, J. P., and Poole, F. G., 1970, Reply to "Summary of Regional Evidence for Right-lateral Displacement in the Western Great Basin:", Geological Society of America Bulletin, v. 81, p. 2175-2180

_____and Carlson, J. E., 1978, Geologic Map of Nevada: U. S. Geological Survey and Nevada Bureau of Mines and Geology, scale 1:500,000.

Stuiver, M., 1982, A High-Precision Calibration of the AD Radiocarbon Time Scale: Radiocarbon, v. 24, no. 1, p. 1-26.

_____, Kromer, B., Becker, B. and Ferguson, C. W., 1986, Radiocarbon Age Calibration Back to 13,300 Years BP and the ^{14}C Age Matching of the German Oak and US Bristlecone Pine Chronologies: Radiocarbon, v. 28, no. 2B, p. 969-979.

_____and Pearson, G. W., 1986, High-Precision Calibration of the Radiocarbon Time Scale, AD 1950-500 BC: Radiocarbon, v. 28, no. 2B, p. 805-838.

Swadley, W. C., Hoover, D. L., and Rosholt, J. N., 1984, Preliminary Report on Late Cenozoic Faulting and Stratigraphy in the Vicinity of Yucca Mountain, Nye County, Nevada: U.S. Geological Survey Open-File Report 84-788, 42 p.

Sylvester, A. G., 1988, Strike-Slip Faults: Geological Society of America, Bulletin, v. 100, p. 1666-1703.

Taber, S., 1930, The Mechanics of Frost Heaving: Journal of Geology, v. 38, p. 303-317.

Taylor, E. M., 1986, Impact of Time and Climate on Quaternary Soils in the Yucca Mountain Area of the Nevada Test Site: University of Colorado, Masters Thesis, 216 p. (unpublished).

_____1988, Instructions for the Soil Development Index Template - Lotus 123: U.S. Geological Survey Open File Report 88-233A, 23 p.

Thenhaus, P. C. and Wentworth, C. M., 1982, Map Showing Zones of Similar Ages of Surface Faulting and Estimated Maximum Earthquake Size in the Basin and Range Province and Selected Adjacent Areas: U. S. Geological Survey, Open-file Report 82-742, 18 p.

Thompson, G. A. and Burke, D. B., 1973, Rate and Direction of Spreading in Dixie Valley, Basin and Range Province, Nevada, Geological Society of America, Bulletin, v. 84, p. 627-632.

Tocher, D., 1958, Earthquake Energy and Ground Breakage, Seismological Society America, Bulletin, v. 48, p. 147-153.

Troxel, B. W. and Wright, L. A., 1976, Geologic Features Death Valley, California: California Division of Mines and Geology, Special Report 106, 33 p.

____and Butler, P. R., 1986, Time Relations Between Quaternary Faulting, Volcanism, and Fan Development, Southern Death Valley, California, Field Guide, Pacific Cell, Friends of the Pleistocene, p. 31-36.

VanWormer, J. D. and Ryall, A. S., 1980, Sierra Nevada-Great Basin Boundary Zone: Earthquake Hazard Related to Structure, Active Tectonic Processes, and Anomalous Patterns of Earthquake Occurrence, Bulletin of the Seismological Society of America, v. 70, no. 5, p. 1557-1572.

Vetter, U. R., 1984, Focal Mechanisms and Crustal Stress Patterns in Western Nevada and Eastern California: Annales Geophysicae, v. 2, p. 699-710.

Vreeken, W. J., 1975, Principal Kinds of Chronosequences and Their Significance in Soil History: Journal of Soil Science, v. 26, no. 4, p. 379-394.

Walcott, C. D., 1897, The Post-Pleistocene Elevation of the Inyo Range, and the Lake Beds of Waucobi Embayment, Inyo County, California, The Journal of Geology, v. 5, p. 340-348.

Wallace, R. E., 1978a, Geometry and Rates of Change of Fault-Generated Range Fronts, North-Central Nevada: U. S. Geological Survey, Journal of Research, v. 6, p. 637-650.

_____1978b, Patterns of Faulting and Seismic Gaps in the Great Basin Province, in Proceedings of Conference VI, Methodology of Identifying Seismic Gaps and Soon-to-break Gaps, U. S. Geological Survey, Open-file Report 78-943, p. 857-868.

_____, Hill, D. P., Ryall, A. S., and Cockerham, R. S., 1983, Potential for Large Earthquakes in the Central Nevada-Eastern California Seismic Belt [abst.]: Seismological Society of America, Earthquake Notes, v. 54, p. 46-47.

_____1984, Patterns and Timing of Late Quaternary Faulting in the Great Basin Province and Relation to Some Regional Tectonic Features: Journal of Geophysical Research, Vol. 89, No. B7, pp. 5763-5769.

Washburn, A. L., 1947, Reconnaissance Geology of Portions of Victoria Island and Adjacent Regions, Arctic Canada: Geological Sococciety America, Memoir 22, 142 p.

_____1956, Classification of Pattern Ground and Review of Suggested Origins, Geological Society of America Bulletin, v. 67, pp. 823-866.

Wernicke, B., 1981, Low-Angle Normal Faults in the Basin and Range Province, Nappe Tectonics in an Extending Orogen:

_____and Burchfiel, B. C., 1982, Modes of Extensional Tectonics, Journal of Structural Geology, v. 4, p. 105-115.

_____1984, Uniform-sense Normal Simple Shear of the Continental Lithosphere, Can. J. Earth Sci, 22, p. 108-125

_____, Axen, G. J., and Snow, J. K., 1988, Basin and Range Extensional Tectonics at the Latitude of Las Vegas, Nevada, Geological Society of America, Bulletin, v. 100, p. 1738-1757.

Wilding, L. P., Odell, R. T., Fehrenbacher, J. B. and Beavers, A. H., 1963, Source and Distribution of Sodium in Solonetzic Soils in Illinois, Soil Science Society of Ammerica, Proceedings 27, p. 432-438.

Willams, P. J., 1962, An Apparatus for Investigation of the Distribution of Movement with Depth in Shallow Soil Layers, Building Note 39, Division of Building Research, N.R.C. Canada.

Wills, C. J., 1989, A Neotectonic Tour of the Death Valley Fault Zone, California Geology, September 1989, p. 196-200.

Wright, L. A. and Troxel, B. W., 1967, Limitations on Right-Lateral, Strike-Slip Displacement, Death Valley and Furnace Creek Fault Zones, California, Geological Society of America, Bulletin, v. 78, p. 933-950.

_____and Troxel, B. W., 1970, Summary of Regional Evidence for Right-Lateral Displacement in the Western Great Basin: Discussion, Geological Society of America, Bulletin, v. 81, p. 2167-2174.

_____1976, Late Cenozoic Fault Patterns and Stress Fields in the Great Basin and Westward Displacement of the Sierra Nevada Block: Geology, v. 4, p. 489-494.

_____and Troxel, B. W., 1984, Geology of the Northern Half of the Confidence Hills 15-minute Quadrangle, Death Valley Region, Eastern California: The Area of the Amargosa Chaos, California Division of Mines and Geology, Map Sheet 34, 31 p.

Zellmer, J. T., 1983, Holocene Faulting and "Pull-Apart" Tectonics in Saline Valley, Inyo County, California: Geological Society of America, Abstracts with Programs, Salt Lake City, Utah.

Zoback, M. L. and M. Zoback, 1980, State of Stress in the Conterminous United States, Journal of Geophysical Research, v. 85, p. 6113-6156.

_____and Beanland, S., 1986, Temporal Variations in Stress Magnitude and Style of Faulting Along the Sierran Frontal Fault System: Geological Society of America, Abstracts with Programs, v. 18, p. 801.

APPENDIX I

SOLIFUCTION STEPS ON ALLUVIAL FAN REMNANTS OF THE WESTERN GREAT BASIN

ABSTRACT

Many mid and late Pleistocene alluvial fan remnants in the western Great Basin have pattern ground surfaces consisting of small, micro-relief steps arranged in flights. The pattern ground features are identified between 37° to 39° N. Lat., at 1000 to 2000 m elevation, on gentle slopes, and apparently independent of aspect. Step in flights increase in height and decrease in width with increasing slopes. The steps comprise flattish treads with well-sorted interlocking stone pavements, and gently sloping risers oriented parallel to contour, that are as much as 1 m high. The steps generally have soils that consist of an Av horizon in fine-grained gravel-free parent materials; probable eolian sediments. This desert loess layer overlies strongly developed argillic B horizons and prominent Stage III (or greater) Bk or K horizons, formed in gravelly sandy loam parent materials.

The pattern ground results from mass wasting of saturated desert loess veneers on gently sloping alluvial fan remnents by solifluction. This rather unique process depends less on the previaling climatic conditions than on time, pedogensis and eolian influx. Prominent secondary accumulations of clay and carbonate in soils associated with the steps, impede infiltration of water and thereby promote saturation within the fine-grained surface layer. This silt-rich layer exhibits a plasmatic behavior and thus fail by solifluction when saturated.

Flights of steps on alluvial fan remnants of the western Great Basin are evidence of both current solifluction activity and relict landscape evolution. The Quaternary paleoclimatic significance of these pattern ground features is not well understood. Formation of this type of pattern ground is apparently favored under conditions that were wetter than the current arid climate of the Great Basin. Hence, formation of steps appears to be favored during pluvial and prehaps periglacial climates of the Quaternary.

INTRODUCTION

Pattern ground consisting of uniformily spaced steps occurs on many mid and late Pleistocene alluvial fan remnants of the western Great Basin. The steps preferentially occur adjacent to hills and mountain fronts on flattish interfluves, stranded by modern drainages from their provenance. The pattern ground features are identified at 1000 to 2000 m elevation on gentle slopes that have a multitude of aspects. Individual steps are from 3 to 80 m long, as much as 1 m high, and range from narrowly arcuate to broadly elliptical in plan. The micro-relief steps comprise flattish treads, that display well-sorted interlocking stone pavements, and risers with 3° to 18° slopes that are as much as 1 m high. Flights of steps are prominent on many mid and late Pleistocene alluvial fan remnants, but apparently have not formed on latest Pleistocene and Holocene fan surfaces of the western Great Basin.

More than a thousand aerial photographs were examined during this thesis, to establish a preliminary distribution of piedmont slopes in southwestern Nevada that exhibit pattern ground consisting of small-scall steps arranged in flights (Fig. 42). The pattern ground is identified on fan remnant from south of the Nevada Test Site (37° N. Lat.) to north of Walker Lake (39° N. Lat.), and from the California-Nevada border to east of Tonopah. The steps are particularly well-defined over relatively large areas in northwestern Fish Lake Valley, in eastern Crater Flat, and in northeastern Yucca Flat, Nevada.

Pattern ground on alluvial fan remnants in northwestern Fish Lake Valley, eastern Crater Flat, and eastern Stingaree Valley, southwestern Nevada (Fig. 42), were examined in the field. The author first examined the pattern ground features during preliminary field studies in Fish Lake Valley for this thesis. Stingaree Valley and Crater Flat, Nevada were selected for study based on the abundances of prominent steps arranged over relatively large areas. Additionally, Crater Flat was selected because preliminary cation-ratio dating of rock varnish (Dorn, 1987) was availible for several previously described geomorphic surfaces (Peterson, 1988), some of which exhibit pattern ground. Further, the author, assisted by A.R. Ramelli (1989, Nevada Bureau of Mines and Geology) mapped a portion of east-central Crater Falt, as part of the Yucca Mountain project at the University of Nevada Reno (in prep.). These three study areas seemingly illustrate the broad range in form of individual steps.

Flights of steps form a distinctive pattern that can be readily identified on aerial photographs at 1:24,000 (or about 1:35,000 if well-defined) and at larger scales. The air-photo pattern is one of alternating light and dark tonal-stripes oriented nearly parallel to contour, that impart a "wrinkled" appearance to fan surfaces (Fig. 43). The generally anastomosing stripes are curvilinear with downfan bulges. Light tonal-stripes represent tightly packed, well-sorted stone pavements on flattish tread surfaces. The dark stripes are often narrower than the light stripes, and represent concentrations of desert shrubs along riser slopes. This air-photo pattern apparently is more distinct and uniform with increasing slopes (disscussed in a following section).

The wide distribution of mid and late Pleistocene alluvial fan remnants that have pattern ground, and the ease of identifing flights of steps on aerial photographs, provide a useful means of distingushing latest Pleistocene and Holocene surfaces form many older surfaces. The presence of pattern ground suggests that fine-grained sediments occur as relatively thick mantles over pedogenic horizons of prominent clay and carbonate accumulation.

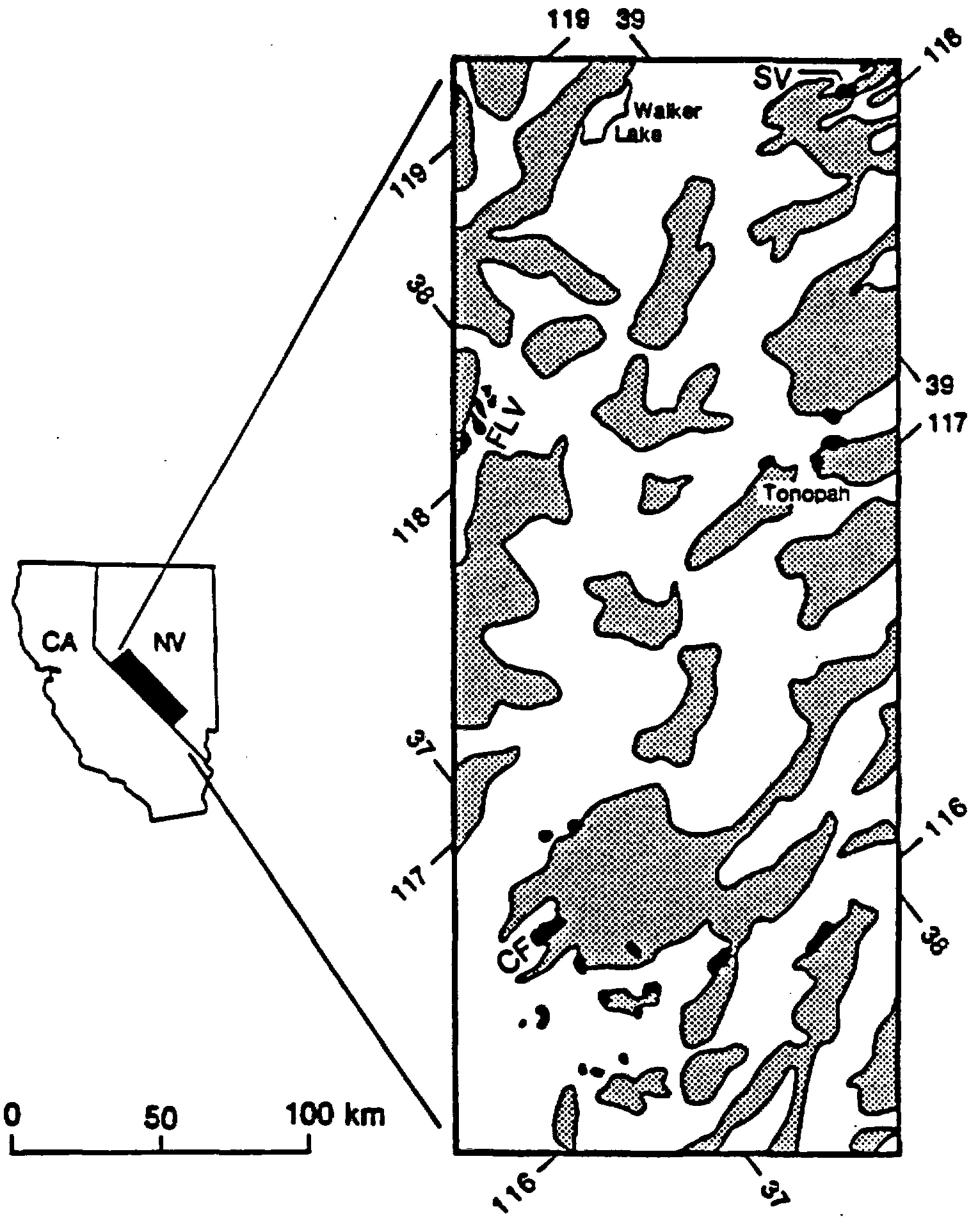

Figure 42. Map of a portion of west-central Nevada showing the distribution of piedmont slopes (blackened areas) that have solifluction steps. The shaded areas are mountains and the unshaded areas are intermountane valleys. CF, Crater Flat; FLV, Fish Lake Valley; SV, Stingaree Valley.

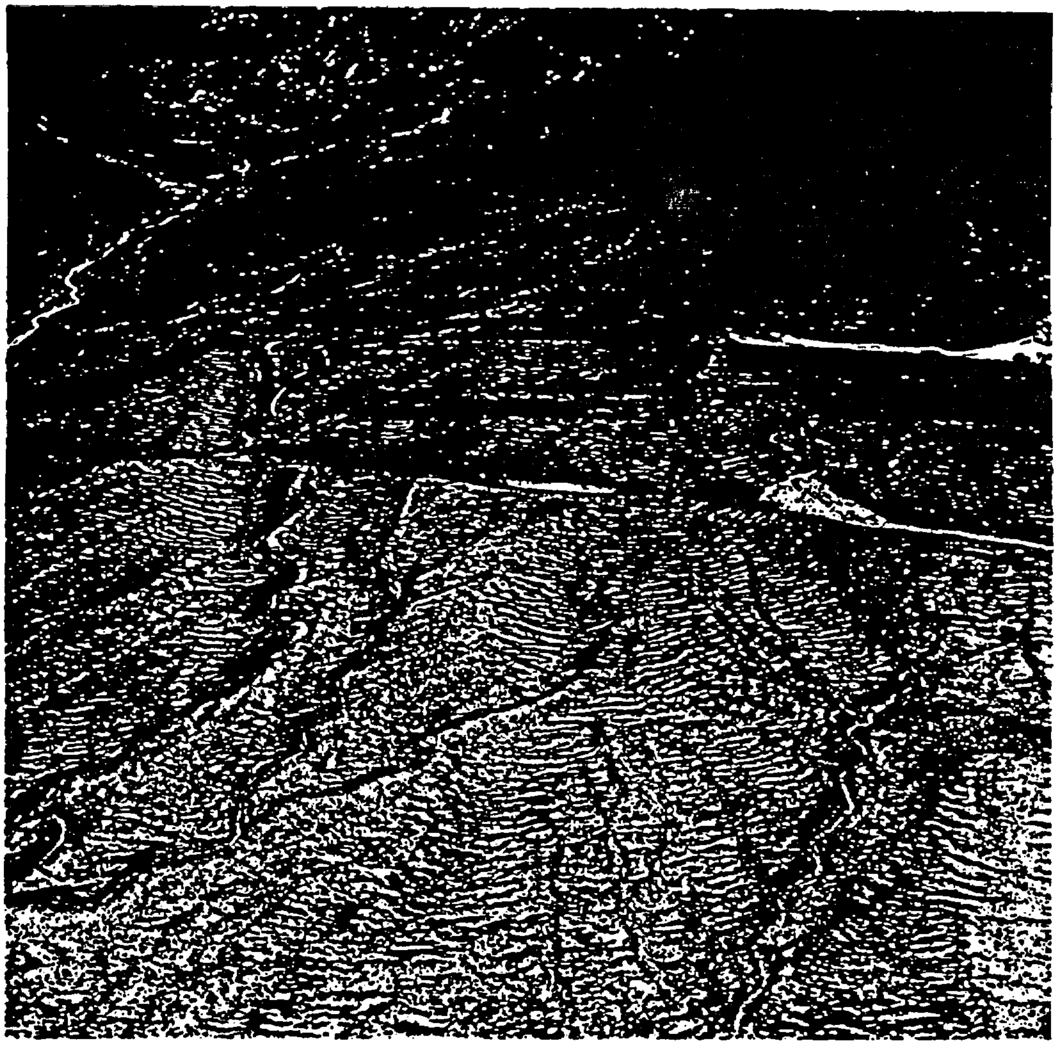

Figure 43. Low-oblique aerial photograph taken towards the southwest of solifluction steps on the lower Indian Creek fan in Fish Lake Valley, Nevada. Note the numerous fault scarps that strike across the midground of the photograph.

PREVIOUS INVESTIGATIONS

Anderson (1933) was the first to describe small-scale steps on alluvial fan remnants in the western Great Basin. Anderson postulate that pattern ground on alluvial fans in northwestern Fish Lake Valley was the result of downslope creep of alluvial materials. Beaty (1968 and 1969) also studied the "wave-like" pattern on alluvial fans in this part of the valley. Beaty considered several modes of formation, but favored an explanation involving mass-wasting of surficial materials. Beaty (1968) postulated that the steps are relict features formed during a climate regime that was wetter and/or colder, however not much different than the modern climate (Beaty, 1969). Brogan (1979) also noted "rounded" steps in Fish Lake Valley, that were characteristic of the oldest fan surfaces (Brogen's Q2).

On alluvial fans of the Death Valley region similar pattern ground features were described by Denny (1965, 1967), Denny and Drewes (1965), Hunt and Washburn (1960, 1966), and Cooke (1970). Denny and Drewes (1965) and Denny (1965, 1967) described miniature terraces with risers less than an inch high and tens of feet in length in many pavement surfaces in the western Amargosa Desert of Nevada. They attributed the formation of these micro-terraces to downslope flow of saturated silty materials. Following a heavy rain, Denny (1967) observed that material beneath the pavement had the consistency of "jelly" and when a stone was removed from the surface the surrounding silty materials tended to flow into the depression left by the stone. Somewhat larger terraces with risers up to m high also form on alluvial fan in the Amargosa Desert (Denny and Drewes, 1965). Denny and Drewes (1965) concluded that both sizes of terraces formed by downslope movement of water-saturated materials.

Hunt and Washburn (1960) described small-scale steps with risers m (or more) high and as much as 5 m long, where stone pavements are well developed on the oldest alluvial fans in Death Valley, California. Hunt and Washburn (1966) used rows of dowels across the terraces to show that no significant movement had occurred in a 4-year period. They concluded that the terraces likely are the result of past movements, possibly during a pluvial paleoclimate. Hunt and Washburn (1960) inferred that the steps were restricted to soils having prominent secondary accumulations of salt. Hence these features may differ from those described in the following section.

DESCRIPTION OF PATTERN GROUND

MORPHOLOGY OF STEPS

The orderly arrangement of small-scale steps in flights, characterizes many Pleistocene alluvial fan remnants in the western Great Basin (Fig. 43). In plan, the micro-relief features vary from narrow and arcuate to broad and elliptical, with bulges that are convex downslope (Fig. 44). These pattern ground features generally occur on 2° to 6° slopes, but are identified in Fish Lake Valley on slopes as steep as about 10°. The dimensions of the steps vary widely, they are 3 to 80 m long, 2 to 15 m wide, and as much as 1 m high. Individual steps consist of two

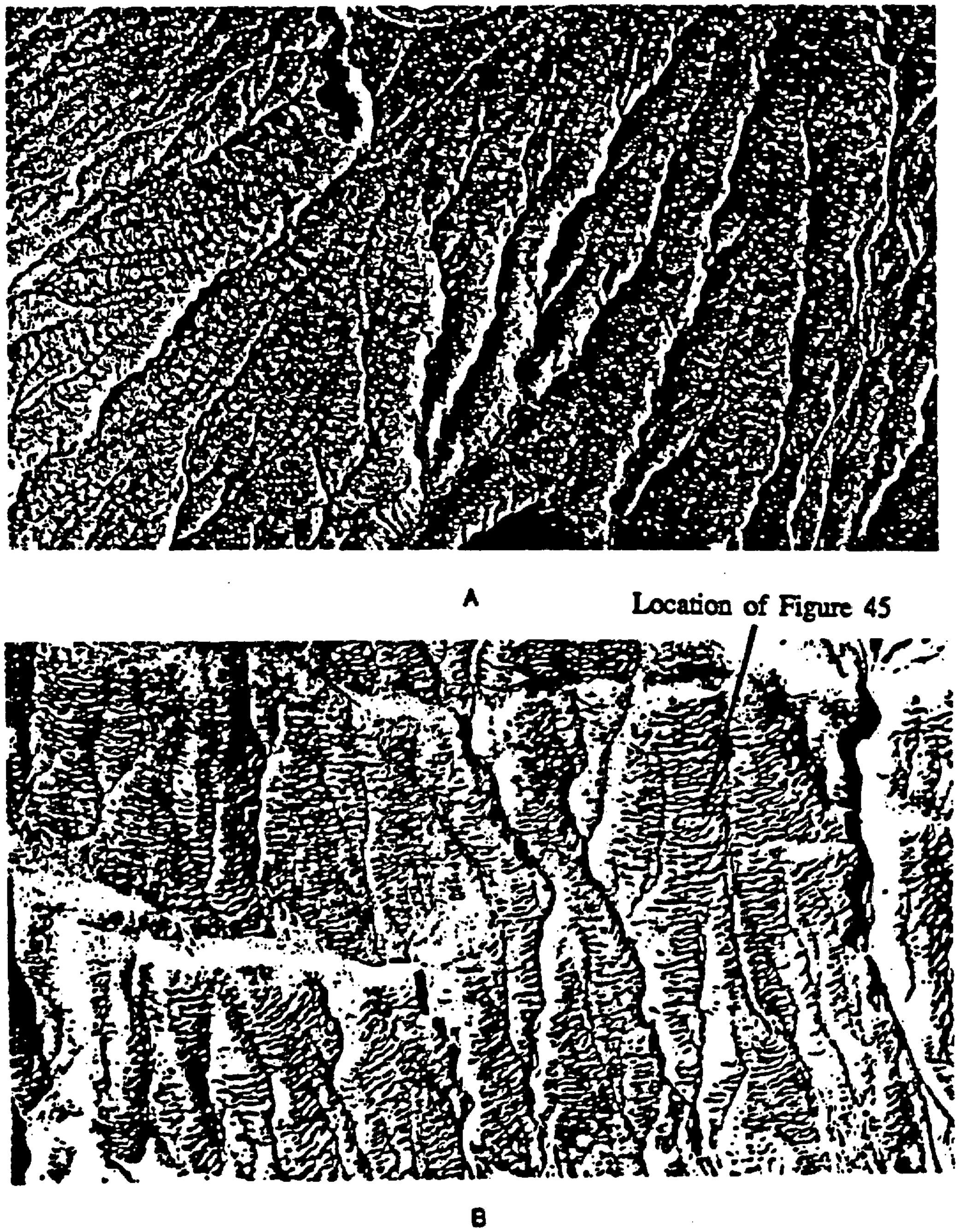

Figure 44. Aerial photographs of solifluction steps in Crater Flat (A) and Fish Lake Valley (B), Nevada. Note that the steps in Fish Lake Valley are generally more distinct and uniform than those in Crater Flat.

components a flat, nearly horizontal tread, and a gently sloping riser (Fig. 45; Appendix IV, Profile P22). Treads are commonly are widest in the middle, and narrow toward the ends. The planar tread surfaces exhibit well-sorted, interlocking stone pavement with strongly varnished lithic fragments, but lack vegetation. Riser lack pavement and have slopes as steep as 18° (or more), that are oriented parallel to contour. Vegetation tends to concentrate along the risers.

A gradual transition in size and shape of the pattern ground features, from broad elliptical forms to narrow arcuate forms, is apparent with an increase in slope from about 2° to 6° or more. In general, with increasing slope, treads are narrower and longer, and risers are steeper, more distinct, and higher. Flights of steps appear to exhibit a decrease in wavelength (e.g., riser to riser distance) and an increase in amplitude (heigth) with increasing slope.

Alluvial fans in southeastern Fairview Valley, west-central Nevada exhibit pattern ground consisting of broad elliptical steps with diffuse risers, on slopes of about 2°. On fan surfaces with similar slopes (2° to about 3°) in eastern Crater Flat, southwestern Nevada, broad elliptical to lobate treads and gradually sloping risers have formed (Fig. 44a). Pattern ground forms on slopes of 3° to 5° in Fish Lake Valley (Fig. 44b), and locally as steep as about 10°. The steps are prominent on these steeper slopes, and have narrow (2 - 5 m) elongate (up to 80 m) treads and relatively steep, well-defined risers.

Washburn (1956), Malde (1961), Denny and Drewes (1965), Ollier (1966), and Revel (1980) have described similar variations in the morphology of patterned-ground features with increasing slope.

SOIL-STRATIGRAPHIC RELATIONS OF PATTERN GROUND FEATURES

The internal composition of the pattern ground features was examined in two exploratory trenches and in numerous shallow pits in various positions (e.g., risers and treads) on the steps. The soil and stratigraphic relations of the pattern ground features are discussed in this section.

A trench was excavated across two tread surfaces and the intervening riser on the late Pleistocene Indian surface in Fish Lake Valley, Nevada (Fig. 44b). Trench exposures show two markedly contrasting stratigraphic units (Fig. 46). A layer of well sorted silts and fine sands (silt loam to loam; field textures) overlies poorly sorted, coarse gravelly deposits (sandy loam to sandy clay loam). This abrupt textural change is apparently representive of the parent materials, and thus suggests two different modes of sedimentation.

The underlying gravelly material is fan alluvium, that is similar to debris flow deposits exposured in many fanhead trenches of the Fish Lake Valley region. The overlying fine grained materials are similar in texture and sorting to deposits that mantle alluvial fans in Mojave Desert of California. Wells and others (1984) have shown that these mantles comprise primarily eolian sediments. Similar loess deposits occur on alluvial fans in the pluvial Lake Lahaton basin (Chadwick and Davis, 1988), and in northern Las Vegas Valley (Davis and Chadwick, 1988). The fine grained surficial layers, in which the pattern ground features form, are assummed to also be eolian in origin.

The "desert loess" layer exposed in the Fish Lake Valley trench, is about 10-

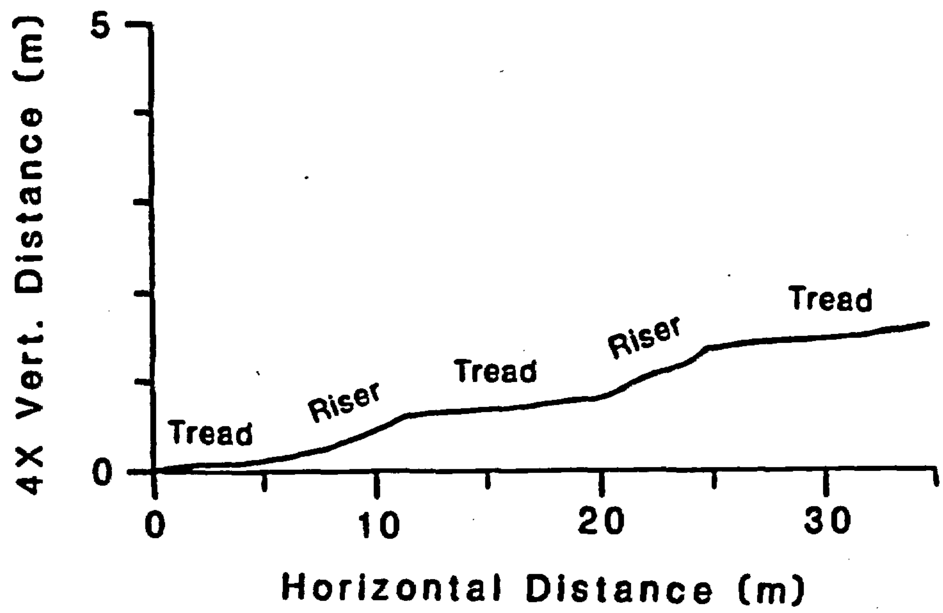

Figure 45. Topographic profile of solifluction steps on the lower Indian Creek fan, see Fig. 44b for location. Note that the flattish treads are separated by more steeply sloping risers. The profile was constructed perpinduclar to the steps using the Brunton and slope stick method of Buchman and Anderson (1979).

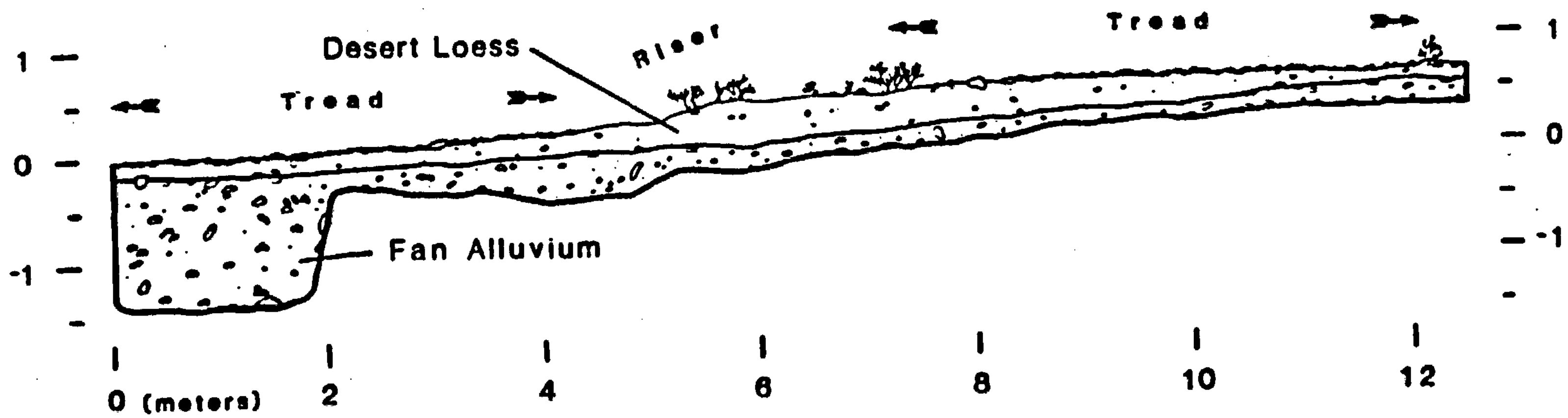

Figure 46. Log of a shallow trench excavated across a riser and two treads (between 15 and 27 m in Fig. 45) in Fish lake Valley, Nevada. The surficial stratigraphic unit is composed of fine grained (eolian?) sediment, and strongly differs from the underlying unit, which is composed of rather typical fan alluvium.

15 cm thick below the treads, and is as much as about 50 cm thick below the riser (Fig. 46). The base the loess layer has a thin (1-2 cm) zones of laminar clay "seams", suggesting that water is impeded along the boundary with the underlying fan alluvium. This abrupt (<2 cm) contact is relatively planar, whereas the surface is clearly stepped. This difference suggests that steps form only in the desert loess layer, and not in the underlying alluvium.

The soil formed in eolian parent materials of the tread has a prominent Av horizon with a distinct crust below the tightly-packed pavement. The subjacent horizon (Bkv) is also vesicular and has modest accumulations of carbonate on pebble bottoms, and a thin laminar clay subhorizon (Pedon 5, Appendix II). The soil under the riser differ somewhat, in that a crusting Av horizon is absent and a Stage I Bk horizon occurs just above the alluvial parent material. The soil profile in the alluvial parent material comprises a prominent, 30 cm thick, argillic B horizon (10YR7/4) over a Stage III Bkm horizon (Fig. 47; Appendix II, Pedon 5).

A second trench was excavated across a pattern ground step in Fairview Valley, Nevada; part of the pluvial Lake Lahaton basin. The trench was oriented perpendicular to the strike of a rather steep (18°) riser. Soil-stratigraphic relations in this trench (Figs. 48 and 49) are similar to those of the Fish Lake Valley trench (cf. Figs. 46 and 47), including a planar, abrupt contact between a nearly gravel-free, desert loess layer and the underlying fan gravels. A strongly developed argillic B horizon exposed in this trench was apparently truncated and subsequently buried by loess deposition. The argillic horizon is massively engulfed by secondary carbonate that clearly disrupts translocated clays on ped faces. The base of the soil profile consists of a mostly cemented Stage III K horizon over a Stage II Bk horizon.

In northeast Crater Flat, Nevada pattern ground occurs on two different geomorphic surfaces that have been cation-ratio dated by Dorn (19887). The steps are prominent on the Yucca surfaces, dated at 360 to 380 ka, and somewhat less prominent on the Early Black Cone surfaces, dated at 118 to 136 ka. These geomorphic surfaces were identified and described by Peterson (1988), and have been mapped in east-central Crater Flat by the author, A.R. Ramelli, and J. W. Bell (Ramelli and others, 1989). Soils associated with both surfaces have relatively thick, crusting Av over Bw horizons (Peterson, 1988). The Yucca soils exhibit thick, clay-rich argillic horizons over strongly cemented K horizons. Whereas, the Late Black Cone soils display Stage I Bk horizons with weakly cemented Stage II-III lenses, or a minimual argillic horizon over weakly cemented duripans (Peterson, 1988).

Similar stratigraphic and pedogenic relations were also observed in numerous hand-dug pits in Fish Lake Valley, Fairview Valley, and in Crater Flat, Nevada.

MODE OF PATTERN GROUND FORMATION

Wells and McFadden (1985) described seemingly similar pattern ground features on alluvial fan in the eastern Mojave Desert of California, and determined

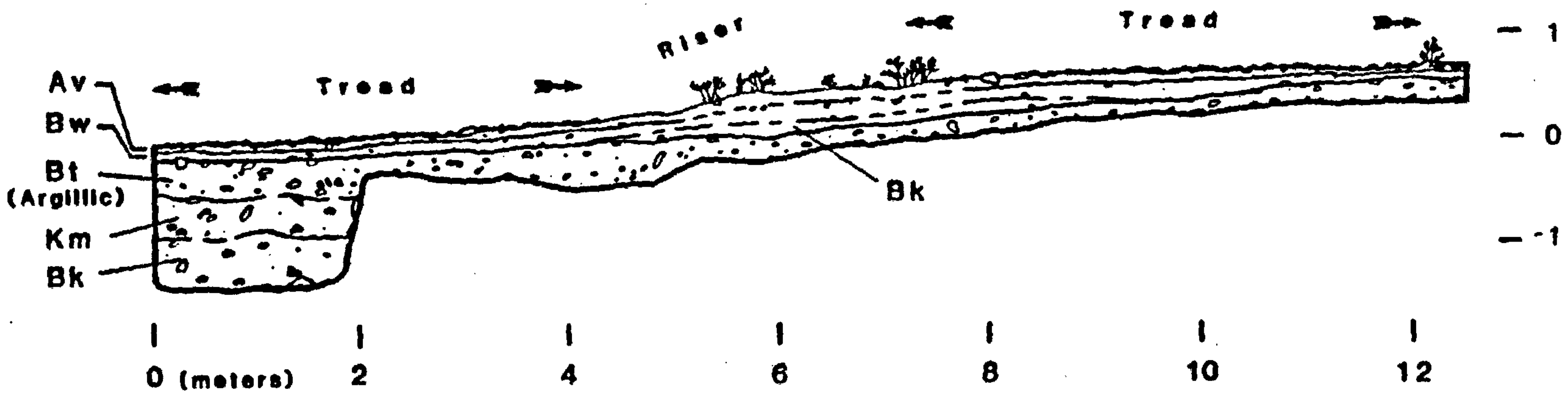

Figure 47. Log of the trench in Fish Lake Valley, Nevada showing soil horizons, which are described in more detail in Appendix II (Pedon 4). A comparison with Figure 46 indicates that the Av and AB horizons have formed in the fine grained surficial deposit, whereas the argillic and Bk horizons have formed in the fan alluvium.

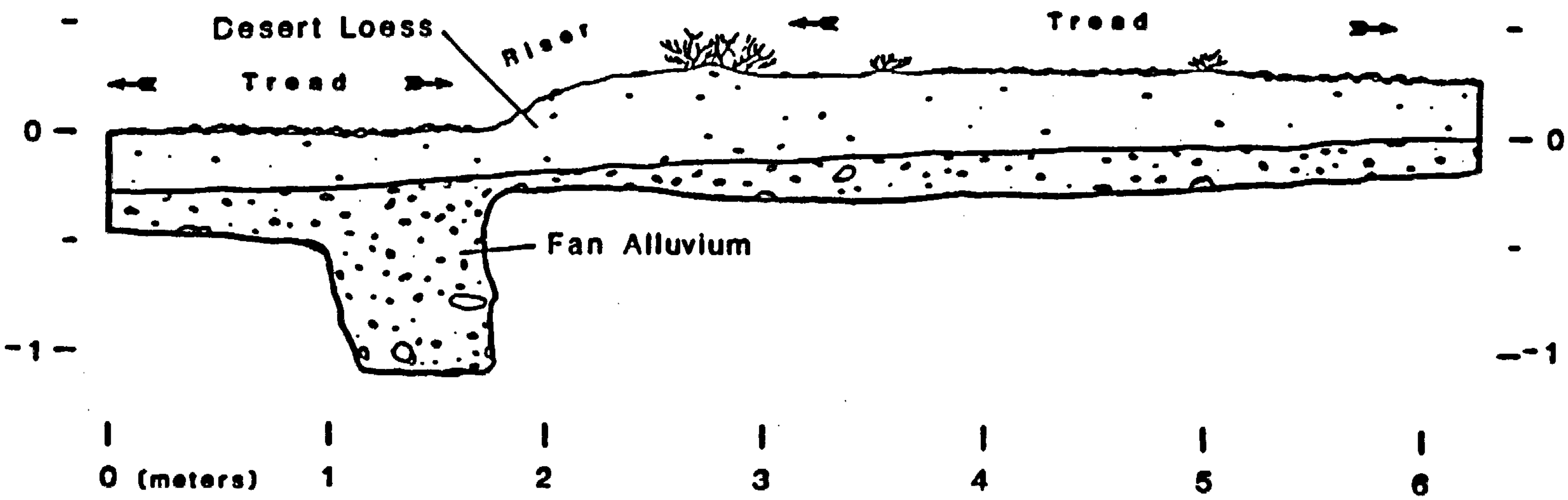

Figure 48. Log of a shallow trench excavated across a rather steep riser and two treads in the Stingaree Valley, Nevada. Note that the contact between the fine grained surficial deposit (desert loess?) and the underlying alluvium is planar, whereas the surface is stepped.

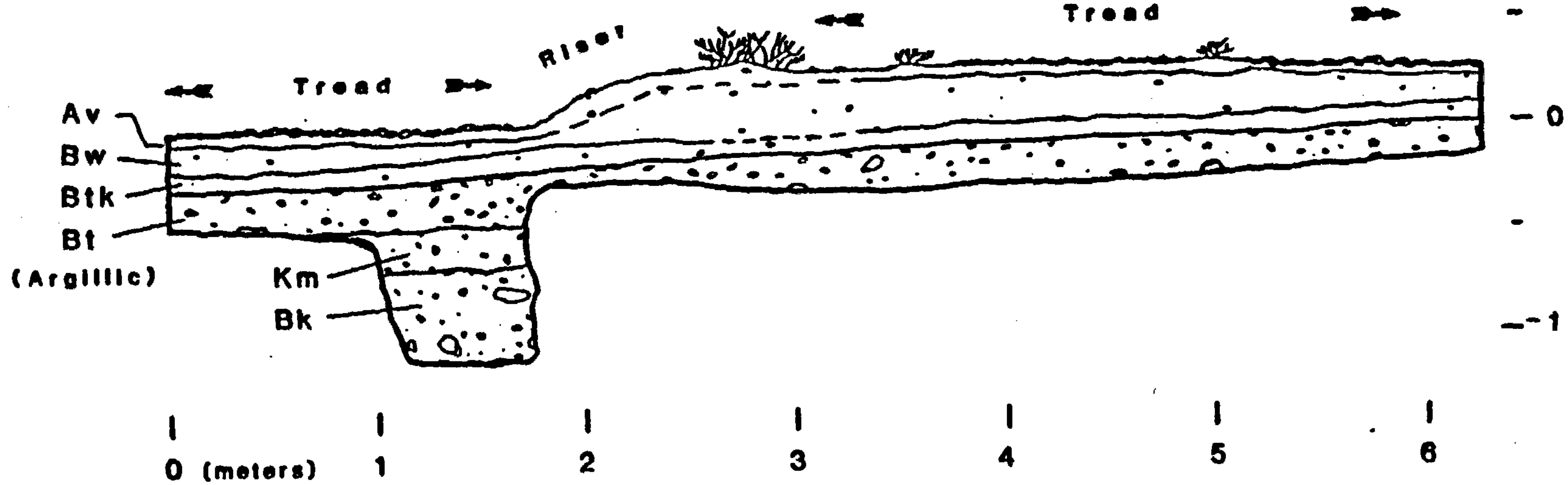

Figure 49. Log of the trench in Stingaree Valley, Nevada illustrating soil horizons. The Av through Btk horizons have formed in the fine grained surficial layer and the Bt and Km horizons have formed in the underlying fan alluvium (cf. Fig. 48).

they formed by sheet wash. The author has identified pattern ground on alluvial fans in northern most Death Valley that is very similar to that described by Well and McFadden (1985). The sheet wash features in both areas however, are clearly different from the micro-relief steps described herein. In particular the air-photo pattern of the sheet wash features is essentially a negatives of the micro-relief steps, and their internal composition is dissimilar. For example, rather than the light tonal-stripes representing interlocking pavement as with the steps, they are rather gravely lag deposits. Further, the sheet wash features consists not of well sorted, fine grained materials below pavements, but of poorly sorted, coarse sands and gravels that largely overly pavements. These (and other) fundamental differences in the pattern ground features, suggest two distinctly different modes of formation. Hence. the steps were not formed by sheet wash.

As described above the micro-relief steps form in fine-grained surficial layers on alluvial fans in the western Great Basin. The bulk of this material is apparently eolian sediment. Perhaps these features are fine sand and silt dunes, stabilized by vegetation.

Several lines of evidence however, suggest the pattern ground features are the result of mass wasting. The most compelling evidence of downslope movement is that risers are consistently parallel to contour and have downslope buldges, and flights of steps exhibit a gradual transition in morphology with increasing slope. These relations strongly suggest that the pattern ground formed by mass wasting, and (for example) not by eolian sedimentation.

Pattern ground comprising uniformilly spaced steps on alluvial fan remnants of the western Great Basin (e.g., Figs. 43 and 44), is likely formed by solifluction. The term solifluction, as used herein, was originally defined by Anderson (1906) as the process of "... slow flowing from higher to lower ground of masses of waste saturated with water." Solifluction is encouraged by impeded drainage over an impermeable layer (Davies, 1969). Solifluction features occur in regions with or without permafrost, but are most common where mean annual temperatures are 1 C or less (Williams, 1962). Several investigators however, such as Paterson (1940), Washburn (1947, 1956), Smith (1949), and Hunt and Washburn (1966), recognized that solifluction may operate under diverse environmental conditions, provided that the primary requisite of saturation is satisfied.

The pattern ground features are apparently restricted to gentle slopes, based on air-photo examination. Stratigraphic relations observed in the trenches (Figs. 46 and 48) and in several exploratory pits, indicate that the steps are formed in fine grained surficial layers rich in silt; M.C. Reheis (1987, unpub. data) determined about 43 % silt and an equal amount of primarily fine and very fine sizes in the Av horizon of an Indian soil in northwestern Fish Lake Valley. These vesicular surficial layers are in abrupt contact with subjacent, clay-rich argillic B horizons over Stage III K (or Bk) horizons. All of the above relationships are consistent with mass wasting by solifluction.

The pattern ground features differ from typical solifluction features however, in that drainage is probably impeded by argillic and K horizons rather than permafrost or frozen ground. The drainage imped by these less permeable soil horizons promots saturation of the silt-rich loess layers, and thus induces gradual downslope flow under the influence of gravity, or solifluction. The processes results in formation of flights of steps on many mid and late Pleistocene alluvial fan remnants of the western Great Basin.

This rather unique process of solifluction depends more on soil development and eolian sedimentation, than on the prevailing climatic. Since pedogenesis is time dependent (Chapter V), this type of solifluction also depends on time. Thus, initiation of solifluction on alluvial fan remnants of the western Great Basin requires a sufficient duration of time to (1) develop less permeable pedogenic horizons (e.g., argillic and K horizons), and (2) accumulate a relatively thick surficial loess layer on alluvial fan surfaces. The latter requisite apparently depends on the formation of desert pavements to trap eolian sediment (Peterson, 19??), and on translocation of fine materials that eventually plug or partly plug the soil sprofile (Taylor, 1986). Once the two requisites are satisfied, all that is necessary for solifluction is sufficient water to saturate and induce flow within the layer of loess.

The interval of time required to develope less permeable soil horizons, hence flights of solifluction steps, is apparently significant. In Fish Lake Valley solifluction steps occur on two distinctively different geomorphic surfaces. They are the post-Bishop tuff (740 ka) McAfee Creek surface and the younger (late Pleistocene) Indian surface. In Fairview Valley the steps form on probable late Pleistocene fan surfaces.

In northeast Crater Flat the steps are abundant on two geomorphic surfaces of significantly different age. They are the Yucca and Early Black Cone surfaces as defined and described by Peterson (1988), and mapped in east-central Crater Flat by the author and A.R. Ramelli (in prep.). Dorn (1987) used preliminary cation-ratio analysis on rock varnish from surficial boulders to date these surfaces. The Yucca surface has cation-ratio dates of 360 to 380 ka, and the Early Black Cone surface of 128 to 137 ka. The next youngest geomorphic surface (Late Black Cone surface) lacks pattern ground, and has radiocarbon dates on organic material extracted from rock varnish of 30 ka or less (Dorn, 1987).

Hence, solifluction steps form on late Pleistocene (380 to 130 ka) geomorphic surface, but not on latest Pleistocene (30 ka) and younger fan surfaces in Crater Flat. This implies that a substantial time interval is required to develope the soil and stratigraphic requistes for solifluction. Thus, the pattern ground features are significantly younger than the alluvial deposits on which they flow.

Soil creep due to volume changes in desert loess layers, may be a secondary process in the formation of solifluction steps on alluvial fan remnants. Two likely volume change processes, shrink-swell and frost heave, are commonly associated with soil creep (Benedict, 1976). Soil expansion (i.e., swell or heave) contibutes a minor component of downslope movement that is proportional to the angle of slope and the magnitude of displacement. For example, with increasing slope (and/or heave) the resulting component of downslope movement increases.

Shrink-swell produced by cycles of saturation and desiccation is an important process in the development of vesicular pores (Miller, 1971), and results in vertical movement of clasts in the formation of stone pavements (Springer, 1958; Cooke, 1970; Dan and others, 1982). Denny (1965) concluded that expansion of silts upon wetting resulted in a slight net movement of material downslope on fans in the

Death Valley region. Polygonal cracks in stone pavements have commonly been attributed to desiccation of the underlying materials following a period of saturation (e.g., Cooke, 1970; Hunt and Washburn, 1966). The cracks define large columnar peds and were observed in all three study areas. The peds shrink as the soil drys, and fine grained materials accumulate in dilated inter-ped voids. This material is apparently incorporated into the soil when soil moisture is retained. Thereby increasing soil volume and resulting a net downslope component of movement (i.e., soil creep).

Mcfadden and others (1986) concluded that accumulations of clay in loess mantles formed on the Cima volcanic field in the eastern Mojave Desert, have profoundly increase the shrink-swell capacity of the loess. They observed markedly domed caps on columnar peds in vesicular A horizons, that they attributed to seasonal formation of the domes in association with that of vesciular pores. Apparently collapse of domes results when soil moisture increases during the winter season.

Repeated freeze-thaw cycles result in volume-changes, and may contribute to the development of the solifluction steps. Repeated freeze-thaw cycles in saturated materials cause coarse particles to migrate upwards (Corte, 1963) in manner that is probably similar to vertical movement associated with the shrink-swell process (described above). The amount of vertical movement, and hence the amount of downslope movement, is closely associated with soil texture and is greatest for silty soils (Davison, 1889, and Taber, 1930), such as the desert loess in which the steps have formed.

Soil creep is probably a secondary factor in the formation of the pattern ground features. Since, only minor down-slope movement is likely, due to the gentleness of the pattern ground slopes and to the present climate of the region.

DISCUSSION

Springer (1958) and Miller (1971) showed that vesicular pores form when loamy soils are in a semi-fluid state, that Miller found to be "very unstable". Miller concluded that the number and size of vesicles increased with repeated cycles of wetting and drying. Vesicular pores are also important characteristics of moving soils (Benedict, 1976).

Hence, numerous, large vescicular pores in Av horizons, and smaller and less frequent vesciles in subjacent B horizons, suggest that the desert loess has been repeatedly saturated. At which point the loess exhibits a plasmatic or dilatent behavor. Thus, the silt-rich surficial layers on aluvial fan surfaces of the western Great Basin are apparently susceptible to failure by solifluction.

Since the presence if an infiltration impeding layer below the loess (i.e., less permeable soil horizons) is independent of the prevailing climate, frigid climatic conditions are not required for formation of the pattern ground features. Thus, there is no compelling reason to assume that solifluction is currently inactive in this arid region. The process is however, favored during prolonged precipitaion events or melt of substantial snow packs, resulting in saturation of the surficial loess layers.

Indirect evidence of plasmatic behavior of the loess layers was shown by numerous viscous "flow- and drip-structures" (similar in appearance to melted wax on a candle), observed draped over the Fish Lake Valley trench walls in January 1988, six months following excavation. These distinctly vesicular structures comprise material that flowed out from under the crusting Av sub-horizons of the tread surfaces. The stone pavements bordering the trench were slight deflated. These relations suggest that solifluction is active, in at least the upper part of the loess layer.

Circumstanial evidence suggests solifluction is currently active on piedmont slopes in the western Great Basin. Specifically, many solifluction steps have steep (up to 18 degrees) riser and exhibit a non-dissected morphology, dispite being composed of easily erodible, fine grained materials not protected by desert pavement. Thus current solifluction activity is apparently capiable of maintianing the step morphology.

Shrink-swell within loess layers is evidentent by the "self-healing" nature of stone pavements. Footprint about 2 to 4 cm deep, were made during the summer season of 1987 in tightly packed stone pavements on tread surfaces in Fish Lake Valley. The impressions were obliterated and nearly reclaimed by pavement the following winter season. Similarily footprints made during the winter of 1988 were reclaimed by the following summer. Vesicular pores destroyed by the impressions have subsequently reformed. These observations suggest that shrink-swell of the loess is seasonal and is associated with the formation of vesicular pores. Thus, shrink-swell is currently active and probably contributes somewhat to the formation of the pattern ground features.

Although the solifluction steps display limited evidence of current activity, they are apparently relict landforms. The steps likely formed during past environmental conditions that were wetter (and/or colder) than currently in the western Great Basin. Two lines of evidence support this hypothesis. 1) Stage I Bk and/or incipient Bt horizons have developed in the lower part of loess layers (e.g., Figs. 47 and 49). This suggests little or no movement occurs in the basal portions of these layers. 2) Many solifluction steps in the western Great Basin have risers that are parallel to contour. However, where there has been relatively recent (late Holocene?) incision of onfan drainages, the risers have failed to reorient into parallism with contour. These observations suggest that solifluction activity is limited to the upper part of loess layers, and the rate of solifluction is exceedingly slow at present.

SUMMARY AND CONCLUSIONS

Soil-stratigraphic studies suggest solifluction steps form in surficial loess layers on alluvial fan remnants. Less permeable, strongly developed argillic and K horizons are requisites critical to solifluction in the arid western Great Basin. Thus these solifluction features differ from their frigid environment counterparts, in that an infiltration impeding layer is not dependent on climate or season, but rather on pedogenic processes. These studies further suggests that relatively thick accumulations of desert loess are necessary for solifluction. Once these requisistes are satisfied, all that is required for solifluction is sufficient water to saturate and induce flow in the layer of loess.

The abundance of prominent solifluction steps on many mid and late Pleistocene alluvial fan remnants, and their apparent absents on latest Pleistocene and Holocene surfaces (e.g., Crater Flat), implies that the time required to satisfy the pedogenic and/or stratigraphic requisites is substantial. Therefore, solifluction steps provide a means of distinguishing and isolating geomorphic surfaces by relative age.

Flights of steps formed in loess on piedmont slopes of the western Great Basin indicate that solifluction is currently active, and has resulted in relict landscape evolution. The rates of solifluction are likely to be exceedingly slow however, due to infrequent saturation of the eolian materials under the previaling climate of the region.

The paleoclimatic significance of these features is not well understood and warrants further investigation. It appears reasonable to assume that solifluction, as described above, would operate more efficiently during wetter periods with more frequent and deeper saturation than occur in the region currently. Perhaps during pluvial climates more moisture is available to saturate the eolian fines and to facilitate mass wasting, thus favoring formation of solifluction steps.

Solifluction steps on alluvial fan remnants, imply characteristic soil-stratigraphic relations. Specifically, (1) the fan surface exhibits moderate to well sorted, interlocking stone pavements, and is probably older than latest Pleistocene in age. (2) A relatively thick, fine grained, surficial layer overlies fan alluvium. (3) The soil profile comprises an argillic horizon and (or?) a horizon of prominent carbonate (and opal) accumulation.

Solifluction of desert loess layers probably result in the near-horizontal and flattish nature of the treads, and in smoothing irregularities (e.g., levee and channel topography) on alluvial fan surfaces. Thus, this study supports the conclusions of Denny (1965) and Denny and Drewes (1965), that the depositional morphology on alluvial fans of the region has been influenced by saturated flow of silt-rich surficial layers. The overlying stone pavements are apparently rafted in a passive and semi-coherent manner during solifluction.

APPENDIX II
PEDON DESCRIPTIONS

PEDONS 1 TO 13

EXPLANATION OF PEDON DESCRIPTIONS

The following pedon descriptions were described according to procedures and nomenclature of the Soil Survey Manual (USDA Agr. Handbook 18, 1951) and revised by the Soil Survey Staff (1966), and a further revision of the procedures in the New Soil Survey Manual (1981, p. 39-49 & 105-107). Pedon description sites are shown in Plate I.

Carbonate morphology was described following Gile and other's (1966) classification of morphogenetic sequences of calcium carbonate accumulations. Postscript addenda, "-" and "+", are used in conjunction with stages of carbonate accumulation to denote the distinctness of carbonate morphology; where "-" indicates the stage-morphology is weakly expressed and "+" is equivalent to Gile and other's (1966) "late stage-morphology" which is transitional to the next higher stage. Where the morphology of a horizon is dominated by carbonate accumulations, a K horizon designation, as proposed by Gile and others (1965), is used. Taylor's (1986) classification of pedogenic sequence of silica opal accumulations is used to describe opal morphology. The informal subordinate distinction "j" for master horizons, is used to describe juvenile or incipient pedogenic accumulations of carbonate and opal. Another informal subordinate distinction, "v" is used to denote horizons with coarsely-vesicular pores (Peterson, 1977; Nettleton and Peterson, 1983). The postscript "c" is used to denote the color of carbonate coats. In a similar manner, "s" and "m" denote the color of opal and mottles, respectively. The terminology for "Physiographic Position" is that of Peterson (1981). The phrase "desert shrubs" includes Sagebrush (Artemisia tridentata), Rabbit Brush, Grease Wood, Shadscale (Artiplex confertifolia), and Spinney Hop sage.

PEDON #: 1

PEDON DESCRIPTION: Morphostratigraphic Unit: middle Marble; Describer: Tom Sawyer Date: 6-22-87 Area: Marble Creek, NW Fish Lake Valley, Nevada. Location: About 0.6 km south of Marble Creek, on the Marble Creek fan immediately north of an unnamed drainage that heads near knob 7937 - W1/2, SW1/4, Sec 23, T2S, R34E, Mt Barcroft 15' Quad, NV-CA; 37 44'49'' N. Lat., 118 09'27" W. Long. Physiographic Position: Apex of inset-fan remnant; dissected to a depth of 1-1.5 m; displaced about 30 cm down to the east along master fault of northern FLVFZ; clearly inset below the Leidy surface. Varnish Development: none; Pavement Development: none; Pavement area: 0 %; Slope: 3 ; Aspect: E; Elevation: 1850 m, 6080 ft; Runoff: medium; Drainage: well; Parent Material: Quartz monzonitic alluvium with subordinate carbonate and metasedimentry lithic fragments; parent material for Av horizon is probably largely eolian sediments; calcareous throughout. Vegetation: Low (<30 cm) desert shrubs up to 1.5 m apart and rare cacti, and sparse grasses. Soil Temperature Regime: warm mesic; Moisture Status: Dry.

	Depth	Color				Consistence						Secondary		Clay	Est. % Wt.	
Horizon	(cm)	Dry	Moist	Text.	Struct.	Dry	Moist	Wet	Bndry.	Pores	Roots	Carb.	Opal	Films	Grv.	Cob.
Av[a]	0-4	2.5Y7/2	2.5Y5/2	fsl	sg to m	so	vfr	ss/ps	gs	1vf,1f	2vf,1f	ev none	none	none	30	5
Bkj[b]	4-23	2.5Y7/2	2.5Y4/2	gsl	1mabk	sh	vfr	so/po	gw		2vf	ev I-	"	"	40	15
2Bk1	23-42	2.5Y6/2	2.5Y4/2	gsl	1m-vcabk	h	fr	so/po	as		1f	ev I	"	"	45	5
2Bk2	42-63	2.5Y6/2	2.5Y4/2	gsl	1m-vcabk	vh	fr	so/po	aw		3vf	I	"	"	45	10
3Bk[c]	63-73	2.5Y6/2	2.5Y4/2	gsl	sg	lo	lo	so/po	aw		1f,1m 1c,1vc	I	I-	"	40	5
4Bk1[c]	73-115	2.5Y7/2	2.5Y4/2	gsl	1m-vcabk	h	fr	so/po	gs		2vf, 1f,1m	I	I-	"	50	10
4Bk2	115-157	2.5Y7/6	2.5Y5/4	gsl	1cabk	sh	vfr	so/po	gw			I-	none	"	40	15
4BC	157-185+	2.5Y7/4	2.5Y4/2	gsl	sg	lo	lo	so/po				"	"	"	40	15

Comments: A detrital wood fragment (Sample # 5-TS-1-28PC; Radiocarbon Site 3) was collected from the north wall of the unnamed drainage channel, about 50 cm below the middle Marble relict surface, and dated at 1555 cal B.P. A tephra sample (5-TS-1-28PC-B; Tephra Site 2), that possibly correlates with one of several Mono Crater ashes that range in age from 3400-8000 yr B.P., but matches most closely with those ranging from 3400-4100 yr B.P. (Sarna-Wojcicki, 1987, written commun.), was collected at a depth of about 1.8 m below the middle Marble surface. [a]Av horizon occurs discontinuously and only between coppice dunes. [b]Carbonate accumulation is displayed as "powdery" filaments in dendritic arrangement. [c]Opal accumulation is on the bottom of pebbles and is displayed as discontinuous coats.

PEDON #: 2

PEDON DESCRIPTION: Morphostratigraphic Unit: middle Marble; Describers: Tom Sawyer, Marith Reheis, and Janet Slate
Date: 6-23-87 Area: Marble Creek, NW Fish Lake Valley, Nevada. Location: About 0.6 km south of Marble Creek, on the Marble Creek fan, immediately north of a unnamed drainage that heads near knob 7937 - W1/2, SW1/4, Sec 23, T2S, R34E, Mt Barcroft 15' Quad, NV-CA; 37 44'49" N. Lat., 118 09'27" W. Long. Physiographic Position: Apex of inset-fan remnant; dissected to a depth of 1-1.5 m; displaced about 30 cm, down to the east, along a fault; clearly inset below the Leidy fan-remnant.
Varnish Development: none; Pavement Development: none; Pavement Area: 0 %; Slope: 3 ; Aspect: E; Elevation: 1850 m, 6080 ft; Runoff: medium; Drainage: well; Parent Material: Quartz monzonitic alluvium with subordinate carbonate and metasedimentry lithic fragments; parent material of Av horizon is probably composed largely of eolian sediments; calcareous throughout.
Vegetation: Low (<30cm) desert shrubs up to 1.5 m apart and rare cacti, and sparse grasses. Soil Temperature Regime: warm mesic; Moisture Status: Dry.

	Depth	Color				Consistence						Secondary		Clay	Est. % Wt.	
Horizon	(cm)	Dry	Moist	Text.	Struct.	Dry	Moist	Wet	Bndry.	Pores	Roots	Carb.	Opal	Films	Grv.	Cob.
Av[a]	0-3	2.5Y7/2	2.5Y4/2	fsl	2vf - csbk	so	n/a	so/po	aw	2vf, 2f,1m	1vf	ev none	none	none	15	5
Bw	3-13	2.5Y6/2	2.5Y4/2	gsl	2f-msbk	sh	n/a	so/po	cw	3vf,1f	1vf,2f	"	"	"	40	10
Bkj[b]	13-39	2.5Y7/2	2.5Y5/2	gsl	1f-msbk	so	n/a	so/po	aw	3vf, 1f,1m	2f,1m	ev I-	"	"	50	5
2Bk1[c]	39-72	2.5Y7/2	2.5Y5/3	vgsl	1f-cabk	sh	n/a	so/po	gw	3vf,1f	2vf, 1f,1m	ev I	"	"	60	5
2Bk2	72-112	2.5Y7/2	2.5Y5/3	vgsl	1f-cabk	sh	n/a	so/po	aw	3vf	2vf,1f	ev I	"	"	55	5
3Bkq	112-130+	2.5Y6/2	2.5Y4/2	vgs	sg	lo-so	n/a	so/po	-	-	-	ev I-	"	"	60	15

Comments: A detrital wood fragment (Sample # 5-TS-1-28FC; Radiocarbon Site 3) was collected from the north wall of the unnamed creek channel, about 50 cm below the middle Marble relict surface, and dated at 1555 cal B.P. A tephra sample (5-TS-1-28FC-B; Tephra Site 2), that possibly correlates with one of several Mono Crater ashes that range in age from 3400-8000 yr B.P., but matches most closely with those ranging from 3400-4100 yr B.P. (Sarna-Wojcicki, 1987, written commun.), was collected at a depth of 1.8 m. [a]Av horizon occurs discontinuously and only between coppice dunes. [b]Carbonate accumulation is displayed as "powdery" filaments in a dendritic arrangement. [c]Secondary carbonate forms nearly continuous to continuous coating on bebble undersides.

PEDON #: 3

PEDON DESCRIPTION: **Morphostratigraphic Unit:** early Marble **Describers:** Tom Sawyer, Marith Reheis, and Janet Slate **Date:** 6-23-87 **Area:** Marble Creek, NW Fish Lake Valley, Nevada. **Location:** North wall of the Marble Creek fanhead trench, about 1 km downstream from where the creek emerges from range front - W1/2, SW1/4 of Sec 23, T2S, R34E, Mt Barcroft Quad. CA-NV; 37 45'00" N. Lat., 118 09'45" W. Long. **Physiographic Position:** Middle-fan-piedmont-remnant summit; inset below the Leidy unit and locally burying the Indian paleosol; **Varnish Development:** Incipient, few fragments are lightly varnished; **Pavement Development:** weakly packed fragments; **Pavement Area:** 40%; **Slope:** 3.5 ; **Aspect:** N80E; **Elevation:** 1785 m, 5860 ft.; **Runoff:** medium; **Drainage:** well; **Parent Material:** Quartz monzonitic alluvium with subordinate carbonate and metamorphic lithic fragments and eolian sediments; calcareous throughout; **Vegetation:** Low (20-30cm) desert shrubs separated by 0.5-1 m. and few cacti; **Soil Temperature Regime:** warm mesic; **Moisture Status:** Dry;

	Depth	Color				Consistence						Secondary		Clay	Est. % Wt.	
Horizon	(cm)	Dry	Moist	Text.	Struct.	Dry	Moist	Wet	Bndry.	Pores	Roots	Carb.	Opal	Films	Grv.	Cob.
Av	0-6	2.5y7/2	2.5Y4/4	fsl	1vfp 2f-csbk	so	n/a	vss/po	av	1vf	3vf,2f 1m,1c	ev none	none	none	30	0
Bw	6-14	2.5Y7/3	2.5Y4/2	gsl	3f-mg 1f-msbk	so	n/a	so/po	cw	3vf, 1f,1m	2vf,1f	ev I-	I-	"	40	5
Bkq	14-68	2.5Y7/3	2.5Y5/3	gsl	1f-csbk	sh	n/a	so/po	gw	3vf, 2f,1m	2vf, 1f,1m	ev I+	I-	"	40	10
Bkj	68-106	2.5Y6/3	2.5Y5/4	gsl	1f-vcsbk	sh	n/a	so/po	cw	2vf,1f	1vf,1f	ev I-	none	"	50	5
B	106-156	2.5Y7/4	2.5Y4/4	vgsl	1f-vcsbk	sh	n/a	so/po	aw	2vf,1f	2vf	ev I-	"	"	60	5
2Btb[a]	156-221+	2.5Y7/4	2.5Y5/4	gsl	f-vcsbk	sh	n/a	so/po				ev I	"	"	50	10

Comments: Two detrital, wood logs were collected from this location (Radiocarbon Site 2) at a depth of 2.2 m and about 5 m below the early Marble relict surface in the north fanhead trench-wall, and were dated at 2155 cal B.P. (5-TS-1-22A) and 2340 cal B.P. (5-TS-1-10MC), respectively. [a]Stratigraphic relations observed in fanhead trench-wall indicates that the lowermost horizon is a buried soil.

PEDON # 4

PEDON DESCRIPTION: Morphostratigraphic Unit: late Marble; **Describer:** Tom Sawyer **Date:** 6-25-87 **Area:** Marble Creek, NW Fish Lake Valley, Nevada. **Location:** Immediately (4 m) south of Marble Creek about 250 m downfan from the mouth of the Marble Creek fanhead trench - W1/2, NW1/4, Sec 23, T.2S., R.34E., Mr Barcroft 15' Quad. CA-NV; 37 45'03" N. Lat., 118 09'48" W. Long. **Physiographic Position:** Upper-inset-fan (near apex) on a gently sloping backslope; dissected to a depth of about 2m; the late Marble unit can be traced upfan to where it is clearly inset below the middle Marble thru Indian units. **Varnish Development:** none; **Pavement Development:** none; **Pavement Area:** 0%; **Slope:** 3.5 ; **Aspect:** E; **Elevation:** 1780 m, 5840 ft; **Runoff:** medium; **Drainage:** well; **Parent Material:** Quartz monzonitic alluvium with subordinate carbonate and metasedimentry lithic fragments; calcareous throughout. **Vegetation:** Low (<30cm) desert shrubs spaced from 1-3 m apart and sparse grasses; **Soil Temperature:** warm mesic; **Moisture Status:** Dry;

	Depth	Color				Consistence						Secondary		Clay	Est. % Wt.	
Horizon	(cm)	Dry	Moist	Text.	Struct.	Dry	Moist	Wet	Bndry.	Pores	Roots	Carb.	Opal	Films	Grv.	Cob.
A	0-5	2.5Y7/2	2.5Y4/3	gsl	2fp	lo - so	lo	so/po	aw	2vf, 2f,2m	1vf,1f	ev none	none	none	30	5
AB	5-26	2.5Y7/3	2.5Y5/4	gsl	3f-csbk 3f-cabk	h	fi	vss/ps	aw	1vf, 2f,2m	1vf,2f	ev "	"	"	50	5
Bkj1[a]	26-37	2.5Y6/2	2.5Y5/3	gsl	2f-csbk	sh	fr	so/po	aw	3vf, 1f,1m	2vf, 1f,1m	ev I-	"	"	45	10
Bkj2[a]	37-80	2.5Y6/2	2.5Y5/3	gsl	2m-csbk	h	fr	so/po	aw	1vf, 3vf,2f	ev 2f,1m	I-	"	"	45	5
2Bkqb[b]	80-93	2.5Y7/2	2.5Y5/2	gsl	sg & 1fsbk	so	vfr	so/po	cw	3vf	1f,1m	ev I-	I	"	40	10
2Bk1	93-109	2.5Y7/2	2.5Y4/3	gsl	2f-cabk	so-sh	vfr	so/po	cw	3vf,1f	1f,1m	ev I-	none	"	50	5
2Bk2	109-148	mot-10YR7/8 2.5Y7/2	2.5Y5/3	vgsl	2f-csbk	sh	vfr	so/po	cw	3vf	1f	ev I-	"	"	55	5
2CB	148-180+	mot-10YR7/6 2.5Y8/2	2.5Y6/3	gsl	sg & 1f-csbk	sh	vfr	so/po		3vf,1f	1f	ev none	"	"	40	10

Comments: Three detrital wood fragments were collected at this site (Radiocarbon Site 1); two from south wall of the shallowly incised Marble Creek channel and the third form this soil pit (Pedon # 4), that is about 4 m to the south of the channel. Radiocarbon dates of 120 cal B.P. (5-TS-1-51MC-I), 660 cal B.P.(5-TS-1-7MC), and 680 cal B.P. (5-TS-1-49-B) were obtained from depths of 5-26 cm, about 80 cm, and at about 2 m, respectively, below the relict surface of the late Marble unit. A tephra sample (5-TS-1-7MC-C) was also collected from a depth of about 2 m. The tephra possibly correlates with an ash erupted from Mono Craters dated at 640 14C yr B.P. (Sarna-Wojcicki, 1989, written commun.). [a]Carbonate accumulation is displayed as "powdery" filaments in dendritic arrangement. [b]Opal has accumulated on a few pebble bottoms as thin, discontinuous "flakes".

PEDON # 5

PEDON DESCRIPTION: **Morphostratigraphic Unit:** Indian; **Describer:** Tom Sawyer **Date:** 7-29-87 **Area:** Indian Creek, NW Fish Lake Valley, Nevada. **Location:** About 4 km from the range front and about 1.5 km south of Indian Creek - E1/2, NW1/4, Sec 7, T.2S., R35E., Davis Mtn. 15' Quad, NV-CA; 37 46'03" N. Lat, 118 07'36" W. Long; in arcuate pavement surface of solifluction step at east end of a trench excavated across a solifluction step (Appendix A, Fig. 4a). **Physiographic Position:** Lower-fan-piedmont-remnant on flattish summit; moderately-wide remnant with prominently expressed solifluction steps. **Varnish Development:** continuous, darkly varnished; "greasy" luster. **Pavement Development:** well sorted & tightly packed; deeply etched limestone fragments; **Pavement Area:** 80%; **Slope:** 3o; **Aspect:** E; **Elevation:** 1590 m, 5240 ft.; **Runoff:** Medium; **Drainage:** well; **Parent Material:** Granitic alluvium with subordinate carbonate, metasedimentry, and andesitic lithic fragments; parent material for the Av & Bwv horizons is probably eolian sediments; calcareous throughout. **Vegetation:** Low (<30cm) desert shrubs that are primarily restricted to subparallel, arcuate bands that follow risers of the solifluction steps. **Soil Temperature Regime:** warm mesic; **Moisture Status:** dry;

	Depth	Color				Consistence						Secondary		Clay	Est. % Wt.	
Horizon	(cm)	Dry	Moist	Text.	Struct.	Dry	Moist	Wet	Bndry.	Pores	Roots	Carb.	Opal	Films	Grv.	Cob.
Avk	0-6	2.5Y7/2	2.5Y7/3	fsl	f-msbk	so	vfr	vss/ps	as	3m,3c	1vf	ev I	none	none	15	5
BA [a]	6-17	2.5Y7/2	2.5Y7/3	gsil	f-vcsbk	sh	fr	so/ps	as	3m,3c	3f,1m	ev I+	I	"	25	5
2Btkq [b]	17-45	10YR7/4	10YR5/4	gsicl	1m-vcsbk	vh	fr	s/p	gw	2vf,2f	3f,1m	ev I-II	II	2npf& 2mkco	30	5
2Bkm [c]	45-95	2.5Y7/3	2.5Y5/3	gsl	1m-csbk	h	fi	so/po	cw	2f	3f	ev III	II-III	none	50	10
2Bk	95-135+	2.5Y7/2	2.5Y5/3	vgsl	1m-csbk	h	fi	ss/ps		2f	1f	ev,I+ to II	I	"	55	5

Comments: Soil Pit # 5 is in a nearly horizontal tread surface of a narrow, moderately high, solifluction step (Fig. 4a).
[a]The Bwv horizon is "cambic-like", but does not meet the required 25 cm depth for the lower horizon-boundary, and therefore is not formally a cambic horizon. [b]Authigenic silicate clays accumulate as films on pores and colloid stains on mineral grains; argillans or clay films were probably present on ped faces, but were likely obliterated by polygenitic engulfment by carbonate; this horizon is considered to be a agrillic horizon. [c]This horizon is dominated by K-fabric; a lack of a laminar zone is evidence that the horizon is not entirely plugged.

PEDON # 6

PEDON DESCRIPTION: **Morphostratigraphic Unit:** Leidy; **Describer:** Tom Sawyer **Date:** 9-12-87 **Area:** Indian Creek, NW Fish Lake Valley, Nevada. **Location:** Immediately (about 25 m) north of Indian Creek; within the stepped sequence of the fanhead trench; about 600 m downfan from mouth of canyon - SW 1/4 of Sec. 3, T.2S., R.34E., Davis Mountain 15' Quad., NV-CA; 37 47'15" N. Lat., 118 11'22" W. Long. **Physiographic Position:** Upper-inset-fan-remnant flattish, narrow summit (stream terrace) with moderately angular shoulders; clearly inset below the Indian unit (Pedon 7) and clearly above the early Marble unit (Pedon 9); dissected to a depth of about 15 m. **Varnish Development:** In general thinly and discontinuously varnished, however a few fragments are darkly varnished having "greasy" luster; **Pavement Development:** Incipient; loosely packed and poorly sorted; **Pavement Area:** 30 %; **Slope:** 3.5o; **Aspect:** ENE; **Elevation:** 1905 m, 6250 ft.; **Runoff:** medium; **Drainage:** well; **Parent Material:** Granitic alluvium with subordinate carbonate, andesite, and metasedimentry lithic fragments; eolian sediments; calcareous nearly throughout. **Vegetation:** Low (<30cm) desert shrubs up to 1m apart; few cacti, and some grasses. **Soil Temperature Regime:** warm mesic; **Moisture Status:** Dry;

Horizon	Depth (cm)	Color Dry	Color Moist	Text.	Struct.	Consistence Dry	Consistence Moist	Consistence Wet	Bndry.	Pores	Roots	Secondary Carb.	Secondary Opal	Clay Films	Est. % Wt. Grv.	Est. % Wt. Cob.
Av[a]	0-13	2.5Y6/2	2.5Y4/3	fsl	3m-cp	so	fr	so/po	cw	2vf,1f	1vf	ev none	none	none	15	3
Btkq[b]	13-28	2.5Y7/2	2.5Y5/4	gsl	1mcsbk	vh	fr	so/po	gw	1f	1vf,2f 2m,1c	nr I-II	II-	2nbr 1npo	45	5
Bkq	28-79	2.5Y7/2	2.5Y5/4	gsl	1mcsbk	vh	fr	so/po	gw	1f	2m,1c	I-II	II-	none	45	5
Bk	79-92	2.5Y7/3	2.5Y5/3	gsl	1mcsbk	sh	vfr	so/po	cw	2f	1f,1m	ev II	I	"	40	10
2Bk1[c]	92-137	2.5Y7/4	2.5Y5/4	gsl	1cvcabk	vh	fi	so/po	cw	1f	1m	ev I+	none	"	50	10
2Bk2	137-150	2.5Y7/3	2.5Y4/3	gsl	sg	lo	lo	so/po	cw	2f	1f,1m	ev I+	"	"	45	5
2Bk3	150-205+	2.5Y7/4	2.5Y4/3	gsl	1mcabk	vh	fr	so/po		1f	1f	ev I	"	"	45	5

Comments: [a]Av horizon occurs continuously between coppice dunes; thin, powdery, discontinuous carbonate coats between some platy peds; somewhat dilatent. [b]Carbonate coats are moderately thick and continuous on the underside of clasts; few coats have a pendant morphology, suggesting the presence of opal (M.C. Reheis, 1988, personal commun.). [c]Carbonate accumulations occur as discontinuous coats on the underside of pebbles, often arranged in a dendritic pattern.

PEDON # 7

PEDON DESCRIPTION: Morphostratigraphic Unit: Indian; **Describer:** Tom Sawyer **Date:** 9-11-87 **Area:** Indian Creek, NW Fish Lake Valley, Nevada. **Location:** Immediately (20 m) north of Indian Creek, on the next to highest (i.e. oldest) member of stepped sequence, about 600 m downfan from the mouth of the canyon; SW1/4, Sec. 3, T.2S., R.34E., Davis Mountain 15' Quad., NV-CA; 37 47'15" N. Lat., 118 11'22" W. Long. **Physiographic Position:** Narrow, flattish, inset-fan-remnant-summit with moderately rounded shoulders; clearly inset below the McAfee Creek unit and above the Leidy unit; depth of dissection about 30-35 m. **Varnish Development:** Continuous, darkly varnished lithic fragments with "greasy" luster; **Pavement Development:** up to well sorted and tightly packed; **Pavement Area:** 60 %; **Slope:** 3 ; **Aspect:** E; **Elevation:** 1610 m, 5270 ft; **Runoff:** somewhat poorly drained; **Drainage:** somewhat poorly drained; **Parent Material:** Granitic alluvium with subordinate carbonate and metasedimentry clasts; parent material for the Av and Bwk horizons is likely eolian sediment; **Vegetation:** Low (<30 cm) desert shrubs and few cacti; **Soil Temperature Regime:** warm mesic; **Moisture Status:** dry.

	Depth	Color				Consistence						Secondary		Clay	Est. %	
Horizon	(cm)	Dry	Moist	Text.	Struct.	Dry	Moist	Wet	Bndry.	Pores	Roots	CaCO3	SiO2	Films	Grv.	Cob.
Avk	0-5	2.5Y7/2	2.5Y7/3	sil	2vcpr 2csbk	sh-h	fr	vss/ps	gw	-	1vf	ev I	none	none	15	0
BA[a]	5-14	2.5Y7/2	2.5Y6/3	l	1fsbk 2mpl	h	fi	vss/ps	as	-	1vf	ev I+	"	"	15	0
2Btkq[b]	14-25	10YR7/3	10YR5/4	scl	3fsbk	sh	vfi	s/p	gw	-	3f,3m	ev I-II	I+	2npr 2nbr	25	5
3Btkq[c]	25-40	10YR7/3	10YR5/4	gsl	2f-msbk	vh	vfi	ss/ps	gw	-	1f,1m	ev,II III	II	2nbr 1npr	40	5
3Bkm[d]	40-58	2.5Y7/3	2.5Y5/3	gsl	2cpl	vh	vfi	so/po	cw	-	1f	ev III	II	"	40	5
3Bk	58-118+	2.5Y7/3	2.5Y5/3	gsl	1sbk	h	fi	so/po	-	-	1f	II	I	"	40	5

Comments: This pit was excavated into the north-wall of the Indian Creek fanhead trench where shoulder rounding is minimal. [a]The Bwv horizon is "cambic-like", but does not meet the required 25 cm depth for the lower horizon-boundary, and therefore is not formally a cambic horizon. [b]Authigenic silicate clays accumulate as films on pores and bridges on mineral grains; argillans or clay films were probably present on ped faces, but were likely obliterated by polygenitic engulfment by carbonate; this horizon is considered to be a agrillic horizon. [c]The 2Btkq horizon contains lenses and pods of cemented material. [d]The K horizon is dominated by K-fabric; a lack of a laminar zone is evidence that the horizon is not entirely plugged.

PEDON # 8

PEDON DESCRIPTION **Morphostratigraphic Unit:** middle Marble; **Describers:** Tom Sawyer and Steve P. Mitchman **Date:** 10-21-87
Area: Indian Creek, NW Fish Lake Valley, Nevada. **Location:** Northwestern corner of interfan valley between the Indian Creek fan and the Leidy Creek fan; immediately south of the southern margin of the Indian Creek fan and about 10 m ESE of Trench Site 2; W 1/2, NE 1/4, Sec 23, T.2S., R.34E. Mt. Barcroft 15' Quad., CA-NV; 37 47'29" N. Lat., 118 10'25" W. Long.
Physiographic Position: Summit of inset-fan-remnant; the relict middle Marble surface is displaced about 2/3 m along the master fault of the northern FLVFZ near Excavation Site 2. **Varnish Development:** none; **Pavement Development:** incipient concentration of lithic fragments on surface. **Pavement Area:** 20 %; **Slope:** 3 ; **Aspect:** E; **Elevation:** 1780 m, 5840 ft; **Runoff:** medium; **Drainage:** well; **Parent Material:** Granitic alluvium with subordinate carbonate, metasedimentry, and andesitic lithic fragments; **Vegetation:** Sparse desert shrubs (<30 cm high), few cholla cactus and grasses; **Soil Temperature Regime:** warm mesic; **Moisture Status:** dry.

Horizon	Depth (cm)	Color Dry	Color Moist	Text.	Struct.	Consistence Dry	Consistence Moist	Consistence Wet	Bndry.	Pores	Roots	Secondary Carb.	Secondary Opal	Clay Films	Est. % Wt. Grv.	Est. % Wt. Cob.
A	0-5	2.5Y8/2	2.5Y3/2	gsl	sg	lo-so	lo	so/po	gs	1vf,2f	1vf,2f	ev none	none	none	30	0
Bk1[a]	5-55	2.5Y7/2	2.5Y8/6	gls	1f-c abk	sh	vfr	so/po	as	1f,2m	3f,1m	ev I	•	•	30	10
Bk2[a]	55-75	2.5Y7/2	2.5Y6/6	s	1c sbk	lo-sh	lo	so/po	cs	1f,3m	1vf,2f	ev I	•	•	5	0
Bkqj[b]	75-95	2.5Y7/2	2.5Y6/6	ls	1c sbk	sh	lo	so/po	cs	2f,1m	1f	ev I-	I-	•	15	15
Bkj[c]	95-145+	2.5Y7/2	2.5Y7/4	sl	1c sbk	sh	lo	ss/ps		2f,2m	1f	ev I-	•	•	15	5

Comments: [a]Carbonate accumulations form nearly continuous coats on the underside of pebbles. [b]Opal accumulations form discontinuous coats on the underside of pebbles. [c]Carbonate accumulates as thin, discontinuous coats on peddle bottoms generally arranged in a dendritic patterns.

PEDON # 9

PEDON DESCRIPTION: **Morphostratigraphic Unit:** early Marble; **Describer:** Tom Sawyer **Date:** 9-11-87 **Area:** Indian Creek, NW Fish Lake Valley, Nevada. **Location:** Immediately (15 m) north of Indian Creek; the second major step above the creek within the stepped sequence of the fanhead trench; about 600 m downfan from range front; SW1/4, Sec 3, T.2S., R.34E. Davis Mountain 15' Quad, NV-CA; 37 47'15" N. Lat., 118 11'22" W. Long. **Physiographic Position:** Summit of inset-fan-remnant (stream terrace); Unit 4 is clearly inset below the Leidy surface. **Varnish Development:** Discontinuous, thinly varnished lithic fragments; **Pavement Development:** Incipient concentration of lithic fragments; **Pavement Area:** 30%; **Slope:** 3.5 ; **Aspect:** ENE; **Elevation:** 1900 m, 6230 ft; **Runoff:** medium; **Drainage:** well; **Parent Material:** Granitic alluvium with subordinate carbonate, andesite, and metasedimentry lithic fragments and eolian sediments; calcareous throughout. **Vegetation:** Low (<30 cm) desert shrubs separated up to 1.5 m apart, few cacti, and very minor grasses. **Soil Temperature Regime:** warm mesic; **Moisture Status:** dry.

	Depth	Color				Consistence						Secondary		Clay	Est. % Wt.	
Horizon	(cm)	Dry	Moist	Text.	Struct.	Dry	Moist	Wet	Bndry.	Pores	Roots	Carb.	Opal	Films	Grv.	Cob.
Av	0-12	2.5Y6/3	2.5Y4/4	fsl	sg & 1vf-fp	lo	lo	vss/po	cw	1vf, 1f	2vf	ev none	none	none	30	5
Bw[a]	12-37	2.5Y7/3	2.5Y5/4	gsl	1vcsbk	sh	vfr	so/po	ci	1f	1f, 2m,1c	ev "	"	"	40	10
2Bkq[a]	37-57	2.5Y7/3	2.5Y5/4	gsl	1vcabk	h	vfr	so/ps	gs	1vf,1m	1vf, 1f,1m	ev I	I	"	45	15
2Bk1[b]	57-95	2.5Y7/2	2.5Y5/4	gsl	1vcabk	vh	fr	so/ps	gw	1vf,1f	1f,1m	ev,I+ to II	I	"	50	10
2Bk2	95-122	2.5Y7/4	2.5Y5/4	gsl	1vcabk	vh	fr	so/ps	cw	1vf,1f	ev 1f,1m	I	"	"	50	20
3Bk1	122-168	2.5Y6/3	2.5Y4/4	gsl	1vcabk	h	fr	ss/ps	cw	1vf,1f	1vf, 1f,2m	ev I-	"	"	50	10
3Bk2	168-190+	2.5Y7/2	2.5Y5/4	vgsl	1mcsbk	sh	vfr	so/ps		2vf 1f,1m	1vf, 1f,2m	ev I-	"	"	60	10

Comments: [a]Discontinuous and dendritic accumulations of carbonate near base of horizon. [b]Carbonate coats on underside of clasts display botryoidal to stalactite-like micro-morphology where opal is observed and smooth, continuous carbonate coats where opal is not observed.

PEDON # 10

PEDON DESCRIPTION: Morphostratigraphic Unit: Leidy; Describer: Tom Sawyer Date: 6-8-88 Area: Marble Creek, NW Fish Lake Valley, Nevada. Location: In the south wall of the Marble Creek fanhead trench about 600 m downfan from mouth of canyon; 37 47'29" N. Lat., 118 10'08" W. Long. Physiographic Position: Summit of middle-fan-piedmont; Varnish Development: Thinly varnished fragments with rare "greasy" luster; Pavement Development: Weakly to moderately sorted and packed. Pavement Area: 60 %; Slope: 3.5 ; Aspect: E; Elevation: 1815 m, 5950 ft; Runoff: medium; Drainage: well; Parent Material: Quartz monzonitic alluvium with subordinate carbonate lithic fragments and eolian sediments; Vegetation: Sparse desert shrubs (<40 cm high) and spaced from 0.4 to 1m apart, few cholla cactus and grasses. Soil Temperature Regime: warm mesic; Moisture Status: dry.

	Depth	Color				Consistence						Secondary		Clay	Est. % Wt.	
Horizon	(cm)	Dry	Moist	Text.	Struct.	Dry	Moist	Wet	Bndry.	Pores	Roots	Carb.	Opal	Films	Grv.	Cob.
Av[a]	0-5	2.5Y7/2	2.5Y5/3	gsl	1cpr 3cpl	so	fr	vss/po	cw	3f,3m	1vf	ev none	none	none	30	0
Btkq[b]	5-14	2.5Y7/3	2.5Y5/4	gsl	1fsbk - sg	lo-so	vfr	so/po	gw	1f	1vf,1f	sr I-	I	1npr 2nbr	50	0
Bkq1	14-42	2.5Y7/2	2.5Y4/4	gsl	2csbk	sh	fr	so/po	gw	2f	1vf,2f 1m	ev I+	I	none	50	0
Bkq2[c]	42-68	2.5Y7/3	2.5Y5/4	gsl	1msbk	sh	fr	so/po	gw	2f	2m,1f	ev II	II	"	50	0
Bkq3[c]	68-111	2.5Y7/3	2.5Y5/4	gsl	1msbk	sh-h	fr	so/po	gw	2f	1f,2m	ev II	II	"	50	0
Bk1	111-150	m-10YR6/8 2.5Y7/4	10YR5/8 2.5Y5/5	gsl	1m-csbk	sh-h	fr	so/po	gw	1f	1f,m,c	ev I+	I	"	50	0
Bk2	150-185+	m-10YR6/8 2.5Y7/4	10YR5/8 2.5Y5/5	gsl	1m-csbk	sh-h	fr	so/po		1f	2f	ev I	none	"	50	0

Comments: The pedon was described in an exposure excavated from the south trench wall of the Marble Creek fanhead trench where "rounding" of the shoulder slope component was minimal. [a]Horizon is slightly dilatent. [b]Opal accumulation is displayed as thin, discontinuous "flakes" or coats on the underside of pebbles. [c]Moderately thick carbonate/opal coatings with pendants.

PEDON # 11

PEDON DESCRIPTION: Morphostratigraphic Unit: middle Marble; Describer: Tom Sawyer Date: 6-9-88 Area: Indian Creek, NW Fish Lake Valley, Nevada. Location: Within the interfan valley between Indian Creek and Liedy Creek fan, about 2 km north of Marble Creek and about 1/2 km south of Trench Site 2; 37 46'17" N. Lat., 118 10'25" W. Long. Physiographic Position: Summit of middle-inset-fan; dissection about 2 m; Immediately downfan the middle Marble unit is buried by the late Marble unit.
Varnish Development: none; Pavement Development: none; Pavement area: 0 %; Slope: 3 ; Aspect: E;
Elevation: 1765 m, 5780 ft; Runoff: medium; Drainage: well; Parent Material: Granitic alluvium with subordinate carbonate and metasedimentry lithic fragments; Vegetation: Sparse desert shrubs (<30 cm high), minor cacti and grasses; Soil Temperature Regime: warm mesic; Moisture Status: dry above 110 cm; slightly moist below 110 cm.

	Depth	Color				Consistence						Secondary		Clay	Est. % Wt.	
Horizon	(cm)	Dry	Moist	Text.	Struct.	Dry	Moist	Wet	Bndry.	Pores	Roots	Carb.	Opal	Films	Grv.	Cob.
Av	0-7	2.5Y6.5/2	2.5Y5/3	gsl	1vf-f cr	sh	vfr	so/po	cs	1f,3m	1vf	ev none	none	none	20	0
Bw	7-23	c-5Y8/1 2.5Y6/3	c-2.5Y4/4 2.5Y5/4	gsl	2cabk	h	fr	vss/ps	gs	2m	1f,1vf	ev I-	"	"	35	0
Bk1	23-71	2.5Y7/3	2.5Y4.5/3	gsl	1csbk	h	fr	vss/po	gs	1f	1vf, 1f&m	ev I	"	"	35	0
Bk2	71-93	2.5Y6/4	2.5Y5/4	gsl	1-2f-m sbk	sh	fr	vss/ps	cs	1f	1vf,f	ev I+	"	"	35	0
2Bk1	93-128	2.5Y7/4	2.5Y4/4	gsl	1msbk	sh	vfr	so/po	gs	2m	1vf&f, 2m	ev I	"	"	40	0
2Bk2	128-180+	2.5Y7/4	2.5Y4/4	gsl	1csbk	sh	fr	so/po		1f	1f	ev I	"	"	40	0

Comments: A detrital log dated at 1065 cal B.P. (Beta-26170) was collected at a depth of 40-50 cm below the relict middle Marble surface in the south channel-wall of an unnamed creek (Radiocarbon Site 4). This pit was excavated about 2 m downstream from the log.

PEDON # 12

PEDON DESCRIPTION: Morphostratigraphic Unit: McAfee Creek; Describer: Tom Sawyer Date: 6-9-88 Area: Indian Creek, NW Fish Lake Valley, Nevada. Location: Immediately north of Indian Creek on the highest member of the stepped sequence; immediately downfan from mouth of canyon; 37 47'13" N. Lat., 118 11'42" W. Long. Physiographic Position: Crest of fully-rounded ballena; dissected to a depth of about 70-80 m; this unit is not considered to have a "stable" geomorphic surface.
Varnish Development: up to darkly and continuous varnished fragments; Pavement Development: up to tightly packed & moderately to well sorted; Pavement Area: 65 %; Slope: 3.5 ; Aspect: E; Elevation: 1920 m, 6300 ft; Runoff: rapid; Drainage: somewhat poorly drained; Parent Material: Granitic alluvium with subordinate metasedimentry and carbonate lithic fragments and eolian sediments; Vegetation: Low (<30 cm) desert shrubs 1-2 m apart; rare juniper (Juniper utahensis)
Soil Temperature Regime: warm mesic; Moisture Status: Dry.

Horizon	Depth (cm)	Color Dry	Color Moist	Text.	Struct.	Consistence Dry	Consistence Moist	Consistence Wet	Bndry.	Pores	Roots	Secondary Carb.	Secondary Opal	Clay Films	Est. % Wt. Grv.	Est. % Wt. Cob.
Avk[a]	0-19	2.5Y7/2	2.5Y4/3	fsl	3ccpr, 2mpl	sh	fr	so/po	cs	3m	1f,1c	ev I	none	none	15	0
Btkq	19-32	2.5Y7/2	2.5Y5/3	gsl	2vcsbk, 1fpl	h	fi	ss/ps	gw	2f	1f,1c	ev II	II	1nbr 1nco	50	10
2Kmq[b]	32-74	s-5YR7/4 c-5YR8/1 2.5Y7/4	5YR5/4 5YR7/2 2.5Y6/4	gsl	1msbk	vh	fi	so/po	gw	1vf	1f,2c	ev,III to IV	III-IV	none	50	10
2Bkq	74-145+	2.5Y7/3	2.5Y5/4	gsl	1f-m sbk	h	fr	so/po	-	1f	1f	ev III	II	"	50	10

Comments: [a]Few thin carbonate coatings on pebble undersides and between platy peds; abundant laminar carbonate fragments of the underlying 2Kmq horizon have been incorporated into the pavement. [b]This horizon was truncated during development of ballena morphology, hence this is a remnantal horizon; horizon has a 2-3 cm thick, discontinuous, indurated laminar subhorizon, suggesting that the horizon is plugged.

PEDON # 13

PEDON DESCRIPTION: **Morphostratigraphic Unit:** late Marble; **Describers:** Tom Sawyer and Doug Rennie **Date:** 6-10-88 **Area:** About 2 km south of Indian Creek, NW Fish Lake Valley, Nevada. **Location:** Immediately south of the southern margin of the Indian Creek fan; in the north wall of Trench 2; W1/2, NE 1/4, Sec. 23, T.2S., R.34E., Mt Barcroft 15' Quad., CA-NV; 37 47'29" N. Lat., 118o10'25" W. Long. **Physiographic Position:** Summit of a narrow-inset-fan-apex; the late Marbel unit is clearly inset below the middle unit at this site; **Varnish Development:** none; **Pavement Development:** none; **Pavement Area:** 0 %; **Slope:** 3.5 ; **Aspect:** E; **Elevation:** 1770 m, 5800 ft; **Runoff:** moderate; **Drainage:** well; **Parent Material:** Granitic alluvium with subordinate metasedimentry and andesitic clasts; **Vegetation:** Sparse, low (<25 cm) desert shrubs; **Soil Temperature Regime:** warm mesic; **Moisture Status:** dry.

	Depth	Color				Consistence						Secondary		Clay	Est. % Wt.	
Horizon	(cm)	Dry	Moist	Text.	Struct.	Dry	Moist	Wet	Bndry.	Pores	Roots	Carb.	Opal	Films	Grv.	Cob.
A[a]	0-9	2.5Y7/2	2.5Y5/3	vgcosl	1fsbk	so	vfr	so/po	gw	1f,2m	1vf	ev none	none	none	75	0
AB[a]	9-21	2.5Y7/3	2.5Y6/4	vgcosl	1fsbk	so-sh	vfr	so/po	cw	2m	1vf	ev I-	I-	"	65	0
2Bkb	21-38	2.5Y7/3	2.5Y5/3	vgm-cosl	m	lo	lo	ss/po	gw	2m,3c	1vf,2m	ev I	I-	"	75	0
2Bkj	38-55	2.5Y7/2	2.5Y5/4	vgcosl	1fsbk	so	vfr	so/po	cw	2f,1m	1vf,2m	ev I	none	"	75	0
2Bk	55-95	2.5Y7/3	2.5Y6/4	vgcosl	m	lo	lo	so/po	cw	2m,1c	1vf	ev I-	"	"	65	0
2C	95-140+	2.5Y7/3	2.5Y6/3	gcosl	m	lo	lo	so/po		1m	1vf	ev none	"	"	50	0

Comments: [a]Very thin, powdery, discontinuous carbonate coats on the underside of pebbles.

APPENDIX III

DETERMINATION OF SOIL DEVELOPMENT INDICES

In this appendix the soil field descriptions (Appendix II) were evaluated using soil development index of Harden (1982) and Harden and Taylor (1983). Taylor's (1988) computer template, executed by LOTUS 123™, was used for compilation of the various soil development indices.

SOIL DEVELOPMENT   5Y=0, 2.5Y=1, 10YR=2, 7.5YR=3,
INDEX CALCULATIONS: 5YR=4, 2.5YR=5, 10R=6, 5R=7

FIELD DESCRIPTION DATA -------->

Morphostrat. Unit/ Pedon #	Horizon	Depth (cm)		Thickness	SOIL COLOR: Dry #1 hue	Dry #1 value	Dry #1 chroma	Moist #1 hue	Moist #1 value	Moist #1 chroma	Dry #2 hue	Dry #2 value	Dry #2 chroma	PARENT MATERIAL: Dry Color hue	Dry Color value	Dry Color chroma	Moist Color hue	Moist Color value	Moist Color chroma
MIDDLE MARBLE																			
Pedon 1	Av	0	4	4	1.0	7.0	2.0	1.0	5.0	2.0				1.0	7.0	2.0	1.0	4.0	2.0
	Bkj	4	23	19	1.0	7.0	2.0	1.0	4.0	2.0				1.0	7.0	2.0	1.0	4.0	2.0
	2Bk1	23	42	19	1.0	6.0	2.0	1.0	4.0	2.0				1.0	7.0	2.0	1.0	4.0	2.0
	2Bk2	42	63	21	1.0	6.0	2.0	1.0	4.0	2.0				1.0	7.0	2.0	1.0	4.0	2.0
	3Bk	63	73	10	1.0	6.0	2.0	1.0	4.0	2.0				1.0	7.0	2.0	1.0	4.0	2.0
	4Bk1	73	115	42	1.0	7.0	2.0	1.0	4.0	2.0				1.0	7.0	2.0	1.0	4.0	2.5
	4Bk2	115	157	42	1.0	7.0	4.0	1.0	5.0	4.0				1.0	7.0	2.0	1.0	4.0	2.5
	4BC	157	185	28	1.0	7.0	4.0	1.0	4.0	2.0				1.0	7.0	2.0	1.0	4.0	2.0
MIDDLE MARBLE																			
Pedon 2	Av	0	3	3	1.0	7.0	2.0	1.0	4.0	2.0				1.0	7.0	2.0	1.0	4.0	2.0
	Bw	3	13	10	1.0	6.0	2.0	1.0	4.0	2.0				1.0	7.0	2.0	1.0	4.0	2.0
	Bkj	13	39	26	1.0	7.0	2.0	1.0	5.0	2.0				1.0	7.0	2.0	1.0	4.0	2.0
	2Bk1	39	72	33	1.0	7.0	2.0	1.0	5.0	3.0				1.0	7.0	2.0	1.0	5.0	3.0
	2Bk2	72	112	40	1.0	7.0	2.0	1.0	5.0	3.0				1.0	7.0	2.0	1.0	5.0	3.0
	3Bkq	112	130	18	1.0	6.0	2.0	1.0	4.0	2.0				1.0	7.0	2.0	1.0	4.0	2.5
EARLY MARBLE																			
Pedon 3	Av	0	6	6	1.0	7.0	2.0	1.0	4.0	4.0				1.0	6.0	2.0	1.0	4.0	2.0
	Bw	6	14	8	1.0	7.0	3.0	1.0	4.0	2.0				1.0	7.0	3.5	1.0	4.0	3.0
	Bkq	14	68	54	1.0	7.0	3.0	1.0	5.0	3.0				1.0	7.0	3.5	1.0	4.0	3.0
	Bkj	68	106	38	1.0	6.0	3.0	1.0	5.0	4.0				1.0	7.0	3.5	1.0	4.0	3.0
	B	106	156	50	1.0	7.0	4.0	1.0	4.0	4.0				1.0	7.0	3.5	1.0	4.0	3.0
	2bkb - omitted from calculation, because horizon is not related to the Early Marble unit.																		
LATE MARBLE																			
Pedon 4	A	0	5	5	1.0	7.0	2.0	1.0	4.0	3.0				1.0	7.0	2.0	1.0	5.0	3.0
	AB	5	26	21	1.0	7.0	3.0	1.0	5.0	4.0				1.0	7.0	2.0	1.0	5.0	3.0
	Bkj1	26	37	11	1.0	6.0	2.0	1.0	5.0	3.0				1.0	7.0	2.0	1.0	5.0	3.0
	Bkj2	37	80	43	1.0	6.0	2.0	1.0	5.0	3.0				1.0	7.0	2.0	1.0	5.0	3.0
	2Bkqb	80	93	13	1.0	7.0	2.0	1.0	5.0	2.0				1.0	7.0	2.0	1.0	5.0	3.0
	2Bk1	93	109	16	1.0	7.0	2.0	1.0	4.0	3.0				1.0	7.0	2.0	1.0	5.0	3.0
	2Bk2	109	148	39	1.0	7.0	2.0	1.0	5.0	3.0	2.0	7.0	8.0	1.0	7.0	2.0	1.0	5.0	3.0
	2CB	148	180	32	1.0	8.0	2.0	1.0	6.0	3.0	2.0	7.0	6.0	1.0	7.0	2.0	1.0	5.0	3.0
INDIAN																			
Pedon 5	Avk	0	6	6	1.0	7.0	2.0	1.0	7.0	3.0				1.0	7.0	3.0	1.0	4.0	3.0
	Bwv	6	17	11	1.0	7.0	2.0	1.0	7.0	3.0				1.0	7.0	3.0	1.0	4.0	3.0
	2Btkq	17	45	28	2.0	7.0	4.0	2.0	5.0	4.0				1.0	7.0	4.0	1.0	4.0	3.0
	2Bkm	45	95	50	1.0	7.0	3.0	1.0	5.0	3.0				1.0	7.0	4.0	1.0	4.0	3.0
	2Bk	95	135	40	1.0	7.0	2.0	1.0	5.0	3.0				1.0	7.0	4.0	1.0	4.0	3.0
LEIDY																			
Pedon 6	Av	0	13	13	1.0	6.0	2.0	1.0	4.0	3.0				1.0	7.0	2.0	1.0	5.0	4.0
	Btkq	13	28	15	1.0	7.0	2.0	1.0	5.0	4.0				1.0	7.0	2.0	1.0	5.0	4.0
	Bkq	28	79	51	1.0	7.0	2.0	1.0	5.0	4.0				1.0	7.0	2.0	1.0	5.0	4.0
	Bk	79	92	13	1.0	7.0	3.0	1.0	5.0	3.0				1.0	7.0	2.0	1.0	5.0	4.0
	2Bk1	92	137	45	1.0	7.0	4.0	1.0	5.0	4.0				1.0	7.0	4.0	1.0	5.0	4.0
	2Bk2	137	150	13	1.0	7.0	3.0	1.0	4.0	3.0				1.0	7.0	4.0	1.0	5.0	4.0
	3Bk3	150	205	55	1.0	7.0	4.0	1.0	4.0	3.0				1.0	7.0	3.0	1.0	5.0	3.0

SOIL DEVELOPMENT M; vw; M; M; s; vs lo so sh h vh eh so
INDEX CALCULATIONS: ---------- TEXTURE ---------- Pl; O,Cr,Ab,Sb; Pr; C 0 1 2 3 4 5 0
FIELD DESC - USDA Textural Class - 0 0.5 1 2 3 3.5 lo vfr fr fi vfi efi po

Morphostrat. Unit/ Pedon #	Horizon	HZ	Horizon (a)(b)(c)	PM	Parent Material (a)(b)(c)	STRUCTURE primary Grade*	primary Kind	secondary Grade	secondary Kind	CONSISTENCE < Dry > HZ*	Dry PM	< Moist > HZ*	Moist PM	<- - - Wet - - -> stkn*	PM	plst*	PM
MIDDLE MARBLE																	
Pedon 1	Av	FSL	3 -9 -9	FSL	3 -9 -9	0.0	0.0			1.0	1.0	1.0	0.0	1.0	0.0	1.0	0.0
	Bkj	GSL	3 -9 -9	GSL	3 -9 -9	1.0	1.0			2.0	1.0	1.0	0.0	0.0	0.0	0.0	0.0
	2Bk1	GSL	3 -9 -9	GSL	3 -9 -9	0.5	1.0			3.0	2.0	2.0	0.0	0.0	0.0	0.0	0.0
	2Bk2	GSL	3 -9 -9	GSL	3 -9 -9	0.5	1.0			4.0	2.0	2.0	0.0	0.0	0.0	0.0	0.0
	3Bk	GSL	3 -9 -9	GSL	2 -9 -9	0.0	0.0			0.0	0.0	0.0	0.0	0.0	0.0	0.0	0.0
	4Bk1	GSL	3 -9 -9	GSL	3 -9 -9	0.5	1.0			3.0	2.0	2.0	0.0	0.0	0.0	0.0	0.0
	4Bk2	GSL	3 -9 -9	GSL	3 -9 -9	0.5	1.0			2.0	2.0	1.0	0.0	0.0	0.0	0.0	0.0
	4BC	GSL	3 -9 -9	GSL	2 -9 -9	0.0	0.0			0.0	0.0	0.0	0.0	0.0	0.0	0.0	0.0
MIDDLE MARBLE																	
Pedon 2	Av	FSL	3 -9 -9	FSL	3 -9 -9	1.5	1.0			1.0	1.0	9.0	9.0	0.0	0.0	0.0	0.0
	Bw	GSL	3 -9 -9	GSL	3 -9 -9	1.5	1.0			2.0	1.0	9.0	9.0	0.0	0.0	0.0	0.0
	Bkj	GSL	3 -9 -9	GSL	3 -9 -9	0.5	1.0			1.0	1.0	9.0	9.0	0.0	0.0	0.0	0.0
	2Bk1	VGSL	3 -9 -9	VGSL	3 -9 -9	0.5	1.0			2.0	1.0	9.0	9.0	0.0	0.0	0.0	0.0
	2Bk2	VGSL	3 -9 -9	VGSL	3 -9 -9	0.5	1.0			2.0	1.0	9.0	9.0	0.0	0.0	0.0	0.0
	3Bkq	VGS	1 -9 -9	VGS	1 -9 -9	0.0	0.0			0.5	0.0	9.0	9.0	0.0	0.0	0.0	0.0
EARLY MARBLE																	
Pedon 3	Av	FSL	3 -9 -9	S	1 -9 -9	2.0	1.0	2.0	1.0	1.0	0.5	9.0	9.0	0.5	0.0	0.0	0.0
	Bw	GSL	3 -9 -9	S	1 -9 -9	3.0	1.0	1.0	1.0	1.0	0.5	9.0	9.0	0.0	0.0	0.0	0.0
	Bkq	GSL	3 -9 -9	S	1 -9 -9	1.0	1.0			2.0	0.5	9.0	9.0	0.0	0.0	0.0	0.0
	Bkj	GSL	3 -9 -9	S	1 -9 -9	1.0	1.0			2.0	0.5	9.0	9.0	0.0	0.0	0.0	0.0
	B	VGSL	3 -9 -9	S	1 -9 -9	0.5	1.0			2.0	0.5	9.0	9.0	0.0	0.0	0.0	0.0
	2bkb																
LATE MARBLE																	
Pedon 4	A	GSL	3 -9 -9	sl	3 -9 -9	0.5	0.5			0.5	0.5	0.0	0.0	0.0	0.0	0.0	0.0
	AB	GSL	3 -9 -9	sl	3 -9 -9	0.5	1.0			3.0	3.0	3.0	3.0	0.5	0.0	1.0	1.0
	Bkj1	GSL	3 -9 -9	sl	3 -9 -9	0.0	0.0			2.0	1.5	2.0	1.5	0.0	0.0	0.0	0.0
	Bkj2	GSL	3 -9 -9	sl	3 -9 -9	0.5	1.0			3.0	2.5	2.0	1.5	0.0	0.0	0.0	0.0
	2Bkqb	GSL	3 -9 -9	sl	3 -9 -9	1.0	1.0			1.0	1.0	1.0	1.0	0.0	0.0	0.0	0.0
	2Bk1	GSL	3 -9 -9	sl	3 -9 -9	1.0	1.0			1.5	1.5	1.0	1.0	0.0	0.0	0.0	0.0
	2Bk2	VGSL	3 -9 -9	sl	3 -9 -9	1.0	1.0			2.0	2.0	1.0	1.0	0.0	0.0	0.0	0.0
	2CB	GSL	3 -9 -9	sl	3 -9 -9	1.0	1.0			2.0	2.0	1.0	1.0	0.0	0.0	0.0	0.0
INDIAN																	
Pedon 5	Avk	SIL	3 -9 -9	FSL	3 -9 -9	3.0	0.5	2.0	1.0	1.0	0.0	1.0	1.0	0.0	0.0	0.0	0.0
	Bwv	SIL	5 -9 -9	FSL	3 -9 -9	2.0	0.5	2.0	1.0	2.0	0.0	2.0	1.0	0.0	0.0	1.0	0.0
	2Btkq	GSICL	6 -9 -9	S	2 -9 -9	1.0	1.0			4.0	0.5	2.0	1.0	2.0	0.0	2.0	0.0
	2Bkm	GSL	3 -9 -9	S	2 -9 -9	1.0	2.5			3.0	0.5	3.0	1.0	0.0	0.0	0.0	0.0
	2Bk	VGSL	3 -9 -9	S	2 -9 -9	1.0	1.0			3.0	0.5	3.0	1.0	1.0	0.0	1.0	0.0
LEIDY																	
Pedon 6	Av	FSL	3 -9 -9	FSL	3 -9 -9	3.0	0.5	1.0	1.0	1.0	1.5	2.0	0.0	0.0	0.0	0.0	0.0
	Btkq	GSL	3 -9 -9	GSL	3 -9 -9	1.0	1.0			4.0	1.5	2.0	0.0	0.0	0.0	0.0	0.0
	Bkq	GSL	3 -9 -9	GSL	3 -9 -9	1.0	1.0			4.0	1.5	2.0	0.0	0.0	0.0	0.0	0.0
	Bk	GSL	3 -9 -9	GSL	3 -9 -9	0.5	1.0			2.0	1.5	1.0	0.0	0.0	0.0	0.0	0.0
	2Bk1	GSL	3 -9 -9	GSL	2 -9 -9	0.5	1.0			4.0	2.0	3.0	0.0	0.0	0.0	0.0	0.0
	2Bk2	GSL	3 -9 -9	GSL	2 -9 -9	0.0	0.0			0.5	2.0	0.0	0.0	0.0	0.0	0.0	0.0
	3Bk3	GSL	3 -9 -9	GSL	3 -9 -9	1.0	1.0			4.0	2.5	2.0	0.0	0.0	0.0	0.0	0.0

SOIL DEVELOPMENT vss ss s vs Ovf 1f 2c 3m 4c * NOTE: For missing data enter "9" for structure (1o grade
INDEX CALCULATIONS: 0.5 1 2 3 n mk k clay films (stains), dry, moist and wet consistenc
FIELD DESC ps p vp 1 2 3 4 5 and secondary carbonate; and "999" for pH.

Morphostrat. Unit/ Pedon #	Horizon	stains (1o)* freq	stains (2o)	CLAY FILMS bridges(1o) freq	bridges(1o) thkn	bridges(2o) freq	bridges(2o) thkn	pores(1o) freq	pores(1o) thkn	pores(2o) freq	pores(2o) thkn	ped faces(1o) freq	ped faces(1o) thkn	ped faces(2o) freq	ped faces(2o) thkn	clasts(1o) freq	clasts(1o) thkn
MIDDLE MARBLE																	
Pedon 1	Av																
	Bkj																
	2Bk1																
	2Bk2																
	3Bk																
	4Bk1																
	4Bk2																
	4BC																
MIDDLE MARBLE																	
Pedon 2	Av																
	Bw																
	Bkj																
	2Bk1																
	2Bk2																
	3Bkq																
EARLY MARBLE																	
Pedon 3	Av																
	Bw																
	Bkq																
	Bkj																
	B																
	2bkb																
LATE MARBLE																	
Pedon 4	A																
	AB																
	Bkj1																
	Bkj2																
	2Bkqb																
	2Bk1																
	2Bk2																
	2CB																
INDIAN																	
Pedon 5	Avk																
	Bwv																
	2Btkq	2.5		2.00	2.00	1.00	1.00	3.00	2.00	1.00	1.00	1.0	1.0			3.0	2.0
	2Bkm																
	2Bk																
LEIDY																	
Pedon 6	Av																
	Btkq			3.0	1.0			2.0	1.0								
	Bkq																
	Bk																
	2Bk1																
	2Bk2																
	3Bk3																

SOIL DEVELOPMENT INDEX CALCULATIONS: FIELD DESC

SOIL DEVELOPMENT INDICES

Morphostrat. Unit/ Pedon #	Horizon	CaCO3 STAGE*	DRY COLOR Hue MAX	DRY COLOR Hue MIN	DRY COLOR Value MAX	DRY COLOR Value MIN	DRY COLOR Chroma MAX	DRY COLOR Chroma MIN	MOIST COLOR Hue MAX	MOIST COLOR Hue MIN	MOIST COLOR Value MAX	MOIST COLOR Value MIN	MOIST COLOR Chroma MAX	MOIST COLOR Chroma MIN
MIDDLE MARBLE														
Pedon 1	Av	0.0	1.0	1.0	7.0	7.0	2.0	2.0	1.0	1.0	5.0	5.0	2.0	2.0
	Bkj	0.5	1.0	1.0	7.0	7.0	2.0	2.0	1.0	1.0	4.0	4.0	2.0	2.0
	2Bk1	1.0	1.0	1.0	6.0	6.0	2.0	2.0	1.0	1.0	4.0	4.0	2.0	2.0
	2Bk2	1.0	1.0	1.0	6.0	6.0	2.0	2.0	1.0	1.0	4.0	4.0	2.0	2.0
	3Bk	1.0	1.0	1.0	6.0	6.0	2.0	2.0	1.0	1.0	4.0	4.0	2.0	2.0
	4Bk1	1.0	1.0	1.0	7.0	7.0	2.0	2.0	1.0	1.0	4.0	4.0	2.0	2.0
	4Bk2	0.5	1.0	1.0	7.0	7.0	4.0	4.0	1.0	1.0	5.0	5.0	4.0	4.0
	4BC	0.5	1.0	1.0	7.0	7.0	2.0	2.0	1.0	1.0	4.0	4.0	2.0	2.0
MIDDLE MARBLE														
Pedon 2	Av	0.0	1.0	1.0	7.0	7.0	2.0	2.0	1.0	1.0	4.0	4.0	2.0	2.0
	Bw	0.0	1.0	1.0	6.0	6.0	2.0	2.0	1.0	1.0	4.0	4.0	2.0	2.0
	Bkj	1.0	1.0	1.0	7.0	7.0	2.0	2.0	1.0	1.0	5.0	5.0	2.0	2.0
	2Bk1	1.0	1.0	1.0	7.0	7.0	2.0	2.0	1.0	1.0	5.0	5.0	3.0	3.0
	2Bk2	1.0	1.0	1.0	7.0	7.0	2.0	2.0	1.0	1.0	5.0	5.0	3.0	3.0
	3Bkq	0.5	1.0	1.0	7.0	7.0	2.0	2.0	1.0	1.0	5.0	5.0	3.0	3.0
EARLY MARBLE														
Pedon 3	Av	0.0	1.0	1.0	7.0	7.0	2.0	2.0	1.0	1.0	4.0	4.0	4.0	4.0
	Bw	0.5	1.0	1.0	7.0	7.0	3.0	3.0	1.0	1.0	4.0	4.0	2.0	2.0
	Bkq	1.0	1.0	1.0	7.0	7.0	3.0	3.0	1.0	1.0	5.0	5.0	3.0	3.0
	Bkj	0.5	1.0	1.0	6.0	6.0	3.0	3.0	1.0	1.0	5.0	5.0	4.0	4.0
	B	0.0	1.0	1.0	7.0	7.0	4.0	4.0	1.0	1.0	4.0	4.0	4.0	4.0
	2bkb													
LATE MARBLE														
Pedon 4	A		1.0	1.0	7.0	7.0	2.0	2.0	1.0	1.0	4.0	4.0	3.0	3.0
	AB		1.0	1.0	7.0	7.0	3.0	3.0	1.0	1.0	5.0	5.0	4.0	4.0
	Bkj1	0.5	1.0	1.0	6.0	6.0	2.0	2.0	1.0	1.0	5.0	5.0	3.0	3.0
	Bkj2	0.5	1.0	1.0	6.0	6.0	2.0	2.0	1.0	1.0	5.0	5.0	3.0	3.0
	2Bkqb	1.0												
	2Bk1	1.0	Soil development indices are not calculated with properties											
	2Bk2	1.0												
	2CB	1.0												
INDIAN														
Pedon 5	Avk	0.5	1.0	1.0	7.0	7.0	2.0	2.0	1.0	1.0	7.0	7.0	3.0	3.0
	Bwv	1.5	1.0	1.0	7.0	7.0	2.0	2.0	1.0	1.0	7.0	7.0	3.0	3.0
	2Btkq	2.0	2.0	2.0	7.0	7.0	4.0	4.0	2.0	2.0	5.0	5.0	4.0	4.0
	2Bkm	3.0	1.0	1.0	7.0	7.0	3.0	3.0	1.0	1.0	5.0	5.0	3.0	3.0
	2Bk	2.5	1.0	1.0	7.0	7.0	2.0	2.0	1.0	1.0	5.0	5.0	3.0	3.0
LEIDY														
Pedon 6	Av		1.0	1.0	6.0	6.0	2.0	2.0	1.0	1.0	4.0	4.0	3.0	3.0
	Btkq	1.0	1.0	1.0	7.0	7.0	2.0	2.0	1.0	1.0	5.0	5.0	4.0	4.0
	Bkq	1.5	1.0	1.0	7.0	7.0	2.0	2.0	1.0	1.0	5.0	5.0	4.0	4.0
	Bk	2.0	1.0	1.0	7.0	7.0	3.0	3.0	1.0	1.0	5.0	5.0	3.0	3.0
	2Bk1	1.5	1.0	1.0	7.0	7.0	4.0	4.0	1.0	1.0	5.0	5.0	4.0	4.0
	2Bk2	1.5	1.0	1.0	7.0	7.0	3.0	3.0	1.0	1.0	4.0	4.0	3.0	3.0
	3Bk3	1.0	1.0	1.0	7.0	7.0	4.0	4.0	1.0	1.0	4.0	4.0	3.0	3.0

SOIL DEVELOPMENT
INDEX CALCULATIONS: ----- Quantified Colors for Rubification (+), Melanization (-), Color Paling (-), Color Lightening (+) ----- RUBIFICATION ------> (maximum=190)
FIELD DESC.

Morphostrat. Unit/ Pedon #	Horizon	Dry hue (+)	Dry hue (-)	Dry value (+)	Dry value (-)	Dry chroma (+)	Dry chroma (-)	Moist hue (+)	Moist hue (-)	Moist value (+)	Moist value (-)	Moist chroma (+)	Moist chroma (-)	Normalized Rub	X thick	Profile Rub
MIDDLE MARBLE																
Pedon 1	Av	0.0	0.0	0.0	0.0	0.0	0.0	0.0	0.0	10.0	0.0	0.0	0.0	0.00	0.00	
	Bkj	0.0	0.0	0.0	0.0	0.0	0.0	0.0	0.0	0.0	0.0	0.0	0.0	0.00	0.00	
	2Bk1	0.0	0.0	0.0	-10.0	0.0	0.0	0.0	0.0	0.0	0.0	0.0	0.0	0.00	0.00	
	2Bk2	0.0	0.0	0.0	-10.0	0.0	0.0	0.0	0.0	0.0	0.0	0.0	0.0	0.00	0.00	
	3Bk	0.0	0.0	0.0	-10.0	0.0	0.0	0.0	0.0	0.0	0.0	0.0	0.0	0.00	0.00	
	4Bk1	0.0	0.0	0.0	0.0	0.0	0.0	0.0	0.0	0.0	0.0	0.0	-5.0	0.00	0.00	
	4Bk2	0.0	0.0	0.0	0.0	20.0	0.0	0.0	0.0	10.0	0.0	15.0	0.0	0.18	7.74	
	4BC	0.0	0.0	0.0	0.0	0.0	0.0	0.0	0.0	0.0	0.0	0.0	-5.0	0.00	0.00	7.74
MIDDLE MARBLE																
Pedon 2	Av	0.0	0.0	0.0	0.0	0.0	0.0	0.0	0.0	0.0	0.0	0.0	0.0	0.00	0.00	
	Bw	0.0	0.0	0.0	-10.0	0.0	0.0	0.0	0.0	0.0	0.0	0.0	0.0	0.00	0.00	
	Bkj	0.0	0.0	0.0	0.0	0.0	0.0	0.0	0.0	10.0	0.0	0.0	0.0	0.00	0.00	
	2Bk1	0.0	0.0	0.0	0.0	0.0	0.0	0.0	0.0	0.0	0.0	0.0	0.0	0.00	0.00	
	2Bk2	0.0	0.0	0.0	0.0	0.0	0.0	0.0	0.0	0.0	0.0	0.0	0.0	0.00	0.00	
	3Bkq	0.0	0.0	0.0	0.0	0.0	0.0	0.0	0.0	0.0	0.0	0.0	0.0	0.00	0.00	7.74
EARLY MARBLE																
Pedon 3	Av	0.0	0.0	10.0	0.0	0.0	0.0	0.0	0.0	0.0	0.0	20.0	0.0	0.11	0.63	
	Bw.	0.0	0.0	0.0	0.0	0.0	-5.0	0.0	0.0	0.0	0.0	0.0	-10.0	0.00	0.00	
	Bkq	0.0	0.0	0.0	0.0	0.0	-5.0	0.0	0.0	10.0	0.0	0.0	0.0	0.00	0.00	
	Bkj	0.0	0.0	0.0	-10.0	0.0	-5.0	0.0	0.0	10.0	0.0	10.0	0.0	0.05	2.00	
	B	0.0	0.0	0.0	0.0	5.0	0.0	0.0	0.0	0.0	0.0	10.0	0.0	0.08	3.95	6.58
	2bkb															
LATE MARBLE																
Pedon 4	A	0.0	0.0	0.0	0.0	0.0	0.0	0.0	0.0	0.0	-10.0	0.0	0.0	0.00	0.00	
	AB	0.0	0.0	0.0	0.0	10.0	0.0	0.0	0.0	0.0	0.0	10.0	0.0	0.11	2.21	
	Bkj1	0.0	0.0	0.0	-10.0	0.0	0.0	0.0	0.0	0.0	0.0	0.0	0.0	0.00	0.00	
	Bkj2	0.0	0.0	0.0	-10.0	0.0	0.0	0.0	0.0	0.0	0.0	0.0	0.0	0.00	0.00	2.21
	2Bkqb															
	2Bk1															
	2Bk2															
	2CB															
INDIAN																
Pedon 5	Avk	0.0	0.0	0.0	0.0	0.0	-10.0	0.0	0.0	30.0	0.0	0.0	0.0	0.00	0.00	
	Bwv	0.0	0.0	0.0	0.0	0.0	-10.0	0.0	0.0	30.0	0.0	0.0	0.0	0.00	0.00	
	2Btkq	10.0	0.0	0.0	0.0	0.0	0.0	10.0	0.0	10.0	0.0	10.0	0.0	0.16	4.42	
	2Bkm	0.0	0.0	0.0	0.0	0.0	-10.0	0.0	0.0	10.0	0.0	0.0	0.0	0.00	0.00	
	2Bk	0.0	0.0	0.0	0.0	0.0	-20.0	0.0	0.0	10.0	0.0	0.0	0.0	0.00	0.00	4.42
LEIDY																
Pedon 6	Av	0.0	0.0	0.0	-10.0	0.0	0.0	0.0	0.0	0.0	-10.0	0.0	-10.0	0.00	0.00	
	Btkq	0.0	0.0	0.0	0.0	0.0	0.0	0.0	0.0	0.0	0.0	0.0	0.0	0.00	0.00	
	Bkq	0.0	0.0	0.0	0.0	0.0	0.0	0.0	0.0	0.0	0.0	0.0	0.0	0.00	0.00	
	Bk	0.0	0.0	0.0	0.0	10.0	0.0	0.0	0.0	0.0	0.0	0.0	-10.0	0.05	0.68	
	2Bk1	0.0	0.0	0.0	0.0	0.0	0.0	0.0	0.0	0.0	0.0	0.0	0.0	0.00	0.00	
	2Bk2	0.0	0.0	0.0	0.0	0.0	-10.0	0.0	0.0	0.0	-10.0	0.0	-10.0	0.00	0.00	
	3Bk3	0.0	0.0	0.0	0.0	10.0	0.0	0.0	0.0	0.0	-10.0	0.0	0.0	0.05	2.89	3.58

SOIL DEVELOPMENT
INDEX CALCULATIONS: ----- MELANIZATION ------> ----- COLOR-PALING ------> ---- COLOR-LIGHTENING --->

Morphostrat. Unit/ Pedon #	FIELD DESC. Horizon	Normalized Mel	X thick	Profile Mel	Normalized Pale	X thick	Profile Pale	Normalized Light	X thick	Profile Light
		(maximum=85)			(maximum=60)			(maximum=80)		
MIDDLE MARBLE										
Pedon 1	Av	0.00	0.00		0.00	0.00		0.13	0.50	
	Bkj	0.00	0.00		0.00	0.00		0.00	0.00	
	2Bk1	0.12	2.24		0.00	0.00		0.00	0.00	
	2Bk2	0.12	2.47		0.00	0.00		0.00	0.00	
	3Bk	0.12	1.18		0.00	0.00		0.00	0.00	
	4Bk1	0.00	0.00		0.08	3.50		0.00	0.00	
	4Bk2	0.00	0.00		0.00	0.00		0.13	5.25	
	4BC	0.00	0.00	5.88	0.08	3.50	7.00	0.00	0.00	5.75
MIDDLE MARBLE										
Pedon 2	Av	0.00	0.00		0.00	0.00		0.00	0.00	
	Bw	0.12	1.18		0.00	0.00		0.00	0.00	
	Bkj	0.00	0.00		0.00	0.00		0.13	3.25	
	2Bk1	0.00	0.00		0.00	0.00		0.00	0.00	
	2Bk2	0.00	0.00		0.00	0.00		0.00	0.00	
	3Bkq	0.00	0.00	1.18	0.00	0.00	3.50	0.00	0.00	8.50
EARLY MARBLE										
Pedon 3	Av	0.00	0.00		0.00	0.00		0.13	0.75	
	Bw	0.00	0.00		0.25	2.00		0.00	0.00	
	Bkq	0.00	0.00		0.08	4.50		0.13	6.75	
	Bkj	0.12	4.47		0.08	3.17		0.13	4.75	
	B	0.00	0.00	4.47	0.00	0.00	9.67	0.00	0.00	12.25
	2bkb									
LATE MARBLE										
Pedon 4	A	0.12	0.59		0.00	0.00		0.00	0.00	
	AB	0.00	0.00		0.00	0.00		0.00	0.00	
	Bkj1	0.12	1.29		0.00	0.00		0.00	0.00	
	Bkj2	0.12	5.06	6.94	0.00	0.00	0.00	0.00	0.00	0.00
	2Bkqb									
	2Bk1									
	2Bk2									
	2CB									
INDIAN										
Pedon 5	Avk	0.00	0.00		0.17	1.00		0.38	2.25	
	Bwv	0.00	0.00		0.17	1.83		0.38	4.13	
	2Btkq	0.00	0.00		0.00	0.00		0.13	3.50	
	2Bkm	0.00	0.00		0.17	8.33		0.13	6.25	
	2Bk	0.00	0.00	0.00	0.33	13.33	24.50	0.13	5.00	21.13
LEIDY										
Pedon 6	Av	0.24	3.06		0.17	2.17		0.00	0.00	
	Btkq	0.00	0.00		0.00	0.00		0.00	0.00	
	Bkq	0.00	0.00		0.00	0.00		0.00	0.00	
	Bk	0.00	0.00		0.17	2.17		0.13	1.63	
	2Bk1	0.00	0.00		0.00	0.00		0.00	0.00	
	2Bk2	0.12	1.53		0.33	4.33		0.00	0.00	
	3Bk3	0.12	6.47	11.06	0.00	0.00	8.67	0.13	6.88	8.50

SOIL DEVELOPMENT
INDEX CALCULATIONS: ------- TOTAL TEXTURE ---------------------------> ----------- STRUCTURE -------------->
FIELD DESC. (maximum=90) (maximum=60)
Morphostrat. <------ Quantified ------>

Unit/ Pedon #	Horizon	Texture (line Xing)	Wet Con	Total Texture	Normalized Texture	X thick	Profile Texture	Quantified Struc	Normalized Struc	X thick	Profile Struc
MIDDLE MARBLE											
Pedon 1	Av	0.0	20.0	20.0	0.22	0.89		0.00	0.00	0.00	
	Bkj	0.0	0.0	0.0	0.00	0.00		20.00	0.33	6.33	
	2Bk1	0.0	0.0	0.0	0.00	0.00		15.00	0.25	4.75	
	2Bk2	0.0	0.0	0.0	0.00	0.00		15.00	0.25	5.25	
	3Bk	10.0	0.0	10.0	0.11	1.11		0.00	0.00	0.00	
	4Bk1	0.0	0.0	0.0	0.00	0.00		15.00	0.25	10.50	
	4Bk2	0.0	0.0	0.0	0.00	0.00		15.00	0.25	10.50	
	4BC	0.0	0.0	0.0	0.00	0.00	2.00	15.00	0.25	10.50	47.83
MIDDLE MARBLE											
Pedon 2	Av	0.0	0.0	0.0	0.00	0.00		25.00	0.42	1.25	
	Bw	0.0	0.0	0.0	0.00	0.00		25.00	0.42	4.17	
	Bkj	0.0	0.0	0.0	0.00	0.00		15.00	0.25	6.50	
	2Bk1	0.0	0.0	0.0	0.00	0.00		15.00	0.25	8.25	
	2Bk2	0.0	0.0	0.0	0.00	0.00		15.00	0.25	10.00	
	3Bkq	0.0	0.0	0.0	0.00	0.00	0.00	15.00	0.25	8.25	59.42
EARLY MARBLE											
Pedon 3	Av	20.0	5.0	25.0	0.28	1.67		45.00	0.75	4.50	
	Bw	20.0	0.0	20.0	0.22	1.78		50.00	0.83	6.67	
	Bkq	20.0	0.0	20.0	0.22	12.00		20.00	0.33	18.00	
	Bkj	20.0	0.0	20.0	0.22	8.44		20.00	0.33	12.67	
	B	20.0	0.0	20.0	0.22	11.11	35.00	15.00	0.25	12.50	54.33
	2bkb										
LATE MARBLE											
Pedon 4	A	0.0	0.0	0.0	0.00	0.00		10.00	0.17	0.83	
	AB	0.0	5.0	5.0	0.06	1.17		15.00	0.25	5.25	
	Bkj1	0.0	0.0	0.0	0.00	0.00		0.00	0.00	0.00	
	Bkj2	0.0	0.0	0.0	0.00	0.00	1.17	15.00	0.25	10.75	16.83
	2Bkqb										
	2Bk1										
	2Bk2										
	2CB										
INDIAN											
Pedon 5	Avk	0.0	0.0	0.0	0.00	0.00		50.00	0.83	5.00	
	Bw	20.0	10.0	30.0	0.33	3.67		40.00	0.67	7.33	
	2Btkq	40.0	40.0	80.0	0.89	24.89		20.00	0.33	9.33	
	2Bkm	10.0	0.0	10.0	0.11	5.56		35.00	0.58	29.17	
	2Bk	10.0	20.0	30.0	0.33	13.33	47.44	20.00	0.33	13.33	64.17
LEIDY											
Pedon 6	Av	0.0	0.0	0.0	0.00	0.00		45.00	0.75	9.75	
	Btkq	0.0	0.0	0.0	0.00	0.00		20.00	0.33	5.00	
	Bkq	0.0	0.0	0.0	0.00	0.00		20.00	0.33	17.00	
	Bk	0.0	0.0	0.0	0.00	0.00		15.00	0.25	3.25	
	2Bk1	10.0	0.0	10.0	0.11	5.00		15.00	0.25	11.25	
	2Bk2	10.0	0.0	10.0	0.11	1.44		0.00	0.00	0.00	
	3Bk3	0.0	0.0	0.0	0.00	0.00	6.44	20.00	0.33	18.33	64.58

SOIL DEVELOPMENT
INDEX CALCULATIONS: ----- DRY CONSISTENCE ------------> ---- MOIST CONSISTENCE ------------>
FIELD DESC. (maximum=100) (maximum=100)

Morphostrat. Unit/ Pedon #	Horizon	Quantified Dry Con	Normalized Dry Con	X thick	Profile Dry Con	Quantified Mst Con	Normalized Mst Con	X thick	Profile Mst Con
MIDDLE MARBLE									
Pedon 1	Av	0.00	0.00	0.00		10.00	0.10	0.40	
	Bkj	10.00	0.10	1.90		10.00	0.10	1.90	
	2Bk1	10.00	0.10	1.90		20.00	0.20	3.80	
	2Bk2	20.00	0.20	4.20		20.00	0.20	4.20	
	3Bk	0.00	0.00	0.00		0.00	0.00	0.00	
	4Bk1	10.00	0.10	4.20		20.00	0.20	8.40	
	4Bk2	0.00	0.00	0.00		10.00	0.10	4.20	
	4BC	10.00	0.10	4.20	16.40	20.00	0.20	8.40	31.30
MIDDLE MARBLE									
Pedon 2	Av	0.00	0.00	0.00		999.00	999.00	0.00	
	Bw	10.00	0.10	1.00		999.00	999.00	0.00	
	Bkj	0.00	0.00	0.00		999.00	999.00	0.00	
	2Bk1	10.00	0.10	3.30		999.00	999.00	0.00	
	2Bk2	10.00	0.10	4.00		999.00	999.00	0.00	
	3Bkq	10.00	0.10	3.30	15.80	999.00	999.00	0.00	12.60
EARLY MARBLE									
Pedon 3	Av	5.00	0.05	0.30		999.00	999.00	0.00	
	Bw	5.00	0.05	0.40		999.00	999.00	0.00	
	Bkq	15.00	0.15	8.10		999.00	999.00	0.00	
	Bkj	15.00	0.15	5.70		999.00	999.00	0.00	
	B	15.00	0.15	7.50	22.00	999.00	999.00	0.00	0.00
	2bkb								
LATE MARBLE									
Pedon 4	A	0.00	0.00	0.00		0.00	0.00	0.00	
	AB	0.00	0.00	0.00		0.00	0.00	0.00	
	Bkj1	5.00	0.05	0.55		5.00	0.05	0.55	
	Bkj2	5.00	0.05	2.15	2.70	5.00	0.05	2.15	2.70
	2Bkqb								
	2Bk1								
	2Bk2								
	2CB								
INDIAN									
Pedon 5	Avk	10.00	0.10	0.60		0.00	0.00	0.00	
	Bwv	20.00	0.20	2.20		10.00	0.10	1.10	
	2Btkq	35.00	0.35	9.80		10.00	0.10	2.80	
	2Bkm	25.00	0.25	12.50		20.00	0.20	10.00	
	2Bk	25.00	0.25	10.00	35.10	20.00	0.20	8.00	21.90
LEIDY									
Pedon 6	Av	0.00	0.00	0.00		20.00	0.20	2.60	
	Btkq	25.00	0.25	3.75		20.00	0.20	3.00	
	Bkq	25.00	0.25	12.75		20.00	0.20	10.20	
	Bk	5.00	0.05	0.65		10.00	0.10	1.30	
	2Bk1	20.00	0.20	9.00		30.00	0.30	13.50	
	2Bk2	0.00	0.00	0.00		0.00	0.00	0.00	
	3Bk3	15.00	0.15	8.25	34.40	20.00	0.20	11.00	41.60

SOIL DEVELOPMENT
INDEX CALCULATIONS: ---- CLAY FILMS ---------> ---- CLAY FILMS --------->
FIELD DESC. (normalize: -20/130)

Morphostrat. Unit/ Pedon #	Horizon	stains 1o	stains 2o	bridges 1o	bridges 2o	pores 1o	pores 2o	ped face 1o	ped face 2o	clasts 1o	clasts 2o	primary class	Sum of	2o Freqs/2	Normalized Cly Flms	X thick	Profile Cly Flms
MIDDLE MARBLE																	
Pedon 1	Av	0	0	0	0	0	0	0	0	0	0	0 ok	0	0	0.00	0.00	
	Bkj	0	0	0	0	0	0	0	0	0	0	0 ok	0	0	0.00	0.00	
	2Bk1	0	0	0	0	0	0	0	0	0	0	0 ok	0	0	0.00	0.00	
	2Bk2	0	0	0	0	0	0	0	0	0	0	0 ok	0	0	0.00	0.00	
	3Bk	0	0	0	0	0	0	0	0	0	0	0 ok	0	0	0.00	0.00	
	4Bk1	0	0	0	0	0	0	0	0	0	0	0 ok	0	0	0.00	0.00	
	4Bk2	0	0	0	0	0	0	0	0	0	0	0 ok	0	0	0.00	0.00	
	4BC	0	0	0	0	0	0	0	0	0	0	0 ok	0	0	0.00	0.00	0.00
MIDDLE MARBLE																	
Pedon 2	Av	0	0	0	0	0	0	0	0	0	0	0 ok	0	0	0.00	0.00	
	Bw	0	0	0	0	0	0	0	0	0	0	0 ok	0	0	0.00	0.00	
	Bkj	0	0	0	0	0	0	0	0	0	0	0 ok	0	0	0.00	0.00	
	2Bk1	0	0	0	0	0	0	0	0	0	0	0 ok	0	0	0.00	0.00	
	2Bk2	0	0	0	0	0	0	0	0	0	0	0 ok	0	0	0.00	0.00	
	3Bkq	0	0	0	0	0	0	0	0	0	0	0 ok	0	0	0.00	0.00	0.00
EARLY MARBLE																	
Pedon 3	Av	0	0	0	0	0	0	0	0	0	0	0 ok	0	0	0.00	0.00	
	Bw	0	0	0	0	0	0	0	0	0	0	0 ok	0	0	0.00	0.00	
	Bkq	0	0	0	0	0	0	0	0	0	0	0 ok	0	0	0.00	0.00	
	Bkj	0	0	0	0	0	0	0	0	0	0	0 ok	0	0	0.00	0.00	
	B	0	0	0	0	0	0	0	0	0	0	0 ok	0	0	0.00	0.00	0.00
	2bkb																
LATE MARBLE																	
Pedon 4	A	0	0	0	0	0	0	0	0	0	0	0 ok	0	0	0.00	0.00	
	AB	0	0	0	0	0	0	0	0	0	0	0 ok	0	0	0.00	0.00	
	Bkj1	0	0	0	0	0	0	0	0	0	0	0 ok	0	0	0.00	0.00	
	Bkj2	0	0	0	0	0	0	0	0	0	0	0 ok	0	0	0.00	0.00	0.00
	2Bkqb																
	2Bk1																
	2Bk2																
	2CB																
INDIAN																	
Pedon 5	Avk	0	0	0	0	0	0	0	0	0	0	0 ok	0	0	0.00	0.00	
	Bwv	0	0	0	0	0	0	0	0	0	0	0 ok	0	0	0.00	0.00	
	2Btkq	35	0	60	40	60	30	40	0	60	0	60 !!	18	10	0.52	14.54	
	2Bkm	0	0	0	0	0	0	0	0	0	0	0 ok	0	0	0.00	0.00	
	2Bk	0	0	0	0	0	0	0	0	0	0	0 ok	0	0	0.00	0.00	14.54
LEIDY																	
Pedon 6	Av	0	0	0	0	0	0	0	0	0	0	0 ok	0	0	0.00	0.00	
	Btkq	0	0	60	0	40	0	0	0	0	0	60 ok	10	0	0.38	5.77	
	Bkq	0	0	0	0	0	0	0	0	0	0	0 ok	0	0	0.00	0.00	
	Bk	0	0	0	0	0	0	0	0	0	0	0 ok	0	0	0.00	0.00	
	2Bk1	0	0	0	0	0	0	0	0	0	0	0 ok	0	0	0.00	0.00	
	2Bk2	0	0	0	0	0	0	0	0	0	0	0 ok	0	0	0.00	0.00	
	3Bk3	0	0	0	0	0	0	0	0	0	0	0 ok	0	0	0.00	0.00	5.77

SOIL DEVELOPMENT
INDEX CALCULATIONS: ---- SECONDARY CARBONATE ----------->
FIELD DESC <MAXIMUM=240>

Morphostrat. Unit/ Pedon #	Horizon	Quantified Carb	Normalized Carb	X thick	Profile Carb
MIDDLE MARBLE					
Pedon 1	Av	0.00	0.00	0.00	
	Bkj	0.00	0.00	0.00	
	2Bk1	0.00	0.00	0.00	
	2Bk2	0.00	0.00	0.00	
	3Bk	0.00	0.00	0.00	
	4Bk1	5.00	0.02	0.88	
	4Bk2	5.00	0.02	0.88	
	4BC	5.00	0.02	0.88	2.63
MIDDLE MARBLE					
Pedon 2	Av	0.00	0.00	0.00	
	Bw	0.00	0.00	0.00	
	Bkj	10.00	0.04	1.08	
	2Bk1	0.00	0.00	0.00	
	2Bk2	0.00	0.00	0.00	
	3Bkq	0.00	0.00	0.00	2.03
EARLY MARBLE					
Pedon 3	Av	0.00	0.00	0.00	
	Bw	7.50	0.03	0.25	
	Bkq	15.00	0.06	3.38	
	Bkj	7.50	0.03	1.19	
	B	0.00	0.00	0.00	4.81
	2bkb				
LATE MARBLE					
Pedon 4	A	0.00	0.00	0.00	
	AB	0.00	0.00	0.00	
	Bkj1	0.00	0.00	0.00	
	Bkj2	0.00	0.00	0.00	0.00
	2Bkqb				
	2Bk1				
	2Bk2				
	2CB				
INDIAN					
Pedon 5	Avk	20.00	0.08	0.50	
	Bwv	60.00	0.25	2.75	
	2Btkq	20.00	0.08	2.33	
	2Bkm	60.00	0.25	12.50	
	2Bk	75.00	0.31	12.50	30.58
LEIDY					
Pedon 6	Av	0.00	0.00	0.00	
	Btkq	0.00	0.00	0.00	
	Bkq	0.00	0.00	0.00	
	Bk	40.00	0.17	2.17	
	2Bk1	0.00	0.00	0.00	
	2Bk2	30.00	0.13	1.63	
	3Bk3	10.00	0.04	2.29	6.08

SOIL DEVELOPMENT
INDEX CALCULATIONS: HOW DO YOU WANT TO CALCULATE THE PROFILE INDEX?

******** INDEX VALUE - PROPERTIES SELECTED ********

Morphostrat. Unit/ Pedon #	Horizon	FIELD DESC — YOUR CHOICES ARE THE FOLLOWING ---ALL PROPERTIES INCLUDING---	TYPE YES OR NO NEXT TO *	DRY CON, Sum Normalized Properties (R-S)	Sum Normalized Properties (DC-PI)	CARB,CLY FLM, Count Properties (R-S)	Count Properties (DC-PI)	Horizon Index	X thick	SELECTED PROFILE INDEX
MIDDLE MARBLE										
Pedon 1	Av	INCLUDE ONLY THE FOLLOWING	yes	0.00	0.00	0	3	0.00	0.00	
	Bkj			0.00	0.10	0	3	0.03	0.63	
	2Bk1	MELANIZATION (M)	* no	0.00	0.10	0	3	0.03	0.63	
	2Bk2	COLOR-PALING (CP)	* no	0.00	0.20	0	3	0.07	1.40	
	3Bk	COLOR-LIGHTENING (CL)	* no	0.00	0.00	0	3	0.00	0.00	
	4Bk1	TEXTURE (T)	* no	0.00	0.12	0	3	0.04	1.69	
	4Bk2	STRUCTURE (S)	* no	0.00	0.02	0	3	0.01	0.29	
	4BC	DRY CONSISTENCE (DC)	* yes	0.00	0.00	0	3	0.00	0.00	4.65
		MOIST CONSISTENCE (MC)	* no							
MIDDLE MARBLE		CLAY FILMS (CF)	* yes							
Pedon 2	Av	SECONDARY CARBONATE (C)	* yes	0.00	0.00	0	3	0.00	0.00	
	Bw			0.00	0.10	0	3	0.03	0.33	
	Bkj			0.00	0.04	0	3	0.01	0.36	
	2Bk1			0.00	0.10	0	3	0.03	1.10	
	2Bk2			0.00	0.10	0	3	0.03	1.33	
	3Bkq			0.00	0.00	0	3	0.00	0.00	3.13
EARLY MARBLE										
Pedon 3	Av			0.00	0.05	0	3	0.02	0.10	
	Bw			0.00	0.08	0	3	0.03	0.22	
	Bkq			0.00	0.21	0	3	0.07	3.83	
	Bkj			0.00	0.18	0	3	0.06	2.30	
	B			0.00	0.15	0	3	0.05	2.50	8.94
	2bkb									
LATE MARBLE										
Pedon 4	A			0.00	0.00	0	3	0.00	0.00	
	AB			0.00	0.00	0	3	0.00	0.00	
	Bkj1			0.00	0.05	0	3	0.02	0.18	
	Bkj2			0.00	0.05	0	3	0.02	0.72	0.90
	2Bkqb									
	2Bk1									
	2Bk2									
	2CB									
INDIAN										
Pedon 5	Avk			0.00	0.18	0	3	0.06	0.37	
	Bwv			0.00	0.45	0	3	0.15	1.65	
	2Btkq			0.00	0.95	0	3	0.32	8.89	
	2Bkm			0.00	0.50	0	3	0.17	8.33	
	2Bk			0.00	0.56	0	3	0.19	7.50	26.74
LEIDY										
Pedon 6	Av			0.00	0.00	0	3	0.00	0.00	
	Btkq			0.00	0.63	0	3	0.21	3.17	
	Bkq			0.00	0.25	0	3	0.08	4.25	
	Bk			0.00	0.22	0	3	0.07	0.94	
	2Bk1			0.00	0.20	0	3	0.07	3.00	
	2Bk2			0.00	0.13	0	3	0.04	0.54	
	3Bk3			0.00	0.19	0	3	0.06	3.51	15.42

SOIL DEVELOPMENT INDEX CALCULATION: 5Y=0, 2.5Y=1, 10YR=2, 7.5YR=3, 5YR=4, 2.5YR=5, 10R=6, 5R=7

FIELD DESCRIPTION DATA ------->

Morphostrat. Unit/ Pedon #	Horizon	Depth (cm)		Thickness	SOIL COLOR <--- Dry #1 hue	Dry #1 value	Dry #1 ---> chroma	<--- Moist #1 hue	Moist #1 value	Moist #1 ---> chroma	<--- Dry #2 hue	Dry #2 value	Dry #2 ---> chroma	<--- Moist #2 hue	Moist #2 value	Moist #2 ---> chroma	<--- Dry #3 hue	Dry #3 value	Dry #3 ---> chroma
INDIAN																			
Pedon 7	Avk	0	5	5	1.0	7.0	2.0	1.0	7.0	3.0									
	Bwv	5	14	9	1.0	7.0	2.0	1.0	6.0	3.0									
	2Btkq	14	25	11	2.0	7.0	3.0	2.0	5.0	4.0									
	3Btk	25	40	15	2.0	7.0	3.0	2.0	5.0	4.0									
	3Bkm	40	50	10	1.0	7.0	3.0	1.0	5.0	3.0									
	3Bk	50	110	60	1.0	7.0	3.0	1.0	5.0	3.0									
MIDDLE MARBLE																			
Pedon 8	A	0	5	5	1.0	6.0	2.0	1.0	3.0	2.0									
	Bk1	5	55	50	1.0	7.0	2.0	1.0	8.0	6.0									
	Bk2	55	75	20	1.0	7.0	2.0	1.0	6.0	6.0									
	Bkqj	75	95	20	1.0	7.0	2.0	1.0	6.0	6.0									
	Bkj	95	145	50	1.0	7.0	2.0	1.0	7.0	4.0									
EARLY MARBLE																			
Pedon 9	Av	0	12	12	1.0	6.0	3.0	1.0	4.0	4.0									
	Bw	12	37	25	1.0	7.0	3.0	1.0	5.0	4.0									
	2Bkq	37	57	20	1.0	7.0	3.0	1.0	5.0	4.0									
	2Bk1	57	95	38	1.0	7.0	2.0	1.0	5.0	4.0									
	2Bk2	95	122	27	1.0	7.0	4.0	1.0	5.0	4.0									
	3Bk1	122	168	46	1.0	6.0	3.0	1.0	4.0	4.0									
	3Bk2	168	190	22	1.0	7.0	2.0	1.0	5.0	4.0									
LEIDY																			
Pedon 10	Av	0	5	5	1.0	7.0	2.0	1.0	5.0	3.0									
	Btkq	5	14	9	1.0	7.0	3.0	1.0	5.0	4.0									
	Bkq1	14	42	28	1.0	7.0	2.0	1.0	4.0	4.0									
	Bkq2	42	68	26	1.0	7.0	3.0	1.0	5.0	4.0									
	Bkq3	68	111	43	1.0	7.0	3.0	1.0	5.0	4.0									
	Bk1	111	150	39	1.0	7.0	4.0	1.0	5.0	5.0	2.00	6.00	8.00	2.00	5.00	8.00			
	Bk2	150	185	35	1.0	7.0	4.0	1.0	5.0	5.0									
MIDDLE MARBLE																			
Pedon 11	Av	0	7	7	1.0	6.5	2.0	1.0	5.0	3.0									
	Bw	7	23	16	1.0	6.0	3.0	1.0	5.0	4.0	0.0	8.0	1.0	1.0	5.0	3.0			
	Bk1	23	71	48	1.0	7.0	3.0	1.0	4.5	3.0									
	Bk2	71	93	22	1.0	6.0	4.0	1.0	5.0	4.0									
	2Bk1	93	128	35	1.0	7.0	4.0	1.0	4.0	4.0									
	2Bk2	128	180	52	1.0	7.0	4.0	1.0	4.0	4.0									
McAFEE CREEK																			
Pedon 12	Avk	0	19	19	1.0	7.0	2.0	1.0	4.0	3.0									
	Btkq	19	32	13	1.0	7.0	2.0	1.0	5.0	3.0									
	2Kmqb	32	74	42	1.0	7.0	4.0	1.0	6.0	4.0	4.0	8.0	1.0	4.0	7.0	2.0	4.0	7.0	4.0
	2Bkq	74	145	71	1.0	7.0	3.0	1.0	5.0	4.0									
ILAFE MARBLE																			
Pedon 13	A	0	9	9	1.0	7.0	2.0	1.0	5.0	3.0									
	AB	9	21	12	1.0	7.0	3.0	1.0	6.0	4.0									
	2Bkb	21	38	17	1.0	7.0	3.0	1.0	5.0	3.0									
	2Bkj	38	55	17	1.0	7.0	2.0	1.0	5.0	4.0									
	2Bk	55	95	40	1.0	7.0	3.0	1.0	6.0	4.0									
	2C	95	140	45	1.0	7.0	3.0	1.0	6.0	3.0									

SOIL DEVELOPMENT
INDEX CALCULATIONS:
FIELD DESC.

Morphostrat. Unit/ Pedon #	Horizon	PARENT MATERIAL <-- Dry Color --> hue	value	chroma	<- Moist Color -> hue	value	chroma	HZ	TEXTURE - USDA Textural Class - Horizon (a) (b) (c)	PM	Parent Material (a) (b) (c)	M; W; Pl; 0 0.5 —— STRUCTURE —— primary Grade	M; S,Cr,Ab,Sb; 1 Kind	M; Pr; 2 secondary Grade	#; C; 3 Kind
INDIAN															
Pedon 7	Avk	1.0	7.0	3.0	1.0	4.0	4.0	SI	3 -9 -9	FSL	3 -9 -9	2.0	2.0	2.0	1.0
	Bw	1.0	7.0	3.0	1.0	4.0	4.0	L	4 -9 -9	FSL	3 -9 -9	2.0	0.5	1.0	1.0
	2Btkq	1.0	6.0	3.0	1.0	4.0	4.0	SCL	4 -9 -9	GSL	3 -9 -9	3.0	1.0		
	3Btk	1.0	7.0	3.0	1.0	4.0	4.0	GSL	3 -9 -9	GSL	3 -9 -9	2.5	1.0		
	3Bkm	1.0	7.0	3.0	1.0	4.0	4.0	GSL	3 -9 -9	GSL	3 -9 -9	2.0	0.5		
	3Bk	1.0	7.0	3.0	1.0	4.0	4.0	GSL	3 -9 -9	GSL	3 -9 -9	1.0	1.0		
MIDDLE MARBLE															
Pedon 8	A	1.0	8.0	3.0	1.0	7.0	4.0	GSL	3 -9 -9	S	1 -9 -9	0.0	0.0		
	Bk1	1.0	8.0	2.0	1.0	7.0	4.0	GSL	2 -9 -9	S	1 -9 -9	1.0	1.0		
	Bk2	1.0	7.0	2.0	1.0	6.0	5.0	S	1 -9 -9	S	1 -9 -9	1.0	1.0		
	Bkqj	1.0	7.0	2.0	1.0	6.0	4.0	LS	2 -9 -9	S	1 -9 -9	0.5	1.0		
	Bkj	1.0	7.0	2.0	1.0	7.0	4.0	SL	3 -9 -9	S	1 -9 -9	0.5	1.0		
EARLY MARBLE															
Pedon 9	Av	1.0	7.0	2.0	1.0	4.0	4.0	FSL	3 -9 -9	FSL	3 -9 -9	1.0	0.5		
	Bw	1.0	6.5	2.0	1.0	4.0	4.0	GSL	3 -9 -9	GSL	3 -9 -9	1.0	1.0		
	2Bkq	1.0	6.5	3.0	1.0	4.0	4.0	GSL	3 -9 -9	GSL	3 -9 -9	1.0	1.0		
	2Bk1	1.0	6.5	3.0	1.0	4.0	4.0	GSL	3 -9 -9	GSL	3 -9 -9	1.0	1.0		
	2Bk2	1.0	6.5	3.0	1.0	4.0	4.0	GSL	3 -9 -9	GSL	3 -9 -9	0.5	1.0		
	3Bk1	1.0	7.0	2.0	1.0	5.0	4.0	GSL	3 -9 -9	GSL	3 -9 -9	0.5	1.0		
	3Bk2	1.0	7.0	2.0	1.0	5.0	4.0	VGSL	3 -9 -9	GSL	3 -9 -9	0.5	1.0		
LEIDY															
Pedon 10	Av	1.0	6.5	2.0	1.0	4.0	4.0	FSL	3 -9 -9	FSL	3 -9 -9	3.0	0.5	1.0	2.0
	Btkq	1.0	6.5	3.0	1.0	5.0	4.0	GSL	3 -9 -9	GSL	3 -9 -9	0.5	1.0		
	Bkq1	1.0	6.5	3.0	1.0	5.0	4.0	GSL	3 -9 -9	GSL	3 -9 -9	2.0	1.0		
	Bkq2	1.0	6.5	3.0	1.0	5.0	4.0	GSL	3 -9 -9	GSL	3 -9 -9	1.0	1.0		
	Bkq3	1.0	7.0	3.0	1.0	5.0	4.0	GSL	3 -9 -9	GSL	3 -9 -9	1.0	1.0		
	Bk1	1.0	7.0	3.0	1.0	5.0	4.0	GSL	3 -9 -9	GSL	3 -9 -9	1.0	1.0		
	Bk2	1.0	7.0	3.0	1.0	5.0	4.0	GSL	3 -9 -9	GSL	3 -9 -9	1.0	1.0		
MIDDLE MARBLE															
Pedon 11	Av	1.0	7.0	3.0	1.0	4.0	2.0	GSL	3 -9 -9	GSL	3 -9 -9	1.0	1.0		
	Bw	1.0	7.0	3.0	1.0	4.0	2.0	GSL	3 -9 -9	GSL	3 -9 -9	1.0	1.0		
	Bk1	1.0	7.0	3.0	1.0	4.0	2.0	GSL	3 -9 -9	GSL	3 -9 -9	0.5	1.0		
	Bk2	1.0	7.0	3.0	1.0	4.0	2.0	GSL	3 -9 -9	GSL	3 -9 -9	1.0	1.0		
	2Bk1	1.0	7.0	3.0	1.0	4.0	2.0	GSL	3 -9 -9	GSL	3 -9 -9	0.5	1.0		
	2Bk2	1.0	7.0	3.0	1.0	4.0	2.0	GSL	3 -9 -9	GSL	3 -9 -9	0.5	1.0		
McAFEE CREEK															
Pedon 12	Avk	1.0	7.0	3.0	1.0	4.0	3.0	FSL	3 -9 -9	FSL	3 -9 -9	3.0	2.0	2.00	0.50
	Btkq	1.0	7.0	3.0	1.0	4.0	3.0	GSL	3 -9 -9	GSL	3 -9 -9	2.0	1.0	1.50	0.50
	2Kmqb	1.0	6.0	3.0	1.0	4.0	4.0	GSL	3 -9 -9	GSL	3 -9 -9	1.5	1.0		
	2Bkq	1.0	6.0	3.0	1.0	4.0	4.0	GSL	3 -9 -9	GSL	3 -9 -9	1.5	1.0		
LATE MARBLE															
Pedon 13	A	1.0	7.0	2.0	1.0	6.0	3.0	VGSL	3 -9 -9	VGSL	3 -9 -9	0.5	1.0		
	AB	1.0	7.0	2.0	1.0	6.0	3.0	VGSL	3 -9 -9	VGSL	3 -9 -9	1.0	1.0		
	2Bkb	1.0	7.0	2.0	1.0	6.0	3.0	VGSL	3 -9 -9	VGSL	3 -9 -9	0.0	0.0		
	2Bkj	1.0	7.0	2.0	1.0	6.0	3.0	VGSL	3 -9 -9	VGSL	3 -9 -9	0.5	1.0		
	2Bk	1.0	7.0	2.0	1.0	6.0	3.0	VGSL	3 -9 -9	VGSL	3 -9 -9	0.0	0.0		
	2C	1.0	7.0	2.0	1.0	6.0	3.0	GSL	3 -9 -9	GSL	3 -9 -9	0.0	0.0		

SOIL DEVELOPMENT ; vs 1o so sh h vh eh so vss ss s vs 0vf 1f 2c 3m 4c
INDEX CALCULATIONS: 0 1 2 3 4 5 0 0.5 1 2 3 n mk k
FIELD DESC. 3.5 1o vfr fr fi vfi efi po ps p vp 1 2 3 4 5

Morphostrat. Unit/ Pedon #	Horizon	CONSISTENCE < Dry > HZ*	PM	< Moist > HZ*	PM	<- - - Wet - - -> stkn*	PM	plstn*	PM	CLAY FILMS stains (1o)* freq	(2o)	bridges(1o) freq	thkn	bridges(2o) freq	thkn
INDIAN															
Pedon 7	Avk	2.5	0.0	2.0	0.5	0.5	0.0	1.0	0.0						
	Bwv	3.0	0.0	3.0	0.5	0.5	0.0	1.0	0.0						
	2Btkq	2.0	0.5	1.0	0.5	2.0	0.0	2.0	0.0	3.0		3.0	1.0		
	3Btk	4.0	0.5	4.0	0.5	1.0	0.0	1.0	0.0	2.0		3.0	1.0		
	3Bkm	4.0	0.5	4.0	0.5	0.0	0.0	0.0	0.0						
	3Bk	3.0	0.5	3.0	0.5	0.0	0.0	0.0	0.0						
MIDDLE MARBLE															
Pedon 8	A	0.5	0.0	0.0	0.0	0.0	0.0	0.0	0.0						
	Bk1	2.0	0.0	1.0	0.0	0.0	0.0	0.0	0.0						
	Bk2	1.0	1.0	0.0	0.0	0.0	0.0	0.0	0.0						
	Bkqj	2.0	1.0	0.0	0.0	0.0	0.0	0.0	0.0						
	Bkj	2.0	0.5	0.0	0.0	1.0	0.0	1.0	0.0						
EARLY MARBLE															
Pedon 9	Av	0.0	0.0	0.0	0.0	0.0	0.0	0.0	0.0						
	Bw	2.0	1.0	1.0	0.0	0.0	0.0	0.0	0.0						
	2Bkq	3.0	2.0	1.0	0.0	0.0	0.0	1.0	0.0						
	2Bk1	4.0	2.0	2.0	0.0	0.0	0.0	1.0	0.0						
	2Bk2	4.0	2.0	2.0	0.0	0.0	0.0	1.0	0.0						
	3Bk1	3.0	1.0	1.0	0.0	0.0	0.0	1.0	0.0						
	3Bk2	2.0	2.0	1.0	0.0	0.0	0.0	1.0	0.0						
LEIDY															
Pedon 10	Av	1.0	0.5	2.0	0.0	0.5	0.0	0.0	0.0						
	Btkq	0.5	0.5	1.0	0.0	0.5	0.0	1.0	0.0			3.0	1.0		
	Bkq1	2.0	0.5	2.0	0.0	0.0	0.0	0.0	0.0						
	Bkq2	2.0	0.5	2.0	0.0	0.0	0.0	0.0	0.0						
	Bkq3	2.5	0.5	2.0	0.0	0.0	0.0	0.0	0.0						
	Bk1	2.5	0.5	2.0	0.0	0.0	0.0	0.0	0.0						
	Bk2	2.5	0.5	2.0	0.0	0.0	0.0	0.0	0.0						
MIDDLE MARBLE															
Pedon 11	Av	2.0	1.0	1.0	1.0	0.0	0.0	0.0	0.0						
	Bw	3.0	1.0	2.0	1.0	0.5	0.5	0.0	0.0						
	Bk1	3.0	1.0	2.0	0.0	0.5	0.0	0.0	0.0						
	Bk2	2.0	1.0	2.0	0.0	0.5	0.0	0.0	0.0						
	2Bk1	2.0	2.0	1.0	0.0	0.0	0.0	0.0	0.0						
	2Bk2	2.0	2.0	2.0	0.0	0.0	0.0	0.0	0.0						
McAFEE CREEK															
Pedon 12	Avk	2.5	0.5	2.0	0.0	0.0	0.0	0.0	0.0						
	Btkq	3.5	0.5	3.0	0.0	1.0	1.0	1.0	0.0			3.00	1.00		
	2Kmqb	4.0	0.5	3.0	0.0	0.0	0.0	0.0	0.0						
	2Bkq	3.5	0.5	2.0	0.0	0.0	0.0	0.0	0.0						
LATE MARBLE															
Pedon 13	A	1.0	1.0	1.0	1.0	0.0	0.0	0.0	0.0						
	AB	1.5	1.0	1.0	1.0	0.0	0.0	0.0	0.0						
	2Bkb	0.0	0.0	0.0	0.0	0.0	0.0	0.0	0.0						
	2Bkj	1.0	0.0	1.0	0.0	0.0	0.0	0.0	0.0						
	2Bk	0.0	0.0	0.0	0.0	0.0	0.0	0.0	0.0						
	2C	0.0	0.0	0.0	0.0	0.0	0.0	0.0	0.0						

SOIL DEVELOPMENT * NOTE: For missing data enter "9" for structure (1o grade),
INDEX CALCULATION: clay films (stains), dry, moist and wet consistence,
FIELD DESC and secondary carbonate; and "999" for pH.

Morphostrat. Unit/ Pedon #	Horizon	pores(1o) freq	pores(1o) thkn	pores(2o) freq	pores(2o) thkn	ped faces(1o) freq	ped faces(1o) thkn	ped faces(2o) freq	ped faces(2o) thkn	clasts(1o) freq	clasts(1o) thkn	clasts(2o) freq	clasts(2o) thkn	CaCO3 STAGE*
INDIAN														
Pedon 7	Avk													1.0
	Bwv					3.0	2.0							1.5
	2Btkq	3.0	1.0											2.5
	3Btk	2.0	1.0											3.0
	3Bkm													3.0
	3Bk													2.5
MIDDLE MARBLE														
Pedon 8	A													0.0
	Bk1													1.0
	Bk2													1.0
	Bkqj													0.5
	Bkj													0.5
EARLY MARBLE														
Pedon 9	Av													
	Bw													0.0
	2Bkq													1.0
	2Bk1													1.5
	2Bk2													1.0
	3Bk1													0.5
	3Bk2													0.5
LEIDY														
Pedon 10	Av													0.0
	Btkq	2.0	1.0											1.0
	Bkq1													1.5
	Bkq2													2.0
	Bkq3													2.0
	Bk1													1.0
	Bk2													0.5
MIDDLE MARBLE														
Pedon 11	Av													0.0
	Bw													0.5
	Bk1													1.0
	Bk2													1.5
	2Bk1													1.0
	2Bk2													1.0
McAFEE CREEK														
Pedon 12	Avk					3.0	3.0							1.0
	Btkq	2.00	1.00											3.5
	2Kmqb													4.0
	2Bkq													3.0
LATE MARBLE														
Pedon 13	A													0.0
	AB													0.5
	2Bkb													0.0
	2Bkj													0.0
	2Bk													0.0
	2C													0.0

SOIL DEVELOPMENT INDEX CALCULATIONS — SOIL DEVELOPMENT INDICES

Morphostrat. Unit/ Pedon #	Horizon	FIELD DESC. DRY COLOR MAX Hue	MIN Hue	MAX Value	MIN Value	MAX Chroma	MIN Chroma	MOIST COLOR MAX Hue	MIN Hue	MAX Value	MIN Value	MAX Chroma	MIN Chroma
INDIAN													
Pedon 7	Avk	1.0	1.0	7.0	7.0	2.0	2.0	1.0	1.0	7.0	7.0	3.0	3.0
	Bw	1.0	1.0	7.0	7.0	2.0	2.0	1.0	1.0	6.0	6.0	3.0	3.0
	2Btkq	2.0	2.0	7.0	7.0	3.0	3.0	2.0	2.0	5.0	5.0	4.0	4.0
	3Btk	2.0	2.0	7.0	7.0	3.0	3.0	2.0	2.0	5.0	5.0	4.0	4.0
	3Bkm	1.0	1.0	7.0	7.0	3.0	3.0	1.0	1.0	5.0	5.0	3.0	3.0
	3Bk	1.0	1.0	7.0	7.0	3.0	3.0	1.0	1.0	5.0	5.0	3.0	3.0
MIDDLE MARBLE													
Pedon 8	A	1.0	1.0	8.0	8.0	2.0	2.0	1.0	1.0	3.0	3.0	2.0	2.0
	Bk1	1.0	1.0	7.0	7.0	2.0	2.0	1.0	1.0	8.0	8.0	6.0	6.0
	Bk2	1.0	1.0	7.0	7.0	2.0	2.0	1.0	1.0	6.0	6.0	6.0	6.0
	Bkqj	1.0	1.0	7.0	7.0	2.0	2.0	1.0	1.0	6.0	6.0	6.0	6.0
	Bkj	1.0	1.0	7.0	7.0	2.0	2.0	1.0	1.0	7.0	7.0	4.0	4.0
EARLY MARBLE													
Pedon 9	Av	1.0	1.0	6.0	6.0	3.0	3.0	1.0	1.0	4.0	4.0	4.0	4.0
	Bw	1.0	1.0	7.0	7.0	3.0	3.0	1.0	1.0	5.0	5.0	4.0	4.0
	2Bkq	1.0	1.0	7.0	7.0	3.0	3.0	1.0	1.0	5.0	5.0	4.0	4.0
	2Bk1	1.0	1.0	7.0	7.0	2.0	2.0	1.0	1.0	5.0	5.0	4.0	4.0
	2Bk2	1.0	1.0	7.0	7.0	4.0	4.0	1.0	1.0	5.0	5.0	4.0	4.0
	3Bk1	1.0	1.0	6.0	6.0	3.0	3.0	1.0	1.0	4.0	4.0	4.0	4.0
	3Bk2	1.0	1.0	7.0	7.0	2.0	2.0	1.0	1.0	5.0	5.0	4.0	4.0
LEIDY													
Pedon 10	Av	1.0	1.0	7.0	7.0	2.0	2.0	1.0	1.0	5.0	5.0	3.0	3.0
	Btkq	1.0	1.0	7.0	7.0	3.0	3.0	1.0	1.0	5.0	5.0	4.0	4.0
	Bkq1	1.0	1.0	7.0	7.0	2.0	2.0	1.0	1.0	4.0	4.0	4.0	4.0
	Bkq2	1.0	1.0	7.0	7.0	3.0	3.0	1.0	1.0	5.0	5.0	4.0	4.0
	Bkq3	1.0	1.0	7.0	7.0	3.0	3.0	1.0	1.0	5.0	5.0	4.0	4.0
	Bk1	2.0	1.0	7.0	6.0	8.0	4.0	2.0	1.0	5.0	5.0	8.0	5.0
	Bk2	1.0	1.0	7.0	7.0	4.0	4.0	1.0	1.0	5.0	5.0	5.0	5.0
MIDDLE MARBLE													
Pedon 11	Av	1.0	1.0	6.5	6.5	2.0	2.0	1.0	1.0	5.0	5.0	3.0	3.0
	Bw	1.0	1.0	8.0	6.0	3.0	1.0	1.0	1.0	5.0	5.0	4.0	3.0
	Bk1	1.0	1.0	7.0	7.0	3.0	3.0	1.0	1.0	4.5	4.5	3.0	3.0
	Bk2	1.0	1.0	6.0	6.0	4.0	4.0	1.0	1.0	5.0	5.0	4.0	4.0
	2Bk1	1.0	1.0	7.0	7.0	4.0	4.0	1.0	1.0	4.0	4.0	4.0	4.0
	2Bk2	1.0	1.0	7.0	7.0	4.0	4.0	1.0	1.0	4.0	4.0	4.0	4.0
McAFEE CREEK													
Pedon 12	Avk	1.0	1.0	7.0	7.0	2.0	2.0	1.0	1.0	4.0	4.0	3.0	3.0
	Btkq	1.0	1.0	7.0	7.0	2.0	2.0	1.0	1.0	5.0	5.0	3.0	3.0
	2Kmqb	4.0	1.0	8.0	7.0	4.0	1.0	4.0	1.0	7.0	5.0	4.0	2.0
	2Bkq	1.0	1.0	7.0	7.0	3.0	3.0	1.0	1.0	5.0	5.0	4.0	4.0
LATE MARBLE													
Pedon 13	A	1.0	1.0	7.0	7.0	2.0	2.0	1.0	1.0	5.0	5.0	3.0	3.0
	AB	1.0	1.0	7.0	7.0	3.0	3.0	1.0	1.0	6.0	6.0	4.0	4.0
	2Bkb												
	2Bkj												
	2Bk												
	2C												

SOIL DEVELOPMENT
INDEX CALCULATION: ----- Quantified Colors for Rubification (+), Melanization (-), Color Paling (-), Color Lightening (+)
FIELD DESC

----- RUBIFICATION -----> (maximum=190)

Morphostrat. Unit/ Pedon #	Horizon	Dry hue (+)	Dry hue (-)	Dry value (+)	Dry value (-)	Dry chroma (+)	Dry chroma (-)	Moist hue (+)	Moist hue (-)	Moist value (+)	Moist value (-)	Moist chroma (+)	Moist chroma (-)	Normalized Rub	X thick	Profile Rub
INDIAN																
Pedon 7	Avk	0.0	0.0	0.0	0.0	0.0	-10.0	0.0	0.0	30.0	0.0	0.0	-10.0	0.00	0.00	
	Bw	0.0	0.0	0.0	0.0	0.0	-10.0	0.0	0.0	20.0	0.0	0.0	-10.0	0.00	0.00	
	2Btkq	10.0	0.0	10.0	0.0	0.0	0.0	10.0	0.0	10.0	0.0	0.0	0.0	0.11	1.16	
	3Btk	10.0	0.0	0.0	0.0	0.0	0.0	10.0	0.0	10.0	0.0	0.0	0.0	0.11	1.58	
	3Bkm	0.0	0.0	0.0	0.0	0.0	0.0	0.0	0.0	10.0	0.0	0.0	-10.0	0.00	0.00	
	3Bk	0.0	0.0	0.0	0.0	0.0	0.0	0.0	0.0	10.0	0.0	0.0	-10.0	0.00	0.00	2.74
MIDDLE MARBLE																
Pedon 8	A	0.0	0.0	0.0	0.0	0.0	-10.0	0.0	0.0	0.0	-40.0	0.0	-20.0	0.00	0.00	
	Bk1	0.0	0.0	0.0	-10.0	0.0	0.0	0.0	0.0	10.0	0.0	20.0	0.0	0.11	5.26	
	Bk2	0.0	0.0	0.0	0.0	0.0	0.0	0.0	0.0	0.0	0.0	10.0	0.0	0.05	1.05	
	Bkqj	0.0	0.0	0.0	0.0	0.0	0.0	0.0	0.0	0.0	0.0	20.0	0.0	0.11	2.11	
	Bkj	0.0	0.0	0.0	0.0	0.0	0.0	0.0	0.0	0.0	0.0	0.0	0.0	0.00	0.00	8.42
EARLY MARBLE																
Pedon 9	Av	0.0	0.0	0.0	-10.0	10.0	0.0	0.0	0.0	0.0	0.0	0.0	0.0	0.05	0.63	
	Bw	0.0	0.0	5.0	0.0	10.0	0.0	0.0	0.0	10.0	0.0	0.0	0.0	0.05	1.32	
	2Bkq	0.0	0.0	5.0	0.0	0.0	0.0	0.0	0.0	10.0	0.0	0.0	0.0	0.00	0.00	
	2Bk1	0.0	0.0	5.0	0.0	0.0	-10.0	0.0	0.0	10.0	0.0	0.0	0.0	0.00	0.00	
	2Bk2	0.0	0.0	5.0	0.0	10.0	0.0	0.0	0.0	10.0	0.0	0.0	0.0	0.05	1.42	
	3Bk1	0.0	0.0	0.0	-10.0	10.0	0.0	0.0	0.0	0.0	-10.0	0.0	0.0	0.05	2.42	
	3Bk2	0.0	0.0	0.0	0.0	0.0	0.0	0.0	0.0	0.0	0.0	0.0	0.0	0.00	0.00	5.79
LEIDY																
Pedon 10	Av	0.0	0.0	5.0	0.0	0.0	0.0	0.0	0.0	10.0	0.0	0.0	-10.0	0.00	0.00	
	Btkq	0.0	0.0	5.0	0.0	0.0	0.0	0.0	0.0	0.0	0.0	0.0	0.0	0.00	0.00	
	Bkq1	0.0	0.0	5.0	0.0	0.0	-10.0	0.0	0.0	0.0	-10.0	0.0	0.0	0.00	0.00	
	Bkq2	0.0	0.0	5.0	0.0	0.0	0.0	0.0	0.0	0.0	0.0	0.0	0.0	0.00	0.00	
	Bkq3	0.0	0.0	0.0	0.0	0.0	0.0	0.0	0.0	0.0	0.0	0.0	0.0	0.00	0.00	
	Bk1	5.0	0.0	0.0	-5.0	30.0	0.0	5.0	0.0	0.0	0.0	25.0	0.0	0.34	13.34	
	Bk2	0.0	0.0	0.0	0.0	10.0	0.0	0.0	0.0	0.0	0.0	10.0	0.0	0.11	3.68	17.03
MIDDLE MARBLE																
Pedon 11	Av	0.0	0.0	0.0	-5.0	0.0	-10.0	0.0	0.0	10.0	0.0	10.0	0.0	0.05	0.37	
	Bw	0.0	0.0	5.0	-5.0	0.0	-10.0	0.0	0.0	10.0	0.0	15.0	0.0	0.08	1.26	
	Bk1	0.0	0.0	0.0	0.0	0.0	0.0	0.0	0.0	5.0	0.0	10.0	0.0	0.05	2.53	
	Bk2	0.0	0.0	0.0	-10.0	10.0	0.0	0.0	0.0	10.0	0.0	20.0	0.0	0.16	3.47	
	2Bk1	0.0	0.0	0.0	0.0	10.0	0.0	0.0	0.0	0.0	0.0	20.0	0.0	0.16	5.53	
	2Bk2	0.0	0.0	0.0	0.0	10.0	0.0	0.0	0.0	0.0	0.0	20.0	0.0	0.16	8.21	21.37
McAFEE CREEK																
Pedon 12	Avk	0.0	0.0	0.0	0.0	0.0	-10.0	0.0	0.0	0.0	0.0	0.0	0.0	0.00	0.00	
	Btkq	0.0	0.0	0.0	0.0	0.0	-10.0	0.0	0.0	10.0	0.0	0.0	0.0	0.00	0.00	
	2Bkqb	15.0	0.0	15.0	0.0	5.0	-10.0	15.0	0.0	20.0	0.0	0.0	-10.0	0.18	7.74	
	2Bkq	0.0	0.0	10.0	0.0	0.0	0.0	0.0	0.0	10.0	0.0	0.0	0.0	0.00	0.00	15.95
LATE MARBLE																
Pedon 13	A	0.0	0.0	0.0	0.0	0.0	0.0	0.0	0.0	0.0	-10.0	0.0	0.0	0.00	0.00	
	AB	0.0	0.0	0.0	0.0	10.0	0.0	0.0	0.0	0.0	0.0	10.0	0.0	0.11	1.26	1.26
	2Bkb															
	2Bkj															
	2Bk															
	2C															

SOIL DEVELOPMENT
INDEX CALCULATIONS: FIELD DESC

Morphostrat. Unit/ Pedon #	Horizon	MELANIZATION (maximum=85) Normalized Mel	X thick	Profile Mel	COLOR-PALING (maximum=60) Normalized Pale	X thick	Profile Pale	COLOR-LIGHTENING (maximum=80) Normalized Light	X thick	Profile Light
INDIAN										
Pedon 7	Avk	0.00	0.00		0.33	1.67		0.38	1.88	
	Bw	0.00	0.00		0.33	3.00		0.25	2.25	
	2Btkq	0.00	0.00		0.00	0.00		0.25	2.75	
	3Btk	0.00	0.00		0.00	0.00		0.13	1.88	
	3Bkm	0.00	0.00		0.17	3.00		0.13	2.25	
	3Bk	0.00	0.00	0.00	0.17	10.00	17.67	0.13	7.50	18.50
MIDDLE MARBLE										
Pedon 8	A	0.47	2.35		0.50	2.50		0.00	0.00	
	Bk1	0.12	5.88		0.00	0.00		0.13	6.25	
	Bk2	0.00	0.00		0.00	0.00		0.00	0.00	
	Bkqj	0.00	0.00		0.00	0.00		0.00	0.00	
	Bkj	0.00	0.00	8.24	0.00	0.00	2.50	0.00	0.00	6.25
EARLY MARBLE										
Pedon 9	Av	0.12	1.41		0.00	0.00		0.13	1.50	
	Bw	0.00	0.00		0.00	0.00		0.13	3.13	
	2Bkq	0.00	0.00		0.00	0.00		0.00	0.00	
	2Bk1	0.00	0.00		0.17	6.33		0.00	0.00	
	2Bk2	0.00	0.00		0.00	0.00		0.13	3.38	
	3Bk1	0.24	10.82		0.00	0.00		0.13	5.75	
	3Bk2	0.00	0.00	12.24	0.00	0.00	6.33	0.00	0.00	13.75
LEIDY										
Pedon 10	Av	0.00	0.00		0.17	0.83		0.19	0.94	
	Btkq	0.00	0.00		0.00	0.00		0.06	0.56	
	Bkq1	0.12	3.29		0.17	4.67		0.06	1.75	
	Bkq2	0.00	0.00		0.00	0.00		0.06	1.63	
	Bkq3	0.00	0.00		0.00	0.00		0.06	0.00	
	Bk1	0.06	2.29		0.00	0.00		0.00	0.00	
	Bk2	0.00	0.00	5.59	0.00	0.00	5.50	0.25	8.75	13.63
MIDDLE MARBLE										
Pedon 11	Av	0.06	0.41		0.17	1.17		0.19	0.88	
	Bw	0.06	0.94		0.17	2.67		0.19	3.00	
	Bk1	0.00	0.00		0.00	0.00		0.06	3.00	
	Bk2	0.12	2.59		0.00	0.00		0.13	2.75	
	2Bk1	0.00	0.00		0.00	0.00		0.00	0.00	
	2Bk2	0.00	0.00	3.94	0.00	0.00	3.83	0.00	0.00	9.63
McAFEE CREEK										
Pedon 12	Avk	0.00	0.00		0.17	3.17		0.00	0.00	
	Btkq	0.00	0.00		0.17	2.17		0.13	1.63	
	2Kmqb	0.00	0.00		0.33	14.00		0.44	18.38	
	2Bkq	0.00	0.00	0.00	0.00	0.00	19.33	0.25	17.75	37.75
LATE MARBLE										
Pedon 13	A	0.12	1.06		0.00	0.00		0.00	0.00	
	AB	0.00	0.00	5.06	0.00	0.00	0.00	0.00	0.00	0.00
	2Btkb									
	2Bkj									
	2Bk									
	2C									

SOIL DEVELOPMENT
INDEX CALCULATIONS ------- TOTAL TEXTURE ---------------------------> ---------- STRUCTURE ------------>
FIELD DESC (maximum=90) (maximum=60)
Morphostrat. <------ Quantified ------>

Unit/ Pedon #	Horizon	Texture (line Xing)	Wet Con	Total Texture	Normalized Texture	X thick	Profile Texture	Quantified Struc	Normalized Struc	X thick	Profile Struc
INDIAN											
Pedon 7	Avk	0.0	15.0	15.0	0.17	0.83		55.00	0.92	4.58	
	Bw	10.0	15.0	25.0	0.28	2.50		35.00	0.58	5.25	
	2Btkq	10.0	40.0	50.0	0.56	6.11		40.00	0.67	7.33	
	3Btk	0.0	20.0	20.0	0.22	3.33		35.00	0.58	8.75	
	3Bkm	0.0	0.0	0.0	0.00	0.00		25.00	0.42	7.50	
	3Bk	0.0	0.0	0.0	0.00	0.00	12.78	20.00	0.33	20.00	53.42
MIDDLE MARBLE											
Pedon 8	A	20.0	0.0	20.0	0.22	1.11		0.00	0.00	0.00	
	Bk1	10.0	0.0	10.0	0.11	5.56		20.00	0.33	16.67	
	Bk2	0.0	0.0	0.0	0.00	0.00		20.00	0.33	6.67	
	Bkq1	10.0	0.0	10.0	0.11	2.22		15.00	0.25	5.00	
	Bkj	20.0	20.0	40.0	0.44	22.22	31.11	15.00	0.25	12.50	40.83
EARLY MARBLE											
Pedon 9	Av	0.0	0.0	0.0	0.00	0.00		15.00	0.25	3.00	
	Bw	0.0	0.0	0.0	0.00	0.00		20.00	0.33	8.33	
	2Bkq	0.0	10.0	10.0	0.11	2.22		20.00	0.33	6.67	
	2Bk1	0.0	10.0	10.0	0.11	4.22		20.00	0.33	12.67	
	2Bk2	0.0	10.0	10.0	0.11	3.00		15.00	0.25	6.75	
	3Bk1	0.0	10.0	10.0	0.11	5.11		15.00	0.25	11.50	
	3Bk2	0.0	10.0	10.0	0.11	2.44	17.00	15.00	0.25	5.50	54.42
LEIDY											
Pedon 10	Av	0.0	5.0	5.0	0.06	0.28		50.00	0.83	4.17	
	Btkq	0.0	15.0	15.0	0.17	1.50		15.00	0.25	2.25	
	Bkq1	0.0	0.0	0.0	0.00	0.00		30.00	0.50	14.00	
	Bkq2	0.0	0.0	0.0	0.00	0.00		20.00	0.33	8.67	
	Bkq3	0.0	0.0	0.0	0.00	0.00		20.00	0.33	14.33	
	Bk1	0.0	0.0	0.0	0.00	0.00		20.00	0.33	13.00	
	Bk2	0.0	0.0	0.0	0.00	0.00	1.78	20.00	0.33	11.67	68.08
MIDDLE MARBLE											
Pedon 11	Av	0.0	0.0	0.0	0.00	0.00		20.00	0.33	2.33	
	Bw	0.0	0.0	0.0	0.00	0.00		20.00	0.33	5.33	
	Bk1	0.0	5.0	5.0	0.06	2.67		15.00	0.25	12.00	
	Bk2	0.0	5.0	5.0	0.06	1.22		20.00	0.33	7.33	
	2Bk1	0.0	0.0	0.0	0.00	0.00		15.00	0.25	8.75	
	2Bk2	0.0	0.0	0.0	0.00	0.00	3.89	15.00	0.25	13.00	48.75
McAFEE CREEK											
Pedon 12	Avk	0.0	0.0	0.0	0.00	0.00		62.50	1.04	19.79	
	Btkq	0.0	10.0	10.0	0.11	1.44		40.00	0.67	8.67	
	2Bkqb	0.0	0.0	0.0	0.00	0.00		25.00	0.42	17.50	
	2Bkq	0.0	0.0	0.0	0.00	0.00	1.44	25.00	0.42	29.58	80.54
LATE MARBLE											
Pedon 13	A	0.0	0.0	0.0	0.00	0.00		15.00	0.25	2.25	
	AB	0.0	0.0	0.0	0.00	0.00	0.00	0.00	0.00	0.00	10.50
	2Bkb										
	2Bkj										
	2Bk										
	2C										

SOIL DEVELOPMENT
INDEX CALCULATION: ----- DRY CONSISTENCE ------------> ---- MOIST CONSISTENCE ----------->
FIELD DESC (maximum=100) (maximum=100)

Morphostrat. Unit/ Pedon #	Horizon	Quantified Dry Con	Normalized Dry Con	X thick	Profile Dry Con	Quantified Mst Con	Normalized Mst Con	X thick	Profile Mst Con
INDIAN									
Pedon 7	Avk	25.00	0.25	1.25		15.00	0.15	0.75	
	Bwv	30.00	0.30	2.70		25.00	0.25	2.25	
	2Btkq	15.00	0.15	1.65		5.00	0.05	0.55	
	3Btk	35.00	0.35	5.25		35.00	0.35	5.25	
	3Bkm	35.00	0.35	6.30		35.00	0.35	6.30	
	3Bk	25.00	0.25	15.00	32.15	25.00	0.25	15.00	30.10
MIDDLE MARBLE									
Pedon 8	A	5.00	0.05	0.25		0.00	0.00	0.00	
	Bk1	20.00	0.20	10.00		10.00	0.10	5.00	
	Bk2	0.00	0.00	0.00		0.00	0.00	0.00	
	Bkqj	10.00	0.10	2.00		0.00	0.00	0.00	
	Bkj	15.00	0.15	7.50	19.75	0.00	0.00	0.00	5.00
EARLY MARBLE									
Pedon 9	Av	0.00	0.00	0.00		0.00	0.00	0.00	
	Bw	10.00	0.10	2.50		10.00	0.10	2.50	
	2Bkq	10.00	0.10	2.00		10.00	0.10	2.00	
	2Bk1	20.00	0.20	7.60		20.00	0.20	7.60	
	2Bk2	20.00	0.20	5.40		20.00	0.20	5.40	
	3Bk1	20.00	0.20	9.20		10.00	0.10	4.60	
	3Bk2	0.00	0.00	0.00	26.70	10.00	0.10	2.20	24.30
LEIDY									
Pedon 10	Av	5.00	0.05	0.25		20.00	0.20	1.00	
	Btkq	0.00	0.00	0.00		10.00	0.10	0.90	
	Bkq1	15.00	0.15	4.20		20.00	0.20	5.60	
	Bkq2	15.00	0.15	3.90		20.00	0.20	5.20	
	Bkq3	20.00	0.20	8.60		20.00	0.20	8.60	
	Bk1	20.00	0.20	7.80		20.00	0.20	7.80	
	Bk2	20.00	0.20	7.00	31.75	20.00	0.20	7.00	36.10
MIDDLE MARBLE									
Pedon 11	Av	10.00	0.10	0.70		0.00	0.00	0.00	
	Bw	20.00	0.20	3.20		10.00	0.10	1.60	
	Bk1	20.00	0.20	9.60		20.00	0.20	9.60	
	Bk2	10.00	0.10	2.20		20.00	0.20	4.40	
	2Bk1	0.00	0.00	0.00		10.00	0.10	3.50	
	2Bk2	0.00	0.00	0.00	15.70	20.00	0.20	10.40	29.50
McAFEE CREEK									
Pedon 12	Avk	20.00	0.20	3.00		20.00	0.20	3.00	
	Btkq	30.00	0.30	3.90		30.00	0.30	3.90	
	2Bkqb	35.00	0.35	14.70		30.00	0.30	12.60	
	2Bkq	30.00	0.30	21.30	43.70	20.00	0.20	14.20	44.90
LATE MARBLE									
Pedon 13	A	0.00	0.00	0.00		0.00	0.00	0.00	
	AB	0.00	0.00	0.00	2.30	0.00	0.00	0.00	1.70
	2Bkb								
	2Bkj								
	2Bk								
	2C								

SOIL DEVELOPMENT
INDEX CALCULATIONS: ---- CLAY FILMS ----------> ---- CLAY FILMS ---------->
FIELD DESC <normalize: -20/130>

Morphostrat. Unit/ Pedon #	Horizon	stains 1o	stains 2o	bridges 1o	bridges 2o	pores 1o	pores 2o	ped face 1o	ped face 2o	clasts 1o	clasts 2o	primary class	Sum of	2o Freqs/2	Normalized Cly Flms	% thick	Profile Cly Flms
INDIAN																	
Pedon 7	Avk	0	0	0	0	0	0	0	0	0	0	0 ok	0	0	0.00	0.00	
	Bw	0	0	0	0	0	0	70	0	0	0	70 ok	0	0	0.38	3.46	
	2Btkq	40	0	60	0	80	0	0	0	0	0	60 !!	30	0	0.54	5.92	
	3Btk	30	0	60	0	40	0	0	0	0	0	60 !!	20	0	0.46	6.92	
	3Bkm	0	0	0	0	0	0	0	0	0	0	0 ok	0	0	0.00	0.00	
	3Bk	0	0	0	0	0	0	0	0	0	0	0 ok	0	0	0.00	0.00	16.31
MIDDLE MARBLE																	
Pedon 8	A	0	0	0	0	0	0	0	0	0	0	0 ok	0	0	0.00	0.00	
	Bk1	0	0	0	0	0	0	0	0	0	0	0 ok	0	0	0.00	0.00	
	Bk2	0	0	0	0	0	0	0	0	0	0	0 ok	0	0	0.00	0.00	
	Bkqj	0	0	0	0	0	0	0	0	0	0	0 ok	0	0	0.00	0.00	
	Bkj	0	0	0	0	0	0	0	0	0	0	0 ok	0	0	0.00	0.00	0.00
EARLY MARBLE																	
Pedon 9	Av	0	0	0	0	0	0	0	0	0	0	0 ok	0	0	0.00	0.00	
	Bw	0	0	0	0	0	0	0	0	0	0	0 ok	0	0	0.00	0.00	
	2Bkq	0	0	0	0	0	0	0	0	0	0	0 ok	0	0	0.00	0.00	
	2Bk1	0	0	0	0	0	0	0	0	0	0	0 ok	0	0	0.00	0.00	
	2Bk2	0	0	0	0	0	0	0	0	0	0	0 ok	0	0	0.00	0.00	
	3Bk1	0	0	0	0	0	0	0	0	0	0	0 ok	0	0	0.00	0.00	
	3Bk2	0	0	0	0	0	0	0	0	0	0	0 ok	0	0	0.00	0.00	0.00
LEIDY																	
Pedon 10	Av	0	0	0	0	0	0	0	0	0	0	0 ok	0	0	0.00	0.00	
	Btkq	0	0	60	0	40	0	0	0	0	0	60 ok	10	0	0.38	3.46	
	Bkq1	0	0	0	0	0	0	0	0	0	0	0 ok	0	0	0.00	0.00	
	Bkq2	0	0	0	0	0	0	0	0	0	0	0 ok	0	0	0.00	0.00	
	Bkq3	0	0	0	0	0	0	0	0	0	0	0 ok	0	0	0.00	0.00	
	Bk1	0	0	0	0	0	0	0	0	0	0	0 ok	0	0	0.00	0.00	
	Bk2	0	0	0	0	0	0	0	0	0	0	0 ok	0	0	0.00	0.00	3.46
MIDDLE MARBLE																	
Pedon 11	Av	0	0	0	0	0	0	0	0	0	0	0 ok	0	0	0.00	0.00	
	Bw	0	0	0	0	0	0	0	0	0	0	0 ok	0	0	0.00	0.00	
	Bk1	0	0	0	0	0	0	0	0	0	0	0 ok	0	0	0.00	0.00	
	Bk2	0	0	0	0	0	0	0	0	0	0	0 ok	0	0	0.00	0.00	
	2Bk1	0	0	0	0	0	0	0	0	0	0	0 ok	0	0	0.00	0.00	
	2Bk2	0	0	0	0	0	0	0	0	0	0	0 ok	0	0	0.00	0.00	0.00
McAFEE CREEK																	
Pedon 12	Avk	0	0	0	0	0	0	80	0	0	0	80 ok	0	0	0.46	8.77	
	Btkq	0	0	60	0	40	0	0	0	0	0	60 ok	10	0	0.38	5.00	
	2Kmqb	0	0	0	0	0	0	0	0	0	0	0 ok	0	0	0.00	0.00	
	2Bkq	0	0	0	0	0	0	0	0	0	0	0 ok	0	0	0.00	0.00	13.77
LATE MARBLE																	
Pedon 13	A	0	0	0	0	0	0	0	0	0	0	0 ok	0	0	0.00	0.00	
	AB	0	0	0	0	0	0	0	0	0	0	0 ok	0	0	0.00	0.00	0.00
	2Bkb																
	2Bkj																
	2Bk																
	2C																

SOIL DEVELOPMENT
INDEX CALCULATION: ---- SECONDARY CARBONATE ----------->
FIELD DESC (maximum=240)

Morphostrat. Unit/ Pedon #	Horizon	Quantified Carb	Normalized Carb	X thick	Profile Carb
INDIAN					
Pedon 7	Avk	50.00	0.21	1.04	
	Bwk	60.00	0.25	2.25	
	2Btkq	50.00	0.21	2.29	
	3Btk	30.00	0.13	1.88	
	3BkM	60.00	0.25	4.50	
	3Bk	50.00	0.21	12.50	24.46
MIDDLE MARBLE					
Pedon 8	A	0.00	0.00	0.00	
	Bk1	10.00	0.04	2.08	
	Bk2	0.00	0.00	0.00	
	Bkq1	0.00	0.00	0.00	
	Bkj	0.00	0.00	0.00	2.08
EARLY MARBLE					
Pedon 9	Av	0.00	0.00	0.00	
	Bw	0.00	0.00	0.00	
	2Btkq	0.00	0.00	0.00	
	2Bk1	15.00	0.06	2.38	
	2Bk2	10.00	0.04	1.13	
	3Bk1	5.00	0.02	0.96	
	3Bk2	0.00	0.00	0.00	4.46
LEIDY					
Pedon 10	Av	0.00	0.00	0.00	
	Btkq	5.00	0.02	0.19	
	Bkq1	22.50	0.09	2.63	
	Bkq2	10.00	0.04	1.08	
	Bkq3	0.00	0.00	0.00	
	Bk1	0.00	0.00	0.00	
	Bk2	10.00	0.04	1.46	5.36
MIDDLE MARBLE					
Pedon 11	Av	0.00	0.00	0.00	
	Bw	12.50	0.05	0.83	
	Bk1	5.00	0.02	1.00	
	Bk2	15.00	0.06	1.38	
	2Bk1	0.00	0.00	0.00	
	2Bk2	0.00	0.00	0.00	3.21
McAFEE CREEK					
Pedon 12	Avk	10.00	0.04	0.79	
	Btkq	70.00	0.29	3.79	
	2Kmqb	220.00	0.92	38.50	
	2Bkq	60.00	0.25	17.75	60.83
LATE MARBLE					
Pedon 13	A	0.00	0.00	0.00	
	AB	0.00	0.00	0.00	0.00
	2Bwb				
	2Bkj				
	2Bk				
	2C				

HOW DO YOU WANT TO CALCULATE THE PROFILE INDEX? YOUR CHOICES ARE THE FOLLOWING ---ALL PROPERTIES INCLUDING---	TYPE YES OR NO NEXT TO A
INCLUDE ONLY THE FOLLOWING	yes
RUBIFICATION (R)	no
MELANIZATION (M)	no
COLOR-PALING (CP)	no
COLOR-LIGHTENING (CL)	no
TEXTURE (T)	no
STRUCTURE (S)	no
DRY CONSISTENCE (DC)	yes
MOIST CONSISTENCE (MC)	no
CLAY FILMS (CF)	yes
SECONDARY CARBONATE (C)	yes
pH INCREASING (PI)	no
pH DECREASING	no

SOIL DEVELOPMENT INDEX CALCULATIONS: Morphostrat. Unit/ Pedon #	FIELD DESC Horizon	DRY COR, Sum Normalized Properties (R-S)	(DC-PI)	CARB,CLY FLM, Count Properties (R-S)	(DC-PI)	Horizon Index	X thick	SELECTED PROFILE INDEX
INDIAN								
Pedon 7	Avk	0.00	0.46	0	3	0.15	0.75	
	Bwy	0.00	0.93	0	3	0.31	2.80	
	2Btkq	0.00	0.90	0	3	0.30	3.29	
	3Btk	0.00	0.94	0	3	0.31	4.68	
	3BkM	0.00	0.60	0	3	0.20	3.60	
	3Bk	0.00	0.46	0	3	0.15	9.17	24.31
MIDDLE MARBLE								
Pedon 8	A	0.00	0.05	0	3	0.02	0.08	
	Bk1	0.00	0.24	0	3	0.08	4.03	
	Bk2	0.00	0.00	0	3	0.00	0.00	
	Bkqj	0.00	0.10	0	3	0.03	0.67	
	Bkj	0.00	0.15	0	3	0.05	2.50	7.20
EARLY MARBLE								
Pedon 9	Av	0.00	0.00	0	3	0.00	0.00	
	Bk	0.00	0.10	0	3	0.03	0.83	
	2Bkq	0.00	0.10	0	3	0.03	0.67	
	2Bk1	0.00	0.25	0	3	0.09	3.33	
	2Bk2	0.00	0.24	0	3	0.08	2.18	
	3Bk1	0.00	0.22	0	3	0.07	3.39	
	3Bk2	0.00	0.00	0	3	0.00	0.00	9.85
LEIDY								
Pedon 10	Av	0.00	0.05	0	3	0.02	0.08	
	Btkq	0.00	0.41	0	3	0.14	1.22	
	Bkq1	0.00	0.24	0	3	0.08	2.28	
	Bkq2	0.00	0.19	0	3	0.06	1.66	
	Bkq3	0.00	0.20	0	3	0.07	2.07	
	Bk1	0.00	0.20	0	3	0.07	2.60	
	Bk2	0.00	0.24	0	3	0.08	2.02	12.22
MIDDLE MARBLE								
Pedon 11	Av	0.00	0.10	0	3	0.03	0.29	
	Bw	0.00	0.25	0	3	0.08	1.34	
	Bk1	0.00	0.22	0	3	0.07	3.53	
	Bk2	0.00	0.16	0	3	0.05	1.19	
	2Bk1	0.00	0.00	0	3	0.00	0.00	
	2Bk2	0.00	0.00	0	3	0.00	0.00	6.30
McAFEE CREEK								
Pedon 12	Avk	0.00	0.70	0	3	0.23	4.45	
	Btkq	0.00	0.98	0	3	0.33	4.23	
	2Bkqb	0.00	1.27	0	3	0.42	17.73	
	2Bkq	0.00	0.55	0	3	0.18	13.02	39.43
LATE MARBLE								
Pedon 13	A	0.00	0.00	0	3	0.00	0.00	
	AB	0.00	0.00	0	3	0.00	0.00	0.00
	2Bkb							
	2Bkj							
	2Bk							
	2C							

SOIL DEVELOPMENT INDEX VALUES:
Profile Property and Selected Property Indicies.

< Morphostrat. unit >			<------------ Profile Property Indices					------------>	Selected Property Index (Dry Con., Clay, Carb.)
Pedon #	Name	Approx. Age	Pale.	Light.	Struct.	Dry Con.	Clay	Carb.	
13	late Marble	0.1	0.00	0.00	10.50	2.30	0.00	0.50	0.77
4	" "	0.1	0.00	0.00	16.83	2.70	0.00	0.00	0.90
11	middle Marble	1	3.83	9.63	48.75	15.70	0.00	3.21	6.30
1	" "	1	7.00	5.75	47.83	16.40	0.00	2.63	4.65
2	" "	1	3.50	8.50	59.42	15.80	0.00	2.83	3.13
8	" "	1	2.50	6.25	40.83	19.75	0.00	2.08	7.20
3	early Marble	1.8	9.67	12.25	54.33	22.00	0.00	6.42	8.94
9	" "	1.8	6.33	13.75	55.42	26.70	0.00	4.46	9.55
10	Leidy	13	5.50	13.63	60.00	31.75	3.46	9.01	12.22
6	"	13	8.67	8.50	64.50	34.40	5.77	6.08	15.42
7	Indian	230	17.67	18.50	53.42	32.15	16.31	24.46	24.31
5	"	230	24.50	21.13	64.17	35.10	14.54	30.58	26.74
12	McAfee Creek	550	19.33	37.75	75.54	43.70	13.77	60.83	39.43

REGRESSION ANALYSIS FOR HOLOCENE SOILS:
Late Marble through early Marble soils.

Paling with age:

Regression Output:		
Constant		0.29
Std Err of Y Est		0.32
R Squared		0.79
No. of Observations		8.00
Degrees of Freedom		6.00
X Coefficient(s)	0.17	
Std Err of Coef.	0.04	

Lightening with age:

Regression Output:		
Constant		0.12
Std Err of Y Est		0.10
R Squared		0.93
No. of Observations		8.00
Degrees of Freedom		6.00
X Coefficient(s)	0.12	
Std Err of Coef.	0.01	

Structure with age:

Regression Output:		
Constant		-0.30
Std Err of Y Est		0.34
R Squared		0.76
No. of Observations		8.00
Degrees of Freedom		6.00
X Coefficient(s)	0.03	
Std Err of Coef.	0.01	

Dry Consistency with age:

Regression Output:		
Constant		-0.11
Std Err of Y Est		0.19
R Squared		0.93
No. of Observations		8.00
Degrees of Freedom		6.00
X Coefficient(s)	0.07	
Std Err of Coef.	0.01	

Carbonate with age:

Regression Output:		
Constant		0.15
Std Err of Y Est		0.22
R Squared		0.90
No. of Observations		8.00
Degrees of Freedom		6.00
X Coefficient(s)	0.30	
Std Err of Coef.	0.04	

Selected Property Index with age:

Regression Output:		
Constant		0.06
Std Err of Y Est		0.25
R Squared		0.87
No. of Observations		8.00
Degrees of Freedom		6.00
X Coefficient(s)	0.10	
Std Err of Coef.	0.03	

REGRESSION ANALYSIS FOR PLEISTOCENE SOILS:
Leidy, Indian, and McAfee Creek soils.

Paling with age:

Regression Output:		
Constant		-89.08
Std Err of Y Est		101.70
R Squared		0.49
No. of Observations		5.00
Degrees of Freedom		3.00
X Coefficient(s)	19.63	
Std Err of Coef.	11.58	

Lightening with age:

Regression Output:		
Constant		-179.47
Std Err of Y Est		53.23
R Squared		0.96
No. of Observations		5.00
Degrees of Freedom		3.00
X Coefficient(s)	19.43	
Std Err of Coef.	2.40	

Structure with age:

Regression Output:		
Constant		-510.57
Std Err of Y Est		233.08
R Squared		0.16
No. of Observations		5.00
Degrees of Freedom		3.00
X Coefficient(s)	11.02	
Std Err of Coef.	14.58	

Dry Consistency with age:

Regression Output:		
Constant		-1176.70
Std Err of Y Est		129.99
R Squared		0.74
No. of Observations		5.00
Degrees of Freedom		3.00
X Coefficient(s)	39.07	
Std Err of Coef.	13.42	

Clay with age:

Regression Output:		
Constant		-80.32
Std Err of Y Est		177.33
R Squared		0.51
No. of Observations		5.00
Degrees of Freedom		3.00
X Coefficient(s)	27.44	
Std Err of Coef.	15.41	

Carbonate with age:

Regression Output:		
Constant		-54.17
Std Err of Y Est		29.52
R Squared		0.99
No. of Observations		5.00
Degrees of Freedom		3.00
X Coefficient(s)	9.98	
Std Err of Coef.	0.67	

Selected Property Index with age:

Regression Output:		
Constant		-273.03
Std Err of Y Est		30.08
R Squared		0.98
No. of Observations		5.00
Degrees of Freedom		3.00
X Coefficient(s)	20.36	
Std Err of Coef.	1.70	

ESTIMATED HOLOCENE SOIL AGES BASED ON CALIBRATED
SELECTED PROPERTY INDEX:

Age with Selected Property Index:
Regression Output:

Constant		0.06
Std Err of Y Est		0.25
R Squared		0.87
No. of Observations		8.00
Degrees of Freedom		6.00
X Coefficient(s)	0.18	
Std Err of Coef.	0.03	

			Estimated Age Range (ka)		
PEDON #	Name	SPI	Age	Max.	Min.
13	LM	0.77	0.1	0.4	n.a.
4	LM	0.90	0.1	0.5	0.0
11	MM	6.30	1.1	1.4	0.9
1	MM	4.65	0.8	1.1	0.6
2	MM	3.13	0.5	0.9	0.4
8	MM	7.28	1.3	1.6	1.1
3	EM	8.94	1.5	1.9	1.4
9	EM	9.55	1.7	2.0	1.5

Morpho-stratigraphic Unit	Estimated Mean Soil Ages: "Preferred" Age	Max. Age	Min. Age
late Marble	0.1	0.5	0.0
middle Marble	0.9	1.3	0.7
early Marble	1.6	2.0	1.4

APPENDIX IV

NUMERICAL AGE CONSTRAINTS

The results of radiocarbon and tephrochronologic analyses are presented in this appendix. Radiocarbon ages have been converted to calibrated dendroyear ages according to the current high-precision calibration schemes of Stiver and Pearson (1986, Figures 1 and 2). In Chapter IV these results are used to constrain the ages of morphostratigraphic units (e.g. Table 3).

An attempt to date a Bristlecone pine (Pinus longaeva Bailey) by dendrochronology (i.e., tree ring analysis) proved to be inclusive (Harlin, T., 1988, written commun.).

THE UNIVERSITY OF ARIZONA
TUCSON, ARIZONA 85721

LABORATORY OF ISOTOPE GEOCHEMISTRY-ENVIRONMENTAL ISOTOPE RESEARCH
DEPARTMENT OF GEOSCIENCES
GOULD-SIMPSON BUILDING
TEL (602) 621-6014
BITNET % "ALONG @ ARIZRVAX"

23 September 87

Dr. David B. Slemmons
400 PLMEC
Department of Geological Sciences
University of Nevada
Reno, Nevada 89557

Dear Dr. Slemmons:

Here are the results of the carbon isotope analyses on the samples you submitted in May of this year:

A-NUMBER	SAMPLE DESCRIPTION	CONVENTIONAL DATE *	DEL C-13
4765	5-TS-1-7mc Wood	660 +/- 40	-23.6 permil
4766	5-TS-1-10mc Wood	2290 +/- 50	-20.5 permil
4767	5-TS-1-22A Wood	2170 +/- 45	-22.0 permil
4768	5-TS-1-28fc Wood	1670 +/- 40	-23.5 permil

* Normalized to C-13 = -25 permil

Note: Attached are calibrated age ranges for your samples according to the current high precision calibration schemes (See *Radiocarbon* vol 28, 1986).

Sincerely,

Austin Long
Professor

Invoice enclosed

THE UNIVERSITY OF ARIZONA
TUCSON, ARIZONA 85721

LABORATORY OF ISOTOPE GEOCHEMISTRY-ENVIRONMENTAL ISOTOPE RESEARCH
DEPARTMENT OF GEOSCIENCES
GOULD-SIMPSON BUILDING
TEL (602) 621-6014
BITNET: "ALONG @ ARIZRVAX"

December 20, 1988

Dr. Thomas L. Sawyer
University of Nevada, Reno
Reno, NV 89557

Dear Dr. Sawyer:

Here are the results of our carbon isotope analyses of your wood sample, 5-TS-1-49-B:

A-5068: 755 ± 60 years before present, based on the "Libby" half-life, and normalized to $\delta^{13}C = -25‰$. Measured $\delta^{13}C = -22.6‰$.

If you have any questions, please call.

Sincerely,

Austin Long

Austin Long
Professor

BETA ANALYTIC INC.

RADIOCARBON DATING, STABLE ISOTOPE RATIOS, THERMOLUMINESCENCE, X-RAY DIFFRACTION
P.O. BOX 248113 CORAL GABLES, FLORIDA 33124 - (305) 667-5167

February 22, 1988

Dr. Thomas Sawyer
University of Nevada - Reno
Center for Neotectonic Studies
Mackay School of Mines
Reno, Nevada 89557

Dear Dr. Sawyer:

Your wood was pretreated by first examining for rootlets. The sample was then given a hot acid wash to eliminate carbonates. It was repeatedly rinsed to neutrality and subsequently given a hot alkali soaking to take out humic acids. After rinsing to neutrality, another acid wash followed and another rinsing to neutrality. The sample was found to be small after these steps. As per your request, it was canceled and is returned herein.

We are enclosing our invoice for the pretreatment work. Would you please forward this to the appropriate office for payment.

Sincerely yours,

Murry Tamers

Murry Tamers, Ph.D.
Co-director

BETA ANALYTIC INC.

RADIOCARBON DATING, STABLE ISOTOPE RATIOS
P.O. BOX 248113 CORAL GABLES, FLORIDA 33124 · (305) 667-5167
BITNET XNRBET22@SERVAX

June 30, 1988

Dr. Thomas Sawyer
University of Nevada - Reno
Center for Neotectonic Studies
Mackay School of Mines
Reno, Nevada 89557

Dear Dr. Sawyer:

Please find enclosed the results on the two wood samples recently submitted for radiocarbon dating analyses. We hope these dates will be useful in your research.

Your woods were pretreated by first examining for rootlets. The samples were then given a hot acid wash to eliminate carbonates. They were repeatedly rinsed to neutrality and subsequently given a hot alkali soaking to take out humic acids. After rinsing to neutrality, another acid wash followed and another rinsing to neutrality. The following benzene syntheses and counting proceeded normally.

We are enclosing our invoice. Would you forward this to the appropriate office for payment. If there are any questions or if you would like to confer on the dates, my direct telephone number is listed above. Please don't hesitate to call us if we can be of help.

Sincerely yours,

Murry Tamers

Murry Tamers, Ph.D.
Co-director

P.S. I'm including some data sheets for future samples or to give to your friends that might need our service.

United States Department of the Interior

GEOLOGICAL SURVEY
Geologic Division
Branch of Western Regional Geology
345 Middlefield Road M/S 975
Menlo Park, California 94025

December 31, 1987

Tom Sawyer
Tectonics Laboratory
LME #400
University of Nevada
Reno, Nevada 89551

Dear Tom:

Enclosed are results of probe analyses of the three ash samples you sent us. The analyses were done on glass separated from the ash. They were done on a SEMQ electron probe by Charlie Meyer of the USGS, Menlo Park.

Your sample 5-TS-1-17MC matches most closely with the Bishop ash and several ash beds of similar composition erupted from the Long Valley-Mono Glass Mountain complex of east-central California, that range from about 0.74 to 1.0 Ma.

Your sample 5-TS-1-28FC-B matches most closely with several ash beds erupted from the Mono Craters south of Mono Lake, most of which range in age from about 3400 to 4100 years B.P. One sample in this group is as old as 8000 yrs B.P., however.

Your sample 5-TS-1-7MC-C matches best with ash beds erupted from the Mono Craters that range in age from about 1000 to 2000 B.P., but one of which is as old as about 3500 yrs. B.P.

These matches should be considered as tentative guides to what the ages of your samples may be rather than as definitive age ranges. Further work on the minor- and trace-element composition of your ash samples and other putative correlative ash beds should be made to obtain more definitive age control.

Sincerely yours,

Andrei Sarna-Wojcicki

Andrei Sarna-Wojcicki
Geologist

Copy to:
C. E. Meyer
R. Fehr
M. Hamer

United States Department of the Interior

GEOLOGICAL SURVEY
Geologic Division
Branch of Western Regional Geology
345 Middlefield Road
Menlo Park, California, 94025

February 8, 1989

Mr. Tom Sawyer
Graduate Research Assistant
Center for Neotectonic Studies
University of Nevada, Reno
Reno, NV 89557-0047

Dear Tom:

Thank you for your letter of January 25 and the informationon on your radiocarbon dates as they relate to ash sample 5-TS-1-7MC-C from Fish Lake Valley. In light of the maximum 755 ± 60 yr. BP date on the detrital wood associated with this ash, I suspect that the ash may be from the ca-640 ± 40 eruption of Panum Crater in the Mono Crater Chain that was dated by Wood and Brooks (1979; GSA Abstracts With Programs, v. 11, p. 543). Our analyses of samples collected from Panum Crater by Ken Lajoie are given below:

	Ash in debris flow 5-TS-1-7MC-C (ash)	Panum Tuff Ring KRL-82282A(P) (pumice)	Panum Plug Dome KRL-82982KP (pumice; d=1.5 m)
SiO_2	77.27	76.86	76.70
Al_2O_3	12.55	12.85	13.01
Fe_2O_3	1.10	1.05	1.11
MgO	0.03	0.03	0.02
MnO	0.06	0.06	0.06
CaO	0.55	0.54	0.55
TiO_2	0.05	0.05	0.06
Na_2O	3.76	3.87	3.81
K_2O	4.63	4.70	4.67
Total (orig.)	99.22	99.21	98.15

Unfortunately, all the late Holocene ash layers erupted from Mono Craters are chemically very similar, and we can't distinguish among them by probe or XRF analysis. We have greater success using INAA, but that is expensive and time consuming.

Sincerely

Andrei

Andrei Sarna-Wojcicki
Geologist

THE UNIVERSITY OF ARIZONA
TUCSON, ARIZONA 85721

LABORATORY OF TREE-RING RESEARCH
BUILDING #58

January 12, 1988

Tom Sawyer
Mackay School of Mines
University of Nevada Reno
Reno, Nevada 89557-0047

Dear Tom,

I have examined the Bristlecone Pine Log from Marble Creek in Fish Lake Valley. I must report that I am unable to find a convincing cross match with our long Bristlecone Chronology from the White Mountains.

I plotted 211 rings, of which the first 100 were fairly wide, yet with good sensitivity. I would expect that there would be few or no missing rings in this portion of the log.

Many trees, even though growing in an area with a good chronology, do not respond exactly the same as the trees on which the chronology is based, therefore, it is not surprising that I am unable to date this log.

Would you like me to return this material?

I am sorry that this has taken so long. I have been fighting a virus since October and every thing is consequently delayed.

Sincerely,

Thomas Harlan
Research Associate

TH:sr

APPENDIX V

TOPOGRAPHIC PROFILES

The following topographic profiles were measured by the Brunton and slope-stick method of Buckman and Anderson (1979), and are shown graphically in this appendix. The location of the profiles is shown on Plate 1.

[all date in meters or degrees]

PROFILE 1

Interval	Angle	<------Hori. Dist----> Incremental (m)	Cumulative	<-------Vert. Dist----> Incremental (m)	Cumulative
1	1.5	1.00	1.00	0.03	0.03
1	-4.5	1.00	2.00	-0.08	-0.05
1	-1	1.00	3.00	-0.02	-0.07
1	4	1.00	3.99	0.07	0.00
1	9	0.99	4.98	0.16	0.16
1	8	0.99	5.97	0.14	0.30
1	15	0.97	6.94	0.26	0.55
1	8	0.99	7.93	0.14	0.69
1	4	1.00	8.93	0.07	0.76
1	0.5	1.00	9.93	0.01	0.77
1	14	0.97	10.90	0.24	1.01
1	15.5	0.96	11.86	0.27	1.28
1	13	0.97	12.83	0.22	1.51
1	13	0.97	13.81	0.22	1.73
1	11.5	0.98	14.79	0.20	1.93
1	13.5	0.97	15.76	0.23	2.16
1	10	0.98	16.75	0.17	2.34
1	4	1.00	17.74	0.07	2.41
1	5	1.00	18.74	0.09	2.49
1	5	1.00	19.74	0.09	2.58
1	4	1.00	20.73	0.07	2.65
1	3.5	1.00	21.73	0.06	2.71
1	2.5	1.00	22.73	0.04	2.76
1	1	1.00	23.73	0.02	2.77
1	0	1.00	24.73	0.00	2.77
1	0.5	1.00	25.73	0.01	2.78

PROFILE P2

Interval	Slope Degrees	Hori. Dist (m) Incremental	Hori. Dist (m) Cumulative	Vert. Dist (m) Incremental	Vert. Dist (m) Cumulative
2	5	1.99	1.99	0.17	0.17
2	3	2.00	3.99	0.10	0.28
2	2	2.00	5.99	0.07	0.35
2	1.5	2.00	7.99	0.05	0.40
2	-4	2.00	9.98	-0.14	0.26
2	1.5	2.00	11.98	0.05	0.31
2	2	2.00	13.98	0.07	0.38
2	3.5	2.00	15.98	0.12	0.51
2	3.5	2.00	17.97	0.12	0.63
2	6	1.99	19.96	0.21	0.84
2	5	1.99	21.95	0.17	1.01
2	3	2.00	23.95	0.10	1.12
2	3	2.00	25.95	0.10	1.22
2	2	2.00	27.95	0.07	1.29

PROFILE P3

Interval	Slope Degrees	Hori. Dist (m) Incremental	Hori. Dist (m) Cumulative	Vert. Dist (m) Incremental	Vert. Dist (m) Cumulative
2	-3.5	2.00	2.00	-0.12	-0.12
2	-3	2.00	3.99	-0.10	-0.23
2	-3	2.00	5.99	-0.10	-0.33
2	-2.5	2.00	7.99	-0.09	-0.42
2	-4	2.00	9.98	-0.14	-0.56
2	-1.5	2.00	11.98	-0.05	-0.61
2	-1.5	2.00	13.98	-0.05	-0.66
2	0	2.00	15.98	0.00	-0.66
2	0	2.00	17.98	0.00	-0.66
2	12.5	1.95	19.94	0.43	-0.23
2	15	1.93	21.87	0.52	0.29
2	18	1.90	23.77	0.62	0.91
2	19.5	1.89	25.65	0.67	1.57
2	24	1.83	27.48	0.81	2.39
2	15	1.93	29.41	0.52	2.90
2	8.5	1.98	31.39	0.30	3.20
2	3	2.00	33.39	0.10	3.30
2	3	2.00	35.39	0.10	3.41
2	-0.5	2.00	37.39	-0.02	3.39
2	-2	2.00	39.38	-0.07	3.32

PROFILE P4

Interval	Slope Degrees	Hori. Dist (m) Incremental	Hori. Dist (m) Cumulative	Vert. Dist (m) Incremental	Vert. Dist (m) Cumulative
1	5	1.00	1.00	0.09	0.09
1	5.5	1.00	1.99	0.10	0.18
1	10	0.98	2.98	0.17	0.36
1	4.5	1.00	3.97	0.08	0.44
2	-3	2.00	5.97	-0.10	0.33
1	0	1.00	6.97	0.00	0.33
1	1	1.00	7.97	0.02	0.35
1	4.5	1.00	8.97	0.08	0.43
1	7.5	0.99	9.96	0.13	0.56
1	11	0.98	10.94	0.19	0.75
1	6	0.99	11.93	0.10	0.85
2	5	1.99	13.93	0.17	1.03
2	5.5	1.99	15.92	0.19	1.22
1	16	0.96	16.88	0.28	1.49
2	27	1.78	18.66	0.91	2.40
2	28	1.77	20.43	0.94	3.34
2	28	1.77	22.19	0.94	4.28
2	27	1.78	23.98	0.91	5.19
1	23	0.92	24.90	0.39	5.58
2	6	1.99	26.88	0.21	5.79
2	6	1.99	28.87	0.21	6.00
2	4	2.00	30.87	0.14	6.14
2	3	2.00	32.87	0.10	6.24
2	2	2.00	34.86	0.07	6.31
2	0	2.00	36.86	0.00	6.31

PROFILE P5

Interval	Slope Degrees	Hori. Dist (m) Incremental	Hori. Dist (m) Cumulative	Vert. Dist (m) Incremental	Vert. Dist (m) Cumulative
2	-2	2.00	2.00	-0.07	-0.07
2	-1	2.00	4.00	-0.03	-0.10
2	0	2.00	6.00	0.00	-0.10
2	0.5	2.00	8.00	0.02	-0.09
2	1.5	2.00	10.00	0.05	-0.05
2	4.5	1.99	11.99	0.16	0.10
2	11.5	1.96	13.95	0.40	0.50
2	10	1.97	15.92	0.35	0.85
2	15	1.93	17.85	0.52	1.37
2	8	1.98	19.83	0.28	1.65
2	5.5	1.99	21.82	0.19	1.84
2	1	2.00	23.82	0.03	1.87
2	2	2.00	25.82	0.07	1.94
2	2	2.00	27.82	0.07	2.01
2	1.5	2.00	29.82	0.05	2.07
2	3	2.00	31.82	0.10	2.17

PROFILE P5 (Continued)

Interval	Slope Degrees	Hori. Dist (m) Incremental	Cumulative	Vert. Dist (m) Incremental	Cumulative
2	1.5	2.00	33.82	0.05	2.22
2	1.5	2.00	35.82	0.05	2.27
2	0	2.00	37.82	0.00	2.27
2	-0.5	2.00	39.82	-0.02	2.26
2	-0.5	2.00	41.82	-0.02	2.24
2	1	2.00	43.82	0.03	2.27
2	-2	2.00	45.81	-0.07	2.20
2	-0.5	2.00	47.81	-0.02	2.19
2	-0.5	2.00	49.81	-0.02	2.17
2	-2	2.00	51.81	-0.07	2.10
2	-1	2.00	53.81	-0.03	2.07
2	-0.5	2.00	55.81	-0.02	2.05
2	-0.5	2.00	57.81	-0.02	2.03
2	-2	2.00	59.81	-0.07	1.96
2	-1.5	2.00	61.81	-0.05	1.91
2	-0.5	2.00	63.81	-0.02	1.89
2	0.5	2.00	65.81	0.02	1.91
2	1	2.00	67.81	0.03	1.94
2	4	2.00	69.81	0.14	2.08
2	7	1.99	71.79	0.24	2.33
2	12	1.96	73.75	0.42	2.74
2	14.5	1.94	75.68	0.50	3.24
2	11.5	1.96	77.64	0.40	3.64
2	8.5	1.98	79.62	0.30	3.94
2	6	1.99	81.61	0.21	4.15
2	4.5	1.99	83.60	0.16	4.30
2	3	2.00	85.60	0.10	4.41
2	-0.5	2.00	87.60	-0.02	4.39
2	-0.5	2.00	89.60	-0.02	4.37
2	-3	2.00	91.60	-0.10	4.27

PROFILE P6

Interval	Slope Degrees	Hori. Dist (m) Incremental	Cumulative	Vert. Dist (m) Incremental	Cumulative
2	-4	2.00	2.00	-0.14	-0.14
2	-2.5	2.00	3.99	-0.09	-0.23
2	0	2.00	5.99	0.00	-0.23
2	0.5	2.00	7.99	0.02	-0.21
2	4	2.00	9.99	0.14	-0.07
2	5.5	1.99	11.98	0.19	0.12
2	10	1.97	13.95	0.35	0.47
2	4	2.00	15.94	0.14	0.61
2	3.5	2.00	17.94	0.12	0.73
2	2.5	2.00	19.94	0.09	0.82
2	-1	2.00	21.94	-0.03	0.78
2	-0.5	2.00	23.94	-0.02	0.77
2	-1.5	2.00	25.94	-0.05	0.71

PROFILE P6

Interval	Slope Degrees	Hori. Dist (m) Incremental	Hori. Dist (m) Cumulative	Vert. Dist (m) Incremental	Vert. Dist (m) Cumulative
2	-4	2.00	2.00	-0.14	-0.14
2	-2.5	2.00	3.99	-0.09	-0.23
2	0	2.00	5.99	0.00	-0.23
2	0.5	2.00	7.99	0.02	-0.21
2	4	2.00	9.99	0.14	-0.07
2	5.5	1.99	11.98	0.19	0.12
2	10	1.97	13.95	0.35	0.47
2	4	2.00	15.94	0.14	0.61
2	3.5	2.00	17.94	0.12	0.73
2	2.5	2.00	19.94	0.09	0.82
2	-1	2.00	21.94	-0.03	0.78
2	-0.5	2.00	23.94	-0.02	0.77
2	-1.5	2.00	25.94	-0.05	0.71

PROFILE P7

Interval	Slope Degrees	Hori. Dist (m) Incremental	Hori. Dist (m) Cumulative	Vert. Dist (m) Incremental	Vert. Dist (m) Cumulative
2	0	2.00	2.00	0.00	0.00
2	0	2.00	4.00	0.00	0.00
2	-0.5	2.00	6.00	-0.02	-0.02
2	1.5	2.00	8.00	0.05	0.03
2	2	2.00	10.00	0.07	0.10
2	2.5	2.00	12.00	0.09	0.19
2	4	2.00	13.99	0.14	0.33
2	6	1.99	15.98	0.21	0.54
2	10	1.97	17.95	0.35	0.89
1	12.5	0.98	18.93	0.22	1.10
1	11.5	0.98	19.91	0.20	1.30
1	12.5	0.98	20.88	0.22	1.52
1	9	0.99	21.87	0.16	1.68
1	6.5	0.99	22.86	0.11	1.79
1	6.5	0.99	23.86	0.11	1.90
2	4.5	1.99	25.85	0.16	2.06
2	4.5	1.99	27.84	0.16	2.22
2	4	2.00	29.84	0.14	2.36
2	2	2.00	31.84	0.07	2.43
2	1	2.00	33.84	0.03	2.46
2	-0.5	2.00	35.84	-0.02	2.44
2	-2	2.00	37.84	-0.07	2.37

PROFILE P8

Interval	Slope Degrees	Hori. Dist (m) Incremental	Hori. Dist (m) Cumulative	Vert. Dist (m) Incremental	Vert. Dist (m) Cumulative
2	1	2.00	2.00	0.03	0.03
2	2	2.00	4.00	0.07	0.10
2	4.5	1.99	5.99	0.16	0.26
2	3.5	2.00	7.99	0.12	0.38
2	4.5	1.99	9.98	0.16	0.54
2	8.5	1.98	11.96	0.30	0.84
1	10	0.98	12.95	0.17	1.01
1	15	0.97	13.91	0.26	1.27
1	13	0.97	14.89	0.22	1.49
1	15.5	0.96	15.85	0.27	1.76
1	12	0.98	16.83	0.21	1.97
1	12	0.98	17.81	0.21	2.18
1	6.5	0.99	18.80	0.11	2.29
2	8.5	1.98	20.78	0.30	2.59
2	7	1.99	22.76	0.24	2.83
2	4	2.00	24.76	0.14	2.97
2	3	2.00	26.75	0.10	3.07
2	0.5	2.00	28.75	0.02	3.09
2	2	2.00	30.75	0.07	3.16
2	-1	2.00	32.75	-0.03	3.13
2	-2	2.00	34.75	-0.07	3.06

PROFILE P9

Interval	Slope Degrees	Hori. Dist (m) Incremental	Hori. Dist (m) Cumulative	Vert. Dist (m) Incremental	Vert. Dist (m) Cumulative
2	0.5	2.00	2.00	0.02	0.02
2	1	2.00	4.00	0.03	0.05
2	3	2.00	6.00	0.10	0.16
2	5.5	1.99	7.99	0.19	0.35
2	7	1.99	9.97	0.24	0.59
2	9	1.98	11.95	0.31	0.91
2	10.5	1.97	13.91	0.36	1.27
2	15	1.93	15.85	0.52	1.79
1	15	0.97	16.81	0.26	2.05
1	13.5	0.97	17.78	0.23	2.28
1	18	0.95	18.74	0.31	2.59
1	12.5	0.98	19.71	0.22	2.81
1	14	0.97	20.68	0.24	3.05
1	10.5	0.98	21.67	0.18	3.23
1	7	0.99	22.66	0.12	3.35
2	4.5	1.99	24.65	0.16	3.51
2	1	2.00	26.65	0.03	3.54
2	1	2.00	28.65	0.03	3.58
2	-1.5	2.00	30.65	-0.05	3.53
2	-1.5	2.00	32.65	-0.05	3.47
2	-1	2.00	34.65	-0.03	3.44

PROFILE P10

Interval	Slope Degrees	Hori. Dist (m) Incremental	Cumulative	Vert. Dist (m) Incremental	Cumulative
2	0.5	2.00	2.00	0.02	0.02
2	0	2.00	4.00	0.00	0.02
2	1.5	2.00	6.00	0.05	0.07
2	1.5	2.00	8.00	0.05	0.12
2	1.5	2.00	10.00	0.05	0.17
2	-1	2.00	12.00	-0.03	0.14
2	4	2.00	13.99	0.14	0.28
1	8.5	0.99	14.98	0.15	0.43
1	8.5	0.99	15.97	0.15	0.57
1	6	0.99	16.97	0.10	0.68
1	5.5	1.00	17.96	0.10	0.78
1	6	0.99	18.96	0.10	0.88
1	7	0.99	19.95	0.12	1.00
1	2.5	1.00	20.95	0.04	1.05
1	3	1.00	21.95	0.05	1.10
2	4.5	1.99	23.94	0.16	1.25
2	1.5	2.00	25.94	0.05	1.31
2	1	2.00	27.94	0.03	1.34
2	2.5	2.00	29.94	0.09	1.43
2	2.5	2.00	31.93	0.09	1.52
2	2	2.00	33.93	0.07	1.59
2	2	2.00	35.93	0.07	1.66
2	3	2.00	37.93	0.10	1.76
2	3	2.00	39.93	0.10	1.87
2	3	2.00	41.92	0.10	1.97
2	5	1.99	43.92	0.17	2.14
2	7	1.99	45.90	0.24	2.39
2	9.5	1.97	47.87	0.33	2.72
1	12	0.98	48.85	0.21	2.93
1	12.5	0.98	49.83	0.22	3.14
1	8	0.99	50.82	0.14	3.28
1	17.5	0.95	51.77	0.30	3.58
1	16	0.96	52.73	0.28	3.86
1	12	0.98	53.71	0.21	4.07
1	11.5	0.98	54.69	0.20	4.27
1	8	0.99	55.68	0.14	4.40
2	5	1.99	57.67	0.17	4.58
2	2	2.00	59.67	0.07	4.65
2	2	2.00	61.67	0.07	4.72
2	3	2.00	63.67	0.10	4.82
2	2.5	2.00	65.67	0.09	4.91
2	1	2.00	67.67	0.03	4.94
2	3.5	2.00	69.66	0.12	5.07
2	1.5	2.00	71.66	0.05	5.12
2	2	2.00	73.66	0.07	5.19
2	2	2.00	75.66	0.07	5.26

PROFILE P10 (Continued)

Interval	Slope Degrees	Hori. Dist (m) Incremental	Hori. Dist (m) Cumulative	Vert. Dist (m) Incremental	Vert. Dist (m) Cumulative
2	2	2.00	77.66	0.07	- 5.33
2	5	1.99	79.65	0.17	5.50
1	5	1.00	80.65	0.09	5.59
1	5	1.00	81.64	0.09	5.68
1	8.5	0.99	82.63	0.15	5.83
1	2.5	1.00	83.63	0.04	5.87
1	5.5	1.00	84.63	0.10	5.96
1	2.5	1.00	85.63	0.04	6.01
2	1	2.00	87.63	0.03	6.04
1	2	1.00	88.63	0.03	6.08
2	1.5	2.00	90.62	0.05	6.13
2	1.5	2.00	92.62	0.05	6.18
2	2.5	2.00	94.62	0.09	6.27
2	2	2.00	96.62	0.07	6.34
2	0.5	2.00	98.62	0.02	6.36
2	1.5	2.00	100.62	0.05	6.41
2	2.5	2.00	102.62	0.09	6.50
2	2.5	2.00	104.62	0.09	6.58
2	3	2.00	106.61	0.10	6.69
2	4	2.00	108.61	0.14	6.83
2	6.5	1.99	110.60	0.23	7.05
2	9	1.98	112.57	0.31	7.37
2	9.5	1.97	114.54	0.33	7.70
2	11.5	1.96	116.50	0.40	8.10
1	16.5	0.96	117.46	0.28	8.38
1	13.5	0.97	118.43	0.23	8.61
1	17	0.96	119.39	0.29	8.91
1	9.5	0.99	120.38	0.17	9.07
1	7.5	0.99	121.37	0.13	9.20
2	6.5	1.99	123.36	0.23	9.43
2	5	1.99	125.35	0.17	9.60
2	4.5	1.99	127.34	0.16	9.76
2	3	2.00	129.34	0.10	9.86
2	2	2.00	131.34	0.07	9.93
2	3	2.00	133.34	0.10	10.04
2	2	2.00	135.33	0.07	10.11
2	2.5	2.00	137.33	0.09	10.20
2	2.5	2.00	139.33	0.09	10.28
2	1.5	2.00	141.33	0.05	10.34
2	2.5	2.00	143.33	0.09	10.42
2	1.5	2.00	145.33	0.05	10.47
2	2	2.00	147.33	0.07	10.54
2	1.5	2.00	149.33	0.05	10.60
2	2	2.00	151.32	0.07	10.67
2	1.5	2.00	153.32	0.05	10.72
2	1.5	2.00	155.32	0.05	10.77

PROFILE P10 (Continued)

Interval	Slope Degrees	Hori. Dist (m) Incremental	Hori. Dist (m) Cumulative	Vert. Dist (m) Incremental	Vert. Dist (m) Cumulative
2	1.5	2.00	157.32	0.05	10.82
2	0.5	2.00	159.32	0.02	10.84
2	1	2.00	161.32	0.03	10.88
2	-0.5	2.00	163.32	-0.02	10.86
2	1.5	2.00	165.32	0.05	10.91
2	1	2.00	167.32	0.03	10.95
2	1	2.00	169.32	0.03	10.98
2	2.5	2.00	171.32	0.09	11.07
2	1	2.00	173.32	0.03	11.10
2	3	2.00	175.32	0.10	11.21
2	1.5	2.00	177.31	0.05	11.26
2	2	2.00	179.31	0.07	11.33
2	2.5	2.00	181.31	0.09	11.42
2	2	2.00	183.31	0.07	11.49
1	2.5	1.00	184.31	0.04	11.53
1	5.5	1.00	185.30	0.10	11.63
1	9	0.99	186.29	0.16	11.78
1	11	0.98	187.27	0.19	11.97
1	14.5	0.97	188.24	0.25	12.22
1	12.5	0.98	189.22	0.22	12.44
1	13	0.97	190.19	0.22	12.67
1	10	0.98	191.18	0.17	12.84
1	9.5	0.99	192.16	0.17	13.00
1	5.5	1.00	193.16	0.10	13.10
1	8	0.99	194.15	0.14	13.24
2	4	2.00	196.14	0.14	13.38
2	2.5	2.00	198.14	0.09	13.47
2	3.5	2.00	200.14	0.12	13.59
2	1.5	2.00	202.14	0.05	13.64
2	0.5	2.00	204.14	0.02	13.66

PROFILE P11

Interval	<-Slope Degrees	<----Hori. Dist (m)--- Incremental	Cumulative	<---Vert. Dist (m)---> Incremental	Cumulative
2	2.5	2.00	2.00	0.09	0.09
2	2.5	2.00	4.00	0.09	0.17
2	4.5	1.99	5.99	0.16	0.33
2	5	1.99	7.98	0.17	0.51
2	7.5	1.98	9.97	0.26	0.77
2	10.5	1.97	11.93	0.36	1.13
2	11.5	1.96	13.89	0.40	1.53
2	15	1.93	15.82	0.52	2.05
1	15	0.97	16.79	0.26	2.31
1	18	0.95	17.74	0.31	2.62
1	20.5	0.94	18.68	0.35	2.97
1	20.5	0.94	19.61	0.35	3.32
1	19.5	0.94	20.56	0.33	3.65
1	22.5	0.92	21.48	0.38	4.03
1	22.5	0.92	22.40	0.38	4.42
1	24.5	0.91	23.31	0.41	4.83
1	18.5	0.95	24.26	0.32	5.15
1	16.5	0.96	25.22	0.28	5.43
1	15	0.97	26.19	0.26	5.69
1	10	0.98	27.17	0.17	5.86
1	10.5	0.98	28.16	0.18	6.05
1	9.5	0.99	29.14	0.17	6.21
1	7.5	0.99	30.13	0.13	6.34
1	8	0.99	31.12	0.14	6.48
1	5	1.00	32.12	0.09	6.57
2	2.5	2.00	34.12	0.09	6.65
2	2.5	2.00	36.12	0.09	6.74
2	2.5	2.00	38.11	0.09	6.83
2	2.5	2.00	40.11	0.09	6.92

PROFILE P12

Interval	<-Slope Degrees	<----Hori. Dist (m)--- Incremental	Cumulative	<---Vert. Dist (m)---> Incremental	Cumulative
2	2.5	2.00	2.00	0.09	0.09
2	4	2.00	3.99	0.14	0.23
2	4	2.00	5.99	0.14	0.37
2	5.5	1.99	7.98	0.19	0.56
2	5	1.99	9.97	0.17	0.73
2	5	1.99	11.96	0.17	0.91
2	5.5	1.99	13.95	0.19	1.10
2	3.5	2.00	15.95	0.12	1.22
2	3.5	2.00	17.95	0.12	1.34
2	6.5	1.99	19.93	0.23	1.57
1	7	0.99	20.93	0.12	1.69

PROFILE P12 (Continued)

Interval	<-Slope Degrees	<----Hori. Dist (m)--- Incremental	Cumulative	<---Vert. Dist (m)---> Incremental	Cumulative
1	7.5	0.99	21.92	0.13	1.82
1	9.5	0.99	22.90	0.17	1.99
1	3	1.00	23.90	0.05	2.04
2	2	2.00	25.90	0.07	2.11
2	4	2.00	27.90	0.14	2.25
2	3	2.00	29.89	0.10	2.35
2	4.5	1.99	31.89	0.16	2.51
2	5	1.99	33.88	0.17	2.68
2	5.5	1.99	35.87	0.19	2.88
2	4.5	1.99	37.87	0.16	3.03
2	5	1.99	39.86	0.17	3.21
2	2.5	2.00	41.86	0.09	3.29
2	7	1.99	43.84	0.24	3.54
1	6	0.99	44.84	0.10	3.64
1	9	0.99	45.82	0.16	3.80
1	9.5	0.99	46.81	0.17	3.96
1	12	0.98	47.79	0.21	4.17
1	6	0.99	48.78	0.10	4.28
2	2.5	2.00	50.78	0.09	4.36
2	3.5	2.00	52.78	0.12	4.49
2	2.5	2.00	54.77	0.09	4.57
2	4	2.00	56.77	0.14	4.71
2	1	2.00	58.77	0.03	4.75
2	3	2.00	60.77	0.10	4.85
2	3	2.00	62.76	0.10	4.96
2	2.5	2.00	64.76	0.09	5.04
2	4	2.00	66.76	0.14	5.18
2	5.5	1.99	68.75	0.19	5.37
2	6	1.99	70.74	0.21	5.58
2	5.5	1.99	72.73	0.19	5.78
2	3	2.00	74.72	0.10	5.88
2	7	1.99	76.71	0.24	6.12
1	7	0.99	77.70	0.12	6.25
1	10.5	0.98	78.69	0.18	6.43
1	13.5	0.97	79.66	0.23	6.66
1	14.5	0.97	80.63	0.25	6.91
1	14	0.97	81.60	0.24	7.15
1	15.5	0.96	82.56	0.27	7.42
1	14.5	0.97	83.53	0.25	7.67
1	12	0.98	84.51	0.21	7.88
1	5	1.00	85.50	0.09	7.97
2	4	2.00	87.50	0.14	8.11
2	3	2.00	89.50	0.10	8.21
2	2.5	2.00	91.49	0.09	8.30
2	1	2.00	93.49	0.03	8.33

PROFILE P13

Interval	Slope Degrees	<----Hori. Incremental	<---Vert. D Cumulative	<---Vert. Dist (m)-- Incremental	Cumulati
2	-3	2.00	2.00	-0.10	-0.10
2	-3.5	2.00	3.99	-0.12	-0.23
2	-2.5	2.00	5.99	-0.09	-0.31
2	-4.5	1.99	7.99	-0.16	-0.47
2	-3	2.00	9.98	-0.10	-0.58
2	-5	1.99	11.98	-0.17	-0.75
2	-4	2.00	13.97	-0.14	-0.89
2	-5	1.99	15.96	-0.17	-1.06
2	13	1.95	17.91	0.45	-0.61
2	16.5	1.92	19.83	0.57	-0.05
2	13.5	1.94	21.77	0.47	0.42
2	10.5	1.97	23.74	0.36	0.79
2	9	1.98	25.72	0.31	1.10
2	2.5	2.00	27.71	0.09	1.19
2	1	2.00	29.71	0.03	1.22
2	0	2.00	31.71	0.00	1.22
2	-1.5	2.00	33.71	-0.05	1.17
2	-2.5	2.00	35.71	-0.09	1.08
2	-2	2.00	37.71	-0.07	1.01
2	-1.5	2.00	39.71	-0.05	0.96
2	-1.5	2.00	41.71	-0.05	0.91

PROFILE P14

Interval	Slope Degrees	<----Hori. Dist (m)---> Incremental	Cumulative	<---Vert. Dist (m)-- Incremental	Cumulati
2	5	1.99	1.99	0.17	0.17
2	5	1.99	3.98	0.17	0.35
2	6.5	1.99	5.97	0.23	0.58
2	6	1.99	7.96	0.21	0.78
2	7.5	1.98	9.94	0.26	1.05
2	8	1.98	11.92	0.28	1.32
2	9.5	1.97	13.90	0.33	1.65
2	14	1.94	15.84	0.48	2.14
1	14.5	0.97	16.81	0.25	2.39
1	18.5	0.95	17.75	0.32	2.71
1	17	0.96	18.71	0.29	3.00
1	20	0.94	19.65	0.34	3.34
1	16.5	0.96	20.61	0.28	3.62
1	18	0.95	21.56	0.31	3.93
1	16	0.96	22.52	0.28	4.21
1	17	0.96	23.48	0.29	4.50
1	14	0.97	24.45	0.24	4.74

PROFILE P14 (Continued)

Interval	Slope Degrees	<----Hori. Dist (m)---> Incremental	Cumulative	<---Vert. Dist (m)-- Incremental	Cumulati
1	14.5	0.97	25.42	0.25	4.99
2	11.5	1.96	27.38	0.40	5.39
2	8.5	1.98	29.35	0.30	5.69
2	10.5	1.97	31.32	0.36	6.05
2	5.5	1.99	33.31	0.19	6.24
2	4.5	1.99	35.30	0.16	6.40
2	4	2.00	37.30	0.14	6.54
2	5.5	1.99	39.29	0.19	6.73
2	2	2.00	41.29	0.07	6.80

PROFILE P15

Interval	<-Slope Degrees	<----Hori. Dist (m)---> Incremental	Cumulative	<---Vert. Dist (m)-- Incremental	Cumulati
2	0	2.00	2.00	0.00	0.00
2	2	2.00	4.00	0.07	0.07
1	-0.5	1.00	5.00	-0.01	0.06
2	26.5	1.79	6.79	0.89	0.95
1	24.5	0.91	7.70	0.41	1.37
1	18.5	0.95	8.65	0.32	1.69
2	4.5	1.99	10.64	0.16	1.84
2	4.5	1.99	12.63	0.16	2.00
2	3.5	2.00	14.63	0.12	2.12
2	1.5	2.00	16.63	0.05	2.17
1	-3	1.00	17.63	-0.05	2.12
1	12	0.98	18.61	0.21	2.33
1	22.5	0.92	19.53	0.38	2.71
1	19	0.95	20.48	0.33	3.04
2	3	2.00	22.47	0.10	3.14
2	4	2.00	24.47	0.14	3.28
2	1.5	2.00	26.47	0.05	3.33

PROFILE P16

Interval	<-Slope Degrees	<----Hori. Dist (m)---> Incremental	Cumulative	<---Vert. Dist (m)-- Incremental	Cumulati
2	1.5	2.00	2.00	0.05	0.05
1	-3	1.00	3.00	-0.05	0.00
1	12	0.98	3.98	0.21	0.21
1	22.5	0.92	4.90	0.38	0.59
1	19	0.95	5.85	0.33	0.92
2	3	2.00	7.84	0.10	1.02
2	4	2.00	9.84	0.14	1.16
2	1.5	2.00	11.84	0.05	1.21

PROFILE P17

Interval	<-Slope Degrees	<----Hori. Dist (m)---> Incremental	Cumulative	<---Vert. Dist (m)---> Incremental	Cumulative
2	1.5	2.00	2.00	0.05	0.05
2	-0.5	2.00	4.00	-0.02	0.03
1	3.5	1.00	5.00	0.06	0.10
2	23.5	1.83	6.83	0.80	0.89
1	14.5	0.97	7.80	0.25	1.14
2	5	1.99	9.79	0.17	1.32
1	0.5	1.00	10.79	0.01	1.33

PROFILE P18

Interval	<-Slope Degrees	<----Hori. Dist (m)---> Incremental	Cumulative	<---Vert. Dist (m)---> Incremental	Cumulative
2	4.5	1.99	1.99	0.16	0.16
2	2.5	2.00	3.99	0.09	0.24
2	4.5	1.99	5.99	0.16	0.40
2	4.5	1.99	7.98	0.16	0.56
2	3.5	2.00	9.98	0.12	0.68
2	5	1.99	11.97	0.17	0.85
2	6.5	1.99	13.96	0.23	1.08
2	8.5	1.98	15.93	0.30	1.38
2	10.5	1.97	17.90	0.36	1.74
2	11	1.96	19.86	0.38	2.12
2	14.5	1.94	21.80	0.50	2.62
2	7	1.99	23.78	0.24	2.87
2	12	1.96	25.74	0.42	3.28
2	12	1.96	27.70	0.42	3.70
2	11	1.96	29.66	0.38	4.08
2	8.5	1.98	31.64	0.30	4.38
2	11	1.96	33.60	0.38	4.76
2	2.5	2.00	35.60	0.09	4.84
2	5	1.99	37.59	0.17	5.02
2	8.5	1.98	39.57	0.30	5.31
2	7	1.99	41.56	0.24	5.56
2	7	1.99	43.54	0.24	5.80
2	7	1.99	45.53	0.24	6.05
2	8.5	1.98	47.50	0.30	6.34
2	2.5	2.00	49.50	0.09	6.43
2	4	2.00	51.50	0.14	6.57
2	6	1.99	53.49	0.21	6.78

PROFILE P20

Interval	<-Slope Degrees	<----Hori. Dist (m)---> Incremental	Cumulative	<---Vert. Dist (m)---> Incremental	Cumulative
1	3.25	1.00	1.00	0.06	0.06
1	3	1.00	2.00	0.05	0.11
1	5.5	1.00	2.99	0.10	0.20
1	6	0.99	3.99	0.10	0.31
1	5.5	1.00	4.98	0.10	0.41
1	6.5	0.99	5.98	0.11	0.52
1	7.25	0.99	6.97	0.13	0.64
1	11.5	0.98	7.95	0.20	0.84
1	5.75	0.99	8.94	0.10	0.94
1	4.5	1.00	9.94	0.08	1.02
1	4	1.00	10.94	0.07	1.09
1	3.5	1.00	11.94	0.06	1.15
1	4.5	1.00	12.93	0.08	1.23
1	5.5	1.00	13.93	0.10	1.33
1	2	1.00	14.93	0.03	1.36

PROFILE P21

Interval	<-Slope Degrees	<----Hori. Dist (m)---> Incremental	Cumulative	<---Vert. Dist (m)---> Incremental	Cumulative
1	4.5	1.00	1.00	0.08	0.08
1	4	1.00	1.99	0.07	0.15
1	4.5	1.00	2.99	0.08	0.23
1	3	1.00	3.99	0.05	0.28
1	5.5	1.00	4.99	0.10	0.37
1	7	0.99	5.98	0.12	0.50
1	11.75	0.98	6.96	0.20	0.70
1	12.75	0.98	7.93	0.22	0.92
1	14.5	0.97	8.90	0.25	1.17
1	7.25	0.99	9.89	0.13	1.30
1	6.5	0.99	10.89	0.11	1.41
1	5	1.00	11.88	0.09	1.50
1	5.5	1.00	12.88	0.10	1.59
1	3	1.00	13.88	0.05	1.65

Profile P22

Interval	<-Slope Degrees	<----Hori. Dist (m)---> Incremental	Cumulative	<---Vert. Dist (m)---> Incremental	Cumulative
2	1	2.00	2.00	0.03	0.03
2	1.5	2.00	4.00	0.05	0.09
2	2	2.00	6.00	0.07	0.16
2	3	2.00	8.00	0.10	0.26
2	4.5	1.99	9.99	0.16	0.42
1	6	0.99	10.98	0.10	0.52
2	0.5	2.00	12.98	0.02	0.54
2	1.5	2.00	14.98	0.05	0.59
2	1.5	2.00	16.98	0.05	0.65
2	1	2.00	18.98	0.03	0.68
2	2.5	2.00	20.98	0.09	0.77
2	2	2.00	22.98	0.07	0.84
2	2	2.00	24.98	0.07	0.91
2	0.5	2.00	26.98	0.02	0.92
2	2	2.00	28.98	0.07	0.99
2	3	2.00	30.97	0.10	1.10
2	5.5	1.99	32.96	0.19	1.29
1	7.5	0.99	33.96	0.13	1.42
1	3	1.00	34.95	0.05	1.47
2	1	2.00	36.95	0.03	1.51
2	1	2.00	38.95	0.03	1.54
2	1.5	2.00	40.95	0.05	1.60
2	1.5	2.00	42.95	0.05	1.65
2	6.5	1.99	44.94	0.23	1.87
2	5	1.99	46.93	0.17	2.05
0.6	15	0.58	47.51	0.16	2.20
2	1.5	2.00	49.51	0.05	2.26
2	0.75	2.00	51.51	0.03	2.28
2	1	2.00	53.51	0.03	2.32
2	2	2.00	55.51	0.07	2.39
2	2.5	2.00	57.51	0.09	2.47

PROFILE P23

Interval	<-Slope Degrees	<----Hori. Dist (m)---> Incremental	Cumulative	<---Vert. Dist (m)---> Incremental	Cumulative
2	0.5	2.00	2.00	0.02	0.02
2	3.5	2.00	4.00	0.12	0.14
2	3.5	2.00	5.99	0.12	0.26
2	3	2.00	7.99	0.10	0.37
2	3	2.00	9.99	0.10	0.47
2	5.5	1.99	11.98	0.19	0.66
1	5.5	1.00	12.97	0.10	0.76
1	12	0.98	13.95	0.21	0.97
1	10.5	0.98	14.93	0.18	1.15
1	10.25	0.98	15.92	0.18	1.33
1	10.25	0.98	16.90	0.18	1.50
1	9.5	0.99	17.89	0.17	1.67
1	8.5	0.99	18.88	0.15	1.82
1	9	0.99	19.87	0.16	1.97
2	5.5	1.99	21.86	0.19	2.17
2	6	1.99	23.85	0.21	2.37
2	3.5	2.00	25.84	0.12	2.50

PROFILE P24

Interval	<-Slope Degrees	<----Hori. Dist (m)---> Incremental	Cumulative	<---Vert. Dist (m)---> Incremental	Cumulative
2	2	2.00	2.00	0.07	0.07
2	5	1.99	3.99	0.17	0.24
2	5	1.99	5.98	0.17	0.42
1	8.5	0.99	6.97	0.15	0.57
1	13.5	0.97	7.94	0.23	0.80
1	15	0.97	8.91	0.26	1.06
1	7	0.99	9.90	0.12	1.18
1	11	0.98	10.89	0.19	1.37
2	5.5	1.99	12.88	0.19	1.56
2	5.5	1.99	14.87	0.19	1.75
2	4.5	1.99	16.86	0.16	1.91

PROFILE P25

Interval	<-Slope Degrees	<----Hori. Dist (m)---> Incremental	Cumulative	<---Vert. Dist (m)---> Incremental	Cumulative
2	0.5	2.00	2.00	0.02	0.02
2	2.5	2.00	4.00	0.09	0.10
2	2.5	2.00	6.00	0.09	0.19
2	2.5	2.00	7.99	0.09	0.28
2	3.5	2.00	9.99	0.12	0.40
2	3.5	2.00	11.99	0.12	0.52
2	3.5	2.00	13.98	0.12	0.65
2	5	1.99	15.98	0.17	0.82
2	3.5	2.00	17.97	0.12	0.94
2	4	2.00	19.97	0.14	1.08
2	5	1.99	21.96	0.17	1.26
2	12	1.96	23.92	0.42	1.67
2	18.5	1.90	25.81	0.63	2.31
2	20.5	1.87	27.69	0.70	3.01
2	26.5	1.79	29.48	0.89	3.90
2	26.5	1.79	31.27	0.89	4.79
2	28.5	1.76	33.02	0.95	5.75
1	34.75	0.82	33.84	0.57	6.32
2	28	1.77	35.61	0.94	7.25
2	33.5	1.67	37.28	1.10	8.36
2	24.5	1.82	39.10	0.83	9.19
2	20.5	1.87	40.97	0.70	9.89
2	16.5	1.92	42.89	0.57	10.46
2	10	1.97	44.86	0.35	10.80
2	13	1.95	46.81	0.45	11.25
2	14.5	1.94	48.74	0.50	11.75
2	14	1.94	50.68	0.48	12.24
2	13.5	1.94	52.63	0.47	12.70
2	14	1.94	54.57	0.48	13.19
2	14.5	1.94	56.51	0.50	13.69
2	13	1.95	58.45	0.45	14.14
2	14.5	1.94	60.39	0.50	14.64
2	11.5	1.96	62.35	0.40	15.04
2	5.5	1.99	64.34	0.19	15.23
2	7.5	1.98	66.32	0.26	15.49
2	7	1.99	68.31	0.24	15.74
2	16.5	1.92	70.23	0.57	16.30
1	11.5	0.98	71.21	0.20	16.50
2	4.5	1.99	73.20	0.16	16.66
2	3.5	2.00	75.20	0.12	16.78
2	5	1.99	77.19	0.17	16.96

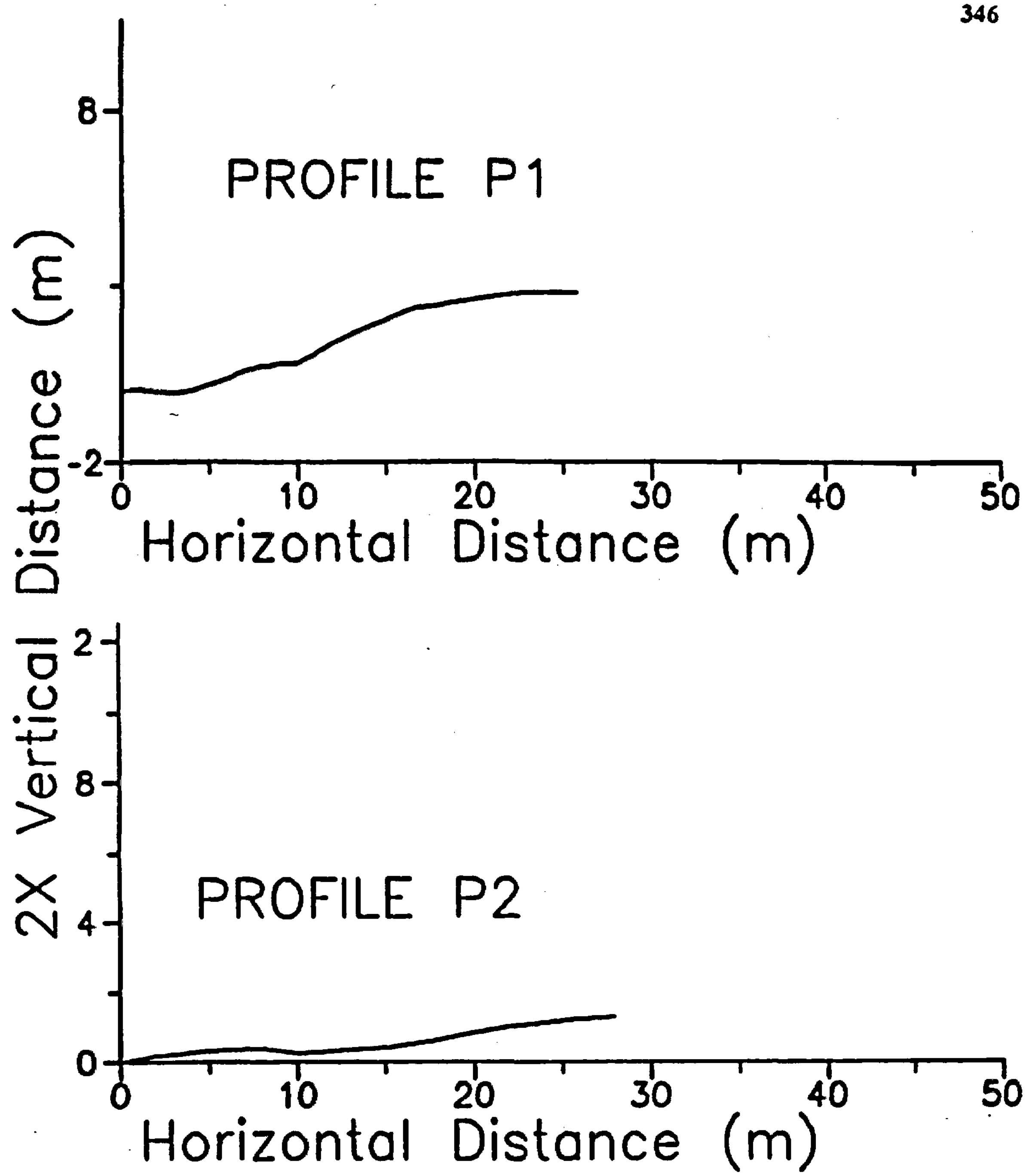
PROFILE P1
8
-2
0
10
20
30
40
50
Horizontal Distance (m)
2X Vertical Distance (m)
PROFILE P2
2
8
4
0
0
10
20
30
40
50
Horizontal Distance (m)

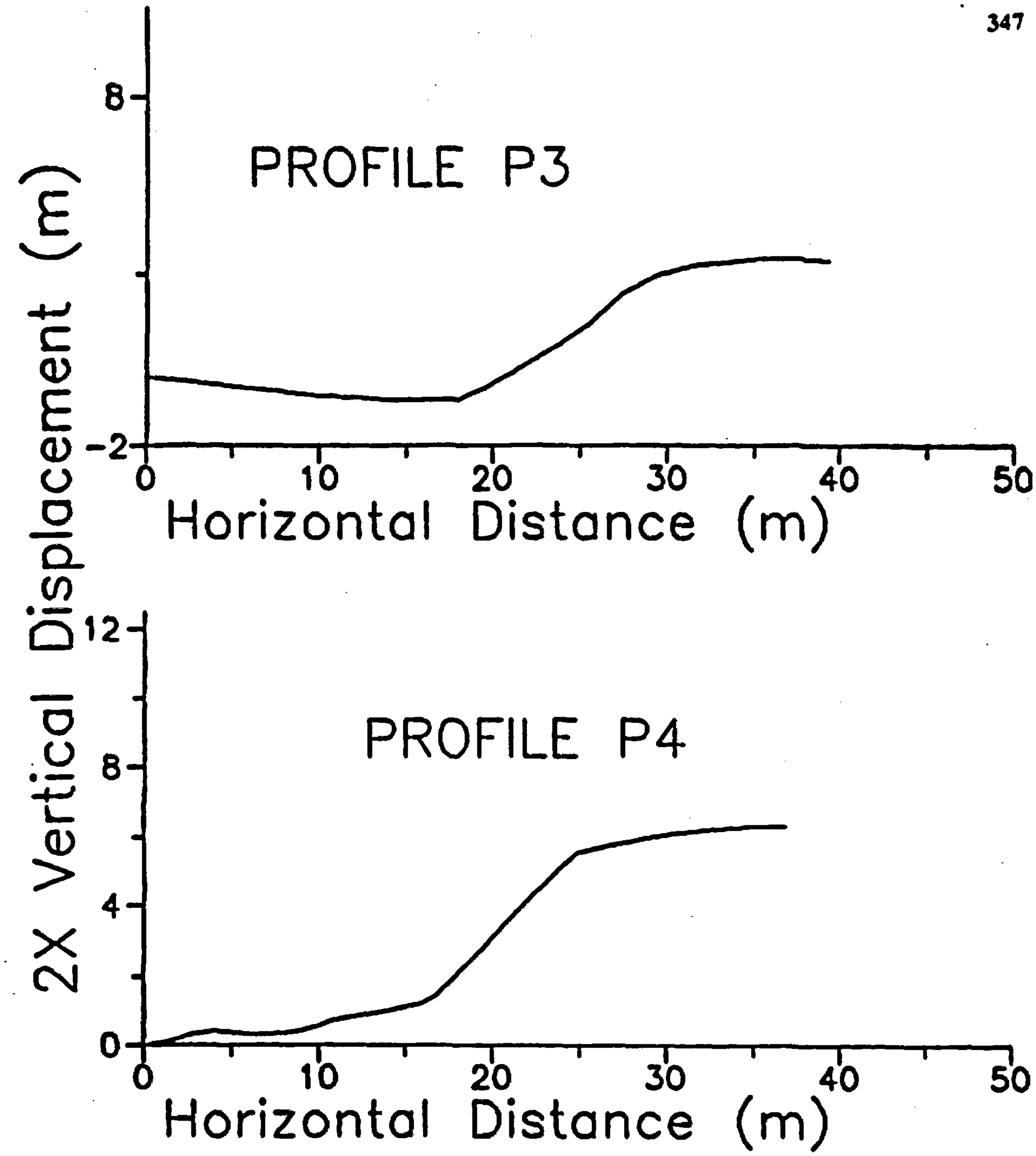
PROFILE P3
8
-2
0
10
20
30
40
50
Horizontal Distance (m)
2X Vertical Displacement (m)
12
PROFILE P4
8
4
0
0
10
20
30
40
50
Horizontal Distance (m)

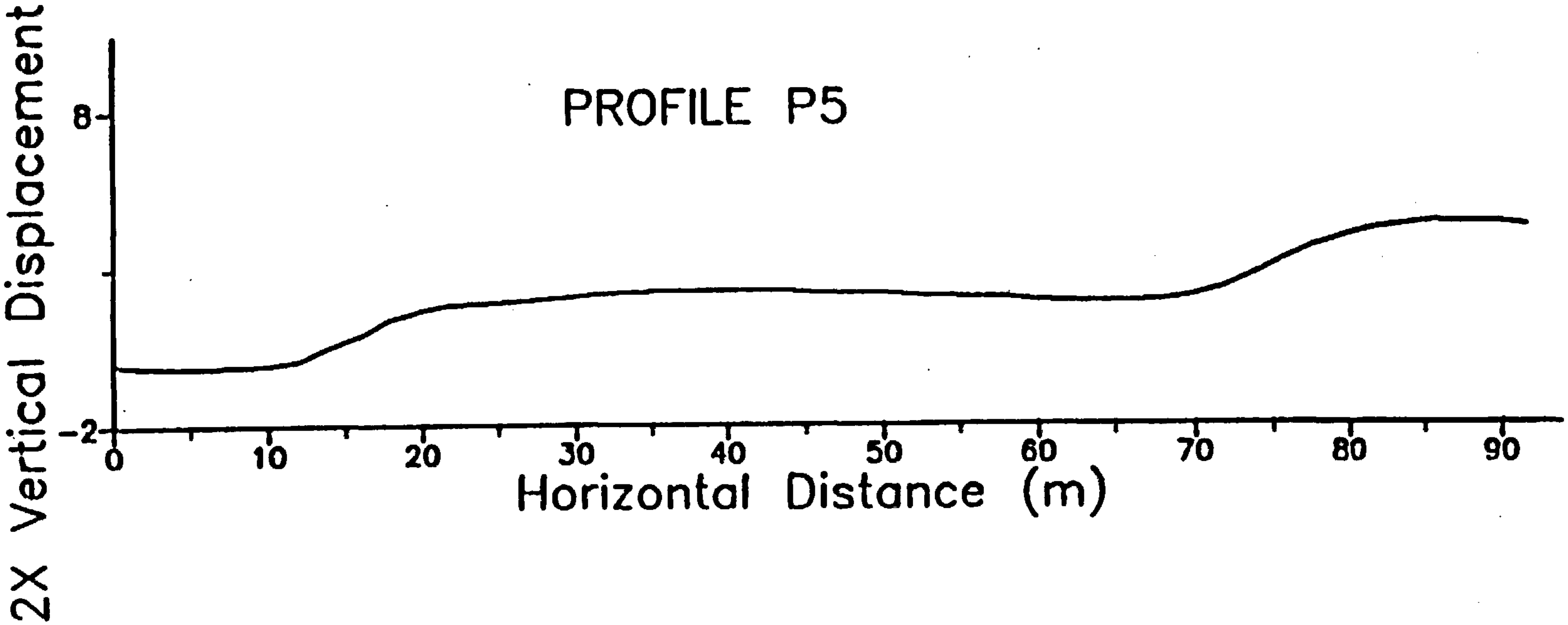
PROFILE P5
2X Vertical Displacement
8
-2
0
10
20
30
40
50
60
70
80
90
Horizontal Distance (m)

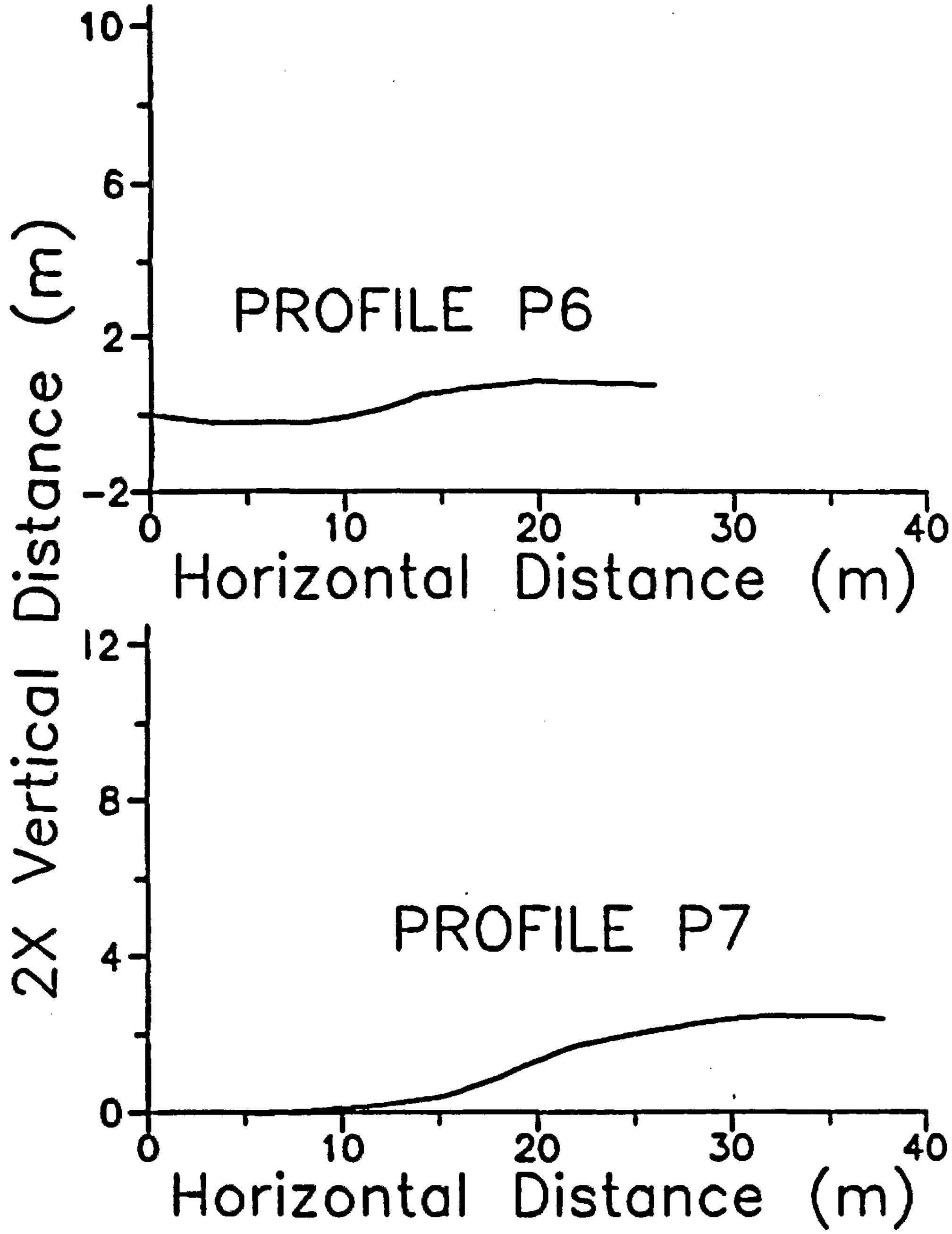
2X Vertical Distance (m)
PROFILE P6
10
6
2
-2
0
10
20
30
40
Horizontal Distance (m)
PROFILE P7
12
8
4
0
0
10
20
30
40
Horizontal Distance (m)

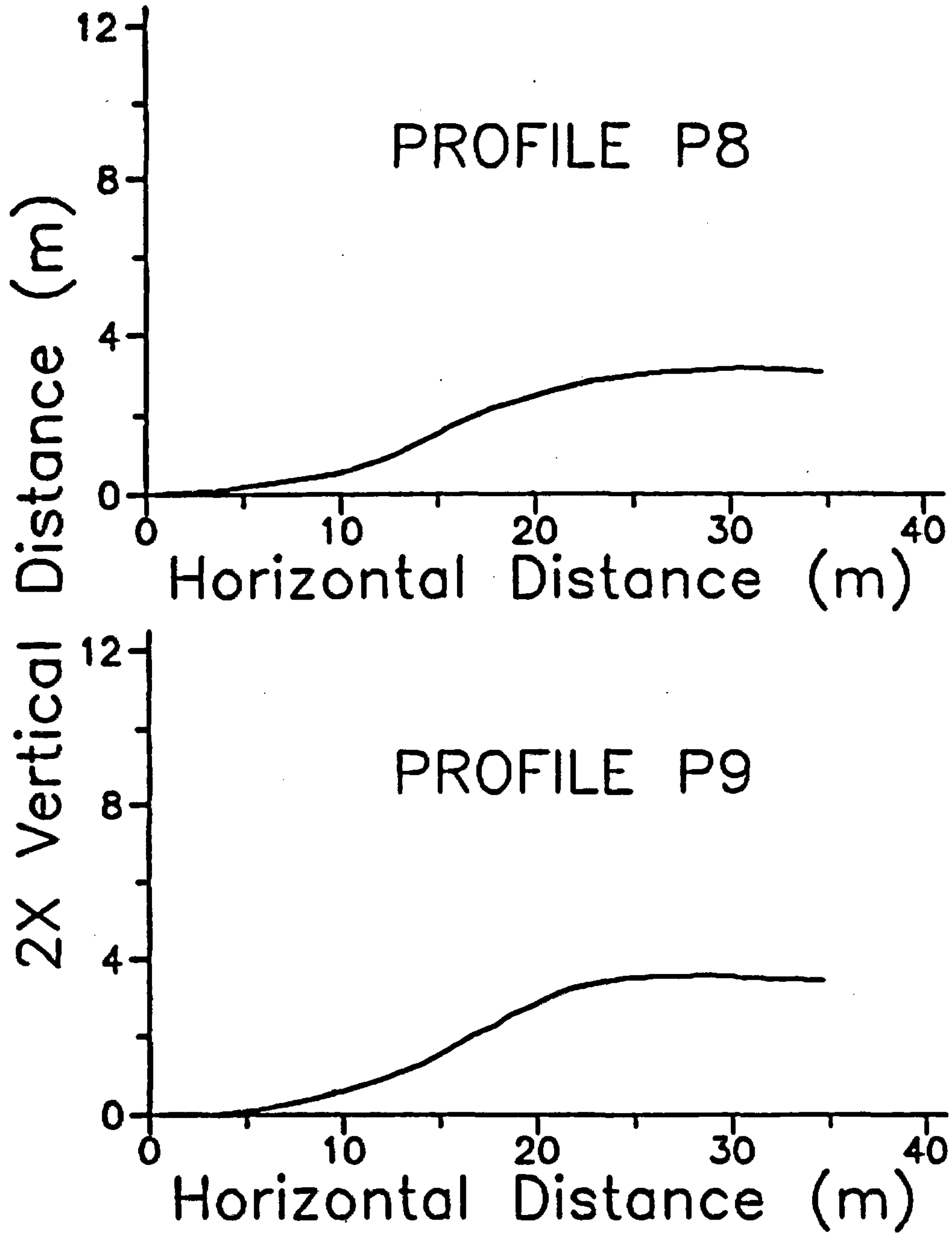
PROFILE P8
PROFILE P9
2X Vertical Distance (m)
Horizontal Distance (m)
Horizontal Distance (m)
0
4
8
12
0
10
20
30
40

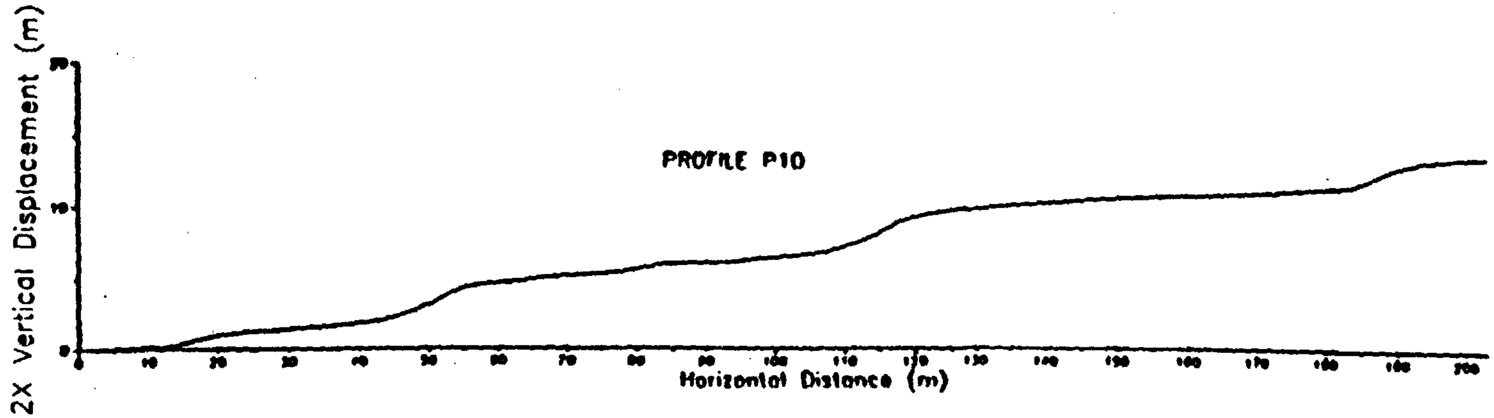
PROFILE P10
-2X Vertical Displacement (m)
Horizontal Distance (m)

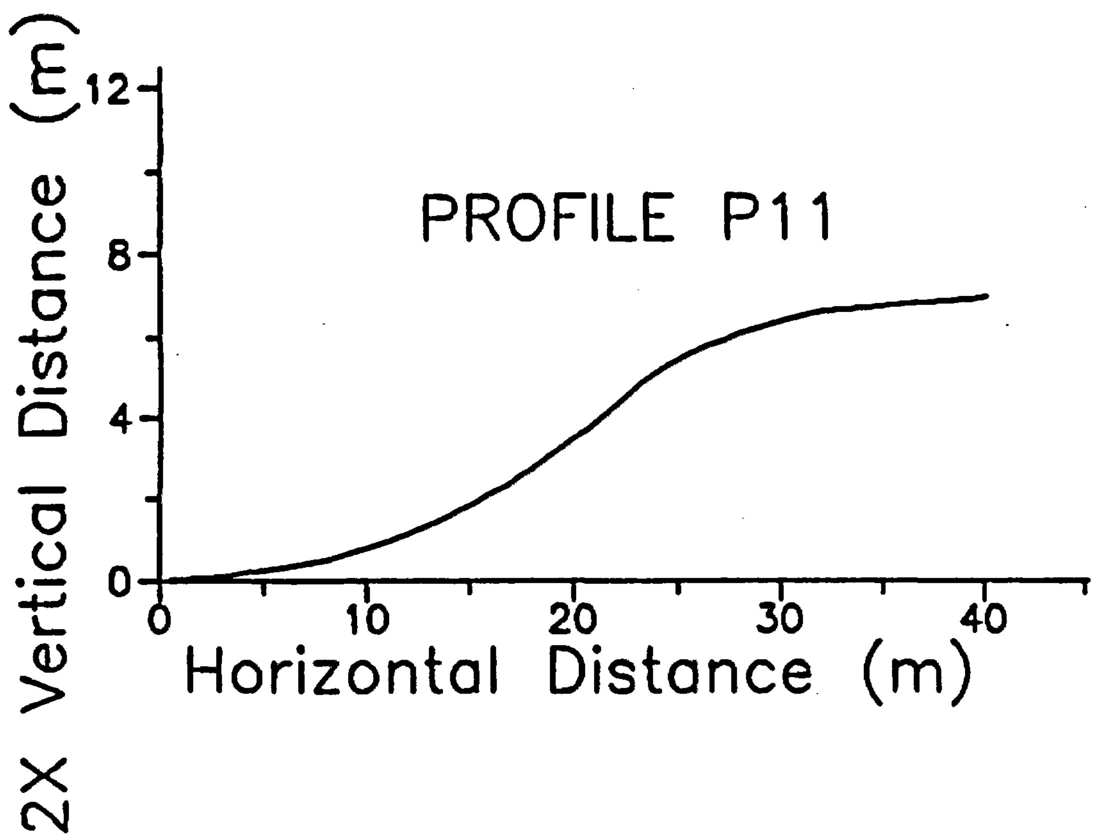
PROFILE P11
2X Vertical Distance (m)
0
4
8
12
0
10
20
30
40
Horizontal Distance (m)

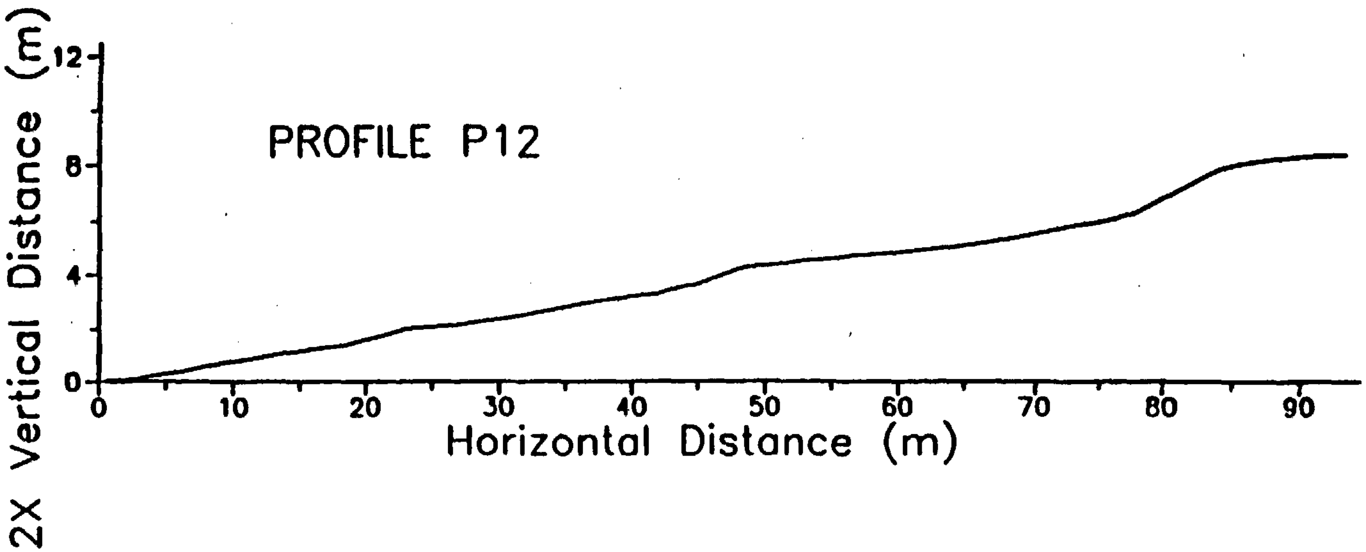
PROFILE P12
2X Vertical Distance (m)
Horizontal Distance (m)
0
4
8
12
0
10
20
30
40
50
60
70
80
90

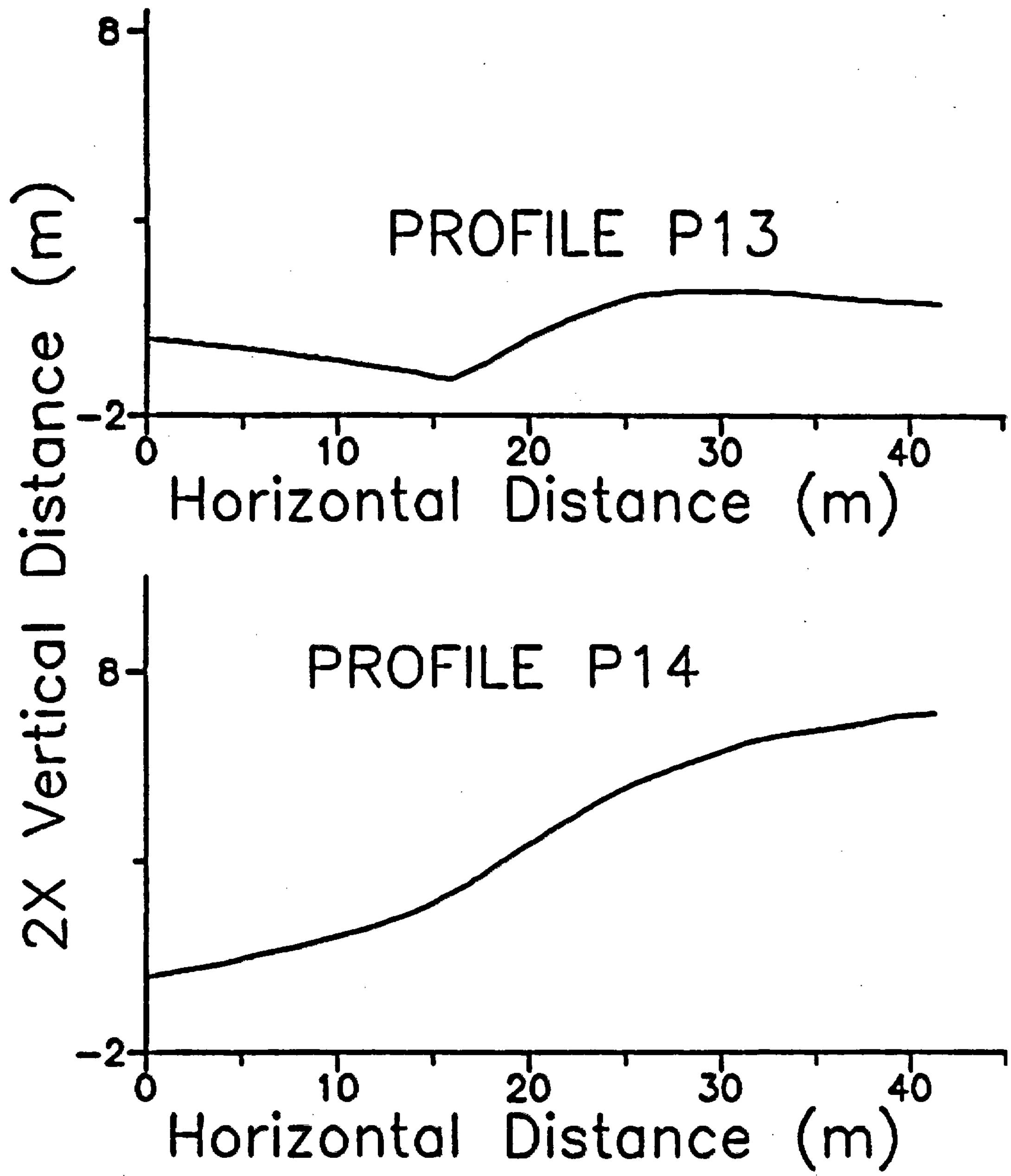

8
-2
PROFILE P13
0
10
20
30
40
Horizontal Distance (m)
2X Vertical Distance (m)
8
-2
PROFILE P14
0
10
20
30
40
Horizontal Distance (m)

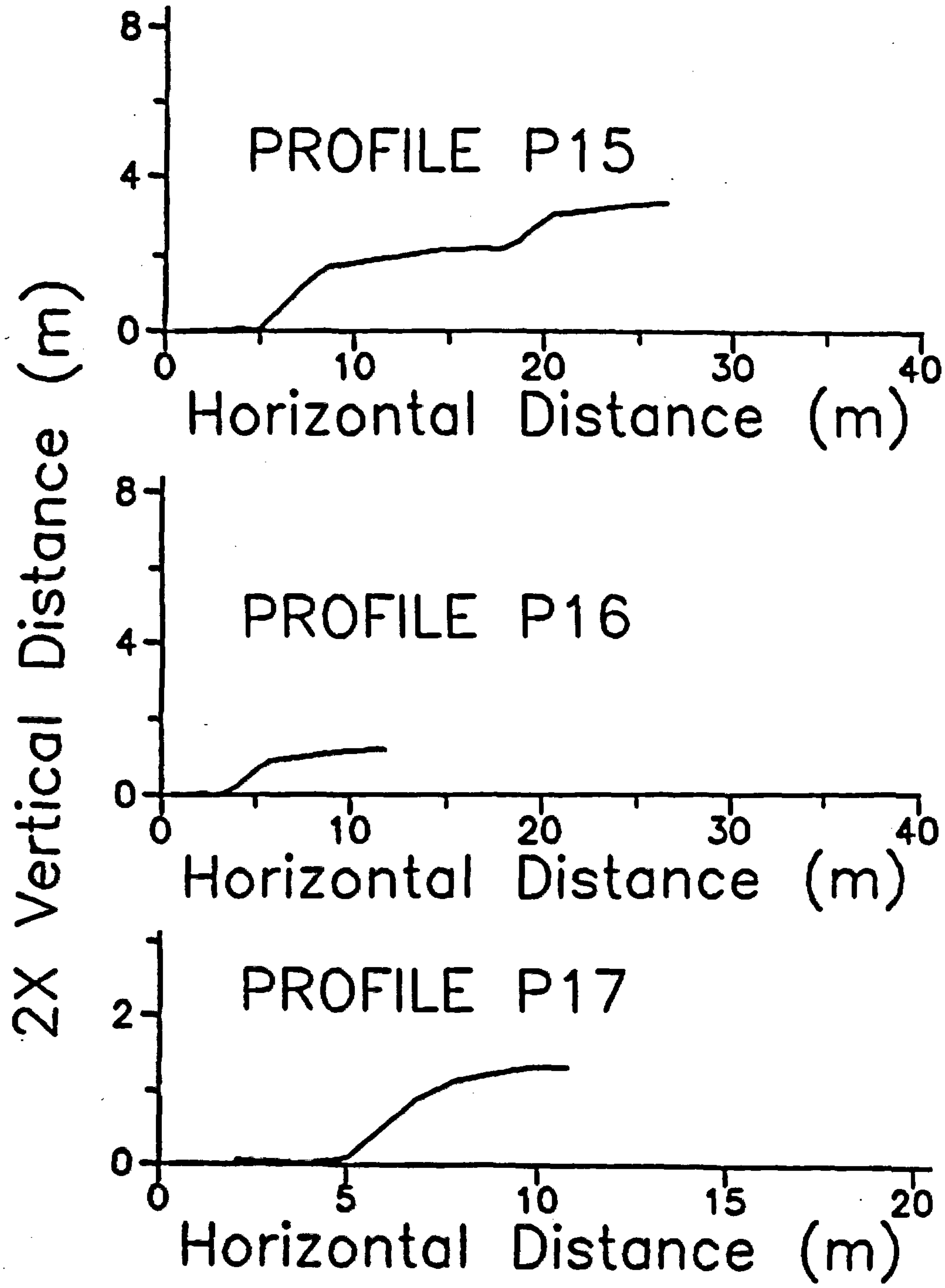
2X Vertical Distance (m)
PROFILE P15
8
4
0
0
10
20
30
40
Horizontal Distance (m)
PROFILE P16
8
4
0
0
10
20
30
40
Horizontal Distance (m)
PROFILE P17
2
0
0
5
10
15
20
Horizontal Distance (m)

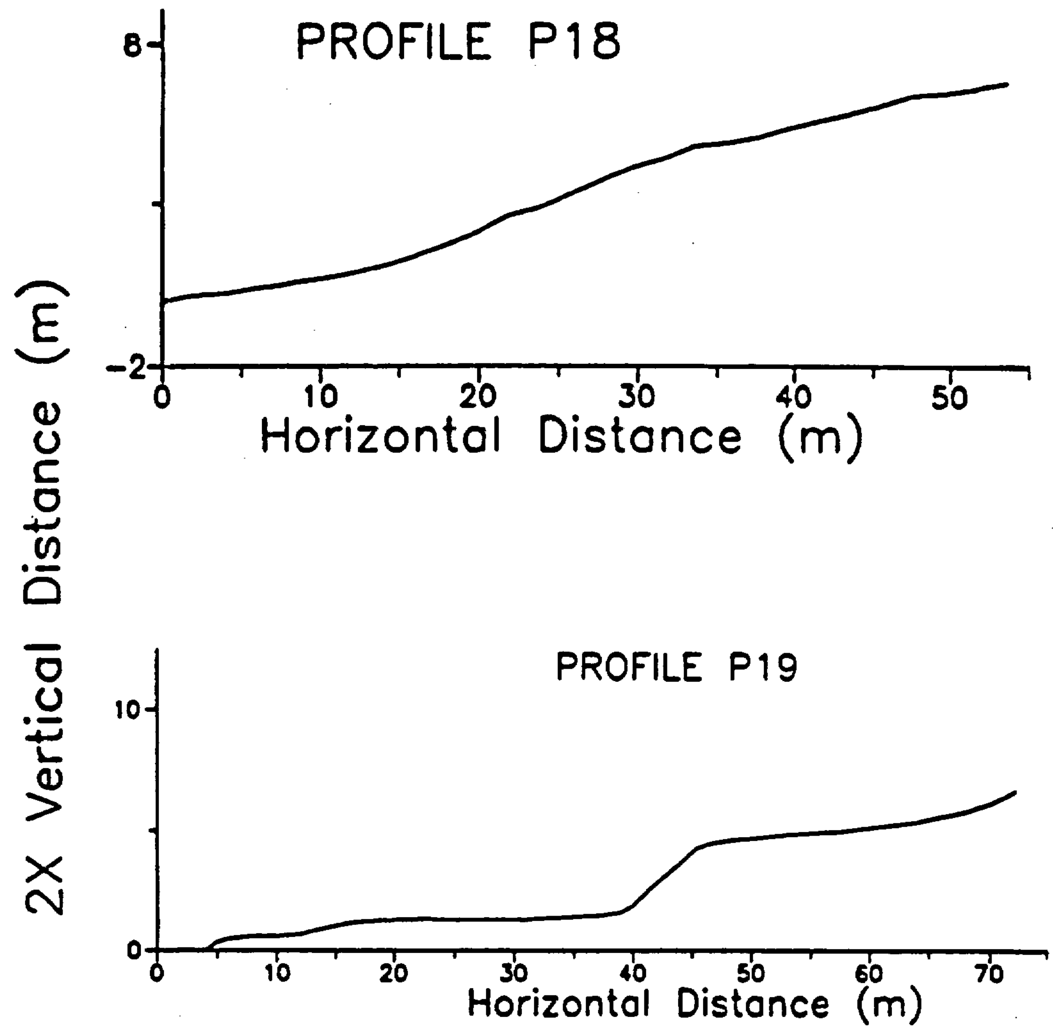
PROFILE P18
8
-2
0
10
20
30
40
50
Horizontal Distance (m)
2X Vertical Distance (m)
PROFILE P19
10
0
0
10
20
30
40
50
60
70
Horizontal Distance (m)

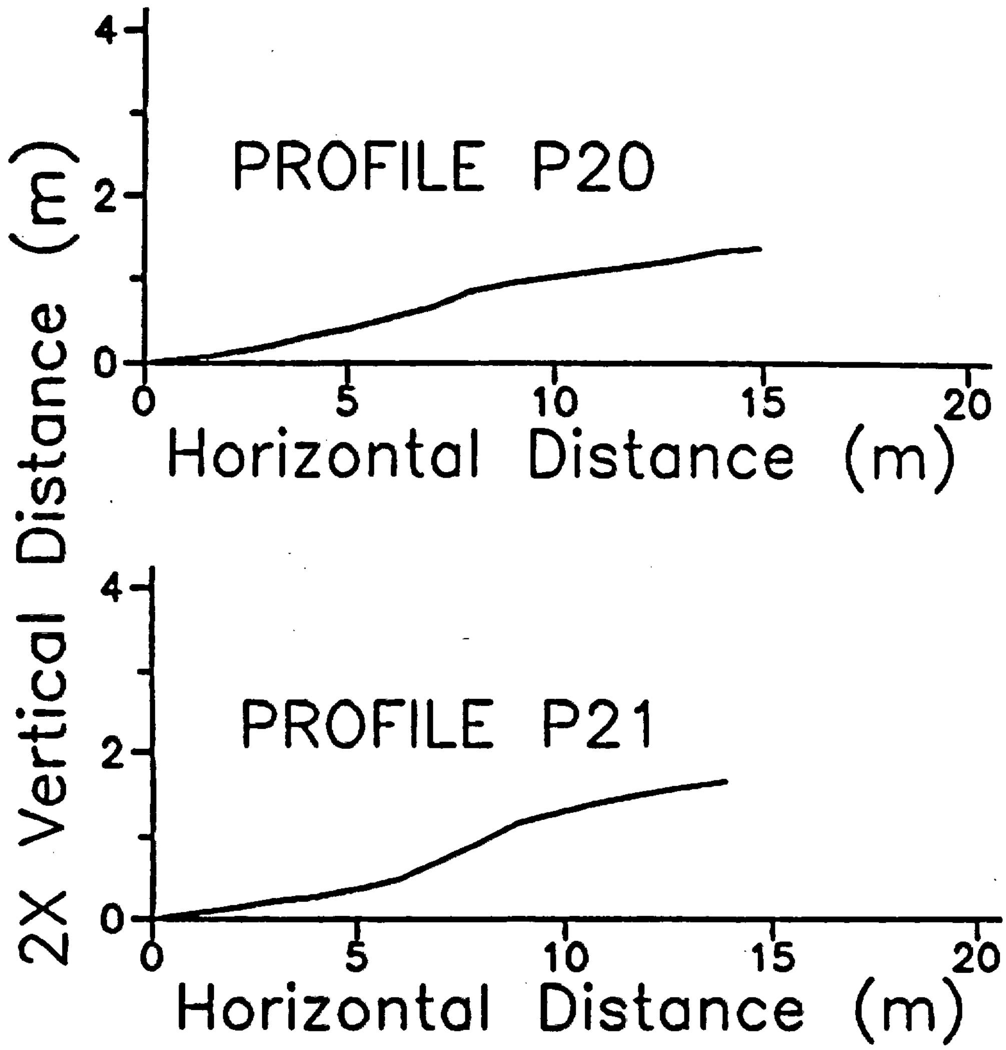
PROFILE P20
PROFILE P21
2X Vertical Distance (m)
Horizontal Distance (m)
Horizontal Distance (m)
0
2
4
0
5
10
15
20

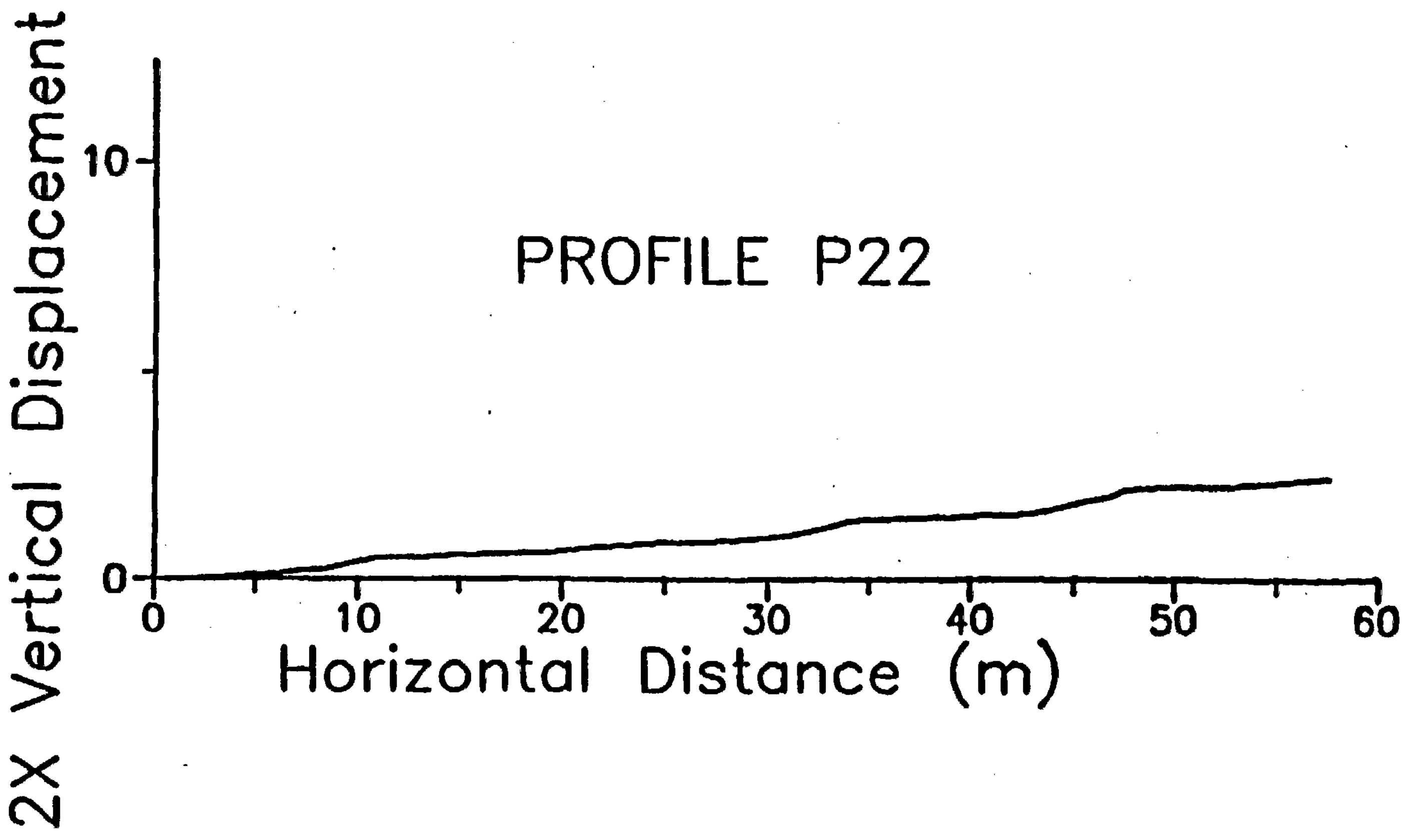
PROFILE P22
2X Vertical Displacement
10
0
0
10
20
30
40
50
60
Horizontal Distance (m)

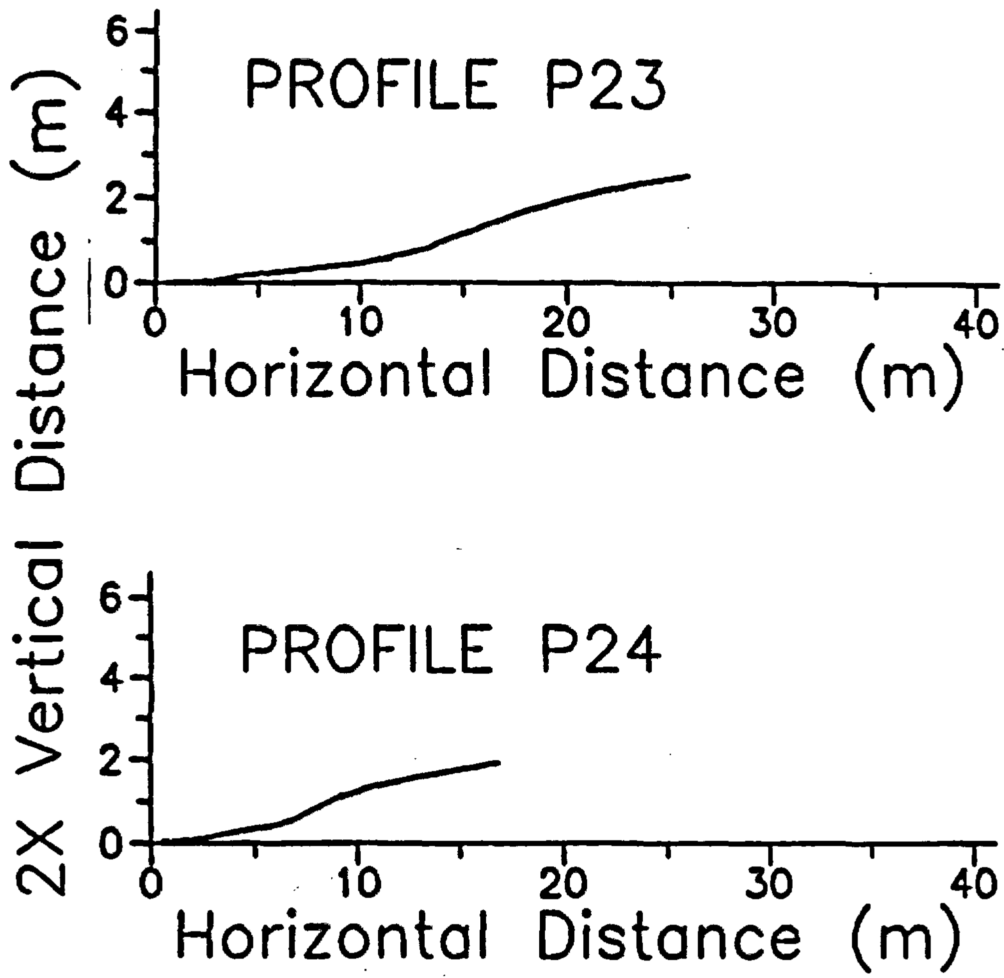
PROFILE P23
2X Vertical Distance (m)
0
2
4
6
0
10
20
30
40
Horizontal Distance (m)
PROFILE P24
0
2
4
6
0
10
20
30
40
Horizontal Distance (m)

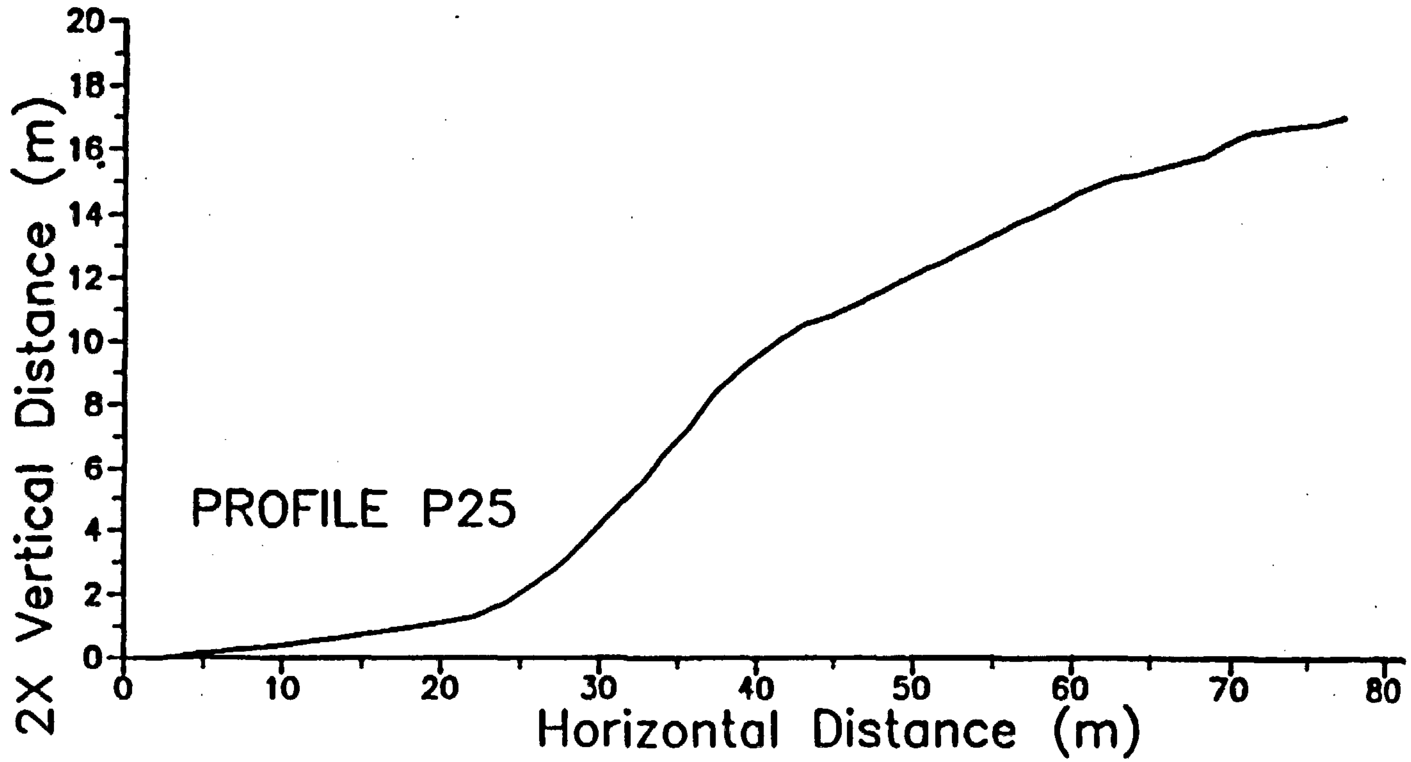
PROFILE P25
2X Vertical Distance (m)
Horizontal Distance (m)
0
2
4
6
8
10
12
14
16
18
20
0
10
20
30
40
50
60
70
80

APPENDIX VI

EDM/THEODOLITE SURVEYS

In this appendix data for three electronic distance meter (EDM) and theodolite surveys of geomorphic features offset along the FLVFZ are presented. The significance of these surveys is discussed in Chapter VI and in Appendix VII. The location of the various surveys are shown in Plate I: EDM Project 1 is shown as EDM 1; EDM Projects 2 and 3 are shown as CS 1 and CS2, respectively.

EDM PROJECT #1

EDM survey across the extensively faulted late Pleistocene Indian surface on
on the mid- and lower-Indian Creek fan.
Participants: Tom and Janet Sawyer, and Scott Lewis
EDM stations (e.g., EDM-A) and Rod # (e.g., 1-1) refer to location of the
EDM/theodolite and the prism, respectively.
This east-west traverse (i.e., azmuith angle constant) has one right step (Fig. E1).
Hence, only zenith angles and slope distances were measured.

	<------- Zenith Angle	------>						< Relative Dist.	>
EDM Station/ Rod #	Angle (deg ' '')	Angle (DD)	Angle (rads)	Slope Dist. (m)	Horiz. Dist. (m)	Height of EDM (m)	Height of Rod (m)	Hori. dist (m) X	Vertical dist (m) Z
EDM-A; shooting east									
1-1	92 59 15	92.988	1.623	122.56	122.39	1.4	1.35	122.39	-6.44
1-2	92 44 20	92.739	1.619	148.38	148.21	1.4	1.35	148.21	-7.14
1-3	92 46 05	92.768	1.619	219.72	219.46	1.4	1.35	219.46	-10.66
1-4	92 35 30	92.591	1.616	510.62	510.10	1.4	1.35	510.10	-23.13
1-5	92 17 05	92.285	1.611	528.09	527.67	1.4	1.35	527.67	-21.11
1-6	92 14 00	92.233	1.610	566.40	565.97	1.4	1.35	565.97	-22.12
1-7	92 06 10	92.103	1.608	586.37	585.98	1.4	1.35	585.98	-21.57
1-8	91 50 00	91.833	1.603	598.70	598.39	1.4	1.35	598.39	-19.20
EDM-B, at Rod 1-8; shooting east									
2-9	92 28 55	92.482	1.614	91.52	91.43	1.4	1.35	91.43	-4.01
2-10	92 26 55	92.449	1.614	225.82	225.61	1.4	2.57	225.61	-8.48
2-11	92 24 40	92.411	1.613	338.94	338.64	1.4	1.35	338.64	-14.31
2-12	92 10 25	92.174	1.609	381.19	380.92	1.4	1.35	380.92	-14.51
EDM-C, at EDM-A; shooting west									
4-16	88 06 45	88.113	1.538	21.42	21.41	1.4	1.35	21.41	0.66
4-17	89 36 50	89.614	1.564	45.55	45.55	1.4	2.57	45.55	1.48
4-18	90 24 30	90.408	1.578	74.16	74.16	1.4	1.35	74.16	-0.58
4-19	88 40 05	88.668	1.548	169.93	169.88	1.4	1.35	169.88	3.90
4-20	89 53 50	89.897	1.569	187.52	187.52	1.4	3.80	187.52	2.74
4-21	88 33 20	88.556	1.546	333.92	333.81	1.4	1.35	333.81	8.36
4-22	88 24 40	88.411	1.543	355.95	355.81	1.4	1.35	355.81	9.82
4-23	88 22 20	88.372	1.542	409.17	409.00	1.4	1.35	409.00	11.57
4-24	88 12 00	88.200	1.539	428.58	428.37	1.4	1.35	428.37	13.41
4-25	88 10 40	88.178	1.539	466.93	466.69	1.4	1.35	466.69	14.80
4-26	87 35 15	87.587	1.529	494.57	494.13	1.4	1.35	494.13	20.77
4-27	87 33 00	87.550	1.528	622.18	621.61	1.4	1.35	621.61	26.55
4-28	87 33 20	87.556	1.528	646.76	646.17	1.4	1.35	646.17	27.53
4-29	87 30 25	87.507	1.527	682.83	682.18	1.4	1.35	682.18	29.65
4-30	87 22 45	87.379	1.525	697.19	696.46	1.4	1.35	696.46	31.83
4-31	87 19 35	87.326	1.524	897.50	896.52	1.4	1.72	896.52	42.19

EDM Station/ Rod #	Zenith Angle: Angle (deg ' '')	Zenith Angle: Angle (DD)	Zenith Angle: Angle (rads)	Slope Dist. (m)	Horiz. Dist. (m)	Height of EDM (m)	Height of Rod (m)	Relative Dist.: Hori. dist (m) X	Relative Dist.: Vertical dist (m) Z
EDM-D, north of Rod 4-31 - i.e., right-step in survey line (see Plate 1).									
5-32	88 41 05	88.685	1.548	280.15	280.08	1.4	1.35	280.08	6.38
EDM-E, at Rod 5-32; shooting west									
6-33	87 33 20	87.556	1.528	95.47	95.38	1.4	1.35	95.38	4.02
6-34	85 27 25	85.457	1.492	127.31	126.91	1.4	1.35	126.91	10.03
EDM-F, at Rod 6-34; shooting west									
7-35	87 35 15	87.587	1.529	328.30	328.01	1.4	1.35	328.01	13.77
7-36	87 46 15	87.771	1.532	532.38	531.98	1.4	1.35	531.98	20.66
7-37	87 31 05	87.518	1.527	556.03	555.51	1.4	1.35	555.51	24.03
7-38	87 21 00	87.350	1.525	659.71	659.00	1.4	1.35	659.00	30.45
EDM-G, at rod 7-38									
8-39	88 06 25	88.107	1.538	114.78	114.72	1.4	1.35	114.72	3.74

EDM PROJECT 1 (Continued)

EDM Station/ Rod #	CUMULATIVE DISTANCE X (m)	Z (m)	EDM Station/ Rod #	CUMULATIVE DISTANCE X (m)	Z (m)
EDM-B					
2-12	0.00	0.00	EDM-D		
2-11	42.28	0.20	5-32	2034.44	75.84
2-10	155.31	6.03			
2-9	289.49	10.50	EDM-E		
			6-33	2129.82	79.87
EDM-A			6-34	2161.35	85.88
1-8	380.92	14.51			
1-7	393.33	12.14	EDM-F		
1-6	413.34	11.59	7-35	2489.36	99.65
1-5	451.64	12.60	7-36	2693.33	106.54
1-4	469.21	10.58	7-37	2716.86	109.91
1-3	759.85	23.05	7-38	2820.35	116.33
1-2	831.10	26.57			
1-1	856.92	27.27	EDM-G		
			8-39	2935.07	120.07
EDM-C					
4-16	878.33	27.93			
4-17	902.47	28.75			
4-18	931.08	26.69			
4-19	1026.80	31.17			
4-20	1044.44	30.01			
4-21	1190.73	35.63			
4-22	1212.73	37.09			
4-23	1265.92	38.84			
4-24	1285.29	40.68			
4-25	1323.61	42.07			
4-26	1351.05	48.04			
4-27	1478.53	53.82			
4-28	1503.09	54.80			
4-29	1539.10	56.92			
4-30	1553.38	59.10			
4-31	1754.36	69.46			

EDM PROJECT #2 - OFFSET BALLENA-PAIR, LIEDY CREEK FAN
FISH LAKE VALLEY

This EDM survey is of a pair of ballenas displaced along the the northwest (N35°W) striking master fault of the FLVFZ, in a predominently right-lateral style. These ballena are remnents of the late Pleistocene Indian morphostratigraphic unit, on the northern Leidy Creek fan in northwwestern Fish Lake Valley, Nevada (37°45' N Lat., 118°10' Long.).

All data is recorded from backsite to foresite.
Prisim 1 (backsite) was approximately due north (± 3°) of EDM-A (i.e., location of the EDM and theodolite).
[* = theodolite optics inverted]

EDM-A:	<--- Azimuth				--->	<--- Zenith			--->									
Prism #	Angle (° ' '')	Angle (DD)	Angle (rad.)	Diff. in Angles	Mean Angle (rad.)	Angle (° ' '')	Angle (DD)	Angle (rad.)	Sum of Angles (DD)	Mean Angle (rad.)	Slope Dist. (m)	Horiz. Dist. (m)	Height of EDM (m)	Height of Prism (m)	Horizontal Dist. (m) X	Horizontal Dist. (m) Y	Vertical Dist. (m) Z
1*	0 00 00	0.000	0.000	n/a	n/a	262 17 55	262.299	4.578	n/a	n/a	50.74	50.21	1.59	1.46	0.00	50.21	-7.01
2	n/a	n/a	n/a	n/a	n/a	096 44 55	96.749	1.689	359.978	1.689	85.10	84.51	1.59	1.63	-16.41	82.90	-9.98
*	348 48 00	348.800	6.088			263 13 45	263.229	4.594									
3	166 54 05	166.902	2.913	179.997	6.055	095 42 40	95.711	1.670	359.946	1.671	133.29	132.62	1.59	2.79	-30.06	129.16	-12.12
*	346 53 55	346.899	6.055			264 14 05	264.235	4.612									
4	169 28 15	169.471	2.958	179.990	6.099	094 23 45	94.396	1.648	360.000	1.641	124.17	123.93	1.59	2.78	-22.66	121.84	-7.46
*	349 27 40	349.461	6.099			266 24 15	266.404	4.650									
5	173 49 00	173.817	3.034	179.993	6.175	093 57 15	93.954	1.640	359.972	1.640	100.84	100.60	1.59	2.60	-10.84	100.01	-5.89
*	353 48 35	353.810	6.175			266 01 05	266.018	4.643									
6	000 07 15	0.121	0.002	180.000	0.002	093 49 15	93.821	1.637	359.967	1.638	76.02	75.85	1.59	2.74	0.16	75.85	-3.93
*	180 07 15	180.121	3.144			266 08 45	266.146	4.645									
7	004 52 55	4.882	0.085	179.990	0.085	094 15 15	94.254	1.645	359.976	1.645	60.69	60.50	1.59	2.75	5.84	60.25	-3.95
*	184 52 20	184.872	3.227			265 43 20	265.722	4.630									
8	012 20 00	12.333	0.215	179.982	0.215	096 12 45	96.213	1.679	359.967	1.680	63.74	63.37	1.59	2.78	13.54	61.90	-5.72
*	192 18 55	192.315	3.357			263 45 15	263.754	4.603									
9	019 29 25	19.490	0.340	180.035	0.340	098 40 00	98.667	1.722	359.964	1.722	58.83	58.16	1.59	3.94	19.39	54.83	-6.53
*	199 31 30	199.525	3.482			261 17 50	261.297	4.560									
10	049 00 25	49.007	0.855	180.011	0.855	098 27 05	98.451	1.718	359.933	1.719	46.75	46.24	1.59	3.01	34.90	30.34	-4.60
*	229 01 05	229.018	3.997			261 28 55	261.482	4.564									
11	063 24 15	63.404	1.107	180.000	1.107	098 26 05	98.435	1.718	359.945	1.718	43.60	43.13	1.59	2.76	38.56	19.31	-5.25
*	243 24 15	243.404	4.248			261 30 35	261.51	4.564									
12	084 55 05	84.918	1.482	180.000	1.482	096 36 15	96.604	1.686	359.954	1.686	41.11	40.84	1.59	1.47	40.68	3.62	-4.86
*	264 55 05	264.918	4.624			263 21 00	263.35	4.596									
13	003 26 25	3.440	0.060	179.998	0.060	098 36 25	98.607	1.721	359.970	1.721	57.36	56.71	1.49	1.38	3.40	56.61	-8.70
*	183 26 15	183.438	3.202			261 21 45	261.363	4.562									
14	018 04 45	18.079	0.316	179.999	0.316	097 32 40	97.544	1.702	359.975	1.703	40.09	39.74	1.49	1.44	12.33	37.78	-5.32
*	198 04 40	198.078	3.457			262 25 50	262.431	4.580									
15	043 11 15	43.188	0.754	179.998	0.754	097 49 40	97.828	1.707	359.979	1.708	33.33	33.02	1.49	1.50	22.60	24.07	-4.53
*	223 11 10	223.186	3.895			262 09 05	262.151	4.575									

EDM-A: <---------- Azimuth ----------> <---------- Zenith ---------->

Prism #	Angle (° ' '')	Angle (DD)	Angle (rad.)	Diff. in Angles	Mean Angle (rad.)	Angle (° ' '')	Angle (DD)	Angle (rad.)	Sum of Angles (DD)	Mean Angle (rad.)	Slope Dist. (m)	Horiz. Dist. (m)	Height of EDM (m)	Height of Prism (m)	Horizontal Dist. (m) X	Horizontal Dist. (m) Y	Vertical Dist. (m) Z
16	082 27 05	82.451	1.439	179.960	1.439	095 33 05	95.551	1.668	359.962	1.668	35.20	35.03	1.49	1.40	34.73	4.59	-3.51
*	262 24 40	262.411	4.580			264 24 40	264.411	4.615									
17	078 07 45	78.129	1.364	180.003	1.364	095 09 20	95.156	1.661	359.646	1.664	46.63	46.44	1.49	1.19	45.45	9.55	-4.63
*	258 07 55	258.132	4.505			264 29 25	264.49	4.616									
18	096 52 30	96.875	1.691	179.997	1.691	093 28 05	93.468	1.631	359.957	1.632	46.89	46.80	1.49	1.30	46.47	-5.60	-3.08
*	276 52 20	276.872	4.832			266 29 20	266.489	4.651									
19	103 26 25	103.440	1.805	179.999	1.805	092 07 25	92.124	1.608	359.982	1.608	63.54	63.50	1.49	1.37	61.76	-14.76	-2.48
*	283 26 20	283.439	4.947			267 51 30	267.858	4.675									
20	115 26 10	115.436	2.015	180.002	2.015	091 42 25	91.707	1.601	359.972	1.601	97.63	97.59	1.49	1.40	88.13	-41.91	-3.01
*	295 26 15	295.438	5.156			268 15 55	268.265	4.682									
21	106 45 55	106.765	1.863	179.996	1.863	092 32 40	92.544	1.615	359.972	1.615	105.88	105.78	1.49	2.67	101.28	-30.51	-3.54
*	286 45 40	286.761	5.005			267 25 40	267.428	4.667									
22	097 46 45	97.779	1.707	180.000	1.707	093 19 30	93.325	1.629	359.964	1.629	133.03	132.81	1.49	3.05	131.58	-17.98	-5.40
*	277 46 45	277.779	4.848			266 38 20	266.639	4.654									
23	081 15 45	81.263	1.418	180.009	1.418	094 10 25	94.174	1.644	359.975	1.644	141.60	141.30	1.49	3.91	139.66	21.47	-7.92
*	261 16 20	261.272	4.560			265 48 05	265.801	4.639									
24	048 51 55	48.482	0.846	180.390	0.843	095 38 25	95.64	1.669	359.973	1.669	160.65	159.87	1.49	1.37	119.34	106.38	-15.95
*	228 52 20	228.872	3.995			264 20 00	264.333	4.613									
25	060 28 15	60.471	1.055	179.996	1.055	094 48 40	94.811	1.655	359.960	1.655	103.15	102.79	1.49	1.35	89.44	50.66	-8.03
*	240 28 00	240.467	4.197			265 08 55	265.149	4.628									
26	090 57 40	90.961	1.588	180.013	1.587	092 59 40	92.994	1.623	359.980	1.623	66.77	66.68	1.49	1.25	66.67	-1.11	-3.73
*	270 58 25	270.974	4.729			266 59 10	266.986	4.660									
27	050 10 35	50.176	0.876	180.005	0.876	095 48 20	95.806	1.672	359.966	1.672	102.81	102.28	1.49	1.18	78.55	65.51	-10.74
*	230 10 50	230.181	4.017			264 09 35	264.16	4.610									
28	038 15 50	38.264	0.668	179.993	0.668	098 19 55	98.332	1.716	359.965	1.717	123.86	122.55	1.49	1.30	75.90	96.22	-18.10
*	218 15 25	218.257	3.809			261 38 00	261.633	4.566									
29	019 58 15	19.971	0.349	180.000	0.349	096 54 25	96.907	1.691	359.971	1.692	88.64	88.00	1.49	1.23	30.05	82.71	-10.94
*	199 58 15	199.971	3.490			263 03 50	263.064	4.591									
30	029 17 25	29.290	0.511	180.010	0.511	098 54 55	98.915	1.726	359.969	1.727	111.67	110.32	1.49	1.42	53.96	96.23	-17.40
*	209 18 30	209.308	3.653			261 03 15	261.054	4.556									

EDM-A: (-------------- Azmuith ----------------)(---------------- Zenith --------------)

Prism #	Angle (° ' '')	Angle (DD)	Angle (rad.)	Diff. in Angles	Mean Angle (rad.)	Angle (° ' '')	Angle (DD)	Angle (rad.)	Sum of Angles (DD)	Mean Angle (rad.)	Slope Dist. (m)	Horiz. Dist. (m)	Height of EDM (m)	Height of Prism (m)	Horizontal Dist. (m) X	Y	Vertical Dist. (m) Z
31	031 14 30	31.242	0.545	179.993	0.545	098 20 45	98.346	1.716	359.967	1.717	173.69	171.85	1.49	1.51	89.14	146.92	-25.24
*	211 14 05	211.235	3.687			261 37 15	261.621	4.566									
32	021 58 50	21.981	0.384	180.007	0.384	095 50 20	95.839	1.673	359.961	1.673	164.38	163.53	1.49	1.42	61.20	151.64	-16.04
*	201 59 15	201.988	3.525			264 07 20	264.122	4.610									
33	016 21 10	16.353	0.285	180.010	0.285	095 33 00	95.55	1.668	360.122	1.669	157.81	157.07	1.49	1.36	44.21	150.72	-15.56
*	196 21 45	196.363	3.427			264 34 20	264.572	4.618									
34	004 22 15	4.371	0.076	180.001	0.076	094 31 40	94.528	1.650	359.960	1.650	79.94	79.69	1.49	1.42	6.07	79.46	-6.40
*	184 22 20	184.372	3.218			265 25 55	265.432	4.633									
35	358 38 30	358.642	6.259	179.991	6.260	094 51 05	94.851	1.655	359.958	1.656	159.22	158.65	1.49	3.09	-3.75	158.61	-11.12
*	178 39 05	178.651	3.118			265 06 25	265.107	4.627									
36	337 05 00	337.083	5.883	180.000	5.883	093 19 00	93.317	1.629	359.943	1.629	163.75	163.48	1.49	2.71	-63.66	150.57	-8.34
*	157 05 00	157.083	2.742			266 37 35	266.626	4.654									
37	341 26 25	341.44	5.959	179.990	5.959	093 58 10	93.969	1.640	359.950	1.641	107.85	107.59	1.49	1.23	-34.24	102.00	-7.77
*	161 27 00	161.45	2.818			265 58 50	265.981	4.642									
38	327 40 15	327.671	5.719	179.996	5.719	091 45 15	91.754	1.601	359.951	1.602	128.17	128.11	1.49	1.43	-68.51	108.25	-3.91
*	147 40 30	147.675	2.577			268 11 50	268.197	4.681									
39	316 32 15	316.538	5.525	179.991	5.525	090 23 55	90.399	1.578	359.782	1.580	166.02	166.02	1.49	3.91	-114.74	121.09	-3.09
*	136 32 50	136.547	2.383			269 23 00	269.383	4.702									
40	296 45 50	296.764	5.180	179.993	5.180	087 19 20	87.321	1.524	359.957	1.524	106.91	106.79	1.49	2.67	-95.35	48.10	3.78
*	116 46 15	116.771	2.038			272 38 10	272.636	4.758									
41	282 11 05	282.185	4.925	179.992	4.925	086 26 30	86.442	1.509	359.961	1.509	93.8	93.62	1.49	2.70	-91.51	19.77	4.50
*	102 11 35	102.193	1.784			273 31 10	273.519	4.774									
42	279 41 30	279.692	4.882	180.004	4.882	086 55 05	86.918	1.517	359.962	1.517	155.16	154.94	1.49	3.96	-152.73	26.08	5.83
*	099 41 15	99.688	1.740			273 02 45	273.044	4.766									
43	261 58 40	261.978	4.572	179.996	4.572	085 14 45	85.246	1.488	359.972	1.488	130.51	130.03	1.49	2.78	-136.60	-19.26	10.24
*	081 58 55	81.982	1.431			274 43 15	274.728	4.795									
44	253 41 15	253.688	4.428	180.002	4.428	089 17 30	89.292	1.558	359.959	1.559	89.4	89.39	1.49	2.69	-85.79	-25.11	-0.12
*	073 41 10	73.686	1.286			270 40 00	270.667	4.724									
45	240 11 45	240.196	4.192	179.992	4.192	086 02 20	86.039	1.502	359.963	1.502	82.23	82.03	1.49	2.49	-71.19	-40.77	4.66
*	060 12 15	60.204	1.051			273 55 25	273.924	4.781									

EDM PROJECT #3

Project 3 is an EDM/theodolite survey of an abandoned drainage channel displaced along the N-NW (N15W) striking master fault of the FLVFS, in a right-divergent style. The channel, which is flanked by degraded lateral debris flow levees, is continuous across the prominent east-facing scarp formed by the master fault on the Indian Creek fanhead (Plate 1).
Participants: Tom and Janet Sawyer.
All data is recorded from backsite (azmith angle = 0 0' 00'') to foresite (rod).
* = inverted optics

	<--------Azmith Angle				------------------>	<--------Zenith Angle				------------------------>							
Rod #	Angle (deg ' '')	Angle (DD)	Angle (rads)	Sum of Angles (DD)	Mean Angle (rads)	Angle (deg ' '')	Angle (DD)	Angle (rads)	Sum of Angles (DD)	Mean Angle (rads)	Slope Dist. (m)	Horiz. Dist. (m)	Height of EDM (m)	Height of Prism (m)	Horizontal Distances X	Y	Vertical Distance Z
Back-site*	0 00 00	0.000	0.000	0.000	0.000	000 00 00	0.000	0.000	0.000	0.000	0.00	0.00	1.61	0.50	0.00	0.00	0.00
1*	320 40 55	320.682	5.597	180.017	2.603	263 50 15	263.838	4.605	359.970	1.693	356.90	354.25	1.61	1.33	181.64	-304.13	-43.72
	140 39 55	140.665	2.455			096 07 55	96.132	1.678									
2*	332 58 20	332.972	5.811	179.998	2.669	263 15 35	263.26	4.595	359.927	1.724	289.40	286.03	1.61	1.33	130.22	-254.66	-44.35
	152 58 25	152.974	2.670			096 40 00	96.667	1.687									
3*	340 35 45	340.596	5.945	180.007	2.806	262 57 20	262.955	4.589	360.054	1.722	246.96	244.15	1.61	1.33	80.38	-230.56	-37.41
	160 35 20	160.589	2.803			097 05 55	97.099	1.695									
4*	350 02 15	350.038	6.109	179.999	2.967	262 16 05	262.268	4.577	359.997	1.707	197.50	195.67	1.61	2.03	33.94	-192.70	-26.03
	170 02 20	170.039	2.968			097 43 45	97.729	1.706									
5*	007 01 15	7.021	0.123	180.012	3.270	264 57 55	264.965	4.625	359.930	1.692	54.46	54.06	1.61	1.33	-6.94	-53.61	-6.89
	187 02 00	187.033	3.264			094 57 55	94.965	1.657									
6*	127 00 35	127.010	2.217	179.972	5.344	272 10 25	272.174	4.750	359.986	1.540	36.47	36.45	1.61	1.33	-29.42	21.52	1.42
	306 58 55	306.982	5.358			087 48 45	87.812	1.533									
7*	119 47 30	119.792	2.091	180.001	5.233	276 28 05	276.468	4.825	359.958	1.478	53.60	53.37	1.61	1.33	-46.30	26.54	5.24
	299 47 35	299.793	5.232			083 29 25	83.49	1.457									
8*	120 40 15	120.671	2.106	179.989	5.242	275 34 55	275.582	4.810	359.954	1.496	149.99	149.57	1.61	2.03	-129.08	75.56	10.45
	300 39 35	300.660	5.248			084 22 20	84.372	1.473									

EDM-A:	<-------------- Azimuth					----------------><	Zenith												
Prism #	Angle (° ' '')	Angle (DD)	Angle (rad.)	Diff. in Angles	Mean Angle (rad.)	Angle (° ' '')	Angle (DD)	Angle (rad.)	Sum of Angles (DD)	Mean Angle (rad.)	Slope Dist. (m)	Horiz. Dist. (m)	Height of EDM (m)	Height of Prism (m)	Horizontal Dist. (m) X	Y	Vertical Dist. (m) Z
46	207 19 25	207.324	3.618	180.000	3.618	084 12 05	84.201	1.470	359.980	1.470	70.63	70.27	1.49	2.58	-32.25	-62.43	6.04
*	027 19 25	27.324	0.477			275 46 45	275.779	4.813									
47	190 48 20	190.806	3.330	179.996	3.330	086 17 40	86.294	1.506	359.969	1.506	76.56	76.40	1.49	1.43	-14.33	-75.04	4.99
*	010 48 35	10.81	0.189			273 40 30	273.675	4.777									
48	158 49 40	158.828	2.772	180.003	2.772	087 44 35	87.743	1.531	359.996	1.531	43.07	43.04	1.49	1.33	15.03	-40.08	1.89
*	338 49 50	338.831	5.914			272 15 10	272.253	4.752									
49	199 09 20	199.156	3.476	179.992	3.476	084 48 40	84.811	1.480	359.964	1.481	23.05	22.96	1.49	1.07	-7.53	-21.60	2.50
*	019 09 50	19.164	0.334			275 09 10	275.153	4.802									
50	079 29 55	79.499	1.388	n/a	1.388	095 07 20	95.122	1.660	n/a	1.660	9.94	9.90	1.49	1.33	9.73	1.80	-1.05
51	340 32 10	340.536	5.943	179.980	5.944	101 27 20	101.456	1.771	359.974	1.771	25.93	25.41	1.49	1.31	-8.46	23.96	-5.34
*	160 33 20	160.556	2.802			258 31 05	258.518	4.512									
52	300 08 50	300.147	5.239	178.994	5.247	091 01 30	91.025	1.589	359.964	1.589	71.33	71.32	1.49	1.31	-61.36	36.36	-1.40
*	120 09 10	121.153	2.115			268 56 20	268.939	4.694									
53	332 27 05	322.451	5.628	180.000	5.628	096 20 50	96.347	1.682	359.971	1.682	61.39	61.01	1.49	1.26	-37.10	48.37	-7.04
*	142 27 05	142.451	2.486			263 37 25	263.624	4.601									

APPENDIX VII

CALCULATION OF SLIP RATE ESTIMATES

Slip rates are calculated in this appendix from displacement and age (i.e., duration of slip accumulation) estimates, discussed in Chapter VI. The horizontal and vertical components of displacement were measured from EDM/theodolite surveys (Appendix V) and during general field investigations (e.g., Appendix VI, Profile 23). These data are used to estimate other components of slip, for example the oblique-slip component that best characterizes the predominant right-divergent style of the FLVFZ.

Figure 32 shows the geometrical and mathematical relations of Clark and others (1984) between the various components of slip. These relations are applied to the measured displacement data in this appendix.

LATE PLEISTOCENE SLIP RATES

CASE STUDY 1

The northwest-striking (N35°W, avg.) master fault of the northern FLVFZ displaces a concordant pair of broad, ridge-like alluvial fan remnants (or ballenas) in a right-lateral sense (Fig. 23). The ballenas are remnants of the late Pleistocene Indian morphostratigraphic unit. One of the remnants forms a shutter ridge that diverts a drainage northward along the fault.

DISPLACEMENT ESTIMATES

A dominant component of right slip is suggested by the ballena pair. The horizontal (H) and vertical (V) components of displacement were measured from an EDM/theodolite survey (Figs. 23 and 24; Appendix V, EDM Project 2). The measured displacement data is used to determine the dip-slip (D) and total-slip (T) components, as shown in Figure 32.

It is frequently necessary in determining components of slip to estimate the dip of a fault. A slight northeastward dip of the master fault in the Case Study 1 area is suggested from a gradual 15° to 20° northward bend in the fault (Fig. 23; Plate I). In calculating components of slip (below), the fault was assumed to dip from 70° (e.g., $\delta = 70°$, $\alpha = 20°$) to vertical ($\delta = 90°$, $\alpha = 0°$ and therefore D = V).

The displacement estimates (shown below) include uncertainties associated with erosional modifications of the ballenas morphology (discussed in Chapter VI). Specifically, the size of the EDM survey points in Figures 23 and 24 are proportional to the inferred maximum shift (lateral or vertical) in the position of the ballena crests, due to erosional modifications. The one exception is the southern ballena remnant east of the fault, which appears to have been modified to a significantly greater degree (discussed below).

Northern Ballena Remnants

The following displacement estimates have been determined form geometrical relations of the northern ballena remnants across the northwest-striking (N35°W) master fault of the northern FLVFZ (Figs. 23 and 24).

H_r = 72 to 107 m, 92 m (preferred) - right slip
V = 0 to 11 m, 5 m (preferred) - (reverse) vertical slip
D = 0 to 12 m, 5 m (preferred) - (reverse) dip slip
T = 72 to 119 m, 97 m (preferred) - right-convergent slip

Southern Ballena Remnants

Air-photo and field examinations suggests the southern ballena remnant east of the fault has been extensively modified by erosion. In particular, little remains of the south side of this remnant adjacent to the fault. These erosional modifications result in an apparent displacement of the southern ballena crest, which is less than the actual displacement. Hence, there is no preferred projection of this crest (Figs. 23 and 24), and therefore no preferred displacement estimates.

The following displacement estimates have been determined form geometrical relations of the southern ballena remnants across the northwest-striking (N35°W) master fault of the northern FLVFZ (Figs. 23 and 24).

$H_r \leq$ 37 to 74 m - right slip
V ≤ 2 m (normal) to 6 m - (reverse) vertical slip
D ≤ 2 m (normal) to 6 m - (reverse) dip slip
T ≤ 39 to 80 m - right-oblique slip

AGE ESTIMATES

The offset ballenas are erosional remnants of the late Pleistocene Indian morphostratigraphic unit, and therefore, are younger than this unit. The Indian unit is younger than the McAfee Creek unit, which is younger than the Bishop tuff (740 ka)(discussed in Chapter IV).

The surface of the ballenas, like the relict Indian surface exhibit "swarms" of prominent solifluction steps, forming patterned ground. The modification of alluvial fan remnants by solifluction is in part, time dependent (Sawyer, 1988a; discussed in Appendix I). In Fish Lake Valley, solifluction steps only occur on late Pleistocene (Indian unit) and older alluvial fan remnants. This suggests a late Pleistocene age for the offset ballena pair.

In Crater Flat, southern Nevada, solifluction steps occur on the Yucca and early Black Cone geomorphic surfaces of Peterson (1988, Appendix I). Dorn (1987) estimated dates of 360 to 380 ka from the Yucca surface and 128 to 137 ka from the early Black Cone surface, based on cation-ratio analysis of desert varnish on surficial lithic fragments.

The surface characteristics (e.g., varnish and pavement development) of the Indian morphostratigraphic unit in Fish Lake Valley (Table 1) are similar to the Yucca surface in Crater Flat, and are generally more prominent than the early Black Cone surface (c.f. Peterson, 1988; Ramelli and others, 1990). The Indian soil has 20 to 30 cm thick argillic horizons (Appendix II), which are apparently similar to those of the Yucca soil (c.f. Peterson, 1988). In contrast, the Indian soil lacks strongly cemented K horizons which are characteristic of the Yucca soil. The stage II to III carbonate development of the Indian soil accords with that development in the early Black Cone soil. These surface and soil characteristics suggest the Indian unit is at least as old as the early Black Cone surface, but younger than the Yucca surface. A numerical age range of 100 to 360 ka is assigned to the Indian unit.

In accordance with the position advocated in Chapter VI, the ballenas are assumed to be roughly half the age of the Indian unit, and hence are assigned an age of 50 to 180 ka. The medial age of 120 ka, was used in "preferred" slip-rate estimates (below). The age of the ballenas is taken to represent the duration of slip accumulation.

SLIP RATE ESTIMATES

The following slip rates are based on age and displacement data from Case Study 1 (Chapter VI; summarized above).

Northern Ballena Remnants

Style Component	Estimated Slip Rate Minimum	Maximum	Preferred
H, - right slip	0.4	2.1	0.8
V - vertical (reverse) slip	0.0	0.2	<0.1
D - dip (reverse) slip	0.0	0.2	<0.1
T - right-oblique slip	0.4	2.4	0.8

Southern Ballena Remnants

As discussed above, erosional modifications of the southern ballena remnant east of the fault result in an apparent offset that is less than the horizontal slip component (H,). Thus, slip rates based on H, provide minimum estimates.

Style Component	Estimated Slip Rate (mm/yr) Minimum	Maximum

H_L - right slip	≥0.2	≥1.5
V - vertical slip (normal)	≥0.0	≥0.1
V - vertical slip (reverse)	≥0.0	≥0.1
D - dip slip	≥0.0	≥0.1
T - right-oblique slip	≥0.2	≥1.6

CASE STUDY 2

The north-northwest-striking (N20°W) master fault of the northern FLVFZ displaces an abandoned drainage channel in a right-divergent style on the Indian Creek fanhead, approximately 5 km north of Case Study 1 (Plate I). The offset channel is associated with the late Pleistocene Indian morphostratigraphic unit (discussed in a following section).

DISPLACEMENT ESTIMATES

The horizontal (H_L) and vertical (V) components of displacement were measured from an EDM/theodolite survey (Appendix V, EDM Project 3), which is shown graphically in Figures 25 and 26. The master fault is inferred to dip 75°E (± 15°), based on observed dips (from 90° to 65°E) of this fault and subparallel faults in the Case Study 2 area.

Erosional modifications of the channel were evaluated (discussed in Chapter VI) and are reflected in the following displacement estimates.

H_L = 83 to 165 m, 122 m (preferred) - right-lateral slip
V = 27 to 52 m, 40 m (preferred) - (normal) vertical slip
D = 27 to 60, 41 m (preferred) - (normal) dip slip
T = 110 to 225 m, 163 m (preferred) - right-divergent slip

AGE ESTIMATES

The drainage channel, offset by the north-northwest-striking master fault of the northern FLVFZ, is only shallowly incised into the late Pleistocene Indian morphostratigraphic unit on the Indian Creek fanhead. The offset channel appears to grade to the Indian surface in the mid-fan area. Degraded lateral debris flow levees, displaying prominent solifluction steps, flank the extent of the channel. These relations suggest that the channel transported debris across and to the Indian surface. Therefore, the channel developed during, or shortly after the Indian surface stabilized. Hence, the numerical age range of the Indian unit (100 to 360 ka, discussed in Case Study 1) is used to represent the age of the offset channel and the duration of slip accumulation. The medial age of 230 ka is used in "preferred" slip-rate estimates.

The following slip rates are based on age and displacement data from Case Study 2.

Style Component	Estimated Slip-Rate (mm/yr) Minimum	Maximum	Preferred
H_s - right-lateral	0.2	1.7	0.5
V - normal	0.1	0.5	0.2
D - normal	0.1	0.6	0.2
T - right-divergent	0.3	2.3	0.7

LATEST-PLEISTOCENE TO HOLOCENE SLIP-RATE ESTIMATES

CASE STUDY 3

An onfan drainage is shallowly incised into the latest-Pleistocene to mid Holocene Leidy morphostratigraphic unit, on the Indian Creek fanhead. The channel is displaced in a right-divergent style along the north-northwest striking (N20°W avg.) master fault of the northern FLVFZ, approximately 1 km north of Case Study 2 (Fig. VIB).

DISPLACEMENT ESTIMATES

Right-slip (H_s) on the master fault was determined from field measurements, considering probable channel projections and erosional modifications. Normal-slip (V) was measured from a slope-stick/Brunton profile of a scarp adjacent to the channel and formed in the Leidy surface by movement along the master fault (Appendix IV; Profile 23). A fault dip of 90° to 60° (75° preferred) is assumed; i.e., same as in Case Study 2.

The channel is wider on the down-thrown side of the fault, than on the relatively upthrown side (Fig. F7). This suggests lateral erosion of the southern channel margin. Thus, the maximum lateral offset of the channel is largely apparent, and thus is greater than the horizontal-slip (i.e., $>H_s$).

H_s = 3 to <15 m, 5 m (preferred) - right-lateral slip
V = 0.7 to 1.3 m, 1 m (preferred) - normal-slip
D = 0.7 to 1.5 m, 1 m (preferred)
T = 4 to <17 m, 6 m (preferred) - right-divergent-slip

AGE ESTIMATES

The offset channel can be no older than the latest- Pleistocene to mid Holocene (Table 3, ≤18 to ≥4 ka) Leidy morphostratigraphic unit, in which it is shallowly incised. Morphostratigraphic relations suggest the channel was beheaded by incision of Indian Creek, before stabilization of the late Holocene

Chapter VI), change with deviations in fault strike. That is, the rate of right slip is greater where the fault strikes northwestward (e.g., at Case Study 1), as compared to where it strikes north-northwestward (e.g., at Case Studies 2 and 3). The converse apparently applies to rates of dip-slip faulting.
(Table 3, 1.5 to 2.4 ka), early Marble unit. Therefore the channel is probably about the same age, or slightly younger than, the Leidy unit. A conservative age estimate of 18 to 6 ka (8 ka preferred) is assigned to the offset channel, used to represent the duration of slip accumulation.

SLIP RATE ESTIMATES

The following slip-rates are based on age and displacement data from Case Study 3.

Style Component	Estimated Slip-Rate (mm/yr) Minimum	Maximum	Preferred
H_s - right-lateral	0.2	<2.5	0.6
V - normal	<0.1	0.2	0.1
D - normal	<0.1	0.2	0.1
T - right-divergent	0.2	<2.8	0.8

DISCUSSION OF SLIP RATE ESTIMATES

The slip rates estimated in this appendix take into account some of the inherent uncertainties in the age (i.e., slip accumulation interval) and displacement data. The late Pleistocene slip rates (i.e., Case Studies 1 and 2) are generally comparable with the latest-Pleistocene to Holocene rates, despite their independent determination. This suggests little (if any?) change in the rate of faulting along the northern FLVFZ is required in the late Quaternary.

The preferred right-lateral (H_s) and right-oblique (T) slip rates are slightly higher, and the preferred dip-slip rates slightly lower, at Case Study 1, relative to the other two case studies. Apparently, slip rates, like faulting styles (discussed in

APPENDIX VIII: DETERMINATION OF MAGNITUDE BY REGRESSION ANALYSIS

The various fault rupture parameters discussed in Chapter VIII are evaluated using the regression equations developed by Slemmons (1982), Bonilla and others (1984), and Slemmons and others (1988). The regressions equations are listed (below) relative to fault rupture parameters.

[Data Set: All and W.N. A = all fault types worldwide and North America, respectively; SS = strike-slip faults only DIP = dip-slip faults (normal and reverse); NORM = normal faults only]

From:	Data Set	Regression eqn.	R squard	Stn. Dev.
LENGTH:				
Slemmons and others 1988				
	All	Ms = 5.39 + 1.03 (Log L)	0.83	0.83
	SS	Ms = 5.50 + 0.95 (Log L)	0.87	0.22
	DIP	Ms = 5.10 + 1.25 (Log L)	0.79	0.34
Extensional events only				
	All	Ms = 5.48 + 0.93 (Log L)	0.71	0.29
	SS	Ms = 5.17 + 1.12 (Log L)	0.82	0.25
	DIP	Ms = 5.57 + 0.87 (Log L)	0.55	0.35
Bonilla and others 1984				
	SS	Ms = 6.24 + 0.619 (Log L)	0.498	0.293
	W.N. A	Ms = 5.17 + 1.237 (Log L)	0.7	0.324
	ALL	Ms = 6.04 + 0.708 (Log L)	0.438	0.306
DISPLACEMENT:				
Slemmons 1982				
	ALL	Ms = 6.821 + 0.847 (Log D)	0.55	0.331
	NORM	Ms = 6.668 + 0.750 (Log D)	0.5	0.422
	SS	Ms = 6.974 + 0.804 (Log D)	0.715	0.323
Bonilla and others 1984				
	SS	Ms = 7.00 + 0.782 (Log D)	0.376	0.331
	W.N. A	Ms = 6.98 + 0.742 (Log D)	0.454	0.442
	ALL	Ms = 6.95 + 0.723 (Log D)	0.398	0.323

PALEOSEISMIC APPROACH TO SIZE DETERMINATION

Fault Parameter: Displacements measured or inferred from exploratory trench studies;
(* calculated with vert. displ; all other calculations based on inferred lateral-slip)

Site where Displacement was measured	Vert. Displ. (m)	Inferred Range Lat. Displ (m)	Slemmons, 1982: All (Range)	All (Mean)	Norm*	SS (Range)	SS (Mean)	Bonilla et al, 1984: SS (Range)	SS (Mean)	NM AN (Range)	NM AN (Mean)	ALL (Range)	ALL (Mean)
Excavation Site 1	0.17	1.7	7.0	6.9	6.1	7.2	7.0	7.2	7.1	7.2	7.0	7.1	7.0
		0.6	6.6			6.8		6.8		6.8		6.8	
	0.21	2.1	7.1		6.2	7.2		7.3		7.2		7.2	
		1.1	6.9			7.0		7.0		7.0		7.0	
Excavation Site 2	0.25	0.8	6.7	6.6	6.2	6.9	6.7	6.9	6.8	6.9	6.7	6.9	6.7
		0.25	6.3			6.5		6.5		6.5		6.5	
	0.31	0.9	6.8		6.3	6.9		7.0		6.9		6.9	
		0.3	6.4			6.6		6.6		6.6		6.6	

Fault Parameter: Paleo-rupture lengths determined by geomorphological analyses;

Section along PLVFZ	Section Length (km)	Slemmons and others, 1988: All Events, All Range	All Mean	All Events, SS Range	SS Mean	Extensional Events, All Range	All Mean	Extensional Events, SS Range	SS Mean	Bonilla et al, 1984: SS Range	SS Mean	NM Range	NM Mean	ALL Range	ALL Mean
Northern Rupture	20	6.7	6.8	6.7	6.8	6.7	6.8	6.6	6.7	7.0	7.1	6.8	6.9	7.0	7.0
	30	6.9		6.9		6.9		6.8		7.2		7.0		7.1	
Southern Rupture	30	6.9	7.0	6.9	7.0	6.9	6.9	6.8	6.9	7.2	7.2	7.0	7.1	7.1	7.1
	40	7.0		7.0		7.0		7.0		7.2		7.2		7.2	

Fault Parameter: Single event displacements based on scarp profiles measured
along the Northern paleoseismic rupture zone (Appendix IV).
(* calculated with vertical displacement, all other calculations based on inferred
inferred lateral-slip (see Chapter VIII))

Fault Scarp Profile #	Single Event Vert. Displ. (m)	Inferred Range in Lat Displ (m)	Slemmons, 1982: All (Range)	All (Mean)	Norm*	SS (Range)	SS (Mean)	Bonilla et al, 1984: SS Range	SS Mean	NM AN Range	NM AN Mean	ALL Range	ALL Mean
Profile P20	0.15	1.5	7.0	6.8	6.1	7.2	7.0	7.2	7.0	7.2	7.0	7.1	7.0
		0.7	6.6			6.8		6.8		6.8		6.8	
Profile P21	0.65	2.0	7.1	6.9	6.5	7.2	7.0	7.2	7.0	7.2	7.0	7.2	7.0
		0.6	6.6			6.8		6.8		6.8		6.8	
Profile P26	0.25	1.5	7.0	6.8	6.2	7.1	7.0	7.1	7.0	7.1	7.0	7.1	7.0
		0.7	6.7			6.8		6.9		6.9		6.8	

Fault Parameter: Arbitrary rupture length scenarios;

Arbitrary Length	Rupture Length (km)	Regression Magnitude Estimate: Slemmons and others, 1982 — All Events (--All --) Range	Mean	(-- SS ---) Range	Mean	Extensional Events (--All --) Range	Mean	(----SS---) Range	Mean	Bonilla et al, 1984 (---SS----) Range	Mean	(--NM AN--) Range	Mean	(-- ALL --) Range	Mean
Total	350	8.0	8.0	7.9	7.9	7.8	7.8	8.0	8.0	7.8	7.8	8.3	8.3	7.8	7.8
DVFZ	320	8.0		7.9		7.8		8.0		7.8		8.3		7.8	
Half	180	7.7	7.7	7.6	7.6	7.6	7.6	7.7	7.7	7.6	7.6	8.0	7.9	7.6	7.6
DVFZ	160	7.7		7.6		7.5		7.6		7.6		7.9		7.6	
Total	70	7.3	7.3	7.3	7.3	7.2	7.2	7.2	7.3	7.4	7.4	7.5	7.5	7.3	7.4
FLVFZ	80	7.4		7.3		7.2		7.3		7.4		7.5		7.4	
Half	35	7.0	7.0	7.0	7.0	6.9	6.9	6.9	6.9	7.2	7.2	7.1	7.1	7.1	7.2
FLVFZ	40	7.0		7.0		7.0		7.0		7.2		7.2		7.2	

SEGMENTATION APPROACH TO SIZE DETERMINATION

Fault Parameter: Rupture-segment length scenarios;

Segment Length	Rupture Length (km)	Regression Magnitude Estimate: Slemmons and others, 1982 — All Events (--All --) Range	Mean	(-- SS ---) Range	Mean	Extensional Events (--All --) Range	Mean	(----SS---) Range	Mean	Bonilla et al, 1984 (-- SS ---) Range	Mean	(--NM AN--) Range	Mean	(-- ALL --) Range	Mean
FLVFZ	65	7.3	7.3	7.2	7.3	7.2	7.2	7.2	7.2	7.4	7.4	7.4	7.5	7.3	7.3
Segment	75	7.3		7.3		7.2		7.3		7.4		7.5		7.4	
Northern	20	6.7	6.8	6.7	6.8	6.7	6.7	6.6	6.7	7.0	7.1	6.8	6.8	7.0	7.0
Segment	25	6.8		6.8		6.8		6.7		7.1		6.9		7.0	
Southern	22	6.8	6.9	6.8	6.9	6.7	6.8	6.7	6.8	7.1	7.1	6.8	7.0	7.0	7.1
Segment	36	7.0		7.0		6.9		6.9		7.2		7.1		7.1	

*Since the Dyer Segment exhibits significant to dominant? vertical-slip, regressions based on dip-slip data sets are used in addition others.

Segment Length	Rupture Length (km)	Regression Magnitude Estimate: Slemmons and others, 1982 — All Events (All)	(Mean)	(Dip)	(Mean)	Extensional Events (All)	(Mean)	(Dip)	(Mean)	Bonilla et al, 1984 (NM AN)	(Mean)	(All)	(Mean)
Dyer	18	6.4	6.6	6.4	6.5	6.4	6.5	6.4	6.6	6.4	6.6	6.7	6.8
Segment	18	6.7		6.7		6.6		6.7		6.7		6.9	

THIS PAGE IS AN OVERSIZED DRAWING OR FIGURE,

THAT CAN BE VIEWED AT THE RECORD TITLED:

PLATE 1
"MORPHOSTRATIGRAPHIC MAP
OF A PORTION OF
NORTHWESTERN FISH LAKE
VALLEY, NEVADA"

WITHIN THIS PACKAGE..

D-01

THIS PAGE IS AN OVERSIZED DRAWING OR FIGURE,

THAT CAN BE VIEWED AT THE RECORD TITLED:

PLATE IIA
"SCHEMATIC FAULT MAP OF THE LATE QUATERNARY FISH LAKE VALLEY AND EMIGRANT PEAK FAULT ZONES IN FISH LAKE VALLEY, NEVADA AND CALIFORNIA"

WITHIN THIS PACKAGE..

D-02

THIS PAGE IS AN OVERSIZED DRAWING OR FIGURE,

THAT CAN BE VIEWED AT THE RECORD TITLED:

PLATE IIB
"DAVIS MOUNTAIN QUADRANGLE
NEVADA-CALIFORNIA"

WITHIN THIS PACKAGE..

D-03

THIS PAGE IS AN OVERSIZED DRAWING OR FIGURE,

THAT CAN BE VIEWED AT THE RECORD TITLED:

PLATE IIC
"MT. BARCROFT QUADRANGLE
CALIFORNIA-NEVADA"

WITHIN THIS PACKAGE..

D-04

THIS PAGE IS AN OVERSIZED DRAWING OR FIGURE,

THAT CAN BE VIEWED AT THE RECORD TITLED:

PLATE IID
"PIPER PEAK QUADRANGLE
NEVADA-CALIFORNIA"

WITHIN THIS PACKAGE..

D-05

THIS PAGE IS AN OVERSIZED DRAWING OR FIGURE,

THAT CAN BE VIEWED AT THE RECORD TITLED:

PLATE IIE
"SOLDIER PASS QUADRANGLE
CALIFORNIA-NEVADA"

WITHIN THIS PACKAGE..

D-06

THIS PAGE IS AN OVERSIZED DRAWING OR FIGURE,

THAT CAN BE VIEWED AT THE RECORD TITLED:

PLATE III
"LOG OF TRENCH AT
EXCAVATION SITE 1"

WITHIN THIS PACKAGE..

D-07

THIS PAGE IS AN OVERSIZED DRAWING OR FIGURE,

THAT CAN BE VIEWED AT THE RECORD TITLED:

PLATE IV
"LOG OF TRENCH AT EXCAVATION SITE 2"

WITHIN THIS PACKAGE..

D-08

THIS PAGE IS AN OVERSIZED DRAWING OR FIGURE,

THAT CAN BE VIEWED AT THE RECORD TITLED:

PLATE 4
"TRENCH 3- ROOKER
ROAD FAULT"

WITHIN THIS PACKAGE..

D-09

THIS PAGE IS AN OVERSIZED DRAWING OR FIGURE,

THAT CAN BE VIEWED AT THE RECORD TITLED:

PLATE 5
"TRENCH 4 - ROOKER
ROAD FAULT"

WITHIN THIS PACKAGE..

D-10

THIS PAGE IS AN OVERSIZED DRAWING OR FIGURE,

THAT CAN BE VIEWED AT THE RECORD TITLED:

PLATE VI
"LOG TRENCH AT
EXCAVATION SITE 4"

WITHIN THIS PACKAGE..

D-11